IASPEI
International Association of Seismology
and Physics of the Earth's Interior

IUGG

IAGA
International Association of
Geomagnetism and Aeronomy

IAGA IASPEI INDIA 2021

IAGA-IASPEI 2021

21-27 August 2021 | Hyderabad, India

60
CSIR NGRI
1961 - 2021

CSIR – NATIONAL GEOPHYSICAL RESEARCH INSTITUTE
(Council of Scientific and Industrial Research)

IAGA-IASPEI 2021

21-27 August 2021 | Hyderabad, India

ABSTRACTS

CSIR – NATIONAL GEOPHYSICAL RESEARCH INSTITUTE
(Council of Scientific and Industrial Research)

PREFACE

After 1969 in Madrid and 2001 in Vietnam, the two IUGG Associations IAGA and IASPEI are meeting the 3rd time for a Joint Scientific Assembly. Initial efforts for the planning of the IAGA-IASPEI Joint Scientific Assembly 2021, to be held at Hyderabad, hosted by CSIR-NGRI and INSA (the National Adhering body of IUGG) started as early as 2019 during the IUGG General Assembly at Montréal, Canada. In February of 2020, the General Secretaries of IAGA and IASPEI made a physical tour of the venue, accommodation, entertainment and transport facilities in Hyderabad to optimize arrangements for delegates, who would attend the conference in August 2021.

These preparations came to a grinding halt when the global pandemic situation started spreading like wildfire from March 2020. It was only in the second half of the year that the decision to not postpone the Joint Assembly, but rather turn it into a virtual one, could be taken. The re-oriented preparations started in earnest again from October 2020. After hundreds of meetings and long days of work, we are now ready for the virtual conference, which will spread over 21 – 27 August, 2021. The 5th IAGA and 1st IASPEI Schools and the GIFT Workshop precede it, the week before. 30 doctoral students will be attending each of the Schools, and more than 50 school teachers will be trained in recent developments in the Earth systems from India and neighboring countries in the GIFT Workshop.

827 scientists and researchers have registered for the conference. 778 abstracts were submitted for presentations during the 53 symposia: 8 Joint symposia, 1 Diamond Jubilee symposium commemorating 60 years of CSIR-NGRI, 27 IAGA symposia and 17 IASPEI symposia, including one from the Asian Seismological Commission (ASC). A major advantage of organizing a joint Assembly is of course the opportunity for interdisciplinary discussion and exchange of research results. Therefore, we are in particular emphasizing that ~20% of all contributions has been submitted to the Joint Symposia.

The 217 poster and 562 oral contributions including 121 invited talks will be presented in virtual mode from all over the world, making optimum time scheduling a big challenge. Three Plenary lectures on topics of interest both for IAGA and IASPEI are scheduled. The Inaugural and Valedictory sessions include participation of policy makers from the Government of India, who will receive a glimpse of the science and its application for human society, which is being deliberated during the conference.

The Scientific Programme Committee has worked hard to balance the parameters of world time zones, overlap of sessions and themes, and preferences of conveners, who have so carefully structured their symposia. Business Meetings, Poster Halls slots had to be accommodated to come up with a best compromise. The journey of transitioning into this new mode has been one of many challenges and learning opportunities. We hope that all delegates make the best of the congregation through virtual sharing of science and casual chats. Virtual conferences are here to stay but we also look forward to meeting each other in person on another scientific occasion.

Scientific Programme Committee
Kusumita Arora (Chair), Monika Korte, Johannes Schweitzer,
Harsh K Gupta, Archana Bhattacharyya, Prakash Kumar

CONTENTS

CONTENTS

Plenary 1

- -

India: A journey in time and space

Trond H. Torsvik

Centre for Earth Evolution and Dynamics (CEED), University of Oslo, 0315 Oslo, Norway

India's journey in time and space can be described in variable detail for the past one billion years. It was once located along the western margin of the Rodinia supercontinent but break-up details and the Late Neoproterozoic-Cambrian formation of Gondwana is complicated by the fact that paleomagnetic data exhibit aberrant and unresolved behavior between 600 and 520 Ma. India was located along the margin of Gondwana and later Pangea together with several Tibetan terranes that drifted off India in the Permian but mysteriously joined again in the end-Cenozoic. But long before that time, Madagascar-Seychelles-India drifted off Africa at 170 Ma, probably triggered by a deep plume sourcing the Karoo large igneous province (LIP). A younger 90 Myr Madagascar LIP heralded the separation of India-Seychelles from Madagascar at 84 Ma. That spearheaded a northward-directed acceleration of India until 60 Ma and shortly after the Deccan Traps, which separated Seychelles from India. The India-Asia collision is traditionally assumed to have happened in the Early Eocene but all plate reconstructions put India too far south of Asia at that time. This has resulted in plentiful models where India is extended northward in order to be adjacent to Asia by the Early Eocene. Some therefore maintain that the Himalayan Orogeny is best divided into two phases, a first phase of collision of a microcontinent to the north of India at 50 Ma, and a second and more substantial India-Asia collision, starting at 25-20 Ma and which has continued until present day.

Plenary 2

- -

Role of core-mantle interaction in the geodynamo

Binod Sreenivasan

Centre for Earth Sciences, Indian Institute of Science, Bangalore, India

The Earth's magnetic field is generated by a dynamo in its fluid outer core, which convects in response to non-uniform heat flow imposed by the mantle. Several observations point to lower-mantle effects on the geodynamo: the high-latitude concentrations of magnetic flux that make up the main dipole field have been found to be relatively stable during the historical period, changes in the frequency of polarity reversals may be correlated to changes in the heat flux at the core-mantle boundary (CMB), and secular variation in the Pacific is weak. Numerical dynamo simulations and laboraory experiments have provided insights into the response of the Earth's field to the inhomogeneity in CMB heat flux. Recent studies indicate that a large variation in CMB heat flux would result in an east-west dichotomy in core convection. This might in turn contribute to the seismic anisotropy of the inner core. In this talk, I shall focus on the role of thermal core-mantle coupling in the geodynamo.

Plenary 3

Seismic structures near the core-mantle boundary

Christine Thomas

Institut für Geophysik Westfälische Wilhelms Universität Münster

In recent years, seismology has provided increasingly detailed images of the interior of the Earth, especially since the onset of the deployment of temporary seismic arrays: Seismic tomography has revealed that some slabs descend into the lower mantle while others seem to stagnate at the mantle transition zone and hot upwellings also seem to show complex behaviour. Topography of seismic discontinuities can provide information the dynamics of the mantle but also on the mineralogy of the Earth's mantle. The region deep in the Earth, the D" layer (the lowest 200-400 km of the Earth's mantle) and core-mantle boundary region, has been studied extensively, revealing more and more complex features for which several hypotheses to explain them have been brought forward. The observed structures in the D" region and the lowermost mantle could for example be partly due to the post-perovskite phase transition but other causes are still discussed while the origin of the large low seismic velocity regions (LLSVP) is still debated. The presence of anisotropy, ultra-low velocity regions as well as scatterers may also shed more light on mineralogy and dynamics of the mantle. Other interesting observations include the topography of the core-mantle boundary and possible detections a layer just beneath the core-mantle boundary. In this presentation we will review some of these observations from above and below the core-mantle boundary region and their connection to dynamics and mineralogy of the Earth's mantle and core. The different hypotheses for causing these structure will be discussed and compared to seismic observations including as much information of the seismic waves as possible.

Joint IAGA IASPEI Symposia

J1 Earth and planetary core structure and evolution from observations and modelling

CONVENERS: Christopher Davies

Swarandeep Sahoo

Kimberly Moore

Christine Thomas

Recent advances in the theory and observation of planetary cores is providing profound insight into these remote and enigmatic regions. The Juno and Cassini missions have revealed the properties of Jupiter's magnetic and gravity fields in unprecedented detail, while results from forthcoming missions such as BepiColombo and InSight promise a step change in our knowledge of the interior structure and dynamics of terrestrial bodies within our solar system. Complementary theoretical developments have advanced our understanding of nucleation and crystallization of solids within planetary cores and how these processes influence the generation of global magnetic fields over geological timescales. Numerical simulations of the dynamo process are pushing towards the extreme conditions of rapidly rotating magnetic turbulence that are thought to characterize many planetary cores, promising new insights into the field generation process and the origin of observed magnetic secular variation. On Earth, novel seismic data processing techniques are being combined with vast datasets to illuminate core-mantle interactions and anomalous structures in the liquid and solid cores, while mineral physics calculations and experiments are now capable of estimating transport properties at the extreme pressure-temperature conditions of the core-mantle boundary. Observations of Earth's magnetic field magnitude and its secular variation have been used to infer various physical processes such as core flow patterns, inner core growth, thermal and compositional evolution of the core, and their fundamental origin.

This session focuses on recent cutting-edge and interdisciplinary activities that advance our understanding of Earth and planetary core structure, dynamics and evolution. We invite submissions from disciplines including, but not limited to: Earth and planetary chemistry, core dynamics, magnetism, mineral physics, seismology, planetary science, and geodesy.

Sr No: I

Our Planet deep interior – a view from the magnetic, gravity and the Earth's rotation observations

CORRESPONDING & PRESENTING AUTHOR:

Mioara Mandea, CNES - Centre National d'Etudes Spatiales, France

Anny Cazenave, CNES - Centre National d'Etudes Spatiales, France

Veronique Dehant, Royal Observatory Belgium, Belgium

Anne Barnoud, Magellium, France

Ilya Firsov, Université Grenoble Alpes – ISTerre, France

Felix Gerick, Royal Observatory Belgium, Belgium

Julia Pfeffer, Magellium, France

Jeremy Rekier, Royal Observatory Belgium, Belgium

Tobias Schwaiger, Université Grenoble Alpes – ISTerre, France

Santiago Andreas Triana, Royal Observatory Belgium, Belgium

Ping Zhu, Royal Observatory Belgium, Belgium

The deep Earth's interior processes, particularly at the core-mantle boundary and in the fluid outer core, are described by indirect observations available from ground and satellite. Invaluable information about the core flow on their own are obtained from magnetic, gravity and Earth's rotation data. The idea to exploit all this information together is appealing and is the core of the GRACEFUL project.

The time dependent magnetic field, originating mainly within the core, can be used to infer the motions of the fluid at the top of the core on decadal and subdecadal time scales. The time dependent gravity field variations that reflect changes in the mass distribution within the Earth and at its surface occur on a broad range of time scales. Decadal and interannual variations include the signature of the flow inside the core, though they are largely dominated by surface contributions related to the global water cycle and climate-driven land ice loss. Earth's rotation changes (or variations in the length of the day) also occur on these time scales, and are essentially related to the core fluid motions through exchange of angular momentum between the core and the mantle at the core-mantle boundary.

Here, we present the first results obtained in the frame of the GRACEFUL ERC project, which aims to combine information about the core deduced from the gravity field, from the magnetic field and from the Earth's rotation in a synergy manner.

KEYWORDS :   satellite magnetic and gravity data, earth's rotation, core-mantle boundary

Sr No: 2

Do preferred structures in paleomagnetic field reconstructions indicate mantle control on the geodynamo?

CORRESPONDING & PRESENTING AUTHOR:

Monika Korte, GFZ German Research Center for Geosciences, Germany

Catherine Constable, University of California San Diego, USA

Chris Davies, University of Leeds, UK

Sanja Panovska, GFZ German Research Center for Geosciences, Germany

Several continuous global geomagnetic field reconstructions spanning up to 100 kyr have been developed in recent years based on paleomagnetic data from sediment cores and volcanic rocks. They indicate preferred longitudinal bands for intensity minima and for virtual geomagnetic pole (VGP) paths during field excursions. Recurring and/or persistent magnetic field structures have long been discussed as potential indications of mantle control on the geodynamo process in Earth's outer core. Preferred longitudinal structures in geomagnetic field characteristics might arise from laterally-varying heat flow through the core-mantle boundary (CMB), as inferred by seismic tomography and global mantle circulation models. Using paleomagnetic field models we investigate statistics associated with magnetic field properties like VGPs and intensity minima that might be indicative of mantle control on the geodynamo. Preliminary results indicate some correlations with models of seismic velocity and heat flow distribution in the lowermost mantle. We also analysis a suite of geodynamo simulations with both homogeneous and laterally-varying CMB heat flow, which allow a full exploration of potential biases arising from limited spatial and temporal resolution in paleofield models. Preliminary results seem to generally support the hypothesis of CMB heat flow heterogeneities influencing the geodynamo process.

KEYWORDS : geodynamo, core-mantle boundary, heat flow heterogeneity

Sr No: 3

The seismic signal of outermost-core stratification (by invitation)

CORRESPONDING & PRESENTING AUTHOR:

Runa Van Tent, Utrecht University, Netherland

Arwen Deuss, Utrecht University, Netharland

Satoshi Kaneshima, Kyushu University, Japan

Christine Thomas, University of Münster, Germany

The presence of a buoyant, stably stratified layer at the top of Earth's liquid outer core, which is otherwise considered to be approximately homogeneous, would change our understanding of outer-core dynamics. The presence of such a layer has been proposed by seismological studies that use SmKS differential travel times to image seismic outermost-core velocity, finding that the outermost core is anomalously slow and that a change in composition is needed to explain the found velocity profile. However, the enrichment in light elements that is required to create buoyant compositional stratification is generally expected to increase,
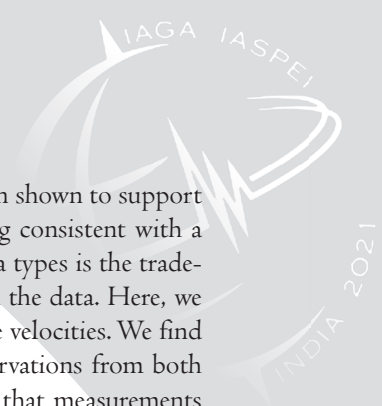
not decrease, seismic velocity. Independent seismic data, Earth's normal modes, have been shown to support the observations of a low-velocity outermost core (Irving et al. 2018), while still being consistent with a homogeneous outer-core composition. An important factor of uncertainty for both data types is the trade-off between the effects of outermost-core structure and lowermost-mantle structure on the data. Here, we assess these trade-offs and determine the robustness of the observed low outermost-core velocities. We find that even though mantle effects are significant, they cannot explain the combined observations from both data types, meaning that a low-velocity outermost core is still required. We also show that measurements of additional normal modes that are particularly sensitive to density need a relatively dense outermost core, which is inconsistent with the presence of buoyant stratification. Finally, we complement our modeling results by performing an inversion on a large normal-mode dataset for mantle and outer-core structure simultaneously.

KEYWORDS : outer core, seismology

Sr No: 4

SYMPOSIUM :   **J1 Earth and planetary core structure and evolution from observations and modelling**

Earth's Outer Core Constrained by the Coda Correlation Wavefield

CORRESPONDING & PRESENTING AUTHOR:

Xiaolong Ma, Australian National University, Australia

Hrvoje Tkalcic, Australian National University, Australia

Abstract : Increasing seismic evidence has suggested that the top of the Earth's outer core has a layer of a P-wave gradient distinct from the bulk of the outer core. This layer could indicate a stable stratification below the core-mantle boundary (CMB) and is essential for understanding the geodynamo and thermochemical interactions between the mantle and core. However, a consistent globally-averaged radial structure of the outermost core has not been obtained due to incomplete coverage of sampling body waves. Here we increase constraints on the seismic structures of Earth's outermost core based on a new concept, termed earthquake-coda correlation wavefield. We construct the observed global correlogram (correlation wavefield) by stacking cross-correlations of the long-duration coda waves (3-9 hours after the event origin time) from ten large earthquakes. The correlogram displays many prominent correlation features that can be used to constrain the outer core structure. We fit both travel times and waveforms of these features by computing synthetic correlograms through different outer-core models. Our results show that Preliminary Reference Earth Model (PREM) displays a too fast P-wave velocity profile in the top of the outer core. Finally, we propose a new outer-core model, which provides an optimal representation of the correlation features in the coda wavefield and informs dynamics of the outer core.

KEYWORDS :   outer core, coda correlation wavefield, body waves

Sr No: 5

Observations of Multiple Podal & Antipodal Reverberations on Dense Seismic Networks

CORRESPONDING & PRESENTING AUTHOR:

Thanh Son Pham, Australian National University, Australia

Hrvoje Tkalcic, Australian National University, Australia

Stacking waveforms recorded by a dense seismic network is a standard method to boost the observation of weak signals, which are otherwise unobservable on individual seismograms. Here we present observations of "exotic seismic phases" in global seismic stacks – PKIKP multiples, which are compressional waves propagating within confined corridors along the Earth's diameter, including its solid inner core, up to five passages. These arrivals are referred to as PKIKP1, PKIKP2, etc., with the last digit indicating the number of passages through the bulk of the Earth. We make these observations on dense arrays at a continental scale and the relatively long-period broadband for specific large earthquakes. We calculate the residuals of differential travel time of PKIKP multiple pairs simultaneously observed, such as PKIKP4–PKIKP2 at small epicentral distances or PKIKP3-PKIKP1 at near antipodal distances. The optimal cylindrical-anisotropy model, which fits the residual measurements, reveals ~2.5% anisotropy for the innermost inner core with a pronounced slow axis residing at ~50° relative to the Earth's rotation axis. These are entirely new, complementary constraints on the centermost part of Earth's inner core to the existing methods that employ relatively high-frequency body waves and low-frequency free oscillations of the Earth.

KEYWORDS : body wave; inner core; exotic observation

Sr No: 6

Possible detection of a stratified layer at the core surface from a geomagnetic field model

CORRESPONDING & PRESENTING AUTHOR:

Masaki Matsushima, Tokyo Institute of Technology, Japan

There is a possibility that a stably stratified layer at the top of the Earth's outer core is present as suggested by recent seismic studies. Upwelling and downwelling flows in the stratified layer would not be present just below the core-mantle boundary (CMB). This means that only toroidal flows contribute to temporal changes in the geomagnetic field. Such fluid flows can be estimated from a geomagnetic field model. In a viscous boundary layer below the CMB, not only the motional induction but also the magnetic diffusion inside the boundary layer are assumed to cause temporal variations of the geomagnetic field. Core surface flows below the boundary layer are assumed to be in the tangentially magnetostrophic state.

To estimate a core surface flow, depths from the core surface are provided as parameters; one is taken to be less than the thickness of the boundary layer, and the other be larger than the thickness of the boundary layer. Therefore, it might be possible to investigate the existence of a stably stratified layer at the top of the
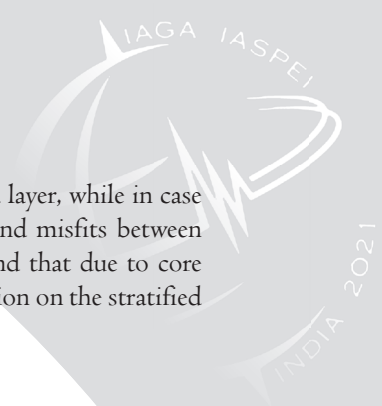
core in the following way. In case 1, only the toroidal flow is allowed inside the stratified layer, while in case 2, both the toroidal and poloidal flows are permitted there. Correlation coefficients and misfits between a temporal variation of the magnetic field obtained from a geomagnetic field model and that due to core surface flows in cases 1 and 2 are compared with each other. The result provides information on the stratified layer.

KEYWORDS : core surface flow, stratified layer, geomagnetic field

Sr No: 7

SYMPOSIUM : **J1 Earth and planetary core structure and evolution from observations and modelling**

Formation of vortices and jet streams in 3D spherical shell convection simulations (by invitation)

CORRESPONDING & PRESENTING AUTHOR:

Rakesh Yadav, Harvard University, USA

Jeremy Bloxham, Harvard University, USA

Moritz Heimpel, University of Alberta, Canada

Decades of observations have painted a rich picture of the atmosphere of Saturn and Jupiter. Both planets have jet streams which circulate unabated around the entire planet, along with numerous storms which could be even larger than the Earth. All these features are striking examples of turbulent self-organization of fluid flows. However, the exact physics behind the formation of these features is still uncertain. Using three simulation cases, I will discuss how rotating convection may form such features: The first simulation shows how rotating convection spontaneously forms jet streams with polygonal shapes, helping to shed light on how Saturn's famous hexagonal jet forms; The second generates several alternating jet streams, as well as numerous storms, similar to what we see on Jupiter; And, the third demonstrates how gigantic storms may form on these planets. I will discuss what we can learn from these cases about the fluid dynamics of Saturn and Jupiter.

KEYWORDS : planetary interior, convection, vortices

Sr No: 8

SYMPOSIUM : **J1 Earth and planetary core structure and evolution from observations and modelling**

Earth and planetary core structure and evolution from observations and modelling

CORRESPONDING & PRESENTING AUTHOR:

Daniel Frost, University of California, Berkeley, USA

Marine Lasbleis, Université de Nantes, France

Brian Chandler, University of California, Berkeley, USA

Barbara Romanowicz, University of California, Berkeley, USA

Progressive crystallisation of Earth's inner core drives convection in the outer core and magnetic field generation. Determining the rate and pattern of inner core growth is thus crucial to understanding the

evolution of the geodynamo. The growth history of the inner core is likely recorded in the distribution and strength of its seismic anisotropy, which arises from deformation texturing constrained by conditions at the inner-core solid-fluid boundary.

Here we show from analysis of seismic body wave travel times (PKP) that the strength of seismic anisotropy increases with depth within the inner core, and the strongest anisotropy is offset from Earth's rotation axis into the western hemisphere. Then, using geodynamic growth models and mineral physics calculations, we simulate the development of inner core anisotropy in a self-consistent manner. We model a range of differential inner core growth rates between the equator and the pole, and a range of asymmetrical growth rates. We test several phases of iron and several iron alloys. From this we find that an inner core composed of hexagonally close-packed iron-nickel alloy, deformed by a combination of preferential equatorial growth and slow translation, can match the seismic observations without requiring hemispheres with sharp boundaries. Our model of inner core growth history is compatible with external constraints from outer core dynamics, and supports arguments for a relatively young inner core ($\sim$0.5–1.5 Ga) and a viscosity $>10^{18}$ Pa-s.

KEYWORDS : inner core, seismology, geodynamics

Sr No: 9

- -

Three Stories about the Core of Venus: Implications for our Solar System and Exoplanets (by invitation)

CORRESPONDING & PRESENTING AUTHOR:

Joseph Orourke, Arizona State University, USA

Venus and Earth are nearly the same size and are thought to have the same bulk composition. However, Earth's dynamo has existed for billions of years, while Venus has no strong, internally generated magnetic field today. Here I will present three different stories for the absence of a dynamo in Venus—all of which are plausible given our vast ignorance about its interior. Discovering which of these three stories is true would provide a key constraint on our models of the accretion and evolution of rocky planets in our Solar System (Earth and Venus) and beyond (Earth- and Venus-like exoplanets). First, Venus may have experienced a "gentle" accretion that preserved chemical stratification in its core, which always prevented dynamo-generating convection. Second, the cores of Venus and Earth might have identical structures and compositions—but relatively slow cooling of the mantle of Venus leads to sub-critical heat flow out of its core. Finally, Venus could have a thick layer of molten silicates (a basal magma ocean) at the bottom of its mantle, which acts as a giant thermal blanket that smothers any chances for a dynamo in the core. Remarkably, each of these stories also make distinct predictions about the fractions and types of rocky exoplanets that will host strong magnetospheres. I will explain how we can test these three stories over the next few decades with both astronomical observations and spacecraft missions to Venus.

KEYWORDS : venus, exoplanets, evolution
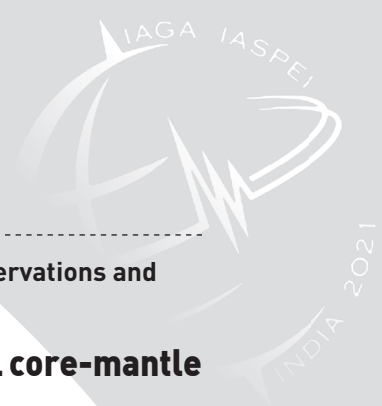
Sr No: 10

Penetrative convection in the Earth's outer core with thermal core-mantle coupling

PRESENTING AUTHOR:

Susmita Garai, Indian Institute of Technology (Indian School of Mines) Dhanbad, India

CORRESPONDING AUTHOR:

Swarandeep Sahoo, Indian Institute of Technology (Indian School of Mines) Dhanbad, India

The heat transfer in the Earth's fluid core is a superadiabatic process. Near the lower mantle, the reduced heat loss or local transfer of heat from the mantle to the core may produce a subadiabatic geothermal gradient which is responsible for developing stably-stratified layers beneath the core-mantle boundary (CMB) as a consequence of accumulation of heat in this zone. In this study, thermal convection between a pair of infinite horizontal isothermal plates is used to model Earth's core convection with stably-stratified layers at its top. A linear stability analysis of this model shows a global stratification with the flow penetrating the stable layers from the unstable fluid regions at the bottom. Such penetration becomes robust for rapid rotation with strong stratification. Finally, a much realistic scenario for the CMB region is considered by imposing thermal heterogeneity in the upper boundary to mimic thermal core-mantle coupling. The effect of this coupling on the flow with and without the stably-stratified layers shows that the thermal heterogeneity together with rapid rotation gives rise to travelling waves with the thermal wind breaking the symmetry of the convective rolls.

KEYWORDS : penetrative convection, thermal core-mantle coupling

Sr No: 11

Topographic effects at the core-mantle boundary

CORRESPONDING & PRESENTING AUTHOR:

Remy Monville, ISTerre (Institut des Sciences de la Terre), France
David Cebron, ISTerre (Institut des Sciences de la Terre), France
Dominique Jault, ISTerre (Institut des Sciences de la Terre), France

Associated with the nutation of the Earth's axis of rotation, there is a quasi-diurnal differential rotation between the outer core and the mantle. This motion provides a core-mantle coupling indirectly inferred from nutation observations. However, the current models of coupling can not fully explain these data. The solution could possibly come from a topographic pressure force that applies to the boundary when a stratified and magnetized fluid flows over a bumpy core-mantle boundary.

We develop a local model in the continuity of the recent works of Glane and Buffett (2018) and Jault (2020). Our code ToCCo, relying on symbolic computation and arbitrary precision, is designed to extend the calculations to orders of Taylor series greater than a linearization, which is commonly done in this

kind of study. This allows us to better constrain the domain of applicability of the results presented in the literature. At this point, we can take into account simultaneously rotation, magnetic field, and stratification to compute the boundary pressure torque. Thus, we can evaluate this coupling over a large panel of parameters and boundary conditions: from core conditions with a conducting mantle, to the ocean and atmosphere situations. Our code is therefore able to reproduce recent studies but also to explore new cases of interest.

REFERENCES

Glane, S. and Buffett, B. (2018). Frontiers in Earth Science, 6:171.

Jault, D. (2020). Geophysical Journal International, 221(2):951–967.

KEYWORDS : core dynamics, dissipation

Sr No: 12

SYMPOSIUM : **J1 Earth and planetary core structure and evolution from observations and modelling**

Magnetic boundary layers in numerical dynamos with heterogeneous outer boundary heat flux

CORRESPONDING & PRESENTING AUTHOR:

Filipe Terra Nova, IAG/USP, Brasil

Hagay Amit, Université de Nantes, France

Magnetic flux expulsion due to outer core fluid upwellings may affect the geomagnetic SV on the CMB. In this process intense horizontal field lines are concentrated below the outer boundary, introducing small radial length scales and consequently strong radial diffusion. We explore such magnetic boundary layers in numerical dynamo simulations with heterogeneous outer boundary heat flux inferred from a tomographic model of lower mantle seismic shear waves velocity anomalies. Our scheme associates magnetic boundary layers to peak horizontal magnetic fields at the top of the shell. In our models mean magnetic boundary layer thickness ranges $\approx 200 - 400$ km and decreases with increasing Rm. Extrapolation or interpolation to Earth's core conditions based on total core flow amplitude or its poloidal part gives mean magnetic boundary layer thickness of ≈ 220 and $\approx 260 - 330$ km, respectively. We find magnetic boundary layers associated with the azimuthal field at the equatorial region, whereas layers associated with the meridional field are found at mid latitudes. Negative outer boundary heat flux anomalies yield preferred locations of expulsion of azimuthal field below Africa and the Pacific, while positive outer boundary heat flux anomalies yield preferred locations of expulsion of meridional field below the Americas and East Asia. Furthermore, we find a tendency of the azimuthal field to low latitudes of the Northern Hemisphere. Our results suggest that the local diffusion time is on the order of several kyr and the local magnetic Reynolds number is on the order of ≈ 10, both much smaller than classical estimates.

KEYWORDS : local diffusion time scale, magnetic boundary layer, reversed flux patches

J2 Application of geophysical studies for understanding lithospheric structure and properties

CONVENERS: Jerome Dyment

Vincent Lesur

Munukutla Radhakrishna

Anand. P. Singh

The main objective of the session is to bring together researchers specialized in geophysical studies, both in potential fields (involving terrestrial, marine, airborne and satellite-based datasets) and in seismology, to present and discuss their new results related to the crustal and lithospheric structure, properties, and geodynamic evolution in both the continental and oceanic realms. Papers involved in regional investigations and/or the development of new methodologies are therefore encouraged.

Considering the original meeting location and host, a special emphasis will be given to the Indian Plate. The plate is bounded by a collision boundary along the Himalayan arc, an active subduction along the Indonesian arc, and a slow to intermediate spreading center along the Carlsberg, Central and Southeast Indian ridges. It comprises of the continental lithosphere of the Indian subcontinent made of an assemblage of several cratons and mobile belts, and the oceanic lithosphere of the northern Indian Ocean. The passive margins of the Indian subcontinent acted as huge sediment depocenters and provide valuable clues on the Himalayan orogeny as well as the ongoing deformation within the Indian plate. A deeper understanding of the continental lithosphere sheds light on the early crust formation as well as the evolution of sub-continental lithospheric mantle. Potential fields and seismology provide images that can be used to delineate lithospheric structures at different spatial scales and, in turn, geodynamic evolution models at different temporal scales.

Sr No: 13

Decreasing magnetization of oceanic crust in subduction zones: a global appraisal

CORRESPONDING & PRESENTING AUTHOR:

Hanjin Choe, Kangwon National University, South Korea

Jerome Dyment, IPGP, France

Seafloor spreading magnetic anomalies of oceanic plates progressively decay and disappear when approaching and entering subduction. Previous studies focused on the Japan Trench showed that before subduction, the flexure of the oceanic lithosphere opens normal faults and rejuvenates hydrothermal circulation which results in the alteration of magnetic minerals. After subduction, thermal demagnetization affects the magnetic minerals of the oceanic crust when the increasing temperature of the subducting slab pass their Curie temperature. No other subduction zone was investigated so far. Here we study the evolution of magnetic anomalies in five subduction zones. The major observed differences are controlled by the age of the lithosphere and related physical properties. Before subduction, magnetic anomalies of the old oceanic lithosphere show a significant decay (20-30%) related to alteration whereas those of the young lithosphere at the Cascadia subduction zone display no such decay as a consequence of negligible flexure on the young Juan de Fuca plate. After subduction, the magnetic anomalies of the subducting plate show a rapid decay reflecting the thermal demagnetization of extrusive basalt, amounting for 30-40% in the old oceanic lithosphere and more than 70% in the young lithosphere of Cascadia. Beyond the complete thermal demagnetization of extrusive basalt, about 40% of the magnetization remains in the old lithosphere and less than 20% in the young lithosphere of Cascadia.

KEYWORDS : subduction zone, magnetic anomaly, curie temperature

Sr No: 14

Comparative analysis of geological lineaments derived from satellite gravity and ASTER data in Cambay area of Gujarat

CORRESPONDING & PRESENTING AUTHOR:

Shiva Shankar Manche, National Remote Sensing Center, India

Arindam Guha, National Remote Sensing Center, India

K. Vinod Kumar, National Remote Sensing Center, India

Study of geological structures is essential in the field of mineral and hydrocarbon exploration as these structures contribute in concentrating mineral deposit and also form hydrocarbon traps. Generally, geophysical data are used to characterize the basement details, and two and three dimensional distribution of deep seated structures. Some of these structures may have surface imprints which can also be mapped from the satellite imagery. In this study, we have processed EIGEN-6C4 satellite gravity data based on implementing Total Horizontal Derivative (THD) to delineate geological structures in the Cambay area, which have subsurface extension. Also, we have processed ASTER multispectral data by implementing
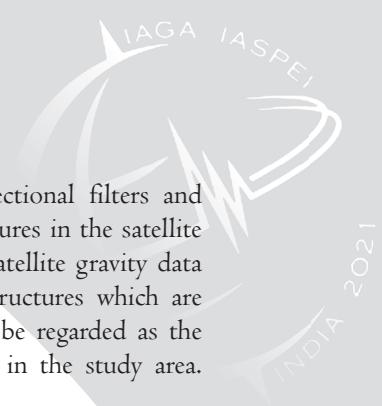
the different edge enhancement techniques such as high pass, Laplacian, and Directional filters and principal component analysis to identify the possible imprints of the geological structures in the satellite image. An attempt has been made to identify important geological structures using satellite gravity data and relate them with the structures that are delineated using ASTER data. The structures which are deep-seated and cutting across the trap rock and also have surface expression could be regarded as the important micro seepage zones; we identified few structures of similar significance in the study area.

KEYWORDS :   lineaments, aster, satellite gravity

Sr No: 15

A new approach via drone magnetometry for chromite exploration – a case study

CORRESPONDING & PRESENTING AUTHOR:

Zeynab Golshadi, University of Tehran, Institute of Geophysics, Iran

Ala Ebrahimi, University of Tehran, Institute of Geophysics, Iran

The Ophiolite originated from the southern margin of the persian Gulf is a larg slab of oceanic crust, made of volcanic and ultramafic rocks connected to the earth's upper mantle, which was overthrust onto a continental crust. Following this, geophysical survey over a harsh topography like the one selected for investigation is not convenient for routine in-situ data aquisition, therfore, we have employed a drone system carrying a GEM magnetometer. the aquired data was processed in 3 different steps: 1-ordinary corrections of magnetic data including geomagnetism, elevation, topography, reduction to pole (RTP), etc. 2- background/flight magnetic noise removal, slope correction, and 3- advanced process which has been tested on synthetic models, to detect presence of podiform and vein types of chromite. Going through the processing steps, after applying basic corrections, we used a separation of potential field anomalies using upward continuation, vertical derivative methods, and RTP. Morover, to calibrate our results, we applied the whole process on a known chromite deposit in the site where satisfying results were found. Field/drilling results on high/low potential areas in this study, confirmed the location of chromite deposits and indicate that the low susceptibility contrast between chromite and surrounding rocks is distinguishable. Building on this, the outcomes suggest that current geophysical mapping system (drone-based magnetic set-up) and utilizing special processing methods, is a feasible option to find small podiform or tabular lens body of chromite resources in harsh topographical places flying at low elevation (<70 m above the ground)

KEYWORDS :   drone magnetometry, chromite, ophiolite mineralization

Sr No: 16

Evolution of the Western Ghats: Constraints from receiver function imaging and Harmonic decomposition

CORRESPONDING & PRESENTING AUTHOR:

Padma Rao B, MoES-National Centre for Earth Science Studies, Govt. of India, India

Ravi Kumar M, CSIR-National Geophysical Research Institute, India

The Western Ghats (WG), with an average elevation of ~1.2 km, is one of the greatest escarpments that spans ~1500 km parallel to the west coast of India. It is a mosaic of disparate geological formations having distinct structural and physical characteristics. In this study, the lithospheric structure and deformation along and across the WG are investigated using receiver functions (RFs) at 25 broadband seismological stations. Techniques like slant-stacking, common-conversion-point imaging and harmonic-decomposition are applied to the RFs. Results reveal a large crustal thickness of ~50 km in the central part of the WG, which decreases to ~36 km both in the southern and northern parts, in conformity with the geology. Moreover, a clear step in the Moho is observed across the WG, with the depths suddenly changing from ~39 km to ~44 km. This marks a clear transition from the Granulites to the Peninsular Gneisses. Further, the RFs reveal a strong low-velocity layer (LVL) along the WG, just below the Moho. This observation gains support from the inference of a sub-Moho low-density zone underneath the west coast of India. Harmonic decomposition of the RFs reveals that this LVL is anisotropic, while the Moho is dipping. The fast axis of symmetry varies from 58.1° to 134.3°, almost perpendicular to the west coast of India. These LVLs could have been formed due to different rifting episodes along the west coast of India since LVLs are manifestations of thermal/chemical anomalies. These results support the rifting model proposed for the evolution of WG.

KEYWORDS :   western ghats, LVL, rifting

Sr No: 17

Surface wave tomography reveals a new mechanism for the fast drift of Indian plate

CORRESPONDING & PRESENTING AUTHOR:

Satish Maurya, Indian Institute of Technology Bombay, India

Jean Paul Montagner, Institut de Physique du Globe de Paris, France

M. Ravi Kumar, CSIR-National Geophysical Research Institute, India

Prior to its collision with Eurasia, the Indian plate accelerated northwards (~80Ma ago) at unprecedented speeds of ~18 cm/year (peak around 65Ma ago). It maintained this speed for another 20Ma and slowed down to 5cm/year after the continent-continent collision. The cause for this anomalous drift of the Indian continental plate is still elusive. Although simulations invoking a double subduction system have been able to generate twice the rate of the present-day Indian plate motion and its average speed during the fast drift, they fail to explain the very high rate of ~18 cm/year. Another study based on magnetic anomalies on the
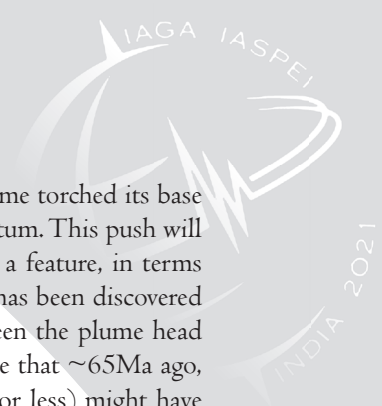
Indian ocean floor advocates that the Indian plate accelerated when the La Réunion plume torched its base and came up to the surface, the upwelling of mantle plume providing additional momentum. This push will be most effective in the presence of a stiff, rigid support in front of the plume. Such a feature, in terms of a deep cratonic keel (down to 250km) in the direction of the Indian plate motion, has been discovered recently from the results of 3D-seismic tomography. The role of the interaction between the plume head and the cratonic keel in the fast drift of the Indian plate cannot be ignored. We propose that ~65Ma ago, significant topography at the Lithosphere-Asthenosphere Boundary (250km to 80km or less) might have caused a lateral sub-lithospheric flow that pushed the Indian plate with considerable acceleration.

KEYWORDS : surface wave tomography, cratonic keel, la réunion plume

Sr No: 18

SYMPOSIUM : **J2 Application of geophysical studies for understanding lithospheric structure and properties**

Delineation of the sedimento-crustal deformation in the Mannar Basin, along the south eastern continental margin of India

CORRESPONDING & PRESENTING AUTHOR:
Nisha Nair, National Centre for Polar and Ocean Research, India
Dhananjai K Pandey, National Centre for Polar and Ocean Research, India
Lachit S Ningthoujam, National Centre for Polar and Ocean Research, India
Khogenkumar Shoraisam, National Centre for Polar and Ocean Research, India

Continental rifting and subsequent rift-to-drift mechanisms led to the genesis of new oceanfloor and surrounding margins containing numerous faults/fractures/shear zones. The Mannar Basin, adjoining southern tip of India, was formed through a similar process. An oblique rifting between Eastern Antarctica and India during early Cretaceous time eventually failed and gave rise to the Mannar basin. The underlying crust in this basin encompasses imprints of rift initiation that took place between India and Sri Lanka during their short-lived separation followed by sediment deposition. Due to inadequate geophysical data coverage in this region, early rifting and associated crustal processes remain far from fully understood. An attempt has been made to utilize closely spaced array of 2D multichannel seismic (MCS) reflection data integrated with litholog information along the Mannar Basin to delineate major sedimentary and upper crustal structures. The detailed seismic interpretation reveals ~2.0-3.0 s (TWT) thick Cretaceous to Recent post-rift sediments across the region. The regional basement appears to be heavily faulted at depths ranging between ~5.0 - 6.0 s (TWT) implying pre-to-syn rift deformation. Our new integrated geophysical interpretation will not only help document precise order of events that shaped up the southern continental margin of India but also shed lights on the inception of the Central Indian Basin. In addition to the high resolution MCS data, combined satellite derived bathymetry and free-air gravity data have been utilized for constraining the sedimento-crustal structure beneath the Mannar Basin.

KEYWORDS : continental margin, crustal deformation, Mannar Basin

Sr No: 19

New insight into the Lithospheric architecture beneath the Bay of Bengal and its adjacent region

PRESENTING AUTHOR:

Prakash Kumar, Indian Institute of Technology Kharagpur, India

CORRESPONDING AUTHOR:

William Kumar Mohanty, Indian Institute of Technology Kharagpur, India

Abstract : The Bay of Bengal is located at the juncture of the passive continental margins of India, Bangladesh, and the Andaman – Sumatra arc – trench systems, whose tectonic framework and evolution are very complex. The present study examines the lithospheric structure of the Bay of Bengal (BoB) and its adjacent region based on joint modelling of potential field data constrained by thermal analysis. The approach assumes local isostasy, thermal steady state, linear density increase with depth in the crust, and temperature-dependent density in the lithospheric mantle. The result elucidates the distinct lithosphere beneath the BoB. The lithospheric thickness beneath the western BoB is greater than 130 km, whereas the eastern BoB has a thinner lithosphere (80–100 km). The thin lithosphere in the eastern BoB is unusual for an ancient ocean. The lithosphere has generally dipping towards the eastern margin of India. The thicker lithosphere in the western basin may be possible due to the continuation of the Indian continental lithospheric or could be due to the conductive cooling of the oceanic basin. In contrast, a relatively thin (80-100 km) lithosphere beneath the eastern basin could be due to the reheating of the lithosphere as a consequence of its interaction with the Kergulean hotspot or slab rollback of subducting Indian lithosphere. The present result is in agreement with previous tomography studies.

KEYWORDS : Bay of Bengal, lithospheric structure, thermal analysis

Sr No: 20

Crust and the upper mantle structure below the Indian Ocean Geoid Low: Constraints from potential field modeling

CORRESPONDING & PRESENTING AUTHOR:

Gokul Venu Sreebindu, IIT Bombay, India

Sreejith K M, Space Applications Centre (ISRO), India

Srinivasa Rao Gangumalla, IIT (ISM) Dhanbad, India

Radhakrishna Munukutla, IIT Bombay, India

Peter Betts, Monash University, Australia

The Indian Ocean Geoid Low (IOGL) is the most intriguing geophysical entity in the globe which lies south of India in the Central Indian ocean. It is characterised by a maximum negative geoid anomaly of 106 m centered at 79°E and 5°S and reduces to ~-50 m at a distance of 2500 km radially. Despite several studies to understand the causative factors contributing to the IOGL, the depth and nature of the sources
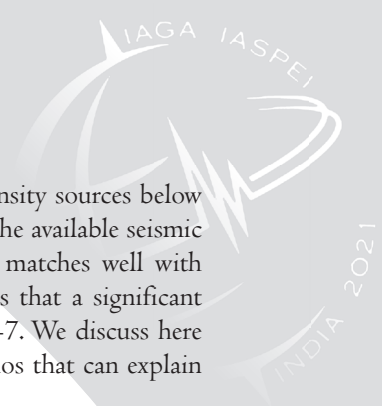
remain enigmatic. In the present study, we made an attempt to unravel the causative density sources below to the IOGL based on the integrated analysis of geoid, gravity, topography along with the available seismic tomographic models within upper mantle. The 3-D density structure modelled here matches well with degree-12 residual geoid anomalies. However spectral decomposition of IOGL reveals that a significant fraction of the mass anomalies comes from the harmonic coefficients less than degree-7. We discuss here the implications of the derived density structure as well as possible geodynamic scenarios that can explain the IOGL.

KEYWORDS : Indian Ocean Geoid Low (IOGL), potential field modeling, upper mantle structure

Sr No: 21

Crustal architecture of Comorin Ridge: new insights from the wide-angle seismic data

CORRESPONDING & PRESENTING AUTHOR:

Lachit Singh Ningthoujam, National Centre for Polar and Ocean Research, Goa, India

Dhananjai Pandey, National Centre for Polar and Ocean Research, Goa, India

Nisha Nair, National Centre for Polar and Ocean Research, Goa, India

Rahul Yadav, National Centre for Polar and Ocean Research, Goa, India

Sanjay Negi, National Centre for Polar and Ocean Research, Goa, India

Amit Kumar, National Centre for Polar and Ocean Research, Goa, India

The Comorin ridge an isolated tectonic block in the Indian Ocean south of Sri Lanka. Knowledge about the crustal structure underneath this aseismic ridge holds key for deciphering India-Madagascar break-up and its links with Marion plume magmatism. The ridge also lies in close proximity to one of the largest geoidal low on Earth. New coincident multichannel seismic reflection (MCS) and 420 km long wide-angle seismic (OBS) data traversing the ridge provide new insights about its tectonics and structural set up. New high quality data successfully image the regional basement and Moho variations.

Here, we present new crustal images using travel-time tomographic inversion of the OBS data. The velocity model is constructed by two-dimensional modeling and inversion approach using the RAYINVR (Zelt and Smith, 1992). The model shows an anomalously thick crust underneath the Comorin ridge, which gradually thins out oceanward. The final model provides very good constraints on the lateral variations on the crust-mantle boundary. Our modelling suggests that the eastern part of the profile images a mature oceanic crust while the western part has a substantially thickened crust with a maximum thickness of $\sim$ 14 km. This thickened crust ($\sim$160 km wide zone) is characterized by an anomalously high velocity lower crust (up to 7.4 km/s), which could be related to magmatic intrusions/crustal underplating.

KEYWORDS : comorin ridge, wide-angle seismic, crustal structure

Sr No: 22

Structural framework of the Western Dalma volcano-sedimentary basin, Eastern Indian shield based on the Bi-dimensional empirical mode decomposition and potential field modelling: implications on metallogeny

CORRESPONDING & PRESENTING AUTHOR:

Santosh Kumar, IIT(ISM), Dhanbad, India

Ramachandrudu Arasada, IIT(ISM) Dhanbad, India

Gangumalla Srinivasa Rao, IIT(ISM) Dhanbad, India

Dalma volcano-sedimentary basin located in the North Singhbhum Mobile Belt (NSMB) is an important crustal province in terms of geodynamic and metallogenic evolution of the Eastern Indian shield. In the present study, integrated interpretation of petrophysical, Bouguer gravity anomaly, and aeromagnetic data was carried out to examine the structural framework of the basin and its implications on concealed mineral deposits. We have decomposed both the gravity and magnetic data into several intrinsic mode functions (IMF-1 to IMF-4) using the Bi-dimensional empirical mode decomposition technique. IMF-1 of both gravity and magnetic data only identifies near-surface random noise and IMF-4 represents signatures of deep-seated sources. In comparison, IMF-2 and IMF-3 reveal two major structures known as Tamar Porapahar shear zones (TPSZ) and Babaikundi-Birgaon lineation. It is observed that both shear zones further extend westward towards the Tamar block of Jharkhand. We also noticed several discrete high gravity (up to 2 to 4 mGal) and magnetic anomalies (400 to 800 nT) with E-W strike direction parallel to the Babaikundi-Birgaon lineament. The inversion of gravity profiles constructed across these anomalies indicates large scale structures and two anomalous high-density (3000-3150 kg/m3) bodies extending down to 1500m depth within the Dalma volcanics and Singhbhum Group of Metapelites. These anomalous bodies could be interpreted as favorable locations for sulfide mineralization. Further, the close spatial association of Babaikundi-Birgaonshear contact with the known sulfide (Au) mineral deposits in this region suggests that mineralization in this region is structurally controlled.

KEYWORDS : north singhbhum mobile belt, potential field modelling, empirical mode decomposition

Sr No: 23

Joint interpretation of potential field data to delineate crustal structure below the Pranhita-Godavari Graben: Tectonic Implications

CORRESPONDING & PRESENTING AUTHOR:

Sumanta Kumar Sathapathy, Indian Institute of Technology Bombay, India

Radhakrishna Munukutla, Indian Institute of Technology Bombay, India

Pranhita Godavari Graben (PGG) is one of the most prominent geotectonic feature located orthogonally at the central east coast of India. This Proterozoic pericratonic rift basin situated between the Dharwar and Bastar cratons and formed through the successive episodes of rifting during the Gondwanaland breakup. The present study area extends from the Central Indian Tectonic Zone in the north and the Godavari basin
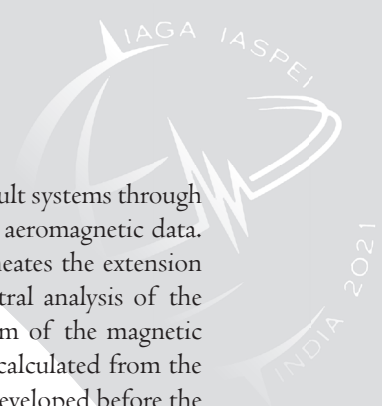
in the south. The potential field data is useful to delineate the geological trends and the fault systems through application of the edge filtering technique and the spectral analysis of both gravity and aeromagnetic data. The joint correlation of tilt angle maps prepared from gravity and magnetic data delineates the extension of PGG towards the offshore up to the ocean continental boundary. The power spectral analysis of the aeromagnetic data using the Centroid method gave rise to average depth to the bottom of the magnetic source (DBMS) of 21 km in the graben to 35 in the craton area. The heat flow value calculated from the DBMS shows a good correlation with published borehole temperature data. As the rift developed before the Gondwana separation, there can be a continuation of the fault in Antarctica which gives the signature of rifting. The joint gravity and magnetic modeling through a transect cutting across the graben will give more insight into the India-Antarctica separation which is done in the current study. The best fit data shows the optimum geological subsurface model and is discussed in detail here in this study.

KEYWORDS : Pranhita Godavari Graben, potential field modelling, crustal structure.

Sr No: 24

SYMPOSIUM : **J2 Application of geophysical studies for understanding lithospheric structure and properties**

Crustal structure and subsidence history of the SE India-Srilanka conjugate margin: constraints from Potential field modelling and Backstripping analysis

CORRESPONDING & PRESENTING AUTHOR:

Ashutosh Singh, IIT(ISM) Dhanbad, India

Gangumalla Srinivasa Rao, IIT(ISM) Dhanbad, India

The rifting history of SE India and its conjugate Srilanka margin is poorly constrained due to the lack of knowledge on the extent of stretched continental crust and unambiguous magnetic anomalies in both the conjugate margins. Here, we have carried out the integrated interpretation of biostratigraphic data from exploration wells, multi-channel seismic lines, and potential field data to understand the tectonic evolution of these conjugate margin. Crustal models obtained from Forward modeling and 2-D flexural back-stripping analysis indicate a thicker crust of 30-37 km below the SE Indian shield and 34-37 km below western Sri Lanka and then decreases gradually to 20-26 below the Mannar basin. Tectonic subsidence data derived from the 1-D back-stripping of wells reveal that the present-day margin was developed in two rifting stages. The oldest episode of rifting is initiated contemporaneous with the separation of the East Indian margin from East Antarctica and resulted in the minor crustal stretching by a factor of $\beta 1=1.07-1.23$. While the second phase of rifting ($\sim$100-65 Ma) also suggests minor stretching factors of $\beta 2=1.09-1.15$. The increase in total crustal stretching factor (β) and width of the extended crust from the north to south supports the anti-clockwise rotation of Sri Lanka during India-Sri Lanka rifting.

KEYWORDS : southeast margin of India, back-stripping, potential field modelling

Sr No: 25

SYMPOSIUM : **J2 Application of geophysical studies for understanding lithospheric structure and properties**

## Ambient Noise Tomography around Ambon Island, Molucca, Eastern Indonesia: Preliminary Results

CORRESPONDING & PRESENTING AUTHOR:

Muhammad Fachrul Rozi Kurniawan, Institut Teknologi Bandung, Indonesia

Shindy Rosalia, Institut Teknologi Bandung, Indonesia

Andri Dian Nugraha, Institut Teknologi Bandung, Indonesia

Zulfakriza Zulfakriza, Institut Teknologi Bandung, Indonesia

David P Sahara, Institut Teknologi Bandung, Indonesia

Abdul Muhari, National Disaster Management Authority of Indonesia

Andi Azhar Nurdin, Agency for Meteorology, Climatology and Geophysics of Indonesia, Jakarta, Indonesia

Sri Widiyantoro, Institut Teknologi Bandung, Indonesia

Nanang T Puspito, Institut Teknologi Bandung, Indonesia

Awali Priyono, Institut Teknologi Bandung, Indonesia

Aditya Lesmana, Institut Teknologi Bandung, Indonesia

Ardianto Ardianto, Institut Teknologi Bandung, Indonesia

M Zain Tuakia, Universitas Pattimura, Indonesia

Erfin Elly, Universitas Pattimura, Indonesia

Ambon Island, part of Northern Banda Arc, Eastern Indonesia, lies in a complex convergence zone between Eurasia, Indo-Australia, and Philippine Sea Plates. The complexity of the tectonic setting caused Ambon Island to have a high potential natural disaster, especially earthquakes. The historical data show that Ambon Island has been struck by major earthquakes, and several of them were followed by a tsunami. On 26 September 2019, Ambon Island was shaken by a shallow strong earthquake of 6.5 Mw and causing many casualties. The mainshock was followed by a dozen of aftershocks for at least two months. The moderate aftershocks in Ambon Island were caused by the reactivation of an onshore fault plane due to the 6.5 Mw mainshock. Our study attempts to image the subsurface of Ambon Island and its's surrounding by performing the first ambient noise tomography (ANT). We use eleven temporary and four permanent stations which were deployed locally around Ambon Island during ~ 2 months. We only use the vertical component to retrieve the Rayleigh wave Green's function. We obtain 52 dispersion curves in the range period of 1–15s from cross-correlating all possible station pairs in the daily segment and then stacked all of the data. Our preliminary results of tomographic group velocity model shows that the low velocity in Ambon and Haruku Islands are associated with volcanic rock, and high velocity in Northern Seram are associated with mica-schist. The low velocity anomalies are also correlated with the epicenter distribution of Ambon aftershock in September 2019.

KEYWORDS :   ambon, disaster, ANT

Sr No: 26

Geological structures in East Antarctica identified from analysis of geophysical potential field data and their correlations with structures of EGMB, India: Implications on the supercontinent Rodinia formation and breakup

CORRESPONDING & PRESENTING AUTHOR:

Giri Yellalacheruvu, IIT Bombay-Monash Research Academy, India

Radhakrishna Munukutla, Indian Institute of Technology Bombay, India

Peter Betts, Monash University, Australia

Tapas Kumar Biswal, Indian Institute of Technology Bombay, India

Robin Armit, Monash University, Australia

East Antarctica along with Greater India played a vital role in the accretion and breakup of the Indo-Antarctic landmasses during the supercontinents Nuna, Rodinia, and Gondwana. The geophysical potential field methods are useful to uncover the masked subsurface geological structures as the ice-covered terranes of Antarctica make it impossible to otherwise delineate them. We use regional-scale magnetic and gravity data to study the structures associated with the supercontinent Rodinia along the India-Antarctica conjugate margins. The distinct magnetic signatures in the aeromagnetic data over East Antarctica allow us to delineate the various rock types and structural links in that area. These magnetically distinct terranes trend at high angles to the Antarctica continental margin at Mac Robertson Land and Mawson station. The recent geochronological investigations on the coastal outcrops of this area yield metamorphic ages of between 0.9-1.0 Ga, suggesting they are part of the global Grenville-age accretionary terranes. Potential field data and modeling constrain the crustal structure of Eastern Ghats Province of East coast of India, which is correlatable with East Antarctica crustal structure. This correlation allowed us to propose a tight fit configuration of these two continents during Rodinia times and also gave important insights to better understand the amalgamation of Grenville age belts in this sector. Based on the observed geophysical signatures, we interpret that these were evolved as a single belt during the amalgamation of Neo Proterozoic supercontinent Rodinia.

KEYWORDS : aeromagnetic data interpretations, East Antarctica, Eastern Ghats Mobile Belt India.

Sr No: 27

Morphotectonics of the Southwest Indian Ridge Between the Melville Fracture Zone and Rodriguez Triple Junction

PRESENTING AUTHOR:

Muhammad Shuhail, National Centre for Polar and Ocean Research, India

CORRESPONDING AUTHOR:

P John Kurian, National Centre for Polar and Ocean Research, India

Kattoju A Kamesh Raju, National Centre for Polar and Ocean Research, India

Detailed geophysical investigations carried out on the Southwestern Indian Ridge, starting from the Rodriguez Triple Junction till Melville Fracture Zone over the past eight years, using multibeam bathymetry, gravity, and magnetic data, complemented with the available published geophysical datasets resulted in a detailed morphotectonic map of the region. Ridge segmentation, Non-transform Discontinuities, Axial Volcanic Highs, and Oceanic Core Complexes are identified using the high-resolution bathymetry. The study suggests the presence of both magmatic and amagmatic crustal accretion in this region. The median valleys are broad and deep at melt-poor ridge segments. Mantle Bouguer Anomalies (MBA) are computed based on multibeam bathymetry and satellite-derived free-air gravity data. The MBA variations observed represent deviations from the assumed crustal thickness and are attributed to crustal thickening or thinning. MBA lows observed at some ridge segments suggest focussed mantle upwelling where the median valleys diminished. The marine magnetic profiles collected over such segments have higher amplitude anomalies, supporting the magmatic crustal accretion. Six new Oceanic Core Complex structures are identified based on the morphology and seabed samples. Based on the seafloor spreading magnetic modeling, the spreading rate and a new set of magnetic anomaly picks representing the age of the crust are delineated towards the east of 66.5°E. The age of the crust varied from 0 to 8.3Ma (4r.1no). The effective spreading rate is computed to be ~13.7 mm/yr and is classified as Slow to Ultraslow spreading mid-ocean ridge.

KEYWORDS : morphotectonics, SWIR, tectonics

Sr No: 28

- -

SYMPOSIUM : **J2 Application of geophysical studies for understanding lithospheric structure and properties**

Discovery of a velocity low beneath Amsterdam Island in Indian Ocean

CORRESPONDING & PRESENTING AUTHOR:

Pratyush Anand, IIT Kanpur, India

Pabitra Singha, IIT Kanpur, India

Dibakar Ghosal, IIT Kanpur, India

Pankaj Kumar, IIT Kanpur, India

The Amsterdam-St. Paul (ASP) plateau has manifested as the interaction of South East Indian ridge (SEIR) and ASP mantle plume. Previous geochemical studies suggest this plateau to be associated with a mantle plume feeding process. Here, we carry out a joint inversion of receiver function and dispersion analysis of the AIS station[1] [2] which is located on the ASP[3] . We have analysed 60 earthquake events in total, of which very few [4] could be used further for computation of radial receiver function and hence inversion. we consider teleseismic events with magnitude (Mw) > 7 for the receiver function computation. We apply an iterative deconvolution technique in time domain and multiple filter analysis (MFT) algorithm to compute Ps receiver function and dispersion curve, respectively. The period used for the computation of Rayleigh wave group velocity distribution curve ranges from 20 to 100s and the receiver function length was 25 s.[5] Our study shows 1D velocity-depth model under the station until a depth of 250 km. We identify evidence of a gradational Moho with a mean depth of ~13 km and observe a drop in velocity at a depth ranging from ~60 - 137 km. Although the estimated thickness of the crust seems to be a bit higher than usual oceanic crust, the additional thickness might be associated with the magmatic underplating. The low velocity suggests either presence of a magmatic plume beneath the island or shallowing up of the Lithospheric-Asthenospheric Boundary (LAB) followed by a Low Velocity Zone (LVZ).

KEYWORDS : joint inversion, receiver function, plume
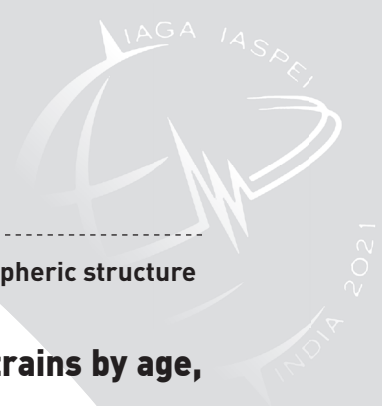
Sr No: 29

Seismicity of the Andaman-Sumatra Subduction Zone: Constrains by age, fracture zones and spreading rate of the lithosphere

CORRESPONDING & PRESENTING AUTHOR:

Jensen Jacob, CSIR-National Institute of Oceanography, India

Jerome Dyment, Université de Paris, Institut de physique du globe de Paris et CNRS, France

Dibakar Ghosal, Indian Institute of Technology Kanpur, India

Pawan Dewangan, CSIR-National Institute of Oceanography, India

The easiness of subduction at the Andaman Sumatra Subduction Zone is represented by the term Subductability', a parameter estimated from the lithospheric age of the subducting northern Wharton lithosphere. We have superimposed the fracture zones, magnetic isochrons and the strike -slip focal mechanism spanning from 2004-2019 to the geometry of the subducting plate as imaged by seismic tomography. A prominent clustering of strike-slip earthquakes along Fracture Zone BC (Jacob et al., Tectonophysics, 2021) is observed, were the contrast of lithospheric subductability, density and thickness is higher. The inception of normal fault earthquakes along ASSZ post 2004 megathrust earthquake is influenced by the reorganisation of the stress field. Correlating the normal focal mechanisms with lithospheric spreading rate shows less events at fast spreading rate than at slow spreading rate; indicating a rougher topography with more asperities for slow spreading lithosphere than the smooth topography of a fast lithosphere

KEYWORDS :   Andaman-Sumatra subduction zone, strike-slip earthquakes, normal-fault earthquakes

Sr No: 30

Seafloor spreading magnetic anomalies in the Gulf of Mexico

CORRESPONDING & PRESENTING AUTHOR:

Andreina Garcia Reyes, Institut de Physique du Globe de Paris, Université de Paris, France

Jerome Dyment, Institut de Physique du Globe de Paris, Université de Paris, France

The Gulf of Mexico is an isolated oceanic basin with its origin likely synchronous to the Central Atlantic Ocean. As marine magnetic anomalies related to seafloor spreading have not been identified and because drilling data reaching the acoustic basement are not available in this basin yet, its nature, structure and age remain controversial. Here we show fan-like structure marine magnetic anomalies related to seafloor spreading in the Gulf of Mexico. The fan-shape structure of these anomalies supports a counterclockwise rotation of the Yucatán Block with respect to a pole located NW of Cuba. Our reconstruction of the initial fit implies that oceanic crust underlies most of the Sigsbee salt province. The older magnetic anomalies seem to abut on the COB, suggesting that oceanization propagated from West to East, in agreement with the location of the rotation pole. We identified the fossil ridge axis and two pairs of conjugate positive anomalies and attempted to decipher the GoM plate tectonic history from the magnetic isochrons, fracture zones as imaged by gravity, and COBs depicted from both gravity and magnetics. Filtering the geomagnetic polarity time scale allowed us to tentatively date the observed anomalies: seafloor spreading in the GoM

predates the Tithonian (> 150 Ma) and stopped in the Berriasian (140 Ma), in agreement with geological constraints. Due to the proximity of the rotation poles, spreading rates increase rapidly westward across the basin. In average, they vary from slow (and probably ultraslow in the easternmost tip of the oceanic basin) to fast spreading.

Sr No: 31

Spectral content distribution of magnetic sources in the Gulf of Mexico and Caribbean plate

CORRESPONDING & PRESENTING AUTHOR:

Andreina Garcia Reyes, Institut de Physique du Globe de Paris, Université de Paris, France
Jerome Dyment, Institut de Physique du Globe de Paris, Université de Paris, France

Spectral methods are part of the techniques to estimate the depth of the magnetic source (e.g. Spector and Grant, 1970). In magnetic exploration, the slopes along the spectrum are used to derive the depth of the magnetic sources. Spectra can provide a valuable information of the magnetic lithosphere structure. Here we explore the bidimensional and tridimensional spatial distribution of the total spectral content from magnetic anomalies to characterize its signature. We use compiled magnetic anomalies from the Caribbean plate and the Gulf of Mexico (García-Reyes, 2018).

At long wavelengths, we identified two types of spectra: 1) 3 layers, high spectral content, for continental blocks and 2) 2 layers, minimal spectral content, for oceanic blocks respectively. Due to the poor coverage and quality of the data in some areas, these results should be interpreted carefully. However, we observe a general consistency with the available geological information. The tridimensional view provides an interesting way of representing the spectral content and possibly, to image the magnetic structures that underlie the seafloor and the surface.

The approach that we are using is quite simple but has not been applied much so far. Although investigating the characteristics of the spectral energy and understanding the meaning of their distribution is a step-backwards to determining the depth of the magnetic source, this approach can give relevant information on the distribution of sources in the subsurface.

Sr No: 32

WDMAM version 2.1: improved global magnetic anomaly map

CORRESPONDING & PRESENTING AUTHOR:

Jerome Dyment, IPGP – CNRS, France

Yujin Choi, IPGP – CNRS, France

Vincent Lesur, IPGP – CNRS, France

Manuel Catalan, Real Instituto y Observatorio de la Armada, Spain

Takemi Ishihara, AIST, Japan

Tamara Litvinova, A.P. Karpinsky Russian Geological Research Institute | VSEGEI, Russia

Mohamed Hamoudi, Université des Sciences et Technologies Houari Boumédiène, Algeria

The World Digital Magnetic Anomaly Map is prepared under the auspices of IAGA and the CGMW (Commission for the Geological Map of the World) of UNESCO. A first version was released in 2007 (Korhonen et al., 2007), and a second one in 2015 (Dyment et al., 2015; Lesur et al., 2016) with the mandate to update the version 2.0 using the same methodology as often as newly available data would make it necessary. The present version 2.1, compiled at 5 km interval and 5 km altitude above continents and at sea-level over the oceans, includes the following new datasets: (1) the complete digital aeromagnetic map of Brasil made available to CGMW by Agência Nacional do Petróleo, Gás Natural e Biocombustíveis; (2) an improved version of the aeromagnetic map of Russia prepared by V-SEGEI; (3) the second version of the Antarctic Digital Magnetic Anomaly maP (ADMAP; Golynsky et al., 2018) which results from a remarkable international effort during and after the Second International Polar Year; (4) a new map of the Caribbean plate and Gulf of Mexico resulting from the compilation and re-processing of existing marine and aeromagnetic data in the area (Garcia, PhD th., 2018); (5) an updated magnetic anomaly map of Eastern Asia prepared by the CCOP (Ishihara and Uchida, 2021); and (6) a new marine magnetic anomaly data compilation prepared by T. Ishihara and coworkers. The new map will be presented and improvements over the previous version will be discussed.

KEYWORDS :   magnetic anomaly, global

Sr No: 33

Marine magnetic anomalies at active and passive margins: what do they tell us about the oceanic lithosphere?

CORRESPONDING & PRESENTING AUTHOR:

Jerome Dyment, IPGP – CNRS, France

Andreina Garcia Reyes, IPGP – CNRS, France

Hanjin Choe, Kangwon National University, South Korea

The magnetic anomalies observed on subducting oceanic plates progressively decrease in amplitude once the flexural ridge passed, revealing (1) the opening of fracture, hydrothermal circulation and alteration of their magnetic minerals between the flexural ridge and the ridge, and (2) their gradual heating and thermal demagnetization once the plate enters subduction, with the titanomagnetite (TCurie ~200 °C) of extrusive

basalt first then the magnetite (TCurie ~580 °C) of the deeper crust successively erased (Choe and Dyment, Geology, 2020; GRL, 2020; EPSL, 2021).

Conversely, the magnetic anomalies observed at passive margins show contrasted signatures, with clear anomalies where the sediment cover is relatively thin to low amplitude, long wavelength anomalies where the sediments are thick. The increased distance to the source is insufficient to explain this effect. Both post-accretion sedimentation resulting in thermal demagnetization of the extrusive basalt layer and syn-accretion sedimentation inhibiting the formation of this extrusive basalt layer result in similar signatures observed in the South Atlantic margins (Granot & Dyment, GRL, 2019), the Red Sea (Dyment et al., AGU Fall Meeting, 2013) and the Gulf of Mexico (Garcia & Dyment, EPSL, revised).

Our observations at active and passive margins better constrain the structure and magnetic properties of the oceanic lithosphere and demonstrate that the first oceanic crust does not necessarily start at the first clear seafloor spreading anomaly, as it is too often considered.

KEYWORDS : magnetic anomaly, oceanic lithosphere, margins

Sr No: 34

Interpretation of Potential Field Data Across the Southeastern Part of the Narmada - Son Lineament, Central India and its Tectonic Implications

CORRESPONDING & PRESENTING AUTHOR:

Naveen P U, Cochin University of Science and Technology, India

Radhakrishna M, Indian Institute of Technology Bombay, India

Singh A.P., CSIR-National Geophysical Research Institute, India

The Narmada – Son Lineament (NSL) is one of the most prominent geo-tectonic features located in central India, characterized by complex geological structures. The present study area lies in the SE part of NSL contains some important geotectonic features such as the Tan Shear zone, Central Indian Suture Zone, and a few major faults. Potential field geophysical data plays an important role in delineating the subsurface geological structure associated with the above features. In this study, we present a detailed analysis of gravity and aeromagnetic anomaly maps using both spectral-based approach and edge-enhancement techniques. We used the Levenberg-Marquardt nonlinear regression method to merge the aeromagnetic data acquired in different surveys and different time periods. Using the spectral analysis, the depth to the bottom of the magnetic basement (DBMS) is estimated by attempting different methods like centroid, modified centroid, spectral peak, and forward modelling of spectral peak techniques, and out of these, the modified centroid method was found to be consistent and suitable in the study area. Nine windows were chosen for calculation and the DBMS values were found to be varying between 21 km to 32 km. The 2D joint gravity and magnetic modelling is carried along a profile cutting across the major geological structures in the region. The proposed 2D model corroborates the north-directed subduction system which was a topic of debate and it gives a better visualization of the crustal structure and evolution of the area. The implications of this model are discussed in the paper.

KEYWORDS : curie depth, Narmada - Son Lineament, modified centroid method
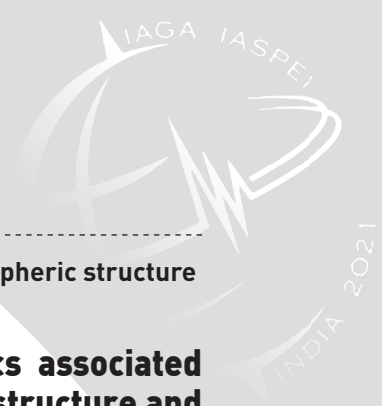
Reactivation of Mahakoshal fold belt and role of tectonics associated with the Gondwana dispersal: constrains from the regional structure and gravity data

PRESENTING AUTHOR:

Devika Maisnam, CSIR- National Geophysical Research Institute, India

CORRESPONDING AUTHOR:

Anand.K Pandey, CSIR- National Geophysical Research Institute, India

Swarnapriya Ch, CSIR - National Geophysical Research Institute (NGRI), India

Anand. P Singh, CSIR - National Geophysical Research Institute (NGRI), India

The E-W trending Proterozoic Mahakoshal supracrustal belt in the northern part of the Central India Tectonic Zone (CITZ) shows a unique large scale left-lateral shearing with >40 km horizontal displacement adjacent to the Mahanadi graben that extends towards Damodar graben. Similar shearing is observed in the ENE-WSW Tan Shear zone across Mahanadi graben. We analyzed the regional geological and structural disposition of different litho-tectonic unite to understand the origin of large-scale shearing and associated deformation across the CITZ and Gondwana grabens. Conspicuously, the western boundary of the Mahanadi graben is sharp with ~1.5-6 km sediment thickness from south to north and decreases gradually towards east. The width and sediment thickness of the Gondwana basin increases northward in Mahanadi graben, with an abrupt increase across the Tan shear zone and other faults up to SNSF. The same is confirmed from the gravity modeling of the region. This suggests lateral oblique-slip sinistral segmentation of basement blocks during Gondwana dispersal. This block rotation involving SNSF extending along the narrow Damodar graben with large lateral displacement is possibly responsible for the regional sinistral deformation of the Mahakoshal belt during the Mesozoic Gondwana dispersal episode, marking the latest phase of deformation in the region.

KEYWORDS :   Mahakoshal, Gondwana, sinistral shearing.

Crustal density and susceptibility structure beneath Achankovil Shear zone: Correlation with Madagascar

CORRESPONDING & PRESENTING AUTHOR:

Chandra Prakash Dubey, National Center for Earth Science Studies

M Prasad, National Center for Earth Science Studies, India

Kumar Batuk Joshi, National Center for Earth Science Studies, India

Virendra Mani Tiwari, National Geophysical Research Institute, India

The southern granulite terrain (SGT) is a large tract of exposed Archean continental crust, divided into the Madurai block (MB), Trivandrum block (TB) and Nagercoil block (NB). These crustal domains are linked

with the NW-SE trending Achankovil Shear Zone (AKSZ). We combine gravity and magnetic data with previously published ground observations and geochronological data to re-evaluate the crustal architecture, evolution of the AKSZ, and possible extension of AKSZ into Madagascar. Analyses indicate that the long wavelength trends of the magnetic anomalies originate at ~ 20 km depth of different SGT blocks. These observations are corroborated with the gravity as well as computed gravity gradient anomalies. The presence of Khondalites outcrops in Trivandrum block implies that high magnetization crust is the main source of positive magnetic anomalies. Such magnetic anomalies advocate that SGT preserves the remanent of Archean crustal blocks in south India, a part due to variation in thermal and geochemical processes. The AKSZ, TB and MB exhibit contrasting magnetic crustal signatures. The results suggest that AKSZ and Ranotsara Shear Zone (RSZ) are crustal structures and interlinked. The joint modelling results reveal a three-layered crustal configuration with varying Moho ranging from 41 to 34 km in NE to SW respectively. It is also noted that AKSZ is a narrow and deep structure near to the Western Ghats Escarpment while it is wide and shallow in the far-east, which implies that the evolution of the Western Ghats is a late geological event.

KEYWORDS : crustal structure, Achankovil shear zone, joint modelling

Sr No: 37

Ambient Noise Love Tomography Investigation of Sub Volcanic Area in Central Java Indonesia: A Preliminary Result

CORRESPONDING & PRESENTING AUTHOR:
Alfan Hidayah Kusuma, Bandung Institute of Technology, Indonesia
Zulfakriza Zulfakriza, Bandung Institute of Technology, Indonesia
Andri Dian Nugraha, Bandung Institute of Technology, Indonesia
Shindy Rosalia, Bandung Institute of Technology, Indonesia
Ahmad Setiawan, Center for Geological Survey, Geological Agency of Indonesia, the Ministry of Energy and Mineral Resources, Indonesia

Abstract : We estimate the ambient noise love cross correlation of sub volcanic area in Central Java, Indonesia. We used 2 months continuous recording of 40 broad-band seismic stations obtained Love wave empirical Green's functions from cross-correlations of the horizontal components. The Love wave group velocity dispersion measurements will be used to construct dispersion maps of 1 to 10-s periods, which will then be inverted to obtain a three-dimensional horizontally polarized S-wave (SH) velocity structure beneath the surface. We expect that the SH model is generally consistent with a previously worked vertically polarized S-wave (SV) model and showed large-scale features that were consistent with geological units, such as the basins and changes in the crustal thickness across the north-west gravity lineament.

KEYWORDS : ambient noise tomography (ANT), love waves, sub-volcanic area
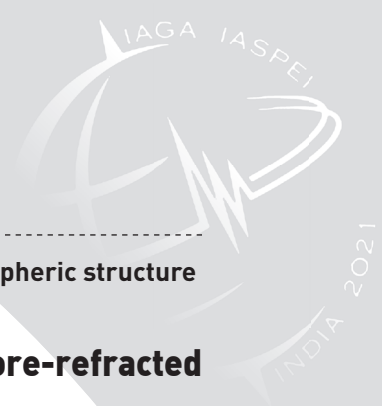
Sr No: 38

Mantle deformation along the Western Ghats: Insights from core-refracted shear wave splitting analysis

PRESENTING AUTHOR:

Sribin C., National Centre for Earth Science Studies, India

CORRESPONDING AUTHOR:

Padma Rao B., National Centre for Earth Science Studies, India

Ravi Kumar M., CSIR-National Geophysical Research Institute, India

Tomson J. K., National Centre for Earth Science Studies, India

Abstract : The Western margin of the Indian sub-continent that hosts one of the world's largest escarpments, called Western Ghats (WG), is a collage of diverse geological formations. Characterizing upper mantle seismic anisotropy offers insights into mantle deformation and its role in the evolution of such regions. In this study, we estimated the upper mantle anisotropy using splitting analysis of SK(K)S and PK(K)S waveforms recorded at 17 stations. Results indicate that the fast axis polarization directions (Φ) are primarily in NE-SW direction, with delay times varying from 0.3s to 1.8s. This direction is parallel to the Absolute Plate Motion of the Indian sub-continent, suggesting that shear at the base of lithosphere is the dominant mechanism for anisotropy along the WG. E-W oriented anisotropy at stations close to the coast, especially in the northern part of WG could be due to lithospheric stretching along the west coast, associated with rifting process. Further, observed coast-parallel Φ (N-S, NNW-SSE) with delay times varying from 0.6s to 1.2s at stations away from the coast, could be due to the edge flow associated with the transition from a thinner to thicker lithosphere. In addition, we observed multilayer anisotropy in-terms of multiple Φ varying from N29.9° to N176.0° with varying delay times of 1.1s to 1.5s at PCH station close to the coast, which is corroborated by the results of two-layer modeling. The variable Φ from coast perpendicular to coast parallel at stations close and away from the west coast of the Indian sub-continent implies different rifting episodes.

KEYWORDS :   seismic anisotropy, SK(K)S & PK(K)S phases, upper mantle

Sr No: 39

Is central Dharwar region, part of south Indian shield, a mid continental paleo rift zone? Evidence from regional gravity anomalies

CORRESPONDING & PRESENTING AUTHOR:

Venkata Rama Rao Jammi, Geological Survey of India, India

Ravi Kumar Bandi, Geological Survey of India, India

Veeraiah Boylla, Centre of Exploration Geophysics, India

Unrelated regional Bouguer gravity anomalies to broad surface geological formations have helped in defining central part of Dharwar Craton, south Indian shield area as transitory block between well-known western Dharwar (WDC) and eastern Dharwar (EDC) occupying about 75000 sq.km in south Indian shield area.

Pronounced longwave length gravity high covering this region to the bordering granulite terrain in south for a length of about 550 km is significant feature of south India. Mid Continental Rifts are characterized with significant tectonic, magmatic and geophysical features. Though passive rift zones of early era may not retain all the topographic evidences such as central depression bordered with shoulder uplifts, the elongated narrow extensional features could be seen in this region in the form of long schist belts and elongated granite body. Bordering normal faults could be identified with abrupt shift in the regional back ground values.

These regions are generally supported with lithospheric thinning and a secondary process of uplifting of local features and crustal doming. Another important factor is type of magmatic activity with alkali basalts and bimodal volcanism. Bouguer gravity anomalies of this region possibly indicate two important inferences as this may be failed rift zone that has stopped before continental break up and filled with linear igneous granite body and basic volcanics. Linear magnetic anomalies also characterize this region. Variations in lithospheric thickness is noticeable in these areas from the other geophysical inputs. Integrated study has led us to believe that central part of Dharwar Craton is paleo rift zone.

KEYWORDS : central Dharwar region, gravity high, paleo rift zone

Sr No: 40

- -

SYMPOSIUM : **J2 Application of geophysical studies for understanding lithospheric structure and properties**

Pn Tomography and Anisotropic Study of the Indian Shield and the Adjacent Regions

PRESENTING AUTHOR:

Bhaskararao Illa, CSIR-NGRI, and PhD registered in Andhra University, Visakhapatnam, India

CORRESPONDING AUTHOR:

Prakash Kumar, CSIR-NGRI, India

Reshma K .S, CSIR-NGRI, Osmania University, Hyderabad, India

High-resolution P- wave velocity and anisotropy structure of the hitherto elusive uppermost mantle beneath the Indian shield and the surrounding regions are presented to unravel the tectonic imprints in the lithosphere. We used high-quality 19500 Pn phases from 172 seismological stations for the earthquakes at a distance range of 2° to 15° with a mean apparent Pn velocity of 8.22 km/s. The Pn velocity anomalies with fast anisotropic directions are consistent with in the Himalaya, Tibet Plateau, Tarim Basin, and Burmese arc. The higher Pn anomalies along the Himalayan arc explicate the subducting cold Indian lithosphere. The cratonic upper mantle of the Indian shield is characterized by Pn velocity of 8.12-8.42 km/s, while the large part in the central Indian shield has higher mantle-lid velocity of ~8.42 km/s with dominant anisotropic value of 0.2-0.3 km/s (~7.5%) indicating the presence of mafic 'lava pillow' related to the Deccan volcanism. Our velocity image clearly reveals the signature of the rift and mobile belts separating the cratons, extending deep at least till the uppermost mantle. Pn anisotropy in the Indian shield displays complex pattern and differs from SKS directions, suggesting the presence of frozen anisotropy, due to the large scale tectonic deformation and alteration after its breakup from Gondwanaland. Our tomographic results in the Bay of Bengal conspicuous that the lower anomaly is bounded by 85° and 90°E ridges in the southern side. Further, 85°E ridge separates the BoB lithosphere into two regions, faster and slower lithospheres, consistent with the gravity observations.

KEYWORDS : Pn wave tomography - uppermost mantle - seismic anisotropy, Indian shield and Asia, crustal structure

Sr No: 41

Sn wave Tomography of the Uppermost Mantle Beneath the Indian Shield and its Adjacent Regions

PRESENTING AUTHOR:

Bhaskararao Illa, CSIR-NGRI, and PhD registered in Andhra University, Visakhapatnam, India

CORRESPONDING AUTHOR:

Prakash Kumar, CSIR-NGRI, India

Reshma K .S, CSIR-NGRI, and PhD registered in Osmania University, Hyderabad, India

Sn velocity image of the uppermost mantle beneath the Indian shield, Himalayan collision zone, Burmese Arc, Bay of Bengal, and Andaman-Nicobar Island regions is generated by tomographic inversion using 11243 Sn travel times data. The uppermost mantle from the Indian shield is hitherto not known. The average apparent Sn velocity obtained for the entire region is ~4.60 km/s with a velocity perturbation of ±0.2 km/s. High velocities are found under most parts of the Indian cratons, the Tarim Basin, the Bay of Bengal, whereas prominent lower Sn velocities are found beneath the Burmese arc region, the Hindu-Kush region, North-west part of India, eastern coastal part of India, and Central part of the Tibetan Plateau. The various cratonic blocks in the shield region show higher anomalies except for the Singhbhum craton, which is highly mineralized and having high surface heat flow values. The intracratonic Cuddapah Basin and Southern Granulitic terrain also exhibit higher uppermost mantle shear velocity. The intriguing observation is the central India high, which is interpreted as the presence of basaltic lava pillows related to the Deccan volcanism. Along the Himalayan arc, we observe higher Sn velocity which supports the idea of subduction of the Indian lithosphere in a piecewise manner into the mantle. Interestingly, the uppermost mantle beneath the Bay of Bengal shows faster and slower Sn values in western and eastern regions respectively implying that the nature of the mantle of the Bay of Bengal has two distinct compositions and low Sn velocities below the Andaman-Nicobar islands.

KEYWORDS : Sn tomography, uppermost mantle, Indian shield and adjacent regions

Sr No: 42

Tectonic forces and Intraplate stress across the Indian Plate: Insights from finite element modelling

CORRESPONDING & PRESENTING AUTHOR:

Akhil Mishra, CSIR-National Geophysical Research Institute, Hyderabad, Inida

R. Yadav, CSIR-National Geophysical Research Institute, Hyderabad, India

V.M. Tiwari, CSIR-National Geophysical Research Institute, Hyderabad, India

Observed In-situ stress orientations over the Indian Plate, is relatively sparse; therefore, numerical modelling of SHmax is needed to comprehend regional stress pattern. In the present work, four cases of stress simulation are carried out to explore the effects of rigidity, lithospheric thickness, basal drag force, and

boundary conditions on the distribution of intraplate stress across the Indian Plate. The rigidity is derived from Effective Elastic plate thickness (EET), which is estimated through joint inversion of admittance and coherence using gravity and topography data. The geometry of the model is created considering plate boundary, lithospheric thickness and EET. The stress field is simulated with ABAQUS software for i) variable lithosphere thickness and constant EET ii) variable EET and constant lithosphere thickness iii) variable EET and lithosphere with fixed Himalayan boundary, and iv) variable EET and lithosphere with force at the Himalayan boundary. For each case, we compared SHmax with in-situ measurements and found that the orientation and magnitude of SHmax obtained in the case (iv) are in remarkable agreement with the available in-situ stress data. The stress field and von-Mises stress over major geological features are also analyzed and discussed. It is inferred that EET, apart from boundary forces, is one of the most significant factors in controlling the stress field distribution. Modelling results also suggest that incorporation of depth dependent rheology and density may further enhance the resulting quality and better predict the stress state.

KEYWORDS : effective elastic thickness; FEM; Indian plate; Maximum horizontal stress; plate boundary forces

Sr No: 43

Deep Electrical and Seismological structural inferences for the Intraplate seismicity of central Brazil

CORRESPONDING & PRESENTING AUTHOR:

Ved Maurya, CSIR-National Geophysical Research Institute, India

Sergio Fontes, Observatorio Nacional, Brazil

Carlos Chaves, Universidade de São Paulo, Brazil

Emanuele Laterra, Observatorio Nacional, Brazil

Antonio Padilha, Instituto Nacional de Pesquisas Espaciais, Brazil

We investigated the intraplate seismicity of the central Brazilian region by passive electromagnetics and seismological observations. For this study, the three-dimensional conductivity and P-wave velocity models were obtained using magnetotellurics (MT), geomagnetic depth sounding (GDS), and seismological data arrays. In the past, one of the major seismic events with a magnitude of ~ 6.2 occurred in the Parecis basin, central Brazil. Previous seismological studies indicated the compressional stress regimes with dominant thrusting in the Northwest direction for the region. To explain the seismicity, a model proposed the flexural crustal deformation associated with isostatic gravity highs, while other models associate it with high heat-flow, lower elastic-thickness, and thinner lithosphere. Whereas, deep electrical observations were somehow missing in this regard which may explain the presence of deep hot fluids from the magmatic materials. The MT+GDS conductivity models have found some weak zones in the crust and upper mantle, which possibly act as the evolution path of the younger alkaline magmatism. The P-wave velocity anomalies, constraining the heterogeneous velocity structure of the crust and upper mantle, also confirm these zones with some deviation. Such mid-crust to upper mantle P-wave velocity and electrical anomalies in the Southeast of Amazon craton somehow links with the ongoing regional compression and upwelling of hot-magmatic materials, activating the thrusting and, or shearing in the upper crust with attendant seismicity.

KEYWORDS : electrical, P-wave velocity, intraplate seismicity
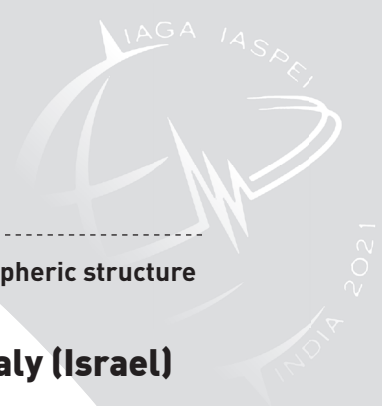
Sr No: 44

Quantitatie multilevel analysis of Hebron magnetic anomaly (Israel)

CORRESPONDING & PRESENTING AUTHOR:

Lev Eppelbaum, Tel Aviv University, Israel

Asaf Yaniv, Soreq NRC, Israel

Nizan Salomonski, Soreq NRC, Israel

Boris Ginzburg, Soreq NRC, Israel

Arie Sheinker, Soreq NRC, Israel

Youri Katz, Tel Aviv University, Israel

Hebron magnetic anomaly is the greatest magnetic anomaly observed at the territory of Israel. Some investigators have associated this anomaly with the magnetic sources occurring at comparatively small depths (5-7 km). Quantitative analysis of airborne data (1000 m over the Earth's surface) indicates that the upper edge of the magnetic anomalous body occurs at a depth of 26-28 km. A rough estimation of the lower edge occurrence is estimated at a depth of about 40 km. Calculated magnetization of this body is about 3000 mA/m. Developed maps of the Moho and Curie discontinuities suggest that the corresponding surfaces in the region are located at the depths of 29-30 and 40-40.5 km, respectively. Thus, the upper edge of this body is located 3 km above the Moho boundary, and the depth of the lower edge of this body and the maximum possible depth of magnetic source occurrence are practically coincided. The recently performed magnetic balloon measurements at the level of about 30 km enabled to preliminary estimate the depth of the upper edge of the anomalous body as 31 km. Tectonically area of the Hebron anomaly is a collision zone between the Judea-Samaria and Negev terranes. In this area several deep (~5-6 km) boreholes were drilled and constructed sequence formation maps show that the Judea-Samaria terrane was subducted under the Negev terrane. It is known that collision zones are characterized by specific geodynamic crust-mantle instability. Thus, we can propose that the Hebron magnetic anomaly is caused by the mantle diapir.

KEYWORDS : advanced quantitative interpretation, multilevel analysis, mantle diapir

Sr No: 45

Geodynamic modeling of lithospheric removal and surface deformation – lithospheric delamination as an explanation for intraplate uplift in central Mongolia

CORRESPONDING & PRESENTING AUTHOR:

Matthew J. Comeau, University of Muenster, Germany

Claudia Stein, University of Muenster, Germany

Michael Becken, University of Muenster, Germany

Ulrich Hansen, University of Muenster, Germany

Intracontinental surface deformation is enigmatic, and the underlying mechanisms responsible are not fully understood. We use self-consistent thermo-mechanical numerical modelling to investigate one explanation:

lithospheric delamination-induced surface deformation. We explore the conditions under which delamination can occur and investigate the timing and amplitude of the consequent surface deformation. As a case study we use central Mongolia, which is an ideal natural laboratory for studying intracontinental surface deformation because of its high topography and its location far in the continental interior.

Rather than imposing an initial dense block in the simulations, we allow lithospheric removal to develop dynamically and self-consistently by applying a phase transition and density jump. This phase transition is hypothesized to be a consequence of metamorphic eclogitization in a thickened crust, due to convergence. We systematically vary parameters and test their influence on lithospheric removal. The analysis confirms that a weak and dense lower crust, a hot crust-mantle boundary, and a moderate convergent regime are critical requirements for delamination-style removal.

The physical parameters and physical structure inferred beneath central Mongolia closely match the conditions and requirements for delamination. The simulations show that the removal of the lithosphere by delamination can reproduce the present-day dome-shaped topographic pattern and generate substantial uplift within a short time period. Furthermore, the duration of the removal event fits geochemical constraints. In addition, the modelled lithospheric structure is consistent with that inferred from geophysical imaging. Therefore, the results suggest that lithospheric removal by delamination is a physically plausible explanation for the observed intracontinental uplift.

KEYWORDS : thermo-mechanical numerical modelling, lithospheric delamination, intraplate uplift

Sr No: 46

Estimation of surface wave dispersion characteristics using ambient noise records in Ulaanbaatar region, Mongolia

PRESENTING AUTHOR:

Lkhagvadorj Dalaijargal, Institute of Astronomy and Geophysics of Mongolian Academy of Science, Mongolia

CORRESPONDING AUTHOR:

Hayashida Takumi, International Institute of Seismology and Earthquake Engineering, Building Research Institute, Japan
Yokoi Toshiaki, International Institute of Seismology and Earthquake Engineering, Building Research Institute, Japan
Demberel Sodnomsambuu, Institute of Astronomy and Geophysics of Mongolian Academy of Science, Mongolia
Odonbaatar Chimed, Institute of Astronomy and Geophysics of Mongolian Academy of Science, Mongolia
Ulziibat Munkhuu, Institute of Astronomy and Geophysics of Mongolian Academy of Science, Mongolia

We applied the seismic interferometry technique to ambient seismic noise data collected from January 2017 to January 2019 recorded at 17 broadband stations in the Ulaanbaatar region, Mongolia. We obtained Rayleigh and Love-wave dispersion characteristics between 5 and 20 s from yearly-stacked cross-correlation functions (CCFs) for 136 station-to-station pairs with nine components. The CCFs show substantially large values (SNR >17) in the target periodic range. For the Rayleigh-wave estimation, we removed P-wave contamination, which exists as precursors, from the stacked CCFs using ZR and RZ components (Takagi et al., 2015) and obtained dominant Rayleigh-wave signals. The estimated Rayleigh and Love-wave phase velocities using the matched-filter FTAN (Bensen et al., 2007) showed little variation over the period between 6 and 10 s, indicating small subsurface heterogeneity in the Ulaanbaatar region. The estimated Rayleigh-wave phase velocity map for 8 s indicated small velocity contrasts between the western
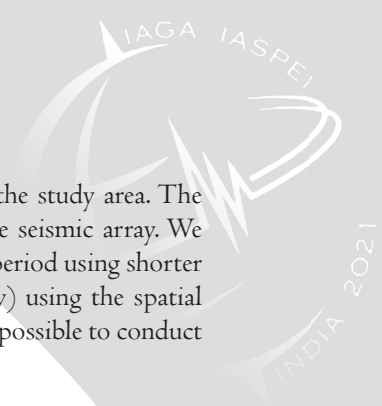
and eastern parts, suggesting the possibility of local seismic velocity heterogeneity in the study area. The resulting velocity trends correspond well with the roughly estimated ones with a sparse seismic array. We also found the possibility of Rayleigh-wave phase velocity estimations in a much longer period using shorter spacing station-to-station pairs, (which are typically excluded in seismic interferometry) using the spatial autocorrelation (SPAC) method. The further combined use of the two methods makes it possible to conduct a tomographic study in the Ulaanbaatar region.

KEYWORDS :   ambient noise cross-correlation, ulaanbaatar, seismic interferometry

Sr No: 47

Symposium :   J2 Application of geophysical studies for understanding lithospheric structure and properties

The deep structure of central Yarlung-Zangbo suture zone (southern Tibet) revealed by 3D inversion of aeromagnetic anomaly

CORRESPONDING & PRESENTING AUTHOR:

Jie Wang, Ministry of Emergency Management of China, China

Changli Yao, China University of Geosciences, China

Zelin Li, Hebei University of Engineering, China

Two subparallel east-west trending linear aeromagnetic anomalies are observed along the central Yarlung-Zangbo suture zone in southern Tibet. The Yarlung-Zangbo suture zone represents the boundary of the Eurasian and Indian plates, and records the subduction of the Neo-Tethyan oceanic slab and subsequent continental collision. The two magnetic lineaments are spatially associated with the Gangdese batholith and Xigaze ophiolites, which are separated by the Xigaze fore-arc basin that is filled with non-magnetic sedimentary sequences. The Mesozoic-Cenozoic Gangdese batholith is characterized by widespread I-type granitoids. The Xigaze ophiolites are dominated by serpentinized mantle peridotites. To investigate the geological origins and deep structures of the magnetic sources of the two magnetic lineaments, a 3D inversion of aeromagnetic anomaly data was undertaken. By analyzing our inversion model and further magnetic modelling, it is proposed that the Gangdese batholith has a magmatic root with higher magnetization than the exposed granitoids, indicating that the deeper part of the Gangdese batholith may contain more mafic constituents than the shallow part. The subsurface part of the Xigaze ophiolites resembles a thin slab dipping to the south, implying that the deep-seated Xigaze ophiolites are also serpentinized and retain complete structure.

KEYWORDS :   aeromagnetic anomaly, 3D inversion, yarlung-zangbo suture

J3 Lithosphere-Atmosphere-Ionosphere Coupling: Seismo Ionospheric and Electromagnetic anomalies

CONVENERS: Mala S. Bagiya

                          Elvira Astafyeva

                          Yasuhide Hobara

This session plans to discuss and understand the "unexplored" characteristics of co- and pre-seismic ionospheric and electromagnetic anomalies and their origin within the framework of lithosphere- atmosphere-ionosphere coupling. A brainstorming discussion towards the advancement of new insights in realizing the pre-seismic imprints in the near space environment is proposed. Observations from ground as well as from space and their validation through model simulations adopting both empirical and physical approaches may assist in understanding the physical mechanisms responsible for these anomalies. This session seeks papers on seismo-ionospheric and electromagnetic anomalies and signatures before and/or after strong earthquakes, tsunamis and volcanic eruptions.
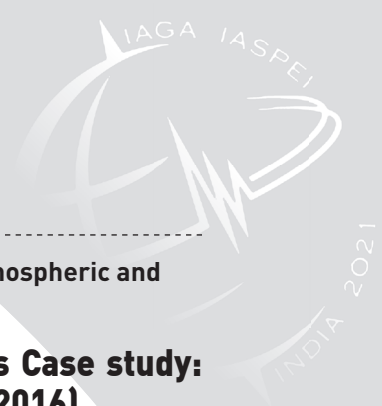
Sr No: 48

Abnormal TEC variations as seismo-ionospheric precursors Case study: The Mw 6.4 Al Hoceima-Morocco earthquake (January 25th, 2016)

CORRESPONDING & PRESENTING AUTHOR:

Abdennasser Tachema, Institute of Sciences and Applied Techniques, University of Tlemcen, Algeria

Abdelmansour Nadji, University of Oran 2, Algeria

The main objective of the current research aims to present a predictive approach to seismic events of significant magnitude (Mw≥5), through anomalous fluctuations in the total electron content 'TEC' of the ionospheric layer. This parameter is derived from geodetic data allowing to model and map the ionized layer of the Earth's upper atmosphere, 'TEC-Mapping'. For this purpose, we took as a sample the study of the GPS_TEC signal related to the strong Al Hoceima-Alboran sea earthquake (January 25th, 2016, Mw 6.4).

The developed seismo-geodetic approach allowed us to detect the time-origin of the seismo-ionospheric precursors, indicating the time delay for the energy transfer between the lithosphere and the ionospheric F2-layer, before the triggering of the mainshock. Thus, the principle concept refers to the existence of a relationship between the prominent ionospheric TEC irregularities and earthquake preparation phase, through the ternary coupling: Lithosphere-Atmosphere-Ionosphere.

To achieve this research we have exploited geodetic datasets derived from about one hundred permanent ground-based GPS/GNSS stations, in order to identify the pre-earthquake ionospheric anomalies which precede a few hours to a few days the mainshock onset of the M6.4 Al Hoceima earthquake.

This work, therefore, permits to valorize the efficiency of this geodetic approach in the field of natural hazards, thus favoring the prediction of the seismic events on regional scale where the GPS/GNSS stations monitoring network is favorable.

KEYWORDS :   seismo-ionospheric precursors, GPS_TEC signal, coupling: lithosphere-atmosphere-Ionosphere.

Sr No: 49

Spatial extent of the resonance ionospheric signatures during the 11 March 2011 Tohoku earthquake

CORRESPONDING & PRESENTING AUTHOR:

Srinivas Nayak, Indian Institute of Geomagnetism, India

Mala S. Bagiya, Indian Institute of Geomagnetism, India

A.S. Sunil, Indian Institute of Geomagnetism, India

Durabha Sai Ramesh, Indian Institute of Geomagnetism, India

The earth and its atmosphere resonantly couple at the frequencies ~3.7 and ~4.4 mHz, leading to efficient energy exchange between them. Earthquakes are one of the potential sources which introduce these frequencies of oscillations into the atmosphere. The induced atmospheric oscillations can lead to the prolonged ionospheric perturbations through ion-neutral collisions. The spatial and temporal evolution

of resonant ionospheric oscillations can be studied using GPS-TEC. The 2011 Tohoku Earthquake (Mw 9.1) that ruptured on 11th March 2011 at 05:46:23 UT has been analysed to characterise the prolonged ionospheric perturbations observed after the event. The earthquake ruptured off the eastern coast of Northern Honshu along a major 200km fault, where the Pacific plate is subducting under the Northern Honshu. It was observed that the resonance phenomena strongly evolved to the south of the epicentre as compared to the north. This anisotropic distribution of resonant ionospheric signatures around the Tohoku epicentre has been scrutinised by referring to seismic and non-seismic parameters. This study suggests that both the non-tectonic parameters and direction of seismic energy released during the rupture played a key role in determining the north-south asymmetry in the resonant ionospheric signatures around the epicentre. It is assumed that this case study is a step forward towards efficient understanding of the earth-atmospheric resonance coupling during great earthquakes.

KEYWORDS :   resonant ionospheric oscillations

Sr No: 50

SYMPOSIUM :   **J3 Lithosphere-Atmosphere-Ionosphere Coupling: Seismo Ionospheric and Electromagnetic**

Seismic Seesaw: Understanding the Binary-earthquakes in a Seesaw Like Fashion Through Short-Term VLF Ionospheric Precursors

CORRESPONDING & PRESENTING AUTHOR:

Prasanna Waichal, Waichal Research, Ichalkaranji (Dist. Kolhapur), Maharashtra, India

It is a common belief that an earthquake is a single event or part of the series of fore-shocks or aftershocks of another major event. However, it has been observed through the Very Low Frequency (VLF) Ionospheric Precursors that there is a systematic "Omega $- (\omega)$" pattern in what can be described as a "Short-Term" earthquake precursor for two major earthquakes of sufficiently strong magnitude in M5-M6 class taking place in succession in a "seesaw" fashion within a few minutes of time-span but separated largely over geographical distances. This paper discusses two such incidents of earthquakes that occurred in the month of February 2021 in the Indonesia-South Pacific region that have shown these (ω) type precursor patterns and have occurred in quick successions in what can be called as a binary system and what is more common with them is the almost identical nature of the precursor pattern observed in the VLF signal variations.

KEYWORDS :   seismic seesaw, binary-earthquakes, VLF ionospheric

Sr No: 51

Simultaneous Detection of Dual-Path Dual-Precursors for Same Earthquake Event in a VLF Monitoring System

CORRESPONDING & PRESENTING AUTHOR:

Prasanna Waichal, Waichal Research, Ichalkaranji (Dist. Kolhapur), Maharashtra, India

This paper discusses for the first time, the simultaneous detection of VLF Ionospheric precursors in two different signal paths at the same time instances which later could be verified with the same earthquake event that took place several days later in the middle of these two VLF Paths. A very interesting phenomenon was detected on 06th March 2021 post mid day. Two VLF signals of 25.500kHz and 19.600kHz originating from the Eastern Europe (Belarus) and the UK are being monitored simultaneously. At 1315 Hrs India Standard Time (IST), both signals detected the Ionospheric precursor at the same time. This trend continued till 1440IST when the signals returned to normal at the same time instance. This clearly indicated that an earthquake of magnitude M5 on the Richter scale is likely to occur within few days and more interestingly, in the area or location that lies between the propagation path of these two signals from their respective transmission location to the receiving or monitoring station in Ichalkaranji in Maharashtra, India (16°42'13"N, 74°28'32"E). An earthquake alert therefore was issued by the author stating the possibility of M5 scale earthquake from 6th March to 11th March 2021 in a geographical area enclosed by these two paths.

KEYWORDS :   very low frequency, VLF ionospheric precursors, earthquake prediction

Sr No: 52

Understanding the M7 and M8 earthquake events of 04 March 2021 in the South Pacific and New Zealand through advance VLF Precursors

CORRESPONDING & PRESENTING AUTHOR:

Prasanna Waichal, Waichal Research, Ichalkaranji (Dist. Kolhapur), Maharashtra, India

In the beginning of March 2021, three major earthquakes of magnitude M7+ and M8+ have taken place near Kermadec Islands region in the South Pacific and in New Zealand [1]. The first from these three events with magnitude M7.3 occurred on 04 March 2021 at 1327UTC/GMT in Gisborne, New Zealand. Just a few hours later, the Kermadec Islands (NZ) south of Tonga in the South Pacific received a major shock of magnitude M7.4 at 1741UTC/GMT. And finally, the strongest of these, a magnitude M8.1 again struck the Kermadec Islands region at 1928UTC/GMT on the same day. This paper discusses the VLF earthquake precursors detected more than 14 days in advance of these events.

The first VLF Ionospheric precursor was detected on 14th February 2021 at 0312UTC/GMT and an earthquake alert [2] was therefore issued stating the possibility of M7+ quake event in the South Pacific and New Zealand with possible dates as 14th Feb 2021 till 26th February 2021. It was anticipated that this particular precursor is the only one and hence the dates were inferred. In reality, there were two more

precursors detected a few days later on 17th February 2021 at 0616UTC/GMT and the other on 19th February 2021 at 0230UTC/GMT. Thus, it is clearly seen that corresponding to the three different earthquakes as described above, three distinct earthquake precursors were detected more than 14 days in advance.

KEYWORDS :   very low frequency, VLF ionospheric precursors, earthquake prediction

Sr No: 53

On the Effects of Non-Tectonic Forcing Mechanisms on GPS measured Coseismic Ionospheric Perturbations: a Geometrical Modelling Approach

CORRESPONDING & PRESENTING AUTHOR:

Mala Bagiya, Indian Institute of Geomagnetism, India
A. S. Sunil, Indian Institute of Geomagnetism, India
Lucie Rolland, Université Côte d'Azur, Géoazur, France
Srinivas Nayak, Indian Institute of Geomagnetism, India
D. S. Ramesh, Indian Institute of Geomagnetism, India

Near and far field coseismic ionospheric perturbations (CIP) have been well studied using Global Navigation Satellite System (GNSS) measured Total Electron Content (TEC). The generation of near field (~500–600 km surrounding an epicenter) CIP is mainly attributed to the coseismic crustal deformation. The azimuthal distribution of near field CIP may contain information on the seismic/tectonic source characteristics of rupture propagation direction and thrust orientations. However, numerous studies cautioned that before deriving the listed source characteristics based on coseismic TEC signatures, the contribution of non-tectonic forcing mechanisms needs to be examined. A 3D model to map the combined effects of non-tectonic forcing mechanisms of geomagnetic field, GNSS satellite geometry, and ambient electron density gradient, on manifestations of GNSS measured near field CIP has been proposed. Further, this model has been tested on earthquakes occurring at different latitudes with a view to quickly quantify the collective effects of these mechanisms. We presume that this model would induce and enhance a proper perception among the researchers about the tectonic source characteristics derived based on the corresponding ionospheric manifestations.

KEYWORDS :   co-seismic ionospheric perturbations, GPS-TEC, non-tectonic forcing mechanism
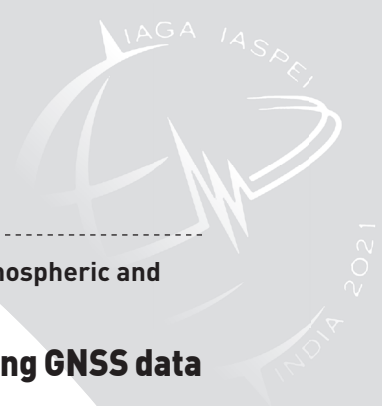
Sr No: 54

Tracing of Ionospheric Signals for Tsunami Early Warning using GNSS data

CORRESPONDING & PRESENTING AUTHOR:

Mala Bagiya, Indian Institute of Geomagnetism, India
Sunil A. S., Indian Institute of Geomagnetism, India
Sunil P. S., School of Marine Sciences, Cochin University of Science and Technology, India
Surendra Sunda, Airports Authority of India, India
Ramesh D. S., Indian Institute of Geomagnetism, India

Giant tsunamis are known to produce two varieties of ionospheric perturbations, the first that travel much faster than ocean water tsunami and another travel along the tsunami. Accordingly, earlier have been captioned as ahead of tsunami travelling ionospheric disturbances while the later as co-tsunami travelling ionospheric disturbances. Using Global Positioning System (GPS) measured Total Electron Content (TEC) in vicinity of the Sumatra 2004 seismic source, tsunamigenic ionospheric perturbations which observed several minutes prior to the arrival of tsunami at Indian east coast were scrutinized. Based on this, here we propose and discuss the potential importance of GPS based real time monitoring of offshore ionosphere for tsunami early warning. Further, the role of varying satellite position geometry in determining the effectiveness of proposed tsunami early warning system has been demonstrated.

KEYWORDS :   ionosphere, GPS-TEC, tsunami early warning

Sr No: 55

Magnetospheric-Ionospheric-Lithospheric coupling analytical model. Observations during the August 5, 2018 Bayan Earthquake

CORRESPONDING & PRESENTING AUTHOR:

Mirko Piersanti, IAPS, Italy
Massimo Materassi, CNR, Italy
Roberto Battiston, University of Trento, Italy
Vincenzo Carbone, Universitá della Calabria, Italy
Giulia D Angelo, IAPS, Italy
Pietro Ubertini, IAPS, Italy

The short-term prediction of earthquakes is an essential issue connected with human life protection and related social and economics matter. Recent papers have provided some evidence of the link between the lithosphere, lower atmosphere, and ionosphere, even though with marginal statistical evidence. The basic coupling hypothesized being via atmospheric gravity wave (AGW)/acoustic wave (AW) channel. In this work we analyse the scenario of the low latitude earthquake (Mw=6.9) occurred in Indonesia on August 5, 2018, through a multi-instrumental approach, using ground and satellites high quality data. As a result, we derive a new analytical lithospheric-atmospheric-ionospheric-magnetospheric coupling model with the aim to provide quantitative indicators to interpret the observations around 6 hours before and at the moment of the earthquake occurrence.

KEYWORDS :   LAIC analytical model, multi-instrumental observations.

Sr No: 56

Simultaneous electric - magnetic and ULF anomalies associated with moderate earthquakes in Kumaun Himalaya

CORRESPONDING & PRESENTING AUTHOR:

Jayashree Bulusu, CSIR-National Geophysical research Institue

Kusumita Arora, CSIR-National Geophysical research Institue, India

Anusha Edara, CSIR-National Geophysical research Institue, India

Shubham Singh, CSIR-National Geophysical research Institue, India

Based on fundamental concepts of variations of electric and magnetic fields at a given location, anomalous EM signatures have been defined based on mediumterm data recording at two sites Dhanachuli site near the Main Boundary Thrust (MBT), and Patiyasar site near the Main Central Thrust (MCT) in Kumaun Himalaya, India. The patterns of anomalous EM signatures are then linked to the occurrence of moderate earthquakes $(3.5 \leq M \leq 5.0)$, which are common occur along the MCT. The vertical component of magnetic field is influenced by prominent positive contributions prior to seven medium magnitude the earthquakes; electric fields also show positive anomalies. Surface wave generation associated with the earthquakes are reflected in the polarization ratios of geomagnetic data in the Pc4 range (0.01 Hz), few days prior to each earthquake. In the case of one earthquake, during which suitable data could be retrieved, we observe a frequency change in ULF (Pc1 range) in addition to the enhancement of the Pc4, prior to the event.

KEYWORDS :   electromagnetic anomaly, ULF waves, earthquake association

Sr No: 57

Ground and Space based observations of the pre and post atmospheric and ionospheric anomalies as investigated using 2015 Nepal earthquake

CORRESPONDING & PRESENTING AUTHOR:

S. Sripathi, Indian Institute of Geomagnetism, India

Rajesh Kumar Barad, Indian Institute of Geomagnetism, India

Ram Singh, Space Pysics Laboratory, India

Sridhar Banola, Indian Institute of Geomagnetism, India

Prabhakar Tiwari, Indian Institute of Geomagnetism, India

We present results of atmospheric/ionospheric anomalies as investigated using ground based and space based measurements using ionospheric density and TIMED/SABER satellite temperature along with thermal anomalies in the Outgoing Long wavelength Radiation (OLR) during pre and post 2015 Nepal Earthquake (28.147°N, 84.708°E) that occurred at 06:11:26 UT on 25 April 2015 (Mw7.8) with major aftershock observed at 07:05:19 UT (Mw7.3) on 12 May 2015. It is noticed in the recent past that atmospheric/ ionospheric anomalies prior to earthquake are significantly increased. So, understanding the atmospheric/ ionospheric behaviour prior to such large earthquakes may provide vital information that is important for early warning systems. Research analysis suggests that atmospheric and ionospheric precursors do exist before

the onset of earthquakes by few days to few 10s of days. But identification is a challenge. In this paper, we examine the ionsopheric parameters such as foF2, foEs and h'Es, h'F and hpF2 at Allahabad station in search of pre-seismic and post-seismic signatures. We also examine the SABER satellite observations of MLT temperature and OLR observations during pre and post seismic event. Our results suggest that there is a strong coupling between seismic activity and ionized density perturbations during co-seismic activity but mixed responses are seen in OLR thermal anomalies as well as atmospheric temperature. Similarly, our results also showed mixed response as well for precursory signatures. Based on the analysed results, attempts are being made to understand their signatures in the light of current understanding on the coupling processes of lithosphere-ionosphere during pre/post seismic event.

KEYWORDS : ionospheric seismology, Nepal earthquake, density variations

Sr No: 58

SYMPOSIUM : **J3 Lithosphere-Atmosphere-Ionosphere Coupling: Seismo Ionospheric and Electromagnetic**

Ionospheric anomalies immediately before large earthquakes: Review and perspective (by invitation)

CORRESPONDING & PRESENTING AUTHOR:

Kosuke Heki, Hokkaido University, Japan

Densification of continuous GNSS receiving stations enabled us to observe changes in ionospheric TEC associated with large earthquakes. Here I focus on TEC enhancements immediately before M8-9 class earthquakes, found first for the 2011 Mw9.0 Tohoku-Oki earthquake (Heki, 2011 GRL) and later for all the earthquakes in this century with Mw 8.2 or more (Heki & Enomoto, 2015 JGR; He & Heki, 2017 JGR). The 18 examples exhibit clear scaling laws, (1) leading times of the anomalies range from ~15 minutes (M8) to ~45 minutes (M9) and scale with fault lengths, and (2) strengths of the anomalies range from ~1 % (M8) to ~10 % (M9) of the background values and scale with fault areas. This suggests that a certain process, sweeping the fault from one end to another, weakens the fault immediately before large earthquake. Occurrences of micro-scale cracks and dislocations there may mobilize positive charges, which temporarily stay on the surface and redistribute ionospheric electrons. 3D tomography of ionospheric electron density anomalies (He & Heki, 2018 JGR; Muafiry & Heki, 2020 JGR) showed that the positive/negative anomalies started to grow simultaneously at low/high altitudes and line-up along the geomagnetic field. The anomalies are also found to exist only above land, suggesting that crustal electric field is responsible for the anomalies.

KEYWORDS : GNSS-TEC, earthquake, ionospheric disturbance

Sr No: 59

Modeling Near-field Co-Seismic Ionospheric Disturbances During the 2015 Illapel Earthquake

CORRESPONDING & PRESENTING AUTHOR:

Xing Meng, Jet Propulsion Laboratory, California Institute of Technology, USA

Michela Ravanelli, Sapienza University of Rome, Italy

Attila Komjathy, Jet Propulsion Laboratory, California Institute of Technology, USA

Olga Verkhoglyadova, Jet Propulsion Laboratory, California Institute of Technology, USA

The Mw8.3 Illapel, Chile earthquake on 16 September 2015 has induced detectable ionospheric disturbances above the near-field region, i.e., within about 1000km from the epicenter. The ionospheric total electron content (TEC) perturbations observed by Global Navigation Satellite System (GNSS) exhibit a strong north-south asymmetry in the perturbation magnitude. The asymmetry is primarily caused by the different ground motion characteristics in the north and south regions of the epicenter. To investigate seismic-ionospheric coupling and reproduce the asymmetric ionospheric disturbances for the Illapel earthquake, we extend the Wave Perturbation - Global Ionosphere-Thermosphere Model (WP-GITM), a three-dimensional time-dependent numerical model for simulating ionospheric disturbances induced by impulsive surface movement, from using a point seismic source to an area seismic source. The area seismic source is specified by a network of GNSS-measured vertical ground velocity data obtained using the Variometric Approach for Displacements Analysis Stand-alone Engine (VADASE) algorithm. The area seismic source well describes the different strengths of ground motions to the north and to the south of the epicenter. We perform WP-GITM modeling with the area seismic source and validate the simulation results against GNSS-observed TEC perturbations. This work represents a significant step forward in WP-GITM development for capturing near-field co-seismic ionospheric disturbances. This is also the first time that seismic ground motion measurements at multiple locations are utilized to drive an earthquake-ionosphere coupling model.

KEYWORDS : co-seismic ionospheric disturbance

Sr No: 60

Ionosonde and satellite data analysis in relation to the 2002 Molise (Italy) seismic sequence

CORRESPONDING & PRESENTING AUTHOR:

Dario Sabbagh, Istituto Nazionale di Geofisica e Vulcanologia, Italy

Loredana Perrone, Istituto Nazionale di Geofisica e Vulcanologia, Italy

Angelo De Santis, Istituto Nazionale di Geofisica e Vulcanologia, Italy

Saioa A. Campuzano, Instituto de Geociencias IGEO (CSIC-UCM), Spain

Gianfranco Cianchini, Istituto Nazionale di Geofisica e Vulcanologia, Italy

Serena D Arcangelo, Universidad Complutense de Madrid – UCM, Spain

Domenico Di Mauro, Istituto Nazionale di Geofisica e Vulcanologia, Italy

Dedalo Marchetti, Jilin University, China

Adriano Nardi, Istituto Nazionale di Geofisica e Vulcanologia, Italy

Orlando Martina, Istituto Nazionale di Geofisica e Vulcanologia, Italy
Alessandro Piscini, Istituto Nazionale di Geofisica e Vulcanologia, Italy
Maurizio Soldani, Istituto Nazionale di Geofisica e Vulcanologia, Italy

A seismic sequence characterized by two moderate magnitude earthquakes within about 24 hours followed by one-month long aftershocks sequence occurred in Molise (Italy) in October and November 2002 [1]. The first mainshock occurred on October 31st (10:33:00 UTC) with local magnitude equal to 5.4, and caused severe damages in terms of destroyed buildings and human losses in the town of S. Giuliano di Puglia. Indeed, despite its moderate intensity, the seismic event killed 30 people, mostly children in a school. A second main event occurred on November 1st (15:09:02 UTC) with local magnitude equal to 5.3. The understanding of the processes that occur during the earthquake preparation phase and the capability to detect the associated signals is of crucial importance in order to prevent such tragic consequences. The combined ground-satellite study of the ionospheric response to the preparation phase of the 2002 Molise seismic sequence intends to contribute to such understanding. Ionospheric anomalies, detected up to a couple of months before the two mainshocks by the Rome ionospheric observatory, are considered, following the multiparametric approach based on ionosonde observations previously applied to the M5.5+ earthquakes occurred in Central Italy since 1984 [2, 3]. The variations for 2-3 hours of specific Es and F2 layers parameters, namely h'Es, fbEs, and foF2, are studied in relation to the geomagnetic activity and the earlier-obtained empirical relations between earthquake magnitude and features (epicentral distance and anticipation time) of anomalies. In addition, in-situ electron density (Ne) measurements over the earthquakes preparation region recorded by the CHAllenging Minisatellite Payload (CHAMP) satellite at altitudes of about 400 km are analyzed, in order to characterize pre-earthquakes anomalies in terms of abnormal changes of the dNe/dt along the tracks acquired under quiet geomagnetic conditions.

[1] C. Chiarabba, P. De Gori, L. Chiaraluce, P. Bordoni, M. Cattaneo, M. De Martin, A. Frepoli, A. Michelini, A. Monachesi, M. Moretti, G.P. Augliera, E. D'Alema, M. Frapiccini, A. Gassi, S. Marzorati, P. Di Bartolomeo, S. Gentile, A. Govoni, L. Lovisa, M. Romanelli, G. Ferretti, M. Pasta, D. Spallarossa, and E. Zunino, "Mainshocks and aftershocks of the 2002 molise seismic sequence, southern Italy", J. Seismol., 9, 2005, pp. 487–494, doi: 10.1007/s10950-005-0633-9. [2] L. Perrone, L. P. Korsunova, and A. V. Mikhailov, "Ionospheric precursors for crustal earthquakes in Italy", Ann. Geophys., 28, 2010, pp. 941–950, doi: 10.5194/angeo-28-941-2010. [3] A. Ippolito, L. Perrone, A. De Santis, and D. Sabbagh, "Ionosonde Data Analysis in Relation to the 2016 Central Italian Earthquakes", Geosciences, 10, 2020, 354, doi: 10.3390/geosciences10090354.

Sr No: 61

Atmospheric Electric Field Fluctuations associated with Earthquakes in Japan

PRESENTING AUTHOR:

Mako Watanabe, University of Electro-Communications, Japan

CORRESPONDING AUTHOR:

Yasuhide Hobara, University of Electro-Communications, Japan
Antrisha Swtiwan, University of Electro-Communications, Japan
Hiroshi Kikuchi, University of Electro-Communications, Japan

In recent years, seismo-electromagnetic phenomena have been reported in various physical quantities and frequency bands. The group of the University of Electro-Communications has discovered several cases of atmospheric electric field anomaly around 30 minutes before and after earthquakes in Iwaki (UEC) and Kakioka (JMA) for medium-sized earthquakes (M>5). In this study, we conducted a frequency analysis of atmospheric electric field data before and after the earthquake in northern part of Japan, Memanbetsu, Hokkaido (JMA). As a result, we confirmed that the atmospheric electric field variation in Memanbetsu was similar to that observed in Iwaki and Kakioka in Honshu (main land Japan). Therefore, the electric field variations with common characteristics at the three spatially separated stations are likely to be related to the occurrence of earthquakes, and are important to understand the generation and propagation mechanism of electromagnetic phenomena preceding earthquakes

KEYWORDS : atmospheric electric field, earthquake

Sr No: 62

Relationship between Atmospheric Electric Fields and Lower Ionospheric Disturbances Associated with Earthquakes

CORRESPONDING & PRESENTING AUTHOR:

Yasuhide Hobara, University of Electro-Communications, Japan

Kakeru Matsuki, University of Electro-Communications, Japan

Mako Watanabe, University of Electro-Communications, Japan

Hiroshi Kikuchi, University of Electro-Communications, Japan

Antrisha Setiwan, University of Electro-Communications, Japan

In recent years, there have been series of reports of ionospheric anomalies detected by GPS TEC immediately before the onset of large earthquakes (M>8.2) (20 to 80 minutes before the earthquake). In addition, the University of Electro-Communications group has discovered several cases of characteristic changes in the atmospheric electric field near the epicenter around 30 minutes of occurrence timings of earthquakes, even for medium-sized earthquakes. In this study, we investigated the relationship between the atmospheric electric field and the amplitude of the VLF/LF transmitter electric field just before and after the earthquake for the first time. As a result, both the atmospheric electric field and the amplitude of the VLF/LF perturbations found to fluctuate within the same period in several cases. The time difference between the observed atmospheric electric field and VLF/LF perturbations suggests that the atmospheric gravity waves generated around the time of the earthquake near the epicenter may have propagated upward and caused ionospheric disturbances.

KEYWORDS : atmospheric electric field, ionospheric anomaly, earthquake

Sr No: 63

Statistical Analysis of Pre-seismic Ionospheric Electron Density Anomalies and Investigation of the Efficiency of Short-time Earthquake Forecasting using Ionosonde, Japan

CORRESPONDING & PRESENTING AUTHOR:

Katsumi Hattori, Chiba University, Japan

Syunya Mitsuishi, Chiba University, Japan

Rui Song, Chiba University, Japan

Chie Yoshino, Chiba University, Japan

Jannyenq LIU, National Central University, Taiwan

Recently, ionospheric anomalies related to earthquakes have been reported and are considered promising for short-term earthquake forecast.

In Japan region, the previous statistical study during 1958-2017 shows a significant anomaly 1-10 days before the earthquakes with $M \geq 6$, depth $D \leq 40$ km, epicenter distance $R \leq 350$ km in NmF2. However, the sensitivity of NmF2 anomalies for earthquakes is not clarified. Therefore, we performed statistical analysis to assess the magnitude, depth, and epicenter distance effects to positive NmF2 anomalies, using ionosonde data at Kokubunji, Japan. We defined the anomaly as the value exceeding median + 1.5 IQR of the NmF2 at the same hour in the previous 15 days and the anomalous day as ten or more hours of the anomalies appear in one day.

We performed Superposed Epoch Analysis (SEA) to investigate statistical significance in the correlation between NmF2 anomalies and earthquakes with the random test. SEA results show that there is a significant NmF2 anomaly 6-10 days before the earthquakes. NmF2 anomalies have sensitivity for earthquakes with magnitude $M \geq 5.8$, depth $D \leq 40$ km, epicenter distance $R \leq 350$ km. Furthermore, these results indicated the magnitude, depth, and epicenter distance dependences.

Then, we performed Molchan's Error Diagram analysis to evaluate the efficiency of NmF2 anomalies for earthquake forecasting. These results indicated that NmF2 anomalies are a precursor of earthquakes and are more precursory for shallower, larger, and closer earthquakes. We found the optimum parameters; $M \geq 6.4$, $D \leq 20$ km, $R \leq 200$ km lead time $\Delta = 10$, and alarm window $L = 1$ can detect about 46% of the targeted earthquakes.

KEYWORDS :   pre-seismic ionospheric electron density anomalies, ionosonde, molchan's error diagram analysis

Sr No: 64

Combination of ground and satellite observations of the August 5, 2018 Bayan Earthquake

CORRESPONDING & PRESENTING AUTHOR:

Coralie Neubueser, INFN, Germany

Early warning systems of earthquakes play a key role in human life protection especially in highly populated areas of the earth. First indications have been found in NOAA satellite data, that particle fluxes of trapped electrons in the Van Allen belts can be correlated to seismic activity on the ground. A recent study on the August 5, 2018 Bayan Earthquake (EQ) shows and explained via an analytical model the coupling among the lithosphere, the atmosphere, the ionosphere and the magnetosphere, through the generation of an acoustic gravity wave (AGW) able to mechanically perturb the ionospheric plasma density which in turn generates electromagnetic waves propagating through the magnetosphere. In this contribution, we will investigate the magnetosphere-ionosphere system from the particle point of view during the same EQ event. We will use the measurements of low-energy electron flux measurements of the HEPD and HEPP instruments on-board CSES-01 satellite to search for particle bursts which can be related to the EQ event.

KEYWORDS : van allen belts, seismic events, electromagnetic wave propagation in magnetosphere

J4 Joint Inversion Methods and Other Interpretation Strategies to Integrate Multidisciplinary Geophysical Data

CONVENERS: Max Moorkamp

Gesa Franz

Alan Jones

Ulrich Achauer

Combining complimentary data sets typically reduces the ambiguity of inversion results and facilitates subsequent interpretation. Hence, integration of multi-disciplinary data has become popular in many disciplines including near-surface geophysics, mineral exploration, sub-basalt and sub-salt problems, gas hydrate investigations, and studies involving deep crustal and mantle structures. Still, many questions remain: Which types of data should be inverted together? How to balance their influence in the inversion? How can we assess the differences between joint inversion, cooperative inversion and other integrated interpretation strategies? This session welcomes research using joint inversion or other approaches to combine different types of geophysical data. Both case studies and technical contributions are welcome.

Sr No: 65

Unstructured grid-based Constrained Inversion of large scale DC and Gravity data

CORRESPONDING & PRESENTING AUTHOR:

Vishnu Kant Verma, IIT Bombay, India

Anand Singh, IIT Bombay, India

The goals of geophysical techniques are to answer the subsurface's actual structure and property under investigation. Geophysical inverse modeling provides a mathematical framework to obtain a reliable model of the Earth's subsurface responsible for the field's measured data. However, a reliable inversion algorithm depends on the following factors: 1) model parameterization, 2) forward and sensitivity computation, and 3) inversion approach. We have parameterized and performed modeling on triangular meshes in the present work to deal with large-scale data sets. We then computed the forward algorithm over topographic variations for DC and gravity data sets using the same model parameterization.

We have tested our inversion algorithm on synthetic and field data sets. From the individual inversions, we have noted the inconsistency in the respective models. Thus, a constrained inversion (CI) approach for DC and gravity data is proposed. In CI, we first perform inversion in one model domain (say gravity) and then use its results with another model domain (say DC) such that both model domains are coupled in some way and invert them simultaneously. The algorithm uses a clustering algorithm to make the petrophysical relationship between density and resistivity. The developed approach reduces the ambiguity arising from incompatible features across individual inversion, and the inverted model shows a high level of structural similarity compared with traditional inversion approaches. The developed methodology is tested on synthetic and actual field data sets, and it provides us with noticeable results.

KEYWORDS :   unstructured grid; constrained inversion, DC resistivity; gravity; large scale.

Sr No: 66

Detection and inversion of UXO and non-UXO sources, exemplified with UAV-borne dual-magnetometer system data from an intertidal flat

CORRESPONDING & PRESENTING AUTHOR:

Mick Emil Kolster, National Space Institute, Technical University of Denmark, Denmark

Magnetic remote sensing remains a common detection approach for Unexploded Ordnance (UXO) disposal campaign in various environments. During the last decade, Uncrewed Aerial Vehicles (UAVs) have provided a brand new approach to such surveying, providing an efficient solution to previously challenging surveying tasks, with the approach constituting a viable alternative to other conventional survey methods. One of these approaches in scalar magnetic UAV surveying, which we briefly present, alongside collected data and inversion results, including detection and postiioining, obtained through different approaches.

A persisting general problem in magnetic UXO methods is false positives, due to the challenges of differentiating between magnetic signatures from UXO and inert objects, e.g., metallic debris. We augment our discussion by presenting some preliminary results on the UXO/non-UXO discrimination problem, and present some preliminary results from ongoing work on reduction in false-positives. Our work includes characterization efforts on size and shape of the source, which requires quality data with good resolution, similar to what is obtainable using UAV methods. Part of our discrimination efforts include utilizing such magnetic data from the UAV system in a probabilistic inversion procedure.

SOME BACKGROUND FOR OUR WORK IS AVAILABLE IN:

- Kolster, M. E., & Døssing, A. (2021). Scalar magnetic difference inversion applied to UAV-based UXO detection. Geophysical Journal International, 224(1), 468-486.
- Wigh, M. D., Hansen, T. M., & Døssing, A. (2020). Inference of unexploded ordnance (UXO) by probabilistic inversion of magnetic data. Geophysical Journal International, 220(1), 37-58.

KEYWORDS : unexoploded ordnance, probabilistic inversion, uncrewed aerial vehicles

Sr No: 67

SYMPOSIUM : **J4 Joint Inversion Methods and Other Interpretation Strategies to Integrate Multidisciplinary Geophysical Data**

Integration of Multi-Geophysical Datasets through Advance Constrained Inversion and ML-based Algorithms

CORRESPONDING & PRESENTING AUTHOR:

Anand Singh, IIT Bombay, India

In the present work, a joint inversion approach for different geophysical datasets is proposed. The algorithm uses machine learning-based techniques to make the relationship among physical properties to obtain common surface features. Here, I have successfully incorporated prior parametric information (such as geologic information) into a deterministic inversion framework using machine learning and advance constrained inversions. As a result, I was able to enhance the quality of the inverted images. We can extract the prior parametric information from lithology observations, geological principles, well logs, and complementary data from other geophysical methods. The resulting subsurface model will satisfy both the observed data and parametric information and, therefore, can represent the earth better than geophysical inversion models that only honor the observed field data.

I demonstrated the results on several field datasets. In the first field data example, it is shown that how ML-based algorithms fulfill two needs. First, the inverted resistivity model honors the fitting between measured and computed data. Second, the recovered resistivity model was guided by other prior well-log information. In the second field data sets, we noted the inconsistencies in both resistivity and density models obtained from the individual inversions. However, the presented joint inversion approach produced similar resistivity and density models while maintaining the same error level of the respective separate inversions. At last, the result of machine learning-assisted 3D joint inversion of gravity and magnetic data was shown as a case study over BIF mineralization.

KEYWORDS : geophysical inversion, multi-geophysical datasets, machine learning algorithms

Sr No: 68

Joint-inversion of receiver functions and dispersion curves: preliminary results from a case of study in Mexico City

CORRESPONDING & PRESENTING AUTHOR:

Manuel J. Aguilar Velazquez, Posgrado en Ciencias de la Tierra, Universidad Nacional Autónoma de México (UNAM), Mexico

Xyoli Perez Campos, Instituto de Geofísica, Universidad Nacional Autónoma de México (UNAM), Mexico

Olivia D. Pita Sllim, Victoria University of Wellington, New Zealand

Receiver functions and dispersion curves have been widely used, separately or jointly, to explore the crustal structure around the world. In this work, we present a study case in which we used the joint-inversion algorithm introduced by Julià et al. (2000) to jointly invert P-wave teleseismic receiver functions and dispersion curves obtained in Mexico City. To estimate shear-wave velocities in-depth, we performed a geostatistical analysis using the 1D resultant models per station previously clustered by ray parameter and back azimuth. Altogether, the receiver-function analysis, the geostatistics, and the corresponding models in-depth suggest the presence of two crustal discontinuities. The first one is located around 8 kilometers below the surface and is a relatively high-velocity zone. The second one is located between the 34 and the 46 kilometers below the surface; we interpreted it as the irregular Moho's geometry, which is consistent with previous results reported in the literature.

KEYWORDS : joint inversion, receiver functions, dispersion curves

Sr No: 69

Identifying the origin of enhanced crustal conductivity with multi-physics inversion

CORRESPONDING & PRESENTING AUTHOR:

Max Moorkamp, LMU Munich, Germany

A region of high electrical conductivity in the lower crust has been observed in regions around the world since the first electromagnetic soundings were made in the 1960s. Traditionally the cause of the high conductivity is interpreted based on the tectonic regime the measurements have been made in. In tectonically active regions melt or fluids or both are inferred, whereas in old stable regions solid phases such as graphite and sulfides are preferred. We perform multi-physics inversion of gravity and magnetotelluric data with a novel coupling criterion based on mutual information of measurements across the western United States. We obtain a combined density and conductivity model that shows geologic structures with high fidelity. In addition, the analysis of the density-conductivity relationship retrieved from the inversion reveals that the simple association of fluid and melts with active regions and solid conductive phases with stable regions is not compatible with our results. Instead we see structures with high conductivity and low density (fluids) juxtaposed against structures with high conductivity and high density (solid conductor). These results demonstrate the multi-physics inversion can help to shed light on composition and processes within the Earth and that the simplistic interpretation employed so far needs to be revised.

KEYWORDS : joint inversion, lithosphere, magnetotellurics

Sr No: 70

Sub-basalt Imaging of Gondwana Sediments, Basement Configuration and Deep Crustal Structures in Different Gondwana Sedimentary Basins of India

CORRESPONDING & PRESENTING AUTHOR:

Laxmidhar Behera, CSIR-National Geophysical Research Institute (CSIR-NGRI), India

Sub-basalt imaging of Gondwana sediments for exploration of hydrocarbon and minerals in different Gondwana sedimentary basins like the Mahanadi, Bengal and Rewa basins of eastern India pose major challenge due to poor penetration, significant attenuation and mode-conversion of seismic energy within the basalts. By using ray-trace inversion and robust tomographic imaging of refraction and wide-angle seismic data, it is possible to delineate very fine details of the sub-surface geological structures like horsts and grabens, faults, dykes and sills. These techniques are successfully employed to delineate low-velocity-layer (LVL) Gondwana sediments hidden below the high-velocity-layer (HVL) basalts having strong lateral and vertical velocity variations, basement configuration and crustal structures along different deep seismic profiles acquired in these sedimentary basins. The shallow velocity models obtained using tomographic imaging are used as input for Pres-stack depth migration (PSDM) to constrain very small and subtle geological features suitable for hydrocarbon and mineral prospecting as well as basement configuration having deep basinal faults. The velocity models derived along different seismic profiles in these basins are further constrained and corroborated by the corresponding density models obtained from the inversion of Bouguer gravity data. The integrated velocity and density models provide an insight of the presence Gondwana sediments hidden below the basalts and deep crustal structures down to the Moho. This study also depicted the tectonic and geodynamic settings of these Gondwana rift basins forming an edifice of both early and late Cretaceous volcanism, which are infested by Rajmahal and Deccan volcanic activities in the eastern India.

KEYWORDS :   seismic tomography, sub-basalt imaging, crustal structure

Sr No: 71

Kiama reverse magnetization zone is unmasked in the oceanic crust of the eastern Mediterranean

CORRESPONDING & PRESENTING AUTHOR:

Lev Eppelbaum, Tel Aviv University, Israel

The Eastern Mediterranean is a tectonically complex region composed of a set of structures of the Tethys Ocean remnant. The initial discovery and mapping of the Kiama zone of inverse polarity has been performed on the basis of 3D combined modeling of magnetic and gravity fields with attraction of paleomagnetic and seismic data. Actually it is the first evidence of discovering such an ancient oceanic crust; therefore additionally integrated analysis of thermal, tectonic, structural and paleogeographical data has been carried out. The recognized Kiama paleomagnetic hyperzone suggests transport along transform faults from the eastern part of the Tethys Ocean (region of the modern Persian Gulf). This hyperzone is discordant to the strike of the Mesozoic terrane belt and the Aegean-Anatolian plate. Study of geophysical, radiometric

and petrological characteristics indicates that the Kiama paleomagnetic zone is bounded by younger ocean floor rocks. Analysis of Moho discontinuity map developed for the Eastern Mediterranean by use of the seismo-gravity analysis testifies that the Kiama zone's crustal thickness is thicker than the adjacent areas. The easternmost Mediterranean is characterized by significant lithospheric thickness (up to 125 km) whereas in the surrounding regions this value is about 100 km. This fact states the significant geodynamic activity during closing of the Neotethys Ocean. The thermal flow data observed over the Kiama hyperzone show extremely low values - until 15 mW/m2 which testifies to the ancient lithosphere. The discrepancy between the Nubian-Arabian foreland, oceanic crust and terrane belt indicates the allochthonous nature of the Eastern Mediterranean.

KEYWORDS : kiama paleomagnetic hyperzone, 3D modeling, integrated analysis

Sr No: 72

Meso-scale upper mantle thermo-chemical structure below ocean basins from a joint analysis of satellite gravity gradients, seafloor topography and seismic tomography

CORRESPONDING & PRESENTING AUTHOR:

Isabelle Panet, Université de Paris, Institut de physique du globe de Paris, CNRS, IGN, France

Marianne Greff Lefftz, Université de Paris, Institut de physique du globe de Paris, CNRS, IGN, France

Barbara Romanowicz, 1. Université de Paris, IPGP, CNRS, France 2. Collège de France Paris, France 3. University of California Berkeley, USA

From a combined analysis of satellite gravity, seafloor topography and seismic tomography of the upper mantle, our aim is to constrain the dynamic origin of enigmatic 1500-2000km wavelength structures in seismic and gravity data : elongated low shear velocity signals along the direction of present-day plate motion (APM) below ocean basins (French et al., 2013), coincident with geoid undulations in the Pacific ocean (Hayn et al., 2012). We first provide evidence for periodic, APM-oriented undulations at the 1600-2000km wavelength over broad oceanic areas, where geoid lows coincide with seafloor topographic lows and upper mantle mass excess, all correlated with the slow seismic velocity fingers at upper mantle depths. We investigate the density structure associated with these signals in the context of a model of bi-dimensional thermal convection. We show that a thermo-chemical interpretation of the seismic velocities is needed, as at least part of the mass excess is likely located within the slow velocity anomalies. We propose a model of secondary convection spanning down to ~1000km depth. As hot upwellings cross a moderately hydrous transition zone, dense partial melt is formed above the 410 km discontinuity, resulting in mass excess within them. We analyze the trade-offs between the temperature of the upwellings and the excess densities and find that the observations favor a sublithospheric low viscosity zone. Because these features are found both beneath fast moving plates and very slow ones, the flow is likely not entirely driven by plate motions, and probably includes a contribution from lower mantle plumes.

KEYWORDS : gravity field, seismology, upper mantle

Sr No: 73

Joint one-dimensional inversion of Magnetotelluric Data and Surface-Wave Dispersion Curves using Correspondence Maps

CORRESPONDING & PRESENTING AUTHOR:

Monica Aquino, Université de Strasbourg, France

Guy Marquis, Université de Strasbourg, France

Jerome Vergne, Université de Strasbourg, France

We use a correspondence map approach to invert jointly surface-wave dispersion curves and magnetotelluric data for subsurface shear velocity and resistivity but also for a possible relationship between them.

Our first experiments consisted of inversions of synthetic data computed from models for which properties are linked by linear and second-order polynomial relationships. Our methodology recovered well both the geophysical models and their relationships. The next experiment involved synthetic data from models of known physical properties, taken from well logs, but without a known relationship. Our approach produced a model closer to the expected result than when separate inversions are used. Having validated the approach with synthetic cases, we have applied our methodology to field data. We compared (i) separate inversions and joint inversions (ii) with and (iii) without correspondence maps. We found that the 1D subsurface models obtained by (i) and (iii) were similar but very different from those obtained by (ii), showing that including correspondence maps in the joint inversion workflow produces superior results.

KEYWORDS :   joint inversion, magnetotelluric, dispersion curves

Sr No: 74

Integrated Geostatistical Inference of Earth Mantle Heterogeneity

CORRESPONDING & PRESENTING AUTHOR:

Alexander Minakov, University of Oslo, Norway

Dmitry Kolyukhin, Trofimuk Institute of Petroleum Geology and Geophysics SB RAS, Russia

The gravity data are essential for imaging the heterogeneous density structure of the Earth mantle but unable to provide a unique solution. The inference of small-scale density structure of deep Earth interior has to rely on physical relations linking density with other geophysical parameters and statistical modeling. The exact relation between seismic velocities and density in the Earth mantle is unknown since it can be affected by temperature, composition, and other factors. However, the assumption that the spatial variation of seismic velocity and density changes might have similar statistics seems reasonable to us. The global seismic tomography models agree well at long wavelengths (1000-3000 km) but often start to diverge at a smaller scale. Thus, detailed regional models have to be considered for geostatistical analysis. Here, the estimation of the covariance or the correlation function is a more robust technique than the estimation of the power spectrum, as the data are spatially localized and band-limited in this case.

We present a new method for the statistical simulation of random fields in the 3D ball using the covariance functions in angular and radial directions as input parameters. We use this method to obtain random realizations of density field and incorporate in a probabilistic inversion of gravity data. The geostatistical prior information provides spatial weighting of the density model consistent with the spatial variation of seismic velocities. We apply this approach to infer thermal and compositional anomalies in the Earth's upper mantle using satellite gravity gradients and seismological data.

KEYWORDS : geostatistics, seismology, gravity

J5 Cratons & Mineral Exploration

CONVENERS: Stephan Thiel

Fiona Darbyshire

Prasanta Patro

We seek contributions pertinent to exploration of cratons and the mapping of mineral systems using electromagnetic and seismic techniques. Contributions that characterize cratons across scales from lithospheric mapping to camp size using array and profile data are invited for this symposium. It includes multi-disciplinary interpretations using other geophysical (e.g. gravity, magnetics, electrical, geoid, heat flow) and geochemical (e.g. xenolith, isotope, geochronology) data, which are able to infer mantle and crustal fertility. We encourage submissions that highlight the importance of lithospheric architecture on position and genesis of mineral systems, including but not limited to iron-oxide-copper-gold (IOCG), sediment-hosted deposits, porphyry deposits, gold and diamond deposits.

Sr No: 75

Crustal magnetotelluric imaging of a Paleoproterozoic graphitic suture zone, Curnamona Province, Australia (by invitation)

CORRESPONDING & PRESENTING AUTHOR:

Graham Heinson, University of Adelaide, Australia

Ben Kay, University of Adelaide, Australia

Kate Roberston, Department for Energy and Mining, Australia

The Curnamona Province is a Paleoproterozoic to Mesoproterozoic domain that hosts the Broken Hill ore body and a number of IOCG deposits, but is mostly covered in Neoproterozoic to Quaternary cover. 3D resistivity modelling of long-period MT from the Australian Lithospheric Architecture Magnetotelluric Project (AusLAMP) identified the Curnamona Conductor with extremely low resistivities ~1 Ohm.m at upper-crustal depths (< 15 km) and lateral extent of >200 km. The conductor dips to the west, centred under the large igneous province Benagerie Suite Volcanics with resistivity ~10-100 Ohm.m in a broader lower crustal region. To yield higher resolution of the Curnamona Conductor, a 56-site broadband MT transect was undertaken with 2 km spacing. We show consistency between AusLAMP 3D models, and new 2D and 3D broadband MT inversions, but with higher spatial and vertical resolution.

The linearity, depth-extent and western dipping morphology of the Curnamona Conductor is remarkably similar to Paleoproterozoic conductors along the eastern margin of the Mount Isa Province in northern Australia, and the eastern margin of the Gawler Craton in southern Australia. Plate reconstructions of Paleoproterozoic Nuna supercontinent suggests that these now disparate cratons were originally contiguous, with extensive subduction along their margin at 1.85 Ga. Marine sedimentation in accretionary wedges prior to collision occurred during the Lomagundi-Jatuli Event of a global increase in $\delta13C$ (2.3-2.0 Ga) with a significant increase in burial of organic carbon. We argue these Paleoproterozoic conductors represent graphitic suture zones that are uniquely representative of a time of enhanced carbon burial in Earth's history.

KEYWORDS : magnetotellurics, curnamona, graphite

Sr No: 76

Integration of geological, geophysical and geochemical methods for exploring the Magmatic Ni-Cu-PGE bearing sulphide mineralization in Betul fold belt, central India

CORRESPONDING & PRESENTING AUTHOR:

Venkata Vijaya Kumar Pachigolla, NGRI, India

Prasanta K Patro, NGRI, India

Abhirami S G, NGRI, India

Dewashish Kumar, NGRI, India

Satyanarayanan M, NGRI, India

K. N. S. S. S. Srinivas, NGRI, India

Khasi Raju, NGRI, India

M. Srihari Rao, NGRI, India

Ujjal K Borah, National Centre for Earth Science Studies, India

Setbandhu Mondal, GSI, India

K Chinna Reddy, NGRI, India

Abstract : The Central Indian Tectonic Zone is one of the most significant footprints of the complex tectonic process that extents a tectono-magmatic history from late Archaean/early Proterozoic to late Proterozoic era in the Indian peninsula. It contains mainly three major Proterozoic supracrustal belts from north to south i.e., Mahakoshal, Betul fold belt (BFB) and Sausar. Magnetotelluric (MT), electrical resistivity tomography (ERT), Induced Polarization (IP), Geochemistry and well logging techniques have been implemented to understand the complex geological processes involved in the generation of Ni-Cu-PGE bearing magmatic sulphide mineralization in the BFB. Geochemical analysis of field samples inferred the presence of potential host rocks for Ni-Cu-PGE bearing sulphide mineralization. MT data from two profiles were analysed and modelled using 2D and 3D inversion algorithms. The 2D and 3D MT models are compared and robust conductivity anomalies are interpreted in connection with geochemistry and physical properties of the core samples explains the origin of Ni-Cu-PGE mineralization in the study region. The near-surface conductors observed in the ERT sections at shallow depth correspond to the sulphide mineralization formed due to secondary hydrothermal fluids and have percolated as veins in the host Padhar mafic-ultramafic complex. They corroborate with the MT results. MT studies reveal an interesting feature is moderately conductor which is associated with magmatic Ni-Cu-PGE deposits are associated with mantle-derived mafic/ultramafic complexes related to lithospheric architecture. The geochemical studies also suggest that the parental magma was generated from subduction modified, metasomatized, enriched mantle source, and emplaced in a continental magmatic arc setting.

KEYWORDS : magnetotellurics, induced polarization, Ni-Cu-PGE-sulphide mineralization, betul fold belt, central India

Sr No: 77

SYMPOSIUM : **J5 Cratons & Mineral Exploration**

Constraints on the crustal architecture of a metallogenic belt – Implications for mineral genesis and emplacement from 3-D electrical resistivity models

CORRESPONDING & PRESENTING AUTHOR:

Matthew J. Comeau, University of Muenster, Germany

Michael Becken, University of Muenster, Germany

Alexey V. Kuvshinov, ETH Zurich, Switzerland

Sodnomsambuu Demberel, Mongolian Academy of Sciences, Mongolia

Erdenechimeg Batmagnai, ETH Zurich, Switzerland

Shoovdor Tserendug, Mongolian Academy of Sciences, Mongolia

Crustal architecture strongly influences the development and emplacement of mineral zones, primarily due to its control on fluid flow. We image the crustal structure beneath a metallogenic belt (Bayankhongor area, central Mongolia), which is narrow and long (~20x100 km) and contains important mineralization zones and sources of copper and gold. Nearby, at the edge of a Precambrian micro-continental block, an ophiolite belt marks the location of an ancient suture zone, providing evidence for the subduction-related closure of a paleo-ocean. However, the crustal structure of these features, and their relationships, are not well studied.

We use natural-source magnetotelluric data to generate three-dimensional electrical resistivity models of the crustal structure. The models show that anomalous, low-resistivity (<50 ohm-m) zones in the upper crust are spatially associated with the surface expressions of known mineral deposits. In contrast, the background is generally resistive (>1, 000 ohm-m). Anomalous low-resistivity zones are also congruent with the suture zone/ophiolite belt, which is revealed to be a major crustal-scale feature.

The low resistivity can be explained by hydrothermal alteration along fossil fluid pathways. This illustrates the pivotal role that crustal fluids play in diverse geological processes. By combining our electrical resistivity results with other geological and petrological data we attempt to gain insights into the emplacement and origin of the mineral resources. The results of this study support the hypothesis that the crustal architecture, including major crustal boundaries, acts as a first-order control on the location of mineral deposits and metallogenic belts.

KEYWORDS : crustal architecture, mineral zones, hydrothermal alteration

Sr No: 78

SYMPOSIUM : **J5 Cratons & Mineral Exploration**

The Thermochemical Structure of Superior Craton from Multi-Observable Probabilistic Inversion

CORRESPONDING & PRESENTING AUTHOR:
Riddhi Dave, UQAM, Canada
Fiona Darbyshire, UQAM, Canada
Juan Carlos Afonso, Macquarie University, Australia
Khaled Ali, De Beers Group, Belgium

Constraining and understanding the thermochemical structure of the lithosphere is an essential step in interpreting the interactions between the lithosphere and the underlying mantle, which can then be incorporated into exploration workflows. Though these features of the lithosphere can be imaged using geophysical inversion or analyzed from xenolith samples, there exists a great deal of inconsistency between competing models and datasets. Multi-observable Thermochemical Tomography (MTT) provides a probabilistic inversion framework that utilizes geology as the fabric to integrate multiple geophysical techniques and incorporates a priori geochemical knowledge.

In this contribution, we present results from an internally consistent thermochemical model of the Superior craton region which comprises the nucleus of the Canadian Shield and has seen modification from processes of localized ductile reworking at its northeastern and northwestern margins, hotspot passage, impingement of the midcontinent rift, and orogenesis along its margins. Combining surface-wave data, body-wave data, absolute elevation (local and dynamic), geoid height, surface heat flow data, gravity anomalies, along with petrological information, this model will directly characterize the Superior craton's origin and tectonic evolution, providing insight into its resource potential.

KEYWORDS : superior craton, thermochemical tomography

Sr No: 79

Mapping IOCG alteration footprints in the Olympic Domain, South Australia using magnetotellurics

CORRESPONDING & PRESENTING AUTHOR:

Stephan Thiel, Geological Survey of South Australia, Australia

Kate Robertson, Geological Survey of South Australia, Australia

Wenping Jiang, Geoscience Australia, Australia

We present results of 334 ultra-wide band MT stations across an area of 100 km x 100 km in the prospective eastern Gawler Craton. The survey area is situated ~100 km south of the supergiant Olympic Dam IOCG deposit, across an area of several IOCG deposits and prospects, including Carrapateena, Oak Dam, and Khamsin. The main aim of this survey was to identify and characterise the lithospheric-scale signature of known and potentially unrecognised IOCG mineral systems and provide insight on the crustal architecture and deep processes that occur in areas that host mineralisation. Regional AusLAMP MT results have highlighted the importance of first order lithospheric architecture along craton margins, and the metasomatised Gawler Craton mantle signature.

Results from detailed 2D and 3D inversion of magnetotelluric data of the in-fill array, airborne EM measurements and geochemical analyses demonstrate a coherent view of the IOCG alteration systems in South Australia. IOCG targets are associated with discrete upper crustal and sub-vertical conductivity pathways beneath IOCG deposits and prospects spanning several kilometres in width and extending to the mid-crust. The conductive pathways align with Bouguer gravity gradients, hinting at deformation pathways along faults. New insights into the geochemical alteration patterns for IOCG mineral systems based on Canadian analogues allow an explanation for the enhanced conductivities.

KEYWORDS :   magnetotellurics, Australia, IOCG

Sr No: 80

Delineating Sulfide Mineralization using Potential Field and Petrographic Data over Western Margin of Greenstone Belt of Dhanjori basin, Eastern Singhbhum craton

CORRESPONDING & PRESENTING AUTHOR:

Ashok Kumar Gupta, Indian Institute of Technology (Indian School of Mines) Dhanabad, India

Shalivahan Srivastava, Indian Institute of Technology (Indian School of Mines) Dhanabad, India

This study presents the analysis of gravity, magnetic data along with petrographic results over the western margin of Proterozoic metavolcanics in Dhanjori basin, Eastern Singhbhum craton. 3D Inversion of any geophysical data set is one of the most efficient technique in visualizing the subsurface mineralized targets on the basis of contrasts in its physical properties. Contrasts in density and magnetic susceptibility values obtained from inversion showed the subsurface information up to a depth of ~300m with different geological domains including metabasalt +/- sulfide, dolerite, quartzite, QPC, granite and magnetite. 2.5D gravity modelling constrained with electrical resistivity tomography (ERT) data delineates two distinct

dimensions of high density and low resistivity indicative of sulfide ores at a depth of ~40m. Traces of these mineralization is also evident from reflected light photomicrographs, electron probe micro analysis (EPMA) and back scattered electron (BSE) over quartzite rocks. These petrographic study, previously published borehole and ERT results links gravity and magnetic data in delineation of possible anomalous country rocks bearing sulfide minerals and also aid in optimizing non uniqueness of potential field data.

KEYWORDS : greenstone belt, 3D inversion of potential field, sulfide mineralization

Sr No: 81

The Temagami Geophysical Anomaly, Superior Craton, Canada: Evidence for Rifting and Mineral Endowment

Ademola Adetunji, Laurentian University, Canada

CORRESPONDING & PRESENTING AUTHOR:

Ian Ferguson, University of Manitoba, Canada

The Temagami Geophysical Anomaly (TGA) is situated in the Paleoproterozoic Huronian Supergroup near the southern margin of Archean Superior craton, along strike from the Temagami Greenstone Belt, 50 km northeast of world-class metal endowment in the Sudbury Igneous Complex. It has been attributed to coincidental geophysical responses from Neoarchean iron formation and a Paleoproterozoic mafic-ultramafic intrusion. The TGA was investigated using integrated magnetotelluric, magnetic, gravity and seismic reflection datasets to define the geometry of its sources and to examine the relationship of Archean basement structure, the mafic-ultramafic intrusion, and Proterozoic rift structures.

Geophysical results reveal a strong conductor, interpreted to be iron formation, extending downwards from the Archean basement surface and enveloping the upper margin of a large magnetic, dense body at 5 km depth. The geometry is consistent with a mafic-ultramafic intrusion adjacent to greenstone rocks. Alignment of the long-axis of the intrusion with the greenstone belt suggests control on the intrusion process by the Neoarchean structures. The 60x10x10 km TGA intrusion lies within the mantle-plume, rift-related Huron-Nipissing magmatic belt and interpreted to be a member of the 2.491-2.475 Ga East Bull Lake intrusive suite. Based on this genetic relationship, it probably contributes significantly to PGE-Ni-Cu endowment of the Sudbury region. The spatial correlation of the intrusion with an overlying 20 km wide, 4.5 km deep, fault-bounded rift basin is attributed to crustal subsidence triggered by the intrusion. Seismic reflection and magnetotelluric results show that younger Huronian Supergroup rocks recorded the transition to sedimentation on a laterally-extensive passive margin.

KEYWORDS : superior craton, magmatism, rifting

Sr No: 82

SYMPOSIUM :   **J5 Cratons & Mineral Exploration**

Utilization of magnetic data from EMAG2 model to identify the structural control in concentrating base metals in the parts of Bhilwara district, Rajasthan

CORRESPONDING & PRESENTING AUTHOR:

Nikhil Kumar Baranval, National Remote Sensing Centre, India

This study presents the role of magnetic anomalies derived from Earth Magnetic Anomaly Grid (EMAG)-2 model to identify the structural control of base metal. We have derived estimated residual magnetic anomaly map from total magnetic anomaly using Gaussian high-pass filter to identify structural controls contributed in concentrating base metal. The residual and regional magnetic targets were separated at 8 km subsurface depth. In this study, we observed high magnetic anomalies surrounded by very low magnetic anomalies along the NE-SW trend in residual magnetic anomaly map. This indicates that the mineralized bodies having high magnetic response are controlled by structure elements striking in the NE-SW direction. These high magnetic anomaly zones were enriched by base metals copper, zinc, etc. confirmed from the mineralization data available in BHUKOSH developed by Geological Survey of India. The upward continuation techniques applied in residual magnetic anomaly estimated the potential field depths of the structural control in concentrating base metals between up to 300 m.

KEYWORDS :   residual magnetic anomaly, EMAG2, upward continuation

J6 Marine Geophysics

CONVENERS: Amir Haroon

Vera Schlindwein

More than 70% of the Earth surface is covered by ocean. Yet, a high percentage of the ocean or the subsurface below the seafloor remains unexplored. This session invites all contributions of marine geophysical research ranging from small to large scales aimed at characterizing various structures of the Earth's interior from water column investigations to deep mantle studies. Fields of research include, but are not limited to synthetic modelling, instrumentation, survey design, data acquisition and novel data processing, visualization, and interpretation procedures. We invite contributions from various fields of geophysical investigations including seismological, electromagnetic, geochemical, magnetic, gravity, and multi-beam surveying. A particular focus will lie on multi-disciplinary interpretation of different data sets, and multi-dimensional imaging of the Earth's interior.

Sr No: 83

Acoustic impedance inversion using well log data based on modified Alternating Direction Method of Multipliers

CORRESPONDING & PRESENTING AUTHOR:

Suman Konar, CSIR - National Geophysical Research Institute, Hyderabad, India

Maheswar Ojha, CSIR - National Geophysical Research Institute, Hyderabad, India

Kalachand Sain, Wadia Institute of Himalayan Geology, Dehradun, India

We use the modified alternating direction method of multipliers (ADMM) method to invert acoustic impedance (AI) of well log data. The proposed method incorporates amplitude compensation and inversion as a single processing step and depends on modification of the convolution between the time-variant wavelet and the hidden reflectivity. In the ADMM solving scheme, the limited memory Broyden-Fletcher-Goldfarb-Shanno (L-BFGS) algorithm and the generalized iterated-shrinkage algorithm (GISA) have been utilized to solve the relative sub-optimization problems. With the assumption that the calculated reflectivity is sparse and the addition of lp-norm ($0<p<1$) regularization in the inversion objective function, the ADMM solving method for nonconvex minimization has been improved to deal with such ill-posed and nonlinear problem. As a distributed optimization approach, ADMM could be flexible enough to search for the global minimum of the objective function. Nevertheless, the poor quality of the seismic data will lead to an unstable inversion and a deviation of the result. These negative impacts should be taken into account and eliminated by certain advanced techniques. We have investigated the performance of the method on synthetic seismic data as generated from sonic and density log, after converting both the logs from depth to time domain. This technique can be used to capture a unique AI solution without strong discontinuity. Furthermore, it is insusceptible to the quality of the input data.

KEYWORDS :   ADMM, L - BFGS, GISA

Sr No: 84

A capillary pressure-based rock physics model for saturation estimation from 4D seismic data in Sleipner field

CORRESPONDING & PRESENTING AUTHOR:

Moumita Sengupta, IIT (ISM) Dhanbad, India

Ranjana Ghosh, NGRI, Hydrabad, India

Saumen Maiti, IIT (ISM) Dhanbad, India

Understanding the effect of fluid saturation in rocks is crucial to characterize the hydrocarbon reservoir. Monitoring of fluid concentration specifically becomes challenging during a sequestration program because the objective is to understand the amount of initial fluid replaced by liquid/gas injection and identify the probability of leakage with time. Conventionally, prediction of saturation requires modelling of elastic properties of the rock by an appropriate rock physics model with an apriori assumption of either uniform or patchy type of distribution. This initial assumption is the basis of choice of rock physics model and practically there is always an additional uncertainty associated with this assumption. Therefore, discrimination between patchy and uniform type of gas distribution in the pore space is essential to predict gas saturation

accurately. Capillary pressure equilibrium theory (CPET) based on the assumption of a state of capillary equilibrium of different phases in the reservoir solves this problem to a certain extent, which is particularly useful for large elastic bounds that cause uncertainties in saturation analysis using conventional rock physics models. In this work, a practical approach based on the CPET has been used to analyse the effect of partial saturation of CO2 gas on the elastic properties of CO2-sequestered reservoir in the Sleipner field, North Sea and interpret the impedance volume obtained by inversion of 4D seismic data in terms of saturation volume. We find that the distribution of gas is uniform type at higher saturation, whereas, it is patchy at low saturation of gas.

KEYWORDS : CPET, 4D, rock physics

Sr No: 85

SYMPOSIUM :   **J6 Marine Geophysics**

Classification of lithology from downhole NMR data using machine learning technique

CORRESPONDING & PRESENTING AUTHOR:

Amrita Singh, CSIR-National Geophysical Research Institute, Hyderabad, India

Maheswar Ojha, CSIR-NGRI, Hyderabad, India

Machine learning techniques are found simple, easy and effective to process large and complex geophysical data. Here, we use machine learning techniques on downhole Nuclear magnetic resonance (NMR) logging data to map gas hydrate-bearing sediments at Hole-01A of the second Indian National Gas Hydrate Program (NGHP-02) in the Krishna-Godavari offshore basin. NMR data contain amplitude distribution with transverse relaxation time (T2) of hydrogen nuclei of the pore fluid, which depends on the fluid type, pore size and grain size distribution in the sediments. We apply unsupervised techniques Davies-Bouldin index, silhouette, k-means clustering and self-organizing map (SOM) on NMR T2 curves to obtain an optimum number of classes with a similar and unique signal shape and interpreted them in terms of lithology with depth. The optimum number of NMR classes is interpreted in terms of clay, silt, sand and pebble/gravel, which are further reconciled with other log data such as gamma ray, density, porosity, resistivity, velocity and photoelectric factor. Our results show five types of classes with lithology dominated by silty-clay and minor sand. The presence of gas hydrate is interpreted by observing an overall low amplitude T2 signal, which is due to the reduction of pore space by solid gas hydrate. The maximum concentration of gas hydrates of about 40% with an average of about 20% of the pore space estimated using NMR- and density-porosity are distributed mainly in silty-clay.

KEYWORDS : Krishna-Godavari basin, NGHP-02, NMR T2 distribution

Sr No: 86

SYMPOSIUM :   **J6 Marine Geophysics**

Estimation of porosity and gas hydrate saturation using VFSA along a 2D seismic line in Krishna Godavari basin, eastern Indian offshore

CORRESPONDING & PRESENTING AUTHOR:

Anju K Joshi, CSIR-National Geophysical Research Institute, India

Maheswar Ojha, CSIR-National Geophysical Research Institute, India

Kalachand Sain, Wadia Institute of Himalayan Geology, India

Gas hydrate saturation and porosity are the two essential parameters for characterizing a gas hydrate reservoir. Generally, porosity derived from well log data is interpolated over the seismic section for the estimation of gas hydrate saturation. Here, we propose a method to invert both porosity and gas hydrate saturation directly by inverting seismic data using the global optimization technique, known as the Very Fast Simulated Annealing (VFSA). The proposed method is first tested on well logs in the Krishna-Godavari offshore Basin. The forward problem is defined using a polynomial equation developed using impedance, water saturation, and porosity. The initial model for the water saturation is directly calculated using the three-phase Biot equation; the initial model for porosity is calculated using the interpolation of available porosity logs. The VFSA selects porosity and gas hydrate saturation (1 - water saturation) in the model space by following a cooling schedule and finally yields the best fit model by minimizing the misfit between the observed and predicted seismic data. The probability density function of the parameters and the correlation matrix between the model parameters (gas hydrate saturation and porosity) are also calculated to determine the associated uncertainty. Inversion results show that the approach used in this study is robust and can be efficiently used for the prediction of porosity and gas hydrate saturation from seismic data.

KEYWORDS :   VFSA, porosity, gas hydrate saturation

Sr No: 87

SYMPOSIUM :   **J6 Marine Geophysics**

Estimation of fracture porosity and gas hydrate saturations in the Krishna Godavari offshore basin, India

CORRESPONDING & PRESENTING AUTHOR:

Laxmi Pandey, AcSIR, CSIR-NGRI, India

Maheswar Ojha, CSIR-NGRI, India

Kalachand Sain, WIHG, India

The study aims to investigate the effect of fractures in prospective gas hydrate zones in the Krishna-Godavari (KG) offshore basin, India. We use logging while drilling (LWD) resistivity and sonic velocity logs at Hole 22A in the KG basin acquired during the second expedition of the National Gas Hydrate Program (NGHP-02). Fracture porosity plays an important role in the characterization of gas hydrate-filled vertical fractures and estimation of gas hydrate saturations. Herein, we propose a joint analysis of resistivity and velocity logs to estimate the appropriate fracture porosity. A modified three-phase Biot type equation for velocity and Archie's empirical equation for resistivity are used to model the isotropic media. The transverse isotropic theory for laminated media is used in the anisotropic analysis of gas hydrate reservoir. The results from joint analysis of resistivity and velocity logs demonstrate the fracture porosity of 7.5% at Hole NGHP-02-22A. It is also found that resistivity and velocity-derived average saturations are 12 and 14% for pore-filling and 36 and 16% for fracture-filling, respectively. These estimates show a good correlation with the pressure core measurements.

KEYWORDS :   fracture porosity, gas hydrates, anisotropy

Sr No: 88

Reservoir characterisation to assess resource potential of hydrocarbon in the Gulf of Khambat, Mumbai offshore, India from seismic and well log analysis

CORRESPONDING & PRESENTING AUTHOR:

Sikha Mondal, IITISM Dhanbad & NGRI; DGH, India

Ranjana Ghosh, NGRI, India

Maheswar Ojha, NGRI, india

Saumen Maiti, IIT ISM Dhanbad, India

The Mumbai Offshore basin is known as the most productive zone among all the petroliferous basins of India after major oil and gas fields were discovered here. However, the Gulf of Khambat situated in northern most part of the Mumbai offshore has not been explored extensively. We aim to locate potential reservoir zones among Paleocene, Eocene and Oligocene sequences in Tapti, Daman, Mahuva, Pipavav, Panna and Deccan Trap formations of the study area. We process all available well logs drilled in Block MB-OSN-2004/1 in detail and conduct petrophysical analysis by multimineral modelling, image log analysis and dipole sonic log analysis to explore hydrocarbon prospects in this area. Whenever available, relevant information from other sources like cuttings report, mud log, and other logs like resistivity data, and local knowledge about field are integrated with the petrophysical analysis study. The inferred lithology of the study area is mainly shaly-sand or shaly-limestone with porosity in the range of ~10-40%. We do well log correlation with the seismic data, joint analysis of both the data and inversion to obtain the impedance volume from the 3D seismic data. Quantitative interpretation of hydrocarbon mainly gas is calculated from the observed sonic impedance at different well locations using standard rock physics modelling. Finally, machine learning tool is used to obtain the 3D gas saturation volume using saturation obtained at well locations and 3D impedance volume. We estimate gas saturation within porous sand layers ranging from 5-60%. Development of new technology is required to exploit the reservoir commercially.

KEYWORDS :   well log analysis, seismic inversion, rock physics machine learning

Sr No: 89

Interpretation of Subsurface Structures from Seismic and Gravity Window: A Study from Krishna-Godavari Offshore Basin, India

CORRESPONDING & PRESENTING AUTHOR:

Satendra Singh, CSIR-NGRI, india

Kalachand Sain, Wadia Institute of Himalayan Geology, India

Maheswar Ojha, CSIR-NGRI, India

Krishna-Godavari (KG), a deltaic sedimentary basin, was evolved as a result of continental rifting and seafloor spreading processes during the Late Cretaceous period (140–120 Ma) between India, Antarctica and Australian plates. The thick sedimentary cover and continuous supply of sediments by the Krishna and Godavari rivers make the basin a suitable womb for hydrocarbon accumulation. The present study aims for a joint interpretation of subsurface structures in the KG offshore basin using seismic, gravity and deep well
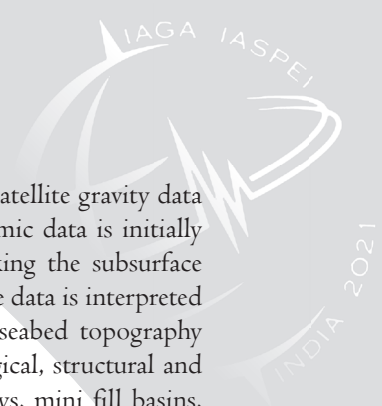
data. The time migrated 2D multi-channel seismic data acquired by CSIR-NGRI and satellite gravity data are utilized for interpreting the geological and tectonic features of the basin. The seismic data is initially conditioned using Dip Steered Median Filter (DSMF), such that noisy events masking the subsurface geology are eliminated to have a well-defined image which can be readily interpreted. The data is interpreted along the dip direction (NW-SE profiles) which shows dominating undulations in seabed topography while it is mostly flattening along the strike direction (NE-SW profiles). Many geological, structural and tectonic features such as faults, folds, horsts/grabens, channels, gas upthrusts/chimneys, mini fill basins, blanking, chaotic reflections, and Mass Transport Deposits (MTDs) are delineated along the seismic lines. The bottom simulating reflector (BSR), which is a prime marker for gas-hydrate, is also identified along the profiles. All the major reflectors are picked on the seismic sections and correlated with the lithological formations of deep well. Gravity responses and their variations along the seismic lines are calculated and modelled to ascertain the subsurface structures.

KEYWORDS : Krishna-Godavari basin, seismic, subsurface features

Sr No: 90

SYMPOSIUM : **J6 Marine Geophysics**

In-Situ Calibration of Differential Pressure Gauges on OBSIP Ocean Bottom Seismometers

CORRESPONDING & PRESENTING AUTHOR:

Gabi Laske, Scripps Institution of Oceanography, UC San Diego, USA

A standard broadband ocean bottom seismometer (OBS) package of the U.S. OBS Instrument Pool (OBSIP) carries a seismometer and a pressure sensor. The purpose of the pressure sensor is manifold and includes the capture of pressure signals not picked up by a ground motion sensor, but also for purposes of correcting the seismograms for unwanted signals generated in the water column. The instrument response of the widely used Cox-Webb DPG remains poorly known, and can vary by individual sensor.

Efforts have been under way to construct and test DPG responses in the laboratory. But the sensitivity and long-period response are difficult to calibrate as they vary with temperature and pressure. Here, we present a way to test the response for each individual sensor and deployment in situ in the ocean. This test requires a relatively minimal and inexpensive modification to the OBS instrument frame that allows a drop of the DPG by 3 inches after the OBS package settled and the DPG equilibrated on the seafloor. The seismic signal generated by this drop is then analyzed in the laboratory upon retrieval of the data.

The results compare favorably with calibrations estimated independently through post-deployment data analyses of other signals such as Earth tides and the signals from large teleseismic earthquakes. Our study demonstrates that observed response functions can deviate from the nominal response by a factor of two or greater with regards to both the sensitivity and the time constant.

KEYWORDS : ocean bottom seismometers; ocean pressure sensors; sensor calibration

Sr No: 91

Successfully proven advancements in autonomous Ocean Bottom Seismometers: Güralp Aquarius

CORRESPONDING & PRESENTING AUTHOR:

Will Reis, Güralp Systems Ltd, UK

Increasing broadband seismic station density in marine environments is crucial for understanding local and distant seismic activity. The recently engineered and successfully commercially deployed Güralp Aquarius OBS system overcomes technical, logistical and financial barriers and redefines boundaries for offshore seismic research.

Aquarius is a portable autonomous OBS combining a broadband seismometer with wireless acoustic communication while deployed at depths of up to 6000m for up to 21 months. Communication on demand allows operators to retrieve specific data for download during deployment period, while a continuous record is preserved on the OBS for full analysis after retrieval. Possible surface acoustic modem platforms vary from fixed buoys with satellite communication, passing ships of opportunity, wave-gliders or small private boats for manned visits. Modular design allows configuration of additional hydrophone and pressure gauge sensors with acoustic modem variations available to suit operator priorities.

Well-proven digital feedback control allows Aquarius to operate at any angle, thereby reducing landing site risks while excluding noise inherently associated with gimbal-controlled levelling systems. Acoustic communication during installation allows operators to assess the quality of the landing site before committing or repositioning. During recovery, ultra-fast recharging facilitates rapid turnaround times for re-deployment (1-hour charge per month deployment) without returning to port.

Further avenues are being explored to adapt Aquarius technology for longer-term autonomous deployments, while current standard configurations continue to be deployed in major ocean basins as part of individual projects and national pools.

KEYWORDS : seismometer, OBS, seismology

Sr No: 92

Offshore–onshore resistivity imaging of freshwater using a controlled source electromagnetic method

CORRESPONDING & PRESENTING AUTHOR:

Keiichi Ishizu, Tokyo Institute of Technology, Japan

Yasuo Ogawa, Tokyo Institute of Technology, Japan

Coastal freshwater provides a water source for more than one billion people living in coastal regions. For sustainable groundwater management in coastal areas, an understanding of the freshwater distribution is necessary. The freshwater distribution in a coastal area can be across the landward and seaward sides. Offshore–onshore seamless mapping of freshwater helps us to gain a comprehensive understanding of

the freshwater distribution in coastal areas. Resistivity imaging using electromagnetic methods has been used to reveal the freshwater distribution in coastal areas because resistivity provides information on porosity and porewater salinity. We used a controlled source electromagnetic (CSEM) method for offshore–onshore seamless resistivity imaging of freshwater at a depth range of 0–500 m below the seafloor. Our CSEM method consists of onshore transmitters and onshore–offshore receivers. We conducted a feasibility study to investigate the ability of the CSEM method for offshore–onshore seamless resistivity imaging of freshwater in a coastal area. We found that the method could image the resistivity distribution of freshwater located at a depth of 500 m below the seafloor. The test results also showed that the detectability of freshwater was high enough at all sea depths between 10 m and 100 m, which is a typical range in coastal areas. These numerical test results imply that the proposed CSEM method is a promising technique for offshore–onshore seamless resistivity imaging of freshwater in coastal areas.

KEYWORDS :   CSEM, freshwater, coastal regions

Sr No: 93

SYMPOSIUM :   **J6 Marine Geophysics**

Crustal Structure of the nascent Fonualei Rift and Spreading Center, Lau basin, derived from Magnetotelluric Measurements

CORRESPONDING & PRESENTING AUTHOR:

Gesa Franz, GEOMAR Helmholtz Centre for Ocean Research Kiel, Germany

Marion Jegen, GEOMAR Helmholtz Centre for Ocean Research Kiel, Germany

Anne Neska, Polish Academy of Science, Germany

Anna Avdeeva, independent consultant, Germany

Florian Schmid, GEOMAR Helmholtz Centre for Ocean Research Kiel, Germany

Heidrun Kopp, GEOMAR Helmholtz Centre for Ocean Research Kiel, Germany

Mark Hannington, GEOMAR Helmholtz Centre for Ocean Research Kiel, Germany

The greater area of the Lau Basin consists of a mosaic of microplates with various spreading centers and arc rifts. Repeated crustal recycling and addition of volatiles and metals in this tectonic setting leads to fertilization of the crust. This assimilation of mineral deposits is associated with building blocks of continental crust, and is thus an important setting to study crustal growth on Earth. During research cruise SO267 in 2018/2019, multi method geophysical and geological data were acquired on the newly formed Niuafo'ou microplate in the Lau Basin to study the links of rifting, magmatism and hydrothermal circulation in the early evolution of back arc spreading. The geophysical data encompass refraction- and reflection seismic, seismological, backscatter, gravity, magnetic and magnetotelluric data. Here we present a first electrical conductivity model derived from 3D inversion of marine magnetotelluric (MT) data. Electrical conductivity is a key proxy for imaging hydrothermal circulation and magmatic processes, since both processes effect the bulk electrical conductivity strongly. Our model exhibits three larger scale crustal conductivity anomalies. Based on the electrical conductivity model alone, we cannot discern whether the anomalies are caused by hydrothermal activity through pathways created by tectonic spreading or by melt accumulation caused by magmatic processes. However, a spatial correlation of our major conductivity anomaly with a seismicity cluster and a comparison with seismic velocity and backscatter data allows us to hypothesizeinfer about the geodynamic processes acting in the region. Our study documents the benefit of integrating different geophysical methods to understand rift arc evolution.

KEYWORDS :   spreading center, marine magnetotellurics, Lau basin

Sr No: 94

Seamount subduction and event locations relative to a reflection interface at Off-Ibaraki region, southeastern part of Japan

Kimihiro Mochizuki1

CORRESPONDING & PRESENTING AUTHOR:

Shinji Yoneshima, Earthquake Research Institute, University of Tokyo, Japan
Kimihiro Mochizuki, Earthquake Research Institute, University of Tokyo, Japan

A subducting seamount is supposed to cause strong stress heterogeneity to its circumstances in subduction zones, likely generating small earthquakes. The understanding of the seismicity might be one key to understand the dynamic process of the subducting seamount. However, the seismicity around the subducting seamount tends to be quite low, thus the details of the seismicity is still unveiled. Unexpectedly, at off-Ibaraki region located southeastern part of Japan, where a seamount subducts, the seismicity became quite active after the 2011 Tohoku-oki earthquake. We performed a double difference event location analysis for an unprecedented number of over 20, 000 events recorded from 2010 to 2011 during the experiment period. The event distribution result exhibited a large number of events in the oceanic plate below the plate boundary. We proceeded to the further investigation since the event location relative to the plate boundary might be still erroneous partly due to a complex topology of the plate boundary around the seamount. We identified vertically aligned sequence of events ranging from about 8 km to 25 km deep around the subducting seamount. From a common station trace gather, highly coherent late arrivals after P and S arrivals were identified at some depth range, which is a reflected wave at some layer interfaces. We will show the analysis result including an example of the late arrivals and discuss the relative location of these events around the seamount whether the seismicity is active above, along, or below the plate boundary.

KEYWORDS : ocean bottom seismometer, event location, seamount subduction

Sr No: 95

Improved Seismic Monitoring with OBS Deployment in the Arctic: A Pilot Study from Offshore Western Svalbard

Zeinab Jeddi, University of Bergen, Norway
Lars Ottemoller, University of Bergen, Norway

CORRESPONDING & PRESENTING AUTHOR:

Mathilde Sorensen, University of Bergen, Norway
Sara Rezaei, University of Bergen, Norway
Steven Gibbons, Norwegian Geotechnical Institute, Norway
Marte Stromme, University of Bergen, Norway
Peter Voss, Geological Survey of Denmark and Greenland, GEUS, Denmark
Trine Dahljensen, Geological Survey of Denmark and Greenland, GEUS, Denmark

The mid-ocean ridge system is the main source of earthquakes within the Arctic region. The earthquakes are recorded on the permanent land-based stations in the region, although smaller earthquakes remain undetected. In this study, we make use of three Ocean Bottom Seismographs (OBSs) that were deployed
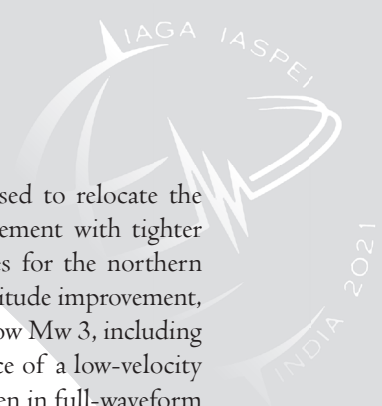
offshore western Svalbard, along the spreading ridges. The OBS arrival times were used to relocate the regional seismicity, using a Bayesian approach, which resulted in a significant improvement with tighter clustering around the spreading ridge. We also extended the regional magnitude scales for the northern Atlantic region for OBSs, by computing site correction terms. Besides location and magnitude improvement, the OBS network was able to detect hundreds of earthquakes, mostly with magnitude below Mw 3, including a swarm activity at the Molloy Deep. Our offshore observations provide further evidence of a low-velocity anomaly offshore Svalbard, at the northern tip of Knipovich ridge that was previously seen in full-waveform inversion. We conclude that even a single permanent OBS near the ridge would make a significant difference to earthquake catalogs and their interpretation.

KEYWORDS : OBS, seismicity, arctic

Sr No: 96

SYMPOSIUM : **J6 Marine Geophysics**

Structure and evolution of oceanic core complexes at the ultraslow Southwest Indian Ridge: insights from three deep-sea surveys

PRESENTING AUTHOR:
Fei Zhou, IPGP, France

CORRESPONDING AUTHOR:
Jerome Dyment, IPGP, France

Oceanic core complexes (OCCs) and detachment faults (DFs) play a key role in crustal accretion at slow and ultraslow spreading centers, resulting in asymmetric flanks, corrugated seafloor, and mantle rocks exhumation. However, factors controlling the structure and evolution of OCCs are still poorly understood at ultraslow spreading ridges. We investigate three OCCs of the Southwest Indian Ridge (SWIR) with high-resolution deep-sea bathymetric and magnetic data. The intensity of magnetic anomalies, amount of extrusive basalt, and therefore degree of magmatism decrease from Yuhuang (49.25°E) to Dragon Flag (49.65°E) to Junhui (51.75°E) OCCs. Conversely, the abundance of serpentinite, evidence of tectonics (e.g., mass wasting), and footwall rotation (measured by the magnetization vector inclination) increase. Combined with results from the amagmatic Easternmost SWIR, our study shows that different degrees of magmatism result in different characters and evolutions of the OCCs and DFs. Their variability therefore offers a mean to approach the heterogeneous along-axis magma supply at ultraslow spreading centers.

KEYWORDS : oceanic core complex, magmatism, ultraslow spreading center

Sr No: 97

Insights on the Indian Ocean Geoid and Gravity Lows: Implications for gradual density heterogeneity

PRESENTING AUTHOR:

Akash Debnath, CSIR-National Geophysical Research Institute, India

CORRESPONDING AUTHOR:

Shib Sankar Ganguli, CSIR-National Geophysical Research Institute, India

Bhaskar Illa, CSIR-National Geophysical Research Institute, India

Prakash Kumar, CSIR-National Geophysical Research Institute, India

In the south of the Indian subcontinent, remarkable geoid and gravity lows on Earth were noticed beneath the Indian Ocean. Hitherto, no general consensus has been reached to explain the origin of such huge geoid and gravity lows in the area. Numerous theories have been postulated to elucidate this negative anomaly including structural undulation in the core-mantle boundary, Mesozoic subducted slab graveyard in the lower mantle, hot mid-mantle anomaly together with cold substance beneath 660 km, low-density material originating from upper mantle (below 1000 km), etc. We took the opportunity to investigate the largest negative anomaly by combining gravity and global seismic tomography models and inferences were drawn. Gravity models of the crust and upper mantle structures were constructed to evaluate the subsurface structures, density heterogeneity, and isostatic state of the region. Scaling spectral inversion of the gravity data indicates that the source lies between 150 to 1000 km. Investigation of GyPSUM and GAP-P4, the global tomography models, suggest a prevalence of low-velocity zone corresponding to the source depth range akin to gravity-derived source depths. Based on the joint analysis of seismic and gravity, we conclude that the source of the largest anomaly attributed to gradual density heterogeneity corresponding to the depth ranging from 150 km to a depth down to 1000 km.

KEYWORDS :   Indian Ocean geoid low, upper mantle structure, density

J9 Analogue Data for the Future: Preservation and Present-Day Utilization of Historical Data in the Geosciences

CONVENERS: Josep Batlló Ortiz

Edward Cliver

Justin Mabie

Anna Skorkina

Masahito Nosé

Started on the second part of the 19th century, the 20th century brought several fold increase in recorded data in the geosciences. These analogue records, largely consisting of seismograms and magnetograms form the basis of climatology and scientific discovery and study in their related fields.

Maintenance of a complete time series of environmental data is necessary for the comprehensive study of a changing world. Availability and usability of old analogue records are needed for understanding of our Earth systems. Historic environmental data in analogue form are, many times, contained in unique formats, difficult to interpret, and at risk of loss. A comprehensive effort on historical data preservation and modernization is needed. Data discovery, availability, interpretation and use for scientific study are necessary for understanding of the changing Earth and extreme events. The sharing of the IASPEI and IAGA accumulated experience is an important step toward comprehensive historical data preservation and modernization. This joint-session symposium welcomes contributions on:

Locating, assessing, preserving, and disseminating historical data mainly obtained from analogue magnetograms and seismograms.

Solutions for batch digitization, recognition and conversion of analog data into digital numerical arrays.

Methodologies and study cases using these historical data to advance our understanding of the Earth system.

Sr No: 98

Digitized Legacy Data: Original Paper v. Microform Copies

CORRESPONDING & PRESENTING AUTHOR:

Thomas Lee, Harvard University, USA

Miaki Ishii, Harvard University, USA

Paul Okubo, University of Hawaii at Manoa, USA

From the beginning of modern seismology, until the dawn of the digital era at the end of the 20th century, nearly all observations of ground movements were recorded on large sheets of paper. Many of these records were subsequently copied onto microforms. Today, there still exist large archives of data on both paper and microform media, and it is highly likely that there exists overlap between these collections. Under the assumption that the microform copies are exact duplicates of the original recordings, holders of paper collections may come under pressure to discard these bulky records in order to use the storage space for other purposes. However, before an informed decision can be made, it is necessary to understand differences between seismic data digitized from microfiche as opposed to from the original paper.

While seismic data on microforms can generally be recovered similarly to that on paper, we undertake a detailed comparison between corresponding records to note the existence of important differences. These arise mainly from distortion of the images, and can give rise to inaccuracies in both the timing of records and in the recovery of accurate waveforms from large amplitude traces – issues that can lead to misinterpretation. Therefore, when decisions regarding the allocation of resources for legacy data preservation efforts are made, it is crucial that the larger size and weight of the original paper records are balanced with the generally higher fidelity of data recoverable from these "master" copies of records.

Sr No: 99

TIITBA GUI for digital historical seismograms vectorization, analysis, and corrections: Case study of the 11/1/1928 (M6.3) Parral, Mexico earthquake.

CORRESPONDING & PRESENTING AUTHOR:

Raul Daniel Corona Fernandez, Earth Sciences Postgraduate, UNAM, Namibia

Miguel Santoyo, Institute of Geophysics, UNAM, Namibia

The Mexico's legacy smoked paper and ink on white paper seismograms, have been recently classified and adequately stored at the Earth-Sciences library of the UNAM University, under the SISMOMex project managed by the National Seismological Service of Mexico (SSN). These seismograms, most of them recorded on Wiechert Seismographs, have significant issues that make them difficult to be vectorized: in most of them time marks among the traces are misaligned, in-homogeneous smoking densities on the paper, unequal distance between traces, among others.
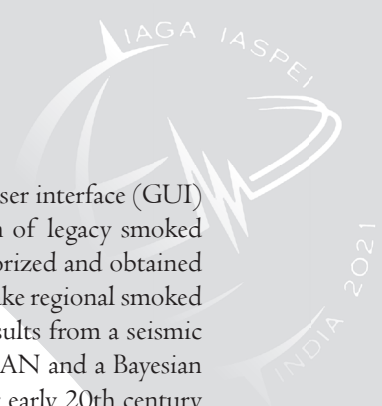
In this work we present TIITBA, a new portable open-source multi-platform graphical user interface (GUI) coded on Python3, specifically developed for the vectorization, analysis and correction of legacy smoked paper seismograms. Also, we present a case study application where we successfully vectorized and obtained the evenly ground motion time-series of the 11/1/1928 (M6.3) Parral, Mexico earthquake regional smoked paper seismograms recorded by the SSN stations at that time. Finally, we present the results from a seismic source analysis based on these corrected time-series, a hypocenter relocation using SEISAN and a Bayesian inversion relocation, and the advantages of using a multi-platform software for studying early 20th century recorded seismicity on smoked paper.

KEYWORDS : legacy seismograms, vectorization tool, historical earthquake re-analisys

Sr No: 100

Preservation and Digitization of Analog Soviet Peaceful Nuclear Explosion Seismograms

Alexei Malovichko, Geophysical Survey Rusian Academy of Sciences, Russia
Yuri Vinogradov, Geophysical Survey Rusian Academy of Sciences, Russia
Pavel Butyrin, Geophysical Survey Rusian Academy of Sciences, Russia
Ruslan Dyagilev, Geophysical Survey Rusian Academy of Sciences, Russia

CORRESPONDING & PRESENTING AUTHOR:
Kevin Mackey, Michigan State University, USA
Daniel Burk, Michigan State University, USA
Kaitlynn Burkhard, Michigan State University,USA
Chris Witte, Michigan State University, USA
Brandi Wheeler, Michigan State University,USA
Anna Dobrynina, Geophysical Survey Rusian Academy of Sciences, Russia

The Geophysical Survey of the Russian Academy of Sciences and Michigan State University are working to recover, preserve, scan, and digitize the historic seismograms of Soviet Peaceful Nuclear Explosions (PNEs). The Soviet Union detonated 122 PNEs from the mid-1960s through the late 1980s. The PNEs were conducted in a wide range of geologic settings and geographic locations, thus representing a unique data set for geophysical studies. These explosions were well recorded by the regional seismic networks, where thousands of seismograms are still retained. We are indexing these irreplaceable legacy analog seismograms and preserving them against loss for future generations by generating high resolution scans of the seismograms and digitizing them for analysis. Most seismograms are from short period SKM instruments and long period SKD, and when combined with the correct station calibration information, the digitization process accurately recovers ground motion signals to at least 5 Hz.

KEYWORDS : explosion, seismogram, digitization

Sr No: 101

Digital Preservation of Analogue Seismograms and Other Documents at Institut Cartogràfic i Geològic de Catalunya (ICGC)

CORRESPONDING & PRESENTING AUTHOR:

Josep Batlló, Institut Cartogràfic i Geològic de Catalunya – ICGC, Spain

Antonio Villaseñor, Instituto de Ciencias del Mar (ICM-CSIC), Spain

Jose Antonio Jara, Institut Cartogràfic i Geològic de Catalunya, Spain

Maite Merino, Observatori Fabra – RACAB, Spain

German Sole, Observatori de l'Ebre, Spain

Judith Unamuno, Ad-Hoc Synectic Systems, Spain

Catalonia, in the NE of the Iberian Peninsula, has a long tradition on seismic recording. The first seismic station in this region, EBR, was installed in 1904. The second one, FBR, started in 1906. Both keep their seismograms and a large amount of complementary information. Since 1984, the Catalan seismic network, presently managed by the Institut Cartogràfic i Geològic de Catalunya (ICGC), was deployed. Analog recording on thermal paper was used up to the end of the XX Century. Altogether, these seismic stations have been generating and preserving a large number of seismograms recorded in analog records (smoke, ink and thermal paper, analog tapes, etc.) and related documents (station notebooks, seismic bulletins, correspondence, etc.). To preserve these records and documents for the future, a campaign to scan them as images was undertaken years ago. At present, around seventy thousand seismograms have been scanned as well as several thousands of pages of bulletins and other records. Access to these data (seismograms, bulletins, etc.) can be obtained at the ICGC website. We show the present status of the project, the adopted strategies for scanning, classification and dissemination of the acquired data and future planning.

Sr No: 102

Digital Archiving of Bromide Paper Records of Ground Tilt Observed in Kii Peninsula, Japan

CORRESPONDING & PRESENTING AUTHOR:

Yasuyuki Kano, University of Tokyo, Japan

Tilt data recorded at two observatories in the Kii Peninsula, southwest Japan are digitally archived. The observatories have been operated by the Disaster Prevention Research Institute, Kyoto University. At Kishu and Yura observatories, ground tilt was recorded on bromide (light-sensitive) papers until at least 1974. The bromide records are stored at the Abuyama Observatory at Kyoto University. At the Kishu observatory, horizontal-pendulum tiltmeters were installed in 1947. The original tilt records until at least 1974 were drawn on bromide papers with a length of 30 cm and height of 8.5 cm, and the recording speed was about 0.2 cm/h. The observation period, as well as note for change in recording speed and the occurrence date of

the earthquakes, was recorded on the back of the paper. The records at Kishu observatory were investigated to detect possible slow slip event beneath the Kii Peninsula in 1973, which is a good example of reexamination of historical records based on modern knowledge of seismology. An opensource software, Omeka, is used to build the archive. The development costs and need for technical knowledge for implementation of the archive are reduced by introducing Omeka. Digital images of bromide records and metadata for each record are registered to Omeka. The place of observatory and time period of observation is linked to each image, which help to find targeted record. Since the images published in the archive are compliant to International Image Interoperability Framework (IIIF), users can display or process the records using any IIIF-compliant viewer.

KEYWORDS : ground tilt, bromide paper, IIIF

Sr No: 103

SYMPOSIUM : **J9 Analogue Data for the Future: Preservation and Present-Day Utilization of Historical Data in the Geosciences**

Observatori Fabra available data and documentation

CORRESPONDING & PRESENTING AUTHOR:

Maria Teresa Merino, Observatori Fabra (RACAB), Spain

Josep Batlló, Institut Cartogràfic i Geològic de Catalunya (ICGC), Spain

Jose Antonio Jara, Institut Cartogràfic i Geològic de Catalunya (ICGC), Spain

Antonio Villaseñor, Institute of Marine Sciences (ICM-CSIC), Spain

Judith Unamuno, Adhoc Synectic Systems, S.A., Spain

Fabra Observatory has been devoted to astronomical, metereological and seismological observations and studies since 1904. Seismic observations have been maintained active since 1906, including instrumental registers and macroseismic data collected mainly from eastern Spain. Its historical archive includes seismograms and complementary documentation such as manuscript and printed butlletins, registers and station notebooks, scientific and divulgative articles in journals and periodicals, letters and scientific correspondence, printed publications from many other institutions, etc. Almost all seismic instruments ever used are conserved in its museum or in use. Besides, it holds regular courses, conferences, scholar visits, and many other divulgation activities.

We have performed record inventories, restorations, studies and scannings to preserve, use and share as much of our scientific heritage as possible with the inestimable advice, help and support from other particular and institutions. Extense summaries of our patrimony and some of those projects up to that date were already presented in the past. Since then, we have significantly increased and improved the detailed inventories, the percentage and diversity of scanned analog seismograms and documentation, and the amount of them that we provide freely from finished and ongoing projects to the scientific community and general public.

Here we aim to expose in detail the current status and projects related to the available analog seismograms and documentation of the seismic section of Observatori Fabra. We present these to detail to a potentially interested audience the available documents and data with their respective explanations and instructions to be accessed and used.

KEYWORDS : analogue records, preservation, digitization

Sr No: 104

Historical data on the Earth's magnetic field for research on magnetosphere physics

CORRESPONDING & PRESENTING AUTHOR:

Nataliya Sergeyeva, Geophysical Center of the Russian Academy of Sciences, Russia

Alexander Zaitsev, Pushkov Institute of Terrestrial Magnetism, Ionosphere and Radio Wave Propagation, Russian Academy of Sciences & Geophysical Center of the Russian Academy of Sciences, Russia

Valery Petrov, Pushkov Institute of Terrestrial Magnetism, Ionosphere and Radio Wave Propagation, Russian Academy of Sciences, Russia

Konstantin Kanonidi, Pushkov Institute of Terrestrial Magnetism, Ionosphere and Radio Wave Propagation, Russian Academy of Sciences, Russia

Ludmila Zabarinskaya, Geophysical Center of the Russian Academy of Sciences, Russia

Dmitry Kudin, Geophysical Center of the Russian Academy of Sciences, Russia

Michael Nisilevich, Geophysical Center of the Russian Academy of Sciences, Russia

Aibulat Khafizov, Geophysical Center of the Russian Academy of Sciences, Russia

Data on the magnetic field variations are the most valuable material for scientific and applied research in magnetosphere physics. Since 1957, WDC for STP collects geomagnetic observational data and provides free access to them. The Center's repository includes digital images of magnetograms, minute, hourly and annual values of field elements, geomagnetic indices, catalogues of magnetic storms and field pulsations. Long data series are created by retrospective supplementation with historical data converted into electronic form. All data are published on website in the public domain. A relational online database "Geomagnetism" containing minute, hour and K-index values functions in WDC http://stp.wdcb.ru/index.php. A simple user-friendly interface is provided for custom query and data extraction.

IZMIRAN data is a significant contribution to WDC funds. In 1973, according to the project "Geomagnetic Meridian 145°", network of magnetometers was installed from Heiss Island, across the Kara Sea, Yamal, Western Siberia and Kazakhstan to India. Analog data from these magnetometers for 1973-1992 collected at IZMIRAN are now stored as microfilms in WDC.

In 1980-1985 IZMRAN, having equipped the observatories with digital magnetometers began to accumulate data. As a result, the base of digital data of 22 Russian observatories for 1983-2000 was formed on CD-ROM become available now at www.cosmos.ru/magbase/ and on the WDC website. Since 2009 IZMIRAN has been working on the renovation of the "Geomagnetic Meridian 145°".
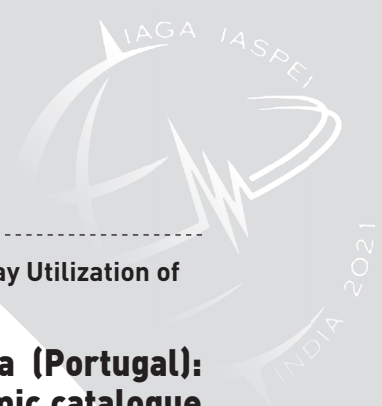
Sr No: 105

The first year of the instrumental seismology in Coimbra (Portugal): revisiting the Milne records for the year 1904 and the seismic catalogue updating.

CORRESPONDING & PRESENTING AUTHOR:

Ana Gomes, CITEUC/University of Coimbra, Potugal

Paulo Ribeiro, CITEUC, Portugal

Fernando Lopes, CITEUC, Portugal

Fernando Figueiredo, CITEUC, Portugal

Josep Batlló, Institut Cartogràfic i Geològic de Catalunya, Spain

The beginning of instrumental seismology in Portugal appears to date back to the end of the 19th century with the installation (circa 1896) of an Angot seismometer at the Meteorological and Magnetic Observatory of the University of Coimbra (OMMUC). However, it was only in May 1903, with the installation of a Milne horizontal E-W pendulum, that the seismic recordings started on a regular basis in Coimbra. Until 1909 in Portugal operated only two seismic stations, one on the mainland (COI) and the other in the Azores archipelago. At that time, the COI seismic station was the most westerly location on the European continent where telluric events were recorded.

The publication of the COI seismic data started in the international catalogue of the International Seismological Association (ISA) with data for the year 1904. The analysis of the ISA's catalogue for the year 1904 showed that the international seismic network had around 139 stations. For that year, the ISA catalogue presents data for 32 major earthquakes, but only 13 have data from the COI seismic station. The meticulous revisitation of the Milne seismograms from the COI station allowed the identification of 11 more events presented in the ISA catalogue, meaning that 75% of the 32 reported earthquakes (24 events) were recorded in Coimbra.

These preliminary results reinforce the need of revisiting and reanalysis old seismograms in the updating knowledge of the seismic activity recorded by the Coimbra station and, in this way, in the enrichment of the World seismic catalogues.

KEYWORDS :   revesiting old seismograms, coimbra 1904 records

Sr No: 106

Preservation of Analogue Data for Nuclear Explosions

CORRESPONDING & PRESENTING AUTHOR:

Victoria Oancea, Leidos, USA

Yu Long Kung, Leidos, USA

Paul Piraino, Leidos, USA

John Murphy, Leidos, USA

Benjamin Kohl, Leidos, USA

Mihaela Popa, NIEP, Berlin

Daniel Paulescu, NIEP, Berlin

Liliya Dimitrova, NIGGG, Bulgaria

Maria Theresia Apoloner, ZAMG, Austria

Ion Ilies, IGS, USA

The purpose of the project is to identify and rescue the analogue nuclear explosion time-series recordings that have been archived in four national institutes in Central and Eastern Europe: ZAMG – Austria, NIGGG – Bulgaria, IGS – Republic of Moldova and NIEP – Romania. The archives cover the entire nuclear explosion era and contain recordings from 78 continually operational stations. Most of the nuclear explosions occurred before digital data recording became common. The analogue paper recordings suffer progressive degradation which is resulting in data loss with time, so their rescue is an urgent task for the community. Inventories of nuclear explosion recordings are being compiled by each institution, based on their national bulletins and seismic catalogues, then recordings are identified in the seismogram archives. These recordings are scanned with high resolution and stored as image files in a data repository. For each scanned recording, a comprehensive set of metadata is prepared, including detailed information on station, instrument and paper recording, as collected from old station books, national catalogues, instrument documentation, and technical publications of the time. Our data rescue project is based on a process of inventory, identification, scanning, and aggregation of metadata and data quality control, followed by collecting the scans and metadata into a common repository to prevent potential loss of digital information. This data set can be converted to digital time-series in the future, allowing the application of modern signal-processing techniques.

KEYWORDS : nuclear explosions, scanning, metadata

Sr No: 107

Digitization of Japanese historical analogue magnetograms – sampling 1-minute and 7.5-second values from the scanned images

Norimichi Mashiko, Japan Meteorological Agency, Japan

CORRESPONDING & PRESENTING AUTHOR:

Shingo Nagamachi, Japan Meteorological Agency, Japan

Kenji Morinaga, Japan Meteorological Agency, Japan

Masahito Nose, Nagoya University, Japan

Japan Meteorological Agency operates magnetic observatories that have as long histories as dating back to 1913 (Kakioka), 1952 (Memambetsu) and 1958 (Kanoya). Their magnetic data with a sampling rate of 1-minute or higher exist for the period posterior to 1976 (Kakioka) or 1985 (Memambetsu and Kanoya). For the earlier periods, however, their numerical data are available only in the form of hourly value, having been manually extracted from the original analogue magnetograms recorded on photographic papers.

At Kakioka Magnetic Observatory (KMO) a project has been under way for years to digitize the historical magnetograms at higher time resolutions (1 minute and 7.5 seconds) by reading the lines of variation record in their digital images scanned at 600dpi. In order to facilitate the tracing of the lines, both automated and manual tools have been developed. For successful reading of quiet-time magnetograms the automated tool
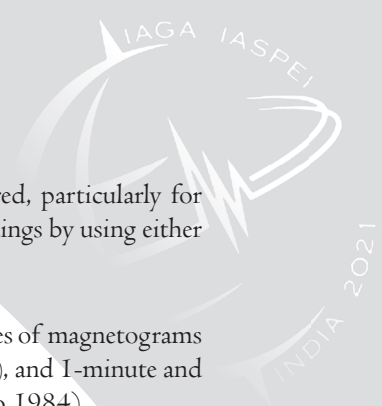
can be simply applied, but otherwise, some elaboration with the manual tool is required, particularly for those involving extreme phenomena like the storm. We present different cases of our readings by using either tool and discuss technical problems we have come across as well as the project outlook.

The deliverables so far at the KMO official data service webpage include: the scanned images of magnetograms for Kakioka (1924 to 1983), Memambetsu (1966 to 1984) and Kanoya (1967 to 1984), and 1-minute and 7.5-second values for Kakioka (1956 to 1983), and Memambetsu and Kanoya (1971 to 1984).

KEYWORDS : digitization, magnetogram, automation

Sr No: 108

SYMPOSIUM : **J9 Analogue Data for the Future: Preservation and Present-Day Utilization of Historical Data in the Geosciences**

Saving Our Seismograms: Successes, Challenges and a Call for Action (by invitation)

CORRESPONDING & PRESENTING AUTHOR:

Allison Bent, Natural Resources Canada, Canada

Lorraine Hwang, University of California, Davis,USA

Peggy Hellweg, University of California, Berkeley, USA

Analog seismograms on paper, film, tape and other media, spanning more than century of seismological recording, comprise a vast and largely untapped data source that is increasingly at risk. Although many seismograms have been lost to natural causes as well as willful destruction, there are still many millions of records in existence. All are at risk from deterioration and large numbers from pressures related to storage space and its associated costs. Many of these data sets are difficult to access and innovative approaches are required to perform any type of modern seismic analysis on them. To unlock their potential, these records and their associated metadata must be scanned and digitized. There have been a number of success stories in this regard at an institutional level but others remain overwhelmed by the task. Until recently, there has been little coordinated effort on a larger scale to develop strategies for preservation, standards and data sharing. With the development of an inventory database now underway, a survey regarding collections and associated metadata, and workshops and discussion groups bringing together interested seismologists, progress is being made. Suggested solutions will be raised for further discussion. Digitized legacy seismograms have the potential to enable discoveries in many fields. These include not only seismotectonics and seismic hazard, but also Earth structure, induced seismicity, ambient noise, tsunamis, landslide, volcanoes and effects associated with climate change. As this data set is rediscovered, researchers have successfully adapted and applied techniques, such as machine learning, developed for use with digital data.

KEYWORDS : seismograms, legacy

Sr No: 109

Metadata for FAIR Legacy Seismic Data

Tim Ahern, IRIS Emeritus

CORRESPONDING & PRESENTING AUTHOR:
Lorraine Hwang, UC Davis, USA

Efforts to preserve analog seismic data and make them available digitally are underway at a number of institutions world-wide. While these preservation efforts provide leadership in best practices in conservation, imaging, and vectorization, community discussions have begun on standards and how the collections can meet FAIR data principles. That these data be Findable, Accessible, Interoperable, and Reusable provides guidance for data management and stewardship in the modern digital ecosystem allowing centers managing these products to develop uniform tools for discovery and return legacy data in formats accompanied with metadata to ensure their usability. Establishing standards before significant work begins will help to ensure continuity and consistency in data preservation projects, high-quality products, and comprehensive capture of key information.

A focus of 2019 Securing Legacy Seismic Data to Enable Future Discoveries held September 18-19, 2019 in Albuquerque, New Mexico was to understand its preservation lifecycle and research uses and provide feedback on the proposed core metadata for legacy data preservation and use. Subsequently, the international community was surveyed on the list of metadata elements revised by workshop participants. Elements were grouped into 6 broad categories that parameterized the data: 1) Time of Data, 2) Station/Channel, 3) Sensor, 4) Recording System, 5) Image File, and 6) Other. Respondents were asked whether each should be Required, Recommended, Optional, or not required. These metadata elements and survey results will be presented. The goal is to set the stage for FAIR legacy data adoption by the larger IASPEI and FDSN communities.

KEYWORDS : legacy seismic data, metadata, FAIR

Sr No: 110

Analogue Seismographs Working in Bulgarian Sismological Stations during the Last Century

CORRESPONDING & PRESENTING AUTHOR:
Liliya Dimitrova, NIGGG – BAS, Bulgaria
Dimitar Dimitrov, NIGGG – BAS, Bulgaria
Dragomir Dragomirov, NIGGG – BAS, Bulgaria

The beginning of Bulgarian seismology dates back to 1891 when a network of correspondents for observation of felt earthquakes in Bulgaria had been formed. In 1905, a seismograph of Omorri-Boch type was installed in the first Bulgarian seismological station in the town of Sofia. During the years, the number of the seismic stations raised and at the end of 2006 the seismological network consisted of 21

analogue stations. The seismic equipment comprised a large number of displacement and velocity sensors. A large archive of seismograms on smoked paper, photo paper and ink record has accumulated in the seismic stations and in the National Institute of Geophysics, Geodesy and Geography of Bulgarian Academy of Sciences. In order to rescue the historical data, the analogue seismograms have being scanned as a first step of its prevention and modernization. This is done in the frame of several national and international projects.

The projects help to collect and reconstruct all the information about the analogue seismological equipment that was in operation at the stations during the analogue era of Bulgarian seismic network. The information is organized in a catalogue includingthe place and the time of operation, the sensitivity, the frequency range, type of recording and other parameters. Accurate information of the parameters of the recording equipment is essential for the subsequent processes of digitization and interpretation of the analog data.

KEYWORDS : analogue seismograph, bulgarian seismological stations, digitization of analogue seismograms

Sr No: 111

SYMPOSIUM : **J9 Analogue Data for the Future: Preservation and Present-Day Utilization of Historical Data in the Geosciences**

Prague-Clementinum Geomagnetic Observations from 1839 to 1926

CORRESPONDING & PRESENTING AUTHOR:
Fridrich Valach, Earth Science Institute of the Slovak Academy of Sciences, Slovakia
Pavel Hejda, Institute of Geophysics, Academy of Sciences of the Czech Republic, Czechia
Milos Revallo, Earth Science Institute of the Slovak Academy of Sciences, Slovakia

Unique geomagnetic records of observations of the geomagnetic field have been preserved in the yearbooks of observatory Clementinum in Prague. In order to make the records directly usable for the geomagnetic and space-weather community, the records had to be digitized and further processed. Our paper focuses on the horizontal intensity and declination, the first being useful to the study of geomagnetic activity, the latter having practical application also in navigation. The data processing included the identification of corrupted portions of records, as well as the conversion of raw data from bifilar magnetometers to physical units of the international system SI. The first decades also required determining or verifying the temperature coefficients of the equipment for measuring the horizontal intensity. The database of these historical observations is presented and an example of the usage of the data for the study of geomagnetic activity is shown. This example shows the first magnetic storm recorded in Prague on 3 September 1839.

KEYWORDS : historical geomagnetic observatory, bifilar magnetometer, geomagnetic field

Sr No: 112

Collecting and Preserving Historical Seismic Data in Romania

PRESENTING AUTHOR:

Raluca Dinescu, University of Bucharest, Romania

CORRESPONDING AUTHOR:

Mihaela Popa, National Institute for Earth Physics, Romania

Daniel Paulescu, National Institute for Earth Physics, Romania

Andreea Chircea, National Institute for Earth Physics, Romania

Cristian Neagoe, National Institute for Earth Physics, Romania

Adina Vanciu Rau, National Institute for Earth Physics, Romania

Victoria Oancea, Leidos, USA

Romania is one of the first countries in the world involved in seismic monitoring and has intense seismicity, both deep and crustal. In 1888, the first station in Romania and one of the first stations in Europe was installed in Bucharest. By 1970, there were 48 analogue stations that functioned in Romania. The seismic "digital era" started there in 1991, but analogue recordings were maintained in several stations until 2017. The archive of the National Institute for Earth Physics (NIEP) in Bucharest contains over one million seismograms and includes records on smoked paper, photo paper, and ink recordings on paper dating since 1900. The analogue recordings are stored on media that suffer continuous physical degradation which results in loss of data over time. Associated with the analogue seismic waveform data is also the metadata to be found archived as national bulletins, seismicity catalogues, instrument documentation, station books, and old publications. These are all needed to properly use the recorded waveforms. Preserving all the archived historical information is a task we started to work on by assessing and creating an inventory of the paper seismograms, scanning the recordings of local or larger teleseismic events, as well as locating, assessing and preserving the metadata.

KEYWORDS : seismic data, analogue recordings, archived historical information

Sr No: 113

Collected Metadata for the Analogue Seismic Stations in Vienna, Austria (VIE and VKA)

CORRESPONDING & PRESENTING AUTHOR:

Mariatheresia Apoloner, Zentralanstalt für Meteorologie und Geodynamik, Austria

Victoria Oancea, Leidos, USA

Maria Del Puy Papi Isaba, Zentralanstalt für Meteorologie und Geodynamik, Austria

Anton Vogelmann, Zentralanstalt für Meteorologie und Geodynamik, Austria

Yan Jia, Zentralanstalt für Meteorologie und Geodynamik, Austria

The first analogue seismic records in Vienna date back to the early 20th century, when the first seismometer (VIE) started recording. During the 20th century, seismic instrumentation advanced. Also the city of Vienna grew, and with it, the background noise. Those factors led to multiple changes in instrumentation and recording sites (VKA). Finally, the last analogue device was switched off in 2006 and replaced by a digital seismometer.

Most of the seismograms are still stored in the archive of the "Zentralanstalt für Meteorologie und Geodynamik" in Vienna. Due to various projects, it was possible to scan selected seismograms and digitize even fewer. However, to interpret this data accurately, additional information is required. This is also referred to as metadata. Often it is available only analogue, on-site and in this case in German language.

Hence, to facilitate future research we focused solely on metadata. We collected information from different resources: the ZAMG archive, numerous publications and the International Seismological Centre. Therefore, we can now give a comprehensive overview of used instrumentation, recording parameters, seismogram availability and quality. In addition, we list relevant publications and online resources.

KEYWORDS : analogue, seismograms, Vienna

Sr No: 114

Preservation and digitalisation of French photographic magnetograms

PRESENTING AUTHOR:

Andreina Garcia, Universite de Paris, Institut de physique du globe de Paris, CNRS, France

CORRESPONDING AUTHOR:

Pierdavide Coisson, Universite de Paris, Institut de physique du globe de Paris, CNRS, France
Vincent Lesur, Universite de Paris, Institut de physique du globe de Paris, CNRS, France
Benoit Heumez, Universite de Paris, Institut de physique du globe de Paris, CNRS, France

The paper archive of the French National Magnetic Observatory includes historical data from the observatories in France, French Polynesia and Africa along the 20th century. The long-time series from Saint-Maur des Fossés, Val Joyeux and Chambon-la-Forêt, and data from the M'bour (Senegal), Bangui (Central Africa) and Pamatai (French Polynesia) observatories, are available. The three orthogonal magnetic components are recorded over 24 hours on photographic magnetograms (excluding the data gap at the time of replacement of the sheets). Although one-hour digitalised data are available at the French Bureau Central du Magnétisme Terrestre (BCMT) or INTERMAGNET, data digitalised at higher resolution may improve the analysis of the geomagnetic storms. The La Cour magnetometer in operation since 1939 was able to record also the values out of scale occurring during geomagnetic storms, while the oldest instruments were unable to handle these large excursions.

We developed a software to extract magnetic data resampled at one-minute from the ancient magnetic records. The latest improvements we realised include a redesigned image processing environment, which conveniently allows to identify the magnetogram traces, removes spurious data and includes trace size as an uncertainty measure on data retrieval. We use the BCMT definitive data to level and calibrate the reconstructed time series and obtain reliable magnetic field values. Further developments are still needed to handle more complex traces.

This software can now be used to reanalyse last century geomagnetic time series. Digitalisation is made on demand, via the website of the BCMT (www.bcmt.fr).

KEYWORDS : magnetic observatories, data digitisation, data archive

Sr No: 115

Preservation of Historical Australian Seismograms, Magnetograms and Geomagnetic Absolute Observations

CORRESPONDING & PRESENTING AUTHOR:

Hugh Glanville, Geoscience Australia, Australia

Efforts are underway to digitally preserve seismograms, magnetograms and geomagnetic absolute observations from Australian observatories. These datasets are stored in original paper and film form and although they are available on request they are not easily discoverable or available at short notice to the public. The retrieval of analogue media is both time-consuming and labour-intensive and can cause further damage to deteriorating records. In this poster, we detail preserved examples of the handwritten records, microfilm, as well as original paper records dating back to 1959 for magnetograms from Wilkes Geomagnetic Observatory, and to 1902 for seismograms from Melbourne Observatory. Different generations of collected data have challenges associated with the preservation efforts, including; legibility, data compression algorithms, stability of the original medium and associated metadata. Additionally, costs and expertise required to create digital copies varies greatly between the different original mediums of data recordings. Our ongoing efforts have prioritised the preservation of the original analogue data through creation of digital copies before the record suffers from further deterioration, and, making those digital records publically accessible through Geoscience Australia's data servers to improve discoverability. Long term efforts following this will then be focused on digitisation for use with modern data analysis techniques.

KEYWORDS :   geomagnetic, seismogram, observatory

Sr No: 116

DigiMAG method for digitizing SMA data

CORRESPONDING & PRESENTING AUTHOR:

Otto Karha, Sodankylä Geophysical Observatory, Finland

Eija Tanskanen, Sodankylä Geophysical Observatory, Finland

The Scandinavian Magnetometer Array (SMA) was part of the International Magnetospheric Study (IMS) (1977-1979). When we consider other magnetometer networks in northern Scandinavia, this nearly 1600 km long SMA chain still has the densest and most regular station spacing. The SMA-instruments were based on modified Gough-Reitzel magnetometers with three wire suspended magnets and a camera. This second generation was called type Münster magnetometer. A considerable amount of data was recorded in the form of magnetograms. Time-consuming optical recording and difficult digitization have been an obstacle to efficient data utilization. Most of the magnetograms has been left non-digitized and unstudied. We have developed a method, named DigiMAG, to digitize these recordings. A custom built device moves the magnetogram and automatically takes photos of it. After photographing the magnetograms, data needs to be collected and this has been done for a great storm which occurred in October 1977. The film height remains constant in pixels, so datasheet nT/mm values can be converted to nT/pixel format. Large amounts of data can be scaled without measuring each photo separately. We found out large regional differences in the auroral region exceeding 500 nT in less than 170 km.

KEYWORDS :   magnetogram, digitization, substorm

Sr No: 117

Comprehensive modernization of historical climate data

CORRESPONDING & PRESENTING AUTHOR:

Justin Mabie, U. of Colorado, USA

A foundation of understanding our environment is the observations that have been made. During the International Geophysical Year, the World Data Centers were established to ensure that data would be available and preserved. Recently, focus has been on preservation and usability of modern data sets which can be large and complex. This has taken focus away from preservation and dissemination of historical data which has not yet been modernized. The World Data Centers were abolished by the International Council of Scientific Unions in 2008, so there is no longer an international mandate to preserve and disseminate this historical data, making it vulnerable to the fiscal and political considerations of its respective hosts. This presentation will discuss the importance of modernization of this data, current and past efforts to modernize data, challenges in data preservation, and propose a combined effort across scientific disciplines towards a comprehensive solution.

KEYWORDS : climate, data, preservation

Sr No: 118

Historical bulletin dataset of World Data Center for Solid Earth Physics (Moscow): Why to save and possible ways to use

CORRESPONDING & PRESENTING AUTHOR:

Anna Skorkina, IEPT RAS, Russia

Boris Dzeboev, GC RAS, Russia

Nataliya Sergeyeva, GC RAS, Russia

World Data Center for Solid Earth Physics (WDC for SEP) is the Regular Member of the International Council for Science World Data System (ICSU WDS). WDC for SEP is responsible for the collection, guaranteed long-term storage, and dissemination of geophysical data. So far, the collection consists of many seismic bulletins for decades from many countries. From time to time, the question arises if we should keep saving paper versions (they have been scanned partly). Recently, after several contacts with International Seismological Centre, we have discovered data that was absent in ISC. Fortunately, the gap was filled. Since 2019, another way of the use of historical data is for educating purposes. Within the "Modern problems of seismology" course (in Lomonosov Moscow State University, Faculty of Physics). there is a hands-on session focusing on work with bulletins.

KEYWORDS : historical seismograms, world data center

J10 Joint session on Education and Outreach

CONVENERS: Manoj Nair

Raju Sarkar

Edgar Bering

Hannah Rogers

Tereza Kameníková

Aaron Velasco

Xyoli Pérez-Campos

Rajib Shaw

Earthquakes and geomagnetism present a substantial hazard worldwide. The significance of geomagnetic hazards lies in its potential impact on man-made technologies on Earth and in space, for example, on satellites, electricity power grids, pipelines, communications and on geophysical exploration. Earthquakes represent a global challenge; seismologists and engineers can minimize earthquake impact by changing the design and construction of buildings to withstand strong ground motions. Social preparedness, community response, and resilience can be advanced through awareness of the underlying science. Involving students and the public in designing experiments and collecting data has been shown to foster a scientific identity, to increase overall interest in science, and to improve the perceived value of scientific research. For many countries, resources and infrastructure for preparedness are a limitation; however, creative, low-cost strategies, such as citizen science, can be implemented.

This inter-divisional symposium calls for papers describing innovations in geoscience instruction methods, citizen science initiatives, seismic engineering approaches, and community learning efforts. Papers are welcome on all aspects of education and citizen-science including methodology, data collection, data analysis, engineering challenges, non-traditional areas of curriculum, case studies etc. Involving students and the public in designing experiments and collecting data has been shown to foster a scientific identity, to increase overall interest in science, and to improve the perceived value of scientific research. For many countries, resources and infrastructure for preparedness are a limitation; however, creative, low-cost strategies, such citizen science, can be implemented. Earthquakes represent a global challenge to resilience that can be overcome by initiatives that improve seismology awareness through education and citizen participation in various countries around the world. We also encourage submissions that describe ways to broaden the public understanding and appreciation of science and to attract non-traditional and under-represented students into the sciences. Papers are welcome describing advances in all levels of instruction, especially inventive approaches to inquiry based learning in all geosciences.

Sr No: 119

The Application of the 5-E Instruction Model to Teaching Undergraduates to Build Spacecraft and Study Geoscience

CORRESPONDING & PRESENTING AUTHOR:

Edgar Bering, University of Houston,USA

Shuhab Khan, University of Houston,USA

Mequanint Moges, University of Houston,USA

Laura Jacobs, University of Houston,USA

Michael Greer, University of Houston,USA

Presley Greer, University of Houston,USA

Bryan Gunawan, University of Houston,USA

Elizabeth Hernandez, University of Houston,USA

Jamie Lehnen, University of Houston,USA

Megan Pina, University of Houston,USA

Itay Porat, University of Houston,USA

John Prince, University of Houston,USA

James Simmons, University of Houston,USA

Chloe Tovar, University of Houston,USA

Alexandra Ulinski, University of Houston,USA

Donald Hampton, University of Alaska, Fairbanks,USA

Nicole Moelders, University of Alaska, Fairbanks,USA

Denise Thorsen, University of Alaska, Fairbanks,USA

The Undergraduate Student Instrumentation Project (USIP) was a NASA program to engage undergraduate students in rigorous scientific research, for the purpose of developing the next generation of professionals in space research. The program is student led and executed from initial ideation of research objectives to the design and deployment of scientific payloads. The University of Houston was selected twice to participate in the USIP programs. The first program (USIP_UH I) ran from 2013 to 2016. USIP_UH II ran from 2016 to 2019. USIP_UH I (USIP_UH II) at the University of Houston was composed of eight (seven) research teams developing six (seven), distinct, balloon-based scientific instruments. This project was a for-credit course two years in duration. The program has been so successful in terms of improved student career outcomes the University has decided to continue the project with purely local funding. The pandemic has produced a substantial instructional challenge since this project is a lab class! The virtual classroom that we designed to meet this need provides tools for ongoing collaboration, revisions, storage, project planning, systems engineering, and a tool to request immediate feedback from faculty and fellow researchers. Additionally, the classroom provides an ongoing place to store data from different students for many years. New students can use this continuity in a consistent and secure way. We also provided tools for conferencing and communication. A combination of several tools were selected and customized to meet this need. These tools include Google Classroom, Microsoft Teams, Slack, Git, Groupme, and Zoom.

Sr No: 120

Diploma in Seismology for High-School Teachers in Mexico

CORRESPONDING & PRESENTING AUTHOR:

Delia Iresine Bello Segura, UNAM, Mexico

Xyoli Perez Campos, UNAM, Mexico

Luis Quintanar Robles, UNAM, Mexico

Jaime Dominguez Rivas, UNAM, Mexico

Jesus Antonio Perez Santana, UNAM, Mexico

Fernando Navarro Estrada, UNAM, Mexico

Antonio De Jesus Mendoza Carvajal, UNAM, Mexico

Jesus Elihu Ruiz, UNAM, Mexico

Brenda Abril Nequiz Guillen, UNAM, Mexico

Leonarda Isabel Esquivel Mendiola, UNAM, Mexico

The high school Physics programs in Mexico do not consider the immediate application of the concepts learned by the students. It is in high school when young people are exploring and looking for experiences to decide the area in which they want to focus their studies. With this in mind, we are working on a project that seeks, through the preparation of high-school teachers, to awake student curiosity in seismology.

Based on the above, and taking as examples the successful programs "Seismographs in Schools" from IRIS and "Geoscience Information For Teachers" from EGU, the Mexican Servicio Sismológico Nacional (National Seismological Service, SSN) has launched a project that includes three stages: 1) Design and delivery of a diploma for high-school teachers; 2) installation of short period seismographs at each teachers' schools; and 3) active participation of teachers and their students in research projects based on the data collected in their schools.

The diploma in Seismology for high-school teachers is a 170 hour course that offers an introduction in topics related to seismology (basic seismology, seismic instrumentation and computer systems applied to seismology). The goals that have been achieved with the diploma have been the modification of the high school programs in which seismology is currently included. Accelerometers have been installed in some schools, there are more and more students of teachers who have completed the diploma presenting experiments at congresses and science contests. But the main objective has been fulfilled for teachers to bring their students closer to seismology.

KEYWORDS :   diploma, high school, teachers

Sr No: 121

Innovation on science outreach in Brazil

CORRESPONDING & PRESENTING AUTHOR:

Katia Pinheiro, Observatório Nacional, Rio de Janeiro, Brazil

MOSAIC (Magnetic Observatories, Stations And Integrated nstagra) Group of Observatório Nacional (Rio de Janeiro, Brazil) develops a variety of outreach projects. The puppets nstagr "A scientific journey to
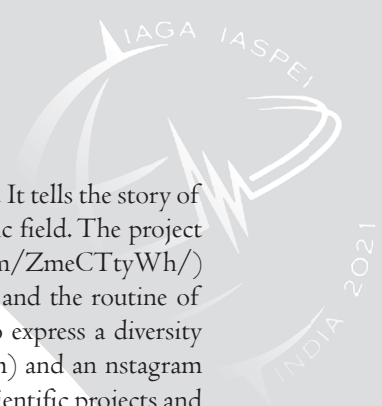
Earth's core" is inspired in Jules Verne's book and designed for children up to 10 years old. It tells the story of seven animals that travel to the Earth's center through seismic waves and Earth's magnetic field. The project "Tique: o Toque da Ciência" (Tique: The Touch of Science in https://vm.tiktok.com/ZmeCTtyWh/) is designed for teenagers that use TikTok social media platform. Videos about science and the routine of scientists are presented by researchers, students and teenagers that use their creativity to express a diversity of scientific contents. We also developed a webpage (www.observatoriosmagneticos.com) and an nstagram account (@grupomosaic) to post information about the geomagnetic field, MOSAIC scientific projects and activities. In these platforms, we aim attract new students, collaborations and stimulate the science diffusion in Brazil.

KEYWORDS : outreach in Brazil, geomagnetism, social media

Sr No: 122

SYMPOSIUM : **J10 Joint session on Education and Outreach**

IAGA has followers! Introducing the IAGA Social Media Working Group

CORRESPONDING & PRESENTING AUTHOR:
Hannah Rogers, University of Edinburgh, UK
Shivangi Sharan, University of Nantes, France
Tereza Kamenikova, Charles University, Czech Republic
Anita Di Chiara, Istituto Nazionale di Geofisica e Vulcanologia, Italy
Barbara Leichter, Central Institute for Meteorology and Geodynamics, Austria
Katia Pinheiro, Observatório Nacional – ON / MCTIC, Brazil
Loren Chang, National Central University Taoyuan City, Taiwan
Leonardo Miquelutti, Universidade Federal Fluminense, Brazil

Initially set up in December 2019, the IAGA social media platforms (Twitter, Instagram, Facebook and a blog) have been dedicated to advertising the work of IAGA. With half the world's population always online, it has become imperative to shift research to a virtual platform and adapt so the general public can access information about science in new ways. IAGA's social media platforms started as an alternative version of mailing lists but have expanded into creating original posts, such as interviews with IAGA members. The IAGA Social Media working group was formed in January 2021 with the main aims:

1. to provide an easily accessible platform for news and an online community for IAGA members

2. to increase awareness of the varied work of IAGA, both within the community (to support cross-disciplinary research) and to the general public

3. to promote the work of early career researchers and under-represented groups in IAGA

In the time of a global pandemic, this working group is forging international connections, advertising opportunities, sharing news, and continuing to grow. As this is the first IAGA meeting since the working group formed, we wish to share our successes and promote our work. Finally, we encourage anyone interested in sharing content or wanting to join the working group to contact us – we would love to hear from you.
Facebook: @IAGAandAIGA
Instagram: @iaga_aiga
Twitter: @IAGA__AIGA
Blog: https://iaga-aiga.blogspot.com/

KEYWORDS : IAGA outreach, social media

Sr No: 123

An Earthquake Early Warning System for Canada

CORRESPONDING & PRESENTING AUTHOR:

Alison Bird, Natural Resources Canada, Canada
Henry Seywerd, Natural Resources Canada, Canada
Stephen Crane, Natural Resources Canada, Canada
John Adams, Natural Resources Canada, Canada
David Mccormack, Natural Resources Canada, Canada

Earthquake Early Warning (EEW) systems have successfully alerted people and infrastructures of imminent strong shaking in several countries where earthquakes poses a substantial risk. A national EEW system is being developed for large regions of moderate to high earthquake risk in Canada, focussing initially on the west coast of British Columbia, eastern Ontario and southern Quebec. In an effort to secure the optimal distribution of EEW sensors, NRCan is collaborating with other Federal Agencies, Provinces, First Nations, and others to host sensors.

We investigate the system's performance for various sensor densities and show that 20km sensor spacing is optimal for effective EEW monitoring. Alert times from the proposed network are presented for a suite of scenario earthquakes to validate the EEW system's capacity to provide practical warning times.

Finally, we demonstrate that the impacts of strong earthquakes can be mitigated by Canada's EEW system, through timely notification of earthquake shaking, enabling appropriate protective actions to be taken by emergency measures organizations, critical infrastructure operators, other industrial facilities, and the public. The national EEW system will be operational in 2024. This will contribute to Canada's efforts to meet the recommendation to "increase the availability of and access to early warning systems" within the United Nations Sendai Framework for Disaster Risk Reduction.

KEYWORDS : earthquake early warning, Canada

Sr No: 124

CrowdMag: Crowdsourcing Earth's magnetic field

CORRESPONDING & PRESENTING AUTHOR:

Manoj Nair, University of Colorado, USA
Rick Saltus, NOAA/University of Colorado, USA

In partnership with the Cooperative Institute for Research in Environmental Sciences (CIRES), NOAA's National Centers of Environmental Information (NCEI) started a crowdsourcing project (CrowdMag) to collect magnetic data from digital magnetometers in smartphones. The primary objectives for the CrowdMag project are (1) validation and improvement of NOAA's magnetic anomaly maps with application not only to navigation, but also for other marine studies as diverse as animal migration and resource exploration, and (2) enhanced engagement of educators and citizen scientists with NOAA's mission and science, thus supporting the next generation of scientists and innovators. Crowdmag uses the phone's internet connection to send magnetic data and location to NOAA. We check the quality of the magnetic data from all users and

make the data available to the public as aggregate maps. Currently, the CrowdMag project has about 65, 000 enthusiastic users who have contributed more than 65 million magnetic data points from around the world. We develop low-resolution global magnetic field models and higher resolution, localized magnetic maps using this data. A second aim of the CrowdMag project is to facilitate Citizen Science and education. One example is the annual summer "CrowdMag Day" campaign at the University of Colorado that engages student interns from CIRES's Research Experience for Community College Students (RECCS) program to collect and examine magnetic data using the CrowdMag app together along a profile in the campus. Our talk will cover the latest scientific and educational aspects of the CrowdMag project and the lessons learned.

KEYWORDS :   geomagnetism, crowdsourcing, crowdmag

Sr No: 125

SYMPOSIUM :   **J10 Joint session on Education and Outreach**

A National University Course on Geohazards in Norway

CORRESPONDING & PRESENTING AUTHOR:
Mathilde Sorensen, University of Bergen, Norway
Louise Vick, UiT The Arctic University of Norway, Norway
Jose Cepeda, University of Oslo, Norway
Felix Halpaap, University of Bergen, Norway

A national consortium consisting of more than 30 experts of earth science and education has developed a national course on geohazards in Norway. The course gives an introduction to various types of geohazards, their potential consequences, and what can be done to prevent natural disasters. Students learn about the geological and physical processes driving geohazards, how society is affected by and can cope with geohazards, and the mitigation measures that can be implemented to prevent disasters. Students thereby develop an understanding of the link between nature and society, and how this link affects the potential consequences of an event. The course focuses on student-active learning and it is taught through a series of thematical modules that are developed by the leading national experts for each theme. Most of the teaching takes place in "flipped classrooms", where students familiarize themselves with the theoretical basis before class, and teaching time is spent on discussion and group activities. The flipped classrooms are supplemented with practical exercises and an excursion where students can observe and identify geohazards and mitigation measures in the field. The course was taught for the first time during the autumn semester 2020 at the universities of Bergen, Oslo and Tromsø.

KEYWORDS :   geohazards, education, national course

Sr No: 126

CORRESPONDING & PRESENTING AUTHOR:

Mohsen Ghafory-Ashtiany, International Institute of Earthquake Engineering and Seismology, IIEES, Iran

Iran with frequent occurrence of devastating earthquakes had experienced high human, social, and property losses due to vulnerability of the built environment and rapid growth of population. Considering the existing knowledge (science, technology, standards, guidelines, etc.), strategy, policy for disaster risk reduction, one would expect that our built environment would have or at least meet the minimum safety and quality standards. Achieving safe and resilience in Iran has been a complex issue that required all sectors of society and experts to work together through the Nexus approach for solving a complex system. In the Nexus system, we should have one objective and all risk-related-discipline should cooperate toward its achievement. This requires the implementation of safety and disaster prevention and management know-how in the development process; which requires making the bridge between science and development policy fully operational.

This paper proposes an approach in which the scientist and decision-makers should close their existing gap in order to provide technical and legislative solutions that safety turned to economic benefit. This can be done through the Integration of all programs, policies, regulations, institutions, and stakeholders by creating synergy through a systematic and NEXUS approach. The Nexus approach is essentially about moving beyond traditional sectoral thinking to achieving overall safety and sustainability of all resources. Nexus in disaster risk management system incorporates the interlinkages, interrelatedness, and interdependencies of all contributing elements, components, players, and parameters affecting the risk as well as their transitions and fluxes across spatial scales and between the components.

KEYWORDS : Iran, seismic risk, nexus

Joint IAGA Division Symposia

DI Exploring Earth's magnetic field from space

CONVENERS: Ciaran Beggan
                        Gauthier Hulot
                        Patrick Alken
                        Yanyan Yang

The magnetic field is a fundamental geophysical characteristic of the Earth, which provides information on a range of processes from core to space. Research related to elucidating these sources is greatly aided by data collected from a fleet of satellite systems around the Earth. Recent years have seen the continued operation of the Swarm constellation with improvements to the quality of the magnetic field measurements, as well as the inclusion of the Cassiope/ePoP mission as Swarm-E. There has also been the successful launch of the CSES mission and the investigation of data from platform magnetometers on other scientific missions. Together these represent new data streams to investigate core, mantle, crust, tidal, ionospheric and magnetospheric sources of the magnetic field. This symposium wishes to combine ideas in modelling, observations and theory applied to Earth's magnetic field as measured primarily from space, also inviting ideas for maintaining and improving observational strategies on the long-term.

Sr No: 127

CSES High Precision Magnetometer and Some Potential Scientific Applications

CORRESPONDING & PRESENTING AUTHOR:

Yanyan Yang, National Institute of Natural Hazards, Ministry of Emergency Management of China, China

Xuhui Shen, National Institute of Natural Hazards, Ministry of Emergency Management of China, China

Zhima Zeren, National Institute of Natural Hazards, Ministry of Emergency Management of China, China

Bin Zhou, National Space Science Center, Chinese Academy of Sciences, China

Gauthier Hulot, Institut de Physique du Globe de Paris, France

Nils Olsen, Technical University of Denmark, Denmark

Chao Xiong, Wuhan university, China

Claudia Stolle, GFZ German Research Centre for Geosciences, Germany

Jianping Huang, ational Institute of Natural Hazards, Ministry of Emergency Management of China, China

Bingjun Cheng, National Space Science Center, Chinese Academy of Sciences, China

Andreas Pollinger, Austrian Academy of Sciences, Austria

Werner Magnes, Austrian Academy of Sciences, Austria

Jie Wang, ational Institute of Natural Hazards, Ministry of Emergency Management of China, China

Feng Guo, ational Institute of Natural Hazards, Ministry of Emergency Management of China, China

The High Precision Magnetometer (HPM) payload assembled on CSES is designed to provide accurate measurement of the magnetic field intensity and vector components. Now, the HPM payload is in good health and is operated continuously to provide data for scientific communities. As a reference for users who are interested in this dataset, we will give an introduction for the data content of the CSES HPM Level 2 scientific data products. In particular, flags for potential magnetic field disturbances from the satellite and its payload are discussed. Recently, we make some progress on in-flight vector calibration using the scalar data and correction for TBB disturbance, which can help to further improve the data quality. Finally, some possible scientific applications of the data on global geomagnetic field modelling, lithosphere observations, Dst index estimation and ionosphere current studies such as FACs and EEJ (CEJ) are outlined. Our analysis demonstrates that the HPM data of CSES are of good quality and suggests a high scientific potential of the data.

KEYWORDS : China seismo-electromagnetic satellite; high precision magnetometer; space magnetometry

Sr No: 128

Towards a true swarm of magnetic satellites - scientific use of measurements taken by navigational magnetometers onboard Low-Earth orbiting satellites

CORRESPONDING & PRESENTING AUTHOR:

Nils Olsen, DTU Space - Technical University of Denmark, Denmark

Most satellites are equipped with magnetometers as part of their attitude control system. The measurements taken by these platform or navigational magnetometers are not only useful for coarse attitude determination for satellite operation but can also be used for scientific investigations, provided they have been properly calibrated.
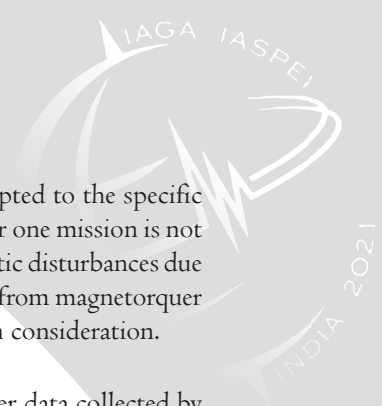
Proper calibration of platform magnetometer data is an endeavour that needs to be adapted to the specific satellite mission. There is no "one-size-fits-all" solution. A procedure that is successful for one mission is not necessarily the optimal approach for other satellites. In particular the correction for magnetic disturbances due to satellite and payload operation -- for instance how to account for magnetic signatures from magnetorquer activity and solar array currents -- usually needs to be adapted for the specific satellite in consideration.

This overview talk describes the preprocessing and calibration of platform magnetometer data collected by Cryosat-2, GRACE and other Low-Earth orbiting satellites and their in studying the dynamics of Earth's core field and current systems in Earth's environment.

KEYWORDS : satellite magnetism, swarm

Sr No: 129

SYMPOSIUM : **D1 Exploring Earth's magnetic field from space**

Satellite Platform Magnetometer Calibration Using Machine Learning (by invitation)

CORRESPONDING & PRESENTING AUTHOR:

Kevin Styp Rekowski, GFZ Potsdam, Germany
Claudia Stolle, GFZ Potsdam, Germany
Ingo Michaelis, GFZ Potsdam, Germany
Odej Kao, Technical University of Berlin, Germany

The use of non-dedicated satellites to improve the data availability for geomagnetic observations of the Earth's magnetic field in space has recently been demonstrated. Making these data accessible enlarged the spatial-temporal coverage of the observations. In this work, we calibrate and characterize platform magnetometer data of different satellite missions (GRACE-FO, GOCE, and others) and make them publicly available for further analysis. By applying machine learning techniques, the measured magnetometer signal is adapted for artificial disturbances. The proposed non-linear regression is able to conduct feature selection as well as feature combination automatically, allowing for a wider range of available features. This approach reduces analytical work for the calibration for platform magnetometers, thus leading to faster and more easily accessible datasets of platform magnetometer measurements. In the future, this approach shall become automatized and generally applicable for other satellite magnetic data sets.

KEYWORDS : platform magnetometer, machine learning, calibration

Sr No: 130

Indices of geomagnetic activity derived from space-born magnetic data from the Swarm mission

CORRESPONDING & PRESENTING AUTHOR:

Constantinos Papadimitriou, National Observatory of Athens, Greece

Georgios Balasis, National Observatory of Athens, Greece

Zoe Adamantia Boutsi, National Observatory of Athens, Greece

Ioannis A. Daglis, National and Kapodistrian University of Athens, Greece

Omiros Giannakis, National Observatory of Athens, Greece

Paola De Michelis, National Institute of Geophysics and Volcanology, Italy

Giuseppe Consolini, National Institute of Astrophysics, Italy

Lorenzo Trenchi, European Space Agency, France

Ground based indices, such as the Dst and AE, have been used for decades to describe the interplay of the terrestrial magnetosphere with the solar wind and provide quantifiable indications of the state of geomagnetic activity in general. These indices have been traditionally derived from ground based observations from magnetometer stations all around the Earth. In the last 7 years though, the highly successful satellite mission Swarm has provided the scientific community with an abundance of high quality magnetic measurements at Low Earth Orbit, which can be used to produce the space-based counterparts of these indices, such the Swarm-Dst and Swarm-AE Indices. In this work, we present the first results from this endeavour, with comparisons against traditionally used parameters, and postulate on the possible usefulness of these Swarm based products for space weather monitoring and forecasting.

KEYWORDS : geomagnetic activity, indices, swarm

Sr No: 131

Core surface flow changes associated with the 2017 Pacific geomagnetic jerk deduced from Swarm secular variation gradient tensor elements

CORRESPONDING & PRESENTING AUTHOR:

Kathy Whaler, School Geosciences, University of Edinburgh, UK

Magnus Hammer, DTU, Denmark

Chris Finlay, DTU, Denmark

Satellite measurements enable spatial magnetic field gradients to be estimated from along track and, in the case of the current Swarm constellation mission, across track differences. Here we produce time dependent core surface advective flow models by inverting time series of geomagnetic virtual observatory (GVO, i.e. 4-monthly values at fixed regular distributed locations in space) elements of the gradient tensor of the secular variation (SV) from Swarm satellite data between 2014 and 2019. Although noisier, their greater sensitivity enable more coefficients of the flow to be resolved. We use a variety of spatial regularizations that result in rather different flow geometries, though they all display the main features seen in previous studies. In the region beneath the Pacific, the flows have non-equatorially symmetric and non-tangentially geostrophic ingredients, notably cross-equator flow in the region below Indonesia. Rapid temporal changes in the Pacific region are seen in both SV and SV gradient tensor GVO time series around 2017, most clearly in the radial
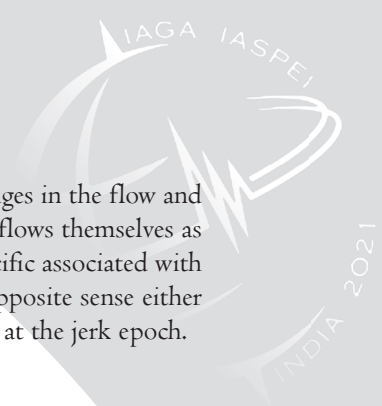
SV component, and also in several of the SV gradient elements. We investigate the changes in the flow and flow accelerations associated with the jerk. We show that, despite the differences in the flows themselves as a result of the spatial regularization, the changes to the core surface flow beneath the Pacific associated with the jerk are consistent. In particular, the east-west component of acceleration has the opposite sense either side of around 160°W longitude, where the acceleration is very small, and changes sign at the jerk epoch.

KEYWORDS : core surface flow, SV gradient data, virtual observatory

Sr No: 132

SYMPOSIUM : **D1 Exploring Earth's magnetic field from space**

NanoMagSat, moving towards permanent space-borne low-cost monitoring of the Earth's magnetic field and ionospheric environment (by invitation)

CORRESPONDING & PRESENTING AUTHOR:

Gauthier Hulot, Université de Paris, Institut de Physique du Globe de Paris, CNRS, France
Jean Michel Leger, CEA-Leti, Université Grenoble Alpes, France
Lasse B. N. Clausen, University of Oslo, Norway
Florian Deconinck, Open Cosmos Ltd, UK
Pierdavide Coisson, Université de Paris, Institut de Physique du Globe de Paris, CNRS, France
Pierre Vigneron, Université de Paris, Institut de Physique du Globe de Paris, CNRS, France
Patrick Alken, University of Colorado Boulder, USA
Arnaud Chulliat, University of Colorado Boulder, USA
Christopher C. Finlay, DTU Space, Technical University of Denmark, Denmark
Alexander Grayver, ETH Zürich, Switzerland
Alexey Kuvshinov, ETH Zürich, Switzerland
Nils Olsen, DTU Space, Technical University of Denmark, Denmark
Erwan Thebault, Universiteé de Nantes, Université d'Angers, CNRS, France
Thomas Jager, CEA-Leti, Université Grenoble Alpes, France
Francois Bertrand, CEA-Leti, Université Grenoble Alpes, France
Tobias Hafner, Open Cosmos Ltd, UK

The geomagnetic field has been continuously monitored from low-Earth orbit (LEO) since 1999, complementing ground-based observatory data by providing calibrated scalar and vector measurements with global coverage. The successful ESA Swarm constellation is expected to remain in operation up to at least 2025. Further monitoring the field from space with high-precision absolute magnetometry is of critical importance for improving our understanding of the dynamics of the multiple components of this field, as well as that of the ionospheric environment. The NanoMagSat project aims to deploy and operate a new constellation concept with a current baseline of three identical 16U nanosatellites, using two 60° inclined and one polar LEO orbits, hosting an innovative payload suite including an advanced Miniaturized Absolute scalar and self-calibrated vector Magnetometer (MAM) combined with a set of precise star trackers (STR), a compact High-frequency Field Magnetometer (HFM), a multi-needle Langmuir Probe (m-NLP) and dual frequency GNSS receivers. NanoMagsat already underwent a consolidation study funded by the ESA Scout programme. This presentation will report on the latest development of the mission, highlighting the way the project is evolving technically, programmatically and scientifically in order to further improve its scope. NanoMagSat intends to complement and improve on many of the science goals of the Swarm mission at a much lower cost, and to bring innovative science capabilities for ionospheric investigations. It aims at forming the basis of a permanent collaborative constellation of nanosatellites for low-cost long-term monitoring of the geomagnetic field and ionospheric environment from space.

KEYWORDS : nanosatellites, earth's magnetism, ionosphere environment

Sr No: 133

In-flight interference and instability calibration of the CSES Fluxgate Magnetometers

PRESENTING AUTHOR:

Tong Yuqi, National Space Science Center, Chinese Academy of Sciences, China

CORRESPONDING AUTHOR:

Zhou Bin, National Space Science Center, Chinese Academy of Sciences, China

According to the in-orbit test and evaluation, High Precision Magnetometer (HPM) onboard China Seismo-Electromagnetic Satellite (CSES) has excellent performance and could provide high-quality data. However, after the three-year launch of CSES, we notice that two Fluxgate Magnetometers (FGM) appear to be influenced when Tri-Band Beacon (TBB) is powered on and emits electromagnetic waves. The other problem is that linear parameters of FGM are found unstable under a linear calibration, there is obvious regularity in scalar deviations which will affect the quality of vector magnetic field data. This paper analyzes possible causes of the TBB interference and the instability of linear parameters and then proposes a solution based on Coupled Dark State Magnetometer (CDSM) measurements. A significant improvement in the scalar deviations is demonstrated, the scalar deviations of TBB disturbed data could be reduced from 9.0nT to around 0.7nT after TBB interference elimination, and the obvious regularity of the scalar deviations disappears after no-linear re-calibration of the FGM parameters.

KEYWORDS : high precision magnetometer, fluxgate magnetometer, data processing

Sr No: 134

Sequential modelling of the Earth's core magnetic field and flow

CORRESPONDING & PRESENTING AUTHOR:

Guillaume Ropp, Université de Paris - Institut de Physique du Globe de Paris, France
Vincent Lesur, Université de Paris, Institut de Physique du Globe de Paris, France

Modern geomagnetic field models, derived using satellite and observatory magnetic data, are now covering more than twenty years, providing information on the numerous external and internal sources generating the field. Therefore, the understanding of the geomagnetic field behaviour, in particular the core field variations, requires field models to describe accurately as much as possible of these sources. This work aims at providing reliable models that describe the short-term evolution of the core magnetic field and of the core surface flow. We use a sequential modelling approach — a Kalman filter, combined with a correlation-based modelling step, together with strong prior information on the spatial behaviour of the geomagnetic field contributions. A sequence of core field snapshot models, 3 months apart, has been built, allowing for a core field temporal resolution of the order of the year. The resulting time series of core field models present the general characteristics of the models based on more classic modelling techniques, thus supporting the reliability of this method. New interesting features were found in both the core field and flow time series, especially at small spatial scales. The flow models display the statistics of the Coupled Earth model (Aubert et al., 2013) - which statistics were used as prior information for the inversion, and a strongly quasi-geostrophic structure.
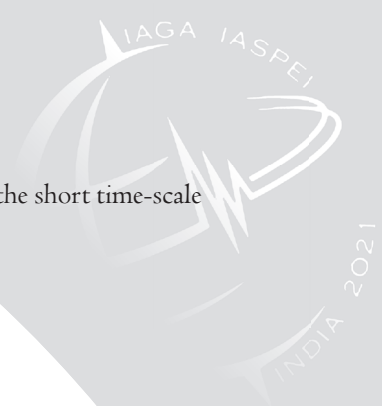
These results suggest that our method is able to provide new, interesting information on the short time-scale behaviour of the core field and on the dynamics in the core inducing these variations.

Sr No: 135

Comparison of field-aligned currents and ground dB/dt variations

CORRESPONDING & PRESENTING AUTHOR

Malcolm Dunlop, Beihang University, China
Xiangcheng Dong, UKRI-STFC, UK
Dong Wei, Southern University of Science and Technology, China
Junying Yang, Beihang University, China
Chao Xiong, GFZ, China

The orientation of field-aligned current sheets (FACs) can be inferred from dual-spacecraft maximum correlations between two Swarm spacecraft (A and C). Statistical analysis of the correlation and inferred orientation shows clear trends in magnetic local time (MLT), which reveal the behaviour of both large and small scale currents. Individual events sampled by higher altitude spacecraft (e.g. the 4 Cluster spacecraft), in conjunction with Swarm (mapping both to region 1 and 2), also show two different domains of FACs: time variable, small-scale (10s km), and more stationary large-scale (>100 km) FACs. Both the statistical trends and individual conjugate events, show comparable effects seen in the ground magnetometer signals (dH/dt) during storm/substorm activity. Intense dB/dt variations particularly take place in the main phase of a geomagnetic storm, particularly during active substorms. Demonstration of intense dB/dt variations which are directly driven by bursty bulk flows (BBFs) at geosynchronous orbit is rare. The characteristics and response during the recovery phase of a geomagnetic storm that occurred on 7 January 2015 were covered by multi-point measurements, combining Cluster and SWARM measurements, and a group of ground-based magnetometer observations. The locations of Cluster and SWARM map to the same conjugate region as the magnetometer ground stations at the time of the BBF. The measurements show that corresponding signals in all measurements occur simultaneously (with suitable time lags) in this region. The most intense dB/dt (dH/dt) variations are associated with FACs corresponding to a modified SCW that are driven by BBFs at geosynchronous orbit around substorm onset.

Sr No: 136

Mie representation of low- and mid-latitude F-region ionospheric currents and magnetic fields using the Swarm satellite data

CORRESPONDING & PRESENTING AUTHOR:

Martin Fillion, Institut de Physique du Globe de Paris, France
Gauthier Hulot, Institut de Physique du Globe de Paris, France

Patrick Alken, CIRES, Colorado

Arnaud Chulliat, CIRES, Colorado

We present a new empirical model of low- and mid-latitude F-region ionospheric currents and associated magnetic fields. This model is build by taking advantage of the unprecedented space-time data coverage provided by theSwarm satellite constellation at two distinct but close altitudes in the F-region. The data are first corrected for some potential fields by removing spherical harmonic representation of the main, lithospheric, E-region ionospheric and magnetospheric fields from the Swarm satellite vector measurements. It is then shown that part of the residual signal in the Swarm data can be represented as a non-potential toroidal magnetic field using the Mie representation in a thin-shell and spherical harmonics expansions. In particular, we derive consistent representations of the toroidal fields and associated poloidal currents both at the altitude of the satellites Alpha and Charlie - around 450 km - and at the altitude of the Swarm satellite Bravo - around 520 km -. These toroidal fields and poloidal currents follow significant average diurnal and seasonal variations. Furthermore, it is possible to identify clear patterns associated with low- and mid-latitude interhemispheric field-aligned currents. The model allows to investigate these currents on a global scale and to more specifically characterize their longitudinal variations in relation with longitudinal variations of the main geomagnetic field.

KEYWORDS : F-region ionospheric currents, swarm satellites, mie representation

Sr No: 137

SYMPOSIUM : **D1 Exploring Earth's magnetic field from space**

Inversion of the satellite-observed tidal magnetic fields in terms of three-dimensional upper-mantle electrical conductivity and water content

CORRESPONDING & PRESENTING AUTHOR:

Libor Sachl, Faculty of Mathematics and Physics, Charles University, Czechia

Jakub Velimsky, Faculty of Mathematics and Physics, Charles University, Czechia

Ondrej Knopp, Faculty of Mathematics and Physics, Charles University, Czechia

The interaction of the oceanic tidal flows with the Earth's main magnetic field provides a powerful natural source of electromagnetic energy suitable for sub-oceanic upper-mantle electrical conductivity sounding. We have developed a new frequency-domain, spherical harmonic-finite element approach to the inverse problem of global electromagnetic (EM) induction. It is set up for an effective inversion of satellite-observed tidally-induced magnetic field in terms of three-dimensional structure of the electrical conductivity in the sub-oceanic upper mantle.

In order to demonstrate that the new approach can successfully reconstruct the 3-D upper mantle conductivity, we performed synthetic tests using a 3-D conductivity model WINTERC-e as a testbed. The WINTERC-e model is independent of any EM data and thus it represents an ideal target for synthetic tests of the 3-D EM inversion.

In the next step, we proceed to the inversion of Swarm-derived models of tidal magnetic signatures. In contrast to the synthetic tests, we take into consideration the imperfections of the satellite measuring devices by including the full covariance matrix to our approach. The resulting 3-D upper-mantle conductivity structure is interpreted in terms of material composition in a thermodynamically consistent way using Perple_X calculation of the thermodynamical database used in Xu et al. (2008). We present preliminary results that quantify the presence of water in the upper mantle.

KEYWORDS : 3-D inverse problem, EM induction, tides

Sr No: 138

The latest results of CSES and follow-up plans (by invitation)

CORRESPONDING & PRESENTING AUTHOR:

Zeren Zhima, National Institute of Natural Hazards, MEMC, China
Xuhui Shen, National Institute of Natural Hazards, MEMC, China
Yanyan Yang, National Institute of Natural Hazards, MEMC, China

The China Seismo-Electromagnetic Satellite (CSES) is the first platform of China Geophysical fields observation satellite mission (Zhangheng mission), with the main objectives to monitor the global geomagnetic field, ionosphere background environment and possible abnormal signals with strong natural disasters. CSES operates in a Sun-synchronous polar orbit with a high inclination degree of 97.4° at an altitude around 507 km, measuring the electromagnetic field, energetic particles and ionosphere plasma parameters. The first-hand scientific observations show that CSES has recorded a number of interesting natural events, showing its good inflight observing capability on natural phenomenon. In this presentation, we mainly introduce the operation status of satellite platform, payloads; as well as the first-hand scientific results obtained from CSES including the geomagnetic field modeling, the electromagnetic waves, the geomagnetic event and earthquake activities etc. The follow-up plans for the Zhangheng mission will be briefly presented.

KEYWORDS :   China seismo-electromagnetic satellite

Sr No: 139

Towards global magnetohydrodynamic simulation of all ACE data

CORRESPONDING & PRESENTING AUTHOR:

Ilja Honkonen, Finnish Meteorological Institute, Finland
Max Van De Kamp, Finnish Meteorological Institute, Finland

We present our approach to modeling over 20 years of the solar wind-magnetosphere-ionosphere system using version 5 of the Grand Unified Magnetosphere-Ionosphere Coupling Simulation (GUMICS-5). As input we use 16 s magnetic field and 1 min plasma measurements by ACE satellite starting from 1998. The modeled interval is divided into 28 h simulations including 4 h overlap. We use a maximum magnetospheric resolution of 0.5 Earth radii (Re) up to about 15 Re from Earth and decreasing resolution further away. In ionosphere we use a maximum resolution of approximately 100 km poleward of +-58 magnetic latitude and decreasing resolution towards equator. We have parallellized the magnetosphere of GUMICS-5 using the Message Passing Interface and have made several improvements which have e.g. decreased its numerical diffusion.

Currently we have simulated almost 9 years of ACE data: 2001-2004, 2010-2011, 2015-2017. On average we obtain new results at a rate of perhaps 30 times faster than real-time and expect to have simulated ACE data from 1998 to 2018 or later by end of this year or early next year. Results for one day and overlap require approximately 15 GB of disk space and final requirement is expected to be about 100 TB. We describe some of the challenges of working with such a large data set. Initial results indicate that GUMICS reproduces the solar cycle in magnetospheric and ionospheric parameters when compared to empirical models.

KEYWORDS :   magnetosphere, ionosphere, solar wind

Sr No: 140

Geomagnetism in the 2030s: Scenarios for Post-Swarm Data Collection (by invitation)

CORRESPONDING & PRESENTING AUTHOR:

Arnaud Chulliat, University of Colorado Boulder, USA

Since 2013, the European Space Agency Swarm tri-satellite mission has collected highly accurate magnetometer measurements in low-Earth, nearly polar orbits. Swarm is a highly successful satellite mission. Its data was used in a broad array of geomagnetism research studies and in innovative data products and services, including those developed by the Swarm Data Innovation and Science Cluster. Swarm's data was fed into the World Magnetic Model 2020 and the 13th Generation International Geomagnetic Reference Field, which are widely used by the research community, government, industry and the general public, e.g., for orientation and navigation. While the end of the Swarm mission is not yet in sight, it is generally expected that the two lower Swarm satellites will re-enter into the atmosphere in the current decade. The third satellite might remain in orbit beyond 2030, but it is unclear if data will still be available, due to funding uncertainties and risk of satellite failure. Various initiatives have been taken in recent years to prepare for the post-Swarm era and ensure that satellite-based geomagnetic field monitoring continues well into the 2030s. This presentation will review some recent initiatives and projects, particularly in the United States and Europe. Future geomagnetic data collection may look quite different from what it is now, with more reliance on platform magnetometers, miniaturized payloads and Cubesats. Magnetic field modeling simulations using Swarm data as a gold standard provide useful insights into the limitations and opportunities of post-Swarm data collection.

KEYWORDS : swarm, IGRF, cubesat

Sr No: 141

The scalar global lithospheric magnetic anomaly map derived from CSES satellite data (by invitation)

CORRESPONDING & PRESENTING AUTHOR:

Jie Wang, Ministry of Emergency Management of China, China
Xuhui Shen, Ministry of Emergency Management of China, China
Yanyan Yang, Ministry of Emergency Management of China, China
Zhima Zeren, Ministry of Emergency Management of China, China
Gauthier Hulot, CNRS, France
Nils Olsen, Technical University of Denmark, Denmark
Bin Zhou, Chinese Academy of Sciences, China
Magnes Werner, Austrian Academy of Sciences, Austria
Angelo De Santis, Via di Vigna Murata, Italy
Jianping Huang, Ministry of Emergency Management of China, China
Andreas Pollinger, Austrian Academy of Sciences, Austria
Roland Lammegger, Graz University of Technology, Austia
Feng Guo, Ministry of Emergency Management of China, China
Wenlong Liu, Beihang University, China
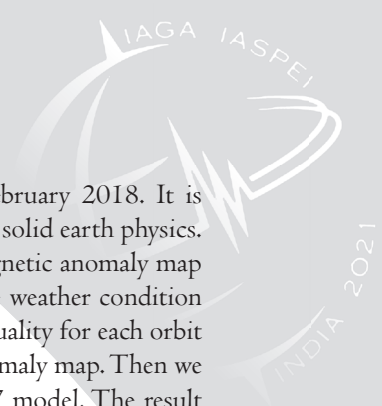
The China Seismo-Electromagnetic Satellite (CSES) was launched successfully in February 2018. It is China's first satellite to measure geophysical fields with scientific goals in both space and solid earth physics. In this work, we used the CSES scalar magnetic data to derive a global lithospheric magnetic anomaly map between ±65° geographic latitude. The night-side data during 2019 under quiet space weather condition (Kp=0o) were selected. After core and external field removal, the tracks with best data quality for each orbit were chosen for further line leveling and gridding to build the lithospheric magnetic anomaly map. Then we compared the grid map obtained from CSES data to that calculated by the CHAOS-7 model. The result shows a good agreement, indicating that the CSES delivers high-quality magnetic data for geophysical and geological studies. To analyze the origins of these satellite magnetic anomalies, we chose eight prominent magnetic anomalies, five in continental and three in oceanic regions. CSES results can clearly reflect the satellite magnetic anomalies which are associated with large-scale magmatic activities, involving the influence of mafic magma and intense crust-mantle interaction during geological history.

KEYWORDS :   lithospheric magnetic anomaly, CSES, long-wavelength magnetic anomaly

Sr No: 142

Forecasting velocity field at the core-mantle boundary using neural networks

CORRESPONDING AUTHOR:

Arban Uka, Epoka University, Albania
Presenting Author: Klaudio Peqini, University of Tirana, Albania
Julian Hoxha, Epoka University, Albania

In the present paper we discuss a model we have constructed with the aim to obtain the velocity field at the Core–Mantle Boundary (CMB). Initially we expand the magnetic field and the velocity field in spherical harmonics by stopping up to maximum degree 6 for the former and 4 for the later. The velocity field is additionally decomposed into a toroidal and a poloidal component. Then we substitute these series into the induction equation under the frozen–flux conditions and invert using standard techniques. The obtained velocity field is approximate and is characterized by large spatial scales. We use the Gauss coefficients of the geomagnetic field and its secular variation given by the global model gufm1, that spans a time period of several centuries. We focus on the period 1935–1990, because the data from this period are more accurate. In order to perform robust forecasting, we use neural networks. First, the networks analyze the velocity field snapshots in order to find typical features that characterize all of them. Also the network searched for particular features and analyze their statistical structure. Lastly, we perform forecasting by using a small number of snapshots. The forecasting seems to be reliable suggesting that the neural network has captured the main characteristics of the velocity field at the CMB.

KEYWORDS :   core-mantle boundary, velocity field, neural networks

Sr No: 143

Understanding the daily to monthly equatorial electrojet variability

CORRESPONDING & PRESENTING AUTHOR:

Gabriel Brando Soares, Observatório Nacional, Brazil

Yosuke Yamazaki, GFZ German Research Centre for Geosciences, Germany

Juergen Matzka, GFZ German Research Centre for Geosciences, Germany

Katia Pinheiro, Observatório Nacional, Brazil

Achim Morschhauser, GFZ German Research Centre for Geosciences, Germany

Claudia Stolle, GFZ German Research Centre for Geosciences, Germany

Patrick Alken, University of Colorado Boulder, USA

Akimasa Yoshikawa, Kyushu University, Japan

Kornyanat Hozumi, National Institute of Information and Communications Technology, Japan

Atul Kulkarni, Indian Institute of Geomagnetism, India

Pornchai Supnithi, King Mongkut's Institute of Technology Ladkrabang, Bangkok

The equatorial electrojet (EEJ) is an electric current that flows in the Earth's ionosphere at a height of about 110 km. The zonal flow of this current along the magnetic equator results in a north-south magnetic field at Earth's surface and at satellite altitudes. By using ground and satellite magnetic data, the seasonal climatology of the EEJ has been extensively studied, leading to the development of climatological models. However, the EEJ temporal variations ranging from few days to one year are not yet well understood nor accurately modeled. It is known that atmospheric solar tides are the main drivers of the observed temporal variations but determining their relative contributions and their respective time series is a challenging task. This occurs because determining the EEJ tidal composition requires good temporal and spatial coverage, which, in earlier work, could be achieved only with accumulation of satellite data over many years. We propose a new technique to determine the tidal composition for a much shorter interval by using a hybrid data set (combining ground and satellite magnetic data) and a mathematical formulation based on the principal component analysis (PCA). With this approach, ground and satellite data play a complementary role covering different local times and longitudes, while the PCA technique helps to map a sparse data set into a dense data set, helping to stabilize the inverse problem. This allows us to show time series of solar tides for shorter time windows, which are compared with tides inverted from neutral atmosphere temperature observations.

D2 Planetary magnetic fields and geomagnetic secular variation

CONVENERS: William Brown

Ingo Wardinski

Christopher Finlay

Swarandeep Sahoo

Katia Pinheiro

Sanja Panovska

Magnetic fields are an intrinsic part of many planetary bodies, including Earth, the study of which informs us of an array of processes and properties. These fields may influence studies of planetary cores, mantles, crusts, oceans, ionospheres and magnetospheres. Planetary magnetic fields operate across a wide range of temporal and spatial scales, of which the secular variations generated by dynamo processes are of particular interest, past, present and future. Observations of these magnetic fields may be contemporaneously observed at the surface, within the atmosphere, or by satellite orbit or fly-by, or derived historically from analysis of various materials. This session aims to cover studies of observations of planetary magnetic fields and their time changes, the incorporation of these data into models, and the theory underpinning these phenomena. A particular focus will be geomagnetic secular variation throughout Earth history and the pressing questions being raised by the wealth of recent observations of Earth and other bodies, as well as rapidly improving geodynamo models.

Sr No: 144

First time-averaged field models for the Miocene, based on new PSVM dataset

CORRESPONDING & PRESENTING AUTHOR:

Yael Engbers, University of Liverpool, UK

Andy Biggin, University of Liverpool, UK

Richard Holme, University of Liverpool, UK

A long-lived hypothesis in geomagnetism is that, if averaged over sufficient time (ca 10 million years), the Earth's magnetic field approximates a geocentric axial dipole (GAD). The significance of the non-GAD features in the time-averaged field is an important and unresolved issue. In the present-day field, the South Atlantic Anomaly (SAA) is the biggest irregularity in the field. Time varying field models for the last 3000 years don't show a persistent anomalous field in the South Atlantic region (Korte et al., 2009). However, recent palaeosecular variation (PSV) data from Saint Helena (8-11 Ma), suggest that the magnetic field contains recurring irregular behaviour in the South Atlantic region on a million-year timescale (Engbers et al., 2020). So far, time-average field (TAF) models have gone back as far as 5 million years, with an overrepresentation of data from the Brunhes period (Cromwell et al., 2018; Johnson et al., 2008). Using our new PSV dataset from the Miocene called PSVM, we present TAF models going further back in time, producing the first images of the average morphology of the magnetic field in the Miocene. With this dataset and these models, we discuss the presence or otherwise of the South Atlantic irregularities in the time-averaged field.

KEYWORDS :   time-averaged field, south atlantic anomaly, miocene

Sr No: 145

Forecasting dipolar geomagnetic field from paleo-models and synthetic models using neural networks

PRESENTING AUTHOR:

Klaudio Peqini, University of Tirana, Albania

CORRESPONDING AUTHOR:

Julian Hoxha, Epoka University, Albania

Arban Uka, Epoka University, Albania

Performing reliable forecasting based on existent palaeo-series of dipolar geomagnetic field is a challenging task. The difficulties arise due to the limited predictability of the dipolar field. Essentially, it is possible to successfully predict the dipolar field for a very short time span of several years but not for geological time scales. In the recent decades several models have been compiled based on magnetic field measurements of the geological past. The palaeo-model used in this study have long time spans of 1.5 - 4 Myr. The length of these series permits to perform statistical analysis in order to analyze their temporal structure. Neural networks are employed to perform such analysis as they can determine key feature vectors that are then afterwards used for prediction. After realizing the statistical properties of the time series, the neural network
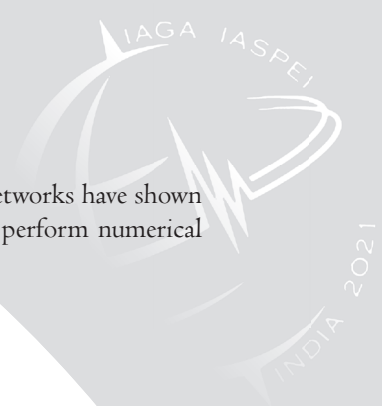
performs numerical realizations, the last being the predictions. Remarkably the neural networks have shown remarkable understanding of the statistical structure of the palaeo-models. Also they perform numerical realizations that are very reliable.

KEYWORDS : palaeomagnetic series, neural networks, forecasting

Sr No: 146

SYMPOSIUM : **D2 Planetary magnetic fields and geomagnetic secular variation**

Time-varying magnetic fields around Mars

CORRESPONDING & PRESENTING AUTHOR:

Shivangi Sharan, University of Nantes, France

Benoit Langlais, University of Nantes, France

Erwan Thebault, University of Nantes, France

Olivier Verhoeven, University of Nantes, France

Although a large part of the observed Martian magnetic field is constituted by crustal fields that are static and invariant in time, there is also a time-varying, transient field formed from the interaction between the static field and the solar wind. Its behavior is driven by both internal and external sources, and can thus be used for investigations of ionosphere as well as internal structure.

For this study, data from two satellites are used. The Mars Global Surveyor (MGS) and Mars Atmospheric and Volatile Evolution (MAVEN) have very different orbit configurations, resulting in different magnetic field observations with respect to local time and altitude. MGS stayed in a polar orbit around Mars providing vector measurements from 1999 to 2006. Currently orbiting Mars in a highly elliptical orbit and providing data from 2014, MAVEN changed its orbit course in early 2019. For each of these datasets, a priori crustal field models are used to subtract the static field from the data to obtain the time varying fields. The resulting residuals are analyzed in both planetocentric and sun-state coordinates and significant differences in field with respect to latitude and altitude are noticed.

These results are useful for modelling the external field to study the internal structure and composition of Mars. It is also useful in removing external variations when modelling the static crustal field.

KEYWORDS : Mars, transient magnetic fields, MGS and MAVEN

Sr No: 147

SYMPOSIUM : **D2 Planetary magnetic fields and geomagnetic secular variation**

Magnetic Rossby waves and torsional Alfvén waves in planetary dynamos (by invitation)

CORRESPONDING & PRESENTING AUTHOR:

Kumiko Hori, Kobe University, Japan

Chris Jones, University of Leeds, UK

Steve Tobias, University of Leeds, UK

Magnetohydrodynamic waves excited in deep interiors of rapidly rotating planets can produce secular variations of the magnetic fields. In strong-field dynamos, in which the inertial and viscous forces are small compared to the magnetostrophic forces, namely Coriolis, pressure, Lorentz, and buoyancy forces, unique wave motions can occur in both axisymmetric and nonaxisymmetric modes: torsional Alfvén waves and magnetic Rossby waves. To explore the relevance of these waves in Earth's core and Jupiter's metallic hydrogen region, we use simple mathematical models, as well as DNS of spherical convection and dynamos. It turned out that the linear theory gave good results for observed wave speeds, whilst nonlinearity might reasonably rule their waveforms or patterns. I will then discuss those waves in data. Now geomagnetic datasets as well as Jupiter's radiance datasets cover a wide range of timescales, although they are still limited and uneven. Newly available data-driven techniques may help to extract wave signals efficiently.

KEYWORDS :   magnetohydrodynamics; waves in rotating fluids; planetary interiors

Sr No: 148

SYMPOSIUM :   **D2 Planetary magnetic fields and geomagnetic secular variation**

Interannual geomagnetic variations reveal equatorially trapped quasi-geostrophic modes in Earth's core

CORRESPONDING & PRESENTING AUTHOR:

Nicolas Gillet, CNRS, France

Felix Gerick, Royal Observatory of Belgium, Belgium

Dominique Jault, CNRS, France

Tobias Schwaiger, CNES, France

Mathieu Istas, CNRS/UGA/CNES, France

Julien Aubert, IPGP, France

We invert for core surface flow motions over the past 20 years covered by satellite magnetic observations, in a stochastic data assimilation framework that incorporates the spatio-temporal information from a recent geodynamo simulation. It reveals coherent, quasi-periodic modes of period about 7 years and azimuthal wave number m=2. It travels westward at the core equator at a speed of about 1500 km/yr (~25°/yr). Perturbations at the core surface are as large as 5 km/yr for the flow parrallel to the equator, while for the radial field it amounts to ~1 μT (corresponding to 0.3 km/yr in Alfvén units). An interpretation of these wave-like patterns as quasi-geostrophic magneto-Coriolis modes trapped at the equator reconciles the observed period (slightly longer than the Alfven time) with the apparent magnetic to kinetic energy ratio (much less than unity). The sharp gradient in the cylindrical radial direction indeed implies an azimuthal field perturbation below the equator ~20 times larger than the one observed at the core surface. This framework offers a deterministic interpretation of interannual geomagnetic field changes observed from above the Earth's surface.

KEYWORDS :   interannual field changes, quasi-geostrophic modes, satellite observations
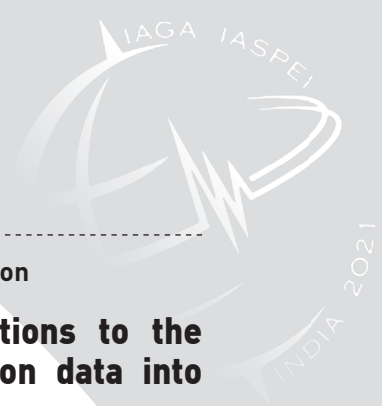
Application of altitude-cognizant spherical Slepian functions to the inversion of virtual observatory satellite secular variation data into localised regions of flow on the core-mantle boundary

CORRESPONDING & PRESENTING AUTHOR:

Hannah Rogers, University of Edinburgh, UK

Ciaran Beggan, British Geological Society, UK

Kathy Whaler, University of Edinburgh, UK

Alain Plattner, University of Alabama, UK

Spherical Slepian functions (or 'Slepian functions') are mathematical functions which can be used to decompose potential fields, as represented by spherical harmonics, into smaller regions covering part of a spherical surface. This allows a spatio-spectral trade-off between aliasing of the signal at the boundary edges while constraining it within a region of interest. While Slepian functions have previously been applied to geodetic and crustal magnetic data, this work applies Slepian functions to flows on the core-mantle boundary. There are two main reasons for restricting secular variation or flow models to certain parts of the core surface: 1) we have reason to believe that different dynamics operate in different parts of the core, such as under LLSVPs; and 2) modelled flow is ambiguous over certain parts of the surface when applying flow assumptions.

In this work, we apply altitude-cognizant Slepian functions to core flow models by directly inverting from satellite virtual observatory secular variation data into regions of interest. We successfully demonstrate the technique and current short comings by showing whole core surface flow models, flow within a chosen region, and its corresponding complement. Unwanted spatial leakage is generated at the region edges in the separated flows but to less of an extent than when using spherical Slepian functions on existing flow models. The limited spectral content of core flows is responsible for most, if not all, of this leakage. We present ongoing investigations into the leakage, and to highlight considerations when applying Slepian functions to core surface flow modelling.

KEYWORDS : regional core flow, spherical slepian functions

Variations of the magnetic declination in Gdansk and London

CORRESPONDING & PRESENTING AUTHOR:

Mikolaj Zawadzki, Institute of Geophysics/Faculty of Physics/University of Warsaw, Poland

In the 17th century, the Polish astronomer Jan Heweliusz and the English astronomer Henry Gellibrand independently measured the declination of the Earth's magnetic field. These types of measurements have been made before, but those made by these two scholars were characterized by their ability to do the right thing interpretation of variations of magnetic declination over time. Heweliusz did a lot long, decades-long measurement series, and Gellibrand compared its measurement with by measurements of other researchers, including Edmund Gunter's research.

Heweliusz was the first person, mentioned that the phenomenon of variations of declination of the Earth's magnetic field is a natural phenomenon. Gellibrand made an identical interpretation these results. Before the time of Heweliusz it was believed that the phenomenon of magnetic declination is caused by an error in the measuring device. Today we can compare the historical research with the contemporary model of declination gufm1 and IGRF.

The declination studies carried out five times in Gdansk were compared by Heweliusz in 1628, 1632, 1642, 1670, 1682 and by Edmund Halley in year 1679 with the gufm1 model. The analysis of these data was aimed at verifying the validity gufm1 model assuming that the research of Jan Heweliusz and Edmund Halley as scientists of high reputation and achievements are characterized by high precision, significantly higher than the studies on which the gufm1 model was based. These studies can be an introduction to further research about the history of declination measurements.

KEYWORDS :   declination, gufm1, IGRF

Sr No: 151

Insights from geodynamo simulations on palaeosecular variation models (by invitation)

CORRESPONDING & PRESENTING AUTHOR:

Richard Bono, University of Liverpool, UK

Andrew Biggin, University of Liverpool, UK

Christopher Davies, University of Leeds, UK

Courtney Sprain, University of Florida, USA

Domenico Meduri, Institut de Recherche en Astrophysique et Planétologie, France

Geodynamo simulations have the potential to provide insights into core processes which generate the geomagnetic field, however, palaeomagnetic observations are necessary to ensure that models realistically simulate the geomagnetic field. We have established a new set of quantitative criteria (QPM) which assess whether a simulation can reproduce palaeomagnetic observations for the past 10 million years. By applying our criteria, we identified a suite of geodynamo simulations which are 'Earth-like' based on palaeosecular variation observations spanning the past 10 million years. We show that common palaeosecular observations reflect fundamental changes in the dipolarity of the geomagnetic field. This insight allows for the construction of a new proxy for dipolarity, the relative contribution of the axial dipole to the non-axial dipole field strength, from observations of the magnitude of VGP scatter at the equator, which can be applied for the past 3 billion years. This proxy reveals that on long time scales, Earth's field dipolarity has remained remarkably stable, even during dramatic changes in other field behaviour, such as superchrons or hyper-reversing intervals. A second application of our dataset of 'Earth-like' dynamo simulations is in the development of statistical field models of palaeosecular variation. We find that dynamo simulations show a pronounced covariance between selected Gauss coefficients. A new family of statistical models, BB18, incorporates this covariance resulting in an improved reproduction of the observed latitudinal dependence in the VGP scatter. Our findings allow for testable predictions in both palaeomagnetic observations as well as constraints for the next generation of geodynamo simulations.

KEYWORDS :   palaeosecular variation, geodynamo simulations, statistical models

Sr No: 152

Geomagnetic semblance and dipolar-multipolar transition in top-heavy double-diffusive geodynamo models

CORRESPONDING & PRESENTING AUTHOR:

Theo Tassin, Institut de Physique du Globe de Paris, France

Thomas Gastine, Institut de Physique du Globe de Paris, France

Alexandre Fournier, Institut de Physique du Globe de Paris, France

Convection in the liquid outer core of the Earth is driven by thermal and chemical perturbations. The main purpose of this study is to examine the impact of double-diffusive convection on magnetic field generation by means of three-dimensional global geodynamo models, in the so-called ``top-heavy'' regime of double-diffusive convection, when both thermal and compositional background gradients are destabilizing. Using a linear eigensolver, we begin by confirming that, compared to the standard single-diffusive configuration, the onset of convection is facilitated by the addition of a second buoyancy source. We next carry out a systematic parameter survey by performing 79 numerical dynamo simulations. We show that a good agreement between simulated magnetic fields and the geomagnetic field can be attained for any partitioning of the convective input power between its thermal and chemical components. On the contrary, the transition between dipole-dominated and multipolar dynamos is found to strongly depend on the nature of the buoyancy forcing. Classical parameters expected to govern this transition, such as the local Rossby number -a proxy of the ratio of inertial to Coriolis forces- or the degree of equatorial symmetry of the flow, fail to capture the dipole breakdown. A scale-dependent analysis of the force balance instead reveals that the transition occurs when the ratio of inertial to Lorentz forces at the dominant length scale reaches 0.5, regardless of the partitioning of the buoyancy power. The ratio of integrated kinetic to magnetic energy provides a reasonable proxy of this force ratio.

KEYWORDS : dynamo: theories and simlations, core, numerical modelling

Sr No: 153

Impact Plasmas and Ancient Dynamos: Crustal Magnetization on the Moon and Mercury (by invitation)

CORRESPONDING & PRESENTING AUTHOR:

Rona Oran, Massachusetts Institute of Technology, USA

Banjamin Weiss, Massachusetts Institute of Technology, USA

Katarina Miljkovic, Curtin University, Australia

Catherine Johnson, University of British Columbia, Canada

Gabor Toth, University of Michigan, USA

Yuri Shprits, Helmholtz Center GFZ, Germany

Alexander Evans, Brown University, USA

The crusts of Moon, Mars, Mercury, and meteorite parent bodies contain remanent magnetization thought to be records of past core dynamos. The Moon constitutes a unique laboratory for understanding the dynamo process because of the apparently strong and long-lived magnetic field. In particular, paleointensity

estimates from Apollo samples seem to require a power source ~100 times larger than what could be continuously supplied by an Earth-like thermochemical dynamo. This motivated the alternative proposal that the source of magnetization is not a dynamo at all, but rather fields induced by the solar wind field and impact plasmas that are recorded by heated and shocked rocks. To assess this, we conducted the first study combining impact-physics and magnetohydrodynamic simulations. We found that impact-amplified fields are ~1, 000 times weaker than the Apollo paleointensities, demonstrating that the Moon was not magnetized solely by external fields. Because this still leaves the high paleointensities unexplained, we are currently exploring the possibility of a hybrid model in which impact plasmas could amplify a dynamo field. This model might also explain magnetization on other airless bodies.

KEYWORDS : impacts, plasmas, crustal magnetization

Sr No: 154

SYMPOSIUM : **D2 Planetary magnetic fields and geomagnetic secular variation**

Inversion for the quasi-geostrophic stream function in the fluid outer core from geomagnetic observations

CORRESPONDING & PRESENTING AUTHOR:
Ilya Firsov, Université Grenoble Alpes, France
Nicolas Gillet, Université Grenoble Alpes, France
Dominique Jault, Université Grenoble Alpes, France
Mioara Mandea, CNES Centre National d'Etudes Spatiales, France

We examine the inverse problem of determining the quasi-geostrophic stream function in the equatorial plane, using a geomagnetic field model at the core surface. We follow Holdenried-Chernoff et al. (2020), and derive the flow from a unique scalar function of the cylindrical polar coordinates. This stream function directly enters the radial induction equation at the core surface.

The quasi-geostrophic assumption theoretically ensures the unicity of the solution. Difficulties remain as large scale secular variation – rate of change of the core magnetic field – may result from the interactions involving the small scale velocity and magnetic fields. These difficulties can be partly alleviated because we are able to estimate the radial induction in such a way that it does not involve gradients in the velocity field. We still need to regularize the inversion, and compare the solutions obtained with various kinds of a priori information and observation error models.

Here, we present the first results obtained in estimating the quasi-geostrophic stream function from different field models.

KEYWORDS : geomagnetic secular variation, dynamics in the Earth's core, geomagnetism
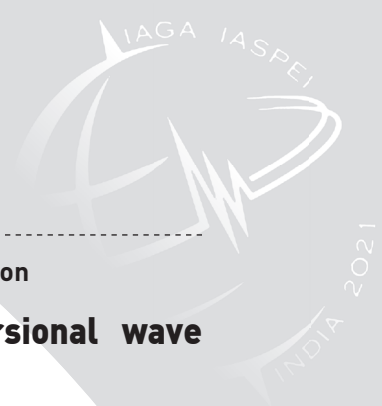
Sr No: 155

The effect of asymmetric background field on the torsional wave propagation in the Earth's core

PRESENTING AUTHOR:

Long Chen, ISTerre, France

Dominique Jault, ISTerre, France

Philip Livermore, University of Leeds, UK

CORRESPONDING AUTHOR:

Long Chen, ISTerre, France

Due to magnetic tension and a dominant Coriolis force, a disturbance in the Earth's fluid outer core could generate torsional waves. Recent inverse models have shown the variation of the length of the day is correlated with the period of torsional oscillations. An accurate description of torsional waves is therefore essential for the interpretation of geomagnetic secular variations. In this study, we focus on the influence of asymmetric background magnetic field, particularly at the tangent cylinder (TC) where an inward propagating wave splits into two. Many past studies on torsional waves have assumed symmetry, and treated the regions above and below the inner core on equal footing. Recent observations and analytical models of the outer core have suggested that the imposition of this symmetry is not realistic. We develop 1D models, as well as running complementary 3D numerical simulations assuming asymmetric background fields to quantify how much a torsional wave can be modified separately in the two regions inside TC. While the fluid viscosity and the magnetic diffusivity are small, they may play a role in the boundary layers at TC. I will discuss various new insights into the torsional wave propagation in this talk.

KEYWORDS :   torsional waves, asymmetry, tangent cylinder

D3 Coupling Processes in the Atmosphere-Ionosphere System

CONVENERS: Christina Arras
             Subramanian Gurubaran
             Loren Chang
             Petra Koucka Knizova

The objective of this symposium is to bring new insights into the understanding of the coupling processes in the atmosphere-ionosphere system. The symposium will address fundamental physical, chemical, and electrodynamical processes covering whole atmosphere system. The coupled effects can be expressed in terms of the modulation of waves from the lower to the upper atmosphere as well as from low- to high-latitudes, electrodynamic and compositional changes, plasma drifts, electric fields and plasma irregularities at different latitudinal regions of the globe due to the varying energy inputs.

The manner in which the couplings take place due to varying energy inputs from the Sun and from the lower atmosphere is a question that is not completely understood. This symposium solicits papers dealing with experiments, observations, modelling and data analysis that describe the effects of atmospheric coupling processes within the whole atmosphere-ionosphere system.

Sr No: 156

Atmosphere-ionosphere response to fireballs revealed by VLF/LF transmitter signals

CORRESPONDING & PRESENTING AUTHOR:

Takeru Suzuki, Chiba University, Graduate School of Science and Engineering, Japan

Hiroyo Ohya, Chiba University, Graduate School of Science and Engineering, Japan

Fuminori Tsuchiya, Tohoku University, Japan

Kazuo Shiokawa, Nagoya University, Jpan

Hiroyuki Nakata, Chiba University, Japan

There are several studies for ionospheric variations associated with fireballs based on GPS-TEC data(e.g., Perevalova et al., 2015). However, few quantitative studies for the D-region ionosphere associated with meteors and fireballs have been reported. In this study, we investigate the variations in the D-region ionosphere during a fireball occurred in Hokkaido at 11:55:55 UT on 18 October, 2018, using VLF/LF transmitter signals. The transmitters used in this study were JJY40kHz (Fukushima, Japan, 37.37° N, 140.85° E), JJY60kHz (Saga, Japan, 33.47° N, 130.18° E), and JJI (Miyazaki, Japan, 22.2 kHz, 32.05° N, 130.82° E). The receiver was located at RKB (Rikubetsu,, Japan, 43.45° N, 143.77° E). Periodic variations of 100-200 s were identified by a wavelet transformation of the signal intensities for the JJY40kHz-RKB, JJY60kHz-RKB, and JJI-RKB paths at about five minutes (12:01 UT) after the fireball. We consider that these variations of intensity were caused by the D-region variations due to acoustic waves in the atmosphere excited by the fireball. If the acoustic waves were excited at the vanishing end point (25 km altitude) of the fireball, the estimated arrival time (311 s) of the acoustic waves roughly matched with the onset of the VLF/LF variations. From the onset of the VLF/LF variations, we estimated the location where the variations in the VLF/LF intensity along the paths. The estimated location was close to the RKB, therefore the acoustic waves obliquely propagated from the vanishing end point up to the D-region height at the south point of the RKB receiver.

KEYWORDS : atmosphere-ionosphere, fireball

Sr No: 157

Coupling of the Ionospheric Plasma as investigated using OI 630 nm Emissions from Low- and Off-equatorial Latitude locations in Indian Longitudes

CORRESPONDING & PRESENTING AUTHOR:

Sovan Saha, Physical Research Laboratory, India

Duggirala Pallamraju, Physical Research Laboratory, India

Rupesh Ghodpage, Indian Institute of Geomagnetism, India

OI 630 nm (red line) nightglow emissions are good tracers to understand the behaviour of the upper atmosphere. These measurements were made from Mt. Abu (24.6 N, 72.7 E, 16 Mag N), a low-latitude location in Indian longitudes using a High Throughput Imaging Echelle Spectrograph (HiTIES). Various types of nocturnal emission variations have been observed. A study carried out to investigate the fluctuations

in the nocturnal emissions that persist throughout the night reveal that they were concurrent with the presence of spread F irregularities as observed using a digisonde operating from Ahmedabad (23.0 N, 72.6 E, 15 Mag N). All-sky imager observations from Kolhapur (16.8 N, 74.2 E, 8.2 Mag N), which is an off-equatorial location between the magnetic equator and Mt. Abu that lies almost in the same magnetic longitude of Mt. Abu, are compared with the optical emissions that are obtained from Mt. Abu. The depletions in emissions observed in the nightglow emissions over Mt. Abu match with the plasma depletions observed in the all-sky images, which reveal that the plasma depletions observed over Kolhapur extend to the latitudes beyond Mt. Abu. The field line mapping indicates that on such occasions the bubbles have reached to an altitude of over 800 km over the dip equator. In this background, both meridional and zonal scale sizes and the dynamics of the plasma bubble, both in the meridional and zonal direction, have been investigated. These results will be discussed in the context of low and equatorial coupling of ionospheric plasma.

KEYWORDS : OI 630 nm nightglow, plasma irregularities, equatorial-low latitude coupling

Sr No: 158

SYMPOSIUM : **D3 Coupling Processes in the Atmosphere-Ionosphere System**

Stratospheric jet stream as a possible source for the enhanced short-period variability in the ionosphere, upper mesosphere and stratosphere during winter months (by invitation)

CORRESPONDING & PRESENTING AUTHOR:

Anna Yasyukevich, Institute of solar-terrestrial physics SB RAS, Russia

Vera Sivtseva, Yu.G. Shafer Institute of Cosmophysical Research and Aeronomy SB RAS, Russia

Irina Medvedeva, Institute of solar-terrestrial physics SB RAS, Russia

Marina Chernigovskaya, Institute of solar-terrestrial physics SB RAS, Russia

Petr Ammosov, Yu.G. Shafer Institute of Cosmophysical Research and Aeronomy SB RAS, Russia

Galina Gavrilyeva, Yu.G. Shafer Institute of Cosmophysical Research and Aeronomy SB RAS, Russia

We've performed a joint analysis of the short-term variability (within the periods of several hours) in the ionosphere, upper mesosphere and stratosphere at middle and high latitudes. The study is based on the data of Total Electron Content (TEC) and measurements of OH rotational temperature at mesopause as well as ERA-Reanalysis data collected for more than 5-year period. We show that the variability experiences a clear seasonal variation both in the ionosphere and at the mesopause. The variability maximum is observed regularly in winter months with mean values which up to 5-6 times exceeds ones during the summer period. These seasonal changes do not correlate with geomagnetic and solar activities. As a possible source for revealed increase in the variability in winter we consider a high-speed jet stream that appears in the winter subpolar stratosphere. We've developed an index for estimating the level of stratosphere variability. The index is based on the Era Reanalysis data. We show that variability in the stratosphere, assessing with the proposed index, experience the similar regular seasonal variation with a maximum during winter months and has its highest values at subpolar regions where the jet stream evolves. We show that there is a clear correlation between the indexes of variability in the mesosphere, ionosphere and the stratosphere. Our results indicate a strong coupling between the short-period variability in the ionosphere, in the upper mesosphere, and in the subauroral stratosphere. The study is supported by the Russian Science Foundation Grant No. 20-77-00070.

KEYWORDS : ionosphere, variability, jet stream
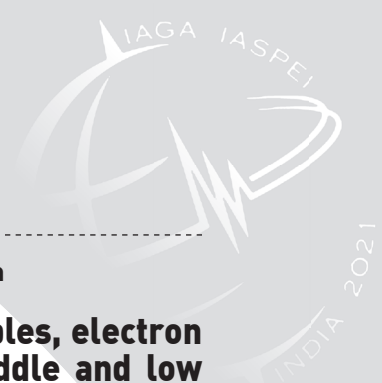
Sr No: 159

A comparison of global distributions between magnetic ripples, electron density fluctuations in the ionosphere and rain fall in middle and low latitudes

CORRESPONDING & PRESENTING AUTHOR:
Toshihiko Iyemori, Kyoto University, Japan
Tadashi Aoyama, Kyoto University, Japan
Yoshihiro Yokoyama, Kyoto University, Japan

Magnetic ripples are small-scale magnetic field variations perpendicular to geomagnetic main field observed along the orbit of low altitude satellites such as the CHAMP or the Swarm satellites in middle and low latitudes (e.g., Nakanishi et al., 2014; Iyemori et al., 2015). They are the spatial structure with scale about a few tens of km - a few hundred km caused by small scale field-aligned currents, and their amplitude depends on the ionospheric conductivities. The electron density (Ne) fluctuations having a similar scale with that of magnetic ripples are observed frequently also in middle or low latitude on dayside along the orbit of the Swarm satellites. However, the location and wave length of Ne fluctuations slightly differ from that of magnetic ripples on the satellite orbits. The cause of magnetic ripples is inferred to be ionospheric dynamo caused by short period atmospheric waves propagated from lower atmosphere. The cause of the Ne fluctuations could also be the atmospheric waves or it could be generated by a plasma instability in the ionosphere. To investigate the generation mechanism of Ne fluctuation, we compare their characteristics with those of magnetic ripples. We also compare their global amplitude distributions with that of rain fall published by JAXA/GSMaP project assuming that the atmospheric waves generated in the troposphere are the source of the magnetic ripples and the Ne fluctuations, and assuming that the rain fall could be an indicator of atmospheric convective motion.

KEYWORDS :   magnetic ripple, electron density, rain fall

Sr No: 160

Thunderstorm Ground Enhancement (TGE) events observed from Tirunelveli, India

CORRESPONDING & PRESENTING AUTHOR:
Gauri Datar, Indian Institute of Geomagnetism, India
Geeta Vichare, Indian Institute of Geomagnetism, India

The existence of a strong electric field in the thunderclouds is known for more than a century; however, many electromagnetic processes associated with it in the atmosphere are not yet clearly understood. It has been known that lightning produces gamma-rays. Recently, thunderstorm ground enhancement (TGE) events have become a subject of interest. A TGE is an enhancement in gamma-ray, electron, and neutron fluxes observed on the ground and can last for several minutes to hours. Gamma-rays detected by a NaI (Tl) detector located near sea level at Tirunelveli, India (near-equator) are used to study TGE events. The present study examines the occurrence of lightning flashes over Tirunelveli along with the enhancements observed in gamma-ray counts and near-surface electric field measurements. This study may help to understand the mechanism of a TGE from a location very different from the previous studies.

KEYWORDS :   atmospheric electric field, TGE, gamma-rays

Sr No: 161

Day-to-day variabilities of Equatorial Electrojet caused by Planetary Waves in the Mesosphere-Lower Thermosphere Region

CORRESPONDING & PRESENTING AUTHOR:
Subramanian Gurubaran, Indian Institute of Geomagnetism, India
Ashish Jadhav, Indian Institute of Geomagnetism, India
Parashram Patil, Indian Institute Of Geomagnetism, India
Rupesh Ghodpage, Indian Institute Of Geomagnetism, India
Rajiv Vhatkar, Shivaji University, India

The low latitude mesosphere-lower thermosphere-ionosphere (MLTI) region forms a coupled system with many of the wave dynamical processes propagating from below influence the ionospheric phenomena to such an extent that the quiet time ionospheric variabilities are often attributed to the waves propagating from below. The day-to-day variability of equatorial electrojet (EEJ) still remains an unresolved issue, primarily due to the complex web of interactions caused by changes in mean winds, tides and planetary waves. In this work our focus is on planetary waves in the low latitude MLT region as we make use of simultaneous observations of geomagnetic field variations and mesospheric winds by medium frequency (MF) radar from Kolhapur (16.8N, 74.2E), India, spanning a period of 5 years (2014-2019). This paper presents recent findings on the role of dominant planetary waves in the low latitude MLTI coupling.

Sr No: 162

Influence of the semidiurnal lunar tide on the equatorial plasma bubble zonal drifts over Brazil

CORRESPONDING & PRESENTING AUTHOR:
Igo Paulino, UFCG, Brazil
Ana Roberta Paulino, UEPB, Brazil
Amauri Medeiros, UFCG, Brazil
Ricardo Arlen Buriti, UFCG, Brazil
Cristiano Max Wrasse, INPE, Brazil
Hisao Takahashi, INPE, Brazil

Using OI6300 airglow images collected over São João do Cariri (7.4°S, 36.5°W) from 2000 to 2007, the equatorial plasma bubble (EPB) zonal drifts were calculated. A strong day-to-day variability was observed in the calculations due to the complex dynamics of the nighttime thermosphere-ionosphere system near the equator. The present work investigated the contribution of the semidiurnal lunar tide (SLT) M2 during the whole period of observation. Influences of the seasons and solar activity on the amplitudes of the SLT tide were investigated as well. On average, the SLT contributes with 5.6% to the variability of the EPB drifts, i.e., it presents an amplitude of 3.1 m/s. The amplitude of the SLT was stronger during the high solar activity reaching over 10% of the average of the EPB zonal drifts. Regarding the seasons, during the summer months the amplitude of the SLT was twice larger (12%) compared to the equinox ones. The results suggest that there are better conditions for the vertical propagation of the SLT when it experiments high temperatures.

Sr No: 163

Ionospheric effects of the 2016 Mt. Aso volcanic eruption based on subionospheric LF observations

CORRESPONDING & PRESENTING AUTHOR:

Hiroyo Ohya, Chiba University, Japan

Yuhi Orito, Chiba University, Japan

Fuminori Tsuchiya, Tohoku University, Japan

Masayuki Yamamoto, Kochi University of Technology, Japan

Hiroyuki Nakata, Chiba University, Japan

Akimasa Yoshikawa, Kyushu University, Japan

Several studies for the F-region ionosphere associated with volcano eruptions based on GPS-total electron content (TEC) data reported that acoustic waves excited by volcano eruptions reach up to the F-region ionosphere and caused F-region perturbations (e.g., Heki, 2006). However, little studies on the D-region ionosphere associated with volcano eruptions have been reported. In this study, we investigate the D-region ionospheric effects of 2016 eruptions of Mt. Aso (32.89N, 131.08E), Japan, using intensity of low frequency (LF, 30-300 kHz) transmitter signals. The LF propagation paths used in this study were JJY (60 kHz) - Sasaguri (SGR, Japan, Kyushu University), JJY (40 kHz) - SGR, and BPC (68.5 kHz) -SGR. Mt. Aso erupted at 16:46 UT on 7 October, 2016. The volcanic explosivity index (VEI) was 3 out of 8, and the eruption height was 11 km. The LF intensity on all paths varied with frequency of 2-5 mHz based on wavelet spectra after the eruptions. We compared the perturbations with atmospheric pressure data obtained by the Kochi university of Technology Infrasound Sensor Network, and seismic waves in the NIED F-net data. The atmospheric pressure and vertical velocity of the seismic waves had the similar frequencies of 3-6 mHz during 16:46-17:20 UT. These similar frequencies suggest that the perturbations would be caused by acoustic resonance between the Earth's surface and lower thermosphere, or by acoustic and atmospheric gravity waves generated by the volcanic eruptions. In the presentation, we will discuss the cause of the LF perturbations in more detail.

KEYWORDS : LF transmitter signals, D-region ionosphere, volcanic eruptions

Sr No: 164

D-region ionospheric signatures associated with the 2015 Nepal earthquake using VLF/LF transmitter signals

CORRESPONDING & PRESENTING AUTHOR:

Tekkan Akashi, Chiba university, Japan

Hiroyo Ohya, Chiba University, Japan

Fuminori Tsuchiya, Tohoku University

Kenro Nozaki, The University of Electro-Communications, Japan

Hiroyuki Nakata, Chiba University, Japan

In the D-region ionosphere, oscillations of LF (low frequency, 30-300 kHz) transmitter signals with a period of 100 s were reported about five minutes after mainshock of the 2011 Tohoku earthquake [Ohya et al.,

JGR, 2018]. This is only one report for coseismic disturbances in the D-region ionosphere. In this study, we investigate the D-region ionospheric variations associated with the 2015 Nepal earthquake using VLF (very low frequency, 3-30 kHz)/LF transmitter signals that reflect in the D-region ionosphere. The mainshock of the Nepal earthquake (Mw 7.9) occurred at 06:11:26 UT on April 25, 2015. The propagation path was BPC (68.5 kHz, 34.63°N, 115.83°E) - TKN (Takine, Fukushima, 37.34°N, 140.67°E). Intensity and phase were observed with a sampling time of 0.1 s. We compared between the VLF/LF transmitter signals and vertical velocity data of seismometers provided by IRIS (Incorporated Research Institutions for Seismology), USA. Based on wavelet analysis, a periodic component of about 100-300 s was seen in both the VLF/LF signals and seismic velocity at arrival time of acoustic waves excited by Rayleigh waves. The coherences between the VLF/LF variation and the seismic velocity were 0.91 and 0.85 for amplitude and phase, respectively, which were significant at the 95% confidence level. If the acoustic waves were excited at the midpoint of BPC-TKN propagation path by the Rayleigh waves that propagated horizontally from the epicenter, and propagate upward up to the D-region height 70 km, the arrival time of the acoustic waves was in good agreement with the VLF/LF oscillations.

KEYWORDS : ionosphere, earthquake, Nepal

Sr No: 165

Numerical modeling of the vertical propagation of atmospheric waves taking into account the neutral wind

CORRESPONDING & PRESENTING AUTHOR:

Yuliya Kurdyaeva, Pushkov Institute of Terrestrial Magnetism, Ionosphere, and Radio Wave Propagation RAS, Russia
Sergey Kshevetskii, Immanuel Kant Baltic Federal University, Russia

Tropospheric disturbances generate a wide range of atmospheric waves that have a significant impact on the upper atmosphere, causing variations of neutral gas and electron density. To give a detailed description of the scene in the atmosphere that is formed as a result of the propagation of waves from the lower atmosphere, the influence of the neutral wind cannot be excluded. Numerical modeling is an effective tool for studying wave processes in the atmosphere. In this work, the propagation of acoustic and internal gravity waves with different periods from local tropospheric thermal monochromatic sources into the upper atmosphere is numerically investigated taking into account several wind profiles. It is shown that the background wind affects the character of the propagation of internal gravity waves. This is manifested in the formation of a thermospheric quasi-waveguide during the start of generation waves of the tropospheric source and in a decrease in the amplitude of IGW propagating downwind and an increase in the opposite direction. Propagation of infrasonic waves forms a heated area, which is the source of secondary waves, which can be influenced by the background wind. Waves with frequencies close to the acoustic cutoff frequency and the Väisälä-Brandt frequency in this frequency range in a non-isothermal atmosphere of the wave can change their properties depending on the stratification.

KEYWORDS : atmospheric waves, thermosphere, neutral wind

Sr No: 166

Features of the generation of atmospheric waves by a meteorological source in the troposphere and relations with pressure variations at the Earth's surface

CORRESPONDING & PRESENTING AUTHOR:

Yuliya Kurdyaeva, Pushkov Institute of Terrestrial Magnetism, Ionosphere, and Radio Wave Propagation RAS, Russia
Sergey Kshevetskii, Immanuel Kant Baltic Federal University, Russia

The work theoretically studies the generation and propagation of waves from model tropospheric meteorological heat sources. It is analytically shown that the generation of internal gravity waves cannot occur without the generation of acoustic waves, and conversely. Due to the resonant properties of the atmosphere, high-frequency sources generate predominantly acoustic waves. Low-frequency sources generate principally internal gravity waves if they run long enough for the resonance properties of the atmosphere to occur. The problem of mistake appearing if the tropospheric source is replaced by a surface source, in which the pressure fluctuations on the surface are recorded pressure fluctuations caused by the tropospheric source is being explored using the numerical experiments. The results of a numerical study of the propagation of infrasonic and internal gravity waves from a local tropospheric heat source and from a boundary source showed that, if a tropospheric source operates at the frequencies of infrasonic waves, means the solutions to the problems of waves from a tropospheric source and from recorded oscillations of surface pressure coincide with sufficient accuracy for many practical applications.

Sr No: 167

Ionospheric variability induced by lower-lying atmosphere

CORRESPONDING & PRESENTING AUTHOR:

Petra Koucka Knizova, Institute of Atmospheric Physics, Czech Academy of Sciences, Czechia
Katerina Podolska, Institute of Atmospheric Physics, Czech Academy of Sciences, Czechia
Daniel Kouba, Institute of Atmospheric Physics, Czech Academy of Sciences, Czechia
Zbysek Mosna, Institute of Atmospheric Physics, Czech Academy of Sciences, Czechia
Katerina Potuznikova, Institute of Atmospheric Physics, Czech Academy of Sciences, Czechia

The ionosphere is permanently changing on a wide range of scales reflecting the variable amount of energy coming from above and coming from below. Upper atmosphere's variability is seen in fluctuations within the observed data on a wide range of scales. Most of the observed variations are intermittent wave/like oscillations with variable life time. Models of the system behavior based mostly on solar forcing capture only main features of ionospheric variability. The complications lay in the fact that ionosphere does not display same sensitivity to the external energy input during entire solar cycle and/or consequent cycles. Besides that, the geographical location seems to play an important role in the geographically conditioned ionospheric

response to the external forcing (solar and geomagnetic). State of ionosphere is significantly affected by the dynamics of lower laying atmosphere. Within the troposphere generation of internal waves is often related to meteorological phenomena. Internal atmospheric waves interact with themselves and/or with the undisturbed atmospheric flow in a complicated dynamical system with long-range dependencies. Our study indicate that not only short-term tropospheric variability impacts upper atmosphere. It seems that similar phenomena predominantly circulation pattern forming the particular type of the climate and related wave fields may be responsible for the observed time shifts in the ionospheric response to the external forcing (solar and geomagnetic).

KEYWORDS : Ionosphere, lower atmosphere, atmospheric waves

Sr No: 168

The role of the plasmaspheric waves in the occurrence of auroral-type sporadic E-layers over South Atlantic Magnetic Anomaly (SAMA) (by invitation)

CORRESPONDING & PRESENTING AUTHOR:

Ligia Da Silva, State Key Laboratory of Space Weather, National Space Science Center, Chinese Academy of Sciences/ National Institute for Space Research, China

Jiankui Shi, National Space Science Center, Chinese Academy of Sciences, China

Laysa Resende, State Key Laboratory of Space Weather, National Space Science Center, Chinese Academy of Sciences/ National Institute for Space Research, China

Oleksiy Agapitov, University of California, USA

Christina Arras, GFZ German Research Centre for Geosciences, Germany

Livia Alves, National Institute for Space Research, Brazil

Inez Batista, National Institute for Space Research, Brazil

David Sibeck, NASA, USA

Luis Eduardo Vieira, National Institute for Space Research, Brazil

Juliano Moro, State Key Laboratory of Space Weather, National Space Science Center, Chinese Academy of Sciences/ National Institute for Space Research, China

Chi Wang, National Space Science Center, Chinese Academy of Sciences, China

Jose Paulo Marchezi, State Key Laboratory of Space Weather, National Space Science Center, Chinese Academy of Sciences/ National Institute for Space Research, China

Claudia Medeiros, National Institute for Space Research, Brazil

Vinicius Deggeroni, National Institute for Space Research, Brazil

Ana Maria Inostroza, National Institute for Space Research, Brazil

Zhengkuan Liu, National Space Science Center, Chinese Academy of Sciences, China

Hui Li, National Space Science Center, Chinese Academy of Sciences, China

Clezio Denardin, National Institute for Space Research, Brazil

The solar wind structures potentially generating strong storms can directly impact the Earth's magnetosphere, affecting the upper atmosphere's ionization through the charged particle precipitation, especially at high-latitudes and the South Atlantic Magnetic Anomaly (SAMA). The impact of low-energy electron precipitation on the high-latitude ionosphere is well understood since the 60's decade. On the other hand, the impact of these particles' precipitation in the ionosphere over the SAMA lacks more information. Therefore, a short period under the influence of the strong geomagnetic-storm associated with an Interplanetary Coronal Mass Ejection is selected for analysis. The Van Allen Probe B recorded the signature of the plasmaspheric Hiss and Magnetosonic wave activities under this solar wind structure's influences. These waves can have interacted
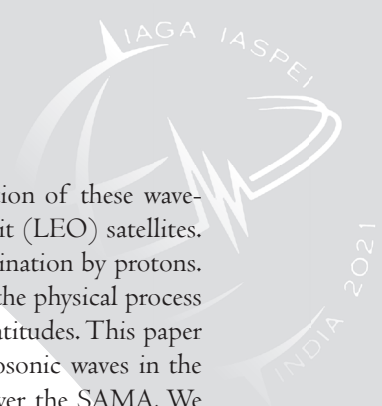
with the low-energy electron flux in the inner radiation belt. Generally, the confirmation of these wave-particle interactions is done by detection of the particles through the Low Earth Orbit (LEO) satellites. For this study, using the LEO's electron detectors is impossible due to the high contamination by protons. It means that the ionization in the Brazilian ionosphere needs more attention regarding the physical process related to the generation of the auroral-type sporadic E-layer, which is unusual in low-latitudes. This paper proposes to discuss the pitch angle scattering mechanism driven by Hiss and Magnetosonic waves in the inner radiation belt during the occurrences of the low-energy electron precipitation over the SAMA. We will use the measurements in situ and ground-based to discuss these physical processes in this region for the first time.

KEYWORDS :   south atlantic magnetic anomaly, plasmaspheric waves, auroral-type sporadic e-layers

Sr No: 169

Sporadic E layer properties at northern polar latitudes

CORRESPONDING & PRESENTING AUTHOR:

Christina Arras, GFZ Potsdam, Germany

Ankur Kepkar, TU Berlin, Germany

Sahar Sobhkhiz Miandehi, GFZ Potsdam, Germany

Jens Wickert, GFZ Potsdam, Germany

GPS radio occultation measurements are used to observe the occurrence and the intensity of sporadic E (Es) layers on a global scale. We analysed data acquired by the FORMOSAT-3/COSMIC satellites. Since their launch in April 2006, the satellites collected about seven million of globally distributed radio occultation profiles.

For our study, we use ionosonde data at midlatitude and low latitude stations as well as Signal-to-Noise Ratio (SNR) GPS L1 radio occultation observations. The SNR is sensitive to vertical changes in the electron density which is reflected in large fluctuations in the according altitude range of the profile. Therefore, vertically thin ionospheric phenomena like sporadic E layers can be identified using numerical filtering techniques.

Currently, the radio occultation time series from FORMOSAT-3/COSMIC comprises 14 years covering more than one solar cycle. In this study, we focus on sporadic E layers that appear in the northern polar region (60°N – 90°N). We will present a climatology of the polar Es events and will discuss their temporal and spatial occurrence. Generally, polar Es layers show a different local time distribution compared to midlatitude sporadic E events which might be caused by electric fields influencing their formation process.

KEYWORDS :   sporadic E, radio occultation, ionosphere

Sr No: 170

Meteorological Storm Influence on the Ionosphere Parameters in Baltic Region

CORRESPONDING & PRESENTING AUTHOR:

Olga Borchevkina, WD IZMIRAN, Russia

Ivan Karpov, WD IZMIRAN, Russia

Mikhail Karpov, WD IZMIRAN, Russia

We present the observations of ionospheric parameters in Baltic region during meteorological storms in 2010-2020. The results of a comprehensive experimental study showed that the passage of meteorological storms had a significant impact on the TEC and foF2 from the median values can reach 1.5–2 times the standard deviations of the value. On days of a meteorological storm, significant changes were noted in the dynamics of the E-layer's critical frequency. When the speed of wind gusts 15 m/s and higher, there was a significant decrease in foEs below the sensitivity threshold of the ionosonde. The observed phenomena at heights of the E region were apparently caused by the propagation of AGWs generated by convective processes in the lower atmosphere during periods of a meteorological storm. Spectral analysis of TEC variations revealed an increase in the amplitudes of ionospheric variations 10–16 min over the area of a meteorological storm. The analysis allowed us to conclude that ionospheric perturbations during the meteorological perturbation were caused by increased AGW generation processes in the lower atmosphere. To interpret the observed disturbances in the upper atmosphere, the experimental measurements are compared with the results of model calculations obtained with the Global Self-Consistent Model of Thermosphere—Ionosphere—Protonosphere (GSM TIP). The results of the GSM TIP modeling with the inclusion of additional thermospheric sources simulating the processes of AGWs dissipation show changes in the ionosphere above the AGWs source.

KEYWORDS : acoustic gravity waves, atmosphere-ionosphere coupling, meteorology disturbances

Sr No: 171

Investigation of Thermosphere-Ionosphere Dynamics Using a Whole Atmosphere Data Assimilation Model

CORRESPONDING & PRESENTING AUTHOR:

Fazlul Laskar, University of Colorado Boulder, USA

Nicholas Pedatella, National Center for Atmospheric Research, USA

Mihail Codrescu, National Oceanic and Atmospheric Administration, USA

Richard Eastes, University of Colorado Boulder, USA

Scott Evans, Springfield, USA

Alan Burns, National Center for Atmospheric Research, USA

William Mcclintock, University of Colorado Boulder, USA

Global-scale Observations of Limb and Disk (GOLD) scans the Earth's disk from geostationary orbit for about 18.5 hours a day, from 0610 UT to 0040 UT. The daylight disk measurements of N2 Lyman-Birge-Hopfield (LBH) bands can be used to retrieve thermospheric neutral temperatures over about one fourth of the globe. The present investigation assesses the impact of GOLD disk temperatures on the Whole Atmosphere Community Climate Model with thermosphere-ionosphere eXtension (WACCMX) using Data Assimilation Research Testbed (DART) framework. Two Observing System Simulation experiments (OSSEs), one with and one without assimilating GOLD thermospheric neutral temperatures, show that assimilating GOLD thermospheric temperatures decreases the model bias and spread by 71% and 49%, when compared to forecast. But compared to lower atmosphere only assimilation the bias and spread is improved by 94% and 83%. Specification of the amplitudes of global DW1 and local diurnal tide in WACCMX+DART are improved by about 7% and about 17%, respectively, when GOLD temperatures are assimilated. Improvements are also observed in ionospheric states and the model states at times and locations where there are no GOLD observations. These results will be presented along with some results from assimilation of actual GOLD disk neutral temperature observations.

KEYWORDS : thermosphere ionosphere coupling, data assimilation

Sr No: 172

All-Sky Imaging Observations of Mesospheric Bore and Ripple events over low latitudes.

CORRESPONDING & PRESENTING AUTHOR:

Nilesh Chauhan, Indian Institute of Geomagnetism, India

Subramanian Gurubaran, Indian Institute of Geomagnetism, India

Krishna Sarkar, Magnetic Observatory, Silchar, Assam, India

All-sky airglow imaging observations of mesospheric bores over Silchar (24.68°N, 92.76°E) and ripple events over Panhala (16.81°N, 74.11°E), India are presented. An All Sky Airglow Imager is operated round the year at the Silchar Magnetic Observatory of Indian Institute of Geomagnetism. Another imager was operated in campaign mode at Panhala. The present work focuses on observations carried out on clear sky nights during January 2020 at Silchar and March 2021 at Panhala. On one of the nights of observations from Silchar, an undular mesospheric bore was observed in OI (557.7nm), sodium (589.3nm) and OH airglow emissions. The bore front appeared bright in OH emission, while it appeared dark in the OI (557.7nm) emission thus displaying a complementarity effect. The observations from Panhala revealed a ripple event of remarkable intensity on one of the nights during the specially conducted campaign. The ripples were observed in OI (557.7nm) emission and they had their phase aligned perpendicular to the background gravity wave front, suggesting that they were generated due to convective instability. This case study on the ripple event was further investigated using SABER temperature measurements and the wind observations from the nearby MF radar. Results from the studies on both kinds of atmospheric disturbances will be presented and discussed.

KEYWORDS : all-sky airglow imaging, mesospheric bore, gravity wave

Sr No: 173

Modulation of ionospheric E-region currents at Indian and African sectors in response to 2013 Sudden Stratospheric Warming

CORRESPONDING & PRESENTING AUTHOR:

Phani Chandrasekhar Nelapatla, CSIR-National Geophysical Research Institute, India

Oluwafisayo Owolabi, Center for Atmospheric Research, NSRDA, Nigeria

Using nine magnetometers data from equatorial and off-equatorial sites in the Indian and African sectors, we investigated the longitudinal dependence of the ionospheric E-region currents during the 2013 major sudden stratospheric warming (SSW) event. The ionospheric E-region currents under the purview of this study are Equatorial electrojet (EEJ), Counter electrojet (CEJ) and Solar quiet (Sq) currents. The results show depletions in EEJ amplitude at both longitudinal sectors during the SSW peak phase, with the significant EEJ depletion in the African EEJ site resulting in CEJ events, unlike the Indian longitudinal sector. On comparing the occurrence of CEJ events in both longitudinal sectors in all the SSW phases, the occurrence frequency of CEJs was found to be more in the African EEJ site with higher amplitude than that of the Indian EEJ sites in all the SSW phases. Unusual enhanced Sq modulation was also observed in the Indian sector, compared to the African sector. Instances of strong and weak correlations were observed between the sites of different longitudinal spacing of the same region relative to the longitudinal spacing of another region during different phases of SSW, highlighting the longitudinal dependence of the E-region ionospheric current system. We also found that the prominent EEJ and CEJ longitudinal variability in the Indian and African sectors was strictly confined to the SSW peak and descending (recovery) phase.

KEYWORDS : sudden stratosphere warming, equatorial electrojet, equatorial counter electrojet

---

Sr No: 174

Dynamical coupling between the low-latitude lower thermosphere and ionosphere via the non-migrating diurnal tide as revealed by concurrent satellite observations and numerical modeling

CORRESPONDING & PRESENTING AUTHOR:

Federico Gasperini, ASTRA LLC, USA

The diurnal, eastward propagating tide with zonal wavenumber 3 (DE3) is an important tidal component due to its ability to effectively couple the ionosphere-thermosphere and the tropical troposphere regions. In this work, we present the first results of the zonal wavenumber 4 (WN4) structure from the Scintillation Observations and Response of The Ionosphere to Electrodynamics (SORTIE) CubeSat mission. Our analyses show the existence of a pronounced zonal wavenumber 4 (WN4) structure in the low-latitude ionosphere during May 27 - June 5, 2020 in concurrent in-situ ion number density measurements from the SORTIE and the Ionospheric Connection Explorer (ICON) satellites. Temperature observations from the Thermosphere Ionosphere Mesosphere Energetics Dynamics Sounding of the Atmosphere using Broad band Emission Radiometry (TIMED/SABER) instrument and output from the Specified Dynamics Whole Atmosphere Community Climate Model with thermosphere and ionosphere eXtension (SD/WACCM-X) demonstrate that the ionospheric WN4 structure is driven by the upward-propagating DE3 tide

KEYWORDS : SORTIE, ICON, DE3
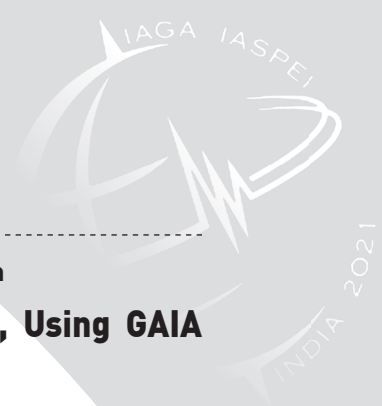
Sr No: 175

Atmospheric Tides Signature Detection in Mid-latitude Es, Using GAIA Model and FORMOSAT-3/COSMIC Radio Occultation Data

CORRESPONDING & PRESENTING AUTHOR:

Sahar Sobhkhiz Miandehi, GFZ German Research Centre for Geosciences, Germany

Yosuke Yamazaki, GFZ German Research Centre for Geosciences, Germany

Christina Arras, GFZ German Research Centre for Geosciences, Germany

Yasunobu Miyoshi, Kyushu University, Jpan

Hiroyuki Shinagawa, NICT, Japan

Sporadic E (Es) is a transient phenomenon where thin layers of enhanced electron density appear in the ionosphere E region (90-120 km altitude). Es can influence radio wave propagation, and its global characteristics have been of great interest to radio communications and navigations. Ions will converge at E-region heights due to neutral wind shear induced by atmospheric tides, forming the so-called Es layers.

This research aims to examine how neutral wind shear influences Es occurrence. For this purpose, radio occultation data of FORMASAT-3/COSMIC, which provide complete global coverage for Ionospheric investigations, have been used. Moreover, GAIA (Ground-to-topside model of Atmosphere and Ionosphere for Aeronomy) model data have been employed to study neutral wind, neutral atmospheric temperature, and composition. The results show both lunar and solar tidal signatures in Es occurrence. The tidal signatures are longitudinally dependent. The effect of non-migrating tides and the modulation of migrating tidal signatures by a zonally changing geomagnetic field are discussed as potential causes.

KEYWORDS :   sporadic E

Sr No: 176

Effects of lower thermospheric winds on the equatorial electrojet

CORRESPONDING & PRESENTING AUTHOR:

Yosuke Yamazaki, GFZ German Research Centre for Geosciences, Japan

Brian Harding, University of California Berkeley, USA

Claudia Stolle, GFZ German Research Centre for Geosciences, Germany

Juergen Matzka, GFZ German Research Centre for Geosciences, Germany

Electric fields and currents in the dayside E-region ionosphere arise from collisional interactions between neutral and plasma particles, and thus understanding electrodynamic processes in the ionosphere can greatly benefit from simultaneous observations of neutral and plasma parameters. This study explores simultaneous observations of the equatorial electrojet (EEJ) from ESA's Swarm satellite mission and equatorial neutral winds in the lower thermosphere (95-180 km) from the Michelson Interferometer for Global High-resolution Thermospheric Imaging (MIGHTI) on NASA's Ionospheric Connection Explorer (ICON) mission. It is demonstrated that there are significant differences in the average zonal wind profiles between periods of eastward and westward EEJ. During the eastward EEJ, the equatorial zonal wind tends to be westward at all heights with small height variation, while during the westward EEJ, the equatorial zonal wind shows larger height variation with the wind being more eastward around 110 km and more westward around 140 km. The results suggest that the equatorial zonal wind plays a role for westward EEJ. The mechanism, by which the equatorial zonal wind influences the EEJ, will be discussed.

KEYWORDS :   EEJ, swarm, ICON/MIGHTI

D4 Advances in Mid, Low Latitude and Equatorial Aeronomy

CONVENERS: Paulo Roberto Fagundes

Geeta Vichare

Venkatesh Kavutarapu

Michael Pezzopane

Yosuke Yamazaki

Ionospheric electrodynamics at equatorial and low latitudes is controlled by the forcing from the lower atmosphere including the effects of SSW , tidal, planetary, and gravity waves; and by the forcing from the magnetosphere through penetration of disturbed time electric fields and neutral winds. The session focuses on the behavior of ionospheric phenomena occurring at equatorial to low latitudes including equatorial ionization anomaly, plasma irregularities, plasma bubbles and blobs, F3-layer, pre-reversal enhancement, etc., with the particular emphasis on the electric fields and current systems associated with solar quiet (Sq) and equatorial electrojet. Recent multi-instrument and multi-site observations, as well as, theoretical and simulation studies have advanced our understanding of these phenomena. Although this has substantially improved our current understanding of the ionospheric electrodynamics during quiet and disturbed periods, solar eclipse, solar flare, and sudden stratospheric warming events, there are still some outstanding questions and challenges, which need to be addressed. Presentations are solicited that focus on the physical understanding of these processes through observations and numerical simulation modeling, and unresolved problems therein.
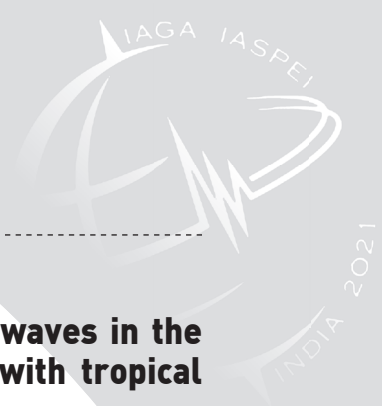
Sr No: 177

Observations of high frequency (20 mins-60 mins) gravity waves in the mesosphere and lower thermosphere and its connection with tropical convection over Tirunelveli and Kolhapur

CORRESPONDING & PRESENTING AUTHOR:

Krishnapriya K, Indian Institute of Geomagnetism, India

High frequency gravity wave is generated primarily due to deep convection and it plays vital role in the tropical middle atmospheric dynamics. We have acquired the Mesosphere and Lower Thermosphere (MLT) winds from MF radar during February – June 2019 over Tirunelveli and Kolhapur in order to examine the high frequency (20-60 mins) gravity waves generation and its propagation direction in the MLT region. The preliminary result shows that strong enhancement in the gravity wave variance in the meridional component over Tirunelveli, however, there is no significant gravity wave   activity over Kolhapur. In particular, an enhancement in the month of June is mainly associated with convection activity over Tirunelveli. The propagation direction of gravity wave activity is followed with convection traces over Tirunelveli. We obtained the mesosphere temperature observations from the Sounding of the Atmosphere using Broadband Radiometry (SABER) to confirm the presence of gravity wave activity during June 2019 and it could be a complementary to our results. Results from a detailed analysis of these observations will be presented and discussed in the context of the dynamics of the middle atmosphere.

KEYWORDS :   gravity waves, convection, M F radar

Sr No: 178

Study on different methods of obtaining the ROTI index on the Brazilian region (by invitation)

CORRESPONDING & PRESENTING AUTHOR:

Carolina Carmo, National Institute for Space Research, Brazil

Clezio De Nardin, National Institute for Space Research, Brazil

Cosme Figueiredo, National Institute for Space Research, Brazil

Laysa Resende, INPE/State Key Laboratory of Space Weather, China

Giorgio Picanco, National Institute for Space Research, Brazil

Paulo Barbosa, Salesian University Center of São Paulo (UNISAL), Brazil

Paulo Alexandre Nogueira, Federal Institute of São Paulo, Brazil

Juliano Moro, INPE/State Key Laboratory of Space Weather, China

Sony Chen, National Institute for Space Research, Brazil

Equatorial Plasma Bubbles (EPBs) are irregularities in the equatorial ionospheric plasma region. One way to observe this kind of irregularity is to calculate the variation of the Total Electron Content (TEC), known as Rate Of TEC Index (ROTI). In this way, we analyze five different methods of calculating the TEC and investigate which one is the best calculation to apply in ROTI in the Brazilian sector. To achieve this goal, we use a set of equipment to observe ionospheric irregularities such as GNSS receivers, ionosonde, and All-Sky imagers at equatorial and low latitudes. The results show that the most adequate and efficient method uses only the Carrier-Phase to calculate the TEC and consequently the ROTI index.

KEYWORDS :   ROTI, plasma bubble, TEC

SYMPOSIUM :   **D4 Advances in Mid, Low Latitude and Equatorial Aeronomy**

Short and long term variability of the lunar semidiurnal tide in the Brazilian ionosphere

Fabiano Araujo, Universidade Estadual da Paraíba, Brazil

Igo Paulino, UFCG, Brazil

Cristiano M. Wrasse, INPE, Brazil

Lourivaldo M. Lima, Universidade Estadual da Paraíba, Brazil

Paulo Batista, INPE, Brazil

Inez Batista, INPE, Brazil

CORRESPONDING & PRESENTING AUTHOR:

Ana Roberta Paulino, Universidade Estadual da Paraíba, Brazil

Using the Total Electron Content over Brazil, the lunar semidiurnal tide was studied from 2011 to 2014. The results showed long and short periods of variation in the amplitude of the lunar semidiurnal tide. The annual component was dominant followed by the semiannual and triannual (~120 days), respectively. Among the short period oscillations in the amplitude of the lunar tide, the most pronounced ones were concentrated between 7-11 days. These oscillations were stronger around the equinoxes, in particular between September and November in almost all latitudes. In some years, as in 2013 and 2014, for instance, they reached large power spectral density in the winter hemisphere. These observed short period oscillations could be a result of a direct modulation of the lunar semidiurnal tide by planetary waves from the lower atmosphere or/and due to electrodynamics coupling of E and F region of the ionosphere. Salient features will be discussed in this work.

KEYWORDS :   lunar tide, TEC, planetary wave

SYMPOSIUM :   **D4 Advances in Mid, Low Latitude and Equatorial Aeronomy**

GPS-TEC Variability in Comparison with IRI-2016 Model at Northern EIA Crest during Solar Cycles 23-24 (2005-2019)

Chintan Jethva, Saurashtra University, India

CORRESPONDING & PRESENTING AUTHOR:

Mala Bagiya, Indian Institute of Geomagnetism, India

H. P. Joshi, Saurashtra University, India

Low latitude ionospheric variability over the period of ~15 years (2005 – 2019), comprising various phases of solar cycles 23 and 24, has been studied at the northern EIA crest region of Rajkot (geographic: 22.29°N, 70.74°E, geomagnetic average: 14.26°N) using Global Positioning System (GPS) – Total Electron Content (TEC) measurements and compared with the International Reference Ionosphere (IRI) – 2016 derived TEC. The salient features of this study are (i) IRI model mostly overestimates the observed ionospheric variability during noon time and underestimates the same during night time. (ii) Seasonal noon time bias was observed for the equinoctial months depending on the phase of the solar cycle, where the model underestimates
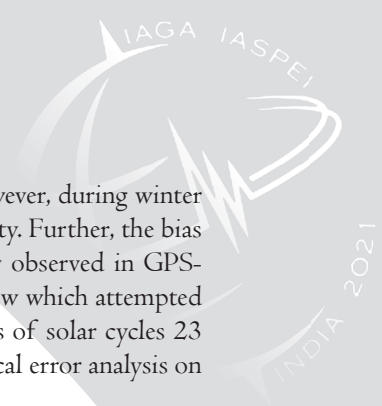
(overestimates) the observed ionospheric variations during high (low) solar activity. However, during winter the model overestimates observed noon time ionospheric TEC irrespective of solar activity. Further, the bias has been found to be least during summer. (iii) Winter anomaly has been prominently observed in GPS-TEC during the high solar activity period. The present study is probably one of those few which attempted to compare the low latitude TEC recorded over ~15 years encompassing various phases of solar cycles 23 and 24 and to our knowledge probably first of its kinds in providing an extensive statistical error analysis on the model derived TEC variations from those of the observed ones.

KEYWORDS :   GPS-TEC, low latitude ionosphere, EIA

Sr No: 181

Tidal signatures in sporadic E occurrence rates at low and middle latitudes

CORRESPONDING & PRESENTING AUTHOR:

Christoph Jacobi, Leipzig University, Germany
Friederike Lilienthal, Leipzig University, Germany
Yosuke Yamazaki, Helmholtz Centre Potsdam German Research Centre for Geosciences – GFZ, Germany
Sahar Sobhkhiz Miandehi, Helmholtz Centre Potsdam German Research Centre for Geosciences – GFZ, Germany
Christina Arras, Helmholtz Centre Potsdam German Research Centre for Geosciences – GFZ, Germany

We analyze sporadic E (Es) occurrence rates (OR) obtained from ionospheric radio occultation measurements by the FORMOSAT-3/COSMIC constellation. Maximum OR are seen at 95 - 105 km altitude at lower midlatitudes. Midlatitude Es are mainly due to wind shear in the presence of tides, and the strongest signals are a migrating diurnal and semidiurnal component. Especially at high latitudes of the southern hemisphere, nonmigrating components such as a diurnal westward wave 2 and a semidiurnal westward wave 1 are also visible. Near the equator, a strong diurnal eastward wavenumber 3 component and a semidiurnal eastward wavenumber 2 component occur in summer and autumn. Terdiurnal and quarterdiurnal components are weaker than the diurnal and semidiurnal ones.

KEYWORDS :   sporadic E, radio occultation, tides

Sr No: 182

Investigation of ionospheric response to 26 December 2019 solar eclise using observations and SAMI2 model simulations

CORRESPONDING & PRESENTING AUTHOR:

Rajesh Kumar Barad, Indian Institute of Geomagnetism, India
S Sripathi, Indian Institute of Geomagnetism, India

Solar eclipse is a unique phenomenon which impacts the atmosphere-ionosphere system and produces short period gravity waves. Here, impact of 26 December 2019 solar eclipse on the ionosphere are studied using both observations and simulations. Since this eclipse passed through Indian equatorial region, CADI

ionosonde located at Tirunelveli has been operated at a high resolution of 2 min. Results show that there is an increase in F-layer height of ~50 km during the eclipse maximum. Near eclipse maximum, strong blanketing Es-layer was observed at Tirunelveli with top frequency ~16 MHz. Same time, fmin also showed a decrease after eclipse maximum showing depletion of D-region ionization. Additional ionogram traces known as satellite traces (ST) were observed for the first time after the eclipse maximum and eclipse end from 04:10 UT to 04:20 UT and 06:24 UT to 06:36 UT respectively. GPS-TEC data as obtained from Tirunelveli and 8 IGS stations along and across the eclipse path are also analysed. A maximum of ~5 TECU decrease in TEC is observed on the eclipse day for IISC and TIRU stations. Periodogram analyses of TEC data showed the presence of wavelike structures with periodicities of 18-24 min for different stations. Simultaneous observations from NASA's Ionospheric connection explorer (ICON) satellite shows an increase and decrease in hmF2 and NmF2 which matches well with CADI, Tirunelveli respectively. These observations have been compared with the SAMI2 model simulations and are discussed in the light of current understanding of eclipse impact on the ionosphere.

KEYWORDS : solar eclipse, gravity waves, satellite traces

Sr No: 183

SYMPOSIUM : **D4 Advances in Mid, Low Latitude and Equatorial Aeronomy**

The Impact of the Disturbed Electric Field in the Sporadic E (Es) layer Development over Brazilian Region (by invitation)

CORRESPONDING & PRESENTING AUTHOR:

Laysa Resende, State Key Laboratory of Space Weather, NSSC/CAS, Beijing, China/National Institute for Space Research INPE,China

Yajun Zhu, State Key Laboratory of Space Weather, China Academy of Science, CAS, China

Jiankui Shi, 1State Key Laboratory of Space Weather, China Academy of Science, CAS, , China

Clezio Denardini, National Institute for Space Research INPE, Brazil

Inez Staciarini Batista, National Institute for Space Research INPE, Brazil

Giorgio Picanco, National Institute for Space Research INPE, Brazil

Juliano Moro, State Key Laboratory of Space Weather, China Academy of Science, CAS, Beijing, China, National Institute for Space Research INPE, China & Brazil

Ronan Chagas, National Institute for Space Research INPE, Brazil

Diego Barros, National Institute for Space Research INPE, Brazil

Sony Chen, National Institute for Space Research INPE, Brazil

Paulo Nogueira, Federal Institute of Education, Science and Technology of São Paulo

Vania Andrioli, 1State Key Laboratory of Space Weather, China Academy of Science, CAS, Beijing, China, National Institute for Space Research INPE, China

Alexander Carrasco, National Institute for Space Research INPE, Brazil

Regia Silva, National Institute for Space Research INPE, Brazil

Chi Wang, State Key Laboratory of Space Weather, China Academy of Science, CAS, China

Liu Zhengkuan, State Key Laboratory of Space Weather, China Academy of Science, CAS, China

E region electric fields during disturbed periods can cause anomalous Es layer behavior, which is observed in the digital ionosonde data. To investigate the influence of these electric fields in the Es layer development, we analyzed a set of 20 magnetic storms from 2015 to 2018 over Boa Vista (2.8°N, 60.7°W), São Luís (2.3°S, 44.2°W), and Cachoeira Paulista (22.41°S, 45°W). The electric field zonal components during the main and recovery phases of each magnetic storm are computed to study the corresponding characteristics of these Es seen in ionograms. Additionally, a numerical model (MIRE, Portuguese acronym for E Region Ionospheric Model) is used to analyze the Es layer dynamics modification around disturbed times. Using
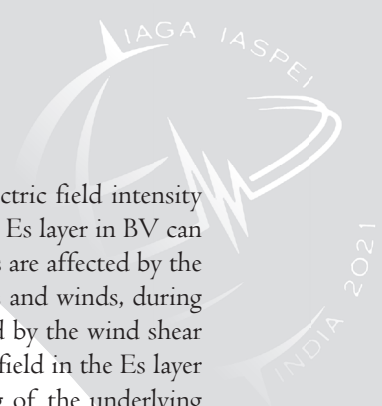
observation data and simulation, we were able to establish a threshold value for the electric field intensity for each region that can affect the Es layer formation. The results sustain that the strong Es layer in BV can be an indicator of the disturbed dynamo event. At SLZ, on the other hand, the Es layers are affected by the competition mechanisms of their formation, as equatorial electrojet (EEJ) irregularities and winds, during the main phase of the magnetic storm. Over CXP, the Es layer dynamics are dominated by the wind shear mechanism. Finally, this study provides new insights into the real impact of the electric field in the Es layer development over the Brazilian sector. Thus, our results lead to a better understanding of the underlying mechanisms related to the Es layer formation and dynamics.

KEYWORDS :   sporadic E layer, electric fields, magnetic storms

Sr No: 184

SYMPOSIUM :   **D4 Advances in Mid, Low Latitude and Equatorial Aeronomy**

The seasonal characteristics of equatorial Electrojet and Counter electrojet in the Indian sector

CORRESPONDING & PRESENTING AUTHOR:

Ms. Archana RK, CSIR-NGRI, Inida

Kusumita Arora, CSIR-NGRI, India

Equatorial electrojet (EEJ) is a current flowing in the ionospheric E-layer along the geomagnetic equator. The studies on the seasonal pattern of EEJ from different sectors have reported the link between EEJ amplitudes and equatorward/poleward movement of Sq focus. Using geomagnetic data from mid-low-equatorial latitudes of both hemispheres in the Indian sector, the seasonal pattern of EEJ, CEJ, and the influence of Sq focus movement on them has been studied. The observations indicate that the equatorial ward movement of Sq focus of both hemispheres might be attributed to the strong EEJ observed in E-season, and weak EEJ amplitudes in D-season might be due to the poleward movement of Sq focus of both hemispheres, whereas during J-season the Sq focus of the northern hemisphere stay close to the equator and the Sq focus of southern hemisphere move poleward, which might have resulted in weak EEJ strength and caused the occurrence of a large number of CEJs.

KEYWORDS :   equatorial electrojet, equatorial counter electrojet, sq focus

Sr No: 185

SYMPOSIUM :   **D4 Advances in Mid, Low Latitude and Equatorial Aeronomy**

Understanding the TEC variability over Europe during 2009 and 2019 SSWs

CORRESPONDING & PRESENTING AUTHOR:

Tarique Siddiqui, IAP Kuehlungsborn, Germany

Yosuke Yamazaki, GFZ Potsdam, Germany

Claudia Stolle, GFZ Potsdam, Germany

Astrid Maute, High Altitude Observatory, USA

J. Lastovicka, Institute of Atmospheric Physics, Czechia

Ilya Edemskiy, Institute of Atmospheric Physics, Czechia

Zbysek Mosna, Institute of Atmospheric PhysicsCzechia

Mani Sivakandan, IAP Kuehlungsborn, Germany

In this work, we focus on the mid-latitude ionospheric variability during SSWs by studying the Total Electron Content (TEC) variability over Europe during 2009 and 2019 Northern Hemisphere (NH) SSW events. Both these SSWs occurred under quiet-to-moderate geomagnetic conditions with the 2009 SSW happening in the beginning of the solar cycle 24 and the 2019 SSW towards its end. The nature of the TEC variability over Europe is investigated during both SSWs using a combination of Global Navigation Satellite System (GNSS) based TEC observations and Thermosphere-Ionosphere Electrodynamics General Circulation Model (TIE-GCM) simulations.

To simulate the SSW effects in TIE-GCM, the dynamical fields from the Whole Atmosphere Community Climate Model with thermosphere and ionosphere extension (WACCM-X) simulations of each SSW is specified at the TIE-GCM lower boundary. The observed and simulated TEC are in overall good agreement and therefore the simulations are used to understand the sources of mid-latitude TEC variability during both SSWs. Through comparison of TIE-GCM simulations with and without geomagnetic forcing, we find that the TEC variability during the 2019 SSW event, was predominantly geomagnetically forced, while for the 2009 SSW , the major variability in TEC was accounted for by the changes in vertically propagating migrating semidiurnal solar (SW2) and lunar (M2) tides. By comparing the TIE-GCM simulations with and without the SW2 and M2 tides, we find that these semidiurnal tides contribute to $\sim$20-25% increase in the quiet background TEC at European mid-latitudes during both SSWs.

KEYWORDS :   vertical coupling, SSWs, tides

Sr No: 186

SYMPOSIUM :   **D4 Advances in Mid, Low Latitude and Equatorial Aeronomy**

Schumann resonance frequency changes with ionosphere for time scales of short and long durations

CORRESPONDING & PRESENTING AUTHOR:

Rahul Rawat, Indian Institute of Geomagnetism, India

Gopi K. Seemala, Indian Institute of Geomagnetism, India

Ashwini Kumar Sinha, Indian Institute of Geomagnetism, India

Schumann resonances (SR) is the global electromagnetic resonance phenomenon generated by global lightning discharges within the Earth-ionosphere cavity. The 1st harmonic is at nearly 8 Hz and subsequent harmonics are separated by approximately 6 Hz. Intensity of Schumann resonance directly depends on overall thunder storm activity over the globe as well as on the source-observation distance, whereas SR frequency depend on the dielectric permeability of the ionospheric D region. The regular diurnal variation of D region ionization resulting from solar zenith angle variation cause a systematic change in SR frequency, whereas a sudden ionospheric disturbance (SID) e.g. Solar flare, gamma ray burst and high-energy particle precipitation not only enhance the ionization in D region, but also modify the altitude of D region which cause a transient change in SR frequency. In this paper, attempt are made to study variation in the first order frequency of the Schumann resonance during such events. Also, the effects of solar cycle variation are also studied, whose results are presented here.

KEYWORDS :   schumann resonances, sudden ionospheric disturbance (SID), solar cycle

Sr No: 187

Ionospheric Disturbances by Solar Coronal Mass ejection in September 2017 over Brazilian and African Sectors

CORRESPONDING & PRESENTING AUTHOR:

Paulo Roberto Fagundes, [1] Universidade do Vale do Paraíba – UNIVAP; [2] Instituto Federal de Tocantins - IFTO, Observatorio de Fisica Espacial, Campus Araguatins, Brazil

Valdir Gil Pillat, [1] Universidade do Vale do Paraíba – UNIVAP; [2] Instituto Federal de Tocantins - IFTO, Observatorio de Fisica Espacial, Campus Araguatins, Brazil

Vera Yesutor Tsali Brown, [1] Universidade do Vale do Paraíba – UNIVAP; [2] Instituto Federal de Tocantins - IFTO, Observatorio de Fisica Espacial, Campus Araguatins, Brazil

Mateus Oliveira Arcanjo, [1] Universidade do Vale do Paraíba – UNIVAP; [2] Instituto Federal de Tocantins - IFTO, Observatorio de Fisica Espacial, Campus Araguatins, Brazil

Francisco Vieira, [1] Universidade do Vale do Paraíba – UNIVAP; [2] Instituto Federal de Tocantins - IFTO, Observatorio de Fisica Espacial, Campus Araguatins, Brazil

A solar coronal mass ejection (CME) is a significant release of solar plasma and is accompanied by a magnetic field from the solar corona. The CME cloud travels outward from the sun to the interplanetary medium and eventually hits the Earth's system. One of the most significant aspects of space weather is the ionospheric response due to SF or CME. Geo-efficiency of the geomagnetic storm occurs when the solar wind speed and number of particles increase and is accompanied by a southward vertical interplanetary field. Usually, the geomagnetic storm starts with sudden storm commencement (SSC) and is afterward followed by the main and recovery phases. In this study, we investigated the ionospheric response (F-region) in the Brazilian and African sectors during the geomagnetic storm event of 07-10/09/2017, using data from networks of GPS-TEC, magnetometers, and ionosondes. Positive ionospheric disturbances in the VTEC during the main phase (08/09/2017) over the Brazilian and African sectors were observed. In addition, two latitudinal chains of GPS-TEC stations from the equatorial region to low latitudes in the East and West Brazilian and another chain in the East African sectors were used to investigate the storm time behavior of the equatorial ionization anomaly (EIA), in both sectors. We noted that the intensity of the disturbance in the Brazilian sector was higher than in the African sector. Furthermore, in the Brazilian sector, there was an occurrence of Spread-F during the night of the main phase (7-8/09/2017) whereas its occurrence was absent in the African sector.

KEYWORDS :   geomagnetic storm, equatorial and low-latitude, F region

Sr No: 188

Characteristics of Equatorial Counter-Electrojet

CORRESPONDING & PRESENTING AUTHOR:

Sreelakshmi J, Indian Institute of Geomagnetism, India

Geeta Vichare, Indian Institute of Geomagnetism, India

The equatorial electrojet (EEJ) is a narrow band of eastward currents flowing in the ionospheric E region during the daytime. Sometimes, the EEJ can reverse and flow in opposite direction (westwards) and these currents are called equatorial counter electrojet (CEJ). The CEJ events show varying amplitude and occurrence

frequency depending on various parameters such as local time (LT), season, longitude, geomagnetic activity, solar flux, lunar phase, etc. There has been a number of studies on the dependence of CEJ on each of these factors using both ground and satellite observations. There is a broad agreement among most of these studies, but some of the dependencies have discrepancies. Almost all the studies have found that CEJ events exhibit prominent longitudinal patterns, however, this has been attributed to different sources such as Wave-4 structure due to non-migrating DE3 tide, migrating tides, etc. The present work shall discuss the characteristics of CEJ and the responsible mechanism.

KEYWORDS : counter electrojet, ionosphere

Sr No: 189

Application of machine learning for detection of ionospheric depletions

CORRESPONDING & PRESENTING AUTHOR:

Gopi Seemala, Indian Institute of Geomagnetism, India

Chandan Kapil, Indian Institute of Geomagnetism, India

Ionospheric electron density depletions play a major role in affecting trans-ionospheric signals of communication and navigation systeThese electron density depletions can be seen as reduction in total electron content (TEC). The algorithms for detection of depletions in TEC use many methods such as difference with de-trended values, filtering etc., but are not fully efficient as the ambient TEC values change the threshold of detection has to be changed. Also, with solar activity the ambient TEC values change as well as the depth of the depletions, hence the threshold values have to be carefully selected to aid in efficient detection, which could even change with geographic region.

In the present study, the machine learning is adapted for the detection of TEC depletions. With this method there is no usage of threshold and hence the bias between smaller and larger depletions is avoided. The detected depletions from this machine learning method are compared with regular TEC depletion detection algorithm, and the results are discussed and presented here.

KEYWORDS : TEC depletions, TEC depletion detection

Sr No: 190

Estimating ionospheric scintillation magnitude from ROTI values in the Indian region

CORRESPONDING & PRESENTING AUTHOR:

Chandan Kapil, Indian Institute of Geomagnetism, India

Gopi Seemala, IIG, India

Ionospheric irregularities is one of the phenomenon that affects trans-ionospheric signals, thereby introducing errors in communication and navigation systems. The ionospheric irregularities manifest as fluctuations in

the received signal amplitude called as scintillations. The magnitude of ionospheric scintillations is calculated from the parameter S4 index, which is a root mean square value of signal to noise ratio of the received signal. However, most GNSS receivers do not provide S4 value due to requirement of high sampling rate of 50 Hz. Ionospheric irregularities can be assessed through the rate of change of total electron content (TEC) index (ROTI), which can be derived from dual frequency GNSS receiver, even with low sampling rate of 30 second. In the past studies it is shown there is some correlation in ROTI and S4, but that was found to vary with geographical locations and other parameters.

In this study, the GPS data from Indian GAGAN network was used to study the correlation between S4 and ROTI values. Apart from correlating the simultaneous values of two indices, the main focus is on to establish a relation or probable S4 values to a given ROTI. The correlation of the two indices are subjected to the various factors like geographical locations, elevation mask angle as well as on the time interval used to calculate ROTI. In this presentation, different methods used to see how the S4 value or the ionospheric scintillation magnitude may be estimated using the ROTI values, and results are discussed.

KEYWORDS : ionospheric scintillations, ROTI/S4,

Sr No: 191

A study on the sources for the excitation of F3 layers at Allahabad (25.3° N, 81.5° E) near anomaly crest region over India during 19-21 December 2015 geomagnetic storm

CORRESPONDING & PRESENTING AUTHOR:

S Sripathi, Indian Institute of Geomagnetism, India

Ram Singh, Space Pysics Laboratory, India

Rajesh Kumar Barad, Indian Institute of Geomagnetism, India

We investigate the causes for simultaneous occurrence of F3 layers and short period oscillations in ionosonde observations at Allahabad (25.3° N, 81.5° E; geom 16.5°N), located at Equatorial Ionization Anomaly (EIA) crest region during intense geomagnetic storm of 20 December 2015. This storm is the third largest storm of 2015 after St. Patrick's Day storm. The isofrequency/isoheight and foF2/h'F analyses were performed to investigate the storm and substorm driven disturbances near EIA crest region. We also analyzed Hokkoido HF radar at mid-latitude, geomagnetic and TEC observations and tropospheric weather to examine their possible sources. The periodogram analysis suggest that isofrequency/isoheights possess period of ~48 min with downward phase propagation velocity of ~46 m/sec that resemble gravity wave characteristics. Based on the dispersion relation, the vertical and the horizontal wavelengths of these gravity waves are found to be ~130 km and 430 km respectively. In addition, due to prolonged southward IMF Bz, our results suggest that low latitude is affected by westward disturbance dynamo electric fields (DDEF). Further analysis using geomagnetic and TEC observations suggest that sources for these height oscillations are located at 50-550N, however, with a phase delay of few hours. This phase delay confirms that the propagation of gravity waves is originated from the high latitudes. These results suggest that F3 layers are possibly generated by equatorward propagating meridional winds and Traveling Ionospheric Disturbances (TIDs). The present investigation highlights the importance of storm-time neutral disturbances vis-à-vis tropospheric weather for the generation of F3 layers at crest region.

KEYWORDS : F3 layers, EIA crest dynamics, geomagnetic storms

Sr No: 192

High-resolution Sporadic E and valley region structures over Arecibo: Implications and current understanding (by invitation)

CORRESPONDING & PRESENTING AUTHOR:

Shikha Raizada, Arecibo Observatory, Puerto Rico

T Nishimura, Boston University, USA

M Sulzer, Arecibo Observatory, Puerto Rico

A Richmond, NCAR, USA

The occurrence of neutral metals and their ions in the upper mesosphere, which overlaps with the E region, is a well known feature of the Earth's ionosphere. A variety of in-situ experiments have extended our knowledge about the seasonal/latitudinal distribution of the ions. While satellites yield information mainly in the F-region and rockets give snapshots of the ionosphere, ground-based instruments offer excellent opportunity to investigate temporal variations of the mesosphere/ionosphere system at a given location. Resonance lidars provide high temporal and altitudinal resolution data sets that promise new insights into a variety of ionospheric processes in the Earth's atmosphere.

High resolution and improved sensitivity of the resonance lidars at Arecibo have led to new observations of neutral metals, and calcium ions in these part of the ionosphere. The simultaneous lidar and Incoherent Scatter Radar observations from Arecibo have shown calcium ions ($Ca+$) act as a proxy for other major ions in the ionosphere. A recent study from Arecibo showed that the metal ion abundance in the $150 - 180$ km region is about half of the one occurring at meteoric altitudes below 120 km. This also allowed us to estimate the concentrations of the major ions like $Fe+$, which are found to be ~ 20 -30 times those of $Ca+$, at the E-region altitudes, and are ~ 5 times of $Ca+$ in the F-region valley. We plan to present such novel observations and discuss ion-neutral interactions, as well as the role of transport in the latitudinal coupling processes.

KEYWORDS :   mesosphere, E-region, ions

Sr No: 193

Mid and Low Latitude Mesosphere-Thermosphere-Ionosphere System Observations by the GOLD Mission (by invitation)

CORRESPONDING & PRESENTING AUTHOR:

Richard Eastes, Laboratory for Atmospheric and Space Physics (LASP), University of Colorado Boulder, USA

GOLD observes the ionosphere-thermospere effects in temperatures, composition and densities of SSWs, tides, waves from the Earth's lower atmosphere in addition to those introduced by forcing from the magnetosphere and solar irradiance. The mission observes the T-I system over the Americas and Atlantic Ocean from geostationary orbit at 47.5 W, approximately over the mouth of the Amazon river in South America. GOLD observations have been successful in revealing aspects of thermospheric and ionospheric phenomena throughout the mid and low latitudes, advancing our understanding of coupling in the mesosphere-thermosphere-ionosphere system and the behavior of the nighttime ionosphere. Coincident

observations from the ground and other satellites - for which GOLD provides a global-scale context — will provide even greater advances in our understanding of the system's behavior, especially when combined with assimilation of these additional data, than has been provided by GOLD alone.

Data are available through either the GOLD Science Data Center or NASA's Space Physics Data Facility (SPDF)

KEYWORDS : thermosphere, ionosphere

Sr No: 194

SYMPOSIUM : **D4 Advances in Mid, Low Latitude and Equatorial Aeronomy**

Investigation on the seasonal and longitudinal variability of Equatorial Plasma Bubble occurrence as observed by GOLD

CORRESPONDING & PRESENTING AUTHOR:

Deepak Karan, Univ. of Colorado Boulder, USA

Richard Eastes, Univ. of Colorado Boulder, USA

Carlos Martinis, Boston Univ, USA

Robert Daniel, Inc., USA

Scott England, Virginia Tech, USA

Alan Burns, NCAR & UCAR, USA

Equatorial Plasma Bubble (EPB) is an interesting nighttime plasma irregularity phenomenon that occurs over the equatorial- and low-latitude ionosphere. After the sunset, plasma density irregularities can occur at the bottom side of the F region. When they are unstable, they can grow rapidly and upwell to higher altitudes. The seeding, development, and persistence of EPBs depend on various factors such as alignment of dusk terminator with the magnetic field lines, trans-equatorial thermospheric winds, electric fields, etc. At a longitude sector, these factors change with seasons and thereby bring the seasonal variability in the occurrence of EPBs. Further, the behaviors of these factors vary at the longitudes observed each night by NASA's Global-scale Observations of the Limb and Disk (GOLD) mission. This causes longitudinal variability in the appearance of EPBs. GOLD observes Earth's ultraviolet emissions from geostationary orbit. On each night GOLD images the ionospheric structure at low-latitudes over the American, Atlantic, and African longitude sectors. In this work, we have investigated the variability of EPB occurrence aver these three longitude sectors during different seasons.

KEYWORDS : bubbles, night, structure

Sr No: 195

Assimilative Modeling of the Day-to-Day Variability of Equatorial Electrojet and its Longitudinal Dependence Using Ground- and Space-Based Magnetometer Data

CORRESPONDING & PRESENTING AUTHOR:

Chuanping Lien, University of Colorado, Boulder, CO, USA

Corresponding Author: Tomoko Matsuo, University of Colorado, Boulder, CO, USA

Astrid Maute, High Altitude Observatory, National Center for Atmospheric Research, Boulder, CO, USA

Claudia Stolle, GeoForschungsZentrum (GFZ), German Research Centre for Geosciences, Germany

The equatorial electrojet (EEJ) is an important manifestation of ionospheric electrodynamics. The day-to-day changes of EEJ result from E-region dynamo processes primarily driven by highly variable atmospheric tides propagating from the lower atmosphere. The extent of day-to-day tidal variability is not well understood due to the sparse spatiotemporal coverage of measurements, and inadequately modeled lower- and middle-atmosphere dynamics. In this study, observations of ground-level magnetic perturbations are utilized to constrain the magnitude and phase of tidal waves specified as lower boundary conditions in the Thermosphere-Ionosphere-Electrodynamics General Circulation Model (TIE-GCM), with the help of an ensemble transform technique. TIE-GCM ensemble simulations are driven by realistic magnetospheric and wave forcing specified by AMGeO analysis and MERRA meteorological reanalysis, respectively, and the 3D Dynamo Model is used as part of forward modeling of ground-level magnetic perturbations. Modeled EEJ is validated with CHAMP magnetometer data. A case study designed for solar minimum March condition showcases the use of routinely available ground-based magnetometer data for improving the model's ability to reproduce the observed characteristics of day-to-day changes of the EEJ.

KEYWORDS : EEJ, ionospheric electrodynamics, data assimilation

Sr No: 196

On the Cause of Post-sunset Enhancement in OI 630 nm Airglow Emission over Low-latitude Thermosphere

CORRESPONDING & PRESENTING AUTHOR:

Sovan Saha, Physical Research Laboratory, India

Duggirala Pallamraju, Physical Research Laboratory, India

Tarun Kumar Pant, Vikram Sarabhai Space Centre, India

Supriya Chakrabarti, University of Massachusetts, Lowell, USA

Airglow emissions act as good tracers of the altitudinal region from where they originate. OI 630 nm nocturnal emission variations, that originate from around 250 km altitude, have been obtained from Mt. Abu (16 Mag-N), Gurushikhar, (a low-latitude location in Indian longitudes) using the High Throughput Imaging Echelle Spectrograph (HiTIES). A photochemical model has been generated by which we can estimate the column integrated emission rates using, as inputs, the electron density from a Digisonde at Ahmedabad (15 Mag-N). A high correlation (> 0.9) has been obtained between these observed and estimated emission rates, which enables us to extend the database when the optical emission measurements

are hindered during moonlit conditions. Around 142 nights of nocturnal emission measurements have been obtained during the months of January, February, and March in the years 2013, 2014, and 2016. Typically, a monotonic decrement in emissions is obtained soon after the sunset. On around sixty percent of these nights an enhancement in OI 630 nm emissions has been observed, that is centred around 20 – 21 LT for about 2 hours. The magnitude of emission enhancements vary from 230 to 15 R over the duration of measurements. Detailed investigations have been carried out on the roles of equatorial electrodynamic phenomena, like the equatorial electrojet, pre-reversal enhancement in electric field to understand the cause of such post-sunset enhancements in emissions. Further, the contribution of neutral winds has also been assessed to understand the cause of this emission enhancements. The findings will be discussed in detail.

KEYWORDS :   OI 630 nm nightglow, thermospheric winds, ionosphere-thermosphere coupling

Sr No: 197

SYMPOSIUM :   **D4 Advances in Mid, Low Latitude and Equatorial Aeronomy**

A quasi-stationary wave-like feature in the nighttime equatorial ionization anomaly

CORRESPONDING & PRESENTING AUTHOR:

Juan Rodriguez Zuluaga, GFZ Potsdam, Germany

Claudia Stolle, GFZ Potsdam, Germany

Yosuke Yamazaki, GFZ Potsdam, Germany

At low magnetic latitudes, the Earth's ionosphere is characterized by a meridional bi-modal distribution of the plasma number density known as the equatorial ionization anomaly (EIA). Previous studies have shown atmospheric tides' effects on the EIA's morphology, focusing primarily on zonal wave numbers less than six (i.e., zonal wavelength > 60°). In this study, we have used far-ultraviolet (FUV) airglow images from the NASA Global-scale Observations of the Limb and Disk (GOLD) mission to report on a wave-like feature in the nighttime EIA with typical zonal wavelengths of about 65 and 35° (i.e., circa 6700 km and 3300 km, respectively.) This feature is seen as poleward and equatorward displacements of the EIA-crests on a synoptic scale. Using GOLD FUV images from October 5, 2018, to June 30, 2020, we found that the wave-like structure is symmetric about the dip equator and appears nearly stationary with time over the night. In quasi-dipole coordinates, maxima poleward displacements of the EIA-crests are seen at about ± 12° latitude and around 20 and 60° longitude (i.e., in geographic longitude at the dip equator, about 53°W and 14°W.) The occurrence and wavelength of the wave-like feature are highly variable on a day-to-day basis with no apparent dependence on geomagnetic activity. Often, clusters of equatorial plasma depletions (EPDs) occur within the wave-like structure suggesting a connection between these two phenomena. We further outline the difference in observing these EPDs from FUV images and in situ measurements during a GOLD and Swarm mission conjunction.

KEYWORDS :   equatorial ionization anomaly, stationary wave, spread F

Sr No: 198

Study of the regular daily variations of the geomagnetic field Sq and SD obtained from the Coimbra Magnetic Observatory (COI) observations by different methods compared to the comprehensive Model CM5 of the quiet-time.

CORRESPONDING & PRESENTING AUTHOR:

Rania Rebbah, University of Coimbra, CITEUC, Department of Physics, Coimbra, Portugal

Anna Morozova, University of Coimbra, CITEUC, Department of Physics, Instituto de Astrofísica e Ciências do Espaço, OGAUC, Coimbra, Portugal

In this work, we show the results of our analysis of the regular daily variations of the geomagnetic field, Sq, and SD, obtained using two methods. The first one is the so-called geomagnetically quiet day (IQD) to calculate mean daily variations. The second one is the principal component analysis (PCA) to decompose the original series into main variability modes.

The primary data were obtained from observations at the Coimbra Magnetic Observatory (COI, Portugal) from 1st January 2007 to 31st December 2017. The geomagnetic field components X, Y, and Z were analyzed separately for every 12 months. The Sq and SD variations obtained with IQD were compared with the principal components' PCs from PCA using the correlation analysis. The PCA ability to extract daily variations similar to ones acquired using the standard approach with IQD was analyzed. The number of the PCs classified either as Sq or SD follows seasonal and decadal variations of the geomagnetic activity.

Our results show that PCA could automatically extract the Sq variation from the observations of Y and Z. For the X component, the automatic extraction of the Sq or SD variations is not possible. A complimentary analysis is always needed to identify a PC corresponding to the SD variation. The corresponding PC1, PC2, and PC3 will be compared to a reference monthly mean curves SqCM5 of the Comprehensive Model CM5 for individual months for all available years using statistical significance of correlation coefficients.

KEYWORDS : solar quiet variation (Sq), solar disturbed variation (SD), principal component analysis

Sr No: 199

Early development of 3-meter scale irregularities in the topside region of a rapidly rising Equatorial Plasma Bubble

CORRESPONDING & PRESENTING AUTHOR:

Tulasiram Sudarsanam, Indian Institute of Geomagnetism, India

K. K. Ajith, Indian Institute of Geomagnetism, India

The non-linear growth of an EPB and/or cascading rate of secondary instabilities is influenced by several factors such as height of the F-layer, local ion-neutral collision frequency, ratio of F- to E-region field-line integrated conductivities, strength of polarization electric fields and the density gradient at the walls of depletion. As the bubble grows into topside ionosphere, the significant reduction of ion-neutral collisions and increased ratio of F- to E-region field-line integrated conductivities give rise to more rapid development of intermediate-to-shorter scale irregularities at topside compared lower altitudes. Though observations
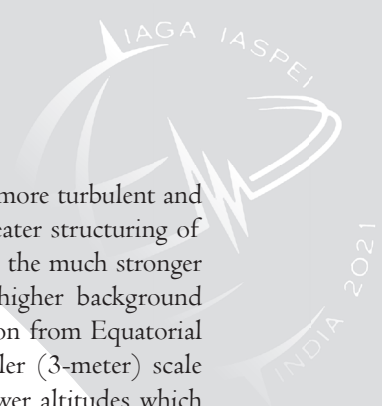
are sparse, the high resolution model simulations often show the early development of more turbulent and smaller scale structures in the topside ionosphere compared to lower altitudes. The greater structuring of EPBs in the topside ionosphere is found to be one of the important factors explaining the much stronger L-band scintillations at low-latitudes compared to equatorial latitudes besides the higher background density and larger density gradients. In this paper, we present a unique EPB observation from Equatorial Atmosphere Radar (EAR) that provides hitherto undisclosed evidence for the smaller (3-meter) scale irregularities initially developing at higher altitudes and subsequently developing to lower altitudes which would have significant impact on the latitudinal development of L-band scintillations. The responsible mechanisms for the early development of shorter scale irregularities in the topside and their subsequent development at lower altitudes will be discussed.

KEYWORDS : equatorial plasma bubbles, ionospheric scintillation

Sr No: 200

SYMPOSIUM : **D4 Advances in Mid, Low Latitude and Equatorial Aeronomy**

Long term investigation of equatorial plasma bubble occurrence using GPS based space and ground measurements

CORRESPONDING & PRESENTING AUTHOR:

Ankur Kepkar, Technical University of Berlin, Germany

Christina Arras, German Research Centre for Geosciences, GFZ, Germany

M. Mahdi Alizadeh, K.N. Toosi University of Technology, Iran

Jens Wickert, German Research Centre for Geosciences, GFZ, Germany

Harald Schuh, German Research Centre for Geosciences, GFZ, Germany

Lung Chih Tsai, National Central University, Hsinchu, Taiwan

In this study, a decade long time series during the years 2007-2017 is used to investigate equatorial plasma bubbles from space based GPS radio occultation measurements obtained from Formosat-3/COSMIC mission as well as observations from about 15 ground based GPS stations situated along the geomagnetic equator. The signal-to noise ratio profiles from radio occultation measurements and Total Electron Content (TEC) measurements from GPS ground station are retrieved, which are susceptible to scintillations caused by plasma bubbles. Furthermore, the study investigates the preconditioning of plasma bubbles through equatorial vertical plasma drift information from International Reference Ionosphere (IRI) Model.

The occurrence of plasma bubbles is investigated in four regions, i.e. America, Africa, Asia and Pacific. Each region showed distinct spatial-temporal visibility caused mainly due to geomagnetic conditions. Overall, a good correlation was observed with a semi-annual double peak structure in both space and ground measurements, especially in the American sectors followed by Asia, Pacific and Africa. A synoptic statistical study with vertical plasma drift is also performed that indicated a good correlation with plasma bubble occurrence mainly in America, and Africa, and followed by other regions. Further, plasma bubble altitude obtained uniquely from radio occultation measurements also had a significant correlation with the vertical plasma drifts. Generally, these plasma bubbles occur soon after the sunset when the Pre-Reversal Enhancement causes an increased upward drift, thus influencing plasma bubble generation.

KEYWORDS : plasma bubbles, radio occultation

D5 Relativistic electrons: Their emergence and loss in geospace, their impact on the upper atmosphere and the role of the cold plasma background

CONVENERS: Ioannis A. Daglis

János Lichtenberger

Jacob Bortnik

Yoshizumi Miyoshi

Gurbax Lakhina

Rajesh Singh

Relativistic electrons in geospace form the Van Allen radiation belts and are a major space weather agent, as they pose a significant threat to space assets. Their emergence and loss are driven, to a large extent, by magnetospheric plasma waves of various frequencies. These processes are mediated by the cold plasma density through wave-particle interactions over a large scale of spatial extent. Loss of relativistic electrons occurs through the magnetopause to interplanetary space and through precipitation to the Earth's atmosphere. Precipitating relativistic electrons have a significant impact on the dynamics of the upper atmosphere, which can cause catalytic destruction of mesospheric ozone and feed back into space affecting the convection electric field.

This session invites studies of the emergence, loss, precipitation and atmospheric impacts of relativistic electrons in geospace, as well as the dynamic behaviour of the plasmasphere and the radiation belt using in-situ and ground based observations, physics-based models, machine learning and/or numerical simulations.

Sr No: 201

Observation of Postsunset OI 135.6 nm Radiance Enhancement Over South America by the GOLD Mission

CORRESPONDING & PRESENTING AUTHOR:

Xuguang Cai, UCAR, USA

Alan Burns, NCAR, USA

Wenbin Wang, NCAR, USA

Liying Qian, NCAR, USA

Stanley Solomon, NCAR, USA

Richard Eastes, U of Colorado, Boulder, USA

The Global-scale Observation of Limb and Disk (GOLD) mission, for the first time, provides synoptic two-dimensional (2D) maps of OI 135.6 nm observations. These maps describe the unambiguous and dynamic evolution of nighttime ionospheric F2-peak electron densities (NmF2) as the 135.6 nm airglow emission radiance correlates well with NmF2 at night. On November 19, 2018, the 135.6 nm radiance measured by GOLD, NmF2measured by a digisonde, and GPS total electron content (TEC) measurements at Cachoeira Paulista (CP) all showed a postsunset enhancement, with an increase near 22:30 universal time. The 135.6 nm radiance map showed that this enhancement was due to the southward movement of the southern equatorial ionization anomaly (EIA) crest. Therefore, the GOLD observation showed the linkage between postsunset enhancement of NmF2 and EIA movement. Furthermore, unlike the southward movement of the southern crest, the corresponding EIA northern crest, however, did not show northward motion. This is the first time that the EIA hemispheric asymmetry, which included both different densities and movement of two crests in a short time period (<2-h), was captured. The cause of this asymmetric movement of the two crests is not clear and requires further investigation.

KEYWORDS : GOLD, EIA, asymmetry movement

Sr No: 202

Energetic electron precipitation detected by balloon and satellite observations and their effect on the middle atmosphere

CORRESPONDING & PRESENTING AUTHOR:

Irina Mironova, Saint Petersburg University, Russia

Miriam Sinnhuber, Karlsruhe Institute of Technology, Germany

Galina Bazilevskaya, Russian Academy of Sciences, Russia

Monali Borthakur, Karlsruhe Institute of Technology, Germany

Dmitriy Grankin, Saint Petersburg University, Russia

Vladimir Makhmutov, Russian Academy of Sciences, Russia

Eugene Rozanov, Saint Petersburg University, Russia

Timofei Sukhodolov, Saint Petersburg University, Russia

A correct description of the Sun-Earth relations requires a deep understanding of atmospheric processes

involving the energetic particle induced ionization in the atmosphere and the formation of chemically active components of the atmosphere capable of affecting the ozone loss and climate. The key question here is the assessment of the atmospheric response to energetic electron precipitation (EEP) both on a regional and global scale. To correctly quantify these effects using chemical-climate models, the spectrum of precipitating particles must be known with high accuracy over the entire range of electrons from 10 keV into the MeV range. Usually, energetic electron precipitation spectra are obtained from space by satellite instruments like the Polar-orbiting Operational Environmental Satellites (POES), which provide global coverage with a sparse temporal and spatial resolution and limited energy coverage. The balloon experiments provide precious additional knowledge on the actual atmospheric precipitating electron fluxes and energy spectra. In this study, we exploit a combination of balloon and satellite data to estimate EEP ozone loss via chemistry-climate models with higher accuracy.

KEYWORDS : energetic electron precipitation, balloon observation, atmospheric response

Sr No: 203

SYMPOSIUM : **D5 Relativistic electrons: Their emergence and loss in geospace, their impact on the upper atmosphere and the role of the cold plasma background**

Precipitation process of electrons in the outer radiation belt associated with oblique whistler mode chorus emissions

CORRESPONDING & PRESENTING AUTHOR:
Yikai Hsieh, Research Institute for Sustainable Humanosphere, Kyoto University, Japan
Yoshiharu Omura, Research Institute for Sustainable Humanosphere, Kyoto University, Japan

Energetic electron accelerations and precipitations in the Earth's outer radiation belt are highly associated with wave-particle interactions between whistler mode chorus waves and electrons. Two main processes take place in the whistler mode wave-particle interactions. One is nonlinear scattering process, which makes electron energy slightly smaller and lowers the equatorial pitch angle of the electron. The other is the nonlinear trapping process, which makes effective energy gain of the resonant electrons. We perform test particle simulation in a 3D dipole field to reproduce the interactions in the radiation belt and investigate the electron precipitation interacting with both parallel and obliquely propagating chorus emissions. We build up a database of Green's functions, which are treated as results of the input electrons interacting with one emission, for a large number of electrons interacting with whistler mode chorus emissions. The formation processes and the loss processes of the outer radiation belt electron fluxes interacting with consecutive chorus emissions are traced by applying the convolution integrals of the electron distribution function and the Green's function sets. We compare the precipitation phenomena between parallel waves and oblique waves and find that oblique chorus emissions result in more electron precipitation than parallel chorus emissions. Electron trajectories show that most cases of precipitation are directly caused by cyclotron resonance. We propose a 2-step precipitation process by nonlinear trapping of Landau resonance and nonlinear scattering of cyclotron resonance to explain the higher precipitation rate in oblique wave-particle interactions.

KEYWORDS : oblique chorus emission, MeV electron loss, nonlinear processes
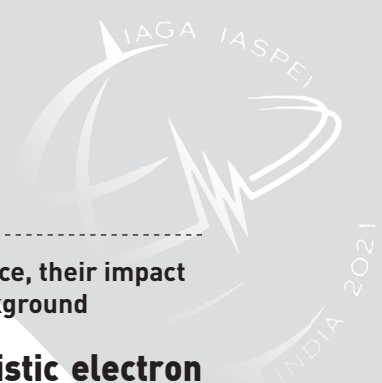
Sr No: 204

The role of the whistler-mode chorus waves in the relativistic electron flux decrease on the outer radiation belt under the influence of an ICME: a case study

CORRESPONDING & PRESENTING AUTHOR:

Vinicius Deggeroni, National Institute for Space Research – INPE, China

Ligia Alves Da Silva, National Space Science Center, Chinese Academy of Sciences, China

Jose Paulo Marchezi, National Space Science Center, Chinese Academy of Sciences, China

Marlos Rockenbach Da Silva, National Institute for Space Research – INPE, Brazil

The electron flux density variability in the Van Allen outer radiation belt can be influenced by the solar wind conditions and interplanetary medium structures. Several dynamic mechanisms can be associated with the outer radiation belt electron flux variability, including the chorus wave-particle interaction. The present work investigates the outer radiation belt electron flux decrease observed under the influence of an ICME. This solar wind structure reached the Earth's magnetosphere on November 6, 2015, associated with a Magnetic Cloud (MC) with rotation south to north. The relativistic electron flux and magnetic field in the outer radiation belt are detected from REPT and EMFISIS instruments, respectively, onboard the Van Allen Probes. The solar wind parameters are obtained by the Advanced Composition Explorer (ACE) satellite. The chorus waves were detected in the lower band (0.1 - 0.5 fce), where fce represents the equatorial electron gyro-frequency. Thereby, these chorus waves can interact with the relativistic electron particles, causing the violation of the first adiabatic invariant. This dynamic mechanism named pitch angle scattering is investigated here through the analysis of the subelements, in which the preliminary results have shown that the opening angle of the loss cone ($D\alpha$) and the interaction time (DT) of the chorus waves package reached ~ 60° and 9 ms, respectively. The physical processes related to this dynamic mechanism are discussed here, as well the influences of this ICME in the chorus waves characteristics detected.

KEYWORDS :   Van Allen probes, wave-particle interaction, whistler-mode chorus

Sr No: 205

The Tverskaya relation and the outer radiation belt formation

CORRESPONDING & PRESENTING AUTHOR:

Elizaveta E. Antonova, Lomonosov Moscow State University, Skobeltsyn Institute of Nuclear Physics; Space Research Institute RAS, Russia

Nikita V. Sotnikov, Lomonosov Moscow State University, Skobeltsyn Institute of Nuclear Physics, Russia

Ilya L. Ovchinnikov, Lomonosov Moscow State University, Skobeltsyn Institute of Nuclear Physics, Russia

Maria O. Riazantseva, Space Research Instituta RAS, Russia

Igor P. Kirpichev, Space Research Instituta RAS, Russia

Maruna V. Stepanova, Universidad de Santiago de Chile (USACH), Chile

Victor Pinto, University of New Hampshire Durham, NH, USA

Pablo S. Moya, Universidad de Chile, Chile

We summarize the latest finding on the validity of Tverskaya relation and the position of the maximum of the outer radiation belt (ORB) formed after a geomagnetic storm and the appearance of large fluxes of relativistic electrons after a storm. Specifically, the Tverskaya relation connects the minimal value of the Dst index observed during a storm and the position of the aforementioned maximum fluxes that correspond to the formation of a new ORB after storm, allowing us to predict the position of ORB maximums for the most of magnetic storms based solely on the Dst predictions. It was shown that large fluxes of ORB relativistic electrons are formed only if the comparatively large substorms are formed during the storm recovery phase, which permits to predict the appearance of large relativistic electron fluxes. Observed dependences were explained theoretically based on the analysis of the ring current formation and stability. This theory had a number of predictions, which have recently been verified, including the dominant role of the adiabatic mechanism of the ORB flux variations and the intersection of the position of the ORB with the position of the source of the auroral oval electrons at the equatorial plane, the local increases of the relativistic electron fluxes during substorms and a number of another effects.

KEYWORDS : outer radiation belt, predictions, auroral oval

Sr No: 206

Association of relativistic electron enhancements with chorus waves and seed electrons

PRESENTING AUTHOR:

Ioannis Daglis, National and Kapodistrian University of Athens, Greece
Afroditi Nasi, National and Kapodistrian University of Athens, Greece
Christos Katsavrias, National and Kapodistrian University of Athens, Greece
Wen Li, Boston University, USA

CORRESPONDING AUTHOR:

Ioannis Daglis, National and Kapodistrian University of Athens, Greece

Acceleration by whistler mode chorus waves is fundamentally important for the acceleration of electrons to relativistic energies in the outer Van Allen belt. Chorus waves growth depends strongly on substorm activity and therefore the acceleration through chorus waves depends on the source electrons (driving chorus) and on the sub-relativistic electrons that form the seed population of the relativistic electrons.

In this work, a selection of geospace disturbance events, emerging from single and isolated interplanetary drivers, is divided into two groups: one resulting in prominent enhancements and one in strong depletions of the relativistic electron Phase Space Density (PSD). Because substorm activity does not always coincide with or depend on magnetic storm occurrence, we have not limited our study to storms, but have included also non-storm events that result in enhancements and depletions of relativistic electrons. We investigate the relation of these enhancements/depletions to solar wind and geomagnetic parameters, wave activity and seed electrons in the outer Van Allen belt, looking for the occurrence of characteristic patterns, by performing a Superposed Epoch Analysis (SEA).
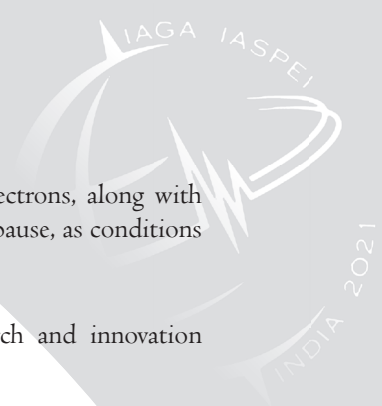
Our study confirms the importance of substorm-associated enhancements of seed electrons, along with prolonged, intense ULF and VLF wave activity and with an earthward displaced plasmapause, as conditions leading to substantial enhancements of relativistic electrons.

Sr No: 207

Designing Radiation Belt Environmental Indicators for the safety of space assets (by invitation)

CORRESPONDING & PRESENTING AUTHOR:

Ioannis Daglis, National and Kapodistrian University of Athens, Greece

Sebastien Bourdarie, ONERA, France

Juan Cueto Rodriguez, Thales Alena Space Espana, Spain

Fabien Darrouzet, IASB-BIRA, Gelgium

Benoit Lavraud, Univ. Bordeaux, France

Stefaan Poedts, Katholieke Universiteit Leuven, Belgium

Ingmar Sandberg, SPARC, Greece

Ondrej Santolik, IAP Prague, Czechia

We are presenting a collaborative project, called SafeSpace, that aims at advancing space weather nowcasting and forecasting capabilities through the delivery of a sophisticated model of the Van Allen electron belt and of a prototype space weather service of tailored particle radiation indicators. SafeSpace will enable forecast capabilities with a target lead time of 2 to 4 days, which is a tremendous advance from current forecasts that are limited to lead times of a few hours. It will improve radiation belt modelling through the incorporation into the Salammbô model of magnetospheric processes and parameters of critical importance to radiation belt dynamics. Furthermore, solar and interplanetary conditions will be used as initial conditions to drive the advanced radiation belt model and to provide the link to the solar origin and the interplanetary drivers of space weather. This approach will culminate in a prototype early warning system for detrimental space weather events, which will include indicators of particle radiation of use to space industry and spacecraft operators. Indicator values will be generated by the advanced radiation belt model and the performance of the prototype service will be evaluated in collaboration with space industry stakeholders. The work leading to this paper has received funding from the European Union's Horizon 2020 research and innovation programme under grant agreement No 870437 for the SafeSpace (Radiation Belt Environmental Indicators for the Safety of Space Assets) project.

Sr No: 208

Energetic electron precipitations with ULF modulation by VLF/LF band standard radio waves

CORRESPONDING & PRESENTING AUTHOR:

Kentaro Tanaka, Chiba University, Japan

Hiroyo Ohya, Chiba University, Japan

Fuminori Tsuchiya, Tohoku University, Japan

Kazuo Shiokawa, Nagoya University, Japan

Yoshizumi Miyoshi, Nagoya University, Japan

Nozomu Nishitani, Nagoya University, Japan

Tomoaki Hori, Nagoya University, Japan

Mariko Teramoto, Kyushu Institute of Technology, Japan

Mrtin Connors, Athabasca University, Japan

Simon G. Shepherd, Dartmouth College, USA

Hiroyuki Nakata, Chiba University, Japan

The Very-low-frequency (VLF;3 kHz to 30 kHz)/low-frequency (LF;30 kHz to 300 kHz) technique is most sensitive to the ionization of the D-region ionosphere, which is caused by energetic electron precipitation (EEP) with energies typically >100 keV (Rodger et al., 2012). Several studies have reported ionospheric modulations due to Ultra-low-frequency (ULF) Pc5 and Pi2 modulations (Asnes et al., 2004). Modulation of D-region due to ULF waves during a substorm was reported (Miyashita et al., 2020). However, there was only one report for the EEP associated with ULF modulation using VLF/LF transmitter signals. In this study, we investigate the EEP associated with the ULF modulation that occurred on May 5, 2011, using the VLF/LF transmitter signals observed in North America. The three transmitters were NDK, WWVB and NLK. One receiver at Athabasca (ATHA), Canada was used.During 05:00 05:30 UT on May 5, 2011 (magnetically quiet oscillations in amplitude of VLF/LF waves with a period of 4-6 minutes were observed on the NDK-ATHA and WWVB-ATHA paths. Furthermore the ground based H-component magnetic field variations and Doppler velocity observed by the SuperDARN HF radars showed similar peropdoc variation. Large Doppler velocity was found near the two paths during the VLF/LF oscillations. This suggests that the EEP occurred over the two paths. Based on ground based magnetic field data, the propagation direction of the ULF wave was eastward (83.5 km/s) from the pre-midnight sector. In this presentation, we will discuss the cause of these VLF/LF oscillations.

KEYWORDS : VLF/LF, EEP, ULF

Sr No: 209

Neural-network-based reconstruction of energetic radiation belt electron fluxes

CORRESPONDING & PRESENTING AUTHOR:

Jacob Bortnik, UCLA, USA
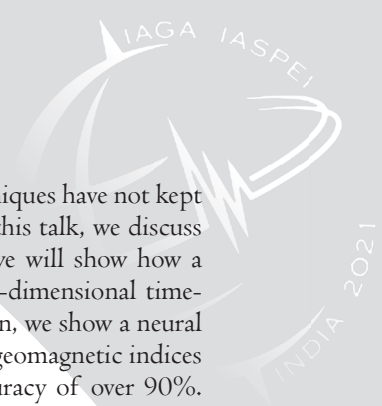
While the volumes of space physics data continue to rise exponentially, our analysis techniques have not kept pace with this rapid growth, and often do not exploit the full potential of the data. In this talk, we discuss how machine learning might provide the solution to this problem, and in particular we will show how a (sparse) time-series of point observations of some quantity can be converted into a 3-dimensional time-varying model of that quantity with the use of neural networks. As a concrete application, we show a neural network based model of the Earth's high energy electron radiation belts, driven only be geomagnetic indices and solar wind parameters, which can reproduce out-of-sample observation to an accuracy of over 90%. These types of machine learning models pave the way for scientific discoveries and practical applications in space weather prediction.

KEYWORDS : radiation belts, machine learning, Van Allen probes

Sr No: 210

SYMPOSIUM : **D5 Relativistic electrons: Their emergence and loss in geospace, their impact on the upper atmosphere and the role of the cold plasma background**

Global effects of whistler mode waves on energetic electron loss in the Earth's magnetosphere (by invitation)

CORRESPONDING & PRESENTING AUTHOR:

Wen Li, Boston University, USA

Qianli Ma, Boston University, USA

Sheng Huang, Boston University, USA

Xiaochen Shen, Boston University, USA

Murong Qin, Boston University, USA

Luisa Capannolo, Boston University, USA

Cold plasma populations play an important role in affecting the generation, propagation, and characteristics of various plasma waves, as well as their interactions with energetic particles in the Earth's magnetosphere. In this presentation we focus on discussing the characteristics of whistler mode waves inside the plasmasphere and plumes, respectively, by analyzing the extensive wave data from the Van Allen Probes mission. Our statistical results show that whistler mode waves in plumes are often stronger than the waves inside the plasmasphere. Moreover, we perform a quantitative analysis of an interesting event to evaluate the dynamic evolution of the total electron density and whistler mode wave intensity therein, and quantify their effects on the energetic electron loss. To achieve the dynamic evolution of whistler mode waves inside the plasmasphere and plumes, we use the machine learning technique, more specifically, artificial neural network to construct the global evolution of total electron density and whistler mode wave amplitude inside the plasmasphere and plume. These constructed whistler mode wave models are used to quantify the effects of whistler mode waves on the global electron loss using the 3D Fokker Planck diffusion simulation.

KEYWORDS : whistler mode waves, electron precipitation

Sr No: 211

Drifting Wormhole Structures observed in the Earth's Radiation Belt

CORRESPONDING & PRESENTING AUTHOR:

Satoko Nakamura, Nagoya University, Japan

Yoshizumi Miyoshi, Nagoya University, Japan

Kazuo Shiokawa, Nagoya University, Japan

Yoshiharu Omura, Kyoto University, Japan

Takefumi Mitani, JAXA, Japan

Nana Higashio, JAXA, Japan

Iku Shinohara, JAXA, Japan

Tomohiro Hori, Nagoya University, Japan

We present an observation of rapid flux depressions in radiation belt electrons, which is referred to as "drifting wormholes (DWHs)". On December 30, 2018, the Arase satellite, Van Allen Probes, and the Time History of Events and Macroscale Interactions during Substorms (THEMIS) detected intense and rapid fluctuations in the flux of relativistic electrons. We investigated the time variation of electron flux by normalizing it with the running average of the flux for a preceding 10 min interval. The time variation of electron flux shows depressions of 1-min scale with clear energy dispersion, which appeared only in the relativistic energy range (500 keV to a few MeV) and small pitch angles. The energy and pitch-angle range of DWH indicates that electromagnetic ion cyclotron (EMIC) waves caused strong pitch-angle scattering in a longitudinally limited region for a short time scale, and relativistic electrons precipitate into the upper atmosphere.

KEYWORDS : EMIC precipitation

Sr No: 212

Relativistic electron microbursts as high-energy tail of pulsating aurora electrons

CORRESPONDING & PRESENTING AUTHOR:

Yoshizumi Miyoshi, Nagoya University, Japan

Shinji Saito, NICT, Japan

Satoshi Kurita, Kyoto University, Japan

Kazushi Asamura, JAXA, Japan

Keisuke Hosokawa, The University of Electro-Communications, Japan

Takeshi Sakanoi, Tohoku University, Japan

Takefumi Mitani, JAXA, Japan

Yasunobu Ogawa, NIPR, Japan

Shin Oyama, Nagoya University, Japan

Fuminori Tsuchiya, Tohoku University, Japan

Sarah Jones, NASA, USA

Allison Jaynes, University of Iowa, USA

We show that sub-relativistic/relativistic electron microbursts form the high energy tail of pulsating aurora (PsA). Chorus waves that propagate along the magnetic field lines at high latitudes cause precipitation bursts of electrons with a wide energy range from a few kiloelectron volts (PsA) to several megaelectron volts (relativistic microbursts). The rising tone elements of chorus waves cause individual microbursts of sub-relativistic/relativistic electrons and the internal modulation of PsA with a frequency of a few Hz. The chorus bursts for a few seconds cause the microburst trains of sub-relativistic/relativistic electrons and the main pulsations of PsA. Our simulation studies demonstrate that both PsA and relativistic electron microbursts originate simultaneously from pitch angle scattering by chorus wave-particle interactions along the field line.

KEYWORDS : microbursts, pulsating aurora, chorus

Sr No: 213

--

SYMPOSIUM :   **D5 Relativistic electrons: Their emergence and loss in geospace, their impact on the upper atmosphere and the role of the cold plasma background**

Outer Radiation Belt Electron Flux Variability and ULF Waves Under the Influence of ICME and HSS Events During the Van Allen Probes Era

CORRESPONDING & PRESENTING AUTHOR:

Jose Paulo Marchezi, National Space Science Center, Chinese Academy of Sciences, National Institute for Space Research, China

Lei Dai, National Space Science Center, Chinese Academy of Sciences, China

Livia Ribeiro Alves, National Institute for Space Research, Brazil

Ligia Alves Da Silva, National Space Science Center, Chinese Academy of Sciences, National Institute for Space Research, China

David Gary Sibeck, Goddard Space Flight Center, USA

Alisson Dal Lago, National Institute for Space Research, Brazil

Chi Wang, National Space Science Center, Chinese Academy of Sciences, China

Hui Li, National Space Science Center, Chinese Academy of Sciences, China

Zhengkuan Liu, National Space Science Center, Chinese Academy of Sciences, China

All the planets and spacecraft inside the heliosphere can be affected by a disturbed solar wind condition. Interplanetary Coronal Mass Ejections (ICME) and Solar wind High-Speed Streams (HSS) cause disturbances in the Earth's magnetosphere, including the Van Allen Radiation Belts. We investigated how the electron's outer radiation belt changes respond to perturbations related to HSS and ICME events that hit the Earth's magnetosphere. We use electron flux density measurements from Van Allen's REPT instrument at 2.10 MeV and ULF waves at the Pc5 frequency range, together with solar wind parameters during the Van Allen Probes era, from October 2012 up to December 2017. We selected 140 HSS events and 49 ICME events, and we were able to compare 51 enhancements and 28 reduction events related to HSS, 17 enhancements, and 16 reduction events related to ICME events. The results show that ULF Pc5 waves are present in all the cases and can play a role in the diffusion of those particles. The cases of electron enhancements, the Interplanetary Magnetic Field (IMF) behavior at z-component, and the substorms with waves signal can help replenish the losses on the outer radiation belt.

KEYWORDS :   Pc pulsations, high-speed streams, enhancement

Sr No: 214

Polar Mesosphere Winter Echoes and Other Phenomena Associated with Energetic Electron Precipitation (by invitation)

CORRESPONDING & PRESENTING AUTHOR:

Yoshimasa Tanaka, National Institute of Polar Research, Japan

Takanori Nishiyama, National Institute of Polar Research, Japan

Akira Kadokura, National Institute of Polar Research, Japan

Mitsunori Ozaki, Kanazawa University, Japan

Yoshizumi Miyoshi, Nagoya University, Japan

Kazuo Shiokawa, Nagoya University, Jpan

Shinichiro Oyama, Nagoya University, Japan

Ryuho Kataoka, National Institute of Polar Research, Japan

Masaki Tsutsumi, National Institute of Polar Research, Japan

Koji Nishimura, Kyoto University, Jpan

Kaoru Sato, The University of Tokyo, Japan

Yoshiya Kasahara, Kanazawa University, Japan

Atsushi Kumamoto, Tohoku University, Japan

Fuminori Tsuchiya, Tohoku University, Japan

Mizuki Fukizawa, Tohoku University, Japan

Mitsuru Hikishima, Japan Aerospace Exploration Agency, Japan

Shoya Matsuda, Japan Aerospace Exploration Agency, Japan

Ayako Matsuoka, Kyoto University, Japa

Iku Shinohara, Japan Aerospace Exploration Agency, Japan

Masahito Nose, Nagoya University, Japan

Tsutomu Nagatsuma, National Institute of Information and Communications Technology, Japan

Manabu Shinohara, National Institute of Technology, Kagoshima College, Japan

Akiko Fujimoto, Kyushu Institute of Technology, Japan

Mariko Teramoto, Kyushu Institute of Technology, Japan

Reiko Nomura, Japan Aerospace Exploration Agency, Japan

Akira Yukimatu, National Institute of Polar Research, Japan

Keisuke Hosokawa, The University of Electro-Communications, Japan

Shoji Masafumi, Nagoya University, Japan

Ralph Latteck, Leibniz-Institute of Atmospheric Physics, Germany

Polar mesosphere winter echoes (PMWE) are enhanced backscatter echoes from the polar mesosphere that are observed with VHF radars during winter periods. Since the PMWE are often observed when electron density in the mesosphere is highly enhanced by energetic proton or electron precipitations, we use them as a proxy of the energetic particle precipitation. We present the PMWE and other various phenomena associated with the energetic electron precipitation (EEP), which were observed in the polar atmosphere and the inner magnetosphere during the passage of corotating interaction region at the leading edge of high-speed solar wind streams (HSS) on 21 March 2017. During this period, the PMWE were observed with the high-power atmosphere radars in both hemispheres, i.e., the PANSY radar at Syowa Station (SYO), Antarctica, and the MAARSY radar at Andoya, Norway. Electromagnetic ion cyclotron (EMIC) waves and whistler-mode chorus waves were simultaneously observed by the Arase satellite when the footprints of Arase were located near SYO and Husafell (HUS), Iceland. It was found that the temporal variations of the PMWE and the magnetospheric plasma waves are similar to each other, therefore, the pitch angle scattering of energetic electrons by the EMIC waves and the chorus waves is a plausible mechanism for the EEP. Pulsating auroras, cosmic noise absorption, and low-altitude (55-70 km) MF radar echoes were also detected at SYO and HUS, which support the EEP. We suggest a possible scenario in which these various phenomena can be explained by the interaction between the HSS and the magnetosphere.

KEYWORDS : polar mesosphere winter echoes, energetic electron precipitation, arase

Sr No: 215

The controlling effect of the plasma density on the acceleration of electrons to ultra-relativistic energies (by invitation)

CORRESPONDING & PRESENTING AUTHOR:

Yuri Shprits, German Research Centre for Geosciences (GFZ), Germany

Hayley Allison, German Research Centre for Geosciences (GFZ), germany

Alexander Drozdov, University of California Los Angeles, USA

Dedong Wang, German Research Centre for Geosciences (GFZ), Germany

Nikita Aseev, German Research Centre for Geosciences (GFZ), Germany

Irina Zhelavskaya, German Research Centre for Geosciences (GFZ), Germany

Maria Usanova, University of Colorado, USA

Measurements from the Van Allen Probes mission clearly demonstrated that the radiation belts cannot be considered as a bulk population above approximately electron rest mass. Ultra-relativistic electrons (~>4Mev) form a new population that shows a very different morphology (e.g. very narrow remnant belts) and slow but sporadic acceleration. We show that acceleration to multi-MeV energies can not only result of a two-step processes consisting of local heating and radial diffusion but occurs locally due to energy diffusion by whistler mode waves. Local heating appears to be able to transport electrons in energy space from 100s of keV all the way to ultra-relativistic energies (>7MeV). Acceleration to such high energies occurs only for the conditions when cold plasma in the trough region is extremely depleted down to the values typical for the plasma sheet.

There is also a clear difference between the loss mechanisms at MeV and multi MeV energies. The difference between the loss mechanisms at MeV and multi-MeV energies is due to EMIC waves that can very efficiently scatter ultra-relativistic electrons, but leave MeV electrons unaffected.

We also present how the new understanding gained from the Van Allen Probes mission can be used to produce the most accurate data assimilative forecast. Under the recently funded EU Horizon 2020 Project Prediction of Adverse effects of Geomagnetic storms and Energetic Radiation (PAGER) we will study how ensemble forecasting from the Sun can produce long-term probabilistic forecasts of the radiation environment in the inner magnetosphere.

KEYWORDS : ultra-relativistic, radiation belts, plasma waves

Sr No: 216

Modeling radiation belt electrons with information theory and neural networks

CORRESPONDING & PRESENTING AUTHOR:

Simon Wing, The Johns Hopkins University, USA

Sasha Ukhorskiy, The Johns Hopkins University, USA

Drew Turner, The Johns Hopkins University, USA

Jay Johnson, Andrews University, USA

Thomas Sotirelis, The Johns Hopkins University, USA

Romina Nikoukar, The Johns Hopkins University, USA

Alex Boyd, The Aerospace Corporation, USA

Giuseppe Romeo, The Johns Hopkins University, USA

Kiley Yeakel, The Johns Hopkins University, USA

An empirical model of radiation belt electrons is developed using RBSP data 2013-2018. The model inputs the solar wind and magnetospheric parameters and outputs radiation belt electron phase space density (psd). The process of selecting input parameters is complex. Many solar wind and magnetospheric parameters are correlated or anticorrelated with one another, making it difficult to determine which parameters would carry relevant and which would carry redundant information. Information theory is used to determine the relevant input parameters and their response lag times. It is also used to determine the effect of solar wind parameters as a function of L^*. The input parameters are ranked based on their information transfer to the radiation belt electrons. Using this ranking as a guide for selecting input parameters, the radiation belt electron model based on neural networks is developed. The preliminary result shows that the model predictive efficiency (PE) is ~0.66, which is comparable to those obtained in some previous models.

KEYWORDS :   radiation belt, empirical model, machine learning

Sr No: 217

Monitoring Plasmapause Dynamics from the Sub-Auroral Ionosphere (by invitation)

CORRESPONDING & PRESENTING AUTHOR:

Balazs Heilig, Mining and Geological Survey of Hungary, Hungary

Claudia Stolle, German Research Centre for Geosciences GFZ, Germany

Guram Kervalishvili, German Research Centre for Geosciences GFZ, Germany

Jan Rauberg, German Research Centre for Geosciences GFZ, Germany

Janos Lichtenberger, Eotvos Lorand University, Hungary

In the past decades researchers have revealed links between a series of sub-auroral ionospheric phenomena and the plasmapause (PP). Many of these ionospheric phenomena are observed by ESA's Swarm mission flying at polar Low-Earth Orbit (LEO), such as the mid-latitude ionospheric trough (MIT), the associated sub-auroral temperature enhancement (SETE), the sub-auroral ion drift (SAID), as well as the inner boundary

of small-scale field-aligned currents (SSB). Moreover, Swarm provides observations of auroral phenomena, such as the auroral oval boundaries (AOB) and the auroral electrojets (AEJ).

Thus, Swarm combined with the contemporarily flying NASA mission, RBSP, presents a unique opportunity to study the relations between all these ionospheric phenomena, as well as their relation to PP dynamics using collocated, simultaneous observations. In the frame of the ESA-funded PRISM project, data products to characterise MIT, SETE and SSB have been developed. AOB and AEJ are also available as Swarm-based products. In this talk, we present the results of a comparative study between the products derived within PRISM and other Swarm products. Then we demonstrate how LEO observations of ionospheric phenomena can be used to contribute to monitor the PP dynamics as one of the goals of a new ESA-funded project PLASMA.

KEYWORDS :   plasmapause, sub-auroral ionosphere, trough

Sr No: 218

On the Semi-Annual Variation of Relativistic Electrons in the Outer Radiation Belt

CORRESPONDING & PRESENTING AUTHOR:

Christos Katsavrias, National and Kapodistrian University of Athens, Greece

Constantinos Papadimitriou, National and Kapodistrian University of Athens, Greece

Sigiava Aminalragia Giamini, National and Kapodistrian University of Athens, Greece

Ioannis Daglis, National and Kapodistrian University of Athens, Greece

Ingmar Sandberg, Space Applications and Research Consultancy (SPARC), Greece

Piers Jiggens, ESA Space Environment, The Netherlands

The nature of the semi-annual variation in the relativistic electron fluxes in the Earth's outer radiation belt is investigated using Van Allen Probes (MagEIS and REPT) and GOES (EPS) data during solar cycle 24. We perform wavelet and cross-wavelet analysis in a broad energy and spatial range of electron fluxes and examine their phase relationship with the axial, equinoctial and Russell-McPherron mechanisms. It is found that the semi-annual variation in the relativistic electron fluxes exhibits pronounced power in the 0.3–4.2 MeV energy range at L-shells higher than 3.5 and, moreover, it exhibits an in-phase relationship with the Russell-McPherron effect indicating the former is primarily driven by the latter. Furthermore, the analysis of the past 3 solar cycles with GOES/EPS indicates that the semi-annual variation at geosynchronous orbit is evident during the descending phases and coincides with periods of a higher (lower) HSS (ICME) occurrence.

KEYWORDS :   radiation belts, semi-annual variation, Russell-McPherron effect

Sr No: 219

On the statistics of radial diffusion coefficients and their application to simulations in the framework of the SafeSpace project

CORRESPONDING & PRESENTING AUTHOR:

Christos Katsavrias, National and Kapodistrian University of Athens, Greece

Ioannis Daglis, National and Kapodistrian University of Athens, Greece

Afroditi Nasi, National and Kapodistrian University of Athens, Greece

Nourallah Dahmen, ONERA, France

Sebastien Bourdarie, ONERA, France

Antoine Brunet, ONERA, France

Constantinos Papadimitriou, National and Kapodistrian University of Athens, Greece

Radial diffusion has been established as one of the most important mechanisms contributing to the acceleration and loss of relativistic electrons in the outer radiation belt. Over the past few years efforts have been devoted to identify empirical relationships of radial diffusion coefficients (DLL) for radiation belt simulations, yet several studies have suggested that the difference between the various models can be orders of magnitude different at high levels of geomagnetic activity, as the observed DLL have been shown to be highly event-specific. In the framework of the SafeSpace project we have used 12 years (2009 – 2020) of multi-point magnetic and electric field measurements from THEMIS A, D and E satellites to create a database of calculated DLL. In this work we present the statistics on the evolution of DLL during the solar cycle 24 with respect to the various solar wind parameters, geomagnetic indices and universal coupling functions. Furthermore, we show the importance of the use of event-specific DLL through simulations of seed and relativistic electrons with the Salammbo code during the intense storm of St. Patricks 2015 and the high-speed stream driven storm of Christmas 2013.

KEYWORDS : radiation belts, radial diffusion, ULF waves

Sr No: 220

Acceleration and loss of relativistic electrons in the outer radiation belt: a delicate interplay between various mechanisms

CORRESPONDING & PRESENTING AUTHOR:

Christos Katsavrias, National and Kapodistrian University of Athens, Greece

Wen Li, Boston University, USA

Constantinos Papadimitriou, National and Kapodistrian University of Athens, Greece

Sandberg Sandberg, Space Applications and Research Consultancy (SPARC), Greece

Sigiava Aminalragia Giamini, National and Kapodistrian University of Athens, Greece

Ioannis Daglis, National and Kapodistrian University of Athens, Greece
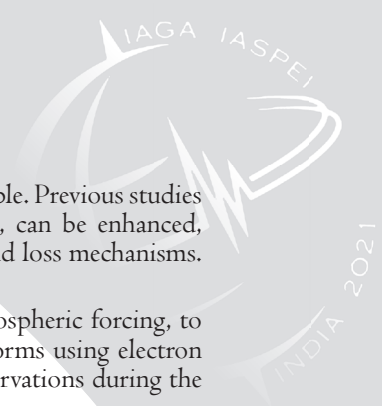
Abstract : Earth's outer radiation belt response to geospace disturbances is extremely variable. Previous studies have shown that the trapped relativistic electron population, in this near-Earth space, can be enhanced, depleted, or even not affected at all due to the interplay between electron acceleration and loss mechanisms.

We investigate outer belt's response to various types of solar wind and internal magnetospheric forcing, to geospace magnetic storms of different intensities and to intense magnetospheric substorms using electron phase space density calculations as well as concurrent Pc5 and chorus wave activity observations during the Van Allen Probes era.

Our results indicate that a degree of repeatability exists as these events share some common features regarding relativistic electron enhancements and losses. Furthermore, analysis of non–storm events, demonstrate that the mechanisms which enhance or deplete the electron population of the outer belt are mainly internal, and as such, are not always associated with geomagnetic storms, at least in terms of Dst (or SYM-H) index.

KEYWORDS : radiation belts, wave-particle interactions, substorm injections

Sr No: 221

SYMPOSIUM : **D5 Relativistic electrons: Their emergence and loss in geospace, their impact on the upper atmosphere and the role of the cold plasma background**

Stochastic variations of whistler-mode emissions in the Van Allen radiation belts (by invitation)

CORRESPONDING & PRESENTING AUTHOR:

Ondrej Santolik, Institute of Atmospheric Physics, Czech Republic

W. S. Kurth, University of Iowa, USA

C. A. Kletzing, University of Iowa, USA

Operational space weather models of the relativistic electron fluxes in the Van Allen radiation belts are becoming an important tool for preventing threats to space assets. These models usually include the influence of naturally occurring whistler mode waves in the geospace through the quasi-linear approximation. An accurate description of statistical properties of whistler mode waves is therefore needed.

Average or median intensities of whistler mode chorus and hiss emissions depend on position in the magnetosphere and on geomagnetic activity indices but their stochastic variations in spacecraft measurements at the same location and for the same geomagnetic activity level are usually comparable to these large-scale spatio-temporal effects.

We use the survey measurements of the Waves instruments of the Electric and Magnetic Field Instrument Suite and Integrated Science (EMFISIS) on board two Van Allen Probes to asses these stochastic variations. We take advantage of the entire data set of these measurements with a nearly 100% coverage from August 31, 2012 till October 13, 2019 (2600 days) for spacecraft A, and from September 1, 2012 till July 16, 2019 (2510 days) for spacecraft B.

KEYWORDS : Van Allen radiation belt, whistler mode hiss, whistler mode chorus

Sr No: 222

Coordinated observations of the effect of consecutive high speed stream pulses on relativistic electron enhancement

Corresponding & Presenting Author:

Afroditi Nasi, National and Kapodistrian University of Athens, Greece

Ioannis A. Daglis, National and Kapodistrian University of Athens, Greece

Christos Katsavrias, National and Kapodistrian University of Athens, Greece

Ingmar Sandberg, Space Applications & Research Consultancy (SPARC), Greece

Wen Li, Boston University, USA

Yoshizumi Miyoshi, Nagoya University, Japan

Shun Imajo, Kyoto University, Japan

Takefumi Mitani, Japan Aerospace Exploration Agency, Japan

Tomo Hori, Nagoya University, Japan

Satoshi Kasahara, University of Tokyo, Japan

Shoichiro Yokota, Osaka University, Japan

Kunihiro Keika, University of Tokyo, Japan

Iku Shinohara, Japan Aerospace Exploration Agency, Japan

Ayako Matsuoka, Kyoto University

Yoshiya Kasahara, Kazanawa University, Japan

During the second half of 2019, a series of recurring, moderate geomagnetic storms (Dstmin ≈ - 70 nT) emerged after a sequence of high-speed solar wind streams (VSW ≥ 600 km/s) impacted the magnetosphere. During one of these storms, intense substorm activity was also recorded (SML ≈ - 2000 nT on August 31 and September 1), as well as a longer-lasting solar wind pressure pulse.

We investigate this series of events, using particle measurements from three missions that recorded significant enhancements of relativistic electron fluxes: the Van Allen Probes, Arase and Galileo 207 & 215 satellites. We use both the flux intensity and the phase space density (PSD) of electrons, along with interplanetary parameters and information on ultra-low frequency (ULF) and chorus wave activity for a detailed analysis of this event.

Our study demonstrates the importance of substorm injections, even during moderate or weak geomagnetic storms. The presence of seed electrons at $L^* = 4$-5, in addition to intense ULF and chorus wave activity, seems to result in very efficient electron acceleration to relativistic and ultra-relativistic energies.

KEYWORDS : relativistic electrons, wave-particle interactions, electron acceleration

Sr No: 223

Plasmashperic products for space weather services (by invitation)

CORRESPONDING & PRESENTING AUTHOR:

Janos Lichtenberger, Eötvös University, Hungary

Balazs Heilig, Eötvös University, Hungary

Anders Jorgensen, New Mexico Institute of Mining and Technology, USA

Peter Steinbach, Hungarian Academy of Sciences, Hungary

David Koronczay, Eötvös University, Hungary

Lilla Juhasz, Eötvös University, Hungary

Nikolett Biro, Eötvös University, Hungary

Bendeguz Bendicsek, Budapest University of Technology and Economics, Hungary

The plasmasphere is torus of cold (~ 1 eV) plasma co-rotating with the Earth. A dynamic region being permanently influenced by the region below (ionosphere) and above (outer magnetosphere) and is controlled by the relative intensities of the solar wind-imposed electric field and the corotation electric field, together with the time-varying background magnetic field. The plasmasphere plays a central role in magnetosphere-ionosphere dynamics and particularly in radiation belts dynamics.

In an ongoing project funded by ESA, we will develop a series of products that can be utilized directly by radiation belt, ring current and ionosphere models and spacecraft operators as well as indirectly by spacercraft designers and launchers, telecommunication and navigation satellite operators and insurance companies.

The products include electron and plasma mass densities based on ground based measurements, empirical and data assimilative models of plasmasphere and plasmapause, and a plasmasphere index based on in-situ and ground based data.

In this talk we present details about the project, products and the plan to integrate it to ESA Space Weather portal.

KEYWORDS :   plasmasphere, space wheather, ESA

Sr No: 224

Uncertainty Quantification for radiation belt physics (by invitation)

CORRESPONDING & PRESENTING AUTHOR:

Enrico Camporeale, University of Colorado, USA

We present a study of the uncertainty quantification relative to radiation belt simulations. In particular, we estimate how uncertainties of some input parameters propagate through the nonlinear simulation, producing a distribution of outputs that can be quite broad. Here we restrict our focus on two-dimensional simulations

(in energy and pitch angle space) of parallel-propagating chorus waves only, and we study as stochastic input parameters the geomagnetic index Kp (that characterizes the time dependency of an idealized storm), the latitudinal extent of waves, and the average electron density. We employ a collocation method, thus performing an ensemble of simulations. The results of this work point to the necessity of shifting to a probabilistic interpretation of radiation belt simulation results and suggest that an accurate specification of a time-dependent density model is crucial for modeling the radiation environment.

KEYWORDS : uncertainty quantification, cold plasma, ensemble modeling

Sr No: 225

SYMPOSIUM : **D5 Relativistic electrons: Their emergence and loss in geospace, their impact on the upper atmosphere and the role of the cold plasma background**

Low L-shell EMIC wave observations by the Van Allen Probes (by invitation)

CORRESPONDING & PRESENTING AUTHOR:

Maria Usanova, University of Colorado at Boulder, USA

Electromagnetic ion cyclotron (EMIC) waves are transverse electromagnetic waves typically generated in the equatorial magnetosphere by anisotropic ion distributions. These waves have been shown to resonantly interact with multiple particle populations in the magnetosphere and are believed to be an important loss process for energetic ring current ions and radiation belt electrons, as well as a cold plasma heating mechanism.

While the outer boundary of EMIC wave generation region is well defined and can be found as far outward as the magnetopause, the location of the inner boundary and the mechanisms that control it are still an open question, partly because low L-shell events are very rare. Here we present a survey of the Van Allen Probes electric and magnetic field data over the entire mission duration and show that EMIC waves can be generated as low as L=1.7 during highly disturbed geomagnetic conditions. We examine properties of these waves, their radial extent and location with respect to the plasmapause. These observations may be important for the dynamics of the inner zone and slot region during geomagnetic storms.

KEYWORDS : EMIC waves, geomagnetic storms, slot region

Sr No: 226

What are the radiation belts doing inside the plasmasphere? (by invitation)

CORRESPONDING & PRESENTING AUTHOR:

Geoffrey Reeves, Los Alamos National Lab., Mexico

The radiation belts consist of the most energetic, magnetically trapped, charged particles in the Earth's magnetosphere. The plasmasphere consists of the least energetic. The two populations are traditionally considered to occupy two distinct spatial domains with the inner edge of the outer radiation belt electrons co-located with the outer edge of the plasmasphere [e.g. Li et al., 2001]. This long-standing framework is misleading. Typically, much of the outer radiation belt can be found inside the plasmasphere where important radiation belt - plasmasphere interactions take place.

Under enhanced geomagnetic activity the outer regions of the plasmasphere are eroded and the plasmapause retreats earthward. At the same time radiation belt electron fluxes are enhanced through both local wave-particle acceleration and inward radial diffusion. There is, however, no single location for the inner edge of the radiation belts. While the boundary is sharp it is highly energy-dependent with lower energies penetrating to lower L-shells than higher energies. Whether the radiation belts are inside, outside, or near the plasmapause depends on energy.

Similarly, in the recovery phase the Alfven layer moves far outward over the outer belt. Once the larger plasmasphere is of sufficient density to support whistler-mode hiss wave-particle interactions begin to scatter radiation belt electrons into the loss cone. This process is also energy (and L-shell) dependent. Therefore, even after long periods, the relationship between plasmapause location and the outer radiation belts is energy-dependent and, particularly at the highest energies, the radiation belts linger inside the plasmasphere.

KEYWORDS :   radiation belts, space weather, storms

D6 Geomagnetic observations for space science, space weather and space climate applications

CONVENERS: Pierdavide Coïsson

Miquel Torta

Ellen Clarke

Magnetic field observations, both from ground and from space, provide information on the current state of space weather and are the corner stone for both scientific understanding and practical applications. Providing timely and accurate geomagnetic measurements is key to generating space weather information in general, and to producing nowcasts and forecasts, in particular. Current and historical geomagnetic data are also relevant for space science studies, including space climate, the long term variation in solar activity and their effects in the near Earth environment. Solar cycle 24 has been relatively weak, but several geomagnetic storms occurred. The complexity of the phenomena occurring during such events still requires significant research efforts to understand the interactions between the various regions of Earth space environment and the induced effects on ground. Space weather events can severely impact modern technologies by disrupting essential services, making it critical to improve their understanding and predictability. Better understanding of the role of longer term changes in the heliosphere and geomagnetic field interactions is also an important factor. Contributions that make use of magnetic field measurements to demonstrate recent advances in the understanding of the space weather hazard and impact are welcome. This could include, but is not limited to, models of both the space environment and the solid earth, to quantify how rapid magnetic variations and sub-surface conductivity impact conducting infrastructures on the ground and improve our physical understanding of electromagnetic fields on, and near, Earth. This session aims to present recent updates in the use of magnetic measurements in space science, space weather and space climate applications.

Sr No: 227

Converting a model of ionospheric reconfiguration timescales into a forecast model of ground level geomagnetic variations (by invitation)

CORRESPONDING & PRESENTING AUTHOR:

Robert Shore, British Antarctic Survey, France

Mervyn Freeman, British Antarctic Survey, France

We summarise some recent and new advances in geomagnetic field modelling, both from during the SWIGS project, and from the new SWIMMR-SAGE project. These advances are aimed at determining the location, extent, and timescales of surface geomagnetic field variations caused by space weather, and also aim to describe the underlying space physics.

Shore et al. (2018) have isolated and identified the spatio-temporal patterns of large-scale surface geomagnetic variations by combining Empirical Orthogonal Functions (EOF) and network analysis. This provides us a toolset and database to understand and quantify the relative contributions to the surface geomagnetic field from different physical processes.

Shore (2019a, b) have related each individual geomagnetic field pattern, or ionospheric equivalent current system, to its driving by the Sun via the solar wind. The authors have shown that different modes of geomagnetic variability have different correlations with the solar wind coupling function epsilon (Perreault and Akasofu, 1978). This research defines the extent to which the solar wind causes a geomagnetic response at each high-latitude location on the Earth's surface, in addition to how big the effect will be, and how long it will persist for.

In the SWIMMR-SAGE project, we are using this new understanding of the physics underlying space weather to build a forecast model of geomagnetic variations at ground level, dependent on solar wind driving and auroral oval boundary proximity. This research is laying the groundwork for the next generation of Met Office space weather forecast models.

REFERENCES

https://doi.org/10.1111/j.1365-246X.1978.tb05494.x

https://doi.org/10.1002/2017JA024420

https://doi.org/10.1029/2019SW002161

https://doi.org/10.1029/2019JA026543

KEYWORDS : space weather forecast

Sr No: 228

Uncertainties on GIC computations: A Portuguese case study

CORRESPONDING & PRESENTING AUTHOR:

Fernando Pinheiro, Centro de Investigação da Terra e do Espaço da Universidade de Coimbra, Portugal

Joana Alves Ribeiro, Centro de Centro de Investigação da Terra e do Espaço da Universidade de Coimbra, Portugal

Rute Santos, Laboratory for Instrumentation, Biomedical Engineering and Radiation Physics - UC

Pedro Soares, Instituto Dom Luiz, Portugal

Maria Alexandra Pais, Centro de Centro de Investigação da Terra e do Espaço da Universidade de Coimbra, Portugal

Joao Cardoso, Laboratory for Instrumentation, Biomedical Engineering and Radiation Physics – UC, Portugal

Fernando A. Monteiro Santos, Instituto Dom Luiz, Portugal

The threat posed by geomagnetically induced currents (GICs) over high voltage transmission networks is an issue of increasing concern as our dependence on technological systems increases. Not all research groups have access to the same amount of information. For instance, some researchers may not know the true path followed by the power lines, while others may not know the resistivity values at transformer stations. This fact forces people to simplify assumptions that may affect GIC computations to a different extent.

This presentation addresses different sources for GIC uncertainties applied to the Portuguese case during solar cycle 24. In particular, we evaluate how uncertainties on the geomagnetic observations and on the conductivity model used to affect the induced geoelectric field computation. Likewise, we assess the impact of different assumptions on the power grid model (e.g., concerning the true line path or the presence of the shield wires) on the GIC computation. This works takes advantage of the most recent conductivity model for the territory and network parameters provided by the national power transmission operator REN – Redes Energéticas de Portugal.

Identification of the main GIC error contributors will become particularly important at the moment there will be GIC measurements available. These will suggest lines of action for improving simulations.

KEYWORDS : gomagnetic induced currents, power network, portugal mainland

Sr No: 229

SYMPOSIUM : **D6 Geomagnetic observations for space science, space weather and space climate applications**

Investigation of the possibility of GIC development in the Mediterranean region during the strongest magnetic storms of solar cycle 24

CORRESPONDING & PRESENTING AUTHOR:

Adamantia Zoe Boutsi, National Observatory of Athens, Greece

George Balasis, National Observatory of Athens, Greece

Ioannis A. Daglis, National and Kapodistrian University of Athens, Greece

Kanaris Tsinganos, National and Kapodistrian University of Athens, greece

Omiros Giannakis, National Observatory of Athens, Greece

Geomagnetically Induced Currents (GIC) constitute an integral part of the space weather research and a subject of ever-growing attention for countries located in the low and middle latitudes. A series of recent studies highlights the importance of considering GIC risks for the Mediterranean region. Here, we exploit data from the HellENIc GeoMagnetic Array (ENIGMA), which is located in Greece, complemented by magnetic observatories in the Mediterranean region (France, Italy, Spain, Turkey and Algeria), to calculate corresponding values of the GIC index, i.e., a proxy of the geoelectric field calculated entirely from geomagnetic field variations. We perform our analysis for the most intense magnetic storms (Dst < -150 nT) of solar cycle 24. Our results show a good correlation between the storm sudden commencement (SSC) and an increase of the GIC index value. These investigations indicate that despite the elevated amplitude of the GIC index the associated risk remains at low level for all magnetic observatories / stations under study during the considered storm events.

KEYWORDS : geomagnetically induced currents, mediterranean region, solar cycle 24
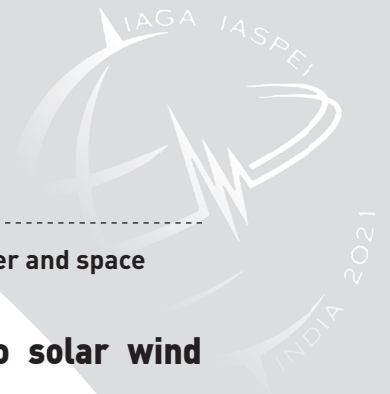
Sr No: 230

The Polar Cap (PC) index combination, PCC: relations to solar wind properties and global magnetic disturbances.

CORRESPONDING & PRESENTING AUTHOR:

Peter Stauning, Danish Meteorological Institute, Denmark

The non-negative Polar Cap PCC index built from PCN (North) and PCS (South) indices correlates better with the solar wind merging electric field, with the development of geomagnetic disturbances represented by the Kp index, and with ring current indices than either of the hemispheric indices. The present contribution builds on the publication of the same name (https://doi.org/10.1051/swsc/2020074) which demonstrates that the ring current index, Dst, to a high degree of accuracy can be derived from a differential source function built from PCC indices. As an example, integration of the PCC-based source function throughout the interval from 1992 to 2018 without attachment to the real Dst indices has generated equivalent Dst values that correlate very well (R=0.86) with the real Dst index values, which are represented with a mean deviation less than 1 nT and an overall rms deviation less than 13 nT. Building the ring current is considered to represent the energy input from the solar wind, which also powers auroral disturbance processes such as substorms and upper atmosphere heating. With currently available PC indices, detailed and accurate SYM-H or Dst index values to represent the ring currents could be derived up to nearly one hour ahead of actual time by integration of the PCC-based source function from any previous quiet state. Thus, the PCC indices enabling accurate estimates of the energy input from the solar wind are powerful tools for space weather monitoring and for solar-terrestrial research.

KEYWORDS : polar cap index, solar wind, geomagnetic ring current

Sr No: 231

Diurnal distribution of whistler in Extremely Low Frequencies observed at LEO altitude by Swarm satellites

CORRESPONDING & PRESENTING AUTHOR:

Pierdavide Coisson, Universite de Paris, Institut de physique du globe de Paris, CNRS, France
Gauthier Hulot, Universite de Paris, Institut de physique du globe de Paris, CNRS, France
Louis Chauvet, Universite de Paris, Institut de physique du globe de Paris, CNRS, France
Pierre Vigneron, Universite de Paris, Institut de physique du globe de Paris, CNRS, France
Olivier Bonnot, Universite de Paris, Institut de physique du globe de Paris, CNRS, France
Vladimir Truhlik, Institute of Atmospheric Physics CAS, China
Dalia Buresova, Institute of Atmospheric Physics CAS, China
Jaroslav Chum, Institute of Atmospheric Physics CAS, China
Janusz Mlynarczyk, AGH University, Poland
Pawel Rzonca, AGH University, Poland
Andrzej Kulak, AGH University, Poland

The Absolute Scalar Magnetometers (ASM) onboard Swarm satellites nominally measure the magnetic field intensity at 1 Hz, but can also be run at 250 Hz, during specific burst-mode data acquisition campaigns. After a few early sessions in 2014, at times of high solar activity, regular 1-week burst acquisition campaigns have been run every month since 2019, during the minimum of the solar cycle.

The Swarm mission has a unique orbital configuration, with polar satellites slowly drifting in local time (LT). The complete coverage of all LT has now been reached, allowing a better understanding of the distribution of whistlers in the Extremely Low Frequency at these orbital altitudes. These whistlers predominantly occur in the evening hours.

We analysed the lightning-generated whistlers, aiming at better understanding their propagation between the lightning source in the troposphere and the satellite in the ionosphere. Data from the World ELF Radiolocation Array (WERA) allowed us to characterise the lightning strikes, and ionosonde data and in-situ electron density measurements from the Electric Field Instrument (EFI) of Swarm were used to constrain the ionospheric medium through which these signals propagate. We also used the IRI Real-Time Assimilative Mapping (IRTAM) for the International Reference Ionosphere (IRI) model to obtain a realistic ionospheric background for events occurring far away from ionosonde locations. The dispersion of whistler signals can be reproduced in a satisfactory way using this technique, showing that opportunistic ionospheric monitoring using these natural signals is possible.

KEYWORDS : whistlers, ionospheric propagation

Sr No: 232

Spatio-temporal statistics of large scale auroral electrojet currents relative to substorm onset latitude and magnetic local time

CORRESPONDING & PRESENTING AUTHOR:

Sebastian Kaki, Finnish Meteorological Institute, Finland

Ari Viljanen, Finnish Meteorological Institute, Finland

Liisa Juusola, Finnish Meteorological Institute, Filand

Kirsti Kauristie, Finnish Meteorological Institute, Finland

The electric currents flowing in the ionosphere change rapidly and a large amount of energy is dissipated in the auroral ionosphere during auroral substorAn important part of the auroral current system are the auroral electrojets whose profiles can be estimated from magnetic field measurements from low Earth orbit satellites. We have combined electrojet data derived from the Swarm satellite mission of ESA with the substorm database derived from the SuperMAG ground network data. We organize the electrojet data in relation to the location of the onset and obtain statistics for the development of the integrated current and latitudinal location of the auroral electrojets relative to the onset. The effect of the magnetic local time of the onset was studied by dividing the data into pre-midnight and post-midnight onsets. We show that the median of the latitudinal location of the maximum of the westward electrojet and the greatest change in the median integrated westward current are co-located with the SuperMAG onset regardless of the magnetic local time sector of the onset.

KEYWORDS : substorms, electrojets, swarm

Sr No: 233

Symposium :   D6 Geomagnetic observations for space science, space weather and space climate applications

# Next Generation Operational Space Weather Nowcasts and Forecasts of Space Weather Impact on UK Ground-level Conducting Infrastructure

CORRESPONDING & PRESENTING AUTHOR:

Alan Thomson, BGS, UK

Ciaran Beggan, BGS, UK

Jeremy Chittenden, Imperial College London, UK

Ellen Clarke, BGS. UK

Jonathan Eastwood, Imperial College London, UK

Colin Forsyth, Dept. Space & Climate Physics, UK

Mervyn Freeman, British Antarctic Survey, UK

Michael Heyns, Imperial College London, UK

Juliane Huebert, BGS, UK

Gemma Richardson, BGS, UK

Rob Shore, British Antarctic Survey, UK

Andy Smith, Dept. Space & Climate Physics, UK

The UK government is funding a range of projects to deliver operational nowcast and forecast services, running in real-time, 24/7, through the Met Office Space Weather Operations Centre. This program is called SWIMMR ('Space Weather Instrumentation, Measurement, Modelling and Risk'). SAGE is the 'SWIMMR Activities in Ground Effects' project and is described here.

SAGE will provide enhanced capability in modelling and forecasting the Geomagnetically Induced Current risk to the UK power transmission network. SAGE will also provide a service for high pressure gas transmission operators, through estimation of Pipe-to-Soil Potential in the UK network. Finally, SAGE will explore assessment of the hazard to the rail signalling network. Operational SAGE models will be run on third-party internet servers and data products will be visualised for ease of forecaster interpretation.

The SAGE research and fieldwork programme will improve elements of the modelling chain, from solar wind measurements through to impact on ground technology, via the conductivity structure of the Earth. SAGE enhances real-time monitoring of geomagnetic variations across the UK through an extended magnetometer array. SAGE also forecasts the ground geomagnetic field through both an empirical model, SPIDER, and the physics-based magnetospheric models, GORGON and SWMF, and couples these to improved models of the ground geoelectric field. SAGE incorporates several Machine Learning products that provide a contextual view for all the deterministic model outputs. Indeed, the variety of input data (real-time, forecast, physics-based and empirical) delivered to the power, pipeline and railway network impact models provides diversity for assessment of model accuracy.

KEYWORDS :   GIC, services, forecasts

Sr No: 234

Mapping the 1989 magnetic superstorm: Geoelectric hazards and North American power-grid anomalies (by invitation)

CORRESPONDING & PRESENTING AUTHOR:

Jeffrey Love, U.S. Geological Survey, USA

Greg Lucas, University of Colorado, USA

E. Joshua Rigler, U.S. Geological Survey, USA

Anna Kelbert, U.S. Geological Survey, USA

Benjamin Murphy, U.S. Geological Survey, USA

A study is made of the spatiotemporal relationship between geomagnetic disturbance, induced geoelectric fields, and operational interference ("anomalies") experienced on the North American power grid during the March 1989 magnetic superstorm. For this, a 1-min time sequence of geomagnetic disturbance maps are constructed by fitting spherical-elementary current functions to magnetometer data time series collected at 24 ground-based observatories by the U.S. Geological Survey and Natural Resources Canada. A time sequence of geoelectric field maps is obtained by convolving the geomagnetic disturbance maps with 3098 magnetotelluric impedance tensors acquired across North America by projects sponsored by the United States National Science Foundation, NASA, the U.S. Geological Survey, and the Canadian Natural Sciences and Engineering Research Council. Geomagnetic and geoelectric maps are compared with the locations and times of the power-grid anomalies. This study's focus is on a sudden commencement of the 1989 storm, when the Hydro-Québec power-grid system collapsed, and on the main-phase of the storm, when numerous power-grid anomalies were experience across the Northern Midwest and the Northeast United States. This study informs understanding of the natural events that caused grid interference across North America during the storm. It demonstrates the importance of long-term monitoring of magnetic storms and large-scale magnetotelluric surveys, as well as the utility of public reports of storm-induced power-grid anomalies. It also highlights the need for a denser network of geomagnetic observatories across North America, the need for complete magnetotelluric surveying across Canada, and the importance of completing the national magnetotelluric survey of the United States.

KEYWORDS : magnetic-storm hazards, geomagnetic monitoring, magnetotelluric surveys

Sr No: 235

Space Weather Impacts on Grounded Structures (SWIGS): A Summary of British Geological Survey (BGS) Results

CORRESPONDING & PRESENTING AUTHOR:

Ciaran Beggan, British Geological Survey, UK

Gemma Richardson, British Geological Survey, UK

Juliane Huebert, British Geological Survey, UK

Adam Collins, British Geological Survey, UK

Natalia Gomez Perez, British Geological Survey, UK

Alan Thomson, British Geological Survey, UK
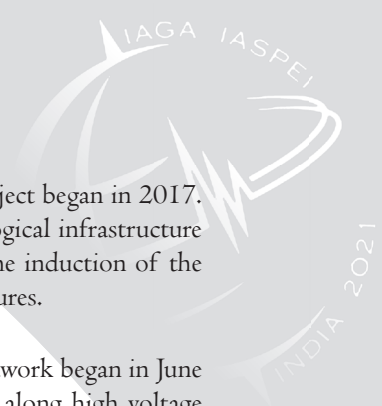
The UK NERC-funded Space Weather Impacts on Grounded Structures (SWIGS) project began in 2017. Its aim was to better understand the various steps of space weather impacts on technological infrastructure starting at the magnetosphere-ionosphere interaction with the solar wind through to the induction of the geoelectric field in the conductive subsurface to the flow of GIC through ground structures.

At British Geological Survey (BGS), planning, procurement, build and initiation of fieldwork began in June 2017, with the main purpose being to make differential magnetometer measurements along high voltage lines across the UK. Other work included magnetotelluric measurements. We also began upgrading the representation of the high voltage power transmission network in the UK to model GIC in a more refined manner at a transformer level, and created the first model of the high-pressure gas pipeline network to compute Pipe-to-Soil potentials. We investigated the use of historic resistivity measurement in a BGS-held database and analysed localised geoelectric field effects. Along with other partners in the SWIGS consortium, efforts were made to introduce forecasting and nowcasting techniques too. We give an overview of progress in the SWIGS project with focus on the main findings of the research within BGS.

KEYWORDS : magnetometer, GIC, hazard

Sr No: 236

SYMPOSIUM : **D6 Geomagnetic observations for space science, space weather and space climate applications**

Dynamics of the ground magnetic field and its time derivative during space weather events

CORRESPONDING & PRESENTING AUTHOR:

Mirjam Kellinsalmi, Finnish Meteorological institute, Finland
Ari Viljanen, Finnish Meteorological Institute, Finland
Liisa Juusola, Finnish Meteorological Institute, Finland
Sebastian Kaki, Finnish Meteorological Institute, Finland

Geomagnetic variations are mainly produced by external currents in the ionosphere and magnetosphere, and secondarily by induced (internal/telluric) currents in the conducting Earth. Large geomagnetically induced currents (GIC) are associated with large time derivatives of the horizontal magnetic field (H). Recent results show that the time derivative (dH/dt) is typically dominated by the contribution from the telluric currents. Our goal is to find measures to quantify the behaviour of the external and internal parts of H and dH/dt during space weather events associated with large dH/dt (and GIC). Results of this study show that the H vector has quite a narrow directional distribution whereas dH/dt is much more scattered. We also demonstrate a notable difference between H and dH/dt, when their directional changes are considered as a function of time. Initial interpretation of the results is given and consequences to the predictability of H and dH/dt are discussed.

KEYWORDS : GIC, geomagnetism

Sr No: 237

Using differential magnetometer measurements to validate GIC modelling in the Spanish power grid

CORRESPONDING & PRESENTING AUTHOR:

J. Miquel Torta, Observatori de l'Ebre, Spain

Santiago Marsal, Observatori de l'Ebre, Spain

Juan Jose Curto, Observatori de l'Ebre, Spain

Victoria Canillas Perez, Observatori de l'Ebre, Spain

Oscar Cid, Observatori de l'Ebre, Spain

Miquel Ibanez, Observatori de l'Ebre, Spain

Alex Marcuello, Universitat de Barcelona, Spain

Geomagnetically induced currents (GIC) are electrical currents induced in conductors operated on the earth's surface in response to geoelectric fields ultimately resulting from space weather events. Given its harmful effects on those systems, GIC modelling has become a practice of increasing interest. However, those geoelectric fields are rarely measured directly, but can be estimated from ground observations of the magnetic field and knowledge of the surface impedance. The geoelectrical source of the GIC is then connected to the load of the circuit, which is provided by the resistances and topology of the network, thus eventually enabling a modeling approach of the GIC. Validation is thus another fundamental step of the process, as it allows assessing the validity of the assumptions made in the models (i.e., earth conductivity structure, network parameters …) by comparing their output with real GIC observations. Geomagnetic observatory practice is also useful for performing differential magnetometric measurements by placing a vector magnetometer under a certain power transmission line, and deducing the GIC flowing in it by comparing its measurements with contemporary measurements of another station located at a distance far enough from the line to exclude the signals derived from the GIC. In this work, we focus on the methodology followed to achieve results concerning the measurement of the GIC flowing in some power lines of the Spanish power transmission grid, and share our experience on the installation of the measuring points.

KEYWORDS : GIC, measurements, validation

Sr No: 238

Forecasting Geomagnetic activity (Dst Index) using Kalman filter

PRESENTING AUTHOR:

Nilam Bhosale, Indian Institute of Geomagnetism, India

CORRESPONDING AUTHOR:

S. Tulasiram, Indian Institute of Geomagnetism, India

In this work, we have adopted the Kalman filter method to make a reliable forecast of geomagnetic activity (Dst index) for real-time applications. In this method, an educated estimate of Dst (forecast) is made based on the ring current state dynamics like injection and decay rates. This estimated Dst is further
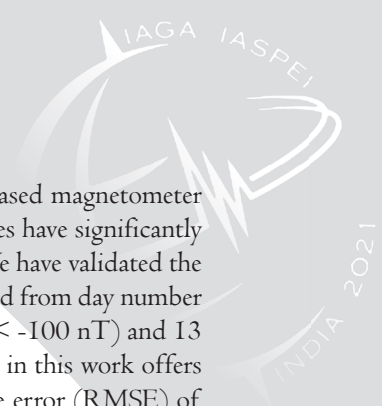
updated (nowcast) with the assimilation of real-time ?H values from a single ground based magnetometer observations at Alibag. Further, the accuracy of both forecasted and nowcasted Dst values have significantly improved by incorporating the effects due to local time asymmetry in the ring current. We have validated the forecasted and nowcasted Dst values with the true Dst during the severely disturbed period from day number 1 to 300 of the year 2001 which consists of 2 super (Dst < -250 nT), 8 intense (Dst < -100 nT) and 13 moderate geomagnetic storms (Dst < -50 nT). The Kalman filter method implemented in this work offers an accurate forecast and nowcast of geomagnetic activity (Dst) with a root mean square error (RMSE) of 12.4 and 11.5 nT, respectively.

Sr No: 239

SYMPOSIUM :   **D6 Geomagnetic observations for space science, space weather and space climate applications**

Forecasting hazardous geomagnetically induced currents for Spanish critical infrastructures by using AI

Florencia Castillo, Universität Heidelberg, Germany

Juan Jose Curto, Observatori de l'Ebre, Spain

CORRESPONDING AUTHOR:

Carlos Escobar, Insituto Física Corpuscular, Spain

Carmen Garcia, Instituto de Física Corpuscular, Spain

PRESENTING AUTHOR:

Jose E. Garcia, Insituto Física Corpuscular, Spain

Juan Ledo, Universitat de Barcelona, Spain

Alex Marcuello, Universitat de Barcelona, Spain

Santi Marsal, Observatori de l'Ebre, Spain

Anna Marti, Universitat de Barcelona, Spain

Pilar Queralt, Universitat de Barcelona, Spain

Veronica Sanz, Instituto de Física Corpuscular, Spain

Joan Miquel Torta, Observatori de l'Ebre, Spain

Bryan Zaldivar, Universidad Autonoma de Madrid, Spain

Extreme space weather events, and its consequent geomagnetic field variations, are sources of electric induction in the Earth that cause geomagnetically induced currents (GIC) in conductors located on its surface. These currents could affect critical infrastructures such as the power transmission grid, railways, and oil and gas pipelines. In this contribution, we present a study to obtain an early warning system to evaluate the impact of violent solar storms on Spanish infrastructures.

The study consists of two distinct stages. First, we will use as input real-time data from the solar wind space probe ACE (located at the L1 point in space) as the input to develop a deep learning model taking into account past conditions to predict the variation of the magnetic field on the Earth's surface at different locations in Spain. Second, we will feed these predictions into a physical model of the 3D Earth's electrical resistivity to generate the geoelectric fields that drive the geomagnetically induced currents.

Various deep learning techniques have been investigated to obtain the best early warning and prediction. In particular, deep neural networks are of interest as they are capable of reproducing a temporal sequence, allowing us to exploit their temporal dynamic behavior and predictive power. Thus, the selected neural

network architectures are Long Short-Term Memory (LSTM) and Convolutional Neural Networks (CNN). Additionally, latest improvements in the machine learning field such as combinations of CNN+LSTM and Attention Mechanism have been explored.

Sr No: 240

The magnetic field investigation on the ARASE (ERG) mission: Data characteristics and scientific results

CORRESPONDING & PRESENTING AUTHOR:

Ayako Matsuoka, Graduate School of Science, Kyoto University, Japan

Mariko Teramoto, Kyushu Institute of Technology, Japan

Reiko Nomura, Japan Aerospace Exploration Agency, Japan

Yoshizumi Miyoshi, Nagoya University, Japan

Masahito Nose, Nagoya University, Japan

Masahiro Kitahara, Nagoya University, Japan

Akiko Fujimoto, Kyushu Institute of Technology, Japan

Yoshimasa Tanaka, National Institute of Polar Research, Japan

Manabu Shinohara, Kagoshima College, Japan

Yuki Obana, Osaka Electro-Communication University, Japan

Satoshi Kurita, Kyoto University, Japan

Shun Imajo, Kyoto University, Japan

Iku Shinohara, Japan Aerospace Exploration Agency, Japan

The acceleration process of the charged particles in the inner magnetosphere is considered to be closely related to the deformation and perturbation of the magnetic field. Accurate measurement of the magnetic field is required to understand the acceleration mechanism of the charged particles, which is one of the major scientific objectives of the ARASE (ERG) mission.

A fluxgate magnetometer (MGF) was built for the ARASE satellite to measure DC and low-frequency magnetic field. We designed MGF which is optimized to investigate following topics; background magnetic field, ULF electromagnetic waves and EMIC waves.

Data from MGF have shown various specific phenomena to the inner magnetosphere. The polarity of the Pc 3-5 ULF waves can be precisely determined by the accurate alignment calibration of the data. It enables us to see the global structure of the magnetospheric oscillation. The original sampling frequency of MGF is 256Hz, and EMIC waves are found at altitudes from the perigee (440 km) to the apogee (32, 000 km), at various magnetic field intensities. The dipolarization and associated waves are observed at substorm events. The accurate measurement of the magnetic field makes it possible to estimate the intensity of the electric current and its temporal variation.

After MGF started the nominal operation in March 2017, it has continuously observed the magnetic field for four years. The stored data shows us the statistical feature if the inner magnetosphere. The superiority of the magnetic field measurement by Arase and derived scientific results are presented.
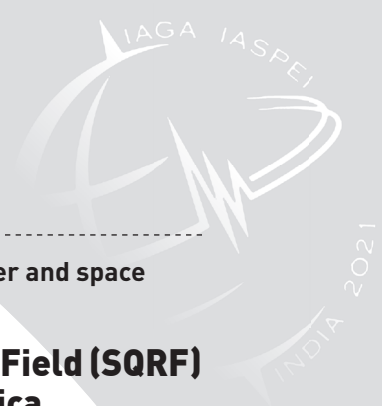
Influence of the uncertainties in the Solar Quiet Reference Field (SQRF) model for deriving geomagnetic indices over South America

CORRESPONDING & PRESENTING AUTHOR:

Sony Chen, INPE, Brazil

Clezio Denardini, INPE, Brazil

Laysa Resende, INPE/State Key Laboratory of Space Weather, Brazil

Ronan Chagas, INPE, Brazil

Juliano Moro, INPE/State Key Laboratory of Space Weather, Brazil

Regia Pereira, INPE, brazil

Carolina Carmo, INPE, Brazil

Giorgio Picanco, INPE, Brazil

Paulo Nogueira, Federal Institute of Education, Science and Technology of São Paulo (IFSP), Brazil

Paulo Barbosa Neto, Salesian University Center of São Paulo (UNISAL), Brazil

Esmeralda Romero Hernandez, Universidad Autonoma de Nuevo Leon (UANL), Brazil

Amanda Piassi, Federal Institute of Minas Gerais (IFMG), Brazil

Giovana Stefani, INPE, Brazil

Jaziel Campelo, INPE, Brazil

In this work, we present the uncertainties of the empirical model developed to predict the solar quiet regular daily field variation (Sq) over the Brazilian sector called the Solar Quiet Reference Field (SQRF) model. The SQRF is based on the magnetic station records from the Embrace Magnetometer Network (Embrace MagNet) during the solar cycle 24. Although the prediction and the magnetic field records have a good agreement, we observe that each magnetic station shows a random error behavior, propagating small errors in the model. Also, some physical aspects, as tidal winds and ionospheric conductivity, may have influenced our predictions. Thus, these uncertainties in the Sq field can propagate errors and influence geomagnetic indices' calculation by erroneously scaling the geomagnetic disturbances. In this context, we introduce a new approach to derive a 'real-time' geomagnetic index based on the SQRF model for the Sq-H field over the South American sector. We analyze one geomagnetic storm event to show that the results have a good representation of the geomagnetic indices. Finally, this analysis yields a new approach to derive the geomagnetic index for space weather applications and studies that requires an Sq field prediction.

Identifying the causes for vertical component geomagnetic field anomaly at Eskdalemuir Magnetic observatory, Scotland

CORRESPONDING & PRESENTING AUTHOR:

Guanren Wang, British Geological Survey, UK

Juliane Huebert, British Geological Survey, UK

Kathy Whaler, University of Edinburgh, UK

Three-component magnetic field observations recorded in the Scottish southern uplands reveal significantly dampened vertical component variations at Eskdalemuir, when compared with the horizontal components, for periods less than an hour. 20th-century literature suggests high-conductivity zones beneath may explain the observed anomaly for different periods. The external magnetic field induces time-varying electric currents flowing through the ground surface, which induces secondary magnetic fields. This study aims to characterise space-weather driven external field contributions at different timescales to the measured vertical field component variations, using modern data recorded at the Eskdalemuir magnetic observatory.

Geomagnetic Depth Sounding uses naturally-occurring magnetic field recorded at the surface as the source to help us map the subsurface lateral conductivity contrast. This technique uses the ratio between the horizontal and vertical magnetic field components for each period, to derive a dimensionless magnetic transfer function called the 'tipper'. Induction arrows derived from the real and imaginary part of the tipper points towards the direction of current concentrations. The magnitude of the induction arrow indicates the strength of the local conductivity.

Reliable tipper estimates are produced when data are collected during times of low-level space weather activity. To analyse quiet-time changes in the tipper, one-minute data recorded in a geomagnetically quiet year are used to establish 'baseline' values so we can visualise monthly changes for both the real and imaginary parts of the tipper above 10-seconds. This set of results are compared against tipper estimates produced using data recorded when the transient external field variations were larger.

Sr No: 243

Correlations of thunderstorm and magnetic records at Conrad Observatory, Austria

CORRESPONDING & PRESENTING AUTHOR:

Niko Kompein, ZAMG, Austria

Patrick Arneitz, ZAMG, Austria

Roman Leonhardt, ZAMG, Austria

Ramon Egli, ZAMG, Austria

Gerhard Diendorfer, Austrian Lightning Detection & Information System, Austria

The Conrad Observatory is particularly exposed to lightning strikes, due to its location on top of Trafelberg mountain (Lower Austria). Lightning strikes produce outliers in 1-second magnetic records, due to the magnetic fields produced by the stroke currents, particularly visible in our GEM systems potassium F-sensors, the so called supergradiometer. Besides the good time correlation between Conrad Observatory events and ALDIS data, we find a correlation between gaussian-weighted stroke peak currents refferring to offsets from F-sensor timestamps and the amplitude of the recorded 1-point outliers in the gradiometer system for selected discharges. More direct comparisons require the explicit calculation of induction and radiation field components predicted by return-stroke models, using a step function current waveform and the data provided by ALDIS. In the case of cloud-to-ground (CG) strokes, the stroke channel can be assumed to be nearly vertical, while no assumption can be made in case of cloud-to-cloud (CC) discharges. Measured fields and field gradients of the F-sensors are ~1 order of magnitude smaller than the calculated counterparts in the case of CG strokes, and a factor ~30 in case of CC discharges. The reason for this discrepancy is unclear

and might be attributed, at least in part, to the fact that observatory magnetometers might not fully integrate the effects of millisecond-long pulses. The unknown stroke channel orientations and the availability of only one gradient axis adds more uncertainty in the case of CC discharges.

KEYWORDS : magnetic timeseries', LLS, lightning effects

Sr No: 244

Surface Magnetic Assessment in Real Time (SMART) Ground-based Magnetometer Network

CORRESPONDING & PRESENTING AUTHOR:

Peter Chi, UCLA, USA

Christopher Russell, UCLA, USA

Brian Anderson, Johns Hopkins University, USA

Anthea Coster, MIT, USA

Jerry Goldstein, Southwest Research Institute, USA

Noel Petit, Augsburg University, USA

Kazue Takahashi, Johns Hopkins University, USA

William Greer, UCLA, USA

Michael Lawson, UCLA, USA

Taylor Lonner, UCLA, USA

Joseph Merrill, UCLA, USA

Peggy Li, UCLA, USA, USA

Alexa Roosnovo, UCLA, USA

Sanchit Agarwal, UCLA, USA

Matt Lacaire, UCLA, USA

Brandon Zhao, UCLA, USA

This NSF-sponsored ground-based magnetometer project consists of four elements: (1) updates and operation of a magnetometer network, (2) data collection and dissemination, (3) magnetoseismic research, and (4) education and public outreach (EPO). We reorganize and reinstate previously built UCLA ground-based fluxgate magnetometers in the United States, forming a network of 14 Surface Magnetic Assessment in Real Time (SMART) stations. Some of the magnetic sensors that experienced man-made damages have been returned to UCLA, and we have refurbished and recalibrated these sensors in the magnetometer laboratory following COVID-19 safety guidelines. We have also adopted Raspberry Pi as the new computer system for these ground-based magnetometer systems and developed software that enables easy on-site operation and enhances network security. We are currently revamping software for receiving, displaying, and disseminating real-time SMART magnetometer data. The calibrated science data will be made available to the public and major Heliophysics data centers, and they will be analyzed with normal-mode and travel-time magnetoseismic methods to investigate the plasmasphere, sudden impulses, and substorm onsets. In addition to the above activities involving high-sensitivity magnetometer measurements for geospace observations, we organize EPO events for the high schools and universities that help operate UCLA ground-based magnetometers. In these events, we introduce space weather phenomena and promote the use of affordable, off-the-shelf microelectromechanical systems (MEMS) magnetometers for citizen science. UCLA students in the SMART team play major roles in all elements of the project.

KEYWORDS : ground-based magnetometers, magnetoseismology, space weather

Sr No: 245

On Using MEMS magnetometers for Ground-based Space Weather Observations

PRESENTING AUTHOR:

Alexa Roosnovo, UCLA, USA

Noel Petit, Augsburg University, USA

CORRESPONDING AUTHOR:

Peter Chi, UCLA, USA

In the past decade, affordable microelectromechanical systems (MEMS) have become available in the commercial market, and some of these compact sensors are sensitive enough to detect the electric currents in geospace during severe space weather events. In this presentation, we examine the performance of several off-the-shelf MEMS magnetometers in terms of the noise level and other measurement characteristics, particularly temperature linearity. As other studies have pointed out, the measurements of the MEMS magnetometers are strongly influenced by the ambient temperature. The Raspberry Pi single-board computer is used for sensor operation and data acquisition. To assess the temperature dependence, we compare the measurements from MEMS magnetometers, such as those utilizing Raspberry Pi, and those by a thermally controlled UCLA fluxgate magnetometer nearby. Coinciding with these sensor evaluations, we assess the cumulative influence on accurately observing and measuring space weather events with such sensors. Our study can provide recommendations for interpreting measurements from MEMS magnetometers and how they may be used most effectively for citizen science.

KEYWORDS : MEMS magnetometers, space weather, education and public outreach

D8 Space weather services: New scientific research to address future needs

CONVENERS: Terry Onsager
                        Juan José Curto
                        Heikki Vanhamäki
                        Anna Naemi Willer
                        Hisashi Hayakawa

The demand for space weather services is continuing to grow as space activities expand and our dependence on the technological infrastructure increase. Space traffic management, space tourism, and human space exploration are among the areas where the expected increase in the utilization of space will require new scientific understanding and new space weather services. This session encourages presentations on advances in modeling and data analysis techniques and scientific understanding that will facilitate space based activities. Of particular interest are efforts to improve the understanding and modeling of neutral atmosphere dynamics impacting satellite orbits and the specification and prediction of the plasma and radiation environment impacting satellites and humans from low-Earth orbit to interplanetary space. In this context, it is equally important to improve our understanding on the extreme space weather events that significantly impact the space activities and technological infrastructure. Therefore, this symposium also encourages discussions on the production, prediction and application of geomagnetic indices and remarkable events. This is a long-running project. About 50 years ago, the Working Group of 'Geophysical Indices' was placed in Division V and Ebro Observatory was entrusted with the activity of the Service of Rapid Magnetic Variations. Also, P. N. Mayaud published a list of 100 years of SSCs measured by himself. Indices and remarkable events data provide clear evidence of the links between solar activity and earth space environment. They are therefore of great importance for Space Weather analysis and required as input in many predictive models. Long term space climate studies benefit from the availability of long time- series of these well-defined indices and remarkable events. Overall, this symposium will bridge discussions on the modelling and data analyses for the space weather services.

Sr No: 246

IUGONET data analysis system for promotion of a study of coupling processes in the solar-terrestrial system

CORRESPONDING & PRESENTING AUTHOR:

Atsuki Shinbori, Nagoya University, Japan

Yoshimasa Tanaka, National Institute of Polar Research, Japan

Norio Umemura, Nagoya University. Japan

Shuji Abe, Kyushu University, Japan

Satoru Ueno, Kyoto University, Japan

Masahito Nose, Nagoya University, Japan

The Inter-university Upper atmosphere Global Observation NETwork (IUGONET) project, consisting of five institutes (Tohoku University, National Institute of Polar Research, Nagoya University, Kyoto University, and Kyushu University), started in 2009 so that users can effectively find and analyze solar and earth's atmospheric observational data for studies of coupling processes in the solar-terrestrial system. In this project, we have added data information for various kinds of ground-based observation data in the solar-terrestrial physics and built a practical database (IUGONET Type-A) to share them on the Internet. We have also developed several plug-in tools (UDAS and UDAS egg) for the integrated data analysis software, SPEDAS, to analyze and visualize various kinds of ground-based and satellite observation data. In the IUGONET Type-A, users can easily learn characteristics of observation data through their quick look images/plots and how to use several basic commands to visualize the data. The IUGONET Type-A has a function of ASCII Downloader (one of the features of UDAS web) to convert CDF into ASCII files on this website so that users can easily read and analyze the observational data with their own tools. Recently, we also started a new promotion style corresponding to the Covid-19 pandemic all over the world. For example, we have held several online tutorial seminars to show how to use the IUGONET products and opened several movies and textbooks used in the previous seminars on the IUGONET website. In this talk, we will show the recent results of the IUGONET activities and future plan.

KEYWORDS :   IUGONET, database, data analysis software

Sr No: 247

Measurements of Thermospheric Density and Temperature from SUVI Solar Occultations

CORRESPONDING AUTHOR:

Ed Thiemann, U of Colorado, LASP, USA

PRESENTING AUTHOR:

Robert Sewell, U of Colorado, LASP, USA

Daniel Seaton, NOAA CIRES, USA

Courtney Peck, NOAA CIRES, USA

Eric Sutton, University of Colorado, USA

Marcin Pilinski, University of Colorado, USA

Direct observations of the thermospheric state can provide direct indicators of space weather activity for constraining models of the thermosphere-ionosphere system. However, no such measurements are currently made in real-time for use in space weather operations, and few have been historically collected for research purposes.

We present results from a NASA Operations to Research project to develop unprecedented operational measurements of the thermospheric state using the Solar UltraViolet Imager (SUVI) onboard the GOES-R series constellation. SUVI images the Sun at extreme ultraviolet (EUV) wavelengths with a primary objective to characterize and track the Sun's morphology as it relates to the source of geoeffective space weather. Since EUV radiation is strongly absorbed in the thermosphere, it can be used to probe the thermosphere via solar occultations. The wavelengths measured by SUVI provide sufficient constraints to distinguish the three major species of the thermosphere: N2, O2 and O. We present measurements made of thermospheric density, temperature and composition from approximately 150 to 300 km. Results are shown to illustrate how EUV images are converted to solar occultation light curves, and how density and temperature are derived from these light curves.

Sr No: 248

Hpo, a half-hourly and hourly, open-ended, Kp-like geomagnetic index for space weather applications

CORRESPONDING & PRESENTING AUTHOR:
Juergen Matzka, GFZ German Research Centre for Geosciences, Germany
Yosuke Yamazaki, GFZ German Research Centre for Geosciences, Germany
Claudia Stolle, GFZ German Research Centre for Geosciences, Germany
Guram Kervalishvili, GFZ German Research Centre for Geosciences, Germany
Jan Rauberg, GFZ German Research Centre for Geosciences, Germany
Sean Bruinsma, CNES, France

The Hpo indices have a derivation scheme and frequency distribution similar to that of the traditional Kp index. However, they have a higher time resolution than Kp and the strongest geomagnetic events with Kp = 9 are subdivided into a finer, open-ended scale. The Hpo indices come in four versions: Hp60 and Hp30 resemble Kp, while ap60 and ap30 resemble the linear ap index, with 60 indicating the hourly and 30 the half-hourly indices. The indices are available from GFZ German Research Centre for Geosciences in near real-time and back to 1995. The index is licensed under CC BY 4.0 and has the DOI 10.5880/Hpo.0001. The index was developed within the EU Horizon 2020 project SWAMI in support of new models for thermospheric density and satellite drag. We will demonstrate the derivation of the index and compare it to the Kp index, the polar cap PC index and solar wind parameters. Examples of applications of the index will be shown.

Sr No: 249

Morphological models for automatic detection of Sfe events

PRESENTING AUTHOR:

Anna Sole Castelli, Observatori de l'Ebre, Spain

CORRESPONDING AUTHOR:

Juan Jose Curto Subirats, Observatori de l'Ebre, Spain

Alba Fisher Carles, Observatori de l'Ebre, Spain

Solar flares produce geomagnetic variations (Sfe) caused by the activation of the ionosphere. They are usually characterized by a rapid rise followed by a smooth decay, which gives place to a crochet-like shape in the magnetograIn view of this particularity, we propose a completely new approach to automatize their detection: an algorithm capable of detecting Sfe based on the morphological signature they leave on magnetograms. Sfe time intervals were analyzed from geomagnetic data recorded at Ebro Observatory. Taking into account the irregularity of the Sfe aspect, we created several morphological models for each magnetic component (X, Y, and Z), as well as for the horizontal, H, and the total, F, modules. Regarding the implementation of the models, two working lines were carried out. Firstly, we aimed to identify a definite Sfe time interval by setting conditions on various parameters such as the correlations of data with the models or model similarities among components and modules. Nevertheless, given the difficulties to discern a common pattern among different intervals known to correspond to Sfe, our attention focused on the F magnetic module. On this second stage, we observed clusters of time intervals whose F variations highly correlated with one of our models. Each of this clusters were attributed to a timespan of event possibility. The high hit ratio of the algorithm gives promising results towards Sfe automatic detection, results that could be improved by combining this new methodology with others already studied.

KEYWORDS : solar flare events, detection, morphology

Sr No: 250

Automatic detection of Sfe: a step forward

PRESENTING AUTHOR:

Alba Fisher Carles, Observatori de l'Ebre, Spain

CORRESPONDING AUTHOR:

Juan Jose Curto Subirats, Observatori de l'Ebre, Spain

Anna Sole Castellvi, Observatori de l'Ebre, Spain

Solar Flare Effects (Sfe) are magnetic variations caused by solar flare events. They only show up in the illuminated hemisphere. Their detection is a difficult task because they do not have a definite morphology pattern and they must be separated from other magnetic perturbations. However, we attempted to automatize these detections. Our algorithm calculates the derivative of the data in order to avoid contamination of the daily variation Sq, and, by means of trigonometric formulas, computes the magnetic radial component, and creates a Sfe index. An a priori assumption of the focus position is no longer needed, since we make a wide patrol of the space area to find it. We have done a massive calculation of Sfe detection (for the period 2000-
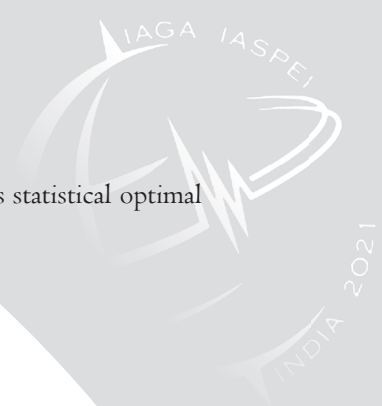
2020) which included 33 Sfe. Through a progressive thresholding process, we found its statistical optimal value (0.4 nT min-1) by using ROC curve method.

KEYWORDS : solar flare effects, detection, thresholding

Sr No: 251

Improvement of the Global Magnetosphere MHD Model at NICT and its Application to Satellite Surface Charging Assessment (by invitation)

CORRESPONDING & PRESENTING AUTHOR:
Aoi Nakamizo, National Institute of Information and Communications Technology (NICT), Japan
Yasubumi Kubota, National Institute of Information and Communications Technology (NICT), Japan
Tsutomu Nakgatsuma, National Institute of Information and Communications Technology (NICT), Japan
Takashi Tanaka, Kyushu University, Japan

In terms of the space weather, global magnetosphere MHD modeling is a powerful tool in simulating (a) the magnetospheric energy input to the ionosphere, which is one of the sources of ionosphere-atmosphere disturbances affecting radio-wave propagation, LEO satellite orbits, and so on, (b) high-latitude geomagnetic disturbances leading to GICs, and (c) keV plasmas causing satellite surface charging.

We have improved the MHD model at NICT so as to make the simulation more realistic, and the first version of the improved model is now running at real-time. Among the above mentioned targets, we have focused our effort on (c) for the past few years and developed a prototype of real-time assessment system of satellite surface charging at GEO, by cooperating with charging analysis tools. Because in general, MHD models do not provide separately the density and temperature of electrons and ions, which are the input of charging analysis tools, we developed an empirical method to estimate those from the output of our MHD model. We talk about the model improvements and details of the assessment system as well as future plans for (a) and (b).

KEYWORDS : global magnetosphere MHD model, plasma environment, satellite surface charging

Sr No: 252

Lowering to the Occasion: Meeting Society's Needs in the Age of Proliferated LEO (by invitation)

CORRESPONDING & PRESENTING AUTHOR:
Paul Obrien, The Aerospace Corporation, USA

As providers launch dozens of low altitude satellites per month and announce plans for constellations reaching into the thousands, the space weather community must ask ourselves: are we pursuing the right research to meet the needs of proliferated use of LEO? There are three significant disconnects between research modeling efforts and the needs of low altitude space systems: inclusion of the drift loss cone

in global electron belt simulations, real-time modeling of geomagnetic cutoffs, and description of field-aligned currents at spacecraft altitudes. So-called "global" simulation models of the electron radiation belts typically do not represent the drift loss cone, where low altitude satellites spend the majority of their lives. Geomagnetic cutoffs, if they are monitored at all, are not represented in a realistic manner that can be used to reconstruct proton and ion fluxes at LEO satellites. Field-aligned currents, which are a meaningful indicator of the location of highest surface charging risk for LEO satellites, are modeled in detail for power grid operators but are not evaluated at LEO altitudes. Addressing these disconnects will likely not require large research investments, but it will require a recognition that society's use of space is rapidly changing. Its needs from the space weather community are changing as well.

KEYWORDS : space weather, energetic charged particles, proliferated LEO

Sr No: 253

Analyses of the Extreme Solar and Geomagnetic Storms in March 1940

CORRESPONDING & PRESENTING AUTHOR:

Hisashi Hayakawa, Nagoya University, Japan
Denny Oliveira, NASA, USA
Ann Shea, SSSRC, France
Don Smart, SSSRC, france
Sean Blake, NASA, USA
Kentaro Hattori, Kyoto University, Japan
Ankush Bhaskar, Vikram Sarabhai Space Centre, India
Juan Jose Curto, Observatori de l'Ebre, Spain
Daniel Franco, National Observatory of Brazil, Brazil
Yusuke Ebihara, Kyoto University, Japan

Solar and geomagnetic storms are of more than just an academic interest for modern civilisation due to its increasing dependency on technological infrastructure and resultant vulnerability to these storms. The March 1940 storm is considered a benchmark event because it triggered one of the earliest contemporary interests for the societal impacts of geomagnetic storms. In this study, we analyse this storm sequence, in terms of the solar eruptions, the subsequent geomagnetic storms, auroral activity, and cosmic-ray variations, based on contemporary observational records. These analyses provide quantitative insights into their magnitudes in these aspects and contextualise these storms with other well-known extreme solar and geomagnetic storms that occurred during the space age.

KEYWORDS : solar flare; geomagnetic storms; aurorae; solar cosmic rays

Sr No: 254

Space Weather and Space Situational Awareness (by invitation)

CORRESPONDING & PRESENTING AUTHOR:

Jennifer Meehan, NOAA NWS, USA

The space operating environment has become more contested and congested. Commercial space missions are growing in number, diversity, and complexity. Orders of magnitude of growth are expected in the number of active satellites in orbit in the next decade. This situation demands improved space situational awareness for conjunction analysis and collision avoidance. The largest uncertainty in determining orbits for satellites operating in low Earth orbit is atmospheric drag related to space weather. In addition to atmospheric drag, space weather poses many other threats to orbiting objects making knowledge of the space environment imperative. Therefore, space weather support, including space environment research, observations, modeling, and forecasting, for the space situational awareness mission is critical. Highly accurate space weather data and predictions will be needed to drive advanced models for precision orbital calculations for collision avoidance measures to ensure a safer operating environment in the space domain for civil, defense, and commercial space operators. This presentation identifies space weather types and their impacts on space assets, and presents the data and forecasts that space operators will need to mitigate the effects of space weather on space missions.

Sr No: 255

International Service of Geomagnetic Indices: Current status and Roadmap (by invitation)

CORRESPONDING & PRESENTING AUTHOR:

Aude Chambodut, University of Strasbourg / CNRS ITES, UMR7063 ; EOST, France

The International Service of Geomagnetic Indices (ISGI) is in charge of the elaboration, validation, dissemination and stewardship of IAGA's endorsed data-products, i.e. geomagnetic indices and lists of remarkable magnetic events.

Six International Institutes (Ebro Observatory, Roquetes, Spain; GFZ, Potsdam, Germany; WDC, Kyoto, Japan; AARI, St Petersburg, Russian Federation; DTU Space, Copenhagen, Denmark; EOST, Strasbourg, France) collaborate in the frame of ISGI. These ISGI-Collaborating Institutes derive and provide the reference data-products relying onto reports and measurements of magnetic observatories distributed all over the planet.

In 2015, ISGI official Web portal and headquarters moved. A complete upgrade and update of the service has been achieved to meet the actual requirements on data management and to answer the needs of the users and stakeholders from international research community and beyond.

We present here the current status of the service and the ISGI roadmap in the frame of various global initiatives.

D9 Geomagnetic disturbance (GMD) benchmarks, case studies and new results in geomagnetically induced currents (GIC) and hazard assessments

CONVENERS: Stefan Lotz
              Antti Pulkkinen

Space weather related GMD can drive GIC in various technological systems such as railways, fuel pipelines and power grid infrastructure, all of which are critical to the activities of modern societies. In order to protect these systems against solar activity, risk planning and hazard assessment efforts need to address a variety of damage modes manifesting at different time scales and in different geomagnetic regions. One critical aspect of this is the identification and design of benchmark events that capture these effects. Accurate benchmarks enable effective vulnerability assessments, assist in the development of mitigation procedures, and help to provide sober risk quantification. Therefore, we invite presentations on (i) assessment of currently proposed or existing benchmarks, (ii) the analysis and design of benchmarks, (iii) case studies of interesting events, and (iv) novel ideas for hazard assessment related to GIC-related effects on the relevant industries.

Sr No: 256

Long-term Evolution of the Polar Cap using Extreme 100-year Dipole Forecasts: Global MHD Simulations

CORRESPONDING & PRESENTING AUTHOR:

Joseph Eggington, Imperial College London, UK
Jonathan Eastwood, Imperial College London, UK
Stefano Maffei, University of Leeds, UK
Phil Livermore, University of Leeds, UK
Jon Mound, University of Leeds, UK
Martin Archer, Imperial College London, UK
Jeremy Chittenden, Imperial College London, UK
Ravindra Desai, Imperial College London, UK
Mike Heyns, Imperial College London, UK
Lars Mejnertsen, Imperial College London, UK

Geomagnetically-induced currents (GICs) present a major risk to ground infrastructure, with the return period of a severe event on the order of 100 years. The location and intensity of the auroral electrojet, responsible for driving these GICs, is dependent on solar wind conditions and is typically confined to high geomagnetic latitudes. However, long-term evolution of the internal magnetic field could affect a given region's susceptibility to GIC risk. At present this evolution results in a shift in the dipole latitude of about 2° per century, accompanied by a decrease in dipole strength of about 5%. Noticeable variations can occur even on decadal timescales, with the migration of the North magnetic pole accelerating over the last 30 years. Hence, investigating possible changes over the 100-year return period is important for predicting the potential impact of a future event, and developing appropriate benchmarks.

In this study we explore the effect of such variations on conditions in the ionospheric polar cap. Extreme scenarios for the future dipole strength and orientation are produced from a 100-year extremal forecast. Using the Gorgon MHD code, we then perform global simulations of the magnetosphere by driving these configurations with both steady and varying solar wind. We identify the variation in the location of the open-closed field line boundary on the ionosphere, and the morphology and intensity of ionospheric current systems and consider the implications for GIC risk over centennial timescales at UK latitudes.

KEYWORDS :   dipole, forecast, GIC

Sr No: 257

A new data set of line GICs measured with the Differential Magnetometer Method in the UK high voltage power grid

CORRESPONDING & PRESENTING AUTHOR:

Juliane Huebert, British Geological Survey, UK
Ciaran Beggan, British Geological Survey, UK

Gemma Richardson, British Geological Survey, UK
Adam Collins, British Geological Survey, UK
Natalia Gomez Perez, British Geological Survey, UK
Alan Thomson, British Geological Survey, UK

Extreme events of space weather can have severe effects on ground-based infrastructure like power lines, railways and gas pipe lines through the induction of geomagnetically induced currents (GICs) not only in mid-to-higher latitude countries. Modelling GICs requires knowledge about the source magnetic field and the electrical conductivity structure of the Earth to calculate electric fields during enhanced geomagnetic activity. The electric field in combination with detailed information about the network topology enable the derivation of GICs in power lines. Directly monitoring GICs in power grid substations is possible with a Hall probe, but scarcely realised in the UK. Therefore we deployed the differential magnetometer method (DMM) to measure GICs at ten sites in the UK power grid. The setup includes the installation of two fluxgate magnetometers, one directly under a power line affected by GICs, and one as a remote site further away. The difference in recordings of the magnetic field in both instruments allows for the calculation of GICs in the respective power line segment via Biot-Savart law during geomagnetically enhanced periods.

We collected data all around the UK power grid starting in 2018, monitoring line segments that in our model connect to transformer substations with high GIC risk. Albeit in the solar minimum with few periods of larger geomagnetic activity, we recorded data during many smaller geomagnetic storms that allow an in detail analysis of the GIC model. The data set provides a base to refine and validate our computational GIC model in the UK power network.

KEYWORDS : space weather, geomagnetically induced currents, HV power lines

Sr No: 258

SYMPOSIUM : **D9 Geomagnetic disturbance (GMD) benchmarks, case studies and new results in geomagnetically induced currents (GIC) and hazard assessments**

Geomagnetically induced currents in conductive crust faults during severe space weather conditions as a possible trigger of earthquakes

CORRESPONDING & PRESENTING AUTHOR:

Victor Novikov, Joint Institute for High Temperatures of Russian Academy of Sciences, Russia

Valery Sorokin, Pushkov Institute of Terrestrial Magnetism, Ionosphere, and Radio Wave Propagation of Russian Academy of Sciences, Russia

Alexey Yaschenko, Pushkov Institute of Terrestrial Magnetism, Ionosphere, and Radio Wave Propagation of Russian Academy of Sciences, Russia

Previous field and laboratory experiments demonstrated that DC pulses injected into the lithosphere through grounded dipole can trigger earthquakes [1, 2]. Based on discovered response of seismicity to artificial electromagnetic impacts we consider a possibility of earthquake triggering by natural electromagnetic phenomena [3] due to excitation of geomagnetically-induced currents (GIC) in the conductive crust faults during strong variations of geomagnetic field. We note that due to saturation of crustal fault with mineralized fluids or the faults graphitization as a result of previous earthquakes its conductivity may exceed the conductivity of host rocks by several orders of magnitude. Numerical estimations with application of the model [3] show that under strong disturbances of the geomagnetic field of $\sim 10^2$ nT, the density of telluric currents in a conductive fault can reach 10^{-6} A/m^2, which is an order of magnitude higher than the current density generated in earthquake source by artificial DC power systems abd injected into the Earth
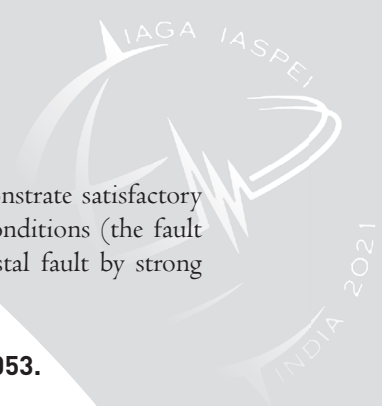
crust [1]. Laboratory experiments on telluric current excitation in a model fault demonstrate satisfactory agreement between numerical and experimental results. Thus, under certain critical conditions (the fault stress-strain state, the fault conductivity and orientation) the GIC excited in the crustal fault by strong variations of space weather can trigger earthquakes.

1. Novikov V.A. et al. (2018) Geophys. Res. Abstr. V.20. EGU2018-15436-1.

2. Novikov V.A. et al. (2017) Earthq. Sci. V.30. P.167.

3. Sorokin V.M. et al. (2019) Earthq. Sci. V.32. P.26.

KEYWORDS : geomagnetically induced currents, conductive crust fault, earthquake triggering

---

Sr No: 259

SYMPOSIUM :   **D9 Geomagnetic disturbance (GMD) benchmarks, case studies and new results in geomagnetically induced currents (GIC) and hazard assessments**

Variations in ground magnetic field and ionospheric electron density over Turkey during geomagnetically disturbed days

CORRESPONDING & PRESENTING AUTHOR:

Ezgi Gulay, Istanbul Technical University, Turkey

Zerefsan Kaymaz, Istanbul Technical University, Turkey

Emine Ceren Kalafatoglu Eyiguler, Istanbul Technical University, Turkey

We present our preliminary results on geomagnetically induced currents (GICs) over Iznik, Turkey (GEO: 40.5°, 29.72°, MAG: 37.75°, 109.52°). Since the time derivative of the geomagnetic field is associated with GICs, in this work, we investigate the GICs at our latitudes by analyzing the deviations in the geomagnetic field and its time derivatives for several geomagnetically active days. We determine the differences between quiet and active day structures in the geomagnetic field variations and make a detailed analysis for each component. In order to bring insights on the behavior of the geomagnetic field at our latitudes during the storm/substorm times, we separate the data into storm and substorm phases using Dst and AE indices. Additionally, correlation between the geomagnetic field variations, solar wind dynamic pressure and IMF orientation are calculated for the purpose of detecting the GIC signatures at our latitudes resulting from the interaction between Earth magnetic field and solar wind. In this presentation, we show geomagnetic field, geoelectric field and ionospheric electron density variations during several storm and substorm cases and indicate the correlation between the response of the ionosphere and ground magnetic field to the solar wind drivers of the storms and substorms at our latitudes.

KEYWORDS :   geomagnetically induced current, ionosphere, space weather

Sr No: 260

Towards more accurate GIC estimations in the Portuguese power network

CORRESPONDING & PRESENTING AUTHOR:

Joana Alves Ribeiro, Coimbra University - Portugal

Fernando J. G. Pinheiro, Coimbra University, Portugal

Pedro Baltazar Soares, Instituto Dom Luiz (IDL), Portugal

Fernando A. Monteiro Santos, Instituto Dom Luiz (IDL), Portugal

Maria Alexandra Pais, Coimbra University, Portugal

Geomagnetically Induced Currents (GICs) computation is gaining importance due to major consequences GICs might cause in modern society (e.g., blackouts). Although their effects are strongest at higher latitudes, there has been evidence of relevant impact at mid and lower latitudes.

To obtain a reasonable estimation of GICs, it is necessary to have a good knowledge of the ground induced electric field and of the topology of the power network. This study aims to improve estimates of this field by using new magnetotelluric (MT) measurements over a 50 x 50 km grid in Portugal mainland. They are used to obtain the first 3D conductivity model for the whole territory, which expresses the response of the regional geoelectric structure to electromagnetic perturbations. The electrical conductivity model is both constrained by and a source of information to the tectonics from the lower crust to the shallow subsurface. Main tectonic features in the territory will be identified.

Finally, in combination with the Coimbra Geomagnetic Observatory (COI) data for the time-dependent geomagnetic field, it will be possible to achieve a better estimation of the spatial distribution of induced geoelectric field variation for each geomagnetic storm studied. We have a good collaboration with the Portuguese national transmission system operator (REN), by which realistic values of power network grid parameters can be brought into play.

In this study, we present results of GIC estimation for Portugal using the new 3D conductivity model for the strongest geomagnetic storms recorded at COI during solar cycle 24.

KEYWORDS : GICs estimation, 3D conductivity model

Sr No: 261

Nighttime Magnetic Perturbation Events Relevant to GICs: Statistical study and Superposed Epoch Analysis

CORRESPONDING & PRESENTING AUTHOR:

Mark Engebretson, Augsburg University, USA

Lidiya Ahmed, NASA/Goddard Space Flight Center, USA

Viacheslav Pilipenko, Russian Academy of Sciences, Russia

Erik Steinmetz, Augsburg University, USA

Mark Moldwin, University of Michigan, USA

Martin Connors, Athabasca University, Canada

David Boteler, Natural Resources Canada, Canada

James Weygand, University of California, Los Angeles, USA

Hermann Opgenoorth, Umea University, Sweden

Shin Ohtani, Applied Physics Laboratory, USA

Jesper Gjerloev, Applied Physics Laboratory, USA

Geomagnetically induced currents (GICs) are generated by intense time-varying electrical currents in the ionosphere that can be detected by ground-based magnetometers. Here we present statistical summaries and superposed epoch analyses of large ($|dB/dt| \geq 6$ nT/s) nighttime magnetic perturbation events (MPEs) observed during 2015 and 2017 at five stations in Arctic Canada. Although ~2/3 of these MPEs occurred within 30 minutes after a substorm onset, ~10% occurred over two hours after the most recent onset. A broad distribution in local time appeared between 1700 and 0100 MLT, and a narrower distribution appeared between 0200 and 0700 MLT. Superposed epoch analyses were produced for premidnight and postmidnight events and for three ranges of time after the most recent substorm onset: A) 0-30 min, B) 30-60 min, and C) >60 min. Of the solar wind and IMF parameters studied, only the IMF Bz component showed any consistent temporal variations prior to MPEs: a 1-2 hour wide 1-3 nT negative minimum beginning ~30 to 80 min before premidnight MPEs, and minima that were less consistent but often deeper before postmidnight MPEs. Median and 25th and 75th percentile SuperMAG auroral indices SML (SMU) showed drops (rises) that were closely associated with both pre- and post-midnight type A MPEs, but most of the MPEs in categories B and C did not coincide with large-scale peaks in ionospheric electrojets. These observations suggest that substorms are neither necessary nor sufficient to cause MPEs, and hence predictions of GICs cannot focus solely on substorms.

KEYWORDS : geomagnetically induced currents, magnetic perturbation events, substorms

Sr No: 262

- -

SYMPOSIUM : **D9 Geomagnetic disturbance (GMD) benchmarks, case studies and new results in geomagnetically induced currents (GIC) and hazard assessments**

Geomagnetically Induced Currents due to Extreme Space Storms: Continental View

CORRESPONDING & PRESENTING AUTHOR:

Ari Viljanen, Finnish Meteorological Institute, Finland

Ilja Honkonen, Finnish Meteorological Institute, Finland

Kirsti Kauristie, Finnish Meteorological Institute, Finland

Geomagnetically induced currents (GIC) flow in technological conductor systems always when the geomagnetic field experiences temporal variations. These variations are accompanied by an induced electric field in the conducting ground, and this geoelectric field is the driver of GIC. We calculate the geoelectric field from measured and simulated ground magnetometer data of very strong geomagnetic storms. We use a 1-D (layered) ground conductivity model to focus on features related only to spatial and temporal variation of the magnetic field. As the power grid model, we use a simplified network that is moved to different locations across Europe. Of special interest are events due to high-amplitude sudden impulses and strong auroral substorm events. A key question is to estimate whether regions south of the typical auroral region could experience as large or even larger events than have occurred at high latitudes, for example, during the Halloween storm in October 2003.

KEYWORDS : GIC

Sr No: 263

Current achievements to assess the vulnerability of the Spanish power grid: systematic construction of a DC-equivalent network and an alternative method for GIC calculation

CORRESPONDING & PRESENTING AUTHOR:

Santiago Marsal, Observatori de l'Ebre, Spain

Joan Miquel Torta, Observatori de l'Ebre, Spain

Victoria Canillas, Observatori de l'Ebre, Spain

Juan Jose Curto, Observatori de l'Ebre, Spain

Juan Jose Ledo, Universitat de Barcelona, Spain

Perla Pina Varas, Universitat de Barcelona, Spain

The threat of Geomagnetically Induced Currents (GIC) driven by severe Space Weather looms over technological systems such as power grids. Assessing their vulnerability is therefore vital to avoid damages to power systems or even disruption of the electrical power supply. This endeavor, however, involves an interdisciplinary approach, ranging from the characterization of the sources of magnetic perturbations causing geoelectric fields, to the modeling of the power network from its parameters and topology, including the characterization of the geoelectrical structure of the Earth beneath and around the area of interest, or the validation of the power network model by means of (direct or indirect) GIC flow measurements. In this talk, we summarize our current achievements focused on mainland Spain, concentrating on a novel procedure to automatically generate a DC-equivalent network from the information provided by the power grid operator, and the subsequent resolution by a computationally improved method that is an alternative to the classical ones (Lehtinen and Pirjola, LP; and Nodal Admittance Matrix, NAM). Plans are underway to go one step further and feed our modeling capabilities with forecasts of the geomagnetic field variations in the Iberian Peninsula from real-time solar wind and IMF data using machine learning techniques.

KEYWORDS :   geomagnetically induced currents, power grid modeling

Sr No: 264

Investigating the Predictive Power of Magnetohydrodynamic Models for Geomagnetically Induced Currents in the UK

CORRESPONDING & PRESENTING AUTHOR:

Ewelina Florczak, University of Edinburgh, UK

Ciaran Beggan, British Geological Survey, UK

Kathy Whaler, University of Edinburgh, UK

Rapid magnetic field fluctuations associated with space weather events can induce geomagnetically induced currents (GICs) in conductive structures on the Earth's surface. Since GICs can be damaging to high-voltage power networks, pipelines or railways, a good forecasting capability is important in order to mitigate their impacts.

We used magnetohydrodynamic models of the magnetosphere and ionosphere, (SWMF/BATS-R-US, SWMF/BATS-R-US+RCM, GUMICS-4 and GORGON) to simulate ground magnetic field variations for the 7/8 September 2017 event, based on solar wind parameters propagated to the simulation domain. Modelled values of the northward and eastward magnetic field components show differences in both amplitude and temporal variability compared to the corresponding measurements from three UK observatories. The BATS-R-US model produces the closest agreement in terms of the northward component, whilst GORGON performs best in terms of the eastward component. The addition of Rice Convection Model (RCM) tend to overestimate the field values. Results indicate the accuracy of ground magnetic field forecast decreases with increasing latitude.

The resulting northward and eastward geoelectric field is calculated from the magnetic field using magnetotelluric transfer functions, which is then extrapolated to compute the GIC for a high-voltage UK power network. The GIC response to a uniform electric field of 1 V/km shows that substations (nodes) located near coastlines are affected the most. It is found that GICs computed from BATS-R-US modelled values are most accurate for nodes located at higher latitudes, whilst GUMICS-4 prediction performs best at lower latitudes.

KEYWORDS : geomagnetically induced currents, MHD models, space weather

Sr No: 265

SYMPOSIUM : **D9 Geomagnetic disturbance (GMD) benchmarks, case studies and new results in geomagnetically induced currents (GIC) and hazard assessments**

Geomagnetically Induced Currents: Assessing the vulnerability of the German power grid

CORRESPONDING & PRESENTING AUTHOR:

Aoife Mccloskey, German Aerospace Center, Germany

Leonie Pick, German Aerospace Center, Germany

Aline Guimaraes Carvalho, German Aerospace Center, Germany

Jens Berdermann, German Aerospace Center, Germany

The vulnerability of power networks to GICs has recently been assessed in several mid- to low-latitude countries such as UK, Ireland, New Zealand amongst others. In contrast, a comprehensive study has yet to be carried out in Germany. Here, we present current progress, results and challenges for assessing the impact of GICs on the German power network.

Firstly, geomagnetic variations within the German region are quantified. The primary data source are 1-min vector magnetic field measurements in the horizontal plane from the four German (incl. neighboring) INTERMAGNET observatories. These are interpolated using the Spherical Elementary Current Systems technique to give maps of magnetic field variability (nT/min).

Following this, in order to model the surface horizontal electric field, information about the conductivity of the sub-surface geology is needed. Here, we outline the availability of data for this purpose for the German geographic region and present initial results applying a plane wave approach to model the induced geoelectric field.

The final step in GIC modelling involves constructing a model of the German high-voltage electricity transmission network, information about which is obtainable from several publicly available datasets. Here,

we present an initial construction of this power network model, including its suitability for our purpose and potential short-comings.

We illustrate our approach by the means of case studies focusing on relatively recent, well-studied periods of elevated geomagnetic activity (e.g., the geomagnetic storm from September 2017).

Sr No: 266

Developing electric field risk maps and geomagnetically induced current models across Europe

CORRESPONDING & PRESENTING AUTHOR:
Gemma Richardson, British Geological Survey, UK
Ciaran Beggan, British Geological Survey, UK
Ellen Clarke, British Geological Survey, Uk
Guanren Wang, British Geological Survey, UK
Adam Collins, British Geological Survey, UK
Alan W P Thomson, British Geological Survey, UK

The EUHFORIA2.0 project aims to address the geoeffectiveness, impacts and mitigation related to coronal mass ejections, solar wind streams and solar energetic particles. A key part of this project is to develop the capability to nowcast and forecast geomagnetically induced currents (GIC) across the continent of Europe.

With the final objective to couple the wider suite of EUHFORIA models from the Sun to the Earth, BGS have been working on the development of a European electric field risk map, and creating examples using historic magnetic storms. The first step in this process is to find all available magnetic field data and interpolate it across the continent. To construct the conductivity model, necessary for computing the geo-electric field and the risk map, a modified version of the EURHOM model (Adam et al 2012) is used, which provides a series of 1D layered blocks of conductivity. A new model of the interconnected European power grid network is also under development, to model the GIC arising from the electric field that results from the conductivity model coupled to the interpolated magnetic field data. In this poster progress and results to date are described. This work is funded by the European Commission Horizon 2020 (H2020) Grant Agreement No. 870405.

IAGA DIVISION I

I.2 Magnetic record of tectonic, geologic and volcanic processes

CONVENERS: Satria Bijaksana

Mathew Domeier

Mamilla Venkateshwarlu

Uwe Kirscher

Ramon Egli

The magnetism of Earth materials presents one of the richest information archives on our planet, with dimensions that extend through time (e.g. geomagnetism to archeomagnetism and paleomagnetism), space (e.g. nanoscale magnetic microscopy to planetary scale satellite surveys) and discipline (e.g. biomagnetism, environmental magnetism and tectonics). Tectonic as well as volcanic processes shape not only the morphology of the Earth but also affect the history of mankind. These processes also change climate as well as environment. These processes might be dated, recorded, or associated with magnetic records in rocks and sediments. This session welcomes contributions, not only, on all types of magnetic record (secular variations, excursions to magnetic stratigraphy) related to tectonic and volcanic processes, but also on changes of magnetic mineralogy and granulometry associated with these processes. We especially welcome contributions that develop new models, simulations, instruments, experimental techniques and analytical approaches to help us better use magnetic methods in understanding tectonic and volcanic processes. Complementary approaches to magnetic methods that help us understand the magnetic record of tectonic and volcanic processes are also welcome.

Sr No: 267

Magnetic fabric characteristics of sediments in and around Dauki fault region, Shillong, India.

PRESENTING AUTHOR:

Mujahed Baba Mohammad, Indian Institute of Geomagnetism, India

CORRESPONDING AUTHOR:

Lakshmi B. V., Indian Institute of Geomagnetism, India

Praveen Gawali, Indian Institute of Geomagnetism, India

K. Deenadayalan, Indian Institute of Geomagnetism, India

D. S. Ramesh, Indian Institute of Geomagnetism, India

Anisotropy of low-field magnetic susceptibility (AMS) analysis is a rapid and sensitive technique for measuring preferred orientations of magnetic grains and, therefore holds great potential for acquiring fabric information. Theoretical and field data show that an idealized suite of AMS ellipsoids develops as primary sedimentary fabrics are progressively overprinted by tectonic fabrics.

AMS has been applied on the sediments recovered from 5 trenches namely DK1, DK2, DK3, DK4 and DK5; in and around Dauki fault region, along Dauki River in order to identify invisible deformation as well as the intensity of deformation. Sediments from DK1 and DK2 sites are characterized mainly by well-developed oblate fabrics (Pj:1.05-1.08; T:0.48-0.52), with Kmin axes clustered around the pole to bedding and Kmax axes that are weakly clustered broadly parallel to the trend of the neighbouring structures. These fabrics could be correspond to the onset of the so-called "earliest deformation" stage. In sites DK3, DK4 and DK5, sediments have magnetic ellipsoids with identical directional properties but with different shapes and degrees of anisotropy. These sediments are characterized by weaker triaxial to prolate fabrics (Pj: 1.03-1.06; T: − 0.03-0.47) in which Kmin axes girdle around Kmax axes, which are tightly clustered around the trend of the neighbouring structures. These fabrics observed correspond to the strong deformation stage. These sediments, in which magnetic fabrics reflect the preferred orientation have typical tectonic magnetic fabrics with varying degrees of tectonic overprint likely controlled by small-scale active faults. The mean orientation of the susceptibility maxima parallels neighbouring active faults.

KEYWORDS : anisotropy of magnetic susceptibility, magnetic ellipsoid, active fault

Sr No: 268

Constraining the Eruption History of Rangitoto Volcano, New Zealand, using Palaeomagnetic Data

CORRESPONDING & PRESENTING AUTHOR:

Megan Allington, Lund University, Sweden

Andreas Nilsson, Lund University, Sweden

Mimi Hill, University of Liverpool, UK

Dimitra Daniil, Uppsala University, Sweden

Ingeborg Hjorth, Lund University, Sweden

Paul Augustinus, University of Auckland, New Zealand

Due to the proximity of Auckland Volcanic Field (AVF), New Zealand, to the densely populated city of Auckland it is important that the eruption histories of the nearby volcanoes are understood in order to assess possible future threats. Rangitoto Island volcano (Rangitoto) has been the subject of a number of studies yet the eruption history remains unclear. Radiocarbon dates taken from marine sediments found at the bottom of a 127-meter core of Rangitoto's lava flows, suggest that there was early volcanic activity as early as 6000BP, after which Rangitoto may have been dormant until the main shield building phase at around 600BP. The radiocarbon data, as well as independently dated ash layers on neighbouring Motutapu Island, suggest that the shield building phase was short-lived, lasting less than 100 years. Distinct multiple eruptions are not considered typical for small basaltic volcanos, such as those in the AVF and could suggest that the volcanic field has entered a new phase. Here we attempt to use palaeomagnetic analyses to provide additional constraints on the eruption rate of Rangitoto. A full palaeomagnetic study on the core has yielded 156 palaeodirectional results and 21 accepted palaeointensity estimates. Magnetic minerology analysis show that much of the core is a reliable recorder of the past geomagnetic field. We use a statistical model to estimate the time duration between lava flows based on the rate of change of the regional geomagnetic field model derived from satellite era models. Preliminary results are incompatible with a short eruption timescale.

KEYWORDS : palaeosecular variation, magnetic inclination, southern hemisphere

Sr No: 269

SYMPOSIUM : **1.2 Magnetic record of tectonic, geologic and volcanic processes**

Magnetic properties evidences of fluid-rock interaction at intraplate shear zones: an example from the Northern Apennines (NW Italy)

CORRESPONDING & PRESENTING AUTHOR:

Claudio Robustelli Test, Università degli Studi di Torino, Italy

Elena Zanella, Università degli Studi di Torino, Italy

Dario Bilardello, University of Minnesota, USA

Enzo Ferrara, Istituto Nazionale di Ricerca Metrologica, Italy

Fluid-rock interaction along plate boundary shear zones influences the faulting processes during the seismic cycle. The circulation of hot fluids during the co-seismic phase commonly triggers thermochemical transformations in a fault zone, producing potential changes of magnetic properties. Thermal generation of newly formed ferromagnetic minerals can be induced by frictional heating, thus, magnetic minerals are suitable indicators of the fluid migration path and seismic frictional heating temperatures.

We present the preliminary results from a rock magnetic investigation of the thrust-wall rocks of an exhumed analogue of actual plate boundary shear zones, cropping out in the Northern Apennines, NW Italy. Here, Geochemical evidence of deeper hot exotic fluids migration during the co-seismic phase was reported.

Our findings reveal changes in magnetic properties at increasing distance from the basal décollement. Temperature dependent remanence experiments show the occurrence of goethite and magnetite assemblages with variable relative abundance, depending on the distance from the main thrust. Variations might be related to alteration processes induced by the migration of fluids along the main faults. Heating signature of the thrust wall-rocks highlights elevated temperatures (Tmax around 350-400 °C) which may constraints the thermochemical reactions occurred in the fault zones.

We suggest that changes in thermomagnetic properties might provide insights into the complex fluid rock-interaction circuit during seismic cycles, as well as their heating-signatures.

KEYWORDS : rock magnetism, fluid-rock interaction, fault rocks

Sr No: 270

Tephra hunt in loess-paleosol sequences – towards an interdisciplinary approach for tephra detection and characterization

CORRESPONDING & PRESENTING AUTHOR:

Christian Laag, Université de Paris, Institut de Physique du Globe de Paris, CNRS, France
Yohan Guyodo, Université de Paris, Institut de Physique du Globe de Paris, CNRS, France
France Lagroix, Université de Paris, Institut de Physique du Globe de Paris, CNRS, France
Daniel Veres, Romanian Academy of Sciences, Romania
Lara Wacha, Hrvatski Geološki Institut & Croatian Geological Survey, Croatia

Loess-paleosol sequences (LPSs) are valuable terrestrial archives of mineral dust and Quaternary environmental evolution. Their paleoclimatic significance depends on reliable age control, which is nowadays often provided by correlative methods such as matching LPS paleoenvironmental data to marine and ice core archives. Almost 40 years ago, Friedrich Heller and Tungsheng Liu succeeded with a seminal breakthrough in LPS chronology by applying a combined paleomagnetic and environmental magnetic approach employing temporal changes of the Earth's magnetic paleo-field in combination with climatically controlled stratigraphical changes in magnetic susceptibility. The limitations of this approach lie mainly in the restricted temporal resolution on shorter timescales constraint by the few existing polarity changes during the Quaternary, and the long wavelengths of climatic changes reflected by environmental magnetic parameters. For shorter time scales, dating techniques like radiocarbon and luminescence dating applied to LPSs also present challenges.

Here, we propose an interdisciplinary tephrostratigraphic approach relying on in-depth mineral magnetic methods for identifying tephra layers in LPS. Tephrochronology employs tephra deposits for linking and dating paleoenvironmental and other archives. As an age-equivalent dating method, tephrochronology represents a precise volcanic-event stratigraphy utilizing age transfers from an independently dated eruption center to tephra deposits.

Our integrated approach relies on the specific magnetic properties of largely non-interacting soft magnetic particles preserved especially in volcanic glass and their characterization by FORC-analyses, IRM composition unmixing and low-temperature magnetic properties. Volcanic glass represents a sample of "frozen" magma and can be unambiguously identified by geochemical and magnetic methods, and linked to known volcanic eruptions.

KEYWORDS :   tephra, FORC analysis, IRM composition unmixing

Sr No: 271

Preliminary paleomagnetism results on 1.88 Ga dyke from Bastar craton, Peninsula India: constraints to Paleogeographic reconstructions

CORRESPONDING & PRESENTING AUTHOR:

Venkateshwarlu Mamilla, CSIR-National Geophysical Research Institute, India

The results of a preliminary paleomagnetic study on 1.9 Ga dyke from Dongargarh Supergroup, Bastar craton, India is reported here. This NW–SE trending dyke which is intruding into the Dongargarh Granite was linked to similarly-aged magmatic activity in the Dharwar craton in India. Seventy-eight samples were collected from 16 sites. The detailed rock magnetic studies indicate that a Single Domain (SD) magnetite [Fe3O4] is the dominant magnetic carrier. The Bastar dyke yield a single polarity magnetization with D = 127°, I = -24° (k = 16, α95 = 12.1°; k = 11.76) and a corresponding paleomagnetic pole at 39° N, 350° E (dp = 6.88, dm = 12.90). The paleogeographic relationship is tested with cratons in the "Columbia" supercontinent including the North China craton, Laurentia, Baltica, Australia, Siberia and the Kaapvaal and Zimbabwe cratons (southern Africa) at 1.9 Ga time.

Sr No: 272

How fast can remagnetization of sedimentary rocks be?

CORRESPONDING & PRESENTING AUTHOR:

Dmitriy Rudko, Schmidt Institute of Physics of the Earth of the Russian Academy of Sciences, Russia

Vladimir Pavlov, Schmidt Institute of Physics of the Earth of the Russian Academy of Sciences, Russia

In terms of completeness of the geological record, the Ordovician key section of the Moyero River valley (North of the Siberian Platform) until recently was considered to be one of the best Ordovician sections of Northern Eurasia. However, until now only the interval from Arenigian (Floian) to Ashgillian (Katian) part of the section have been thoroughly studied. Our new data indicate the occurrence in this section the Cambrian-Ordovician boundary and existence of several hundred meters thick Tremadocian sequence. All this taken together bring this section to the number of the best Ordovician sections of the world. Although a significant part of this section contains primary paleomagnetic record, there are also numerous layers of different lithology, which are completely or partly remagnetized by Permian-Triassic traps, represented in this area by sills sporadically intruded into the sedimentary strata. In this report, we present the data indicating that numerous sedimentary rocks outcropped in the vast area expanding over tens of kilometers along the Moyero river valley had been remagnetized during a very short remagnetization event which duration barely exceeded several hundred years. We consider the origin of this remagnetization and show that it is not due to simple heating or to thermoviscous processes but linked rather with fluid migration ejected to the rocks during the trap intrusion emplacement. This case of very fast magnetization indicates that paleomagnetic directions derived from remagnetized rocks should be used with caution to calculate the position of paleomagnetic poles. This work is supported by RSF #20–17–00198.

Sr No: 273

Magnetic Susceptibility and Magnetic Mineral Morphology of Hot Springs Area in Arjuno-Welirang Mountain as Magnetic Signature of Geothermal System

CORRESPONDING AUTHOR:

Siti Zulaikah, Universitas Negeri Malang, Indonesia

PRESENTING AUTHOR:

Cathlea S. Damayanti, Universitas Negeri Malang, Indonesia

Jason S. Herrin, NTU, Singapore

Bambang H. Iswanto, Universitas Negeri Jakarta, Indonesia

This research aims to study the characteristics of magnetic susceptibility and magnetic mineral morphology as well as the element composition of sediments in the Cangar and Padusan hot springs in the Arjuno-Welirang mountain system. Measurements were made to study in more detail the relationship between magnetic susceptibility, Fe-Silicate content and magnetic mineral morphology and to compare these characteristics in two hot springs in the same mountain system. This information is needed to understand the magnetic properties of rocks as a geothermal system signature. Magnetic susceptibility values ranged from $(7.558 - 62.694) \times 10\text{-}6$ m3/kg with an average of $32.275 \times 10\text{-}6$ m3/kg for Cangar and $(11.821 - 28.101) \times 10\text{-}6$ m3/kg with an average of $18.129 \times 10\text{-}6$ m3/kg for Padusan. From the data on elemental content, it was found that dominant elements such as Al, Si, K, Ca, Ti and Fe. The morphology of the extracted magnetic minerals shows that many magnetic minerals have a crystalline shape, especially hedral with a very fine grain surface and clean, free of impurities. This is thought to be due to the continuous flow of hot water in the depositional environment so that it can remove impurities that often stick to the surface of the extracted magnetic minerals. Some magnetic minerals are also found in spherical shapes, especially in the hot water deposits of Padusan. The existing both crystalline and spherical minerals suggest that there is the lithogenic and anthropogenic source of magnetic minerals.

KEYWORDS : susceptibility, magnetic, geothermal

Sr No: 274

Developing WEPAPIS-60 (Western Pacific Paleointensity-Stacking for the last 60 kyr)

CORRESPONDING & PRESENTING AUTHOR:

Satria Bijaksana, Institut Teknologi Bandung, Indonesia

Ulvienin Harlianti, Institut Teknologi Bandung, Indonesia

Darharta Dahrin, Institut Teknologi Bandung, Indonesia

Kartika Kirana, Universitas Padjadjaran, Indonesia

Silvia Fajar, Institut Teknologi Bandung, Indonesia
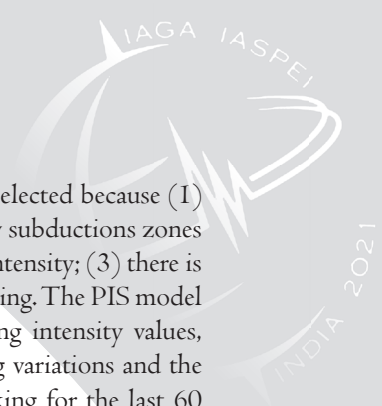
Paleointensity stacking (PIS) applied on six cores data from Western Pacific. This area selected because (1) data from this area has not been represented in the previous PIS; (2) this region has many subductions zones so it can try proving the influence of hematite minerals in the subduction zone to paleointensity; (3) there is a high-resolution RPI from Lake Towuti which can be used as a reference curve in processing. The PIS model made by 4 stages, which are selecting core data from Western Pacific area, normalizing intensity values, interpolating intensity value, and stacking core data. Stacking done with three weighting variations and the resulting model will be referred as WEPAPIS-60 (Western Pacific Paleointensity Stacking for the last 60 kyr). The results obtained can show the pattern of low-intensity values in 41 kyr (Laschamp excursion), 34 kyr (Mono Lake excursion), and the range of 10-20 kyr (which may be related to a young series excursion.

KEYWORDS : WEPAPIS-60, Western-Pacific, paleointensity

Sr No: 275

Tenure of the Nuna supercontinent: possibilities of relative paleolongitudinal constraints and position of surrounding continental blocks

CORRESPONDING & PRESENTING AUTHOR:

Uwe Kirscher, University of Tuebingen, Germany

Ross Mitchell, Institute of Geology and Geophysics, Chinese Academy of Sciences, China

Yebo Liu, Curtin University, Australia

Adam Nordsvan, University of Hong Kong, Hong Kong, China

Paleogeography, chronology and importance of the Paleoproterozoic assembly of the supercontinent Nuna are still debated. In a recent paleomagnetic effort using Australian rocks, we extended the group of building continents of Nuna to Laurentia, Siberia, Baltica, Australia and North China. Using our preferred Nuna configuration, a combined apparent polar wander path can be established for these key constituents. Apart from some minor complexity, the combined path can be seen as the superposition of a presumable tectonic path with oscillatory deviations at the beginning and near the end of Nuna's tenure. Assuming that these oscillatory loops are related to true polar wander events caused by density perturbations in the mantle, could suggest that lower mantle structures were already present during Nuna times. If we further assume that these lower mantle structures were stable during the Nuna interval, similar as the lower mantle provinces in the last several 100 million of years, we can propose a relative paleolongitude framework and establish a well-constrained paleogeographic model for this time. The homogenous structure of the apparent polar wander path also allows us to investigate a potential position of remaining continental blocks during the Nuna time and check if they might have been a part of Nuna or not. In this respect potential options were evaluated considering cratonic India, Amazonia and Congo-Sao Francisco. Due to paleomagnetic limitations and the limited dataset, generally more than one option is permitted, making geological tools inevitable to improve our understanding of the Nuna supercontinent even further.

KEYWORDS : supercontinents, nuna, paleogeography

Sr No: 276

Siberian paleogeography: paleomagnetic and geological constraints

CORRESPONDING & PRESENTING AUTHOR:

Sergei Pisarevsky, Curtin University, Institute of the Earth's Crust, Siberian Branch of the Russian Academy of Sciences, Russia

There are 26 reliable Precambrian paleomagnetic poles for Siberian Craton. Their analysis together with geological data implies low-to middle latitudinal positions of the craton at 1870 – 760 Ma. Geological data suggest that the craton has been completely assembled at ca. 1860 Ma and that at 1800-1100 Ma the western, northern and eastern margins of the craton faced oceans, but the southern margin has been in close proximity or connection with another continent. The analysis of coeval paleomagnetically constrained locations of Siberia and Laurentia at ca. 1735, 1480 and 1380 Ma supports their proximity, but not a close contact. Based on recent geological data it is possible that the Yantze Craton has been located between southern Siberia and northern Laurentia at those times. The analysis of roughly coeval 1100-1000 Ma Apparent Polar Wander Paths for Siberia and Laurentia supports their proximity, but due to age uncertainties a "tight" and "loose" connection between two cratons cannot be distinguished.

KEYWORDS :   paleomagnetism, precambrian, Siberia

Sr No: 277

Middle Eocene onset of Australia-Pacific plate motion in the southwest Pacific inferred from stratigraphy in New Caledonia and New Zealand

CORRESPONDING & PRESENTING AUTHOR:

Edoardo Dallanave, University of Bremen, Germany

The Pacific plate circuit went through a complex reorganization during the early to middle Eocene, which coincides with the onset of subduction along the western Pacific margin. While the subduction initiation of the northwest pacific is well constrained in space and time, the mode and tempo of the southwest Pacific margin evolution and the subduction initiation beneath the Tonga-Kermadec Arc are not fully resolved. We present magneto-biostratigraphic data from an early to middle Eocene sedimentary records exposed in New Caledonia, which is an emerged portion of the Norfolk Ridge. Here it is exposed regionally a transition from pelagic micrite to terrigenous-rich calciturbidite that is interpreted to represent a shift from sedimentation on a stable submarine plateau to slope formation developed under a convergent tectonic regime. Our magnetic polarity-based chronology constrains the age of transition at 45 Ma. We integrate records from New Caledonia with recent magnetostratigraphic data from South Island, New Zealand, where marked variations in terrigenous input occurred during the early and middle Eocene. Synchronous sedimentary changes in the southwest Pacific occurred at the same time as onset of rapid seafloor spreading south of Australia and New Zealand. We infer that the underlying cause of stratigraphic change was inception of slip at a new configuration of the Australia-Pacific plate boundary, which evolved into the Tonga-Kermadec subduction system.

KEYWORDS :   eocene, magnetostratigraphy, southwest pacific

Sr No: 278

SYMPOSIUM :   **1.2 Magnetic record of tectonic, geologic and volcanic processes**

Diagenetic analysis of methane seep (active versus inactive) sediments from Bay of Bengal

CORRESPONDING & PRESENTING AUTHOR:

Virsen Gaikwad, CSIR-National Institute of Oceanography, Dona Paula, Goa, India

Firoz Badesab, CSIR-National Institute of Oceanography, Dona Paula, Goa, India

Pawan Dewangan, CSIR-National Institute of Oceanography, Dona Paula, Goa, India

Mahender Kotha, Goa University, India

ABSTRACT : A comprehensive rock magnetic, mineralogical and petrographic analyses were conducted on the two sediment (gravity) cores retrieved from the active (associated with shallow gas hydrate system) and inactive seep sites from the Krishna-Godavari (K-G) basin, Bay of Bengal. The main focus was to constrain the structural and diagenetic controls on the sediment magnetic properties. In the uppermost sulfidic zone, a systematic downcore diagenetic dissolution of primary magnetic minerals controlled by anaerobic oxidation of methane is observed at active seep site. Presence of chemosynthetic clams and authigenic carbonates provides strong evidence on the methane intensification in this zone. Petrographic analyses of methane derived authigenic carbonates showed the dissolution structures controlled by methane-related diagenetic processes. Reduction and enhancement of magnetic signals in the lowermost methanic zone is manifested by the formation of diagenetic/authigenic iron sulfides (pyrite, greigite). At inactive / non-seep sites, we observed anomalous magnetic signatures in terms of concentration, grain size, and mineralogy. A mixed mineral assemblages comprised of detrital titanomagnetite and authigenic fine-grained iron sulfides are noticed. A typical low-temperature maghemitization shrinkage cracks on the titanomagnetite grains indicates the focal area where preferential dissolution might have started. We proposed that the opening and closing dynamics of the underlying fracture/fault system controlled the variability in methane fluxes, hydrate accumulation and diagenetic processes at the studied sites.

KEYWORDS :   gas hydrate, diagenesis, Krishna-Godavari basin

I.3 Paleo- and rock-magnetic mysteries — quest for solutions

CONVENERS: Maodu Yan

Xiaoqiang Yang

Paleo- and rock-magnetism have played key roles in understanding the geomagnetic field, plate tectonics, and the past and recent environment. However, despite of many great efforts, some fundamental properties of the geomagnetic field and rock magnetic remanence, average strength and its spatial and temporal short and long term variations, inclination bias in sedimentary rocks, remagnetization, etc., remain debated, leading to some ambiguities in the evolution of Earth's interior, plate kinematics, dynamics of the core and mantle, long term climate change, and true polar wander. This inclusive session brings together diverse studies that make use of paleo-, rock, and environmental magnetic data in relation to geological, geomagnetic, and environmental processes. We welcome presentations of innovative studies from both experimental and theoretical aspects of paleo- and rock- magnetism that highlights how the geomagnetic field changes and rock remanence behaves.

Sr No: 279

Revised chronology of central Tibet uplift and its significant implications (by invitation)

CORRESPONDING & PRESENTING AUTHOR:

Xiaomin Fang, Institute of Tibetan Plateau Research, Chinese Academy of Sciences, China

Guillaume Dupontnivet, Université de Rennes, France

Chengshan Wang, University of Geosciences (Beijing), China

Chunhui Song, Lanzhou University, China

Qingquan Meng, Lanzhou University, China

Weilin Zhang, Institute of Tibetan Plateau Research, CAS, China

Junsheng Nie, Lanzhou University, China

Tao Zhang, Lanzhou University, China

Understanding the Tibetan Plateau (TP) topographic history is essential to determining its building mechanisms and its role in driving regional climate, environments and biodiversity. The Lunpola Basin (central-southern Tibet) is the key place to constrain the Tibet building, because it is the first place carried out stable isotope based paleoaltimetry study that supporting for a present elevation of the central TP at least during the past 35 Ma, implying a much earlier uplift of the TP than before. This view was soon widely accepted by international society, but was challenged by a recent finding of low elevation that was estimated by 25.5 Myr tropical fossils. We here use magnetostratigraphic and radiochronologic dating to robustly revise the chronology of both regional elevation estimates in the Lunpola Basin. The results indicate that both ages estimated from stable isotope and fossil are wrong, where the former age of ~40 Ma is revised to ~26-21 Ma, and the latter of ~26 Ma to ~40 Ma. Thus, these revised chronologies demonstrate that central Tibet was generally low (<2.3 km) since at least ~40 Ma and became high (3.5-4.5 km) since at least ~26 Ma. This supports the Eocene existence of a lowland between the Gangdese Shan and Tanggula Shan until their early Miocene uplift. This later uplift of central-southern Tibet has important implications for TP growth mechanisms and agrees well with recently updated studies of the TP-imposed impacts on Asian atmospheric circulations, surface processes and biotic evolution and diversification differentiation.

KEYWORDS : central Tibet, new chronology, tectonic significance

Sr No: 280

Preliminary paleomagnetic results from the Cretaceous Padana and Ngarming Formations in the Xigaze forearc basin, southern Tibet

PRESENTING AUTHOR:

Shihua Xu, Nanjing University, China

CORRESPONDING AUTHOR:

Yongxiang Li, Nanjing University, China

Xinyu Liu, Nanjing University, China

Dengkui Jin, Nanjing University, China

The Xigaze forearc basin (XFB) was formed along the southern margin of Asia when the northward subduction of Neo-Tethys Ocean beneath Asia. The Cretaceous to lower Eocene strata in the XFB are comprised of flysch-dominant Xigaze Group (Sanzugang, Chongdoi, and Ngarming Formations) and Cuojiangding Group (Padana, Qubeiya, Quxia, and Gyalaze Formations). The Padana Formation consists of gray shale interbedded with sandstone and purple-red shale interbedded sandstone, and documents environmental changes in the XFB. To better constrain the chronology of the environmental changes, we conducted a magnetostratigraphic study of Padana and Ngarming Formations of Sangsang section, southern Tibet. Paleomagnetic samples were collected from 73 stratigraphic levels, which are mainly from sandstone, and were subjected to stepwise thermal demagnetization that reveal two-component magnetizations. The high-temperature components (HTC) typically unblocked at ~ 580-680 ? and passed both a reversed test and a fold test at 95% confidence level, suggesting a primary origin of the remanence. The magnetostratigraphic results show a predominantly reversed polarity, which, together with biostratigraphic data, constrain the studied interval to the early Campanian. The environmental changes in the XFB during the early Campanian will be discussed.

KEYWORDS : paleomagnetism, sedimentary environment, xigaze forearc basin

Sr No: 281

SYMPOSIUM : **1.3 Paleo- and rock-magnetic mysteries – quest for solutions**

Low-latitude hydroclimate changes related to paleomagnetic variations during the Holocene in southern China

PRESENTING AUTHOR:

Tingwei Zhang, Sun Yat-sen University, China

CORRESPONDING AUTHOR:

Xiaoqiang Yang, Sun Yat-sen University, China

Recent studies have strongly suggested that cloud cover has a critic influence on precipitation in low latitudes during the relatively warm period. However, it is very difficult to reconstruct cloud cover proxies over the long geological period. We attempt to decipher the potential links between paleo-hydroclimate variability and the Earth's magnetic field (EMF) to understand how cloud cover modulates the paleoclimate change process in southern China. Two sediment cores with different deposition environments were selected, and high-resolution hydroclimate proxies were derived based on the hematite to goethite ratio. The results showed significant centennial-scale variations during the Holocene epoch. There is a positive correlation between the hydroclimate variations and the virtual axial dipole moment, especially during the intervals of rapid changes in the EMF intensity (2.8-2.0 kyr BP and 1.5-0.3 kyr BP). Moreover, spatial correlation analysis reveals that the hydroclimate in southern China is predominantly influenced by cloud feedbacks. Our comparisons among different virtual axial dipole moments (VADM) and sea surface temperature (SST) records support the EMF-galactic cosmic ray-cloud-climate hypothesis. This connection between the EMF and climate does not mean that the EMF is fully responsible for climate change, although the EMF plays an important role that should not be ignored in climate change.

KEYWORDS : earth's magnetic field, climate change, cloud cover

Sr No: 282

Millennial resolution late Miocene northern China precipitation record spanning astronomical analogue interval to the future

PRESENTING AUTHOR:

Peng Gao, Lanzhou University, China

CORRESPONDING AUTHOR:

Junsheng Nie, Lanzhou Universit, china

Much has been learned regarding orbital and millennial timescale climate changes after the onset of Northern Hemisphere glaciations (NHG) at ca. 2.7 Ma. By contrast, little is known about these variations before the NHG due to lack of high-resolution records. Here we report first millennial resolution quantified East Asian summer monsoon (EASM) precipitation record from the north eastern Tibetan Plateau. The record supports astronomical forcing of EASM during the late Miocene, except for the period of 8.13-8.03 Ma when EASM experienced high amplitude variations at the 100-, 20-kyr, and suborbital bands, which is in sharp contrast with the damped astronomical forcing. Detection of strong 100-kyr and millennial cycles during low eccentricity intervals of the warm late Miocene with ephemeral NH ice sheets cast doubt on NH ice sheet size variations as their exclusive forcing in the late Miocene and late Quaternary paleoclimatic records.

KEYWORDS :   east asian summer monsoon, late miocene, astronomical forcing

Sr No: 283

Critical altitudinal shift from detrital to pedogenic origin of the magnetic properties of surface soils in the western Pamir Plateau, Tajikistan

PRESENTING AUTHOR:

Jian Kang, Institute of Tibetan Plateau Research, Chinese Academy of Science, China

CORRESPONDING AUTHOR:

Jinbo Zan, Institute of Tibetan Plateau Research, Chinese Academy of Science, China

Sedimentary archives of the westerlies-influenced Pamir Plateau in Tajikistan, a climatically sensitive region in arid central Asia (ACA), provide information on past climatic changes and the tectonic evolution of the northern Tibetan Plateau. However, due to the scarcity of meteorological stations, knowledge of the recent precipitation history of the region is limited. In this study, we conducted a detailed rock magnetic investigation of 34 surface loess samples from the western Pamir Plateau. The results show that on the windward side, below an altitude of ~2100 m a.s.l., the concentration of magnetic minerals initially decreases and then begins to increase with increasing altitude. Below ~2100 m a.s.l., the surface soils are enriched in multidomain (MD) magnetite particles, suggesting a detrital origin of the magnetic minerals, whereas above this altitude the samples are enriched in fine superparamagnetic (SP) magnetite/maghemite grains of pedogenic origin. The inferred variations in pedogenic intensity, combined with analysis of the available meteorological data and the content of organic matter and clay, support the occurrence of an altitudinal threshold separating a predominantly detrital control on surface soil magnetic mineral assemblages from

a predominantly pedogenic control. Within the plateau interior, the surface loess samples exhibit low and uniform values of magnetic concentration parameters and organic matter and clay content, which is attributed to the decreased supply of moisture from westerly sources because of the rain shadow effect. Our results indicate that rock magnetic investigations can be used to define a critical climatic boundary in ACA.

KEYWORDS : rock magnetism, surface soils, climatic boundary

Sr No: 284

SYMPOSIUM : **1.3 Paleo- and rock-magnetic mysteries – quest for solutions**

Coupled impacts of sea ice variability and North Pacific atmospheric circulation on orbital terrigenous sediment dynamics in the subarctic Pacific Ocean

CORRESPONDING & PRESENTING AUTHOR:

Yi Zhong, Southern University of Science and Technology, China

Qingsong Liu, Southern University of Science and Technology, China

The processes controlling environmental changes in the subarctic Pacific Ocean over millennial timescale to orbital timescales are not well understood. Here we use a 230 kyr long sedimentary record from the northwest Pacific to assess the late Pleistocene sensitivity of sediment dynamics to orbital forcing at a source-to-sink perspective. The paleodata synthesis and model simulations suggest the orbital terrigenous sediment dynamics could be resulted from the obliquity-scale changes in atmospheric climatic modes induced by Aleutian Low forcing. Moreover, we found remarkable shift in the North Pacific circulation involving a strengthened Siberia High at the Last Glacial Maximum. This coupled ocean-atmosphere system represents a potential amplifier of climate variability, such that improved constraints on its past behaviour could provide insight into regional climatic signals are transferred to a hemsispheric scale. In summary, this study provides new insights into the causes of terrigenous dynamic and highlights the relevance of AL-forcing dynamics as an active positive feedback mechanism in the high-latitude climatic changes.

KEYWORDS : sediment provenance; magnetic mineralogy; aleutian low; orbital forcing; north pacific intermediate water; subarctic pacific ocean

Sr No: 285

SYMPOSIUM : **1.3 Paleo- and rock-magnetic mysteries – quest for solutions**

Classification of a complexly mixed magnetic mineral assemblage in Pacific Ocean surface sediment by electron microscopy and supervised magnetic unmixing

CORRESPONDING & PRESENTING AUTHOR:

Jinhua Li, Institute of Geology and Geophysics, Chinese Academy of Sciences, China

Yan Li, Institute of Geology and Geophysics, Chinese Academy of Sciences, China

Shuangchi Liu, Institute of Geology and Geophysics, Chinese Academy of Sciences, China

Andrew P Roberts, Australian National University, Australia

Hongmiao Pan, Institute of Oceanology, Chinese Academy of Sciences, China

Tian Xiao, Institute of Oceanology, Chinese Academy of Sciences, China

Yongxin Pan, Institute of Geology and Geophysics, Chinese Academy of Sciences, China

Unambiguous magnetic mineral identification in sediments is a prerequisite for reconstructing paleomagnetic and paleoenvironmental information from environmental magnetic parameters. We studied a deep-sea surface sediment sample from the Clarion Fracture Zone region, central Pacific Ocean, by combining magnetic measurements and scanning and transmission electron microscopic analyses. Eight titanomagnetite and magnetite particle types are recognized based on comprehensive documentation of crystal morphology, size, spatial arrangements, and compositions, which are indicative of their corresponding origins. Type-1 particles are detrital titanomagnetites with micron- and submicron sizes and irregular and angular shapes. Type-2 and -3 particles are well-defined octahedral titanomagnetites with submicron and nanometer sizes, respectively, which are likely related to local hydrothermal and volcanic activity. Type-4 particles are nanometer-sized titanomagnetites hosted within silicates, while type-5 particles are typical dendrite-like titanomagnetites that likely resulted from exsolution within host silicates. Type-6 particles are single domain magnetite magnetofossils related to local magnetotactic bacterial activity. Type-7 particles are superparamagnetic magnetite aggregates, while Type-8 particles are defect-rich single crystals composed of many small regions. Electron microscopy and supervised magnetic unmixing reveal that type-1 to -5 titanomagnetite and magnetite particles are the dominant magnetic minerals. In contrast, the magnetic contribution of magnetite magnetofossils appears to be small. Our work demonstrates that incorporating electron microscopic data removes much of the ambiguity associated with magnetic mineralogical interpretations in traditional rock magnetic measurements.

KEYWORDS :   magnetic minerals, magnetic techniques, transmission electron microscopy

Sr No: 286

SYMPOSIUM :   **1.3 Paleo- and rock-magnetic mysteries – quest for solutions**

Paleomagnetic constraints on the Cenozoic Altyn Tagh Fault movement and deformation of the NE Tibetan

CORRESPONDING & PRESENTING AUTHOR:

Maodu Yan, Institute of Tibetan Plateau Research, Chinese Academy of Sciences, China

The Altyn Tagh Fault (ATF) is the northern boundary of the Tibetan Plateau. The Cenozoic activities of this fault have played important roles on the adjustment of the India-Asia collision and the uplift of the northeastern Tibetan Plateau. However, the timing of commencement, amount of displacement, strike-slip rate, and the tectonic evolution and uplift of the region are still under debate.

We present here new detailed paleomagnetic rotation studies on two curvatures south of the ATF (Yingxiongling and QMTB) to understand the originality of the curved landform and their relationship with the ATF. We found (1) No significant post-20 Ma rotations at the localities further away from the ATF, but remarkable counterclockwise rotations of ~50° at ~16-11 Ma closer to the fault at the Yingxiongling curvature; (2) significant clockwise rotations of ~32.2 ± 15.4° during ~33–16 Ma, and subsequent statistically insignificant counterclockwise rotations of ~8.7 ± 9.4° after ~16 Ma in the middle NQMTB. Integrated with other lines of geological evidence, we propose that these two arcuate units were most likely caused by the sinistral strike-slip faulting of the ATF, rather than originally curved ones. Through transpressive push and sinistral frictional drag, the two periods of strike-slip faulting have resulted in significant clockwise rotations of the middle NQMTB during ~33-16 Ma, and remarkable counterclockwise rotations of the northwest corner of the NQMTB and the Yingxiongling curvature,

respectively. We argue that the Altyn Tagh Shan and the connected Qilian Shan had corresponding rapid uplifts during those periods.

Sr No: 287

Comparative rock magnetic study of Eocene volcanogenic and sedimentary rocks from Yunnan, southeastern Tibetan Plateau, and its geological implications

PRESENTING AUTHOR:

Miaomiao Shen, Institute of Tibetan Plateau Research, Chinese Academy Sciences, China
Jinbo Zan, Institute of Tibetan Plateau Research, Chinese Academy Sciences, China

CORRESPONDING AUTHOR:

Maodu Yan, Institute of Tibetan Plateau Research, Chinese Academy Sciences, China
Weilin Zhang, Institute of Tibetan Plateau Research, Chinese Academy Sciences, China
Xiaomin Fang, Institute of Tibetan Plateau Research, Chinese Academy Sciences, China
Dawen Zhang, Zaozhuang University, China
Tao Zhang, Institute of Tibetan Plateau Research, Chinese Academy Sciences, China

Many recent biomagnetostratigraphic studies within and around the Tibetan Plateau have resulted in significant age differences, due to lack of radiometric age constraints. It has hindered the knowledge on the tectonic and paleoclimate evolutions of the Tibetan Plateau. Identifying barely visible tephra-bearing layers is urgent to solve the debate. Here we carry out a comparative rock magnetic study of Eocene volcanogenic and sedimentary rocks from the Jianchuan and Qujing Basins of the Yunnan Plateau. Our aim is to establish an effective method for tephra identification in sedimentary sequences. Petrographic and rare earth element analyses demonstrate that the volcanogenic rocks are of basic-intermediate magmatic origin with no sign of deformation or alteration, and the sedimentary rocks are unaffected by volcanic disturbance. Rock magnetic analyses reveal that the primary ferrimagnetic minerals of the volcanogenic rocks are Ti-poor titanomagnetite and/or magnetite, including pseudo-single-domain, viscous superparamagnetic and ultrafine superparamagnetic (true superparamagnetic, nonviscous around room temperature) grains. Hematite is the dominant magnetic mineral in the sedimentary rocks, and paramagnetic minerals are also abundant; pseudo-single-domain/single-domain magnetite and maghemite are also present. The enrichment of ultrafine superparamagnetic grains in the volcanogenic rocks may induce strikingly peaked signals in low-temperature frequency-dependent susceptibility measurement, in sharp contrast with pedogenically produced viscous superparamagnetic particles that show no peaks. Therefore, we attribute the low-temperature frequency-dependent susceptibility parameters to the effective and sensitive magnetic parameters for identifying tephra-bearing layers within the sedimentary sequences of the Yunnan Plateau.

Sr No: 288

Paleomagnetic and Chronologic Data Bearing on the Permian/Triassic Boundary Position of Qamdo in the Eastern Qiangtang Terrane: Implications for the Closure of the Paleo-Tethys

PRESENTING AUTHOR:

Chong Guan, Institute of Tibetan Plateau Research, Chinese Academy of Sciences, China

CORRESPONDING AUTHOR:

Maodu Yan, Institute of Tibetan Plateau Research, Chinese Academy of Sciences, China

The tectonic evolution of the eastern Paleo-Tethys in the Three-Rivers headwater region remains uncertain, especially because of the lack of quality paleomagnetic data from the east Eastern Qiangtang Terrane (EQT). Here, we present an integrated paleomagnetic and zircon U-Pb geochronologic study of the Gadikao Formation (Fm.) volcanic rocks in the EQT. This previously assumed Carboniferous or Permian rock unit is now zircon U-Pb dated to ~254–248 Ma. Our new high quality (29 sites and 257 samples) inferred primary paleomagnetic results yield a robust Permo-Triassic boundary paleopole of 59.7°N and 228.2°E (A95 = 3.3°), with a paleolatitude of 10.0 ± 3.3°N for the study area. Integrated with other reliable Permo-Triassic paleomagnetic data of the EQT and the Tarim Block and other lines of geologic evidence, we propose that the EQT drifted continuously northward during 300–200 Ma and the Paleo-Tethys Ocean probably closed at ~232–220 Ma around the Qamdo region, most likely at 230 Ma.

KEYWORDS :   paleomagnetic, eastern qiangtang terrane, paleo-tethys

Sr No: 289

Hydroclimatic and environmental magnetic record inferred from Baxian Lake: implications for monsoon variations during the last 2000 years in Southern China

PRESENTING AUTHOR:

Shengtan Shang, Sun Yat-sen University, China

CORRESPONDING AUTHOR:

Xiaoqiang Yang, Sun Yat-sen University, China

Understanding the potential mechanisms driving the precipitation pattern in the Asian summer monsoon (ASM) area is significant to reconstructing the environmental and hydrological conditions over the past ~2000 years. However, robust and consistent conclusions have been hampered by the complex processes controlling the dynamics and diverse interconnected linkage of the Asian monsoon. Here, we present a reconstruction of variations in humidity for the past two millennia, based on the ratio of hematite to goethite (Hm/Gt) and other magnetic parameters in the sediments of Baxian Lake, southern China. The record indicates that a dramatic transition from dry to humid climate occurred during AD 800–950, and then returned to extreme drought during the Medieval Warm Period. The fluctuations between a relatively wet climate and weak drought were also demonstrated during the Little Ice Age (AD 1450–1800). Moreover, the

Hm/Gt record indicates that an opposite precipitation pattern occurred in southern China when compared with precipitation records in northern China and India. We ascribe this result to the superimposition of land-ocean-atmosphere dynamics on the traditional model of the intertropical convergence zone (ITCZ) movement forced by the Atlantic Meridional Overturning Circulation, and the migration of western Pacific subtropical high forced by the ITCZ, Walker circulation, and Hadley circulation controlling the route of East ASM and location of precipitation. This is significant for enhancing our understanding of the relationship among the continent-ocean thermal gradient, ASM variation, ITCZ movement, El Niño Southern Oscillation-like events, and extreme climates in areas influenced by the ASM.

KEYWORDS : hematite/goethite, rainfall pattern, southern China

Sr No: 290

Did anoxic Black Sea sediments properly record paleosecular variations during the Holocene ?

CORRESPONDING & PRESENTING AUTHOR:
Jiabo Liu, Southern University of Science and Technology, China
Qinsong Liu, Southern University of Science and Technology, China
Norbert Nowaczyk, Helmholtz-Zentrum Potsdam, Deutsches GeoForschungsZentrum GFZ, Germany

Magnetostratigraphic analyses of sediments, reconstructing directions and relative paleointensity variations, have greatly improved our understanding of the Earth's magnetic field and have been widely used also in chronology. To ensure the fidelity of sedimentary paleomagnetic records, certain depositional environments without magnetic mineral diagenesis is generally a precondition. Consequently, most lakes, marginal seas and tropical coasts which are characterized by anoxic water conditions due to stratification and/or high organic matter input are unsuitable for paleomagnetic studies.

However, such anoxic sediments are often characterized by high sedimentation rates and are the only available paleomagnetic material for specific areas. Recovering the paleomagnetic information from these anoxic sediments thus can achieve better data coverage over temporal and spacial scales.

In this study, the anoxic Holocene Black Sea sediments were systematically investigated by using paleo- and rock-magnetic protocols, as well as transmission and scanning electron microscopy (TEM and SEM) observations. Paramagnetic pyrite framboids were ubiquitously identified in the anoxic sediment. Besides, magnetite particles enclosed in silicates are the sole magnetic carrier that could be observed. The obtained paleomagnetic results from the Holocene sections from sixteen cores show fairly comparable variations among each other, though carried by a weak magnetic remnant magnetization.

Thus, the magnetite inclusions preserved in the anoxic Black Sea sediments likely recorded reliable paleosecular variations, which may have great implications for reconstructing paleosecular variations from other anoxic sediments.

KEYWORDS : paleomagentism, anoxic sediments, Black Sea

Sr No: 291

An Overview of Paleomagnetic data from Deccan traps and the revision of Deccan Super-pole

CORRESPONDING & PRESENTING AUTHOR:

Satish Sangode, Savitribai Phule Pune University, India

Amarjeet Bhagat, Savitribai Phule Pune University, India

Ashish Dongre, Savitribai Phule Pune University, India

Deccan traps representing strongly ferrimagnetic ChRM directions is one of the most widely studied paleomagnetic record over Indian subcontinent. A compilation of total 1666 Paleomagnetic Site mean directions so far published during the last 60 years is processed using Paleomagnetic Analysis Program v4.2 (Zang and Ogg, 2003). Filtering of the data having large scatter and removal of transitional polarity directions yielded 1062 significant mean Paleomagnetic directions that produce total site mean D/I of 152/56. The compilation results in Chrons C30n mean of 333/-38, C29r of 157/47 and C29n of 341/-32. A Deccan Superpole has been calculated based on this data at 284°E and 27°N. The above exercise reveals spatio-temporal disparity by poor representation from Saurashtra, Malwa, Eastern- and Central Deccan provinces compared to the Western Deccan province. Further about 80% of the data belongs to C29r, which also shows an inclination anomaly of >100 and an 80 anticlockwise rotation of the Indian plate within a brief time interval of ~700 Ka. We suggest standardization of demagnetization protocols, interlaboratory calibrations and precise determination of altitudes to further improve the definitions of Chrons and the geomagnetic field intensities during the Deccan event.

KEYWORDS :   deccan traps; palaeomagnetism

I.4 Earth's magnetic field and secular variation on all temporal and spatial scales

CONVENERS: Arnaud Chulliat

Gelvam Hartmann

Phil Livermore

Yoichi Usui

The Earth's magnetic field varies on a wide range of temporal and spatial scales. Geodynamo processes and waves in the Earth's outer core generate magnetic field variations on subdecadal to geological time scales. Some variations are global (e.g., magnetic reversals, the dipole decay) while others have a smaller spatial foot print (e.g., the evolution of the South Atlantic Anomaly, the drift of the North magnetic dip pole). This session aims at bringing together researchers investigating geomagnetic field variations on all temporal and spatial scales, and using a broad range of methods. We welcome observational studies based on paleomagnetic and archeomagnetic records, cosmogenic isotopes, ground-based and satellite geomagnetic measurements, as well as theoretical studies, numerical simulations and laboratory experiments.
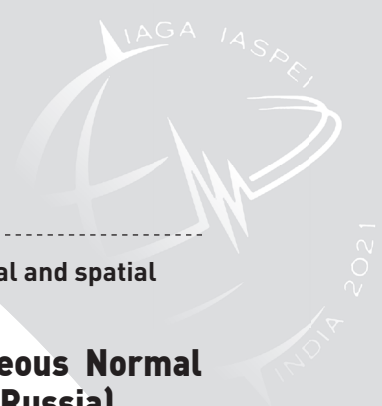
Intensity of the Earth's magnetic field during the Cretaceous Normal Superchron (Okhotsk-Chukotka Volcanic Belt, North-East of Russia)

CORRESPONDING & PRESENTING AUTHOR:

Elizaveta Bobrovnikova, Schmidt Institute of Physics of the Earth, Russian Academy of Sciences, Moscow, Russia

Ivan Lebedev, Schmidt Institute of Physics of the Earth, Russian Academy of Sciences, Moscow, Russia

Existing estimates of the Earth's magnetic field intensity during the Cretaceous Normal Superchron (CNS) allow two opposite points of view: the intensity of geomagnetic field during the most of the Mesozoic was (1) significantly lower than present-day field, or (2) similar to that. Actually, the quantity and quality of paleointensity estimates for the time interval of 80-95 million years is rather high, but large scatter of the virtual dipole moment (VDM) values doesn't provide an unambiguous opportunity to make a final conclusion about the Earth's magnetic field strength during this time.

We present the first paleointensity results from volcanic rocks of the Okhotsk-Chukotka volcanic belt, erupted at the end of the Cretaceous Normal Superchron (126-84 Ma). The paleointensity estimates were determined according to the experimental protocol of the modified Coe Thellier–Thellier procedure and meet the modern reliability criteria. The obtained values of the geomagnetic field intensity are approximately half of the current value, which confirms the hypothesis of the existence of a geomagnetic field with a low dipole moment in the Cretaceous Normal Superchron.

KEYWORDS : intensity, CNS, VDM

Geomagnetic excursions in the past 70 ka: Similarities and differences of the spatiotemporal characteristics (by invitation)

CORRESPONDING & PRESENTING AUTHOR:

Sanja Panovska, GFZ German Research Centre for Geosciences, Potsdam, Germany

Monika Korte, GFZ German Research Centre for Geosciences, Potsdam, Germany

Jiabo Liu, Southern University of Science and Technology, China

Norbert Nowaczyk, GFZ German Research Centre for Geosciences, Potsdam, Germany

Geomagnetic excursions are the most extreme variations of the geomagnetic field during stable polarities. They are characterized by a dramatic field intensity decline and large directional deviations. Geomagnetic excursions are frequently observed in paleomagnetic records and are an intrinsic feature of the field. Yet, we still do not fully understand the mechanism that drives them and many questions remain open.

Here we present a new study of excursions that occurred in the 70-15 ka period based on a high-resolution,

global paleomagnetic field model. The model, named GGFSS70, is built from nine globally distributed, well-dated, sedimentary paleomagnetic records. It includes three geomagnetic excursions: Norwegian-Greenland Sea (65 ka), Laschamps (41 ka), and Mono Lake/Auckland excursion (34.5 ka). We analyzed the dipole moment, paleosecular variation (PSV) index, global field morphology at the Earth's surface and the core-mantle boundary, and dipole and non-dipole energy variations during these events. By investigating these properties, we inferred similarities and differences of these excursions. The PSV index is different for the three events, with the most pronounced peak over the Laschamps, while the Mono Lake/Auckland excursion shows only a slight increase, not reaching the excursion threshold globally, only regionally. At the Earth's surface, the dipole energy is always higher than the non-dipole except over the Laschamps excursion. Thus, the Laschamps excursion is associated with growth and poleward moving of reversed flux patches, and a completely reversed field in the tangent cylinder, which is not the case for the other two excursions.

KEYWORDS :   earth's magnetic field, paleomagnetic data, geomagnetic excursions

Sr No: 294

A Miocene reversed-to-normal polarity transition recorded in a volcanic section on St. Helena, South Atlantic

CORRESPONDING AUTHOR:

Elisabeth Schnepp, Montanuniversitaet Leoben, Austria

PRESENTING AUTHOR:

Patrick Arneitz, ZAMG, Austria

Morgan Ganerod, Geological Survey of Norway, Norway

Robert Scholger, Montanuniversitaet Leoben, Austria

Roman Leonhardt, ZAMG, Austria

Yael Engbers, University of Liverpool, UK

Andy Biggin, University of Liverpool, UK

The first paleomagnetic study of secular variation of St. Helena island was performed only recently. Engbers et al. (PNAS 2020) discovered a profile of six lava flows, which recorded a reversed-to-normal polarity transition with three intermediate directions. The profile was resampled, extended by four lava flows and another parallel profile with twelve lavas was added. Mean characteristic remanent magnetization directions have been obtained from four to seven specimens per flow with alternating field or thermal demagnetizations. They are reasonably defined for sixteen of the sites with Fisher precision parameters k above 50 and ⬚ 95 confidence radii below 12.5° reproducing well paleodirections from Engbers et al. (2020). The upper nine flows of Profile 1 show very similar directions compared to the five uppermost flows of Profile 2 and three (two) transitional directions are in profile 1 (2) with virtual geomagnetic pole latitudes between -7° and 27° followed by three (one) normally magnetized lavas. Therefore, the transitional nature of the lavas is well supported by two independent sampling campaigns and two parallel profiles. Thermomagnetic curves of susceptibility suggest titanomagnetites with high and low Ti-content as remanence carriers. Many curves show strong irreversibility suggesting the presence of primary low-temperature oxidation or maghemitization. Paleointensity determination with the Coe version Thellier experiments and 39Ar/40Ar dating are under work and will allow for field modelling of the polarity transition.

KEYWORDS :   transitional field, paleointensity
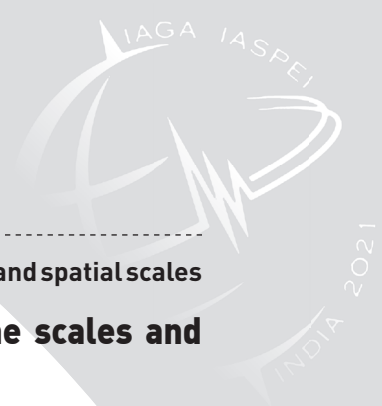
Sr No: 295

Oscillations in the geomagnetic field at sub-centennial time scales and their sources

CORRESPONDING & PRESENTING AUTHOR:

Crisan Demetrescu, Institute of Geodynamics, Romanian Academy, Romania

Venera Dobrica, Institute of Geodynamics, Romanian Academy, Romania

Cristiana Stefan, Institute of Geodynamics, Romanian Academy, Romania

We investigate the variation of the geomagnetic field at sub-centennial time scales, as shown by both time series of annual means provided by geomagnetic observatories and time series of gufm1 annual means on a world-wide 2.5°x2.5° latitude/longitude grid. A Hodrick-Prescott type of analysis, separating a decadal variation and a trend, has been employed. The trend has been in turn decomposed by a Butterworth filtering in two oscillations, at sub-centennial (60-90 years) and inter-decadal (20-30 years) time scales. Similar oscillations are shown to be present in the solar activity described by solar indices and solar wind parameters, particularly in the current systems, ring current included, developed as a result of magnetosphere/ionosphere interaction with the solar wind and the heliospheric magnetic field. We forward the external current systems as a source to oscillations observed in the geomagnetic field, via an inductive response of the Earth's interior (core and mantle levels) to variations of external sources.

KEYWORDS : sub-centennial oscillations, geomagnetic observations, geomagnetic models

Sr No: 296

Spikes in the Geomagnetic Field: A case study of the Levantine Iron Age Anomaly

CORRESPONDING & PRESENTING AUTHOR:

Pablo Rivera Perez, Universidad Complutense de Madrid, Spain

Francisco Javier Pavon Carrasco, Universidad Complutense de Madrid, Spain

Maria Luisa Osete Lopez, Universidad Complutense de Madrid, Spain

The Levantine Iron Age Anomaly (LIAA) corresponds to a short-decadal geomagnetic intensity variation in the Levantine region. The LIAA is characterized by a high intensity maximum (about 160 ZAm2 in terms of the virtual dipole moment) that is related to a large geomagnetic positive anomaly (the so-called spike) at the Earth's surface. The occurrence in both space and time of the LIAA has been constrained by archeomagnetic data coming from Eastern Europe and Western Asia between 1050 BC and 700 BC.

Davies and Constable (2017) indicated that the LIAA spike is characterized by small spatial wavelengths and thus it is due to the contribution of high spherical harmonic degrees. Here, we revisit this work by using the most recent archeomagnetic dataset covering the spatial and temporal period of the LIAA. To reconstruct the spike event, we develop a spherical harmonic global model as a perturbation of the Gauss coefficients from a previous paleomagnetic global model that did not use the LIAA data record. Our results indicate that the LIAA event could be characterized by larger spatial wavelengths and thus it is defined by lower harmonic degrees (between 3 and 6) than expected by the previous work.

KEYWORDS : geomagnetic spike, archaeomagnetism, geomagnetic field model

Sr No: 297

New archaeointensity data from Japan: Evidence of low intensities during the Late Yayoi period.

CORRESPONDING AUTHOR:

Evdokia Tema, Università degli Studi di Torino, Italy

PRESENTING AUTHOR:

Yuri Santos, Università degli Studi di Torino, Italy

Ricardo Trindade, University of São Paulo, Brazil

Gelvam Andre Hartmann, Universidade Estadual de Campinas, Brazil

Tadahiro Hatakeyama, Okayama University of Science, Japan

Naoko Matsumoto, Okayama University, Japan

Jun Mitsumoto, Okayama University, Japan

Monica Gulmini, Universià degli Studi di Torino, Italy

We present new absolute archaeointensity data from Japan obtained from the study of ceramic fragments from four archaeological sites situated at the Okayama prefecture. All studied materials are well dated based on archaeological evidence, with ages ranging from 150 CE to 600 CE, covering the Late Yayoi and Kofun periods. The collected fragments come from pottery and haniwa artifacts from the sites of Tatezaka, Tatetsuki, Tenguyama, and Nima Ohtsuka. Preliminary rock magnetic and archaeomagnetic experiments suggest the presence of magnetite and/or Ti-magnetite as the main carrier of the remanence, with a minor contribution of a higher coercivity mineral. After thermal demagnetization experiments, the most magnetically stable samples were selected for archaeointensity analysis that were performed following the classical Thellier-Thellier method, including partial thermoremanent magnetization (pTRM) checks and pTRM tail-checks. All measurements were corrected for anisotropy and cooling-rate effects. Successful archaeointensity determinations, following strict selection criteria, were obtained for three sites. The new data are compared with previously published archaeointensity records from Japan and with global geomagnetic field models predictions. Such comparison shows an interesting intensity low around the second century CE which was not previously observed and that deserves further investigation.

KEYWORDS :   archaeointensity, Japan, ceramics

Sr No: 298

A statistical evaluation of paleosecular variation and time-averaged field for 0-10 Ma

CORRESPONDING & PRESENTING AUTHOR:

Wellington P. De Oliveira, Universidade Estadual de Campinas, Brazil

Gelvam A. Hartmann, Universidade Estadual de Campinas, Brazil

Filipe Terra Nova, Instituto de Astronomia, Geofísica e Ciências Atmosféricas, Universidade de São Paulo, Brazil

Daniele Brandt, Instituto de Astronomia, Geofísica e Ciências Atmosféricas, Universidade de São Paulo, Brazil

Andrew J. Biggin, University of Liverpool, UK

Jairo F. Savian, Universidade Federal do Rio Grande do Sul, Brazil

Daniel R. Franco, Observatório Nacional, Brazil

Ricardo I. F. Trindade, Instituto de Astronomia, Geofísica e Ciências Atmosféricas, Universidade de São Paulo, Brazil

Thiago R. Moncinhatto, Instituto de Astronomia, Geofísica e Ciências Atmosféricas, Universidade de São Paulo, Brazil

Investigations about long-term geomagnetic variations are essential for a better assessment of the paleomagnetic field behavior. However, on timescales of a few million years the structure of the average field is especially limited by the inhomogeneous spatio-temporal sampling of paleomagnetic records. Here, we assess the latitudinal behavior of the paleosecular variation (PSV) and time-averaged field (TAF) structure for the past 10 Ma from a reviewed and updated the paleodirectional database derived from igneous rocks. The new database provides improvements in the spatial and temporal distribution of the high-quality data compared with the previous compilations. In addition, the new data collection differs significantly in using stricter selection criteria. Results show that the curve of Model G fitted to the estimates of virtual geomagnetic pole (VGP) dispersion produces a low latitudinal dependence of PSV, associated with high and low values for Model G a and b parameters, respectively. Moreover, we propose the first 0-10 Ma TAF model based on the latitudinal distribution of inclination anomaly data. Results also indicate the presence of small non-dipole field contributions, with best estimates for the zonal quadrupole term about 3% of the axial dipole term larger than the zonal octupole term (~1% of the axial dipole term). These new findings suggest that non-dipole structures have persisted over a long-term through observations of geomagnetic field models for the past 100 ka and 0-5 Ma period.

KEYWORDS : paleosecular variation, time-averaged field, database

Sr No: 299

Core field variation studies using satellite data (by invitation)

CORRESPONDING & PRESENTING AUTHOR:

Magnus Hammer, Technical University of Denmark, Denmark

Christopher Finlay, Technical University of Denmark, Denmark

Nils Olsen, Technical University of Denmark, Denmark

We have used 20 years of continuous magnetic field measurements from the Oersted, CHAMP and Swarm satellite missions, supplemented by calibrated platform magnetometer data from the CryoSat-2 satellite, to study sub-decadal variations of the Earth's core magnetic field at the core–mantle boundary (CMB). To do this, we apply the Subtractive Optimally Localized Averages (SOLA) method which allows for radial secular variation (SV) and secular acceleration (SA) field estimates at the CMB to be computed. An advantage of the SOLA approach is that we obtain precise information regarding the spatial and temporal resolution of our SA estimates. During the Swarm era we are able to resolve the time-varying SA at the CMB on timescales down to one year for spatial scales down to 4000 km (corresponding to spherical harmonic degree 10). We find, that along the CMB geographic equator the evolution of the SA displays intense features with amplitudes reaching $\pm 2.5 \mu T/yr^2$ under Indonesia from 2011–2014, under central America from 2015–2019, sequences of SA with alternating sign under the Atlantic during 2004–2019, and strong positive and negative SA features appearing side-by-side in the Pacific in 2017 drifting westward.

KEYWORDS : geomagnetism, secular variation, secular acceleration

Sr No: 300

Recovery of rapid core motions: a synthetic study

CORRESPONDING & PRESENTING AUTHOR:

Tobias Schwaiger, CNES, France

Nicolas Gillet, CNRS, France

Dominique Jault, CNRS, France

Mioara Mandea, CNES, France

Julien Aubert, IPGP, France

The observed secular variation of the geomagnetic field is assumed to reflect the convective dynamics of the Earth's fluid outer core. Time-dependent models of the field are used to invert for the fluid flow just beneath the core surface. However, it is unclear how well rapid core motions on interannual or shorter time scales can be resolved with current geomagnetic field models.

To answer this question, we present a study in which we use a state-of-the-art numerical geodynamo simulation that exhibits such rapid dynamics. From the simulation data, we generate synthetic magnetic field observations with a temporal and spatial distribution equivalent to ground and satellite records. We then construct a magnetic field model by solving the inverse problem constrained by this synthetic data. The obtained model is in turn inverted for the core surface motions.

Based on the comparison of the inverted flow with the reference flow provided by the geodynamo simulation, we discuss how accurately we can expect to recover the Earth's core surface motions when applying the same methods to geomagnetic records. In particular, we focus on whether we can detect torsional oscillations and quasi-geostrophic Alfvén waves, the latter having been associated with geomagnetic jerks.

KEYWORDS :   interannual field changes, core flow, quasi-geostrophic modes

Sr No: 301

Spherical Cap Harmonic Analysis of the Geomagnetic Field over the Indonesian Region for Epoch 2015.5

CORRESPONDING & PRESENTING AUTHOR:

Yosi Setiawan, BMKG, Indonesia

Ten regional geomagnetic field models have been developed using the Spherical Cap Harmonic Analysis (SCHA) method over the Indonesian region and adjacent areas for epoch 2015.5 using the spatial truncation index $k = 1 - 10$. This research aims to obtain a geomagnetic field model with better resolution and accuracy than the International Geomagnetic Reference Field (IGRF) model. The data used are compiled from 68 geomagnetic repeat stations in Indonesia from BMKG (Badan Meteorologi Klimatologi dan Geofisika) Indonesia, combined with definitive data from four BMKG geomagnetic observatories and 10 INTERMAGNET observatories. Synthetic cartesian X, Y, and Z components at sea level at 17 fixed locations, calculated from IGRF-13, are also used to increase the calculation's stability because of the data distribution irregularities. The area covered by the models is the Indonesian region between 92°E and 152°E
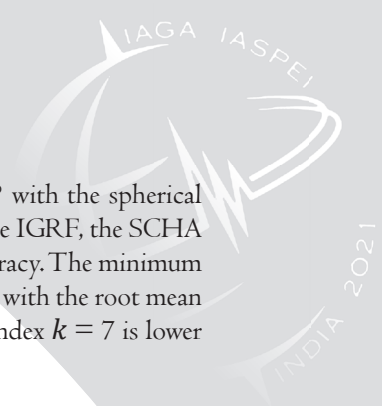
in longitude and 33°S and 27°N in latitude. The spherical cap half-angle is set to 30° with the spherical cap pole's coordinate at 122°E and 3°S. From statistical analysis and comparison with the IGRF, the SCHA model with index $k = 7$ is considered the best SCHA model, both in resolution and accuracy. The minimum wavelength which this SCHA model can represent is approximately 1800 km. Compared with the root mean square difference (RMSD) of the IGRF model, the RMSD of the SCHA model with index $k = 7$ is lower by 27.69 nT, 8.38 nT, and 19.17 nT for X, Y, and Z components, respectively.

KEYWORDS : spherical cap harmonic analysis, regional geomagnetic field modelling, Indonesia

Sr No: 302

The predictions of a new geomagnetic jerk around 2020 come true: insights from observatory and Swarm data

CORRESPONDING & PRESENTING AUTHOR:

F. Javier Pavon Carrasco, Universidad Complutense de Madrid, Spain

Santiago Marsal, Observatori de l'Ebre (OE), Univ. Ramon Llull – CSIC, Spain

Saioa A. Campuzano, Geoscience Institute (CSIC - UCM), Spain

J. Miquel Torta, Observatori de l'Ebre (OE), Univ. Ramon Llull – CSIC, Spain

Following the pattern of a new jerk every 3-4 years, 2020-2021 should see a new event after the one observed around 2017.5. In this work, we explore this scenario by analysing the secular variation of the East geomagnetic field component in both ground and satellite geomagnetic data. At ground, we use the available data from 2015 to 2021 in 10 observatories worldwide distributed. This analysis shows the occurrence of the mentioned jerk in 2017.5 at observatories located in the Pacific region, but also reveals a new jerk between mid-2019 and early 2020 with a clear global character. Swarm satellite data also corroborate these findings by means of the secular variation estimated using virtual observatories at 440 km altitude. In addition, a general view using the most recent CHAOS geomagnetic model confirms the global character of the 2020-jerk with V-shaped secular variation changes in meridional sectors covering the Eastern Pacific, America, Asia and the Indian Ocean; and Λ-shapes in Europe, Africa and Western Pacific. The radial geomagnetic field at the core-mantle boundary is investigated as the origin of the new jerk. Results show that the global-average secular acceleration of the radial field exhibits a new pulse at the end of 2018, establishing the starting epoch of the 2020-jerk.

KEYWORDS : geomagnetic jerks, secular variation, geomagnetic data

Sr No: 303

Application of Time-series and Machine Learning Techniques for geomagnetic main field forecasting

Diana Navarrete Cruz, Universidad Complutense de Madrid, Spain

CORRESPONDING & PRESENTING AUTHOR:

F. Javier Pavon Carrasco, Universidad Complutense de Madrid, Spain

Saioa A. Campuzano, IGEO (CSIC-UCM), Spain

In this study we apply different time-series and machine learning methods to explore the secular variation forecast of the Earth's magnetic main field. In details, we use the traditional autoregressive time series techniques along with the Holt-Winters smoothing exponential method, and we compare them with models based on machine-learning algorithms such as Long Short-Term Memory (LSTM) Recurrent Neural Networks and the Prophet method by Facebook. The study is carried out using the last release of the CHAOS model (7.6) that covers the last 22 years. The different approaches are applied to the Gauss coefficients of the geomagnetic main field using 15 years for training and testing the four models that are used to predict the following 7 years. Forecasts are compared with the CHAOS model itself to investigate the robustness of the predictions.

KEYWORDS : autoregressive methods, machine learning, geomagnetism

Sr No: 304

SYMPOSIUM : **1.4 Earth's magnetic field and secular variation on all temporal and spatial scales**

Rock-magnetic and paleomagnetic investigation of the Dolni Vestonice Loess Paleosol Sequence

Yohan Guyodo, Université de Paris - Institut de Physique du Globe, Paris

CORRESPONDING & PRESENTING AUTHOR:

Robin Heraibi, Université de Paris - Institut de Physique du Globe, Paris
France Lagroix, Université de Paris - Institut de Physique du Globe, Paris

Loess-Paleosol sequences (LPS) are known to record Quaternary continental climate changes as well as reversing magnetic fields, in particular in China. In Europe, their use as archives of paleosecular variation (PSV) would improve their chronology. A high quality PSV record requires that the magnetism-based climate signal be accounted for across the length of the LPS. Here, we present a rock-magnetic and paleomagnetic study of the Dolni Vestonice (DV09) LPS located in the Czech Republic and covering the last 140 kyr. A major objective of this study is to investigate the possibility of extracting a reliable PSV record, both in direction and intensity. Magnetic properties were analysed continuously from 300 bulk samples across the 15 m long DV09 profile. A suite of 632 oriented specimens were analysed for their anisotropy of low-field magnetic susceptibility (AMS). Measurements of remanent magnetizations (natural (NRM), anhysteretic (ARM) and isothermal (IRM)), after stepwise alternating field demagnetizations, were achieved on oriented specimens from 212 sampling depths. Rock-magnetic parameters allowed identifying changes in the magnetic assemblage mineralogy, concentration and grain size. Paleomagnetic directions were isolated through principal component analysis. Relative paleointensity (RPI) proxies were established using ARM and IRM as NRM normalizers. A quantitative comparison between bulk rock-magnetic and paleomagnetic data permitted to describe stratigraphically the influence of changing environmental conditions on the paleomagnetic signal, while AMS data constrained the depositional and post-depositional history providing insight into possible particle orientation biases. The reliability of the DV09 RPI record was further tested through comparisons with other RPI records.

KEYWORDS : loess and paleosol sequences, secular variation, last interglacial and glacial periods
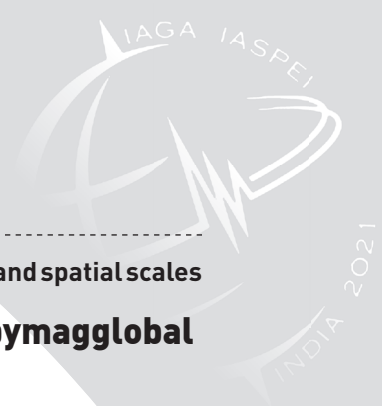
Sr No: 305

A python interface for global geomagnetic field models: pymagglobal

CORRESPONDING & PRESENTING AUTHOR:

Maximilian Arthus Schanner, GFZ German Research Centre for Geosciences, Germany

Stefan Mauerberger, University of Potsdam, Germany

Monika Korte, GFZ German Research Centre for Geosciences, Grmany

We present pymagglobal, a simple to use python interface for global geomagnetic field models. The main purpose of pymagglobal is to replace some Fortran scripts, which are used in the geomagnetism community to evaluate global field models. Out of the box, pymagglobal can read cubic-spline based geomagnetic field models stored in the same file format as gufm1 or the CALSxk model series, but with minor customization other models can be read as well. The python interface can, e.g., give model curves for any location, time series of dipole moment or spherical harmonic coefficients or grids and maps of magnetic field components.

pymagglobal can be installed by a single command and comes with a command line interface, that allows easy extraction and visualization of information from the models. Additionally, the python backend is available and can be used to access the models, for example to include them in your own plots or to generate synthetic data. The package is available at https://git.gfz-potsdam.de/sec23/korte/pymagglobal.

KEYWORDS :   software, global geomagnetic field models

Sr No: 306

A global Holocene model of the geomagnetic field based on space-time correlations

CORRESPONDING & PRESENTING AUTHOR:

Maximilian Arthus Schanner, GFZ German Research Centre for Geosciences

Monika Korte, GFZ German Research Centre for Geosciences, Germany

Matthias Holschneider, University of Potsdam, Germany

Based on thermoremanent records from the last ten thousand years, we present a preliminary global geomagnetic field model for the Holocene. The model is developed by applying recently proposed algorithms, based on space-time correlations. The geomagnetic potential is assumed to be a Gaussian process whose covariance structure is given by a pyhsically motivated space-time kernel function, including several hyperparameters. Due to the amount of data and complexity of the model, the full Bayesian posterior is numerically intractable. Therefore, we propose approximate computations via sequentialization and linearization. Instead of inverting the full covariance matrix at once, we implement a Kalman-filter with a fixed time step of ten years. Every step consists of a prediction, based on the temporal covariance, and a correction via Gaussian process regression. To apply the latter to the non-linear thermoremanent records, we implement a linearization. Dating errors are accounted for via linearization of a noisy input formulation. The hyperparameters are inferred from the data using a maximum marginal likelihood estimate. Finally, a smoothing algorithm is applied to re-introduce cross-correlations that have been lost due to the sequential approach.

Due to the specific statistical nature of the proposed algorithms, the outcoming model comes with space and time dependent uncertainty estimates. Although a preliminary model, the general evolution is similar to existing models. Less variation is present in the large scale degrees.

KEYWORDS :   global geomagnetic field model, holocene, bayesian inversion

Sr No: 307

Spatial Uncertainty in the IGRF-13 Model: Where is it Most Accurate?

CORRESPONDING & PRESENTING AUTHOR:

Ciaran Beggan, British Geological Survey, UK

The International Geomagnetic Reference Field (IGRF) is a multi-institute model of the Earth's magnetic field, compactly described by 195 spherical harmonic (Gauss) coefficients to degree and order 13, which allows the continuous evaluation of the field at any location on or above the surface. It is developed from satellite and ground-based magnetometers and describes the large-scale (> 3000 km) variation of the magnetic field in space and time. While much effort has been made on improving the forecast of the secular variation of the field over the five-year intervals between release and renewal, less emphasis has been placed on understanding the spatial errors from a user point of view. The call for the IGRF-13 candidate models requested uncertainties in spectral terms on the Gauss coefficient which a few teams provided. However, most non-scientific applications are for directional information, particularly declination and inclination which are more difficult to model as they are non-linear operations on the X, Y and Z components. In this study, we look at estimating the large-scale spatial error of the IGRF to provide indicative maps to users illustrating where the IGRF has larger uncertainties. The errors are based on the globally averaged misfit of IGRF to ground-based measurements (e.g. at repeat stations) and the morphology of the magnetic field itself.

KEYWORDS :   magnetic, uncertainty, IGRF-13

Sr No: 308

Geomagnetic Field Paleointensity Spanning the Past 11 Myr from Marine Magnetic Anomalies in the Southern Hemisphere

CORRESPONDING & PRESENTING AUTHOR:

Yuanjie Li, Southern University of Science and Technology, China
Qingsong Liu, Southern University of Science and Technology, China

Global variations in geomagnetic intensity can provide dating markers for the sedimentary record, which is particularly helpful in precisely reconstructing climate change. However, there are few continuous sedimentary records of relative intensity that span the past 11 Myr, and those that exist can have a high degree of uncertainty. The previous researches indicated that the marine magnetic anomaly profiles have the ability to record the fluctuations of geomagnetic field strength in the past, which could be more easily accessed and be able to provide additional suitable independent evidence to verify the existing paleointensity information. Here, we collected marine magnetic data across three ocean areas in the East Pacific Rise and the Southeast Indian Ridge. The selected magnetic anomaly data were recalculated using the Comprehensive Model 4 as the main field, and then projected in the spreading direction and reduced to the poles. And then, the main reversal boundaries in the profiles were identified and the distance between reversals was transformed into the time domain based on the GPTS2020. Finally, all profiles in each area were stacked. It is discovered that linear tiny wiggles were correlated over the three stacked profiles from three different areas. A comparison with a previous magnetic study on the South Atlantic Ridge and the synthetic profile from relative paleointensity records generated for the past ~8 Myr confirmed that the small wavelength anomalies result from global geomagnetic intensity fluctuations. The newly calibrated timescales from selected marine magnetic anomalies could provide a potential dating reference for sedimentary strata.

KEYWORDS :   paleointensity, marine magneitc anomaly, geomagnetic field

Sr No: 309

Hints about the occurrence of geomagnetic field excursions using Shannon Information

PRESENTING AUTHOR:

Saioa A. Campuzano, IGEO, Spain

CORRESPONDING AUTHOR:

Angelo De Santis, Istituto Nazionale di Geofisica e Vulcanologia, Spain

Martina Orlando, Istituto Nazionale di Geofisica e Vulcanologia, Spain

Francisco J. Pavon Carrasco, Universidad Complutense Madrid, Spain

Alberto Molina Cardin, Universidad Complutense Madrid, Spain

During geomagnetic field excursions, the field intensity exhibits very low values that can result in large-scale fluctuations of local field direction. These fluctuations are similar in magnitude to those observed during reversals, but without producing a persistent polarity change. Recent models of the past geomagnetic field, such as IMOLE, GGF100k and LSMOD2, include the two most recent excursions recorded, i.e. Laschamp (~41 ka) and Mono Lake (~34 ka) events. Knowing more of these events would improve our knowledge about the geomagnetic field and its future.

The Shannon Information or Information Content is a statistical measure which characterises the properties of organisation (maximum value) or disorder (minimum value) of a system. It is possible to define the Shannon Information by an expression including the Gauss coefficients that define a geomagnetic field model [De Santis et al., EPSL, 2004]. It is expected that when approaching to excursions, the Shannon Information decreases, i.e. the disorder of the system increases.

We have calculated the Shannon Information from the Gauss coefficients of the three geomagnetic field reconstructions that span the last excursions. Although the considered reconstructions are based on sedimentary data, which could present some smoothing effects related to the mechanism of the acquisition of the magnetisation, it is observed a generalised decrease of the Shannon Information that seems to anticipate the occurrence of the impending excursions some time in advance.

KEYWORDS : geomagnetic field, shannon information, geomagnetic excursions

Sr No: 310

Oligocene-Miocene relative paleointensity from the Indian Ocean, IODP Site U1443

CORRESPONDING & PRESENTING AUTHOR:

Yoichi Usui, Japan Agency for Marine-Earth Science and Technology, Japan

Sediment archives provide a continuous paleointensity record. However, records older than a few million years are limited. In this contribution, we present a preliminary record of relative paleointensity from the Oligocene to the Miocene at IODP Site U1443, where pelagic carbonates were collected from the Ninety East Ridge in the North Indian Ocean. The sediments were continuously cored to about 200 m using the APC or half-length APC system. Samples from the Late Oligocene to Middle Miocene (~9-23 Ma) were

examined. Sedimentation rates were generally low (~4 mm/kyr), except for ~15 mm/kyr at ~13.5-14 Ma. The paleointensity estimates were consistent with previous records from the eastern equatorial Pacific, where sedimentation rates were ~10 mm/kyr. However, the resolution of the U1443 record appears to be lower by a factor of 5 (13.5-14 Ma) to 15 (elsewhere). Nevertheless, the present results support the idea that these records represent global variations in the geomagnetic field.

KEYWORDS : carbonate, sedimentation rate

Sr No: 311

SYMPOSIUM :   1.4 Earth's magnetic field and secular variation on all temporal and spatial scales

A record of the lower Mammoth geomagnetic reversal from a marine succession in the Boso Peninsula, central Japan (by invitation)

CORRESPONDING & PRESENTING AUTHOR:

Yuki Haneda, Geological Survey of Japan, Japan

Makoto Okada, Ibaraki University, Japan

Palaeomagnetic records from geological archives provide significant information about the nature of geomagnetic reversals; however, there are few detailed palaeomagnetic records of pre-Pleistocene reversals. The lower boundary of the Mammoth Subchron (late Pliocene) is recorded in an expanded 10-m interval of a marine succession deposited at high accumulation rates (9–66 cm/kyr) in the Boso Peninsula, central Japan. Here, we report a continuous palaeomagnetic record of the lower boundary interval of the Mammoth Subchron, including the direction and palaeointensity of the geomagnetic field. A hybrid method of thermal demagnetization at 200°C and progressive alternating field demagnetization were used to effectively extract the primary palaeomagnetic component, which is thought to be carried by magnetite. The transitional zone of the lower Mammoth reversal, which is characterized by instability of the palaeomagnetic direction and depletion of the relative palaeointensity, occurred from late Marine Isotope Stage MG3 to MG2, spanning 13 kyr. The virtual geomagnetic pole (VGP), calculated from the direction of the primary palaeomagnetic component, rapidly rebounded twice from a southern high latitude to the North Atlantic within the transitional zone. In contrast to the complex behavior of the lower Mammoth reversal recorded in the Boso Peninsula succession, records from a lava sequence in O'ahu show a rebound following a 180° directional change, and those from a marl succession in Sicily show a single rapid directional change. Highly diverse geomagnetic field evolution among these three on-land sections indicates that a strong influence of a non-axial dipole field during the reversal.

KEYWORDS :   paleomagnetic reversal, pliocene, chiba

Sr No: 312

SYMPOSIUM :   1.4 Earth's magnetic field and secular variation on all temporal and spatial scales

Isolating core field signals in Geomagnetic Virtual Observatory time series using Principle Component Analysis

CORRESPONDING & PRESENTING AUTHOR:

William Brown, British Geological Survey

Ciaran Beggan, British Geological Survey, UK

Magnus Hammer, Technical University of Denmark

Chris Finlay, Technical University of Denmark

Geomagnetic Virtual Observatories (GVOs) are a method for processing magnetic satellite data in order to simulate the observed behaviour of the geomagnetic field at a fixed location. Signals at a given GVO location will be strongly correlated with its neighbours due to the influence of large-scale external field sources and the biased sampling effect caused by local time precession of the satellite orbit. Using Principal Component Analysis we identify and remove signals related to these noise sources in secular variation residuals, to better resolve core field variations on sub-annual timescales.

We apply our methodology to monthly GVOs for the Ørsted, CHAMP, CryoSat-2 and Swarm missions. We identify common principle components representing local time sampling biases and external field sources across all missions. Our analysis is enhanced by focussing on regions of geomagnetic latitude where different external field sources dominate, identifying distinct polar, auroral and low-to-mid latitude regions. Annual differences are often used to calculate SV so as to remove annual and semi-annual external field signals, but these signals can be re-introduced if our corrected SV is integrated back to main field. We find representing secular variation with monthly first differences allows us to identify and remove annual and semi-annual external field variations from the SV, which leads to improved main field series. We are able to produce global grids of GVO time series which better represent core field secular variation at monthly time resolution.

KEYWORDS : geomagnetism, secular variation, observations

Sr No: 313

SYMPOSIUM : **1.4 Earth's magnetic field and secular variation on all temporal and spatial scales**

A record of the lower Mammoth geomagnetic reversal from a marine succession in the Boso Peninsula, central Japan

CORRESPONDING & PRESENTING AUTHOR:

Dr. Yuki Haneda, IAGA, Geological Survey of Japan, Tsukuba, Japan

Palaeomagnetic records from geological archives provide significant information about the nature of geomagnetic reversals; however, there are few detailed palaeomagnetic records of pre-Pleistocene reversals. The lower boundary of the Mammoth Subchron (late Pliocene) is recorded in an expanded 10-m interval of a marine succession deposited at high accumulation rates (9–66 cm/kyr) in the Boso Peninsula, central Japan. Here, we report a continuous palaeomagnetic record of the lower boundary interval of the Mammoth Subchron, including the direction and palaeointensity of the geomagnetic field. A hybrid method of thermal demagnetization at 200°C and progressive alternating field demagnetization were used to effectively extract the primary palaeomagnetic component, which is thought to be carried by magnetite. The transitional zone of the lower Mammoth reversal, which is characterized by instability of the palaeomagnetic direction and depletion of the relative palaeointensity, occurred from late Marine Isotope Stage MG3 to MG2, spanning 13 kyr. The virtual geomagnetic pole (VGP), calculated from the direction of the primary palaeomagnetic component, rapidly rebounded twice from a southern high latitude to the North Atlantic within the transitional zone. In contrast to the complex behavior of the lower Mammoth reversal recorded in the Boso Peninsula succession, records from a lava sequence in O'ahu show a rebound following a 180° directional change, and those from a marl succession in Sicily show a single rapid directional change. Highly diverse geomagnetic field evolution among these three on-land sections indicates that a strong influence of a non-axial dipole field during the reversal.

KEYWORDS :

I.5 The theory and applications of rock and environmental magnetism

CONVENERS: Liao Chang

Joshua M. Feinberg

Fundamental rock magnetic properties and magnetic recording processes underpin our understanding of magnetic signals encoded in terrestrial and extraterrestrial materials. Advances in rock magnetic theories and analytical methods expand our ability to obtain important information in Earth, environmental and planetary research, including reconstructing past geomagnetic field variations and environmental parameters, and understanding a wide range of geological and geophysical processes. This session focuses on recent advances in fundamental rock magnetism and environmental magnetism across all scales, from theories to experiments. We welcome a range of contributions, including new rock magnetic theories, analytical methods, anisotropy, fundamental investigations of magnetic minerals and their grain size/domain state dependent properties, magnetic mineral unmixing, and magnetic modelling. We also welcome studies establishing links between rock and mineral magnetic properties and environmental variables, and those that apply magnetic proxies to environmental issues related to climatic, geochemical and biological processes on Earth.
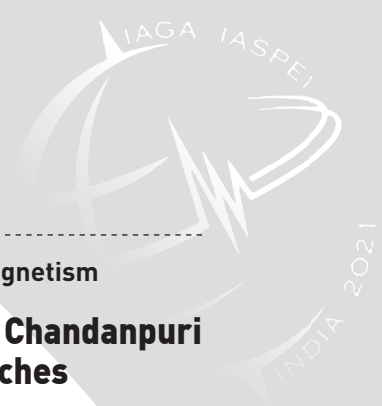
Sr No: 314

Reconstruction of paleoenvironmental changes from Chandanpuri Formation, Deccan Traps: Magnetic and Geochemical approaches

CORRESPONDING & PRESENTING AUTHOR:

B.V Lakshmi, Indian Institute of Geomagnetism, India

K. Deenadayalan, Indian Institute of Geomagnetism, India

Pravin B. Gawali, Indian Institute of Geomagnetism, India

The Quaternary deposit of the Deccan Trap (DT) region is although important to evaluate the climatic history in DT, little information on this sequence is available till date. In this presentation, we focus on the 9 m thick sediment sequence of Chandanpuri Formation (CHF), Western Maharashtra, DVP to reconstruct the paleoenvironmental changes of sediments from variations in the magnetic susceptibility and geochemical data. Sediment magnetic records have become a useful proxy for reconstructing the paleoclimatic history of a given area and can provide an alternate method of reconstruction that may capture environmental change from a different perspective. Magnetic susceptibility (MS), which is a measure of concentration of total magnetic minerals in the sample, is used as proxy for palaeoclimate/palaeo-monsoon estimations. Magnetic study shows that the MS signal of Chandanpuri (CHF) sediments is derived from the catchment and ruled out biogenic and anthropogenic magnetite contributing to the MS signal or its obliteration due to magnetite dissolution. The geochemical assemblage often provides vital clues in terms of the provenance, transport processes and weathering in the catchment area. All chemical weathering intensity (CWI) indices and magnetic properties register an increasing trend in top of the section suggesting that chemical weathering was more intense whereas slackened monsoon decreased the CWI indices and MS at the bottom. However the highlight of this study turns out to be the efficacy of combined magnetic and geochemical study in elaborating the depositional processes influenced by climatic and geotectonic vicissitudes.

KEYWORDS : Deccan Trap, magnetic susceptibility, chemical weathering

Sr No: 315

Magnetic properties of cave sediments at Gran Dolina site in Sierra de Atapuerca (Burgos, Spain)

CORRESPONDING & PRESENTING AUTHOR:

Serena Darcangelo, Universidad Complutense de Madrid, Spain

Fatima Martin Hernandez, Universidad Complutense de Madrid, Spain

Josep Maria Pares, CENIEH, Spain

We report new rock magnetic results from a cave in the "Sierra de Atapuerca" (Burgos, North of Spain), that is one of the most important archaeological and palaeontological sites of Lower to Middle Pleistocene in Europe. We consider the principles of environmental magnetism to furnish a new proxy for understanding the climatic – paleoenvironmental conditions at the time the earliest hominins began to migrate into Europe, its remains were found in the Atapuerca site. Our samples are taken in cave sediments of Gran Dolina Cave.

Rock magnetic analyses allowed us to determine changes in grain size, composition, and concentration in both cave-entrance and cave-interior sediments. Generally, the cave-entrance sediments are characterized by a high concentration of magnetic minerals while the cave-interior presents a more variable concentration. We compare our results to the others proxies applied in this archaeological site and expose a correlation between them.

KEYWORDS : environmental magnetism, Sierra de atapuerca, rock magnetism

Sr No: 316

- -

SYMPOSIUM :   **1.5 The theory and applications of rock and environmental magnetism**

Mineral magnetic record of orbital-scale redox changes in the Cretaceous eastern Tethys Ocean

CORRESPONDING & PRESENTING AUTHOR:

Yongxiang Li, Nanjing University, China
Benjamin Gill, Virginia Tech, USA
Isabel Montanez, UC Davis, USA
Lifeng Ma, Nanjing University, China
Matthew Leroy, Virginia Tech, USA
Kenneth Kodama, Lehigh Univ, USA

Iron species analysis is a commonly used geochemical approach to reconstruct paleo-redox conditions. Ratios of fractions of different reactive iron species in sedimentary rocks are used to infer paleo-redox state of bottom water in oceans. Analysis of the magnetic properties of minerals corresponding to different iron species allows to tentatively establish an analogous magnetic proxy, that is the ratio of hard isothermal remanent magnetization to magnetic susceptibility, HIRM/χ, for bottom water redox conditions. This magnetic proxy was employed to investigate the redox conditions during the Cenomanian-Turonian Oceanic Anoxic Event 2 (OAE2) (~94 Ma) in the eastern Tethys Ocean by carrying out a high-resolution rock magnetic study of the OAE2 interval in southern Tibet. The mineral magnetic data of the Tibetan section show repeated fluctuations between relatively oxic and dysoxic/anoxic conditions in the eastern Tethys of the Southern Hemisphere during OAE2. Spectral analysis of a log (HIRM/χ) time series reveals cyclical variations at orbital frequencies and the subtle cyclic redox changes are found to occur within the obliquity frequency band. Moreover, variability in redox conditions at the onset of OAE2 correlates well with that recently documented for the OAE2 interval at Tarfaya, Morocco using the iron speciation approach, implying that the cyclic redox variations spanned both hemispheres. Therefore, the magnetic proxy, HIRM/χ, shows high potential for reconstructing high-resolution redox variability during past OAEs and hyperthermals as it is non-destructive, relatively rapid, and more economical than typically applied geochemical approaches.

KEYWORDS : redox state, OAE2, southern Tibet

Sr No: 317

How far could the environmental magnetism be a useful tool for evaluating urban PM removal capacities by plants?

CORRESPONDING & PRESENTING AUTHOR:

Sarah Letaief, CNRS, Université de Montpellier, France
Pierre Camps, CNRS, Université de Montpellier, France
Thierry Poidras, CNRS, Université de Montpellier, France
Patrick Nicol, CNRS, Université de Montpellier, France

Do urban hedges act as a sink for particles matter (PM) which could improve urban air quality? Regarding the numerous studies mainly based on CFD modelling, no consensus was already made in the efficiency of plants to trap PM. Some of them show an effectiveness extraction by the foliage with dry deposition processes, whereas other emphasize the negative role of hedges in the obstruction of atmospheric dispersion of pollutants and therefore increase pollution. For possible answer to the issues raised, it is essential to precisely determine the deposition velocity (Vd) parameter, which is specific to each plant species, and environmental conditions. Most of the time, it is underestimated in modeling-based studies by taking standard values.

From this standpoint, a wind tunnel (6 m x 86 cm x 86 cm) was designed to perform analogical experiments on different endemic species. It allows us to control parameters such as wind speed, the nature and the injection time of pollutants. Beforehand, physical hedge characterization as resistance (%) and the leaf area index (LAI) have been estimated for each specie and allow comparison between plants removal potential. PM concentrations upwind and downwind of natural reconstituted hedges are provided by 6 optical particles counter (OPC). The aim would correlate PM concentration measured by size bins from the OPC with remanence measurements (ARM80, 100mT, IRM100mT, IRM300mT and SIRM) of PM deposition on plant leaves by using transfer function. Finally, rock magnetism measurements (IRM cumulative acquisition curves and hysteresis parameter) would allow the understanding of these transfer functions.

KEYWORDS : environmental magnetism; wind tunnel; urban PM; deposition velocity.

Sr No: 318

First-order reversal curve characteristics of pigmentary and specular hematite (by invitation)

CORRESPONDING & PRESENTING AUTHOR:

Andrew Roberts, Australian National University, Australia
Xiang Zhao, Australian National University, Australia
David Heslop, Australian National University, Australia

Hematite carries magnetic signals of interest in tectonic, paleoclimatic, and planetary studies. First-order reversal curve (FORC) diagrams have become an important tool for assessing the domain state of, and magnetostatic interactions among, magnetic particles in such studies. We present here FORC diagrams for diverse pigmentary and specular hematite samples, which provides a catalog of results for comparison

with other studies and explains key FORC features observed for hematite. Central ridge-type signatures typical of non-interacting single domain particle assemblages and "kidney-shaped" FORC signatures, and combinations of these FORC distribution types, occur commonly in natural and synthetic hematite. Central ridge-type distributions are even obtained when synthetic hematite particles are packed in contact with each other. Lack of vertical spreading in these FORC distributions indicates that magnetostatic interactions are not an important determinant of the magnetic properties of hematite, in contrast to magnetite. This also indicates that vertical spreading in "kidney-shaped" distributions is not due to interactions. Rather, it is due to the particle size spectrum of assemblages with more complex asymmetric FORC distributions that arise from the hexagonal anisotropy of hematite, which provides multiple easy axes for magnetization switching within the basal plane. The dominant FORC distribution type in a sample (central ridge, kidney-shaped, or mixture) depends on the balance between out-of-plane/in-plane anisotropy due to uniaxial or hexagonal magnetization switching. These results help to identify and explain magnetization switching and anisotropy features that are intrinsic to the magnetic properties of hematite.

KEYWORDS : rock magnetism, hematite, FORC

Sr No: 319

A Preisach-based Model of Chemical Remanent Magnetisation Acquisition, Comparisons to Thermoremanent Magnetisations and Behaviour During Thellier-type Palaeointensity Determination

CORRESPONDING & PRESENTING AUTHOR:

Evelyn Baker, Imperial College London, UK

Adrian Muxworthy, Imperial College London, UK

David Heslop, Australian National University,Australia

Chemical remanent magnetisations (CRM) are ubiquitous in nature, but are usually 'unwanted' and their magnetic remanence signals are often discarded. There is a need for a better understanding of CRM growth and how it contributes to palaeointensity determination. Thermoremanence (TRM) acquisition has previously been successfully modelled using a thermally activated Preisach model and used to determine TRM palaeointensity estimates, without the need to heat samples. Here we use a similar approach to model grain-growth CRM. It is based on interacting single-domain grains, including a solution to the relaxation time equation accounting for the effect of growth rate on blocking volume. We use this model to explore how CRM intensity varies as a function of growth rate and when varying the input Preisach distribution. We also make comparisons to TRMs and model Thellier-type palaeointensity determination and produce Arai plots for CRMs.

KEYWORDS : chemical remanent magnetisation, palaeointensity, preisach model

Sr No: 320

New progresses of paleo- and environmental magnetic studies from the North Pacific Ocean (by invitation)

CORRESPONDING & PRESENTING AUTHOR:

Qingsong Liu, Southern University of Science and Technology, China

Yi Zhong, Southern University of Science and Technology, China

Xiaodong Jiang, Southern University of Science and Technology, China

Congcong Gai, Southern University of Science and Technology, China

Ting Chen, Chongqing Normal University, China

The North Pacific Ocean (NPO) plays an important role in modulating the climatic system. However, it is difficult to construct reliable d18O curves for both chronological and paleoclimatic studies due to the shallower Carbonate Compensation Depth (CCD). In contrast, paleomagnetism provides an independent master curve for dating, and environmental magnetism bears invaluable information for paleocimatic constructions. During the past 5 years, the CM2 group at SUStech systematically investigated sediments, manganese nodules and crusts from the NPO, and revealed a sophisticated coupling systems including the Asian dust, westerly transportation, provenance chemical weathering, sub-circulation systems, and the Kuroshio current, etc. In this review, we summarize major progresses of these relevant studies and show the importance of paleo- and environmental magnetism methods in handling the complicated NPO system.

Sr No: 321

Early low-temperature and later high-temperature diagenetic processes and their influence on magnetic mineral assemblages in marine sediments from IODP Site C0023, Nankai Trough, Northwestern Pacific Ocean (by invitation)

CORRESPONDING & PRESENTING AUTHOR:

Myriam Kars, Kochi University

Male Koester, Alfred Wegener Institute Helmholtz Centre for Polar and Marine Research, Germany

Susann Henkel, Alfred Wegener Institute Helmholtz Centre for Polar and Marine Research, Germany

Stephen Bowden, University of Aberdeen, UK

Xiang Zhao, Australian National University, Australia

Andrew Roberts, Australian National University, Australia

Diagenesis, including geochemical and microbial processes, can have a major impact on sediment mineralogy during burial. Primary magnetic mineral assemblages can be modified significantly by dissolution or formation of new magnetic minerals as a result of early or late post-depositional processes. At International Ocean Discovery Program Site C0023, which was drilled in the protothrust zone of Nankai Trough during Expedition 370, offshore Japan, non-steady state diagenesis has led to mineral alteration that is largely decoupled from current redox conditions. We use different and complementary rock magnetic and geochemical analyses (I) to characterize magnetic mineral assemblages in terms of abundance, grain size,

and composition to assess the magnetic mineralogy alteration and the diagenetic overprint, and (2) to reconstruct the evolution of (bio-)geochemical processes, especially of sedimentary iron. Four magnetic zones are identified downcore and explained by specific (bio)-geochemical processes. Zone 1 contains ferrimagnetic greigite, which forms at a shallow sulfate-methane transition (SMT) and is preserved because of rapid sedimentation. Zones 2 and 4 have fewer magnetic minerals, mainly iron oxides, and result from diagenetic alteration associated with a reverse SMT, several millions of years after sediment deposition. Zone 3, between Zones 2 and 4, contains authigenic single-domain magnetic particles that likely formed as a result of fluid circulation through faults above and below the décollement. Varying sediment supply and organic matter input through time, burial temperature, and tectonic fluids circulation seem to primarily be responsible for the current diagenetic magnetic mineral assemblages and geochemical patterns.

KEYWORDS : nankai trough, magnetic mineral diagenesis, iron cycle

Sr No: 322

SYMPOSIUM : **1.5 The theory and applications of rock and environmental magnetism**

Grain size analyses for paleo-environmental proxies using Time-Asymmetric FORCs

CORRESPONDING & PRESENTING AUTHOR:

Thomas Berndt, Peking University, China

Liao Chang, Peking University, China

Huapei Wang, China University of Geosciences, China

Junxiang Miao, China University of Geosciences, China

Zhaowen Pei, Peking University, China

Pengfei Xue, Peking University, China

Shishun Wang, Peking University, China

Jos Augusto Proena Maia Devienne, Peking University, China

Magnetic minerals, such as precisely size- and shape-controlled biogenic magnetic particles, may be highly sensitive indicators of past environments. Such minerals give rise to very characteristic magnetic properties that are easy and fast to measure using FORC diagrams. Quantitatively reconstructing magnetic grain sizes, shapes and arrangements from FORC diagrams, remains, however, a challenge, since the inversion is generally non-unique. Key to using magnetic particles as palaeoenvironmental proxies is the correct and complete characterization purely from magnetic measurements. In this talk we explore how this can be achieved with the novel experimental technique of time-asymmetric First-Order Reversal-Curves (FORC): a simple adjustment to FORC diagrams that allow to quantify thermal relaxation in addition to coercivity. It is possible to mathematically invert these diagrams to obtain a complete description of magnetic grain geometry. We show experimental and theoretical insights on how this technique can be used to quickly measure and characterize samples for use as paleoenvironmental tracer.

KEYWORDS : rock magnetism, grain size, FORC

Sr No: 323

Magnetic properties and paleomagnetic stability of bent and collapsed magnetosome chains: a finite-element micromagnetic approach

PRESENTING AUTHOR:

Zhaowen Pei, Peking University, China

Thomas Berndt, Peking University, China

CORRESPONDING AUTHOR:

Liao Chang, Peking University, China

Fan Bai, Peking University, China

Biogenic magnetite chains (magnetosomes) produced by magnetotactic bacteria (MTB) are important paleoenvironmental and paleomagnetic recorders. It has been shown that magnetic properties of intact magnetosome chains are closely related to their morphology and chain structures. Magnetosomes in sediments are subject to compression and are therefore unlikely to be in their intact shape. In this study, we use the finite element micromagnetic simulation tool MERRILL to study quantitatively changes in magnetic properties and paleomagnetic recording stability of magnetosome chains in response to chain alteration, in particular, as a function of variable degrees of bending and collapse. Hysteresis loops, isothermal remanent magnetism (IRM) curves, and ?rst-order reversal curves (FORC) for more than 200 modeled magnetosome microstructures were calculated. Our results indicate that bending or collapse leads to a significant coercivity reduction and domain states transition. Therefore, we suggest that hysteresis parameters and FORC diagrams can be used to assess bending or collapse degree of magnetosome chains in sediments. The natural remanent magnetization (NRM) and thermal stability of magnetosome chains were simulated to model processes associated with potential chain alteration after sediment deposition. We show that NRM records remain both faithful to a pre-collapse/bending NRM, and thermally stable over geological timescales, indicating that even strongly bent or collapsed magnetosome chains are still excellent paleomagnetic recorders.

KEYWORDS :   magnetosomes, micromagnetic simulations, magnetic properties

Sr No: 324

Micromagnetic calculations of the effect of magnetostatic interactions on isothermal remanent magnetization curves: implications for magnetic mineral identification

PRESENTING AUTHOR:

Fan Bai, Peking University, China

CORRESPONDING AUTHOR:

Liao Chang, Peking University, China

Thomas A. Berndt, Peking University, China

Isothermal remanent magnetization (IRM) curves are used widely in rock magnetic and environmental magnetic studies to characterize magnetic properties of natural samples. Previous theoretical and experimental investigations indicate that magnetostatic interactions can have a strong effect on the IRM

behavior. In order to investigate this effect of magnetic interactions, we modelled IRM curves and hysteresis properties for magnetite assemblages with variable morphologies (grain size, elongation, and shape) using the finite-element micromagnetic modeling code MERRILL. We also conducted an analytical study of IRM behavior for non-interacting single domain grains utilizing the Stoner–Wohlfarth model. It is found that multiple Gaussian components do not necessarily reflect multiple magnetic mineral populations. For example, interactions can produce coercivity distributions that resemble results of some samples containing a detrital and extracellular (D+EX) and a biogenic soft or hard (BS/BH) coercivity components. Simulated IRM curves for different morphologies of interacting flattened grains are similar, which indicates that the effect of interactions can overshadow the effect of grain morphologies. Our micromagnetic and analytical calculations also consistently indicate that the IRM curves for noninteracting fine-grained assemblages is mostly determined by grain shape and elongation distributions of the magnetic mineral assemblages. Our numerical and analytical calculations provide important constrains on the behavior of IRM curves and hysteresis for characterizing complex magnetic mineral components in natural samples.

KEYWORDS : IRM curves, micromagnetic simulation, magnetostatic interactions

Sr No: 325

Application of rock magnetic techniques in a floodplain sediment environment: A study from the Lower Morava River Basin (Czech Republic)

CORRESPONDING & PRESENTING AUTHOR:
Eduard Petrovsky, Institute of Geophysics CAS, Czech Republic
Jaroslav Kadlec, Institute of Geophysics CAS China, Czech Republic
Hana Grison, Institute of Geophysics CAS, Czech Republic

Mineral magnetic studies are widely used as a tool for understanding the past environmental processes. They also help in interpreting the results of archeological research and/or anthopogenically-induced pollution assessment. The floodplain sedimentary archives can reflect various natural and human induced processes influencing the river catchment. These may play significant role in magnetic record stored in in floodplain sequences. The Morava River (Czech Republic) floodplain archive should also record a significant period related to the first large settlement centres built in the river floodplain during the 9th century. These contemporary inhabitants possibly affected the natural floodplain environmental balance causing a large forest clearance around the settlements. These activities could change natural groundwater oscillation regime leading to flood frequencies. Our study uses magnetic properties for reconstructing the floodplain processes controlled by both natural and anthropogenic events. Magnetic susceptibility, natural and anhysteretic remanent magnetization, and hysteresis loops were measured on samples from vertical profiles of flodplain sediments. Our results reveal continuous increase of ferrimagnetic mineral (magnetite) input to the floodplain related to the field soil erosion increase in the catchment. The erosion accelerated since the 1950s due to incorrect land use methods and introduction of modern agriculture techniques. Finally, the industrial pollution significantly contributes to the magnetic enhancement of the topmost 50 cm of the floodplain sequences.

KEYWORDS : magnetite, river sediments, catchment

Anisotropy of Magnetic Susceptibility (AMS) as sediment fabrics in a variety of depositional environments from the Indian Subcontinent

CORRESPONDING & PRESENTING AUTHOR:

Satish Sangode, Savitribai Phule Pune University, India

Rohtash Kumar, Wadia Institute of Himalayan Geology, India

Sumit Ghosh, Wadia Institute of Himalayan Geology, India

J Malsoma, Mizoram University, India

Raghvendra Tiwari, Mizoram University, India

N Suresh, Wadia Institute of Himalayan Geology, India

Dhananjay Meshram, Savitribai Phule Pune University, India

Nitin Kadam, Savitribai Phule Pune University, India

A large variety of depositional environments extensively sampled from the Himalaya, Indo-Bermese ranges, coastal dunes, soil-paleosols and laterites representing fluvial, marine, estuarine, lacustrine, pedogenic and aeolian facies are examined for AMS using standard methods. We discuss various controls over the AMS fabrics including mineralogy, grain size and shapes, and the energy conditions as chief factors responsible to fabric characteristics associated with the given depositional environment. The advanced tensorial solutions represented by AMS are often biased to sampling points, whereas their inferences are routinely restricted to flow regimes. AMS integration with the knowledge of facies opens new arena for several qualitative and quantitative estimates on depositional environments including their correlation and interrelation. Whereas, the variable rates of sedimentation and the variability within facies architecture demands a rational approach of sampling to correctly represent the depositional environment of the sediment unit in question. Further we suggest methods of fabric enhancement using heat treatment, demagnetization and high field inductions. Changes due to the effect of burial, lithification and early cementation is considered. The fabrics amongst laterites and paleosols on the other hand are typically non-oblate and are governed by the solution-precipitation activities. Finally the comparison of fabrics amongst different depositional environments is made to explore the applicability of AMS in sedimentologic studies. We demonstrate that the AMS in sedimentary environments is the collective representation of depositional milieus rather than the flow regime alone.

KEYWORDS :   anistorpy of magnetic susceptibility, sediment, depositional environment

Sr No: 327

A case study of magnetic biomonitoring applied to cultural heritage: Villa Farnesina, Rome, Italy

CORRESPONDING & PRESENTING AUTHOR:

Aldo Winkler, Istituto Nazionale di Geofisica & Vulcanologia, Italy

Tania Contardo, University of Siena, Italy

Stefano Loppi, University of Siena, Italy

Antonio Sgamellotti, Accademia Nazionale dei Lincei, Italy

Virginia Lapenta, Accademia Nazionale dei Lincei, Italy

Villa Farnesina (Rome, Italy) is considered one of the finest historical buildings of the Italian Renaissance, with its interiors frescoed by, among others, Raphael Sanzio, Sebastiano del Piombo, Giovanni Bazzi known as il Sodoma and Giulio Romano.

The magnificent gardens of the Villa - which include pine and cypress trees, together with ornamental and shrub species - extend along the right bank of the Tiber river, and separate the busy Lungotevere road from the main building.

The aim of this study was to assess the sources and the spatial distribution of the airborne particles emitted by vehicles, as inferred from the magnetic properties of the leaves collected from the trees located along the roadway and inside the gardens of the Villa, integrated with the magnetic and chemical characterization of the lichen samples (Evernia prunastri), transplanted on the same sites and inside the frescoed halls.

The compositional and magnetic properties of the samples suggested that brake abrasion from vehicles is the main source of the bioaccumulated particles, being their concentration crucially influenced by the distance from the road.

This multidisciplinary approach demonstrated that the combined protective role offered by the distance from the roadside and the urban gardens can successfully mitigate the inauspicious effects of pollution on fine arts.

KEYWORDS :   magnetic biomonitoring, airborne particulate matter, cultural heritage

I.6 Paleo- and rock-magnetic data: archiving, mining, (re)use

CONVENERS: Lisa Tauxe

Sergei Pisarevsky

Patrick Arneitz

Paleo- and rock-magnetic data have been generated since the early 1900s and many data sets remain beyond the reach of modern paleomagnetists. Discovering and preserving legacy data is urgently needed, particularly for materials that can no longer be sampled (e.g., archaeological sites or outcrops that have been destroyed or are no longer accessible). The data may be in paper or outmoded digital format (floppy disks) and their retrieval requires considerable effort. This session will be devoted to the general topic of identifying, digitizing and archiving of legacy data. Topics will include populating databases with rescued legacy data, examples of how to amalgamate large data sets of geomagnetism and paleomagnetism data and/or re-interpreting archived data with new methods/ideas.

Sr No: 328

A magnetostratigraphy database from Siwalik sequence in the Himalayan foreland basin

CORRESPONDING & PRESENTING AUTHOR:

Satish Sangode, Savitribai Phule Pune University, India

Pushkar Nalawade, Savitribai Phule Pune University, India

We present a compilation of published magnetostratigraphic data for Neogene Siwalik sequence from the Himalaya developing a database for site mean, formation mean and sub-basins means using a common palaeomagnetic software platform. We discuss the disparity in the data due to variety of demagnetization protocols apart from the uncertainties over identification of ChRM, unknown tectonic deformations, manual errors, laboratory practices and the instrumental standards. After filtering the data with large statistical scatter, the formation-wise data plotted on GIS platform indicate a large diversity amongst D/I values depicting internal deformation, the intensity of which is increased after ~5 Ma. Prior to 5 Ma, there is coherency at the order of sub-basins and their means indicate a pattern of deformation along the axis of Himalaya. The Sediment accumulation rates show three orders of variation in magnitudes depicting regional tectonic pulses, basin partitioning due to intra-foreland thrusts and the basin fill conditions vis-a-vis depocenter migration. Nevertheless, we demonstrate that the magnetostratigraphic data from Siwalik sequence have preserved significant information on the style of syn-tectonic and internal deformation apart from the magnetic reversal pattern. Further the closer look at the palaeomagnetic directions from Upper Siwalik leads to understand the distributed deformation providing a genetic linkage to Neotectonics in the Himalayan foreland basin.

KEYWORDS :   Himalaya, Siwalik

Sr No: 329

Simple Uncertainty Propagation For New And Legacy Paleomagnetic Data (by invitation)

CORRESPONDING & PRESENTING AUTHOR:

David Heslop, Australian National University, Australia

Andrew P. Roberts, Australian National University, Australia

Estimation of paleomagnetic directions plays a crucial role in archeomagnetism, magnetostratigaphy, paleogeographic reconstruction, and constraining past geomagnetic field behavior. While analysis and aggregation of paleomagnetic directional data is performed in a hierarchical fashion, the standard statistical framework employed by paleomagnetists does not consider uncertainty propagation through each level of the hierarchy (i.e., uncertainty of specimen-level principal component analysis, site mean, pole, etc.). With this limitation, inferences drawn from paleomagnetic data will be affected by underestimated uncertainties. We present an approximate directional uncertainty propagation scheme that applies to Fisher distributions and, thus, to a number of paleomagnetic data processing tasks. Our uncertainty propagation scheme is a straightforward addition to the existing statistical framework used to aggregate paleomagnetic directions.

Importantly, this scheme can be applied readily to legacy data, even when sample-level demagnetization records are not available. Using illustrative case studies, we show how uncertainties can be propagated through different stages of the paleomagnetic data processing chain.

KEYWORDS :   paleomagnetism, fisher statistics, uncertainty propagation

Sr No: 330

- -

SYMPOSIUM :   **1.6 Paleo- and rock-magnetic data: archiving, mining, (re)use**

MagIC as a FAIR repository for America's archaeomagnetic legacy data

CORRESPONDING & PRESENTING AUTHOR:

Shelby Jones, New Mexico Office of Archaeological Studies, USA

Eric Blinman, New Mexico Office of Archaeological Studies, USA

Lisa Tauxe, University of California, San Diego, USA

Jeffrey Royce Cox, New Mexico Office of Archaeological Studies, USA

Stacey Lengyel, East Tennessee State University, USA

Robert Sternberg, Franklin and Marshal College, USA

Jeffrey Eighmy, Colorado State University, USA

Beginning in 1964, an academic lineage of Robert DuBois and his students, Daniel Wolfman and Jeffrey Eighmy, developed dedicated United States-based archaeomagnetic research programs. Collectively, they analyzed over 5377 archaeomagnetic sites, primarily from North America, dated to less than 2000 years old. Yet despite their decades of effort, few journal publications resulted. Instead, most of their published results are in archaeological reports, often without technical data, which limits the data's accessibility. Furthermore, when published, the results are generally averaged at the site-level using statistical conventions different from today's standards, limiting the data's comparability and (re)usability.

In 2015, we undertook a salvage archival study to digitize the surviving data and metadata from the scientists' individual estates and emeritus collections. We digitized measurement data from more than 51, 000 specimens, reinterpreted them using modern conventions, and uploaded them to the FAIR-adhering magnetic data repository – MagIC. The reinterpreted site-level results from the three laboratories are mutually consistent, permitting the individual datasets to be combined and analyzed as single regional entities.

Through incorporation into the MagIC repository, these legacy data are now accessible for incorporation into archaeomagnetic and global magnetic field modeling efforts, critical to understanding Earth's magnetic field variation through time. In the Four Corners region of the United States Southwest, this digitized archive advances the development of a new regional paleosecular variation curve used in archaeomagnetic dating. This project highlights the both value and complexities of managing legacy data; the many lessons learned set a precedent for future paleomagnetic data recovery efforts.

KEYWORDS :   archaeomagnetism, FAIR compliant, magic database

Sr No: 331

Robust determination of palaeosecular variation (PSV) reference curves for archaeomagnetic dating

CORRESPONDING & PRESENTING AUTHOR:

Simo Spassov, Royal Meteorological Institute of Belgium, Belgium

Elina Aidona, Aristotle University of Thessaloniki, Greece

The difficulty in establishing PSV reference curves draws back to rather large uncertainties of individual database points, their uneven distribution over time / geographic space and unknown or often not verified distributions of experimental errors. The majority of PSV calculation methods assume or simulate particular marginal probability density functions for age and direction and thus incorporate informative priors that are difficult to estimate correctly. The methodology here proposed follows therefore an inverse logic, i.e. neglecting inconsistent knowledge of informative priors in archaeomagnetic databases and using uninformative priors instead.

A stochastic approach is being proposed, based on a bundle of weighted non-uniform rational B-spline curves that are determined through sets of spline control point sequences. The three dimensional (3D) control points (age, declination, inclination) are drawn for each spline by simple random sampling with replacement from the 3D uncertainty region (UR) of each datum. The URs are taken as uniform (uninformative prior). Weighting accounts for the extent of the 3D uncertainty region, Euclidean distances between uncertainty regions and between control points and eventually geographical distances with respect to the relocation centre. The PSV uncertainty envelope is determined from the convex hull of the bundle and integrated into an archaeomagnetic dating routine based on computational geometry. Dating examples from Bulgaria and France reveal a precision common to that of usual PSV dating methods. The asset of the present method is that it relies exclusively on uncertainty ranges without making assumptions about the marginal probability distributions (cf. principle of insufficient reason).

KEYWORDS :   archaeomagnetism, palaeosecular variation, dating

Sr No: 332

Precambrian Paleomagnetic Data Archiving: The Need for Accurate Reporting and Quality Evaluation

CORRESPONDING & PRESENTING AUTHOR:

Joseph Meert, University of Florida, USA

Anthony Pivarunas, US Geological Survey, USA

Scott Miller, University of Florida, USA

Manoj Pandit, University of Rajasthan, India

Anup Sinha, Indian Institute of Geomagnetism, India

Precambrian paleomagnetic studies have matured over the past 30 years. A simple (albeit uncritical) search in google scholar shows that articles containing the word paleomagnetism were 2200 in the 1990-1991 interval, 2500 in the 2000-2001 interval, 14, 600 in the 2010-2011 interval and as of April this year 8380
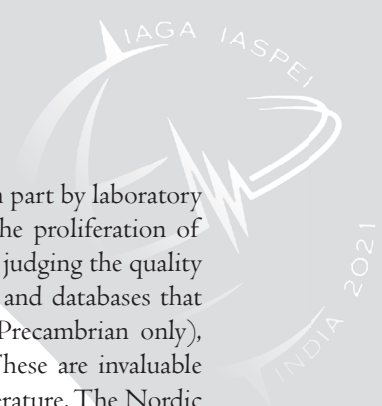
in the 2020-2021 interval. The increasing number of paleomagnetic studies are driven in part by laboratory automation and efficiency along with the relative ease of electronic submission and the proliferation of venues in which to publish. Easy access to these data and some evaluative mechanism for judging the quality of those data is therefore of critical importance. There are now several hosts for data and databases that depend in part on user participation or dedicated database personnel. Paleomagia (Precambrian only), MAGIC and the GPMDB are examples of recent and older database compilations. These are invaluable resources, but are often used uncritically and errors are often propagated through the literature. The Nordic Paleomagnetic workshops began in the late 1980's and have continued to the present day. These workshops are focused on quality reviews of new and existing data as well as filtering out errors. In this talk, we will give some far too common errors in published paleomagnetic studies and the problems in interpreting paleomagnetic data in the Precambrian. I will also present the new reliability criteria (R-Value; Meert et al., 2020) that supercedes the valuable Q-index of Van der Voo (1990).

KEYWORDS :   reliability, India, precambrian

Sr No: 333

The GEOMAGIA archaeomagnetic and volcanic database: overview, issues and solutions

CORRESPONDING & PRESENTING AUTHOR:

Maxwell Brown, University of Minnesota, USA

Gwenael Herve, Universite Paris-Saclay, France

Monika Korte, GFZ German Research Centre for Geosciences, Germany

Agnes Genevey, Sorbonne Universites, University Paris 6, France

The GEOMAGIA50 database currently holds over 11, 000 archaeomagnetic and volcanic entries spanning the past 10, 000 years. It is a major resource for studies on Earth's magnetic field and for archaeomagnetic dating. The database includes magnetic results, chronological data, and associated metadata to these fields, such as specimen/sample/site information and dating methods. The variety of approaches taken in archaeomagnetic and volcanic studies, as well as the large range of materials used to obtain data, mean that cataloguing data in a consistent way is challenging and results in compromises. We outline these issues, what they mean for users of the database, and propose possible solutions that could be implemented in the future. A significant hurdle is the documentation of age data and its importance cannot be understated. Most challenging is the archival of radiocarbon ages, both calibrated and uncalibrated. Radiocarbon dating is an ever evolving area of research that necessitates periodic reevaluation of already collected radiocarbon dates. As atmospheric radiocarbon has varied with time, experimental ages must be calibrated against data-driven calibration curves. These curves have evolved through time and GEOMAGIA50 does not automatically recalibrate experimental ages stored in the database. Furthermore, radiocarbon ages and associated metadata in the database are not comprehensive. We discuss how future iterations of the database could tackle this problem. Finally, we address how data obtained from novel materials, such as speleothems, could be integrated into GEOMAGIA50, as we envision these burgeoning data sources will contribute significant new data in the coming years.

KEYWORDS :   GEOMAGIA50, databases, dating

Sr No: 334

Legacy Paleomagnetic Collections: The Need for Preservation and Archiving of Key Sample Sets (by invitation)

CORRESPONDING & PRESENTING AUTHOR:

Phil Mccausland, University of Western Ontario, Canada

All paleomagnetic data are derived from measurements that were done on carefully collected and prepared samples and specimens. These paleomagnetic collections represent targeted sampling of geological units (such as dyke swarms) and contexts (such as ore bodies/host rock), that are also of interest for other investigations such as geochronology, isotope geochemistry, and paleointensity studies. Once paleomagnetic collections have been worked on, they may not be preserved in some form to be available for later sample requests. Most researchers do not have the mandate or ability to store research samples long term, let alone maintain them in archival form, even if the collections were sampled from locations that are difficult or impossible to revisit.

As we work to archive paleomagnetic data for future (re)use, preserving legacy collections arguably has the same rank of importance, for the samples offer the opportunity for followup work and fuller context for the existing paleomagnetic data. Preservation of entire collections is difficult, but key samples could include unused specimens, AF specimens (not chemically altered), "waste" cored contact test block samples, and specimens from sites that "didn't work." Collection documentation is vital, especially to preserve orientations, but also for other context metadata. Related documented material such as rock powders and rock magnetic samples as well as petrographic thin sections are also useful to preserve. While there is no centralized archive for preserved paleomagnetic collections, an effort by researchers and institutions to curate well-documented legacy paleomagnetic collections can nevertheless pay dividends in future research opportunities using improved techniques.

KEYWORDS :   paleomagnetic collections, curation, research infrastructure

Sr No: 335

BiCEP – A new method for reanalysis of legacy paleointensity data.

CORRESPONDING & PRESENTING AUTHOR:

Brendan Cych, University of California San Diego, USA
Matthias Morzfeld, University of California San Diego, USA
Lisa Tauxe, University of California San Diego, USA

Paleomagnetists obtain estimates of the Earth's ancient magnetic field strength (paleointensity) using Thellier-type experiments, which involve a double heating of a specimen in zero field and in a known lab field to compare to the original magnetization. Unfortunately, for many real world geological materials, the assumptions of these experiments are violated. Paleomagnetists employ sets of "selection criteria" to determine whether data from a paleointensity experiment violate these assumptions. There are many existing sets of criteria, with various threshold values, and there is little agreement on a best set to use.
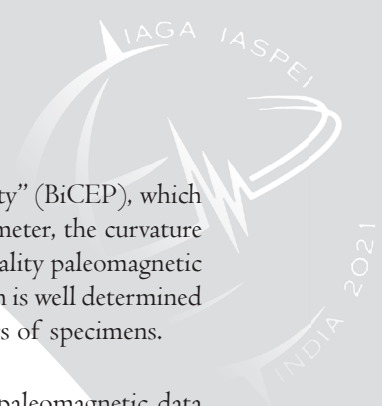
We present a new statistical approach called "Bias Corrected Estimation of Paleointensity" (BiCEP), which assumes that paleointensity data are biased by an amount that depends on a single parameter, the curvature criterion of Paterson (2011). Using this relationship we can estimate the bias in poor quality paleomagnetic data and correct for it. We apply BiCEP to a set of 30 sites where the original field strength is well determined and obtain accurate and precise paleointensity estimates without excluding large numbers of specimens.

The BiCEP method highlights the importance of data archival of measurement level paleomagnetic data adhering to FAIR principles. Without archived measurement level data, we would not have been able to test our assumptions. We hope that BiCEP can be used in future compilations of paleomagnetic data, as it is able to provide consistent analysis between different datasets and can use more data for analysis that would have been excluded in the past.

KEYWORDS : paleointensity

Sr No: 336

SYMPOSIUM : **1.6 Paleo- and rock-magnetic data: archiving, mining, (re)use**

Precambrian Paleomagnetic Data Archiving: The Need for Accurate Reporting and Quality Evaluation

CORRESPONDING & PRESENTING AUTHOR:

Dr. Joseph Meert, University of florida

We present a compilation of published magnetostratigraphic data for Neogene Siwalik sequence from the Himalaya developing a database for site mean, formation mean and sub-basins means using a common palaeomagnetic software platform. We discuss the disparity in the data due to variety of demagnetization protocols apart from the uncertainties over identification of ChRM, unknown tectonic deformations, manual errors, laboratory practices and the instrumental standards. After filtering the data with large statistical scatter, the formation-wise data plotted on GIS platform indicate a large diversity amongst D/I values depicting internal deformation, the intensity of which is increased after ~5 Ma. Prior to 5 Ma, there is coherency at the order of sub-basins and their means indicate a pattern of deformation along the axis of Himalaya. The Sediment accumulation rates show three orders of variation in magnitudes depicting regional tectonic pulses, basin partitioning due to intra-foreland thrusts and the basin fill conditions vis-a-vis depocenter migration. Nevertheless, we demonstrate that the magnetostratigraphic data from Siwalik sequence have preserved significant information on the style of syn-tectonic and internal deformation apart from the magnetic reversal pattern. Further the closer look at the palaeomagnetic directions from Upper Siwalik leads to understand the distributed deformation providing a genetic linkage to Neotectonics in the Himalayan foreland basin.

KEYWORDS :

IAGA Division II

2.1 Electrodynamics of the ionosphere-atmosphere system and its coupling to the space environment

CONVENERS: Irina Mironova

Martin Fullekrug

Andrei Demekhov

Electrodynamics of the global electrical circuit and the polar ionosphere-atmosphere system depends on solar wind magnetosphere interaction from above as well as the thunderstorm activity maintaining a time varying, globally uniform electrical potential difference between the ionosphere and the Earth as well as downward electric currents in the fair weather regions. The symposium solicits contributions on interdisciplinary studies that emphasize the electrodynamic connection between the ionosphere- atmosphere system and the magnetosphere, as well as the coupling between atmospheric layers, ionospheric potential, electrical currents, lightning physics, energetic radiation, energetic particles, and their impact on the Earth's atmosphere, ionosphere and the magnetosphere. In particular, we welcome reports on the impact of energetic particle precipitation on the Earth's ionosphere and atmosphere, the formation of ionospheric potential, electrical currents and conductivity, meteorological effects of the global atmospheric electric circuit, lightning physics, and energetic radiation. This symposium is focused on both satellite and ground based observations, as well as modeling studies of electrodynamics of the ionosphere-atmosphere system and its coupling to the space environment.
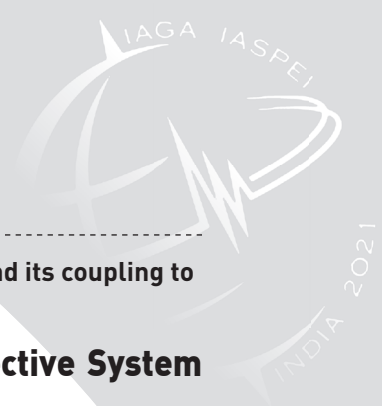
Sr No: 337

D-, E-, F-region ionosphere coupling due Mesoscale Convective System (MCS) generated lightning discharges

CORRESPONDING & PRESENTING AUTHOR:

Rajesh Singh, Indian Institute of Geomagnetism, India

Navin Parihar, Indian Institute of Geomagnetism, India

Ajeet K. Maurya, Doon University, India

A Mesoscale Convective System (MCS) associated lightning discharges during May 2014 generated a group of Transient Luminous Events (TLEs), which in altitude range reached the upper mesosphere region. Further the event manifested in rare simultaneous observations of columniform sprites and associated gravity waves (GWs) using Transient Luminous Events (TLEs) camera and All-sky imager over Prayagraj (25.5° N, 81.9° E, geomag. lat. ~ 16.5° N), India. The investigation showed presence of GWs (period ~ 14 min) in OH broadband airglow (emission peak ~ 87 km) imaging that propagated in the direction of sprite's occurrence and dissipated in the background atmosphere thereby generating turbulence. It was also observed that after the sprite event, another set of GWs (period ~ 11 min) was observed in OH imaging. The Very Low Frequency (VLF) navigational transmitter signal JJI (22.2 kHz) analysis showed the presence of GWs with ~20 min periodicities in D-region. In the F-region we observed waves with ~18 min period in the ionospheric Total Electron Content (TEC) variations recorded at a nearby GPS site (LKO). The presentation will focus on a study which report the first time the GWs associated with MCS and its electrical coupling manifestations starting from the troposphere to D-, E- and F-region ionosphere simultaneously.

KEYWORDS : metorology, lightning physics, gravity waves

Sr No: 338

Long-term mesospheric record of EPP-generated NO, measured with Odin/SMR

CORRESPONDING & PRESENTING AUTHOR:

Francesco Grieco, Chalmers University of Technology, Sweden

Kristell Perot, Chalmers University of Technology, Sweden

Donal Murtagh, Chalmers University of Technology, Sweden

Particles originating from the sun or from its magnetosphere can dramatically alter the chemistry of the Earth's atmosphere. One of such alterations is the increase of reactive nitrogen species such as nitric oxide (NO) in the mesosphere and the stratosphere. Solar protons cause the production of NO and other species in the stratosphere and lower mesosphere. This is known as energetic particle precipitation (EPP) direct effect and the amount of NOy species that are generated in this way is today relatively well understood. Moreover, less energetic particles such as magnetospheric electrons interact with molecules in the upper mesosphere and lower thermosphere, giving rise to the production of NO and other NOy species which, at the winter pole, are then transported by the mean meridional circulation (MMC) down to the lower

mesosphere and stratosphere. This is called EPP indirect effect, and the amount of reactive nitrogen species present in the stratosphere due to this process is still not well estimated. In our study, utilizing 20 years of observations performed with the Sub-Millimeter Radiometer (SMR) on board the Odin satellite, we investigate the correlation between mesospheric NO and tracers of the MMC. We do so to estimate the amount of EPP-generated NO descending during polar winters through the mesosphere via the MMC, distinguishing it from NO produced locally at lower altitudes through photochemistry and EPP direct effect. Our study leads to a unique climatological record of NO due to EPP indirect effect over a long period in both hemispheres.

KEYWORDS :   epp, no, mesosphere

Sr No: 339

- -

SYMPOSIUM :   **2.1 Electrodynamics of the ionosphere-atmosphere system and its coupling to the space environment**

Evaluation of calculated ionospheric conductivities using python

CORRESPONDING & PRESENTING AUTHOR:

Ms. Clara Oliveira, University of Brasilia, Brazil

To understand the behavior of ionospheric electricity and the coupling of the atmosphere and magnetosphere, studying the conductivity of the ionosphere is of fundamental importance. Currently, models of the ionosphere, neutral atmosphere, and geomagnetic field, IRI, NRMSISE-00, and IGRF, respectively, are available online. This makes it so that more researchers in emergent countries can implement algorithms for calculating conductivity. Here, a new algorithm in python was developed for calculating Pedersen and Hall conductivity, and its results were compared with the model developed by the University of Kyoto. The models adjusted very well to each other (~15% difference) to altitudes up to 165 km. That altitude is slightly above the expected. However, above that altitude, the calculated values of Hall's conductivity are very erratic and diverge strongly from the Kyoto model, while the Pedersen conductivity starts to readjust to the Kyoto model at about 200 km. The most likely cause is that the equations used for calculating the collision frequency only consider the O+ and a fictional ion called ion 1 that represents a mixture of NO+ and O2+. The influence of this and others parameters on the conductivity calculus will be discussed.

KEYWORDS :   ionospheric conductivity, conductivity, ionospheric electricity

Sr No: 340

- -

SYMPOSIUM :   **2.1 Electrodynamics of the ionosphere-atmosphere system and its coupling to the space environment**

Investigation of the horizontal displacement between lightning and sprites

CORRESPONDING & PRESENTING AUTHOR:

Dakalo Mashao, University of KwaZulu-Natal/ South African National Space Agency, South Africa

Michael Kosch, University of KwaZulu-Natal/ South African National Space Agency, South Africa

Martin Fullekrug, University of Bath, UK

Nickolay Ivchenko, KTH Royal Institute of Technology, Sweden

The optical emissions of 5 sprites in the middle atmosphere were observed simultaneously from Sutherland and Carnarvon in South Africa, separated by 192 km, during the 2019 sprites campaign. These two distinctive locations have low radio interference, and they are free from air and light pollution. The lightning occurrence times, positions, and polarities supplied by the South African Lightning Detection Network and Earth Networks were used to identify the lightning flashes which initiated the observed sprites events. The parent lightnings' vertical electric fields associated with the sprite events were recorded by a wideband low-frequency radio receiver, in the frequency range ~4 Hz to ~400 kHz (Füllekrug, 2009). The lightning vertical electric field waveforms were used to identify the type of lightning associated with each sprites event. We also investigate the horizontal displacement between the parent lightning and sprites events. Sprites tend to appear on average ~20 km away from their parent lightning strike, which is consistent with previous studies (Mlynarczyk et al., 2015; Bór et al., 2018).

KEYWORDS : sprites, lightning, triangulation

Sr No: 341

SYMPOSIUM : **2.1 Electrodynamics of the ionosphere-atmosphere system and its coupling to the space environment**

On the relationship between Travelling Ionospheric Disturbances (TIDs) and SuperDARN Near Range Echoes (NREs)

CORRESPONDING & PRESENTING AUTHOR:

Alicreance Hiyadutuje, South African National Space Agency/ University of KwaZulu Natal, South Africa

Michael Kosch, South African National Space Agency/University of KwaZulu Natal, South Africa

Judy Stephenson, South African National Space Agency/University of KwaZulu Natal, South Africa

The Super Dual Auroral Radar Network (SuperDARN) forms a global network of coherent high frequency (HF) radars located at mid-to high latitudes. Atmospheric Gravity Waves (AGWs) are ubiquitous throughout the atmosphere and can transport enormous energy and momentum from above or below into the mesosphere. AGWs are readily detected by HF radars as Travelling Ionospheric Disturbances (TIDs) (Oinats et al., 2015). Different mechanisms cause SuperDARN Near Range echoes (NREs) around 100 km altitude. One example is the Gradient Drift Instability (GDI) known as Far-aspect Angle Irregularity Region (FAIR) Echoes (Maurice and Nishitani, 2020). Near-simultaneous occurrence of F-region TIDs and E-region NREs are identified in the radar data during winter and summer. By using cross-correlation and statistical significance analysis, a moderate correlation between the two phenomena was found. FFT of their time series show that both phenomena have the same periods.

REFERENCES

1. Oinats, Alexey V., Vladimir I. Kurkin, and Nozomu Nishitani. "Statistical study of medium-scale travelling ionospheric disturbances using SuperDARN Hokkaido ground backscatter data for 2011." Earth, Planets and Space 67.1 (2015)

2. St.-Maurice, J-P., and N. Nishitani. "On the Origin of Far-Aspect Angle Irregularity Regions Seen by HF Radars at 100-km Altitude." Journal of Geophysical Research: Space Physics 125.6 (2020)

KEYWORDS : TIDs, GDI, NREs

Sr No: 342

A sensitivity of cloud microphysical parameters to changes in fair-weather Jz of GEC due to solar activity

PRESENTING AUTHOR:

Arseniy Karagodin, St. Petersburg State University, Russia

CORRESPONDING AUTHOR:

Irina Mironova, St. Petersburg State University, Russia
Eugene Rozanov, PMOD/WRC, Switzerland

During the last decades, the meteorological response to changes in By component of the interplanetary magnetic field (IMF) in high latitudes, known as the Mansurov effect, has been broadly studied. However, the role of the global electric circuit (GEC) in this effect is still unclear. Recent studies suggested that a reaction of cloud microphysics on IMF-induced changes in fair-weather current density Jz of GEC might be a possible way for this solar-weather coupling. Such a mechanism has to be confirmed but there were no numerical studies that showed the Mansurov effect found in observations. In this work, we carried out the ensemble sensitivity experiment with the chemistry-climate model SOCOLv3 to understand the sensitivity of cloud microphysical parameters to changes in Jz current density. We found that even small changes +/- 12% in Jz and corresponding changes of autoconversion rate in regions where IMF By-induced anomalies in electric potential of ionosphere occur might result in large anomalies in surface pressure and temperature in high latitudes. The work shows the importance of further investigation of the solar-weather coupling through GEC using global climate models.

KEYWORDS :   solar-weather coupling, GEC, chemistry-climate models

Sr No: 343

Direct Connection Between Auroral Oval Streamers/Flow Channels and Equatorward Traveling Ionospheric Disturbances

CORRESPONDING & PRESENTING AUTHOR:

Larry Lyons, University of CA, Los Angeles, USA
Toshi Nishimura, Boston University, USA
Shunrong Zhang, Massachusetts Institute of Technology, USA
Anthea Coster, Massachusetts Institute of Technology, USA
Jiang Liu, UCLA, USA
Bill Bristow, The Pennsylvania State University, USA
Ashton Reimer, SRI International, USA
Roger Varney, SRI International, USA

We use simultaneous auroral imaging, radar flows, and total electron content (TEC) measurements over Alaska to examine whether there is a direct connection of large-scale traveling ionospheric disturbances (LSTIDs) to auroral streamers and associated flow channels having significant ground magnetic decreases. Auroral observations allow identification of streamers and TEC observations detect ionization enhancements associated with streamer electron precipitation. Radar observations allow direct detection of flow channels. The TEC observations show direct connection of streamers to TIDs propagating equatorward from the equatorward boundary of the auroral oval. The TIDs are also distinguished from the streamers to which they connect by their wave-like TEC fluctuations moving more slowly equatorward than do the TEC enhancements from streamer electron precipitation. TIDs previously observed propagating equatorward from the auroral oval have been identified as LSTIDs. Thus, the TIDs here are likely LSTIDs, but we lack sufficient TEC coverage necessary to demonstrate that they are indeed large scale. Furthermore, each of our events show TIDs' connection to groups of a few streamers and flow channels over a period on the order of 15 min and a longitude range of ~10-15o, and not to single streamers. (Groups of streamers are common during substorms. We do not know of evaluation of whether streamers and associated flow channels typically occur in such groups.) We also find evidence that a flow channel must lead to a sufficiently large ionospheric current for it to lead to a detectable LSTID, a few tens of nT ground magnetic field decrease being not sufficient.

KEYWORDS :   TIDs, flow channels, auroral streamers

Sr No: 344

SYMPOSIUM :   **2.1 Electrodynamics of the ionosphere-atmosphere system and its coupling to the space environment**

Charge moment change-based characterization of global lightning activity via the inversion of Schumann resonance measurements

CORRESPONDING & PRESENTING AUTHOR:

Tamas Bozoki, Institute of Earth Physics and Space Science (ELKH EPSS), Hungary

Erno Pracser, Institute of Earth Physics and Space Science (ELKH EPSS), Hungary

Gabriella Satori, Institute of Earth Physics and Space Science (ELKH EPSS) , Hungary

Joszef Bor, Institute of Earth Physics and Space Science (ELKH EPSS) , Hungary

Earle Williams, Massachusetts Institute of Technology, USA

Yakun Liu, Massachusetts Institute of Technology, USA

Anirban Guha, Tripura University, India

Mike Atkinson, HeartMath Institute, USA

Ciaran Beggan, British Geological Survey, UK

Alexander Koloskov, National Academy of Sciences of Ukraine, Ukraine

Andrzej Kulak, AGH University of Science and Technology, Poland

Janusz Mlynarczyk, AGH University of Science and Technology, Poland

Joan Montanya, Polytechnic University of Catalonia, USA

Robert Moore, University of Florida, USA

Mariusz Neska, Polish Academy of Sciences, Poland

Pascal Ortega, University of French Polynesia, France

Rahul Rawat, Indian Institute of Geomagnetism, India

Ashwini Kumar Sinha, Indian Institute of Geomagnetism, India

Ryan Said, Vaisala, Finland

Yuri Yampolski, National Academy of Sciences of Ukraine, Ukraine

Detailed investigation of lightning climatology on global scales is currently hindered by the incomplete and spatially uneven detection efficiency of ground-based VLF networks and by the restricted spatio-temporal

coverage of satellite observations. Currently available technology does not allow the detailed quantitative evaluation of lightning activity on continental scales on time scales ranging from the diurnal to the interannual. Our group proposes a cost-effective technique to infer the distribution and intensity of global lightning activity based on the inversion of Schumann resonance (SR) measurements. Due to the extremely weak attenuation of lightning-radiated electromagnetic (EM) waves in the SR-band (~3-50 Hz) all lightning strokes with vertical extent contribute to the globally detectable EM field which makes SR measurements very much suitable for climatology-related investigations. Vertically separated charged regions form in thunderstorms because ice-based charge separation is dominantly driven by vertically oriented processes, i.e., gravity and updraft. This implies that practically every lightning flash in the atmosphere (intracloud and cloud-to-ground alike) has a vertical component of its charge moment change and is guaranteed to contribute to the ELF intensity. Furthermore, this approach gives the intensity of lightning activity in terms of an absolute physical quantity: the vertical charge moment change (CMC) in the unit of C2km2/s, not biased by chosen event selection criteria as in case of statistics based on the number density of strokes or flashes. Here we describe our inversion algorithm and present CMC-based lightning distributions from a few selected days. Considerable variability in the chimney-to-chimney activity is evident.

KEYWORDS : Lightning, Schumann resonances, Extremely low frequency

Sr No: 345

Long-term changes in the Earth-ionosphere cavity caused by solar X-rays and energetic electron precipitation

CORRESPONDING & PRESENTING AUTHOR:

Tamas Bozoki, Institute of Earth Physics and Space Science (ELKH EPSS), Hungary

Gabriella Satori, Institute of Earth Physics and Space Science (ELKH EPSS), Hungary

Earle Williams, Massachusetts Institute of Technology, USA

Irina Mironova, St. Petersburg State University, Russia

Peter Steinbach, Eötvös Loránd University, Hungary

Emma Bland, University Centre in Svalbard, Norwegian

Alexander Koloskov, National Academy of Sciences of Ukraine, Ukraine

Yuri Yampolski, National Academy of Sciences of Ukraine, Ukraine

Oleg Budanov, National Academy of Sciences of Ukraine, Ukraine

Mariusz Neska, Polish Academy of Sciences, Poland

Ashwini Kumar Sinha, Indian Institute of Geomagnetism, India

Rahul Rawat, Indian Institute of Geomagnetism, India

Mitsuteru Sato, Hokkaido University, Japan

Ciaran Beggan, British Geological Survey, UK

Sergio Toledo Redondo, University of Murcia, Spain

Yakun Liu, Massachusetts Institute of Technology, USA

Robert Boldi, Zayed University,UAE

Anirban Guha, Tripura University, India

The Earth–ionosphere cavity resonator is occupied primarily by the electromagnetic radiation from lightning below 100 Hz. This phenomenon is known as the Schumann resonances (SR). We present long-term SR intensity records from eight different SR stations each equipped with a pair of induction coil magnetometers. All the records exhibit a pronounced in-phase solar cycle variation and our aim is to reveal the underlying reason for this effect. The long-term SR intensity records are compared on the annual and

interannual timescales with the fluxes of precipitating 30-300 keV medium energy electrons provided by POES NOAA satellites and on the daily timescale with electron precipitation events identified using a SuperDARN radar in Antarctica. The long-term variation of the Earth–ionosphere waveguide's effective height as inferred from its cutoff frequency is independently analyzed based on spectra recorded by the DEMETER satellite. It is shown that to account for all our observations one needs to consider both the effect of solar X-rays and EEP which modify the quality factor of the cavity and deform it predominantly over low- and high latitudes, respectively. The increase in the quality factor is linked with decreases in dissipation in the altitude range of the ELF 'magnetic' height where ionization by both X-rays and EEP increases the electrical conductivity. Our results suggest that SR measurements should be considered as an alternative tool for collecting information and thus to monitor changes in the ionization state of the lower ionosphere associated with EEP.

KEYWORDS : energetic electron precipitation, earth-ionosphere cavity, schumann resonances

Sr No: 346

SYMPOSIUM : **2.1 Electrodynamics of the ionosphere-atmosphere system and its coupling to the space environment**

Complex analysis response of the ionosphere-atmosphere system on solar flares and energetic particle precipitation during September 2017

CORRESPONDING & PRESENTING AUTHOR:

Irina Mironova, Saint Petersburg University, Russia

Maxim Klimenko, Saint Petersburg University, Russia

Polina Pikulina, Saint Petersburg University, Russia

Eugene Rozanov, Saint Petersburg University, Russia

Timofei Sukhodolov, Saint Petersburg University, Russia

Olesya Yakovchuk, Saint Petersburg University, Russia

The ionosphere-atmosphere response on exceptional solar activity in early September 2017 at a minimum of solar cycle 24 is analysed. The beginning of the intensive solar-terrestrial disturbances was the Sun active region AR2673, which produced several powerful solar flares class X with the strongest flare X9.3 of solar cycle 24 on September 6, 2017, and X1.3 on September 7, 2017. This flare produced increasing in irradiance in the extreme ultraviolet and soft X-ray ranges of the solar spectrum that are important the most for the sunlit regions of the upper mesosphere and the lower thermosphere. After these flares and coronal mass ejections began G4 - severe geomagnetic storm on September 7-8, 2017 with Ap = 106. Moreover, the second strongest flare X8.2 of Solar Cycle 24 on September 10, 2017, generated instantly the Ground Level. Energetic particle precipitation during disturbances of September 2017 led to increasing the total electron abundance and electron density in the F region and in the upper ionosphere at low and middle latitudes increases as well as increases chemical components of the middle polar atmosphere leading to ozone destruction.

This work presents new results that add to our growing understanding of how impulsive solar and magnetospheric energetic particle precipitation as well as solar flares affect the Earth's ionosphere - atmosphere system and provides a foundation for understanding their cumulative impacts on the atmosphere and climate.

KEYWORDS : solar flares, energetic particle precipitation, ionosphere-atmosphere

2.2 Solar Influence on the Atmosphere and Climate

CONVENERS: Christoph Jacobi

                     Nicholas Pedatella

                     Luc Damé

Solar influence on climate keeps attracting much interest presently. This includes in particular the role of the Sun both in the past climate as in future climate variability as an important aspect. State-of the art climate models include a well resolved stratosphere and mesosphere. This allows the prediction of global climate and its changes, taking into account expected solar related variability at short to long time scales.

In the middle and upper atmosphere solar related electromagnetic and particle variability is one dominant forcing mechanism for atmospheric variability at time scales from days to decades. From available datasets it is not always straightforward to distinguish between solar and meteorological influences. Time series are often too short to clearly identify, e.g., the 11- and 22- year solar cycles in the presence of nonlinear trends owing to lower atmospheric variability. The effect of planetary waves at time scales of days to weeks is difficult to extract from time series in the presence of the solar rotation effect and harmonics.

Results from observations, including observation and modeling solar forcing, theoretical work and modeling efforts to quantify meteorological and solar effects on the lower, middle, and upper atmosphere are welcome. Reports on progress in reconstructing past climate and future climate projections and the role of extraterrestrial forcing in these are desired.

Sr No: 347

Inter-annual variability of lightning activity and its external drivers

CORRESPONDING & PRESENTING AUTHOR:

Marzieh Khansari, Sodankylä Geophysical Observatory, Finland

Eija Tanskanen, Sodankylä Geophysical Observatory/ Aalto University, Finland

Shabnam Nikbakhsh, Sodankylä Geophysical Observatory, Finland

INTRODUCTION

The possible effect of solar activity on lightning has been studied for a long period of time. Specifically, the relationship between sunspot number and lightning activity has been investigated, although the results still remain inconclusive across regions and time. In some regions a positive correlation is found, at others a negative one. Thus, it is important to explore other external drivers possibly influencing lightning activity, such as geomagnetic index or high-speed solar wind streams (HSS).

METHOD

In order to investigate the impact of solar activity on lightning activity, we investigated the relationship between lightning count, HSS, proton flux (with energy higher than 60 Mev) and westward electrojet index at the high latitudes between 65° to 71° during solar cycle (SC) 23 (1998 to 2009).

RESULTS

Our analysis showed strong correlation between HSS and lightning activity as well as proton flux ($>$ 60 Mev) during SC23. We found that this correlation exists when HSS rate and proton flux are above a certain threshold. Furthermore, our finding showed that lightning activity and geomagnetic IL index strongly correlates during SC23. All of the above mentioned variables peaked together in 2003 when geomagnetic activity was the strongest during SC23.

CONCLUSION

Based on our results, we hypothesize that under some circumstances, like high rates of HSS, solar activity influences lightning.

KEYWORDS : lightning activity, HSS, Proton flux

Sr No: 348

Influence of Seasonal and Solar Flux Variations on the Low-latitude OI 630 nm Thermospheric Nightglow

CORRESPONDING & PRESENTING AUTHOR:

Sovan Saha, Physical Research Laboratory, India

Duggirala Pallamraju, Physical Research Laboratory, India

OI 630 nm nightglow emissions originate from around 250 km altitude due to dissociative recombination of molecular oxygen. High Throughput Imaging Echelle Spectrograph (HiTIES) is used to measure the OI 630 nm nightglow emissions over Mt. Abu (16 Mag N), Gurushikhar, India, a low-latitude location. Around five years of data (2013 to 2017) with varying solar fluxes have been analysed to characterise

the nocturnal emission variations. A photochemical model has been developed, which estimates column integrated emission rates using measured electron densities obtained from digisonde, as input. Different kinds of variations in the nightglow emission are observed, like, monotonic decrement of airglow after sunset due to absence of solar photons, post-sunset and post-midnight enhancement in emissions, fluctuations in emission rates, etc. HiTIES has a field of view (FOV) of 54 degree, which gives latitudinal information of these emissions. On some occasions, it is observed that the emission rates in the northern side of HiTIES's FOV show higher values as compared to those in the southern side. This suggests that the location of the equatorial ionization anomaly (EIA) crest is situated towards higher latitudes. Further, on some occasions, later in the night, the emissions in the northward direction reduce and those in the zenith increase. This is viewed as a reversal of the EIA. The overall dynamics of OI 630 nm nocturnal variation will be discussed in detail in the context of the varying effect of equatorial electrodynamics with that in the solar flux conditions and seasons.

KEYWORDS : OI 630 nm nightglow, photo-chemical model, seasonal and solar flux variation

Sr No: 349

The 11-year solar cycle UV irradiance effect and its dependency on the Pacific Decadal Oscillation

CORRESPONDING & PRESENTING AUTHOR:
Sigmund Guttu, University of Oslo, Norway
Yvan Orsolini, NILU, Norway
Frode Stordal, University of Oslo, Norway
Odd Helge Otteraa, Norce Research, Norway
Nour Eddine Omrani, University of Bergen, Norway

The stratospheric and tropospheric impacts from the 11-year ultraviolet solar spectral irradiance (SSI) variability have been extensively studied using climate models and observations. In this study, we demonstrate using idealized model simulations that the Pacific Decadal Oscillation (PDO), which has been shown to impact the atmospheric circulation on several timescales, strongly modulates the solar-induced atmospheric response. We use a high-top version of the coupled ocean-atmosphere Norwegian Climate Prediction model (NorCPM) forced by the SSI dataset recommended for CMIP6. We perform a 24-member ensemble experiment over the solar cycle 23 in an idealized framework. To assess the PDO modulation of the solar signal, we divide the model data into the two PDO phases, PDO+ and PDO-, for each solar (maximum or minimum) phase. By compositing and combining the four categories, we hence determine the component of the solar signal that is independent of the PDO and the modulation of the solar signal by the PDO, along with the solar signal in each PDO phase. Our results show that the intensification of the polar vortex under solar maximum is much stronger in the PDO- phase. This signal is transferred into the troposphere, where we find a correspondingly stronger polar jet and weaker Aleutian Low. We further show that the amplification of the solar signal by the PDO- phase is driven by anomalous meridional advection of solar-induced temperature anomalies over northern North America and the North Pacific, which contributes to a decreased meridional eddy heat flux.

KEYWORDS : SSI, PDO, circulation

Sr No: 350

Solar Irradiance Variability and Climate (by invitation)

CORRESPONDING & PRESENTING AUTHOR:

Margit Haberreiter, PMOD/WRC, Switzerland

Solar irradiance is the key energy input to Earth and varies on timescales from minutes to days, years and centuries. For a full understanding of its impact on the Earth atmosphere and climate it is important to understand solar variability on all timescales. We will discuss the latest advances in both Total and Spectral Solar Irradiance (TSI, SSI) observations and modeling and its impact on the Earth atmosphere and climate. In addition, the Earth radiation budget is an important measure for the long-term trend of the climate system. A positive Earth Energy Imbalance (EEI) is the energy, which is continuously stored by the Earth and will ultimately be released to the atmosphere, causing global warming. In order to exactly quantify it, the TSI and the Top of the Atmosphere (ToA) Outgoing Radiation (TOR) need to be measured with unprecedented accuracy and precision. Latest advances towards determining the Earth Radiation Budget will also be discussed..

KEYWORDS : solar Irradiance, sun-earth connection, earth climate

Sr No: 351

Similar patterns of tropical precipitation and circulation changes under solar and greenhouse gas forcing (by invitation)

CORRESPONDING & PRESENTING AUTHOR:

Stergios Misios, National Observatory of Athens, Greece

Mathew Kasoar, Imperial College London, UK

Elliott Kasoar, Imperial College London, UK

Lesley Gray, Oxford University, UK

Joanna Haigh, Imperial College London, UK

Theory and model evidence indicate a higher global hydrological sensitivity for the same amount of surface warming to solar as to greenhouse gas (GHG) forcing, but regional patterns are highly uncertain due to their dependence on circulation changes. I will discuss results of a multi-model ensemble of idealized experiments of solar and GHG forcing and a set of simulations of the last millennium to demonstrate similar patterns of forced response in the tropical Pacific, of higher amplitude for the solar forcing. Both solar and GHG warm the equatorial Pacific, enhance precipitation in the central Pacific, and weaken and shift the Walker circulation eastward. I will conclude that tropical Walker circulation and precipitation might be more susceptible to solar variability rather than GHG variations during the pre-industrial period, assuming comparable global mean surface temperature changes.

KEYWORDS : solar cycle, walker circulation, precipitation

Sr No: 352

Influence of geomagnetic disturbances on midlatitude mesosphere/lower thermosphere mean winds and tides

CORRESPONDING & PRESENTING AUTHOR:

Christoph Jacobi, Leipzig University, Germany

Friederike Lilienthal, Leipzig University, germany

Dmitry Korotyshkin, Kazan (Volga Region) Federal University, Russia

Evgeny Merzlyakov, RPA Typhoon, Russia

Gunter Stober, University of Bern, Switzerland

Observations of upper mesosphere/lower thermosphere (MLT) wind have been performed at Collm (51°N, 13°E) and Kazan (56°N, 49°E), using two SKiYMET all-sky meteor radars with similar configuration. Daily vertical profiles of mean winds and tidal amplitudes have been constructed from hourly horizontal winds. We analyze the response of mean winds and tidal amplitudes to geomagnetic disturbances. To this end we compare winds and amplitudes for very quiet (Ap < 5) and unsettled/disturbed (Ap > 20) geomagnetic conditions. Zonal winds in both the mesosphere and lower thermosphere are weaker during disturbed conditions for both summer and winter. The summer equatorward meridional wind jet is weaker for disturbed geomagnetic conditions. Tendencies over Collm and Kazan for geomagnetic effects on mean winds qualitatively agree during most of the year. For the diurnal tide, amplitudes in summer are smaller in the mesosphere but greater in the lower thermosphere, but no clear tendency is seen for winter. Semidiurnal tidal amplitudes increase during geomagnetic active days in summer and winter. Terdiurnal amplitudes are slightly reduced in the mesosphere during disturbed days, but no clear effect is visible for the lower thermosphere. Overall, while there is a noticeable effect of geomagnetic variability on the mean wind, the effect on tidal amplitudes, except for the semidiurnal tide, is relatively small and partly different over Collm and Kazan.

Sr No: 353

Mechanism Studies of Madden-Julian-Oscillation Coupling into the Mesosphere/Lower Thermosphere Tides using SABER, MERRA-2, and SD-WACCMX

CORRESPONDING & PRESENTING AUTHOR:

Komal Kumari, Clemson University, USA

Haonan Wu, Clemson University, USA

Abigail Long, Clemson University, USA

Xian Lu, Clemson University, USA

Jens Oberheide, Clemson University, USA

Tidal deconvolution of SABER temperature observations allows one to resolve intraseasonal (30-90-day) tidal variability that occurs as a response to the recurring Madden-Julian Oscillation (MJO) in tropical convection. In this study, we make effort for a better understanding of the physical causes of intraseasonal
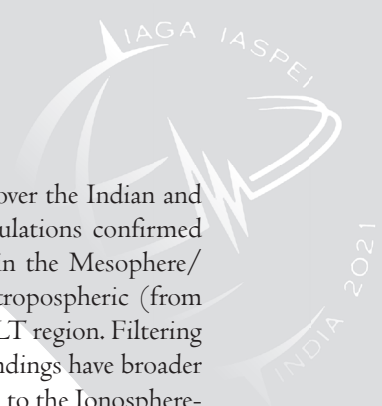
variability in the diurnal tides as a function of various locations of active-MJO events over the Indian and Pacific Ocean. A statistical analysis of SABER observations and SD-WACCMX simulations confirmed previously unverified model predictions of a 10-25% tidal modulation by the MJO in the Mesophere/Lower Thermosphere (MLT) region. The tides largely respond to the MJO in the tropospheric (from MERRA-2) tidal forcing, and the tidal advection and gravity wave drag forcing in the MLT region. Filtering by tropospheric/stratospheric background winds is comparably less important. These findings have broader implications as tides can also couple variability on MJO timescales from the MLT region to the Ionosphere-Upper Thermosphere region.

KEYWORDS : atmospheric tides, madden-julian oscillation, mesosphere/lower thermosphere

Sr No: 354

Delayed ionospheric response to Solar EUV variations using satellite observations and CTIPe model simulations

CORRESPONDING & PRESENTING AUTHOR:

Rajesh Vaishnav, Institute Meteorologie, Universite Leipzig, Germany

Christoph Jacobi, Institute für Meteorologie Universität Leipzig, Germany

Jens Berdermann, German Aerospace Center, Germany

Erik Schmaqter, German Aerospace Center, Germany

Mihail Codrescu, Space Weather Prediction Centre, NOAA, Boulder, Colorado, USA

We investigate the ionospheric delayed response to solar EUV variations at the 27 days solar rotation time scale using the ionospheric Total Electron Content (TEC) provided by the International GNSS Service (IGS), and the Coupled Thermosphere Ionosphere Plasmasphere Electrodynamics (CTIPe) model simulated TEC. The ionospheric delay estimated using model simulated TEC is in good agreement with the delay estimated for observed TEC against Solar Dynamics Observatory (SDO) EUV Variability Experiment (EVE) measured flux. The ionospheric delay strongly varies with latitude and time and depends on the solar activity. Furthermore, modelling effort has been made to quantify the effect of eddy diffusion on the delayed ionospheric response. Enhanced eddy diffusion leads to increased loss rates resulting in a decrease of the ionospheric time delay.

KEYWORDS : Solar EUV variations, CTIPe model

2.3 Stratosphere-Mesosphere-Thermosphere-Ionosphere System – Long-Term Changes

CONVENERS: Liying Qian

Jan Lastovicka

Long term changes of greenhouse gas concentrations and other drivers, such as the long term change of the Earth's magnetic field, cause long term changes in the upper atmosphere, which are often much larger than tropospheric trends. Note that in atmospheric science, long term changes, or trends, refer to changes on a time scale longer than one solar cycle (~ 11 years). We welcome papers on investigating trends in the stratosphere, mesosphere, thermosphere and ionosphere, dealing with ground based as well as satellite borne observations, model simulations, theoretical analyses, long term data quality issues, methods of determination of trends, and related laboratory experiments.

Sr No: 355

Trends in the mesosphere-thermosphere-ionosphere system: Progress report (by invitation)

CORRESPONDING & PRESENTING AUTHOR:

Jan Lastovicka, Institute of Atmospheric Physics, Czech Acad. Sci., Czech Republic

Long-term trends are important phenomenon of predominantly anthropogenic origin in the mesosphere, thermosphere and embedded ionosphere. In the last two years since the IUGG Assembly in 2019 some progress in trends has been reached, for example in modeling or in specifying the role of secular changes of the Earth's magnetic field in trends. A review of progress in terms of main results in the field of long-term trends in the mesosphere-thermosphere-ionosphere system, reached over the last two years, will be briefly presented.

KEYWORDS :   long-term trends, ionosphere, upper atmosphere

Sr No: 356

The best solar proxy for ionospheric long-term trend studies

CORRESPONDING & PRESENTING AUTHOR:

Jan Lastovicka, Institute of Atmospheric Physics, Czech Acad. Sci. , Czech Republic

To select the best solar activity proxy and the dependence of ionospheric parameters on this proxy is important for long-term trend or climatological studies of ionospheric parameters as well as for modeling. The problem consists of three questions: (1) Is the dependence of ionospheric parameters on solar proxies stable with time? (2) Is the relative role of solar proxies the same for foF2 and foE? (3) What is the most suitable solar proxy for calculating trends in foF2? We use the yearly average and partly monthly median values of foE and foF2 from selected European stations with long (1976-2019) and high-quality data. Six solar proxies are utilized: F10.7, F30, Mg II, He II, sunspot number R and H Lyman-alpha flux Fα.

Results: (1) The dependence of foF2 and foE on F10.7 is not stable; it is stronger in recent years (since ~1996 for foF2 and since ~2000 for foE). (2) The relative role of solar proxies for foF2 and foE is different. Results (1) and (2) were derived for yearly average values. (3) Mg II and F30 followed by F10.7 are found to be the best solar proxies for both yearly and monthly foF2 values as well as for years of deep solar minima (2008-09, 2018-19). The variability of yearly values of foF2 is almost fully described by solar proxies and this relation is highly linear.

KEYWORDS :   Ionosphere, solar activity proxies

- -

SYMPOSIUM : **2.3 Stratosphere-Mesosphere-Thermosphere-Ionosphere System – Long-Term**

Climate Changes in the Upper Atmosphere: Contributions by the Changing Greenhouse Gas Concentrations and Earth's Magnetic Field From the 1960s to 2010s

CORRESPONDING & PRESENTING AUTHOR:

Liying Qian, National Center for Atmospheric Research, USA

Joseph Mcinerney, National Center for Atmospheric Research, USA

Stanley Solomon, National Center for Atmospheric Research, USA

Hanli Liu, National Center for Atmospheric Research, USA

Alan Burns, National Center for Atmospheric Research, USA

Previous studies have established the importance of the increasing greenhouse gas concentrations in causing trends in the thermosphere and ionosphere (T-I). Recent work indicates that the changing Earth's magnetic field is also important. We conduct whole atmosphere model simulations to examine T-I trends driven by these two drivers and their relative importance. We found that, (1) trends in the T-I, driven by either of the two drivers, exhibited significant latitudinal and longitudinal variability; (2) in the thermosphere, trends were predominantly driven by the greenhouse gas driver except that the magnetic field driver played a small role in the neutral temperature trend ($\sim 25\%$) in some regions mainly in the longitude sector ~ 120oW – 20oE. The magnetic field driver played a more important role in the ionosphere in the longitude sector ~ 120oW – 20oE. In this longitude sector, the two drivers were comparable in driving the trends of hmF2, NmF2, and electron temperature; the relative importance of the two drivers to the ion temperature trend additionally depends on altitude, with the greenhouse gas driver being the dominant driver at lower altitudes (~ 200 km – 320 km), and the two drivers becoming comparable above; (3) although the magnetic field driver is important in the longitude sector ~ 120oW – 20oE, it drove both negative and positive trends in roughly equal amounts, consequently, its contributions to the global average trends in the T-I are negligible.

KEYWORDS : upper atmosphere trends, greenhouse gases, magnetic field

- -

SYMPOSIUM : **2.3 Stratosphere-Mesosphere-Thermosphere-Ionosphere System – Long-Term**

Determination of vortex current structure in the high-latitude ionosphere with associated GIC bursts from ground magnetic data

CORRESPONDING & PRESENTING AUTHOR:

Vladislav Chinkin, Geophysical center of the Russian Academy of Sciences, Russia

Anatoly Soloviev, Geophysical center of the Russian Academy of Sciences, Russia

Vyacheslav Pilipenko, Geophysical center of the Russian Academy of Sciences, Russia

One of the most harmful factors of space weather for industrial power transmission lines are electric geomagnetically induced currents (GICs) caused by abrupt changes of the geomagnetic field. Nighttime magnetic impulses observed at auroral zone latitudes may be organized into quasiperiodic sequence of pulses, named Ps6 pulsations. Such meso-scale disturbances on short timescales may be considered as the space weather proxy of tornadoes during severe terrestrial weather. These "tornados", that are isolated and multiple magnetic pulses, may be responsible for significant bursts of GICs.

We proposed a new method, which makes it possible not only to automatically determine several simultaneous vortex structures using the data from a 2D network of magnetometers, but also to determine their instant dynamic parameters (position, radius, speed, trajectory, current direction and intensity, …). The method is based on the determination of local minima in functions of the magnetic field obtained by interpolation and subsequent correction by potential functions.

This new technique of data analysis has confirmed that extreme GIC (>100A) in the power transmission line in northwest Russia on June 29, 2013 was caused by geomagnetic Ps6 pulsations produced by a sequence of localized (radius ~ 200–250 km) eastward propagating vortices driven by FACs with densities up to 5 A/km2.

The proposed technique may be helpful for studying fine temporal/spatial structures of meso-scale geomagnetic disturbances of different physical origins. The research was conducted under the RSF project # 21-77-30010.

KEYWORDS : geomagnetically induced current, magnetometer, vortex structure

Sr No: 359

SYMPOSIUM : **2.3 Stratosphere-Mesosphere-Thermosphere-Ionosphere System – Long-Term**

Trents in noctilucent (by invitation)

CORRESPONDING & PRESENTING AUTHOR:

Franzjosef Luebken, Leibniz Institute of Atmospheric Physics, Kuehlungsborn, Germany

Gerd Baumgarten, Leibniz Institute of Atmospheric Physics, Kuehlungsborn, Germany

Noctilucent clouds are often cited as potential indicators of climate change in the middle atmosphere. They owe their existence to the very cold summer mesopause region (~130K) at mid and high latitudes. We analyze trends derived from the Leibniz-Institute Middle Atmosphere Model (LIMA) and the MIMAS ice particle model (Mesospheric Ice Microphysics And tranSport model) for the years 1871-2008 and for middle, high and arctic latitudes, respectively. Model runs with and without an increase of carbon dioxide and water vapor (from methane oxidation) concentration are performed. Trends are most prominent after ~1960 when the increase of both carbon dioxide and water vapor accelerates. Negative trends of (geometric) NLC altitudes are primarily due to cooling below NLC altitudes caused by carbon dioxide increase. Increases of ice particle radii and NLC brightness with time are mainly caused by an enhancement of water vapor. Several ice layer and background parameter trends are similar at high and arctic latitudes but are substantially different at middle latitudes. NLC altitudes decrease by approximately 15-20m per increase of carbon dioxide by 1ppmv. The number of ice particles in a column and also at the altitude of maximum backscatter is nearly constant with time. We will also present first results on effects of future climate scenarios on NLC and will discuss a potential future (regional) increase of Earth's albedo caused by NLC.

KEYWORDS : mesospheric ice layers, climate change in the MA, earth's albedo

Sr No: 360

MLT Summer Length Defined by Mean Zonal Wind Features Observed for More Than One Solar Cycle at Mid- and High-Latitudes in the Northern Hemisphere

CORRESPONDING & PRESENTING AUTHOR:

Juliana Jaen, Leibniz- Institute of Atmospheric Physics (IAP), Germany

Toralf Renkwitz, Leibniz- Institute of Atmospheric Physics (IAP) , Germany

Peter Hoffmann, Leibniz- Institute of Atmospheric Physics (IAP) , Germany

Maosheng He, Leibniz- Institute of Atmospheric Physics (IAP) , Germany

Yosuke Yamazaki, GFZ German Research Centre for Geosciences, Germany

Christoph Jacobi, University of Leipzig, Germany

Chris Hall, The Arctic University of Norway, Norway

Masaki Tsutsumi, National Institute of Polar Research, Japan

Vivien Matthias, German Aerospace Center (DLR) , Germany

Jorge Chau, Leibniz- Institute of Atmospheric Physics (IAP), Germany

Specular meteor radars (SMRs) and partial reflection radars (PRRs) have been observing mesospheric winds for more than a solar cycle over Germany (~54°N) and northern Norway (~69°N). In this work, we investigate mesospheric mean zonal wind over these two regions between 2004 and 2019. We also include zonal mean geostrophic zonal wind from microwave limb sounder (MLS) at 55°N and 70°N. Our study focuses on the summer, considering that strong planetary waves are absent and lower atmosphere conditions are relatively stable. We established two definitions of the summer length (SL) based on the zonal wind reversal: (1) the mesosphere and lower thermosphere summer length (MLT-SL) using SMR and PRR winds, and (2) the mesosphere summer length (M-SL) using PRR and MLS. Under both definitions, the summer begins around April and ends around mid-September. The largest variability is found in the summer beginning, particularly at high latitudes, possibly due to the polar vortex behavior. The years 2004 and 2013 show an abnormal behavior compared to the mean value for MLT-SL, as well as 2012 for both definitions. M-SL exhibits an increasing trend over the years, while MLT-SL does not have a well-defined trend. We complement our work with an extended time series of 30 years at mid-latitudes using only PRR winds. In this case, the SL shows a breakpoint, suggesting a non-uniform trend and periods similar to those known for El Niño-southern oscillation and quasi-biennial oscillations.

Sr No: 361

A 28-year trend of water vapor in stratosphere and mesosphere from observation and model simulation

CORRESPONDING & PRESENTING AUTHOR:

Wandi Yu, Hampton University, USA

Jia Yue, NASA GSFC, USA

Rolando Garcia, NCAR, USA

James Russell, Hampton University, USA

Water vapor in the stratosphere and mesosphere is an important greenhouse gas, and its budget plays an essential role in climate sensitivity. However, previous studies on its long-term trend have ambiguous conclusions. We use a merged data combining the observation from the Sounding of the Atmosphere using Broadband Emission Radiometry (SABER), Halogen Occultation Experiment (HALOE), and Microwave Limb Sounder (MLS) to estimate water vapor trends over the SABER period (2003-2020) and a longer period (1993-2020). The specified dynamics versions of the Whole Atmospheric Community Climate Model (SD-WACCM) can well represent the water vapor trend in both periods of time. Both the merged data and SD-WACCM result indicates that although water vapor increases about 2%-6% per decade over 2003-2020, its trend over the longer period of time is neglectable. The increase of water vapor from methane oxidation stably is about 1% per decade. Changes in the tropical tropopause temperature are the main reason for the large positive trend after 2003, but its contribution to 28 years of record is negative. We conclude that though on higher altitudes of stratosphere more methane oxidation stably produces more water vapor, in the lower stratosphere, the amount of water vapor entering the stratosphere from the troposphere may yield to low-frequency variation in the past three decades and does not have a significant trend.

KEYWORDS : stratospheric water vapor, long term trend, WACCM

Sr No: 362

SYMPOSIUM : **2.3 Stratosphere-Mesosphere-Thermosphere-Ionosphere System – Long-Term**

How does long-term changes in geomagnetic activity regulate the CO2-driven trend in the thermosphere and ionosphere? (by invitation)

CORRESPONDING & PRESENTING AUTHOR:

Huixin Liu, Kyushu University, Japan

Increasing CO_2 in the atmosphere is predicted to produce long-term trend in the thermosphere and ionosphere, along with tropospheric warming. However, the thermosphere and ionosphere are first and foremost dominated by the solar and geomagnetic activity (GA) forcing, making it challenging to search CO_2-driven signal in observations. In this study (Liu et al, JGR, https://doi.org/10.1029/2020JA028607, 2021), we examine the interaction between GA forcing and CO_2 forcing using the GAIA whole atmosphere model. The model reveals three salient features. (1) increasing GA always weakens the CO_2-driven trend at a fixed altitude. (2) increasing GA forcing can either strengthen or weaken CO_2-driven trend in hmF2 and NmF2, depending on local time and latitudes. This renders invalid the widely used linear fitting methods for GA removal. (3) An interdependency exists between the efficiency of CO_2 and GA forcing, with the former enhances at lower GA levels while the latter enhances at higher CO_2 concentration. This implies that the CO_2-driven trend would accelerate in periods of declining GA, while effects of magnetic storms will become larger with increasing CO_2 in the future. These effects are closely related to circulation and tidal changes in the thermosphere as well (Liu et al., GRL, https:// doi.org/10.1002/2020GL087413). These model experiments provide a preliminary framework to understand interactions between meteorological forcing from from below and the geomagnetic forcing from above.

KEYWORDS : long-term trend, ionosphere and thermosphere, geomagnetic activity

Sr No: 363

TIRO: A project to gain insight into the topside ionosphere using LEO satellites

CORRESPONDING & PRESENTING AUTHOR:

Lucas Schreiter, German Center for Geoscience, Potsdam, Germany

Guram Kervalishvili, German Center for Geoscience, Potsdam, Germany

Claudia Stolle, German Center for Geoscience, Potsdam, Germany

Jose Van Den Ijssel, TU Delft, Netherland

Jan Rauberg, German Center for Geoscience, Potsdam, Germany

Daniel Arnold, Uni Bern, Switzerland

Chao Xiong, Wuhan University, China

Bernhard Fluche, German Center for Geoscience, Potsdam, Germany

Observations from Low Earth Orbiting (LEO) satellites are the only means to access the topside ionosphere globally. The upper atmosphere, including the ionosphere, has been known to be sensitive to long-term trends, e.g., in neutral composition, geomagnetic field, or solar radiation, among others. Continuous long-term data sets are thus of large importance to allow for possible quantification. Topside Ionosphere Radio Observations from multiple LEO-missions (TIRO) is a project in ESA's Swarm DISC framework, which will provide accurate radar-leveled in situ electron density from GRACE and GRACE-FO K-Band observations. Furthermore, GPS-TEC obtained from zenith-looking GPS antennas at CHAMP, GRACE, and GRACE-FO will be provided, which will be consistent with already existing products from the Swarm and GOCE missions. With the expected public release of the project results in early 2022, the data allows covering periods from 2000 until today, e.g., almost two solar cycles, without significant observation gaps. The altitudes covered are as low as 250 km for GOCE and near 500 km for GRACE(-FO).

We will show the first results for the calibrated data and will discuss comparisons to independent models and observations collected by other missions. Conjunctions between different LEO satellites will be shown as they are of particular interest to evaluate the consistency, and in addition allow to investigate dynamic of small-scale phenomena in the ionosphere, such as describing the morphology of irregularities.

KEYWORDS :   GPS, GRACE, Ionosphere

Sr No: 364

Multi-decadal study of geocoronal hydrogen Balmer-alpha emission intensity from Northern mid-latitudes

CORRESPONDING & PRESENTING AUTHOR:

Susan Nossal, University of Wisconsin-Madison, USA

Edwin Mierkiewicz, Embry-Riddle Aeronautical University, USA

Liying Qian, National Center for Atmospheric Research, USA

R. Carey Woodward, University of Wisconsin-Oshkosh at Fond du Lac campus, USA

L. Matthew Haffner, Embry-Riddle Aeronautical University, USA

Joseph Mcinerney, National Center for Atmospheric Research, USA

Stan Solomon, National Center for Atmospheric Research, USA
Hanli Liu, National Center for Atmospheric Research, USA
Arianna Ranabhat, University of Wisconsin-Madison, USA

Ground-based Fabry-Perot observations of geocoronal hydrogen Balmer-alpha emissions taken from Northern mid-latitudes span multiple solar cycles, facilitating investigation of decadal scale variations, including natural variability in the hydrogen response to solar geophysical changes. The observations suggest a somewhat surprising increase in hydrogen emission intensity between the solar-maximum period of 1990-1991 (S.C. 22) and the near-solar-maximum period of 2000-2001 (S.C. 23), with the caveat that this is a limited data set and that there are calibration uncertainties. The apparent intensity increase is counter to previous midlatitude observations for which the observed hydrogen Balmer-alpha column intensity increases with higher solar activity. We will discuss the extended Northern hemisphere hydrogen emission data set, including strategies for assessing uncertainty and data quality. We will also discuss interpretation of these observations in the context of climate simulations with the NCAR Whole Atmosphere Community Climate Model-eXtended (WACCM-X).

KEYWORDS : thermosphere, solar-terrestrial, airglow

Sr No: 365

SYMPOSIUM : **2.3 Stratosphere-Mesosphere-Thermosphere-Ionosphere System – Long-Term**

EUV Solar Occultations of the Thermosphere Reveal Unexpectedly Cool Temperatures at the Evening Terminator

CORRESPONDING & PRESENTING AUTHOR:
Ed Thiemann, University of Colorado, USA
Marie Dominique, Royal Observatory of Belgium, Belgium

The LYRA instrument onboard the PROBA2 spacecraft measures total number density (O+N2) in the thermosphere between 150 and 350 km via solar occultations. Measurements have been made annually beginning in 2010 through the present, over the northern hemisphere during the spacecraft's eclipse season which spans mid-November to mid-February. Recent data processing updates have enabled the measurement of temperature profiles form 150 to 350 km with an estimated accuracy better than 5%. Temperatures from 2010 to 2017 are compared with estimates from the MSIS empirical model and show good agreement at the dawn terminator but LYRA is markedly cooler at the dusk terminator, with the MSIS-LYRA temperature difference increasing with solar activity. Anthropogenic cooling can explain this discrepancy at periods of lower solar activity, but the divergence of temperature with increasing solar activity remains unexplained. In this presentation, we review both the LYRA data processing updates and comparisons with MSIS.

KEYWORDS : thermosphere density, thermosphere cooling, solar occultations

Sr No: 366

The energy budget of the upper mesosphere and lower thermosphere from 20 years of TIMED data

CORRESPONDING & PRESENTING AUTHOR:

Martin Mlynczak, NASA Langley Research Center, USA

Linda Hunt, SSAI, USA

We present an evaluation of the energy budget of the upper mesosphere and lower thermosphere (0.1 hPa to 1 e-04 hPa; 65 km to 105 km) using 20 years of data from instruments on the TIMED satellite. Heating due to the absorption of solar radiation from the near-infrared to Lyman-alpha is included as is heating due to seven exothermic chemical reactions. Radiative cooling from carbon dioxide, ozone, and water vapor is included. Zonal and global annual averages of the total heating and cooling are developed. In general, we find that the total heating and cooling terms are in approximate balance in the annual global average. In the lower thermosphere we find that radiative cooling exceeds the total heating. This result implies non-radiative sources of energy (possibly turbulent dissipation?) to achieve long term balance in the energy budget. Substantial variation in the energy budget observed over the two solar cycles has been observed.

KEYWORDS :   climate, energy budget, solar cycle

IAGA Division III

3.1 Reporter review for Div III (by invitation)

CONVENERS: Simon Wing

George Balasis

This session presents reviews of the scientific progress in the Div III in the last few years.

Sr No: 367

Recent progresses in machine learning applications to space physics (by invitation)

CORRESPONDING & PRESENTING AUTHOR:

Giovanni Lapenta, KULeuven, Belgium

Turbulent systems are host to two key processes: reconnection and energy exchanges between particles and electromagnetic fields. An important aspect is the ability to detect where such processes happen and what correlations exist between these two processes and between them and other processes or conditions observed within the system. We report on the activities of the European Horizon 2020 project AIDA (www.aida-space.eu) and describe some new approaches to investigate these processes and to analyse their correlations. We will focus on two approaches. First are physics-based methods that use intrinsic properties to identify processes. An example is the use of peculiar properties of the Lorentz transformation to identify reconnection regions [1].

Second, machine learning techniques can be used to classify local conditions and flag areas of interest [2]. Both approaches will be shown in simulation results and in data from the MMS mission. We will focus on the turbulent outflows of reconnection sites. The primary sites form large outflow jets that become turbulent and produce energy exchanges and additional secondary reconnection sites.

[1] Lapenta, Giovanni. "Detecting reconnection sites using the Lorentz Transformations for electromagnetic fields." The Astrophysical Journal 911.2 (2021): 147.

[2] Dupuis, Romain, et al. "Characterizing magnetic reconnection regions using Gaussian mixture models on particle velocity distributions." The Astrophysical Journal 889.1 (2020): 22.

KEYWORDS : turbulence, energization, reconnection

Sr No: 368

Reporter review: Earth's ring current (by invitation)

CORRESPONDING & PRESENTING AUTHOR:

Kunihiro Keika, The University of Tokyo, Japan

The Earth's ring current, the westward current flowing in the inner magnetosphere, is primarily responsible for a decrease in the geomagnetic field at low latitudes, called a magnetic storm. The ring current is determined by the plasma pressure and its spatial gradient in the inner magnetosphere. The pressure is dominated by ions with energies of a few to a few hundreds of keV. O+ ions of ionospheric origin makes a significant contribution to the ion pressure during geomagnetically active periods. The spatio-temporal variations are affected by the electromagnetic coupling with the ionosphere and the magnetotail.

Recent in-situ observations of oxygen ions as well as protons in the severe radiation environments by multiple spacecraft from successful missions have made a significant contribution to advancing our understanding of the ring current dynamics such as spatio-temporal variations and composition. Advances in numerical modeling, particularly the coupling between different simulation models, have also contributed to quantifying the ring current dynamics and connections with other surrounding regions such as the ionosphere and

magnetotail. Simultaneous observations of space- and ground-based observations have provided important clues in the detailed structures of energetic ion spatial distributions. This reporter review will present new scientific results selected from these contributions during the past two years.

Sr No: 369

SYMPOSIUM : **3.1 Reporter review for Div III**

Magnetic reconnection (by invitation)

CORRESPONDING & PRESENTING AUTHOR:

Mikhail Sitnov, JHU/APL, USA

Magnetic reconnection, a key mechanism transferring energy from sheared and stretched magnetic fields to plasma heating and acceleration, remains in the focus of the main magnetospheric missions and modeling studies. Recent MMS observations helped evaluate the reconnection electric field near dayside X-lines. It is found that mass-loading by O+ ions can slow the rate of magnetopause reconnection, but the effect is transient. THEMIS and GOES observations demonstrated that, for a strong solar wind driving, the magnetic storms can be directly powered by near-Earth magnetotail reconnection. Particle acceleration mechanism unique to time-dependent magnetotail reconnection is found in consecutive jet fronts. Electron-only reconnection has been detected in the bow shock, turbulent magnetosheath and the magnetotail. Onset of reconnection in the latter goes through the phase when diverging flows already exist, while the X-lines are not formed yet. Agyrotropy parameters have been found to quantify demagnetization of ion and electron species on the way to magnetotail reconnection onset. Data mining of substorms revealed regimes of unsteady and steady reconnection in the tail, consistent with mining-guided simulations of the reconnection onset. Energetic electrons as tracers of a complex magnetic topology reveal interesting features of the magnetotail reconnection, combining chaotic motion and surprisingly coherent gyrophase bunching within a few thousand kilometers of the reconnection site. Combined MHD and particle description of plasma electrons explain the formation of their power-law spectra over more than two decades in energy. These and other results of the last two years of reconnection studies in the magnetospheric plasmas are discussed.

Sr No: 370

SYMPOSIUM : **3.1 Reporter review for Div III**

IAGA Reporter Review: Magnetosphere-Ionosphere Coupling (by invitation)

CORRESPONDING & PRESENTING AUTHOR:

James Weygand, University of California, Los Angeles,USA

The coupled magnetosphere ionosphere system is highly complex. The ionosphere influences the magnetosphere through ion outflow, the magnetosphere influences the ionosphere through energetic particle precipitation, and both exchange momentum and energy through field aligned currents and waves. Unraveling the coupling between different regimes is accomplished and understood through in-situ and remote sensing observations and the importance and understanding of various coupling process in the system is tested by modelers and experimentalists. Big data analysis techniques, multi-point observations, and improved

modeling capabilities are providing us the means by which to study and understand the complex interactions in the magnetosphere ionosphere system. In this review we will focus on recent advances in our understanding of magnetosphere-ionosphere coupling, including observational and modeling based.

KEYWORDS :   magnetosphere-ionosphere coupling

Sr No: 371

Reporter review: Magnetotail plasma transport (by invitation)

CORRESPONDING & PRESENTING AUTHOR:

Masaki Nishino, JAXA/ISAS, Japan

Supply, transport and loss of plasma in the magnetotail are fundamental processes of magnetospheric physics, particularly from the viewpoint of Magnetosphere-Ionosphere coupling as well as connection between the outer magnetosphere and the inner magnetosphere. For the southward IMF condition, plasma transport through magnetic reconnection is a dominant process in the magnetosphere, and turbulence in the magnetotail also likely plays an important role in plasma heating as well as transport. On the other hand, for the northward IMF cases, plasma transport processes in the magnetotail has not yet been fully understood. However, from both observations and simulations, there have been remarkable progresses of understanding the phenomena during northward IMF including plasma supply from the solar wind as well as plasma transport inside the magnetotail. In particular, recent observations of cold ion jets in the cold-dense plasma sheet will be focused on. Finally, plasma transport in the magnetotail under the very low-density solar wind will be mentioned. The low-beta plasma environment in the magnetosheath facilitates magnetic reconnection at the tail flank magnetopause, which may change plasma transport path in the magnetotail.

KEYWORDS :   magnetotail, plasma transport, solar wind entry

Sr No: 372

Earth's Radiation Belts: Recent Results and Outstanding Mysteries (by invitation)

CORRESPONDING & PRESENTING AUTHOR:

Sasha Ukhorskiy, JHU/APL

Near-Earth space permeated with strong dipolar magnetic field produces radiation belts: relativistic electrons and penetrating ions trapped in the magnetic field on quasi-periodic trajectories around the planet. Ever since the discovery of radiation belts by pioneering space missions in 1050s the mechanisms sculpting their intensities have been a subject of scientific debate. Recent observations throughout the solar system and beyond showed the universality of processes that generate intense particle radiation within magnetized environments such as Earth's. Earth's radiation belts are a unique natural laboratory for developing our understanding of the particle energization processes that operate across the universe. Moreover, increased levels of particle radiation can damage and destroy orbiting spacecraft and is hazardous for astronauts health, hence, understanding to the level of predictability, of how particle radiation is produced and vary is critical for mitigating their adverse impacts. Due to a remarkable increase in wealth of the radiation belt data due
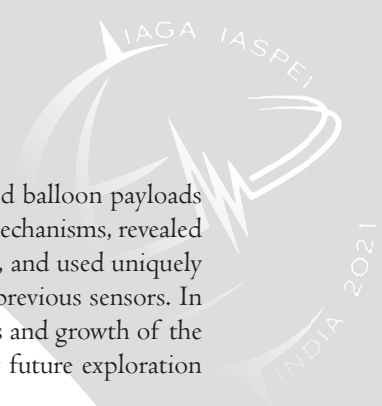
to recent space Van Allen Probes (NASA), Arase (JAXA) and low-altitude CubeSats and balloon payloads we quantified previously suggested energization processes, discovered new energization mechanisms, revealed the critical importance of dynamic plasma injections into the innermost magnetosphere, and used uniquely capable instruments to unveil inner radiation belt features that were all but invisible to previous sensors. In this paper we outline recent advancements in our understanding of radiation belt physics and growth of the predictive capabilities and discuss some of the outstanding mysteries to be resolved by future exploration mission into Earth's inner magnetosphere.

KEYWORDS : radiation belts, energetic particles

Sr No: 373

SYMPOSIUM : **3.1 Reporter review for Div III**

Reporter review on ULF waves (by invitation)

CORRESPONDING & PRESENTING AUTHOR:

Kazue Takahashi, Johns Hopkins University Applied Physics Laboratory, USA

This presentation provides an overview of ULF wave research in the past two years. The topics include wave excitation by solar wind disturbances and instabilities in the ion foreshock, wave generation within the magnetosphere, interaction of waves with energetic particles, and waves at other planets. The presentation covers both observations and theoretical analyses. Also included are measurement techniques and diagnostic use of the waves.

KEYWORDS : ULF waves, observation, theory

Sr No: 374

SYMPOSIUM : **3.1 Reporter review for Div III**

Recent Advances in Understanding the Physics of the Dayside Solar Wind-Magnetosphere Interaction (by invitation)

CORRESPONDING & PRESENTING AUTHOR:

Katariina Nykyri, Embry-Riddle Aeronautical University, USA

NASA Magnetosphere Multi-Scale Mission was launched in March 2015 from Cape Kennedy in Florida. The in-situ four-point measurements at ion and electron scales have helped understand and uncover microphysics of magnetic reconnection, plasma waves and plasma instabilities at shocks, dayside magnetosheath and magnetosphere. Together with other space missions (e.g., THEMIS, Cluster, Geotail and Van Allen Probes) and ground-based observatories, combined with progress in numerical modeling, have made it possible to make major breakthroughs understanding both the microphysics and global-scale processes associated with the dayside solar wind-magnetosphere interaction. This reporter review will discuss progress and highlights of these discoveries from recent years.

KEYWORDS : solar wind -magnetosphere coupling

Sr No: 375

Space weather: Progress in recent years (by invitation)

CORRESPONDING & PRESENTING AUTHOR:

Minna Palmroth, University of Helsinki, Finland

This presentation reviews first the status of space weather activities during the last few years from the perspective of scientific and operational activities. In terms the science of space weather, emphasis is laid on the modelling activities, which form the basis for space weather predictions. Recent observational capabilities including monitoring of the Sun are reviewed as well.

The presentation then goes on to review the operational capabilities within space weather, indicating the newest progress in building space situational awareness systems working 24/7.

Finally, the presentation reviews the gaps in our knowledge both in terms on science of space weather, as well as from the monitoring and predicting point of view. The future needs are presented, emphasising especially the need to monitor and model the near-Earth space systematically to accurately describe the impacts of space weather. It is also of vital importance to prepare for the most extreme space weather, and to develop protocols and procedures that can protect the critical societal infrastructure against the fury of the Sun.

3.2 The expanding regimes of ULF wave research

CONVENERS: Jayashree Bulusu

Kazue Takahashi

Masahito Nose

ULF wave research has a long-standing history and equally significant ongoing efforts in explaining some of the fundamental problems of magnetospheric research viz: energy transport during dynamic coupling of solar wind-magnetosphere, wave particle interaction, flux rope disruptions during active geomagnetic conditions. The research has a far-reaching implication in modelling the mass densities using field line resonances and extends to higher frequencies covering the IAR (Ionospheric Alfven resonator) and ELF bands in probing the lowest ionospheric layers. This ULF session focuses on the advancement in the understanding of ULF wave propagation and transport of energy in the geospace and other planetary environments. Papers are invited from observations of ULF waves with satellites and ground based experiments depicting transmission of energy from the solar wind, internal ULF instabilities, magnetosphere-ionosphere coupling, field line resonances, investigations of IAR and SR (Schumann Resonances) and their relation to ULF waves. Papers depicting the developments in analytic, numerical, and machine learning techniques are also encouraged regarding generation and propagation of ULF waves and the role of the waves in probing the magnetosphere.

Sr No: 376

An analysis of some critical aspects of the comparison between solar wind and magnetospheric fluctuations: a case study.

CORRESPONDING & PRESENTING AUTHOR:

Dario Recchiuti, Università degli Studi dell'Aquila - Consorzio "Area di Ricerca in Astrogeofisica",Italy

Umberto Villante, Universià degli Studi dell'Aquila - Consorzio "Area di Ricerca in Astrogeofisica", Italy

Simone Di Matteo, Catholic University of America, USA

Several critical aspects may influence the analysis of the relationship between the solar wind (SW) and the magnetospheric fluctuations: for example, the characteristics and the frequency of the SW fluctuations that are expected to impinge the magnetosphere may be not the same when they are observed by spacecraft at different places in front of the magnetosphere; similarly, the choice of the analytical methods adopted for the spectral analysis might influence the frequency estimate (as well as the wave identification itself) both in the SW and in the magnetosphere (Di Matteo and Villante, 2017, 2018).

Focusing attention on these aspects, we present a case study analyzing the compressional fluctuations (f ≈ 1-5 mHz), following an interplanetary shock, showing that some differences in the characteristics of the SW fluctuations emerge when the same stream is observed at different places.

Our results also confirm the critical role of the analytical methods in determining the fluctuation characteristics. We then compared the aspects of the SW fluctuations with those of the magnetospheric fluctuations following the corresponding sudden impulse, as observed by two satellites at geostationary orbit and at several ground-based stations.

We found that the fluctuations observed in the magnetosphere were related to compressional SW fluctuations approximately at the same frequencies, with no evidence for wave activity of internal origin, or directly driven by the shock impact.

KEYWORDS :   solar wind and magnetospheric waves, event identification, frequency estimate

Sr No: 377

Statistical analysis of Pi2 wave fields detected by Van Allen Probes

CORRESPONDING & PRESENTING AUTHOR:

Kazue Takahashi, Johns Hopkins University Applied Physics Laboratory, USA

Robert Lysak, University of Minnesota, USA

Massimo Vellante, University of L'Aquila, Italy

John Wygant, University of Minnesota, USA

Craig Kletzing, University of Iowa, USA

We have analyzed electric and magnetic field data from Van Allen Probes to understand the spatial variation of Pi2 waves in the inner magnetosphere. Pi2 wave events were selected by using an automated algorithm that identifies peaks in the power spectra computed from magnetic fields measured at low-latitude ground

stations located between 22 and 02 MLT. This algorithm is capable of selecting two peaks (fundamental and second harmonic modes) at a given time step. For the selected Pi2 events we computed the coherence, amplitude ratio, and cross-phase between the magnetic field components (H and D) on the ground and all field components at the spacecraft. We statistically processed data covering the entire spacecraft mission period (2012-2019) and generated 2d images of the magnetospheric Pi2 wave fields covering L < 6 and all MLT. The images reveal radial Pi2 mode structures of the fundamental and second harmonic in the midnight sector, which confirm cavity mode oscillations. The images also show MLT variations of Pi2 wave fields that were not obvious in previous statistical studies. We compare the observations with numerical simulations that incorporate a realistic magnetospheric mass density distribution.

KEYWORDS : Pi2 waves, van allen probes

Sr No: 378

MMS Observations of waves in the Pc1 band with constant frequency across L shells: Wave curl analysis of propagation vectors and investigation of their source mechanisms

CORRESPONDING & PRESENTING AUTHOR:

Mark Engebretson, Augsburg University, USA

Sarah Vines, Applied Physics Laboratory, USA

Brian Anderson, Applied Physics Laboratory, USA

Robert Allen, Applied Physics Laboratory, USA

Kristoff Paulson, Smithsonian Center for Astrophysics, USA

Richard Denton, Dartmouth College, USA

Jay Johnson, Andrews University, USA

Christopher Russell, University of California, Los Angeles, USA

Magnetospheric Pc1 waves are usually attributed to ion cyclotron instabilities driven by positive temperature anisotropies, and have frequencies that are determined by, and are generally proportional to, the ion gyrofrequencies at the location of their origin. Paulson et al. (2014, 2017) observed a large number of wave events in data from the equatorially-orbiting Van Allen Probes spacecraft with frequency independent of the local ion cyclotron frequency, many of them characterized by a pearl structure. This study reports observations of similar waves in data from the Magnetospheric Multiscale (MMS) spacecraft, and applies a newly developed technique, wave curl analysis (Vines et al., 2021) to accurately determine the propagation vector (k) of these waves. Energetic particle data from the HPCA instrument on MMS and available ground-based magnetometer data are used to further characterize selected wave events. Preliminary results suggest that these waves are either triggered by mode conversion from magnetosonic waves or are themselves specific modes of magnetosonic waves.

KEYWORDS : ULF Waves, EMIC Waves

Sr No: 379

Generation of Non-Substorm Pi2s at Low and Middle Latitudes

CORRESPONDING & PRESENTING AUTHOR:

Manjula Lingala, CSIR-NGRI, India

This study analyses the characteristics of non-substorm Pi2 (3 – 25 mHz) from low and middle latitudes. Pi2 events are identified from geomagnetic H-component data from low and middle latitude observatories Hyderabad (HYB, L¼ 1.03) and Paratunka (PET, L¼ 2.1) respectively, during solar maximum period (2015 – 2016) for quietest geomagnetic conditions, with stringent criteria of interplanetary parameters and activity indices. Data from five high-latitude stations from THEMIS ground magnetometer chain, covering all local time sectors are additionally analysed to verify the absence of substorms, pseudo substorms, etc. which may also generate Pi2 signatures. Variation of non-substorm Pi2 periods with geomagnetic activity index Kp and solar wind speed (Vsw) show inverse relations with Pi2 period at HYB. In addition, non-substorm Pi2s are distributed equally in all local time sectors with ratio of second harmonic to fundamental Pi2 ranging within 1.3 –2.2. These trends of non-substorm Pi2s indicate plasmaspheric cavity resonance (PCR) as the dominant source at low latitude, confirmed using a theoretical model. In contrast, non-substorm Pi2 periods do not show a steady trend with Kp and Vsw at mid-latitude station PET. Local time variations show an increased period in the pre-midnight sector at PET. A close agreement between theoretical estimates and observed periods of non-substorm Pi2-s at PET, leads to the inference of Alfven nature of these modes, attributable to a resonant oscillation.

KEYWORDS :   Non-substorm Pi2s, plasmaspheric cavity resonance (PCR), Pi2 periods

Sr No: 380

What Control Excitation of Quarter Waves? (by invitation)

CORRESPONDING & PRESENTING AUTHOR:

Yuki Obana, Osaka Electro-Communication University, Japan
Robert L. Lysak, University of Minnesota, USA
Colin L. Waters, University of Newcastle, USA
Murray D. Sciffer, University of Newcastle, USA

The low beta plasma of the inner magnetosphere supports two ULF wave modes, the shear Alfven mode and fast mode. The fast mode can exhibit cavity mode resonances, whereas, the shear Alfven mode forms standing wave structures well-known as field line resonances (FLRs). These modes are coupled due to the magnetosphere geometry and plasma distribution, and also from the anisotropic ionospheric conductivities. In studies of ULF waves, it is often assumed that the ionospheric signatures are very similar at conjugate points, however, differences between the two hemispheres can occur. When the ionosphere has very different conductance between conjugate points, the FLR forms a node-like structure in the electric field in the sunlit side with an antinode-like structure in the dark ionosphere. These waves are called "quarter wave".

Using magnetic field data from latitudinally separated stations in New Zealand, we have investigated the detailed wave characteristics of quarter wave modes. Furthermore, we have simulated FLRs using the
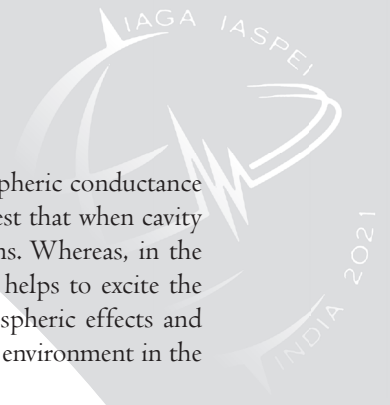
three-dimensional model of ULF waves in a dipolar magnetosphere that includes ionospheric conductance effects. The observational results are well supported by the simulations which also suggest that when cavity resonances are pronounced, quarter waves may be masked by the fast mode oscillations. Whereas, in the dark ionosphere, the waves are attenuated and the "moderate" cavity mode amplitude helps to excite the quarter waves. This implies that an understanding of ULF waves should include ionospheric effects and that quarter waves are a key phenomenon to include in understanding the complex wave environment in the magnetosphere.

KEYWORDS : ULF wave, Magnetosphere-Ionosphere coupling, inner-magnetosphere

Sr No: 381

SYMPOSIUM : **3.2 The expanding regimes of ULF wave research**

Second harmonic poloidal standing Alfvén waves excited by a steep gradient of proton phase space density at the edge of the nose structure (by invitation)

CORRESPONDING & PRESENTING AUTHOR:

Kazuhiro Yamamoto, Graduate School of Science, The University of Tokyo, Japan

Kanako Seki, Graduate School of Science, The University of Tokyo, Japan

Masahito Nose, Nagoya University, Japan

Ayako Matsuoka, Kyoto University, Japan

Mariko Teramoto, Kyushu Institute of Technology Faculty of Engineering, Japan

Reiko Nomura, Japan Aerospace Exploration Agency (JAXA) , Japan

Satoshi Kasahara, Graduate School of Science, The University of Tokyo, Japan

Shoichiro Yokota, Graduate School of Science, Osaka University, Japan

Kunihiro Keika, Graduate School of Science, The University of Tokyo, Japan

Kazushi Asamura, Japan Aerospace Exploration Agency (JAXA) , Japan

Yoshiya Kasahara, Kanazawa University, Japan

Atsushi Kumamoto, Tohoku University, Japan

Fuminori Tsuchiya, Tohoku University, Japan

Masafumi Shoji, Nagoya University, Japan

Yoshizumi Miyoshi, Nagoya University, Japan

Iku Shinohara, Japan Aerospace Exploration Agency (JAXA), Japan

Geoff Reeves, Los Alamos National Laboratory, USA

Harlan Spence, University of New Hampshire, USA

Poloidal standing Alfvén waves can obtain their energy from energy gradient or radial gradient in the phase space density of resonant particles through the drift-bounce resonance. Because the temporal and spatial variations of low energy (1-10 keV) ions are more complicated than high energy (> 100 keV) ions, the importance of the low energy ions in the excitation of the poloidal waves is not fully understood.

In this study, we examine the second harmonic poloidal wave observed by the Arase satellite and demonstrate that the poloidal waves were excited by ~12 keV protons. The azimuthal wave (m) number was estimated to be positive (eastward propagation) and ~180 from the finite Larmor radius effect of protons and the theory of the drift-bounce resonance. The steep outward gradient of the proton phase space density well corresponds to the exciting regions of waves (L = 5.7-6.1), suggesting the outward gradient of protons supplies free energy to the waves.

The time variation of radial distributions of the resonant protons was measured by the Arase and RBSP-B satellites. At L ~ 5.7, RBSP-B measured a sudden increase of ~10 keV protons 1.5 hours after the wave excitation detected by Arase. From the analytical formulae of diffusion coefficient (DLL) and energy variations with L (dW/dL), we found that protons can move ~0.4 Re inward in 1.5 hours, decreasing their energy by ~2 keV through the drift-bounce resonance. We interpret the sudden increase at ~10 keV as a result of the radial diffusion of ~12 keV protons.

KEYWORDS : poloidal standing Alfvén wave, drift-bounce resonance, radial diffusion

Sr No: 382

Observation of the dayside Pc4-5 wave before the substorm

CORRESPONDING & PRESENTING AUTHOR:

Aleksandr Rubtsov, Institute of Solar-Terrestrial Physics of the Siberian Branch of the Russian Academy of Sciences, Russia
Olga Mikhailova, Institute of Solar-Terrestrial Physics of the Siberian Branch of the Russian Academy of Sciences, Russia
Dmitri Klimushkin, Institute of Solar-Terrestrial Physics of the Siberian Branch of the Russian Academy of Sciences, Russia
Jie Ren, Peking University, China
Qiugang Zong, Peking University, China

We present a preliminary analysis of the observation of the poloidal Pc4-5 wave on the dayside of the magnetosphere 30 minutes before the substorm. This wave was observed for ~15 hours by widely spaced satellites of three missions (Van Allen Probes, THEMIS, GOES): 7-17 MLT and L = 4.5-8 RE. The substorm injection on the nightside observed by GOES15 was 20 minutes after the wave appearance. The AE index started to increase ~10 minutes later. Note that the solar wind conditions were quiet, and there were no magnetic storm or substorm activities within at least 12 hours before. The combined observations demonstrate discrete frequency dependence on L-shell and no specific azimuthal frequency distribution. The measurements at the same L-shell at different times show frequency increase with time. Some oscillations were observed in the energy range 30-500 keV in both ion and electron data, but it didn't cover the whole interval under consideration. The azimuthal wave number was preliminary calculated using the finite gyroradius effect and equals –(20-80).

KEYWORDS : ULF waves, substorm, data analysis
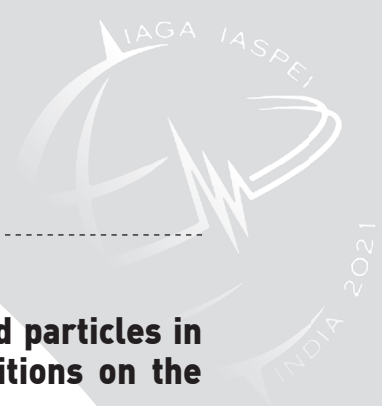
Sr No: 383

Resonance interaction between Alfvenic waves and charged particles in Earth's magnetosphere under asymmetric boundary conditions on the ionosphere: the quarter-wave case

CORRESPONDING & PRESENTING AUTHOR:

Ekaterina Smotrova, ITMO University, Russia

Dmitri Klimushkin, Institute of Solar-Terrestrial Physics, Siberian Branch of the Russian Academy of Science, Russia

Pavel Mager, Institute of Solar-Terrestrial Physics, Siberian Branch of the Russian Academy of Science, Russia

The ULF waves are a significant factor of space weather because they participate in the processes of interaction with high-energy charged particles in Earth's magnetosphere. This work is concerned with the wave-particle interaction according to the theory of drift-bounce resonance suggested by Southwood and Kivelson (1981). We have studied the dynamics of motion of a charged particle, such as proton or electron, in the electric field of ULF waves by means of numerical calculations. In our study, we mainly considered poloidal Alfvenic waves in the magnetosphere under asymmetric boundary conditions on the ionosphere: the so-called quarter-waves. The simulation was provided in two cases: the equatorial one, when the particle moves near the magnetic equator, and the general. For both cases, the dipole approximation of the Earth's magnetic field was adopted, also the bounce and the drift motion of particles were taken into account. Based on the obtained results, we made a conclusion that the theory of drift-bounce resonance is applicable for the quarter-wave case and conditions for its occurrence are not different from resonance for the half-wave case. Specifically, the resonance between the charged particle and the ULF-waves in the case of the quarter-wave is only possible, when the bounce harmonic number and azimuthal wave number are integers.

KEYWORDS : wave-particle interaction, drift-bounce resonance, ULF waves

Sr No: 384

ULF Wave Power During Geomagnetic Storms and Implications for Radial Diffusion Processes (by invitation)

Jonathan Rae, Northumbria University, UK

CORRESPONDING & PRESENTING AUTHOR:

Jasmine Sandhu, Northumbria University, UK

John Wygant, University of Minnesota, USA

Aaron Breneman, NASA Goddard Space Flight Center, USA

Sheng Tian, University of Minnesota, USA

Frances Staples, University College London, UK

Mariatheresia Walach, Lancaster University,UK

David Hartley, University of Iowa,USA

Clare Watt, Northumbria University, UK

Tom Elsden, University of Leicester, UK

Richard Horne, British Antarctic Survey, UK

Louis Ozeke, University of Alberta, Canada

Marina Georgiou, National and Kapodistrian University of Athens, Greece

Kyle Murphy, n/a

ULF waves drive radial diffusion of radiation belt electrons, where this process contributes to energisation, loss, and large scale transport of the outer radiation belt. In this study we quantify the changes and variability in ULF wave power during geomagnetic storms, through a statistical analysis of Van Allen Probes data. The results show global wave power enhancements during the main phase of storms. Local time asymmetries show sources of ULF wave power are both external solar wind driving as well as internal sources.

The statistical analysis demonstrates that storm time ULF waves are able to access lower L values compared to pre-storm conditions. We assess how magnetospheric compressions and cold plasma distributions shape how ULF wave power propagates through the magnetosphere. Results show that the Earthward displacement of the magnetopause is a key factor in the low L enhancements. Furthermore, the presence of plasmaspheric plumes during geomagnetic storms plays a crucial role in trapping ULF wave power, and contributes significantly to large storm time enhancements in ULF wave power.

The results have clear implications for enhanced radial diffusion of the outer radiation belt during geomagnetic storms. Estimates of storm time radial diffusion coefficients are derived from the ULF wave power observations, and compared to existing empirical models of radial diffusion coefficients. We show that current Kp-parameterised models, such as the Ozeke et al. [2014] model, do not fully capture the large variability in storm time radial diffusion coefficients or the extent of enhancements in the magnetic field diffusion coefficients.

KEYWORDS : ULF, radiation belts

Sr No: 385

Using ULF Standing Alfvén Waves to Remotely Sense the Plasmasphere Dynamics (by invitation)

CORRESPONDING & PRESENTING AUTHOR:

Alfredo Del Corpo, University of L'Aquila, Italy

Massimo Vellante, University of L'Aquila, Italy

Balazs Heilig, Mining and Geological Survey of Hungary, Hungary

The plasmasphere is a torus-like region of dense and cold plasma that encircle the Earth and continuously changes its configuration in response to geomagnetic disturbances. Plasmasphere monitoring is an essential task to accomplish due to its central role in the space weather context. The magnetosphere is populated by traveling magnetohydrodinamic (MHD) compressive waves in the Ultra Low Frequency (ULF) range. Whenever the frequency of these forcing waves matches with the eigenfrequency of a given field line a ULF standing Alfvén wave is produced and resonance takes place. Field line resonances (FLRs) can be conveniently used to monitor the plasma mass density in the inner magnetosphere. Indeed, the FLR frequency is physically linked to the magnetic field topology and to the plasma mass density distribution along the geomagnetic field lines. FLR can be estimated by performing cross-spectral analysis of magnetic signals simultaneously recorded by latitude separated magnetic stations aligned along the same magnetic meridian. By using a network of station pairs at different latitudes it is possible to obtain the latitudinal FLR frequency profile. Starting from the FLR frequencies detected by such a network, the equatorial radial profile of the plasma mass density can be inferred by numerically solving the governing MHD wave equation, making assumptions on the magnetic field topology and on the plasma distribution along the field lines. We present recent developments of this technique applied to the European quasi-Meridional Magnetometer Array (EMMA) a network set up to monitor the plasmasphere in quasi real time.

KEYWORDS : field line resonances, plasmasphere dynamics, EMMA

Sr No: 386

Properties of Pc5 ULF waves at discrete frequencies during the impact of solar wind periodic density structures on the magnetosphere: a case study

CORRESPONDING & PRESENTING AUTHOR:

Simone Di Matteo, Catholic University of America, USA

Umberto Villante, University of L'Aquila, Italy

Nicholeen M. Viall, NASA - Goddard Space Flight Center, USA

Larry Kepko, NASA - Goddard Space Flight Center, USA

There are challenges in the identification of the nature and source of Pc5 ULF waves ($f \approx 1$–5 mHz) at discrete frequencies in the Earth's magnetosphere due to the variety of external and internal generation mechanisms and the ability to robustly identify such perturbations. To tackle the latter, we developed a spectral analysis procedure, based on the multitaper method, able to distinguish narrow-band and broad-band enhancements in power spectral density. We apply this procedure to magnetospheric field measurements at geostationary orbit and ground during the interaction of the magnetosphere with two interplanetary shocks followed by a train of solar wind periodic density structures (PDS) on November 9, 2002. After the first Sudden Impulse, we observed a damped fluctuation at $f \approx 1.9$ mHz at high latitude ground observatories, while after the second one a global oscillation at $f \approx 1.5$ mHz is detected at the geostationary orbit and ground. Shortly after, a train of ≈ 90-minute PDSs modulate the dimension of the magnetosphere cavity resulting in similar global oscillations of the magnetospheric field. At the impact of the first PDS, we identified additional waves at $f \approx 2.3$ and ≈ 3.5 mHz. In the second PDS, solar wind density fluctuations at $f \approx 2.6$ mHz drive global magnetosphere fluctuations. Towards the end of the PDS-magnetosphere interaction, we observed waves at $f \approx 1.9$ mHz and fluctuations encompassing a broad frequency range ($f \approx 2.4$–3.3 mHz). For the waves at discrete frequencies, the combination of satellites and ground magnetometers observations revealed their mode structure, locations and creation mechanism.

KEYWORDS :   ULF waves at discrete frequencies, global magnetospheric modes, solar wind mesoscale structures

Sr No: 387

Modelling the Varying Location of Field Line Resonances During Geomagnetic Storms

CORRESPONDING & PRESENTING AUTHOR:

Tom Elsden, University of Leicester, UK

Samuel Wharton, University of Leicester, UK

Jonathan Rae, Northumbria University, UK

Jasmine Sandhu, Northumbria University, UK

Maria Walach, Lancaster University, UK

Matthew James, University of Leicester, UK

Darren Wright, University of Leicester, UK

Tim Yeoman, University of Leicester, UK

Previous observational studies have shown that the natural Alfvén frequencies of geomagnetic field lines vary significantly over the course of a geomagnetic storm, decreasing by up to 50% from their quiet time values. This was recently demonstrated statistically using ground magnetometer observations across 132

geomagnetic storm events. This then brings into question where field line resonances (FLRs) will form in storm-time conditions relative to quiet times. Using 3D magnetohydrodynamic (MHD) simulations, we investigate how changes in the Alfvén frequency continuum of the Earth's dayside magnetosphere over the course of a geomagnetic storm affect the fast-Alfvén wave coupling. By setting the model Alfvén frequencies consistently with the observations, and permitting a modest change in the plasmapause/magnetopause locations, we show that FLR locations can change substantially during storms. The combined effects of higher fast waveguide frequencies and lower Alfvén frequencies during storm main phases act together to move the FLR locations radially inwards (by up to two Earth radii for the cases considered).

KEYWORDS :   ULF Waves, field line resonance, magnetosphere

Sr No: 388

Traveling through Field Line Resonances

CORRESPONDING & PRESENTING AUTHOR:

Tom Elsden, University of Leicester, UK

David Southwood, Imperial College London, UK

Using a 3D MHD simulation refined for analysis of terrestrial ULF signals in a dipole background field, we have reproduced multiple features of MHD waves observed during the final stages of the Saturn Cassini orbiter mission by the Cassini spacecraft magnetometer. We do this by reproducing what a spacecraft would see by analysing fields in the simulation as a time series along a curve through the simulation volume, representing the actual spacecraft orbit. Despite needing to allow for amplitude variation with latitude and magnetic shell, the Cassini measurements can be well modelled in this way. In particular, the complex phase structure of the azimuthal component in the vicinity of field line resonance is found to provide significant Doppler shifts. This effect leads to a counterintuitive result, that the resonant structure means the azimuthal field measured in the spacecraft frame may show a different apparent frequency to that of the meridional components. We shall provide both direct comparisons of field line resonance signals in data from Saturn's magnetosphere and the computer simulation, including crossing the same resonance north and south of the equator.

KEYWORDS :   ULF Waves, field line resonance, saturn

Sr No: 389

Excitation mechanism of internally driven ULF waves by the drift-bounce resonance with ring current ions based on the Magnetosphere-Ionosphere coupled model

CORRESPONDING & PRESENTING AUTHOR:

Tomotsugu Yamakawa, The University of Tokyo, Japan

Kanako Seki, The University of Tokyo, Japan

Takanobu Amano, The University of Tokyo, Japan
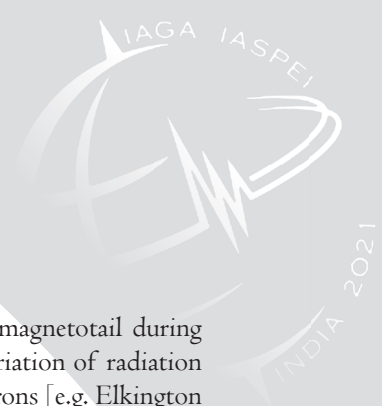
Naoko Takahashi, National Institute of Information and Communications Technology, Japan

Yoshizumi Miyoshi, Nagoya University, Japan

Aoi Nakamizo, National Institute of Information and Communications Technology, Japan

Internally driven ULF waves can be generated by ring current ions injected from the magnetotail during substorms. The excitation mechanism of ULF waves is a key to understand dynamic variation of radiation belt, since Pc5 (1.67-6.67 mHz) waves can drive radial diffusion of radiation belt electrons [e.g. Elkington et al., 2003]. Drift-bounce resonance [Southwood, 1976] has been considered as a candidate excitation mechanism. Previous spacecraft observations suggested drift-bounce resonance excitation of ULF waves [e.g. Takahashi et al., 2018]. However, excitation mechanism and global distribution of these waves are far from understood. This study aims to investigate the excitation of internally driven ULF waves based on the drift-kinetic model.

We performed a kinetic simulation by using GEMSIS-RC model [Amano et al., 2011], in which five-dimensional drift-kinetic equation for ion PSD and Maxwell equations are solved self-consistently. Simulation results have indicated that Pc5 waves are excited by the drift resonance under an isotropic Maxwellian PSD ion injection [Yamakawa et al., 2019]. We also found the drift-bounce resonance excitation of Pc3 waves under asymmetric butterfly type injection [Yamakawa et al., 2020].

Recently, we made Magnetosphere-Ionosphere coupling between GEMSIS-RC and GEMSIS-POT model [Nakamizo et al., 2012] in order to improve ionospheric boundary condition. GEMSIS-POT is a 2-D ionospheric potential solver. Simulation results have shown the excitation of Pc5 waves in the dayside (drift resonance) and Pc4 waves in the duskside (drift-bounce resonance). We will also report on the effects of R1FAC and R2FAC related electric field on the excitation of ULF waves.

KEYWORDS :   ULF waves, drift-bounce resonance, drift-kinetic simulation

Sr No: 390

SYMPOSIUM :   **3.2 The expanding regimes of ULF wave research**

THEMIS observations of double frequency Pc5 pulsations in the morning sector magnetosphere

CORRESPONDING & PRESENTING AUTHOR:

Galina Korotova, University of Maryland, USA

David Sibeck, NASA/GSFC, USA

We survey THEMIS magnetometer observations of double-frequency compressional Pc5 pulsations in the morning sector magnetosphere as a function of latitude and local time. We employ finite gyroradius techniques to determine the properties of these waves. We investigate their nodal structure. We use three distinct methods to study the propagation velocities of these double-frequency pulsations and find that they propagate antisunward. We test three proposed pulsation generation mechanisms and find that the drift-mirror instability provides the best explanation.

KEYWORDS :   PC5, pulsation

Sr No: 391

Generation of the ULF waves by a moving surface impulse on the magnetopause

CORRESPONDING & PRESENTING AUTHOR:

Dmitri Klimushkin, Institute of Solar-Terrestrial Physics, Russia

Pavel Mager, Institute of Solar-Terrestrial Physics, Russia

Qiugang Zong, Peking University, China

The spatio-temporal structure of ULF waves generated by a moving pressure impulse on the magnetopause is analytically explored. Two cases are considered: the slow impulse with the velocity much smaller than the Alfven speed, and the case when the source's velocity is larger than the Alfven speed. In the first case, it is found that the impulse generates two Alfven wave modes coined as the primary and the secondary modes. Superposition of the primary and secondary modes produces plasma vortices behind the source. In the second case, the moving source generates the fast mode which propagates into the magnetosphere as expanding Mach cone. Every point of the cone moves with the local Alfven speed. The magnetic shell where the local Mach number becomes equal 1 is the boundary for the mode propagation. This surface can be coined as the reflection surface. The wave cannot penetrate deeper than this surface. The Mach cone is reflected from the reflection surface, then expands outside and reflects from the magnetopause. Reflections from the reflection surface and the magnetopause leads to turning the Mach cone into the curved polyline.

KEYWORDS :   moving source, impulse excitation, ULF waves

Sr No: 392

Normal modes of Poloidal Field Line Oscillations: An Analytic Approach

CORRESPONDING & PRESENTING AUTHOR:

Adhitya Pavithran, Indian Institute of Geomagnetism, India

Jayashree Bulusu, National Geophysical Research Institute, India

Ashwini Kumar Sinha, Indian Institute of Geomagnetism, India

Geeta Vichare, Indian Institute of Geomagnetism, India

We develop an analytical model to study the normal modes of poloidal Alfven waves in the Earth's magnetosphere using idealistic, highly conducting ionospheric conditions at both ends of the field line. The ideal, cold, magnetohydrodynamic (MHD) equation is solved for transverse magnetic perturbations in a dipolar magnetic field. The plasma density distribution is assumed to be given by a power law, $1/r^m$, where r is the geocentric distance of any point on the field line and m is the density index. This model is an improvement over the traditionally used formal WKB approach to solve the field line equation, as it overcomes the inability of WKB method to deal with the singularities in the vicinity of the turning points. The eigenfrequencies and spatial structures are obtained analytically for guided poloidal oscillations, for different density indices, ranging from 0 to 6, at different L-values. Further the analytical results are compared with eigenfrequencies and spatial structures computed numerically.

KEYWORDS :   analytic model, poloidal mode, shear alfven waves

3.3 Recent advances in the system level understanding of solar wind – magnetopshere – ionosphere – thermosphere coupling

CONVENERS: Jone Peter Reistad

Kazuo Shiokawa

Geeta Vichare

The amount of available data describing the electrodynamics in geospace has significantly increased during the past decades. In addition, the improved physical understanding, computing power, and efforts to optimize numerical methods, has vastly improved the capabilities of modern physics-based models to describe in great detail the interactions taking place in this huge and complex system. This session welcomes presentations on all aspects of recent advances in our system level description of the coupled solar wind – magnetosphere – ionosphere – thermosphere system, including their evaluation using observations.

Sr No: 393

Mesoscale-resolving global modeling of stormtime geospace

CORRESPONDING & PRESENTING AUTHOR:

Viacheslav Merkin, The Johns Hopkins University Applied Physics Laboratory, USA

Kareem Sorathia, The Johns Hopkins University Applied Physics Laboratory, USA

Kevin Pham, NCAR, USA

Dong Lin, NCAR, USA

Shanshan Bao, Rice University, USA

Wenbin Wang, NCAR, USA

Frank Toffoletto, Rice University, USA

John Lyon, Dartmouth College, USA

Stormtime geospace exhibits some of the most complex and least understood interactions in space physics. This complexity is in large part due to both the cross-scale and cross-domain nature of these interactions. Indeed, during stormtime all domains of geospace become active while their interactions are mediated or driven by processes occurring across a broad range of scales. Therefore, a crucial requirement for any model of stormtime geospace is that it include all of its key domains while resolving all of the critical scales. In this presentation, we will review recent work by the team of the NASA DRIVE Center for Geospace Storms on the development of such a model that we call the Multiscale Atmosphere-Geospace Environment (MAGE) model. The mesoscale-resolving capabilities of MAGE across the domains of geospace will be demonstrated using simulations of resolution previously not accessible to community models, reaching the ion kinetic scales in the magnetotail and sub-100km scale in the ionosphere-thermosphere. Examples of several processes that are known to play a significant role in stormtime energy or mass redistribution throughout geospace will be shown including: the build-up of the ring current by mesoscale plasmasheet transport, magnetopause boundary instabilities, subauroral polarization streams, F-region ionosphere polar cap density patches, and travelling ionospheric and atmospheric disturbances. We will conclude with a discussion of further steps that need to be taken to ensure a more self-consistent representation of stormtime geospace in community models.

KEYWORDS : stormtime, geospace, mesoscale

Sr No: 394

The Two-Dimensional Evolution of Thermospheric $\sum$O/N 2 Response to Weak Geomagnetic Activity During Solar-Minimum Observed by GOLD

CORRESPONDING & PRESENTING AUTHOR:

Xuguang Cai, NCAR, USA

Alan Burns, NCAR, USA

Wenbin Wang, NCAR, USA

Liying Qian, NCAR, USA

Stanley Solomon, NCAR, USA

Richard Eastes, U of Colorado Boulder, USA

We conduct observational and modeling studies of thermospheric composition responses to weak geomagnetic activity (nongeomagnetic storms). We found that the thermospheric O and N2 column density ratio ($\sum$O/N2) in part of the Northern Hemisphere measured by Global-scale Observations of the Limb and Disk (GOLD) exhibited large and long-lived depletions during weak geomagnetic activity in May and June 2019. The depletions reached 30% of quiet time values, extended equatorward to 10°N and lasted more than 10 hr. Furthermore, numerical simulation results are similar to these observations and indicate that the $\sum$O/N2 depletions were pushed westward by zonal winds. The $\sum$O/N2 evolution during weak geomagnetic activity suggests that the formation mechanism of the $\sum$O/N2 depletions is similar to that during a geomagnetic storm. The effects of weak geomagnetic activity are often ignored but, in fact, are important for understanding thermosphere neutral composition variability and hence the state of the thermosphere-ionosphere system.

Sr No: 395

Role of magnetosphere-ionosphere coupling in evolution of auroral substorm as viewed from global MHD simulation (by invitation)

CORRESPONDING & PRESENTING AUTHOR:

Yusuke Ebihara, Kyoto University, Japan

Takashi Tanaka, Kyushu University, Japan

Recent global magnetohydrodynamics (MHD) simulations can reproduce large- and meso-scale features of an auroral substorm from quiet time to recovery phase seamlessly in spite of inherent limitations of the MHD approximation. When the interplanetary magnetic field (IMF) is northward, complicated aurorae are developed as a consequence of the interchange-like instability arising from the magnetosphere-ionosphere coupling. When IMF turns southward, the growth phase begins. Elongated arcs move equatorward, which manifest complicated distribution of the plasma pressure at high latitudes. When the near-Earth reconnection takes place, 3-dimensional plasma flows are excited in the magnetosphere, generating field-aligned current (FAC) that manifests the expansion onset. Due to overflow of the ionospheric Hall current, additional upward FAC is developed, resulting in westward traveling surge. We overview the role of the magnetosphere-ionosphere coupling in the evolution of auroral substorms, and discuss a perspective to acquire an understanding of the auroral substorms as a whole system.

KEYWORDS :   magnetosphere-ionosphere coupling, auroral substorm, global MHD simulation

Sr No: 396

Characteristics during the Impulse-Induced Supersubstorms: A new type of Substorm

CORRESPONDING & PRESENTING AUTHOR:

Shipra Sinha, Indian Institute of Geomagnetism, India

Geeta Vichare, Indian Institute of Geomagnetism, India

Ashwini Kumar Sinha, Indian Institute of Geomagnetism, India

Rahul Rawat, Indian Institute of Geomagnetism, India

Gopi Seemala, Indian Institute of Geomagnetism, India

Substorms are more general phenomena than long been used description of nighttime increase in precipitation and auroral activity. Auroral morphology during nighttime substorm represents only a part of a more general and more widely distributed disturbances that occupies a substantial portion of the magnetosphere. This idea was first proposed by Jelly and Brice in 1967. The idea did not become very popular maybe because of lack of observational evidences, until now. We present case studies of Impulse-Induced supersubstorms occurring during ~0 nT IMF Bz. These substorms appear to have its onset as a result of various injection mechanisms other than just magnetic reconnection. Thus, we suggest that any mechanism leading to particle injection and precipitation should comprise and describe the substorm phenomena in general, irrespective of how and from which local time sector the injection and precipitation has taken place. We believe that, particle injection only through magnetic reconnection and precipitation from night side following the field line, should not limit the description of any substorm. Viscous interaction, adiabatic compression, field aligned current intensification can also lead to particle injection during impulse induced substorms. In this study we have discussed the satellite and ground based observations of impulse induced supersubstorm events. We have shown how these events are different from normal Akasofu-type substorm and why we call it a new type of substorm.

REFERENCE:

1. Jelly, D., and N.Brice (1967), Changes in Van Allen radiation associated with polar substorms, J. Geophys. Res., 72(23), 5919–5931, doi:10.1029/JZ072i023p05919

KEYWORDS : 1. Southward IMF Bz component prior to substorm onset is not a necessary condition for impulse-induced substorms, 2. Impulse induced substorms can have its onset at MLT sectors other than midnight.

Sr No: 397

Investigating magnetospheric particle injections and associated drift echos induced by interplanetary shocks (by invitation)

CORRESPONDING & PRESENTING AUTHOR:

Ankush Bhaskar, Space Physics Laboratory, VSSC, India

David Sibeck, NASA/GSFC, USA

Suk Bin Kang, NASA/GSFC, USA

Mei Ching Fok, NASA/GSFC, USA

Denny Oliveira, NASA/GSFC, USA

Shrikanth Kanekal, NASA/GSFC, USA

Tarun Pant, Space Physics Laboratory, VSSC, India

Geeta Vichare, Indian institute of Geomagnetism, India

The impact of Interplanetary (IP) shocks causes sudden compressions of the magnetosphere and ion and electron injections deep inside the magnetosphere. Sometimes these particle injections appear in the form of multiple particle drift echoes. Observations within the Van Allen radiation belts indicate the frequent occurrence of recurrent drift-echoes with periodic enhancements (or, as recently reported, decreases) in energetic particle intensities. The present study surveys drift echoes associated with the impact of IP shocks and observed by Van Allen Probes during 2012-2019. We use the Advanced Composition Explorer (ACE) and the Wind spacecraft to determine IP parameters near the L1 libration point. The Van Allen Probes Relativistic Electron Proton Telescope (REPT) and Magnetic Electron Ion Spectrometer (MagEIS) were used to identify drift echoes in the Earth's magnetosphere. We infer the origin and spatial extent of the drift echoes, as well as how their properties depend on energy and L-shell. The underlying mechanisms for their evolution are discussed in the framework of our present understanding.

KEYWORDS :   radiation belt, drift echos, interplanetary shock

Sr No: 398

SYMPOSIUM :   **3.3 Recent advances in the system level understanding of solar wind – magnetopshere – ionosphere – thermosphere coupling**

Explicit IMF By-effect in solar wind–magnetosphere coupling (by invitation)

CORRESPONDING & PRESENTING AUTHOR:

Lauri Holappa, University of Oulu, Finland

Robert Robinson, Catholic University of America, USA

Antti Pulkkinen, NASA GSFC, USA

Timo Asikainen, University of Oulu, Finland

Kalevi Mursula, University of Oulu, Finland

Geomagnetic activity is mainly driven by the southward (Bz) component of the interplanetary magnetic field (IMF), which dominates all solar wind coupling functions. Coupling functions also depend on the absolute value of the dawn-dusk (By) component of the IMF, but not on its sign. However, recent studies have shown that for a fixed level of solar wind driving, auroral electrojets in the Northern Hemisphere are stronger for By > 0 than for By < 0 during Northern Hemisphere winter. In Northern Hemisphere summer the dependence on the By sign is reversed. While this By sign dependence, also called the explicit By-dependence, is very strong in the winter hemisphere, it is weak in the summer hemisphere. While the physical mechanism of this effect is still unknown, significant progress has been made in several recent studies. Here we study how IMF By modulates the large-scale field-aligned currents (FAC), measured by the Active Magnetosphere and Planetary Electrodynamics Response Experiment (AMPERE). We also model the coupling between FACs and auroral electrojets using an empirical conductance model. We show that the IMF By component modulates Region 1 and 2 FACs in the dawn sector of the winter hemisphere which leads to an explicit By-dependence in ionospheric conductance and the westward electrojet. We also show that the By-dependence of FACs and conductance is weak in the dusk sector, which explains the earlier observation of the weak By-dependence of the eastward electrojet.

KEYWORDS :   space weather, geomagnetic activity, field-aligned currents

Sr No: 399

Global development of magnetospheric ELF/VLF waves observed by multi-point ground stations and satellites and modeled by the RAM-SCB simulations

CORRESPONDING & PRESENTING AUTHOR:

Kazuo Shiokawa, Nagoya University, Japan

Yuhei Takeshita, Nagoya University, Japan

Yoshizumi Miyoshi, Nagoya University, Japan

Vania Jordanova, Los Alamos National Laboratory, USA

Mitsunori Ozaki, Kanazawa University, Japan

Jyrki Manninen, Sodankylä Geophysical Observatory, Finland

Shinichiro Oyama, Nagoya University, Japan

Yoshiya Kasahara, Kanazawa University, Japan

Martin Connors, Athabasca University, Canada

Dmitry Baishev, Siberian Branch of the Russian Academy of Sciences, Russia

Vladimir Kurkin, Siberian Branch of the Russian Academy of Sciences, Russia

Alexey Oinats, Siberian Branch of the Russian Academy of Sciences, Russia

Magnetospheric ELF/VLF waves are an important process for generation and loss of energetic electrons in the inner magnetosphere. The spatial and temporal distribution of these waves have not been well known due to limitation of multi-point spectral measurements. In this presentation, based on Takeshita et al. [2019; 2021], we report recent studies of magnetospheric ELF/VLF waves (1) observed by multi-point ground stations by the PWING project and the Arase and NOAA POES satellites and (2) modeled by RAM-SCB simulations. The typical longitudinal extent of ELF/VLF waves is estimated to be ~76 degree at subauroral latitudes based on ~2-month measurements of magnetospheric ELF/VLF waves at six ground-based stations by the PWING project. The spatio-temporal development of the waves is shown by using these ground and satellite observations and RAM-SCB model for the geomagnetic storms of March and November 2017. The waves show repeating eastward expansion from midnight to the morning and noon associated with substorms. We also observed dayside ELF/VLF wave enhancement, possibly driven by magnetospheric compression by solar wind.

PWING: Study of dynamical variation of Particles and Waves in the INner magnetosphere using Ground-based network observations

- Takeshita, Y., Shiokawa, K., Ozaki, M., Manninen, J., Oyama, S.-I., Connors, M., et al. (2019). Journal of Geophysical Research: Space Physics, 124. https://doi.org/10.1029/2019JA026810

- Takeshita, Y., Shiokawa, K., Miyoshi, Y., Ozaki, M., Kasahara, Y., Oyama, S.-I., et al. (2021). Journal of Geophysical Research: Space Physics, 126, e2020JA028216. https://doi.org/10.1029/2020JA028216

KEYWORDS :   magnetospheric ELF/VLF waves, PWING project RAM-SCB model

Sr No: 400

Simulation of storm time equatorial ionospheric plasma drifts: IMF By effects

CORRESPONDING & PRESENTING AUTHOR:

Geeta VICHARE, Indian Institute of Geomagnetism, India

Debrup Hui, Ghani Khan Choudhury Institute of Engineering and Technology, India

The influence of east-west component of interplanetary magnetic field (IMF-By) on ionospheric dynamics over polar region is a well-studied topic. However, its effects beyond the polar latitudes have rarely been addressed and still remains very obscure. We have designed storm-time simulation experiments with varying IMF-By conditions, using Thermosphere Ionosphere Electrodynamics General Circulation Model (TIEGCM). It is observed that strong IMF-By and its polarity have effects on the storm time ionosphere-thermosphere dynamics even near equator. It can affect the equatorial zonal electric field, magnitude of morning/evening time pre-reversal-enhancements (PRE) and meridional winds. The details of the simulation results will be presented and discussed.

KEYWORDS :   IMF by, equatorial ionosphere

3.6 Magnetotail dynamic processes

CONVENERS: Jay Johnson
                      Xuzhi Zhou
                      Meng Zhou

Decades of space explorations have shown that plasma and energy transport processes in the magnetotails of Earth and other planets play a critical role in the dynamics of their magnetospheres. These processes occur over a diverse range of spatial and temporal scales, involving steady and/or intermittent mass loading, momentum, and energy transport often culminating in explosive events that completely reorganize the plasma sheet and drive processes in the inner magnetosphere, ionosphere, and boundary layer. Multipoint observations within the boundary layers, the plasma sheet and the ionosphere have been key to developing a more comprehensive view of the role of various transport processes. However, many unsolved questions remain about the underlying transport mechanisms and their coupling to the inner magnetosphere and ionosphere, which can only be resolved using multiple approaches that include theory, simulation, and observation. This session provides a forum to present the latest results on magnetotail processes at earth and other planets.

Sr No: 401

A Space Hurricane over the Earth's Polar Ionosphere (by invitation)

CORRESPONDING & PRESENTING AUTHOR:

Qinghe Zhang, Shandong University, China

Yongliang Zhang, The Johns Hopkins University, USA

Chi Wang, Center for Space Science and Applied Research, Chinese Academy of Sciences, China

Kjellmar Oksavik, University of Bergen, Norway

Larry R. Lyons, University of California, Los Angeles, USA

Michael Lockwood, University of Reading, UK

Huigen Yang, Polar Research Institute of China, China

Binbin Tang, Center for Space Science and Applied Research, Chinese Academy of Sciences, China

Joran Idar Moen, University of Oslo, Norway

Zanyang Xing, Shandong University, China

Yuzhang Ma, Shandong University, China

Xiangyu Wang, Shandong University, China

Yafei Ning, Shandong University, China

Lidong Xia, Shandong University, China

In Earth's low atmosphere, hurricanes are destructive due to their great size, strong spiral winds with shears, and intense rain/precipitation. However, disturbances resembling hurricanes have not been detected in Earth's upper atmosphere. Here we report a long-lasting space hurricane in the polar ionosphere and magnetosphere during low solar and otherwise low geomagnetic activity. This hurricane shows strong circular horizontal plasma flow with shears, a nearly zero-flow center, and a coincident cyclone-shaped aurora caused by strong electron precipitation associated with intense upward magnetic field-aligned currents. Near the center, precipitating electrons were substantially accelerated to ~10 keV. The hurricane imparted large energy and momentum deposition into the ionosphere despite otherwise extremely quiet conditions. The observations and simulations reveal that the space hurricane is generated by steady high-latitude lobe magnetic reconnection and current continuity during a several hour period of northward interplanetary magnetic field and very low solar wind density and speed.

KEYWORDS :   solar wind-magnetosphere coupling, space hurricane, magnetic reconnection

Sr No: 402

Mercury's Nightside Magnetosphere under Extreme Solar Wind Conditions: MESSENGER Observations (by invitation)

CORRESPONDING & PRESENTING AUTHOR:

Weijie Sun, University of Michigan, USA

James Slavin, University of Michigan, USA

Mercury's nightside magnetosphere is investigated with MESSENGER observations under the impact of a coronal mass ejection (CME) and a high-speed stream (HSS). In the plasma sheet, flux ropes and dipolarization fronts were produced with high frequent and large numbers, which correspond to occurrence rates for the two structures approximately two orders of magnitude higher than under average conditions.

Interestingly, the flux ropes are appeared as quasi-periodic flux rope groups. Each flux rope group contains a number of tens of flux ropes and lasts approximately one minute. Moreover, in each flux rope group, a few large flux ropes appear first and are followed by several smaller flux ropes. In the CME event, the tail magnetic reconnection produced a distorted Hall magnetic field pattern and the X-line had a dawn-dusk extent of 20% of the tail width. The lobe magnetic flux accounted for around half of Mercury's available magnetic flux. Surprisingly, no magnetic flux loading and unloading events were observed during these intense driving conditions, which suggest that Mercury's magnetosphere responded with a type of quasi-steady convection. The quasi-steady convection feature is opposed to the tail flux loading-unloading events seen at Earth under the extreme solar wind driving.

KEYWORDS : mercury's magnetosphere, extreme magnetotail, flux rope

Sr No: 403

SYMPOSIUM : **3.6 Magnetotail dynamic processes**

Magnetotail reconnection onset caused by electron kinetics with a strong external driver

CORRESPONDING & PRESENTING AUTHOR:

San Lu, University of Science and Technology of China, China

Magnetotail reconnection plays a crucial role in explosive energy conversion in geospace. Because of the lack of in-situ spacecraft observations, the onset mechanism of magnetotail reconnection, however, has been controversial for decades. The key question is whether magnetotail reconnection is externally driven to occur first on electron scales or spontaneously arising from an unstable configuration on ion scales. Here we show, using spacecraft observations and particle-in-cell (PIC) simulations, that magnetotail reconnection starts from electron reconnection in the presence of a strong external driver. Our PIC simulations show that this electron reconnection then develops into ion reconnection. These results provide direct evidence for magnetotail reconnection onset caused by electron kinetics with a strong external driver.

KEYWORDS : magnetotail, magnetic reconnection

Sr No: 404

SYMPOSIUM : **3.6 Magnetotail dynamic processes**

Effects of ion slippage in Earth's ionosphere and the plasma sheet (by invitation)

CORRESPONDING & PRESENTING AUTHOR:

Jian Yang, Southern University of Science and Technology, China

Wenrui Wang, Southern University of Science and Technology, China

Yukitoshi Nishimura, Boston University, USA

Richard Wolf, Rice University, USA

Frank Toffoletto, Rice University, USA

Vassilis Angelopoulos, University of California, Los Angeles

David Knudsen, University of Calgary, Canada

Eric Donovan, University of Calgary, Canada

Jun Cui, Sun Yat-sen University, China
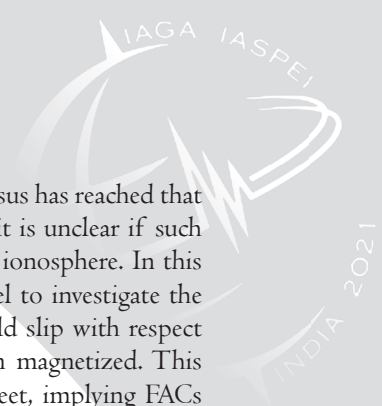
Although triggering mechanisms for substorm onsets remain highly controversial, consensus has reached that violation of frozen-in flux condition in the central plasma sheet is required. However, it is unclear if such violation in the early stage of substorms would lead to any detectable signatures in the ionosphere. In this study, we carry out a numerical gedanken experiment using the Rice Convection Model to investigate the effects of the violation without specifying the microphysics. We assume that ions would slip with respect to the magnetic field lines in the late substorm growth phase while electrons remain magnetized. This essentially creates an additional radially tailward Hall current in the central plasma sheet, implying FACs that may give rise to discrete auroral arcs. The simulation results predict (1) a thin arc and a strong westward electrojet associated with downward-upward-downward field-aligned currents and westward-eastward-westward horizontal flows in the ionosphere, which are found to be consistent with a pre-onset arc observed by the Swarm and the THEMIS all-sky imager; (2) a rapid creation of a bubble-blob pair in the plasma sheet with a tailward hump of Bz that may lead to tearing instability.

KEYWORDS : substorm, magnetosphere-ionosphere coupling, aurora

Sr No: 405

Simulation of Magnetotail Fast Flows and Their Coupling to the Inner Magnetosphere and Ionosphere (by invitation)

San Lu, UCLA, USA

Lei Cheng, FIT, USA

Jay R. Johnson, Andrews University, USA

Simon Wing, JHU/APL, USA

Meiching Fok, NASA/GSFC, USA

Natalia Buzulukova, NASA/GSFC, USA

Lijen Chen, NASA/GSFC, USA

CORRESPONDING & PRESENTING AUTHOR:

Yu Lin, Auburn University, USA

Xueyi Wang, Auburn University, USA

Joseph D. Perez, Auburn University, USA

Using the Auburn Global Hybrid Code in 3-D (ANGIE3D), we investigate the kinetic structure and roles of magnetotail fast flows in the global transport. The simulation shows that magnetotail reconnection, which has a dawn-dusk size of 1-5 RE, recurs with a period of several minutes, resulting in recurring localized fast flow injections and entropy bubbles. Strong ion temperature anisotropy and non-Maxwellian distributions are present in the fast flows, and the braking of fast flows due to the dipole-like field results in further perpendicular heating in the injection sources. Kinetic Alfvén waves (KAWs) are generated in reconnection around fast flows, carrying transverse electromagnetic perturbations, parallel Poynting fluxes, parallel currents, and parallel electric field. By tracking the wave propagation from the plasma sheet to the ionosphere, it is found that shear Alfven waves/KAWs are significantly altered due to interaction with the dipole-like field, mainly by the flow shear associated with the azimuthal convection at the flow braking. The fraction of Poynting flux transmitted from the tail to the ionosphere is examined. Finally, using the combined ANGIE3D and the Comprehensive Inner Magnetosphere-Ionosphere (CIMI) model, we study the connection of fast flow injections and the inner magnetosphere. Multiple fast flow injections are found to lead to multiple peaks in the particle fluxes in the inner magnetosphere as well as layers of upward and downward field-aligned currents at the ionosphere. Low energy particles are found to penetrate deeper radially than the high energy particles.

KEYWORDS : magnetotail-inner magnetosphere-ionosphere simulation, fast flows, kinetic alfven waves

Sr No: 406

Structure and dynamics of the magnetotail plasma sheet at lunar distances (by invitation)

CORRESPONDING & PRESENTING AUTHOR:

Andrei Runov, UCLA, USA

We present analysis of the lunar orbiting Turbulence and Electrodynamics of Moon's Interaction with the Sun (ARTEMIS) dual probe observations in the magnetotail at geocentric distances R~60 RE. The near-Moon magnetotail is unique plasma and magnetic field regime. In many respects, the physical conditions in the near-Moon magnetotail are quite different from those in the neat-Earth plasma sheet and opposite the those in the inner magnetosphere: contrary to a strong, quasi-dipolar magnetic field with fluctuations of a fraction of a percent of the mean field strength, with electrons and ions fully magnetized and obeying the adiabatic motion with the first adiabatic invariant conserved, the lunar-distant magnetotail is a region with a weak and highly fluctuating magnetic field, where not only thermal and suprathermal ions, but thermal and suprathermal electrons are unmagnetized in the vicinity of a strong magnetic gradient, the magnetotail current sheet. Using comprehensively instrumented ARTEMIS probes we study i) structure of the magnetotail plasma sheet during quiet geomagnetic conditions (AE<100 nT, |Dst|<20 nT |V|<50 km/s), ii) characteristics of tailward and earthward fast plasma flows and associated magnetic structures, and iii) configurations of the magnetotail current sheet at geocentric distances 50<R<70 RE.

KEYWORDS : magnetotail, plasma sheet, current sheet

Sr No: 407

Fast Magnetic Field Annihilation in Magnetotail Electron-scale Current Sheet (by invitation)

CORRESPONDING & PRESENTING AUTHOR:

Hiroshi Hasegawa, Institute of Space and Astronautical Science, JAXA, Japan

Richard Denton, Dartmouth College, USA

Takuma Nakamura, University of Graz, Austria

Kevin Genestreti, Southwest Research Institute, USA

Tai Phan, University of California, Berkeley, USA

Magnetic reconnection is the key to fast release of magnetic energy in many space and astrophysical plasma systems, such as during magnetospheric substorms, but little observational information is available to understand exactly how magnetic-to-electron energy conversion occurs in electron-scale diffusion regions (EDRs). It is generally believed that the EDR has an X-type magnetic field geometry around which the energy of anti-parallel magnetic fields is mostly converted to electron bulk-flow energy. We present multi-spacecraft observations in Earth's magnetotail and a fully kinetic simulation of an elongated EDR in which, contrary to the standard model of reconnection, the fast energy conversion is caused mostly by magnetic field annihilation, rather than magnetic topology change. The discovery of the annihilation-dominated EDR reveals a new form of energy conversion in the collisionless reconnection process.

KEYWORDS : magnetic reconnection, magnetotail, magnetic-field annihilation

Sr No: 408

Two-dimensional Structure of auroral oval/plasma sheet flow channels

CORRESPONDING & PRESENTING AUTHOR:

Larry Lyons, University of CA, Los Angeles, USA

Toshi Nishimura, Boston University, USA

Chihping Wang, UCLA, USA

Jiang Liu, UCLA, USA

Bill Bristow, The Pennsylvania State University, USA

Flow bursts in the tail plasma sheet are often viewed as seen in MHD simulations, where entropy is conserved and the energy dependent magnetic drift is neglected. On the other hand, Rice Convection Model (RCM) simulations show a considerable deepening of the low entropy plasma "bubbles" that comprise a flow burst. The lack of entropy conservation is the result of a divergence of the heat flux vector resulting from the energy dependent magnetic drift. A signature of this divergence is strong azimuthal flows that form within the inner plasma sheet. These flows are predicted to be within the subauroral and dawnside auroral polarization stream (SAPS and DAPS, respectively) region of the plasma sheet. The SAPS/DAPS flows are predicted to dominate when a flow burst is within the dusk/dawn convection cell, with flow bursts between the two cells being deflected roughly equally in both azimuthal directions. These flow bursts map to the auroral ionosphere as channels of enhanced flows, where the flows and the deflections to the SAPS and DAPS region can be measured in two-dimensions versus time. We take advantage of a relatively new approach to obtain two-dimensional SuperDARN flow patterns to show that the two-dimensional structure of flow channels qualitatively agrees with the RCM predictions.

KEYWORDS : flow burst, flow channels, auroral streamers

Sr No: 409

Mesoscale plasmasheet dynamics (by invitation)

CORRESPONDING & PRESENTING AUTHOR:

Viacheslav Merkin, The Johns Hopkins University Applied Physics Laboratory, USA

Kareem Sorathia, The Johns Hopkins University Applied Physics Laboratory, USA

Adam Michael, The Johns Hopkins University Applied Physics Laboratory, USA

Evgeny Panov, Austrian Academy of Sciences, Austria

Sasha Ukhorskiy, The Johns Hopkins University Applied Physics Laboratory, USA

Frank Toffoletto, Rice University, USA

John Lyon, Dartmouth College, USA

Michael Wiltberger, NCAR, USA

In this presentation, we review recent work using high-resolution global magnetosphere models to study mesoscale processes in the Earth's plasmasheet, their effects on particle energization, plasma and magnetic flux transport, and magnetosphere-ionosphere coupling. By mesoscale plasmasheet processes we understand here azimuthally localized (~1 Earth radius) structures including transient flow channels known as bursty bulk flows along with embedded in them enhanced magnetic field structures (dipolarizing flux bundles and dipolarization fronts) as well as ballooning-interchange "fingers" closer to the Earth. These structures

are known to be depleted of flux tube entropy, i.e., they are buoyant, and are sometimes called bubbles. We demonstrate the effects of these processes during geomagnetically active times, via both idealized and real event simulations, including: the contribution of the bubbles to the magnetic flux transport into the inner magnetosphere during substorms, as well as the contribution of the corresponding localized field-aligned currents to the substorm current wedge; the role of the ballooning-interchange instability in driving auroral beads; the role of the bubbles in non-adiabatic particle energization, especially for heavy ionospheric ions (O+); and the critical contribution of the bubbles to the build-up of the ring current and the radiation belts, including via particle trapping within them. We conclude with a discussion of future research directions stemming from this work, including the need for non-MHD treatment in order to properly capture the global geospace impacts of these mesoscale plasmasheet processes.

KEYWORDS : plasmasheet, ring current, mesoscale transport

Sr No: 410

Space-Ground Observations of Substorm Onset Beads (by invitation)

CORRESPONDING & PRESENTING AUTHOR:
Toshi Nishimura, Boston University, USA
Anton Artemyev, University of California, Los Angeles, USA
Larry Lyons, University of California, Los Angeles, USA
Eric Donovan, University of Calgary, USA
Vassilis Angelopoulos, University of California, Los, USA

Substorm auroral onset is characterized by auroral beads along the onset arc. The periodic nature of the bead structure suggests a critical role of waves in the near-Earth plasma sheet. It has been difficult to identify what magnetotail features are related to beads because of the lack of satellite observations in a possible onset region at the time of substorm onset. In this study, we present coordinated satellite-ground observations at substorm onset and describe modulation of plasma and magnetic field structures that are possibly related to the auroral beads. We also discuss how those signatures are connected to theoretical estimations of substorm onset instability.

KEYWORDS : substorm onset, aurora, near-earth plasma sheet

3.8 Recent Advances in Observations and Modeling of the Ring Current System

CONVENERS: Vania Jordanova
Ioannis Daglis
Yoshizumi Miyoshi
Yiqun Yu

The dynamics of energetic particles forming the ring current populations, the main signature of a geomagnetic storm, have been studied for many decades. However, the development of predictive ring current models and the forecast of severe geomagnetic storms remain challenging due to gaps in our understanding of the complex and strongly coupled magnetosphere-ionosphere system. The ring current populations interact with the surrounding plasmasphere and radiation belts and with the outer magnetosphere and ionosphere through a variety of physical processes leading to particle injections, acceleration, and loss. Coordinated multi-satellite and ground based observations combined with numerical modeling are essential to understand these processes. This session invites presentations on research advancing our knowledge of ring current dynamics and its coupling with the magnetosphere and ionosphere, as well as capabilities for their nowcast and forecast.

Sr No: 411

Stormtime Ring Current Heating of the Plasmasphere and Ionosphere

CORRESPONDING & PRESENTING AUTHOR:

Jonathan Krall, Naval Research Laboratory, USA

Mei Ching Fok, NASA, USA

Joseph Huba, Syntek Technologies, USA

Alex Glocer, NASA, USA

The energy deposition from ring current ions into the high density "cold" plasma of the ionosphere and plasmasphere is analyzed, based on a Comprehensive Inner Magnetosphere-Ionosphere (CIMI) simulation of the 2015 October 7 storm. In addition, the Naval Research Laboratory (NRL) Sami3 is Also a Model of the Ionosphere (SAMI3) ionosphere/plasmasphere code is used to simulate the effect of ring current heating on the ionosphere and plasmasphere. We find that energy is deposited at altitudes as low as 100 km. We find that heating along the entirety of any given field line, both in the ionosphere and plasmasphere, contributes to the heating effect and subsequent cold O+ outflows. Relative to the heating of the plasmasphere, the direct heating of the ionosphere by ring current ions produces only a small contribution to the thermal O+ outflow that forms the O+ shell.

KEYWORDS : ring current, oxygen torus, plasmasphere

Sr No: 412

Using Polar Cap (PC) indices to monitor magnetic storm developments

CORRESPONDING & PRESENTING AUTHOR:

Peter Stauning, Danish Meteorological Institute, Denmark

The present contribution discusses the relations between Polar Cap (PC) indices and the 1-min SYM-H and hourly Dst indices characterizing total (symmetrical) magnetospheric ring current intensities with particular emphasis on possible space weather applications. It is demonstrated that using simulated real-time PC indices in a PC-based source function may provide gradient values for the ring current intensities which upon integration during magnetic storm events would provide actual ring current index values in a close approximation to the real indices. In a study of the strongest storm events in 2009-2018, the average correlation between real and simulated real-time Dst index values was 0.82. In real-time applications equivalent Dst (or SYM-H) index values are provided currently 1 h ahead of time. It is also demonstrated that amplitude relations and timing differences for peak polar cap and ring current indices suggested in publications over the years and in a recent report from the International Standards Organisation (ISO) are not valid for the stronger magnetic storms (Dst(peak)<-90 nT) and could be seriously misleading.

KEYWORDS : polar cap index, geomagnetic ring current, solar wind
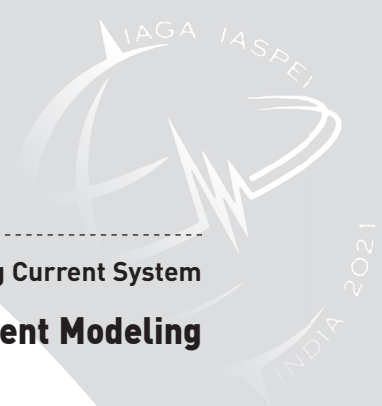
Key Observations (Or The Lack Thereof) To Guide Ring Current Modeling (by invitation)

CORRESPONDING & PRESENTING AUTHOR:

Matina Gkioulidou, JHU/APL, USA

The Earth's ring current has been a subject of interest and considerable study for nearly a century, from the days of ground-based geomagnetism to the satellite era. Protons, helium ions, and oxygen ions, of 10s – 100s keV, originating both from the solar wind and Earth's ionosphere, are known to contribute to the ring current species population and energy density content. The development of the ring current in the inner magnetosphere during geomagnetic storms controls the global electrodynamics of the coupled magnetosphere-ionosphere system. The global reconfiguration of the magnetic field due to the ring current development also controls the depletion of radiation belt electrons > MeV, both due to adiabatic depletion at lower L shells, as well as due to magnetopause losses. Therefore, the ring current is the key element of geomagnetic storms in the near-Earth space and understanding its buildup is essential. Van Allen Probes mission's comprehensive, unique instrumentation, provided data within geosynchronous orbit for seven years that shed light to ring current dynamics and composition. These key new observations have enabled the augmentation of state-of-the-art ring current models by providing critical constraints. Nonetheless, predictions made by these newly developed models have also illustrated major observational gaps that need to be addressed in order to unlock the physical processes that determine the storm-time energy buildup in the inner magnetosphere.

KEYWORDS : ring current, inner magnetosphere

EMIC wave-induced proton precipitation during the 27-28 May 2017 storm: Comparison of BATSRUS+RAM-SCBE simulations with ground/space-based observations

CORRESPONDING & PRESENTING AUTHOR:

Shreedevi P R, Beihang University, China

Yiqun Yu, Beihang University, China

Yoshizumi Miyoshi, Nagoya University, Japan

Xingbin Tian, Beihang University, China

Chaewoo Jun, Nagoya University, Japan

Kazuo Shiokawa, Nagoya University, Japan

Vania Jordavnova, Los Alamos National Laboratory, USA

Electro Magnetic Ion Cyclotron (EMIC) waves are known to initiate ion precipitation into the mid-latitude ionosphere during geomagnetic storms. Recent studies have shown that the EMIC wave-induced ion precipitation can contribute significantly to the total energy flux deposition into the ionosphere and severely affect the magnetosphere-ionosphere coupling. In this study, the temporal and spatial evolution of the proton precipitation into the ionosphere and its correspondence to the EMIC wave activity in the

inner magnetosphere is examined using simulations from the BATSRUS+RAM-SCB model. During the geomagnetic storm of 27-28 May 2017, the Van Allen Probes satellite observed typical signatures of EMIC waves in the inner magnetosphere i.e., at 4 to 6 Re in the evening sector. Ground magnetometers at high latitude stations also showed the presence of PC1/EMIC waves after 1600 UT on 27 May 2017. During the main phase of the storm, the DMSP satellites observed enhanced proton precipitation at locations where the ground/space-based magnetic field measurements showed the presence of enhanced EMIC wave activity. The plasma source and distributions of associated temperature anisotropy in the equatorial plane are investigated to understand the excitation of the waves. A comparison of the precipitating proton fluxes obtained from the simulations with the particle measurements from the DMSP satellites shows that EMIC wave scattering can account for the 30 keV proton precipitation at sub auroral latitudes. This study shows that the EMIC wave-particle interaction plays a significant role in the Spatio-temporal evolution of the ion precipitation in the mid-latitude ionosphere.

KEYWORDS : proton precipitation, emic wave-particle interaction, geomagnetic storms

Sr No: 415

Identifying electromagnetic 1 ion cyclotron (EMIC) wave-driven ring current proton precipitation through Van Allen Probes and POES conjugate measurements (by invitation)

CORRESPONDING & PRESENTING AUTHOR:

Binbin Ni, Wuhan University, China
Yang Zhang, Wuhan University, China

Based on a rigorous conjunction between Van Allen Probe B and NOAA-19, we perform a detailed analysis to capture simultaneous enhancements of EMIC waves and ring current proton precipitation. By assuming that ring current proton precipitation is mainly caused by EMIC wave scattering, we establish a physical model between the wave-driven proton diffusion and ratio of precipitated-to-trapped proton flux. By inferring the intensity of EMIC waves required to cause the observed proton precipitation, we find that the model results of wave intensity, obtained using either the observed or empirical Gaussian wave frequency spectrum, are quite consistent with the wave observations, within a factor of ~ 1.5. Our study therefore strongly supports the dominant contribution of EMIC waves to ring current proton precipitation, and offers a valuable means to construct the global distribution of EMIC waves using low-altitude POES proton measurements, which generally have a broader L-shell coverage and higher time resolution.

KEYWORDS : ring current proton precipitation, wave-particle interactions, conjugate measurements

Sr No: 416

Variation of energetic ions during magnetic storm and substorm time: ERG (Arase) and Van Allen Probe Observations

CORRESPONDING & PRESENTING AUTHOR:

Bhaskara Veenadhari, Indian Institute of Geomagnetism, India

Yoshizumi Miyoshi, Nagoya University, Japan

Megha Pandya, Indian Institute of Geomagnetism, India

Trunali Shah, Indian Institute of Geomagnetism, India

Tomo Hori, Nagoya University, Japan

Kazushi Asamura, JAXA, Japan

The energetic ions, O+, H+ and He+ (10 to 100 of keV) are rapidly enhanced in the inner magnetosphere, responsible for the main contribution for the ring current. The ring current is a highly variable region, and understanding the energization processes provides the information into how substorm-ring current coupling may contribute to the generation of storm conditions. The O+, H+ and He+ data from Radiation Belt Storm Probes Ion Composition Experiment (RBSPICE)and Helium Oxygen Electron ion flux (HOPE) onboard of VAP for some magnetic storms and substorms. The relationship between the ion flow in the plasma sheet and fresh ion plasma injections in to the ring current region will be examined during substorm intervals. The latest the Exploration of energization and Radiation in Geospace(ERG) satellite observations will also be analyzed for the same events. The characteristics of energetic ions will be quantitatively analyzed for variations at different energy, L-value and MLT and the PADs during different phases of the magnetic storm will investigated.

KEYWORDS : ring current, radiation belts, innermagnetosphere

Sr No: 417

On the long-term evolution of the ring current

CORRESPONDING & PRESENTING AUTHOR:

Crisan Demetrescu, Institute of Geodynamics, Romanian Academy

Venera Dobrica, Institute of Geodynamics, Romanian Academy, Romania

Cristiana Stefan, Institute of Geodynamics, Romanian Academy, Romania

The intensity and the evolution of the ring current are currently proxied by the storm-time geomagnetic index Dst, and by shorter time series of the indices SYM-H and ASY-H. In this paper we infer the evolution of the ring current before the information provided by these indices, by noting that there is a similar interdecadal evolution of magnetosphere and ionosphere current systems, as seen in geomagnetic indices, that allows extending back in time the information to 1868, based on the aa index. Besides the expected 11-year variability, sub-centennial and inter-decadal variations are observed in aa. Annual means provided by geomagnetic obsrvatories are contaminated not only by the 11-year variability, but also by the sub-centennial and inter-decadal variations. We used a Hodrick-Prescott type of analysis and Butterworth filtering to get the two sub-centennial variations. These data are compared to Hale and Gleissberg cycles of the solar activity, detected in other parameters that illustrate this variability (sunspot number, reconstructed magnetic

heliospheric field, reconstructed solar wind parameters, reconstructed total solar irradiance etc). A good correlation is present, allowing to extrapolate the evolution of the ring current to cca 1600 AD, using the gufm1 model (Jackson et al., 2000). Two types of information is used in this enterprise, namely the 11-year signal in the annual means time series of the geomagnetic elements, and the so-called sub-centennial variation in the horizontal and vertical components of the geomagnetic main field provided by the gufm1 model.

KEYWORDS : ring-current, geomagnetic indices, Hale and Gleissberg cycles

Sr No: 418

Storm-time Ion Composition Variations Inferred from Arase and Van Allen Probes Observations (by invitation)

CORRESPONDING & PRESENTING AUTHOR:

Robert Haaser, Los Alamos National Laboratory, USA

Vania Jordanova, Los Alamos National Laboratory, USA

Erin Lay, Los Alamos National Laboratory, USA

Steven Morley, Los Alamos National Laboratory, USA

Kateryna Yakymenko, Los Alamos National Laboratory, USA

Yoshizumi Miyoshi, Nagoya University, Japan

Brian Larson, Los Alamos National Laboratory, USA

Lynn Kistler, University of New Hampshire, USA

The September(2017) solar-storm induced significant effects on the Magnetosphere when Solar-Coronal Mass Ejection arrived 09/08/2017. Dst dipped <-140nT and Kp-indices >8 near peak. This time-span occurred when the precessions of the Van Allen Probes (RBSP) and Arase satellites brought them to nearly opposite day/night sectors. At their highest orbit altitudes (L>5), RBSP(A/B) occupied sun-ward positions, while Arase occupied mostly anti-sunward positions. Data collected by the Helium-Oxygen-Proton-Electron(RBSP/HOPE) and Low-Energy Particle Experiments/Ion Mass Analyzer (Arase/LEPi) instruments measured low energy ion densities/fluxes for H+/He+/O+(<20 keV/q). From our analyses of data near the peak of the storm, the RBSP/HOPE instrumentation report O+/H+ density ratios greater than 1 (L>5, day-side), larger than previous theoretical fits derived from geosynchronous observations (Young et al., 1982). At the same time, the Arase/LEPi instrument reports much smaller numbers (night-side), more in-line with such previous predictions. Though increases in O+/H+ ratio with Kp in the range of L~6 is expected (Fernandes et al., 2017), we are currently interested in reproducing its large magnitude with our Magnetosphere-Ionosphere Coupling(MIC) modeling efforts. Efforts are also underway to verify instrument parity. We will also consider a (smaller) storm in the range of March/17-19/2019 when precession brought the RBSP/Arase probes to the same night-side sector. From this, we will determine how ratios from HOPE/MOM and LEPi(<25keV/q) compare under similar conditions (quiescent and perturbed). Ions density/flux data up to 180 keV(from RBSP/MAGEIS&RBSPICE and Arase/MEPI) are used improving cross-instrument consistency Resulting O+/H+ storm ratios will be used to specify plasma boundary conditions for future MIC modeling studies.

KEYWORDS : solar storm, RBSP, MIC
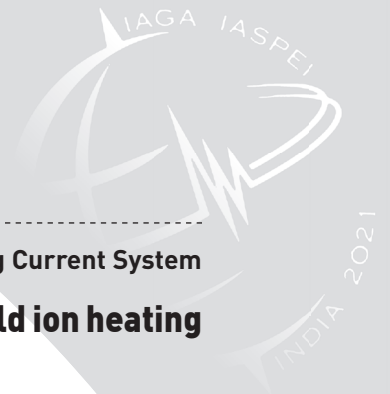
Sr No: 419

Cross-energy couplings from MSW to EMIC waves through cold ion heating inside the plasmasphere

CORRESPONDING & PRESENTING AUTHOR:

Kazushi Asamura, ISAS/JAXA, Japan

Yoshizumi Miyoshi, Nagoya University, Japan

Masafumi Shoji, Nagoya University, Japan

Yasumasa Kasaba, PPARC, Tohoku University, Japan

Yoshiya Kasahara, Kanazawa University, Japan

Ayako Matsuoka, Kyoto University, Japan

Fast magnetosonic (MS) waves are commonly observed in the equatorial region of the inner magnetosphere. Past numerical simulations show MS waves can accelerate low-energy ions through cyclotron resonance, although the observational evidence is still unclear. Arase (ERG) satellite found events of perpendicular heating of cold ions simultaneously with plasma wave activities of the MS waves. We have applied the WPIA (wave-particle interaction analysis) method to the selected ion heating event with the MS waves. The results show that the MS waves accelerate the low-energy ($<\sim$10keV) ions with pitch angles near 90 degrees. We also found these ions give their energy to EMIC waves which appears just below the local proton cyclotron frequency. Since MS waves are considered to be generated by the ring distribution of energetic ions, this analysis indicates energy transfer from higher-energy ions to the lower-energy ions in the inner magnetosphere.

KEYWORDS :

Sr No: 420

Contribution of electron pressure to ring current and ground magnetic depression using RAM-SCB simulations and Arase observations during 7-8 November 2017 magnetic storm

CORRESPONDING & PRESENTING AUTHOR:

Sandeep Kumar, Nagoya University, Japan

Yoshizumi Miyoshi, Nagoya University, Japan

Vania Jordanova, Los Alamos National Laboratory, USA

Miles Engel, Los Alamos National Laboratory, USA

Kazushi Asamura, Japan Aerospace Exploration Agency (JAXA) , Japan

Shoichiro Yokota, Graduate School of Science, Osaka University, Japan

Satoshi Kasahara, The University of Tokyo, Japan

Yoichi Kazama, Academia Sinica, Taiwan

Shiang Yu Wang, Academia Sinica, Taiwan

Takefumi Mitani, Japan Aerospace Exploration Agency (JAXA) , Japan

Kunihiro Keika, The University of Tokyo, Japan

Tomoaki Hori, Nagoya University, Japan

Chae Woo Jun, Nagoya University, Japan

Iku Shinohara, Japan Aerospace Exploration Agency (JAXA) , Japan

Understanding the physical processes that control the dynamics of energetic particles in the inner magnetosphere is important for both space-borne and ground-based assets essential to modern society. The storm time distribution of ring current particles in the inner magnetosphere depends strongly on their transport in evolution of the electric and magnetic field along with acceleration and loss. In this study, we investigated the ring current particle variations using observations and simulations. We compared ions (H+, He+, and O+) and electron fluxes and plasma pressure variations of Arase observations with the self-consistent inner magnetosphere model: Ring current Atmosphere interactions Model with Self Consistent magnetic field (RAM-SCB) during 7-8 November 2017 geomagnetic storm. We examined the contribution of the different species (ions and electrons) to the magnetic field deformation observed at ground magnetic stations (09-45° MLat) using RAM-SCB simulations. The results show that the ions are the major contributor with ∼ 88 % and electrons contribution is ∼ 12% to the ring current pressure. It is also found that the electrons' contribution to the ring current in dawn to morning sector is non-negligible during the main phase of the storm. Thus, electron contribution to the storm time ring current is important and should not be neglected.

KEYWORDS :   inner magnetosphere, ring current

Sr No: 421

Composition of the Ring Current Source Region During Storm Main Phase (by invitation)

CORRESPONDING & PRESENTING AUTHOR:

Lynn Kistler, University of New Hampshire, USA

The ionospheric and solar wind contributions to the magnetosphere can be distinguished by their composition. While both sources contain significant H+, the heavy ion species from the ionospheric source are generally singly ionized, while the solar wind consists of highly ionized ions. Both the solar wind and the ionosphere contribute to the plasma sheet. It has been shown that with both enhanced geomagnetic activity and enhanced solar EUV, the ionospheric contribution increases. However, the details of this transition from a solar wind dominated to more ionospheric dominated plasma sheet are not well understood. An initial study using AMPTE/CHEM data shows that the transition can occur quite sharply during storms, with the ionospheric contribution becoming dominant during the storm main phase. However, during the AMPTE time-period, there were no continuous measurements of the upstream solar wind, and so both the simultaneous solar wind composition and the driving solar wind and IMF parameters were not known. The HPCA instrument on MMS and both the LEPi and MEPi instruments on Arase are able to measure He++. With these data sets, the He++/H+ ratio can be compared to the simultaneous He++/H+ ratios in the solar wind to more definitively identify the solar wind contribution to the plasma sheet. This allows the relative contributions to be determined. We find that when the IMF turns southward the dominant source of the hot plasma sheet change from solar wind to ionospheric. This composition change explains why the storm time ring current also has a high ionospheric contribution.

KEYWORDS :   ring current source, geomagnetic storm, heavy ions
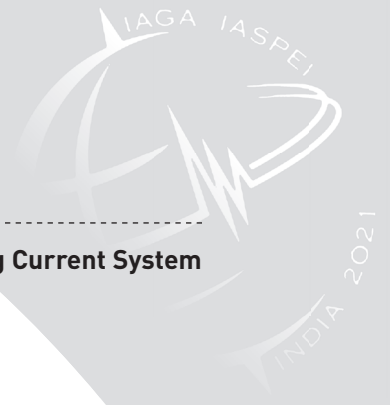
Sr No: 422

Ring current injection and its effects in the ionosphere (by invitation)

CORRESPONDING & PRESENTING AUTHOR:

Jian Yang, Southern University of Science and Technology, China

Wenrui Wang, Southern University of Science and Technology, China

Yukitoshi Nishimura, Boston University, USA

Weiqin Sun, Southern University of Science and Technology, China

Dong Wei, Southern University of Science and Technology, China

Fei Zhang, Southern University of Science and Technology, China

Frank Toffoletto, Rice University, USA

Richard Wolf, Rice University, USA

Stanislav Sazykin, Rice University, USA

Vassilis Angelopoulos, University of California, Los Angeles, USA

Jun Cui, Sun Yat-sen University, China

Substorm injections are believed to play an important role in the formation of the ring current. Associated with the enhanced partial ring current, the Region-2 field-aligned current (FAC) is also elevated related to the pressure gradient in the inner magnetosphere. The closure of the FAC through the pre-midnight subauroral region implies strong westward drifts, called subauroral ion drifts (SAIDs). In this study, we use the state-of-the-art RCM to simulate recurrent injections of fast flows, in which a particularly intense SAID (>5000 m/s) is reproduced. Such subauroral drift is found to occur simultaneously with the STEVE (Subauroral Thermal Emission Velocity Enhancement), an upper atmospheric emission phenomenon that has been extensively studied recently. Our modeling shows that SAIDs map to the sharp inner edge of a strongly enhanced partial ring current at r≈4 Re. The simulation also predicts that the peak of the SAIDs, the center of the downward FAC, the subauroral boundary, the plasmapause, the inner edge of the proton and electron partial ring current and the maximum azimuthal drift in the magnetosphere are pressed tightly within 0.5° latitude or 0.2 Re in the equatorial plane.

KEYWORDS : substorm, magnetosphere-ionosphere coupling, subaurora

Sr No: 423

SYMPOSIUM :   3.8 Recent Advances in Observations and Modeling of the Ring Current System

Meridional Distribution of Ring Current Ions and Pressure-Driven Currents in the Nightside Inner Magnetosphere: Arase Observations (by invitation)

CORRESPONDING & PRESENTING AUTHOR:

Shun Imajo, Kyoto University, Japan

Masahito Nose, Nagoya University, Japan

Satoshi Kasahara, University of Tokyo, Japan

Shoichiro Yokota, Osaka University, Japan

Ayako Matsuoka, Kyoto University, Japan

Kunihiro Keika, University of Tokyo, Japan

Tomoaki Hori, Nagoya University, Japan

Mariko Teramoto, Kyushu Institute of Technology, Japan

Kazuhiro Yamamoto, University of Tokyo, Japan

Reiko Nomura, Japan Aerospace Exploration Agency, Japan

Akiko Fujimto, Kyushu Institute of Technology, Japan

Iku Shinohara, Japan Aerospace Exploration Agency, Japan

Yoshizumi Miyoshi, Nagoya University, Japan

We examined the average meridional distribution of middle-energy protons (10–180 keV) and pressure-driven currents in the nightside (20–04 hr magnetic local time) ring current region during moderately disturbed times using the Arase satellite's data. Because the Arase satellite has a large inclination orbit of 31°;, it covers the magnetic latitude (MLAT) in the range of -40°; to 40°; and a radial distance of <6RE. We found that the plasma pressure decreased significantly with increasing MLAT. The plasma pressure on the same L–shell at 30°<MLAT<40° was ~10–60% of that at 0°<MLAT<10°, and the rate of decrease was larger on lower L*–shells. The pressure anisotropy, derived as the perpendicular pressure divided by the parallel pressure minus 1, decreased with radial distance and showed a weak dependence on MLAT. The magnitude of the plasma beta at 30°<MLAT<40° was 1 or 2 orders smaller than that at 0°<MLAT<10°. The plasma pressure normalized by the value at 0°<MLAT<10° estimated from the magnetic strength and anisotropy was roughly consistent with the observed plasma pressure for L*=3.5°–5.5. The azimuthal pressure-gradient current derived from the plasma pressure was distributed over MLAT~0–20°, while the curvature current was limited within MLAT0–10°. We suggest that the latitudinal dependence should be taken into account in interpretations of plasma parameters in successive orbits during magnetic storms.

KEYWORDS :   meridional distributions, ring current ions, pressure-driven current

Sr No: 424

Multisatellite observations of field-aligned low-energy O+ ion flux enhancements in the inner magnetosphere: September 22, 2018, Event

CORRESPONDING & PRESENTING AUTHOR:

Institute for Space-Earth Environmental Research, Nagoya University,Nagoya, Japan

Ayako Matsuoka, Graduate School of Science, Kyoto University, Kyoto, Japan

Yoshizumi Miyoshi, Institute for Space-Earth Environmental Research, Nagoya University, Nagoya, Japan

Kazushi Asamura, Institute of Space and Astronautical Science, Japan Aerospace Exploration Agency, Sagamihara, Japan

Tomoaki Hori, Institute for Space-Earth Environmental Research, Nagoya University, Nagoya, Japan

Mariko Teramoto, Department of Space Systems Engineering, Kyushu Institute of Technology, Kitakyusyu, Japan

Iku Shinoahara, Institute of Space and Astronautical Science, Japan Aerospace Exploration Agency, Sagamihara, Japan

C. A. Kletzing, Department of Physics and Astronomy, University of Iowa, Iowa City, IA, USA

Masfumi Hirahara, Institute for Space-Earth Environmental Research, Nagoya University,
Nagoya, Japan

C. W. Smith, Institute for the Study of Earth, Oceans, and Space, University of New Hampshire, Durham, NH, USA

R. J. Macdowall, Solar System Exploration Division, Goddard Space Flight Center, Greenbelt, MD, USA

H. E. Spence, Institute for the Study of Earth, Oceans, and Space, University of New Hampshire, Durham, NH, USA

G. D. Reeves, Space Sciences and Applications Group, Los Alamos National Laboratory, Los Alamos, NM, USA

Masahito Nose, Nagoya University, Japan

Recent studies employing the Arase and Van Allen Probes satellites have shown that unidirectional / bidirectional energy-dispersed O+ flux appears a few minutes after substorms in the inner magnetosphere and lasts for ~10 min with a decrease in its energy from ~5 keV to 10–100 eV. This may contribute to the O+ content of the inner magnetospheric plasma such as the warm plasma cloak and the oxygen torus.

The present study examines the low-energy O+ ion flux variations simultaneously observed by multiple satellites, Arase, Van Allen Probe A and B satellite, on September 22, 2018. The O+ fluxes are enhanced after a substorm onset at 05:24 UT, at which three satellites are located in the nightside inner magnetosphere (Arase at MLT=0.3 hr, L=6.2, GMLAT=−9.6 deg; Probe A at MLT=0.7 hr, L=5.5, GMLAT=14.7 deg; Probe B at MLT=0.0 hr, L=5.3, GMLAT=10.6 deg). Arase observes O+ flux enhancements only in the parallel direction to the magnetic field in the energy range from a few keV to 200 eV. Probe A and B, however, identify O+ flux enhancements in both parallel and antiparallel directions starting at 1 keV down to 10 eV. Multiband flux enhancements are detected only by Probe A. We perform numerical calculation of O+ ion trajectories to reproduce the observed E-t spectrograms at three satellites. In the presentation, we will show results of data analysis and numerical simulation in more detail, and discuss the contribution of the low-energy O+ ion flux enhancements to the O+ content of the inner magnetospheric plasma.

KEYWORDS : field-aligned low-energy O+ ion, warm plasma cloak, oxygen torus

3.10 Machine learning in space physics

CONVENERS: Peter Wintoft

                     Irina Zhelavskaya

Over the past decades there has been a tremendous increase in the amount of data from ground based and space based measurements and observations. The data enables us to explore our solar-terrestrial environment and other planets, and to develop and verify models with increasing accuracy and detail. Due to the large datasets, the large number of variables, and the complex interactions between different physical regions in the heliosphere, the exploration and modelling is a great challenge. The past decades have also seen great development and maturity in the area of machine learning (ML) driven by performance increase in hardware, increased availability of ML software, and theoretical development. In this session we invite contributions on ML in space physics which may include, but are not limited to, aspects of: data mining; data preprocessing; supervised, unsupervised, and reinforcement learning; feature selection; physics-informed ML; predictions and verification. Both theoretical and applications- oriented presentations are welcome. Theoretical aspects should primarily be focused on the incorporation of prior knowledge (physics) into the ML process and the interpretation of the derived ML relations. On the application aspect, we invite presentations concerned with practical challenges related to preprocessing of data, ML algorithms and frameworks, and validation.
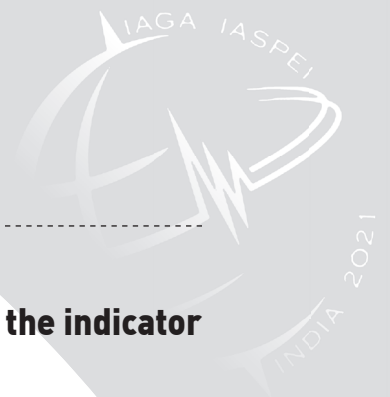
Sr No: 425

Identification of extreme events in magnetosphere based on the indicator functions system for the URAGAN hodoscope data

PRESENTING AUTHOR:

Roman Sidorov, Geophysical center of the Russian Academy of Sciences, Russia

CORRESPONDING AUTHOR:

Vladislav Chinkin, Geophysical center of the Russian Academy of Sciences, Russia
Viktor Getmanov, Geophysical center of the Russian Academy of Sciences, Russia
Alexei Gvishiani, Geophysical center of the Russian Academy of Sciences, Russia
Michael Dobrovolsky, Geophysical center of the Russian Academy of Sciences, Russia
Anna Dmitrieva, National Research Nuclear University MEPhI, Russia
Anna Kovylyaeva, National Research Nuclear University MEPhI, Russia
Igor Yashin, National Research Nuclear University MEPhI, Russia
Leo Tsibizov, Geophysical center of the Russian Academy of Sciences, Russia

Identification of extreme events in the magnetosphere is an urgent problem in geomagnetism and aeronomy. The necessary observations for the considered identification problem are implemented by the muon hodoscope (MH) URAGAN developed by NRNU MEPhI, registering muon flux intensities. In the MH, the numbers of muons falling on its detector per unit time are counted. Time series of matrix MH data are formed with angular and temporal modulations. The proposed identification is based on the mathematical apparatus of indicator matrices (IM) and space-time filtering.

For the reference interval, matrices of estimates of mathematical expectations and standard confidence intervals are calculated. Based on the comparison of the matrices of the reference and current confidence intervals, matrices of anomalies are formed, which are compared with a given threshold matrix. Exceeding the thresholds corresponds to anomalous events. Binary MI events are formed, where anomalies correspond to one, and the absence of anomalies is equal to zero. Identification includes the analysis of MI and the detection of areas of concentration of units in them.

The proposed identification method based on IM was tested on experimental MH data with model extreme events. The possibility of identifying decreases in the level of 2-3% was confirmed.

IM-based identification for MH data can be successfully applied to the problems of identifying extreme events in the magnetosphere and early diagnostics of geomagnetic storms.

KEYWORDS : muon hodoscope

Sr No: 426

Modeling radiation belt electrons with information theory and neural networks

CORRESPONDING & PRESENTING AUTHOR:

Simon Wing, The Johns Hopkins University, USA

Sasha Ukhorskiy, The Johns Hopkins University, USA

Drew Turner, The Johns Hopkins University, USA

Jay Johnson, Andrews University, USA

Thomas Sotirelis, The Johns Hopkins University, USA

Romina Nikoukar, The Johns Hopkins University, USA

Alex Boyd, The Aerospace Corporation, USA

Giuseppe Romeo, The Johns Hopkins University, USA

Kiley Yeakel, The Johns Hopkins University, USA

An empirical model of radiation belt electrons is developed using RBSP data 2013-2018. The model inputs the solar wind and magnetospheric parameters and outputs radiation belt electron phase space density (psd). The process of selecting input parameters is complex. Many solar wind and magnetospheric parameters are correlated or anticorrelated with one another, making it difficult to determine which parameters would carry relevant and which would carry redundant information. Information theory is used to determine the relevant input parameters and their response lag times. It is also used to determine the effect of solar wind parameters as a function of L^*. The input parameters are ranked based on their information transfer to the radiation belt electrons. Using this ranking as a guide for selecting input parameters, the radiation belt electron model based on neural networks is developed. The preliminary result shows that the model predictive efficiency (PE) is ~0.66, which is comparable to those obtained in some previous models.

KEYWORDS :   radiation belt, machine learning, empirical model

Sr No: 427

Recognition of extreme magnetospheric processes based on neural network technologies using data from the URAGAN muon hodoscope and a system of neutron monitors

CORRESPONDING & PRESENTING AUTHOR:

Vladislav Chinkin, Geophysical center of the Russian Academy of Sciences, Russia

Viktor Getmanov, Geophysical center of the Russian Academy of Sciences, Russia

Alexei Gvishiani, Geophysical center of the Russian Academy of Sciences, Russia

Michael Dobrovolsky, Geophysical center of the Russian Academy of Sciences, Russia

Sidorov Roman, Geophysical center of the Russian Academy of Sciences, Russia

Soloviev Anatoly, Geophysical center of the Russian Academy of Sciences, Russia

Anna Dmitrieva, National Research Nuclear University MEPhI, Russia

Anna Kovylyaeva, National Research Nuclear University MEPhI, Russia

Igor Yashin, National Research Nuclear University MEPhI, Russia
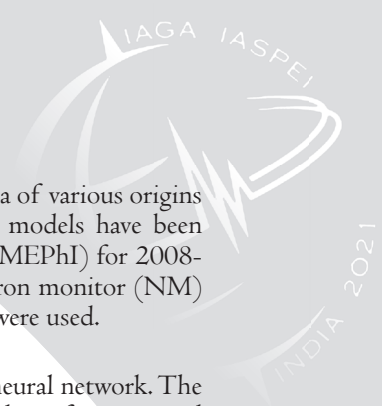
Recognition of extreme magnetospheric processes using circumterrestrial monitoring data of various origins is an urgent problem of solar-terrestrial physics. Two types of Dst index estimation models have been developed. For the first type, the data from the URAGAN muon hodoscope (NRNU MEPhI) for 2008-2018 were, used: for the second type the global survey data from the IZMIRAN neutron monitor (NM) system for 2002-2018 were used. For the objective function of the model, Dst indices were used.

The model for estimating the Dst index was calculated on the basis of a convolutional neural network. The structure was implemented, to the input of which the time series segments of the input data of size 48 and output with dimension 1, which was compared with the reference Dst indices during training.

After training on test samples, two variants of estimation models were obtained - MH-Dst indices and NM-Dst indices; then they were compared with the reference Dst indices for the test period. The probabilities of correct and false recognition were calculated. It turned out that recognition according to MH data reaches 30%, while according to NM data it exceeds 50%, and their combined use improved the probabilistic characteristics of recognition up to 60%.

Based on the obtained dependencies, we can say about the possibility of building a predictive model based on this recognition model. Now we can only say that the NM and MH data complement each other.

Sr No: 428

SYMPOSIUM : **3.10 Machine learning in space physics**

Automatic detection of Ionospheric Alfvén Resonances in Induction Coil Data Using U-net

CORRESPONDING & PRESENTING AUTHOR:

Ciaran Beggan, British Geological Survey, UK

Paolo Marangio, University of Edinburgh, UK

Rosa Filgueira, Heriot Watt University, UK

Vyron Christodoulou, DataLab, UK

Hannah Rogers, University of Edinburgh, UK

Ionospheric Alfvén Resonances (IAR) are weak oscillations along magnetic field lines generated by waves temporarily trapped in the F-region (100-1000km) of the ionosphere. The IAR typically appear as a variable number of bright thin diffuse fringes between 0.5-20 Hz in spectrograms generated from induction coil magnetometer data, changing dynamically throughout local night-time. Analysis of IAR parameters such as their frequency and the gap between the fringes can provide quantitative measurements of density in the upper atmosphere.

Since 2012, two induction coils running at a cadence of 100 Hz have been in operation at Eskdalemuir Observatory in the UK. IAR are common and visible on a majority of the days, though with a seasonal and solar cycle dependence. To more efficiently analyse their properties, we have developed a machine learning method to identify and automatically extract IAR using a convolution neural network method known as U-net.

The U-net model was trained using hand-picked examples of IAR from 178 days of data recorded between 2012 and 2019, achieving 90% success. One of the issues with training such a model is that the standard metric of accuracy does not work well when only a few pixels in an image are of the target class (i.e. IAR). Instead, the Intersection over Union metric was used to ensure that the model correctly identified the bright fringes. After training the model was run on the remaining 2300 days of data to identify IAR in the data, and importantly returning a null result when none were present.

KEYWORDS : U-net, magnetic, spectrograms

Sr No: 429

Forecasting ground magnetic field variations in the UK using L1 solar wind data with CNN and LSTM networks

CORRESPONDING & PRESENTING AUTHOR:
Frederik Madsen, University of Edinburgh, UK
Kathy Whaler, University of Edinburgh, UK
Ciaran Beggan, British Geological Survey, UK

Extreme space weather can have large impacts on infrastructure important to our technology-based society. Machine learning techniques have proven successful as a tool for forecasting space weather and its effects from interplanetary observations. Recent scientific advances have involved forecasting geomagnetic indices rather than ground magnetic field perturbations. Here, nowcast and forecast models are constructed to predict the horizontal geomagnetic field, B_H, and its time derivative, dB_H/dt, as a result of extreme space weather at the three UK observatories Hartland, Eskdalemuir and Lerwick. The dB_H/dt predictions are made from solar wind plasma and IMF observations from DSCOVR by using Long Short- Term Memory (LSTM) networks and hybrid Convolutional Neural Network (CNN)-LSTM models. 5-fold grid search cross-validation is used for tuning the hyperparameters in each model.

Forecasts were made with 5-, 15- and 30-minute lead time. The LSTM models are generally found to outperform the hybrid CNN-LSTM models. LSTM nowcasts all yield a correlation coefficient of 1. The forecast models are found to only be able to predict the directly driven parts of geomagnetic storms. Of all the forecasting models, only the ones for Lerwick and the B_H 15- and 30-minute forecasts for Eskdalemuir were successful. The 5-minute B_H forecast as well as all the dB_H/dt models for Eskdalemuir and all the Hartland models were found to have little or no forecasting dB_H/dt power. This suggests that the machine learning models have better forecasting power closer to the auroral zones, when the ground magnetic variation field is larger.

KEYWORDS :   geomagnetic, forecast, LSTM
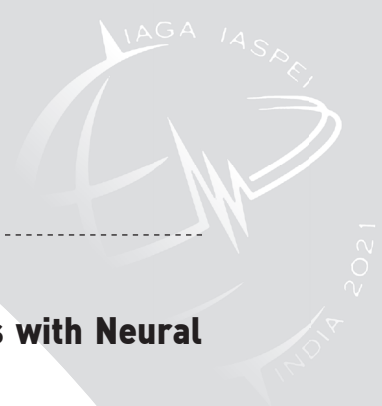
Sr No: 430

Automatic Calibration of Satellite Platform Magnetometers with Neural Network-based Time Shift Approximation

CORRESPONDING & PRESENTING AUTHOR:

Kevin Styp Rekowski, GFZ Potsdam, Germany

Claudia Stolle, GFZ Potsdam, Germany

Ingo Michaelis, GFZ Potsdam, Germany

Odej Kao, Technical University of Berlin, Germany

Abstract : Additional datasets of magnetic space-based observations of the Earth's magnetic field are of high interest for space physics and geomagnetism. Filling gaps of data from high-precision magnetic missions, such as between CHAMP and Swarm, as well as a higher spatio-temporal coverage make the use of satellite's platform magnetometer data attractive. Nevertheless, these platform magnetometers need to be carefully calibrated as other satellite payload systems introduce artificial disturbances to their measurements. This is a tedious analytical task where machine learning can help to improve Feature Selection and Feature Generation. In contrast to existing work, we propose a Feedforward Neural Network architecture for a non-linear regression of the magnetometer measurements. This results in several challenges, such as a lack of ground truth for high latitudes where auroral field-aligned currents occur that are not included in the ground truth, e.g., high precision magnetic field models. In addition, a neuron is introduced to find a possible time shift within the data alongside the training. First results on the GRACE-FO satellite mission show promising results, e.g., outperforming results of analytical calibrations.

KEYWORDS :   platform magnetometer, calibration, time shift approximation

Sr No: 431

Using Physics Informed Neural Network in Radiation Belts Physics

CORRESPONDING & PRESENTING AUTHOR:

Enrico Camporeale, University of Colorado, USA

We approach the problem of solving the one-dimensional Fokker-Planck equation for radiation belt electrons from a data-driven standpoint. We use a physics-informed neural network (PINN) to discover the optimal drift and diffusion coefficients that, once used in the Fokker-Planck equation, yield the solution with smaller discrepancy with respect to Van Allen Probes observations. Further, we train a machine learning algorithm that generalizes such coefficients for any radiation belt condition (boundary conditions and initial values). Interestingly, a feature selection analysis shows that the drift and diffusion coefficients are weakly dependent on the value of the geomagnetic index Kp, in contrast with all previous parameterizations presented in the literature.

We show that using PINN-discovered coefficients in a forward model yields much smaller errors with respect to the tradiational diffusion and loss terms used in the literature.

This approach, although well rooted in our physical understanding of the process in play, seeks to extract the

largest amount of information from the data with minimal assumptions, and we believe it promises to shed light on the physics of resonant and non-resonant wave-particle interactions in the radiation belts.

KEYWORDS : Physics Informed Neural Network, Inverse Problem, Van Allen Probes

Sr No: 432

Modelling of the AL index time series with echo state network

CORRESPONDING & PRESENTING AUTHOR:

Shinya Nakano, The Institute of Statistical Mathematics, Japan

The AL index indicates the strength of westward electrojet and it is widely used for monitoring geomagnetic activity in the auroral region. It is interpreted that the westward electrojet consist of two component. One is related with the magnetospheric convection driven by solar wind electric field, and the other is related with substorm expansion. Although the behavior of the westward electrojet is believed to be controlled by the solar wind input to the magnetosphere, it is not easy to model the behavior of the AL index because of the complicated physical processes of the westward electrojet. In order to obtain some insights to understand key processes of the westward electrojet, this study modelled the behavior of the AL index with an echo state network. An echo state network is a kind of recurrent neural networks where the connections and weights between hidden state variables are fixed, and it is used for modelling dynamical systems and time series data. The echo state network mostly reproduced temporal variations of the AL index. However, it did not necessarily well reproduce some of impulsive patterns, which might suggest that some impulsive variations in the AL index should be treated as a stochastic process. We also conduct some analyses for investigating the features of the residuals which cannot be explained by the echo state network model.

KEYWORDS : AL index, auroral electrojet, echo state network

Sr No: 433

ULF wave classification in Swarm time series using convolutional neural networks

CORRESPONDING & PRESENTING AUTHOR:

Georgios Balasis, National Observatory of Athens, Greece
Alexandra Antonopoulou, National Observatory of Athens, Greece
Constantinos Papadimitriou, National Observatory of Athens, Greece

Ultra-low frequency (ULF) magnetospheric plasma waves play a key role in the dynamics of the Earth's magnetosphere and, therefore, their importance in Space Weather studies is indisputable. Magnetic field measurements from recent multi-satellite missions are currently advancing our knowledge on the physics of ULF waves. In particular, Swarm satellites have contributed to the expansion of data availability in the topside ionosphere, stimulating much recent progress in this area. Coupled with the new successful developments in artificial intelligence, we are now able to use more robust approaches for automated ULF
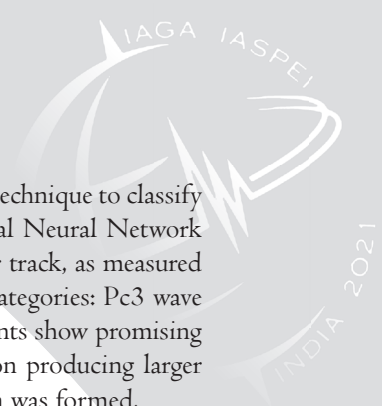
wave identification and classification. The goal of this effort is to use a machine learning technique to classify ULF wave events using magnetic field data from Swarm. We construct a Convolutional Neural Network that takes as input the wavelet power spectra of the Earth's magnetic field variations per track, as measured by each one of the three Swarm satellites, aiming to classify ULF wave events in four categories: Pc3 wave events, background noise, false positives, and plasma instabilities. Our primary experiments show promising results, yielding successful identification of 90% accuracy. We are currently working on producing larger datasets, by analyzing Swarm data from mid-2014 onwards, when the final constellation was formed.

KEYWORDS : ULF waves, deep learning, swarm mission

Sr No: 434

SYMPOSIUM : **3.10 Machine learning in space physics**

A machine learning approach for Field Line Resonance frequency identification

CORRESPONDING & PRESENTING AUTHOR:
Raffaello Foldes, University of L'Aquila, Italy
Alfredo Del Corpo, University of L'Aquila, Italy
Ermanno Pietropaolo, University of L'Aquila, Italy
Massimo Vellante, University of L'Aquila, Italy

A consolidated technique employed for monitoring the plasmasphere consists of remotely inferring the equatorial plasma mass density in the inner magnetosphere using Field Line Resonance (FLR) frequencies. FLR frequencies are obtained via cross-phase analysis of ultra-low frequency (ULF) signals recorded from pairs of latitude separated stations.

In this work we survey several supervised machine learning (ML) algorithms for identifying FLR frequencies by using measurements of the European quasi-Meridional Magnetometer Array (EMMA).

Our algorithms take as input the 30-min cross-phase spectra of magnetic signals and return the FLR frequency as output; we evaluate the algorithm performance on four different station pairs from $L = 2.4$ to $L = 5.5$. Results show that tree-based algorithms are those who reach the highest accuracy and precision, even if their performance slightly decreases with increasing latitude and tend to deteriorate during nighttime. We test our algorithms on a particular geomagnetic storm occurred the 1st June 2013; the estimation error does not seem to depend on the geomagnetic activity, although at high latitudes the error increases during highly disturbed geomagnetic conditions such as the main phase of a storm.

Our approach may represent a prominent space weather tool included into an automatic monitoring system of the plasmasphere, but this work represents only a preliminary step in this direction. The application of this approach on a more extensive data set and on more pairs of stations is straight-forward and necessary to create more robust and accurate models.

KEYWORDS : field line resonances, plasmasphere, ULF waves

3.11 Magnetospheric processes

CONVENERS: Simon Wing

Matthew Argall

Steve Petrinec

Larry Kepko

Kevin Genestreti

George Balasis

Karlheinz J. Trattner

Rumi Nakamura

Planetary magnetospheres have long been known to be spatially bounded by the fast solar wind, such that plasmas and fields observed earthward of the boundary (magnetopause) are distinct from plasmas and fields outside the boundary. Additional boundaries associated with the presence of a magnetosphere are at the outer edge of the magnetotail plasmasheet, the upstream bow shock, and other places. These boundaries topologically and spatially separate the different regions from one another and are of finite thickness. Recent spacecraft missions and ground-based observatories have made it possible to make observations from multiple vantage points, at varying spatial scales, and at high temporal resolution. In particular, the next thrusts of magnetospheric research involve system science, and the cross-scale coupling and energization of space plasmas. In this context, cross-scale can mean across plasma regimes (i.e, Micro <-> Meso <-> Global) and across magnetospheric regions (e.g., tail -> ring current, Ionosphere <-> magnetosphere).

Magnetic reconnection is a universal process of plasmas by which magnetic energy is converted to particle kinetic energy via a topological change in the magnetic field. Reconnection has a profound impact on the geospace environment as it often explosively develops and redistributes mass and energy over a variety of scale sizes. Rapid progress in understanding the micro-physics of reconnection in space has been largely enabled by NASA's Magnetospheric Multiscale (MMS) mission and the development of computational resources required to describe complex systems with physics-based models. Multi-spacecraft conjunctions, data-driven and theoretical models are often used to advance our understanding of how the micro-physics impacts and/or is impacted by the large-scale magnetosphere.

This session welcomes contributions that highlight processes within the magnetosphere, solar wind-magnetosphere interactions, and magnetosphere-ionosphere interactions. Studies that involve satellite and ground observations, modeling and simulations, theory, specially those which address that address the physics of magnetospheric boundary layers and their influence on magnetospheric dynamics and laboratory experiments are welcomed. This session encourages contributions on the micro-physical aspects of reconnection and the impact of reconnection on geospace.
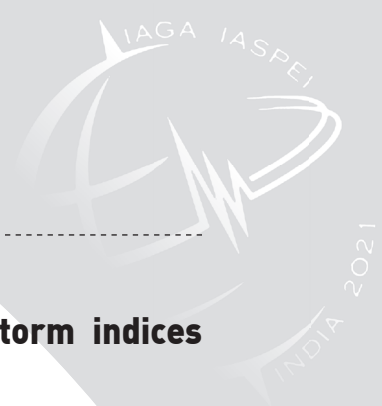
Sr No: 435

Dynamical complexity in Swarm-derived storm and substorm indices using information theory measures

CORRESPONDING & PRESENTING AUTHOR:

Georgios Balasis, National Observatory of Athens, Greece

Constantinos Papadimitriou, National Observatory of Athens, Greece

Adamantia Zoe Boutsi, National Observatory of Athens, Greece

For 7 years now, the European Space Agency's Swarm fleet of satellites surveys the Earth's magnetic field, measuring magnetic and electric fields at low-Earth orbit (LEO) with unprecedented detail. We have recently demonstrated the feasibility of Swarm measurements to derive Swarm AE-like and Dst-like indices. We have shown that the newly proposed Swarm indices monitor magnetic storm and magnetospheric substorm activity at least as good as the standard AE and Dst indices. Herein, we employ a series of information theory measures, namely Hurst exponent and various entropy measures, for analyzing Swarm-derived indices. The results show that information theory techniques can effectively detect the dissimilarity of complexity between the pre-storm activity and intense magnetic storms (Dst < 150 nT), which is convenient for space weather applications.

Sr No: 436

What are the fundamental modes of energy transfer in the coupled Magnetosphere-Ionosphere system? (by invitation)

CORRESPONDING & PRESENTING AUTHOR:

Jonathan Rae, Northumbria University, UK

The fundamental processes responsible for energy exchange between large-scale electromagnetic fields and plasma are well understood theoretically, but in practice these theories have not been tested. These processes are ubiquitous in all plasmas, especially at the interface between high and low beta plasmas in planetary magnetospheres and other magnetic environments. Although such boundaries pervade the plasma universe, the processes responsible for the release of the stored magnetic and thermal plasma energy have not been fully identified and the importance of the relative impact of each process is unknown.

Despite advances in understanding energy release through the conversion of magnetic to kinetic energy in magnetic reconnection, how the extreme pressures in the regions between stretched and more relaxed field lines in the transition region are balanced and released through adiabatic convection of plasma and fields is still a mystery. Recent theoretical advances and the predictions of large-scale instabilities must be tested. In essence, the processes responsible remain poorly understood and the problem unresolved. The aim of this white paper is to highlight three outstanding open science questions that are of clear international interest; the interplay of local and global plasma physics processes, the partitioning during energy conversion between electromagnetic and plasma energy, what processes drive the coupling between low and high beta plasmas. We present a discussion of the new measurements and technological advances required from current state-

of-the-art, and several candidate mission profiles with which these international high-priority science goals could be significantly advanced.

Sr No: 437

Study of Slow-mode shocks in Magnetic Reconnection Based on 2.5 D Hybrid Simulations

CORRESPONDING & PRESENTING AUTHOR:

Nehpreet Walia, University of Tokyo, Japan
Kanako Seki, University of Tokyo, Japan
Takanobu Amano, University of Tokyo, Japan

The rate of magnetic reconnection predicted by the Petschek's model [1965] is closest to the one seen in observations of reconnection in space. It requires the presence of a structure called slow-mode shocks (SSs) to produce particle acceleration as the particles transverse from lobe (upstream) to exhaust (downstream). However, SSs are observed sporadically in space as reported by Saito et al. [1995] (10% detection in magnetotail) and Walia et al. [2018] (20% detection in magnetopause). We analyzed the structure of the magnetic reconnection region and the acceleration locations of particles using 2.5D hybrid simulations. We observed that the reconnection boundary can be interpreted as a SS from as close as ~ 6.5 ion inertial length from the X-point, and its detection probability increases with the increase of distance from the X-point and with the increase of plasma beta. Also, it was observed that if the angle at which the artificial satellite crosses the boundary is very oblique, the detection probability can decrease to ~ 10%. We found that the particles which enter SSs closer to the X-point are accelerated and they gain high energies. Further from the X-point, the acceleration effect of the SS decreases and a non-classical picture of SSs appears. The hot beam population at those SS downstreams helps in satisfaction of SS conditions. However, this beam population gains a significant part of its total energy via the acceleration at the SSs closer to X-point and from reflecting between these SS.

Sr No: 438

Geomagnetic and auroral observations from the Gjøa and Discovery Expeditions

CORRESPONDING AUTHOR:

Charles Deehr, University of Alaska Fairbanks Geophysical Institure, USA

PRESENTING AUTHOR:

Alv Egeland, University of Oslo, Norway

Amundsen's expedition through the Northwest Passage included measurements of the Earth's magnetic field and visual observations of the northern lights at Gjøahavn station (GH) for the period 1903-05. Simultaneous recordings were carried out at Cape Armitage (CA) by Scott's Discovery Expedition in Antarctica, geomagnetically conjugate to GH, for the years 1903-04. Contemporary analysis of both data sets showed that the magnetic dip poles move their location with large diurnal, 28-day and annual variations. The conjugate stations were separated in solar time by 6.5 hours, so the effects of solar radiation and the magnetosphere could be separated in both the magnetic and visual auroral data. Similar to CA, aurora was reported on 90 nights at GH, maximizing in mid-winter. The maximum diurnal occurrence frequency of polar cap aurora was found at geomagnetic dusk and dawn at both stations. Auroral substorm intensification occurs simultaneously in the magnetic data 1.5 hours before magnetic midnight at the two stations. The visual aurora was often not accompanied by local magnetic disturbances. Analysis of magnetic data, using the separation of solar effects between the two stations, indicates that a field-aligned current system associated with the visual aurora near 80° geomagnetic latitude and +/- six hours around geomagnetic noon is the source of the Svalgaard-Mansurov Effect.

KEYWORDS : polar cap aurora, conjugate observations, svalgaard-mansurov effect

Sr No: 439

Insights from coupled simulations on directions of magnetospheric research

CORRESPONDING & PRESENTING AUTHOR:
Michael Wiltberger, NCAR, USA
Kevin Pham, NCAR, USA
Dong Lin, NCAR, USA
Kareem Sorathia, JHU, USA
Viacheslav Merkin, JHU, USA
Jeffery Garretson, JHU, USA
John Lyon, Dartmouth College, USA

Simulations have long been a useful tool in studying the dynamics of the magnetosphere. The coupling of magnetohydrodynamic simulations of the magnetosphere to simulations of ionosphere-thermosphere and inner magnetosphere provided insights into how the connections between these regions can impact the evolution of the entire system. For instance, simulations with polar wind flowing into the magnetosphere have shown an impact on the subsequent dynamics of the magnetosphere with respect to storage and release of energy in the magnetotail. Simulations have also shown how ionospheric conductivity can lead to global geospace responses by regulating dayside and nightside reconnection location and rate. Currently, the high resolution results from the Multiscale Atmosphere-Geospace Environment (MAGE) model produced by the Center for Geospace Storms are showing the importance of treating the system as a coupled whole while at the same time resolving critical mesoscale processes that may have global-scale consequences. This work has included connections between bursty bulk flows and the energization of the ring current and radiation belts, the role of the magnetopause Kelvin Helmholtz Instability in particle entry and loss from the magnetosphere, and the role of flux transfer events in transfer of energy from the solar wind into the geospace system. The coupling of these simulations with modern data analysis methods, especially machine learning, and constellations of spacecraft and widely distributed observing systems has the potential to transform the way we study geospace.

KEYWORDS : magnetosphere, simulation, mesoscale

Sr No: 440

Effects of a Velocity Shear on Explosive Reconnection and Particle Acceleration in High Lundquist Number Double Tearing Modes

CORRESPONDING & PRESENTING AUTHOR:

Arghyadeep Paul, Indian Institute of Technology Indore, India

Bhargav Vaidya, Indian Institute of Technology Indore, India

The presence of multiple current sheets in reconnection environments is expected due to the inherent turbulence associated with the process. A velocity shear in reconnection environments is also common due to the dynamic nature of the process. We have investigated the effect of a velocity shear on the explosive phase of the double tearing mode (DTM) within the 2D resistive magnetohydrodynamic framework in a high Lundquist number system. We further explore the effect of this shear flow on the mechanism of particle acceleration in DTMs. We find that the theoretical scaling of the reconnection rate with a shear flow is dependent on the magnetic island structure and larger islands tend to enhance the reconnection rate drastically. We have also investigated the modification on the energy spectrum of the particles in the presence of a shear flow. The velocity shear has negligible effects on the power law index, however, it has a significant effect on the maximum energies attained by the particles. Individual particle trajectories also help to identify the exact machanism of the acceleration process and the mechanism is found to vary based on the location of the particles. We highlight the importance of the convective electric field in the inflow as well as the outflow region inside large magnetic islands in the acceleration of particles. The interaction and bounce-back of the particles with the reconnection exhausts inside the large scale primary magnetic islands is found to have a significant effect on the energization of the particles.

KEYWORDS : explosive reconnection, particle acceleration, double tearing modes

Sr No: 441

Average plasma sheet thickness at lunar distances based on ARTEMIS observations

CORRESPONDING & PRESENTING AUTHOR:

Iklim Gencturk Akay, Istanbul Technical University, Turkey

Zerefsan Kaymaz, Istanbul Technical University, Turkey

ARTEMIS probes spend around 4.5 days per pass in the magnetotail at lunar distances. ARTEMIS probes observe the plasma sheet from 20 to 30 hours per orbit, each collecting 100 days (2400 hours) of magnetotail data, including 20-30 days (500-700 hours) in the plasma sheet. The spatial coverage of the magnetotail in XZ- plane for the interval of 2 years (08.2011-08.2013) shows the diamagnetic effect of the plasma sheet, which causes a decrease in the magnetic field magnitudes. The stretched dipolar field lines with an average of about 8 nT is found for $|Z|>7$ RE, where we expect to see plasma sheet.

Bx parameter is also used to separate the north and south parts of the magnetotail or as the neutral sheet denominator. Usage of Bx, sort the observations such that the dynamic neutral sheet region seems now to be aligned with the x-axis. In XBx- projection most of the Bx is populated around the positive and negative 10nT region.
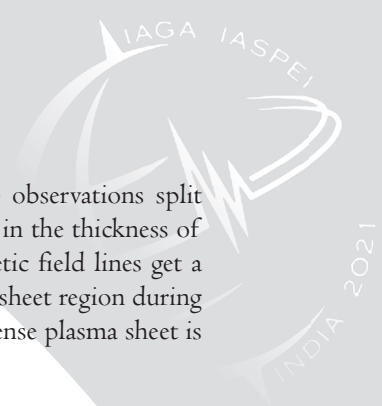
To investigate the effect of IMF direction on the XZ-plane, the magnetic field line observations split into categories in according to the interplanetary magnetic field direction. The increase in the thickness of the plasma sheet is observed for northward IMF case such that the magnetotail magnetic field lines get a vertical component nearly equal to the x-component. Not only the expansion in plasma sheet region during northward IMF but also the stretching of the field lines can be observed. Thick, cold-dense plasma sheet is also investigated during northward IMF.

KEYWORDS :   ARTEMIS, plasma sheet, magnetotail

Sr No: 442

SYMPOSIUM :   **3.11 Magnetospheric processes**

Statistical Test of the Linear Mode Conversion Theory Beaming Formula for Non-thermal Continuum Radiation

CORRESPONDING & PRESENTING AUTHOR:

Scott Boardsen, GPHI/NASA-GSFC, USA

Eunhwa Kim, Princeton University, USA

William Kurth, University of Iowa, USA

Chio Cheng, Princeton University, USA

Iver Cairns, University of Sydney, Australia

Linear mode conversion theory (LMCT) predicts that free space radiation will be emitted from the radio window at the equatorial plasmapause with a beaming angle of $\theta b = \tan^{(-1)}(\sqrt{(fpe/fce)})$ where the wave frequency f equals the plasma frequency fpe at the window and θB is measured with respect to the ambient magnetic field direction or anti-direction, fce is the electron cyclotron frequency. In a statistical study covering a large range of geomagnetic conditions the plasmapause location will cover a range of equatorial radial distances with the plasmapause moving outwards as KP index decreases. Therefore, statistically, spacecraft observations for fixed f and radial distance, under the assumption of outward beaming, the beaming formula predicts that θb versus magnetic latitude will form an inverted V signature with the apex at the magnetic equator. Statistical analysis of the beaming angle derived from Van Allen Probes High Frequency Receiver observations over the entire mission qualitatively reproduces an inverted V pattern in magnetic latitude between frequencies of 17 and 100 kHz, and the relationship between θb and KP index is qualitatively consistent with changing plasmapause location. However, the observed beaming angle is much larger than that of the theory for observations near the magnetic equator. For frequencies from 100 kHz to 400 kHz the emissions are strongly beamed with θb near 90° making it difficult to explain this strong beaming using LMCT.

KEYWORDS :   continuum radiation, waves, plasmapause

Sr No: 443

Visualization of Multiple Wave Fronts in Magnetospheric Multi Scale Fast Plasma Imager Phase Space Measurements

CORRESPONDING & PRESENTING AUTHOR:

Scott Boardsen, GPHI/NASA-GSFC, USA

Daniel Gershman, NASA-GSFC, USA

Naritoshi Kitamura, University of Tokyo, Japan

Barbara Giles, NASA-GSFC, USA

Various Wave Vector estimation methods like Bellan's method, multi-phase component analysis, and k-filtering rely on the assumption that one dominant wave vector exists per frequency bin. They can't resolve multiple wave fronts in a bin. Wave distribution function analysis could be used to tackle this. However, in this study we explore a different route where the response of phase space density (PSD) of the ions and electrons due the superposition of two wave vectors are visualized in phase space. A plasma wave is characterized by the cyclic exchange of energy between particles and fields that compose the wave mode, along with possible resonant interactions. The response of phase space to both of these interactions is a function of wave vector direction. Burst mode MMS-FPI measurements with a Nyquist frequency of 3 Hz for the ions and 17 Hz for the electrons will be used in this study, allowing the investigation of waves below these frequencies. The focus will be on waves in the ion cyclotron frequency range. First we will use linear theory to explore how FPI PSD should respond to one and two wave vectors as function of wave amplitude and PSD one count level, exploring various projections of PSD. Then we will re-analyze a kinetic Alfven wave (KAW) event in the magnetopause boundary layer for which the FPI PSD is highly unstable to field aligned ion cyclotron waves (ICW) to see if this event could actually be explained as a superposition of an ICW and its reflection.

KEYWORDS :   plasma waves, phase space density

Sr No: 444

The Plasma Observatory: exploring particle energization in space plasmas through multi-point, multi-scale in situ measurements (by invitation)

Anatoly Petrukovich, Russian Academy of Sciences, Russia

Jean Louis Pincon, CNRS, France

Yoshifumi Saito, JAXA, Japan

Luca Sorriso Valvo, CNR, Italy

Rami Vainio, University of Turku, Finland

Robert Wimmer Schweingruber, University of Kiel, Germany

CORRESPONDING & PRESENTING AUTHOR:

Alessandro Retino, CNRS, France

Yuri Khotyaintsev, Swedish Institute of Space Physics, Sweden

Olivier Le Contel, CNRS, France

M. Federica Marcucci, INAF, Italy

Ferdinand Plaschke, OEAW , Austria

Andris Vaivads, KTH, Sweden

Vassilis Angelopoulos, UCLA, USA

Pasquale Blasi, Gran Sasso Science Institute, Italy

James L. Burch, SWRI, USA

Johan De Keyser, BIRA-IASB, Belgium

Malcolm Dunlop, Rutherford Appleton Laboratory, UK

Lei Dai, National Space Science Center, China

Johathan Eastwood, Imperial College, UK

Huishan Fu, Beihang University, China

Stein Haaland, University of Bergen, Norway

Masahiro Hoshino, University of Tokyo, Japan

Andreas Johlander, University of Helsinki, Finland

E. Lawrence Kepko, NASA, USA

Harald Kuchareck, University of New Hampshire, USA

Gianni Lapenta, KU Leuven, Belgium

Benoit Lavraud, CNRS, France

Olga Malandraki, National Observatory of Athens, Greece

William Matthaeus, University of Delaware, USA

Kathryn A. Mc Williams, University of Saskatchewan, Canada

Understanding particle energization in plasmas is a compelling science problem of major importance for the worldwide magnetospheric, solar, and astrophysical plasma communities. In situ measurements are required to study and understand how particles are energized in space plasmas. In the solar system, the near-Earth space is an unique laboratory for studying particle energization since very high resolution in situ measurements can be performed and all data can be transmitted to ground with high cadence. Furthermore, the near-Earth space provides a wide range of different plasma conditions, which can be used as a proxy for solar and astrophysical plasma regimes. This presentation outlines the importance of studying particle energization through future multi-point, multi-scale in situ measurements. Five compelling science questions related to particle energization by shocks, reconnection, waves and turbulence, jets and their combinations, are identified. Answering these questions requires resolving scale coupling, nonlinearity and non-stationarity, which cannot be done with existing 4-point observations. In situ measurements from a multi-point, multi-scale Plasma Observatory consisting of at least 7 spacecraft are needed, covering fluid, ion and electron scales. Such a novel Plasma Observatory will enable a paradigm shift in our comprehension of particle energization processes with very important impact on solar and astrophysical plasmas. The ideas discussed in this presentation are included in the White Paper « Particle Energization in Space Plasmas: Towards a Multi-Point, Multi-Scale Plasma Observatory » (https://arxiv.org/abs/1909.02783) which has been submitted for the future ESA Voyage 2035-2050 science program.

KEYWORDS : space plasmas, particle acceleration, magnetosphere

Sr No: 445

SYMPOSIUM : **3.11 Magnetospheric processes**

Auroral Vortices

CORRESPONDING & PRESENTING AUTHOR:

Jay Johnson, Andrews University, USA

Simon Wing, John Hopkins University, USA

Peter Delamere, University of Alaska, Fairbanks, USA

Steven Petrinec, Lockheed Martin, USA

Shiva Kavosi, University of New Hampshire, USA

Velocity shears serve as effective voltage generators in planetary magnetospheres and drive field-aligned currents, coupling the magnetosphere-ionosphere system and powering auroral emissions. We present a quasi-static magnetosphere-ionosphere coupling model that relates solar wind and ionospheric parameters to the strength and thickness of field-aligned currents in a region of sheared velocity, such as the boundary layer between the solar wind dominated magnetosheath and magnetosphere. We compare the predictions of the model with DMSP satellite observations and find remarkably good scaling of the currents with solar wind and ionospheric parameters in the upward region-I region located at the boundary layer or open field lines. Auroral bright spots have also been observed at Earth, Jupiter, and Saturn in regions that map to the boundary layer. It has been suggested that the bright spots are associated with Kelvin-Helmholtz vortices. We utilize our model to determine how the field aligned current structure depends on ionospheric and boundary layer parameters for vortex structures. In 2D mapping of field-aligned currents differs substantially from the 1D case in that there is competition between geometrical convergence, which strengthens the currents and resistance to the flow field aligned currents as the current channel is reduced. As a result, there is a preferred scale of vortex structures where field-aligned currents and electron energy flux maximize. We find that the size of observed auroral beads in planetary magnetospheres is consistent with the predictions of the preferred scale of vortex structures for typical magnetospheric parameters.

KEYWORDS : vortex, kelvin-helmholtz, aurora

Sr No: 446

Multi-scale structures of dayside current layer and secondary reconnection beside ion-scale flux ropes (by invitation)

CORRESPONDING & PRESENTING AUTHOR:

Malcolm Dunlop, Beihang University, China

Xiangcheng Dong, UKRI-STFC, UK

Tieyan Wang, UKRI-STFC, UK

Karlheinz Trattner, University of Colorado Boulder, USA

Philippe Escoubet, ESA, Europe

Christopher Russell, UCLA, USA

The coordination of different spacecraft missions allows us to investigate multiple scales in the magnetospheric current layers and detailed structure of the reconnection layer, and in FTEs. We first compare the small-scale MMS crossings to simultaneous Cluster crossings at different locations on the MP boundary layer. Cluster currents are an order of magnitude lower than MMS, since the larger separations cannot reveal the detailed current structure. Nevertheless, we find that the MP at two locations may have similar magnetic field structure, suggesting the MP has similar current structure across a wide region during specific IMF conditions. The MMS four spacecraft data show that the small-scale physical process in the magnetopause current, e.g. current carriers and current sources, have features beyond the classic Chapman-Ferraro model. The detailed plasma and field structure of ion-scale flux rope FTEs can be created by secondary reconnection in the exhaust of the primary reconnection site and in the boundary layer electron distributions seen by MMS can show complex IBL electron structure, i.e. three field-line topologies as suggested by different plasma sublayers resulting from reconnection lines forming above and below the spacecraft. The secondary reconnection required for FTE growth has not previously been directly observed, however, and we show in situ observations of a secondary reconnection electron diffusion region (EDR) beside the leading edge of an ion-scale flux rope at the magnetopause. The observation of secondary reconnection beside the flux rope gives direct evidence that flux ropes can be created and evolved in the reconnection exhaust region.

KEYWORDS : magnetopause, currents, reconnection

Sr No: 447

Star planet interactions and atmospheric losses for planets with and without magnetospheres

CORRESPONDING & PRESENTING AUTHOR:

Arnab Basak, Indian Institute of Science Education and Research Kolkata, India

Dibyendu Nandy, Indian Institute of Science Education and Research Kolkata, India

We present results of 3D compressible magnetohydrodynamic (MHD) simulations of the interactions between the solar wind and planets with different magnetospheric strengths, using the Star-Planet Interaction Module (CESSI-SPIM) developed at CESSI, IISER Kolkata. A gravitationally stratified planetary atmosphere is considered which is in hydrostatic equilibrium with the ambient medium. It is found that the solar wind is able to penetrate closer to a planet with weak intrinsic magnetic field, resulting in greater atmospheric loss. The atmospheric loss rate, which dictates the planetary habitability, is higher for a stronger wind. We also study a case analogous to the conditions of present-day Mars, where a non-magnetized planet without atmosphere is considered. The results are found to be in agreement with observations from Mars Global Surveyor (MGS) and Mars Atmosphere and Volatile EvolutioN (MAVEN) missions and is expected to complement data from the recent Mars missions. The study is important from the perspective of planetary habitability in solar and exoplanetary systems.

KEYWORDS :   star planet interactions, magnetospheres, atmospheres

Division IV

4.1 Advances and Upcoming Developments in Solar and Heliospheric Physics

CONVENOR: Mari Paz Miralles

Spiros Patsourakos

Jin-YI Lee

Xochitl Blanco-Cano

John Richardson

Cynthia Lopez Portela

Stefano Livi

Valery M Nakariakov

Bo Li

Raffaella D'Amicis

Continuous observations have advanced our knowledge of the physical and dynamical properties of the Sun, the heliosphere, and the interstellar medium. These observations, along with theory and models, continue to pose challenges to our understanding of the relevant physical processes. This session invites contributions covering new results from space- and ground-based observations, theory, and modeling of different aspects of the Sun and the heliosphere, including the solar interior, magnetic field, atmosphere, solar wind, and interstellar medium. Waves and turbulence in the solar corona and wind are also a critical topic on both theoretical and observational grounds. This session will stimulate exchange and promote discussion of upcoming developments from the latest research and instrumentation in the field. In addition, we also invite contributions from the SCOSTEP/PRESTO program (Pillar 1: Sun, interplanetary space, and geospace).
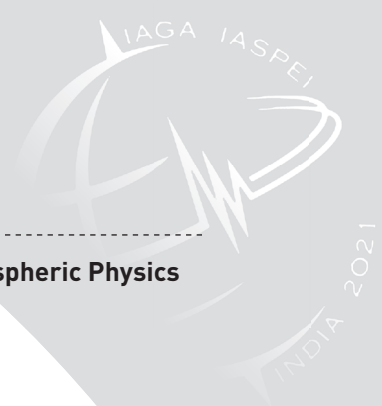
Sr No: 448

On the decay of sunspot groups

CORRESPONDING & PRESENTING AUTHOR:

Judit Murakozy, Institute of Earth Physics and Space Science, Hungary

The development and decay of the sunspot groups are governed by different mechanisms, their detailed examination became possible recently on large samples.

By using the SoHO/MDI - Debrecen data (SDD) the decay of the sunspot groups was studied on more than 100 different groups by distinguishing between their leader and follower spots. The results show that the following spots decay faster while the leading spots decay slower. The schedule of the decay is the following: firstly the following penumbrae and umbrae decay and then the leading penumbrae, while the longest living part of the sunspot group is the leading umbra.

Thanks to the 1.5 hourly temporal resolution of this database the above detailed decomposition process can be observed in its progress. This shows that after the maximum area state of the groups the asymmetry index between the leading and following parts will be at the same level until about 60 % of the maximum area. After this the asymmetry increases which means in most cases that the area of the leading part predominates while the following part gradually disappears until about 25 % of the maximum area, where this condition appears to be stabilizing. This asymmetry depends on the area of the sunspot groups, the higher the area the steeper the variation and it is much more pronounced in the cases of umbrae.

KEYWORDS :   solar magnetic field, sunspot groups, decay,

Sr No: 449

Using synthetic PSP/WISRP J-maps to infer the global properties of slow solar wind

CORRESPONDING & PRESENTING AUTHOR:

Spiros Patsourakos, University of Ioannina, Greece
Alexander Nindos, University of Ioannina, Greece
Angelos Vourlidas, Applied Physics Laboratory, USA

The nature of the slow solar wind is still debated, and its release could be either continuous or fragmented. Indeed, coronagraphs and heliospheric imagers regularly observe a spectrum of transient slow wind flows like for instance blobs, jets. etc. A standard tool used in the study of such flows, is the display of intensity as a function of time and elongation for a given direction, which is frequently called J-map. The launch of the Parker Solar Probe (PSP) mission in 2018, and the availability of high-quality up-close images of the corona by its Wide-Field Imager (WISPR), opened new exciting observational capabilities in solar wind research. He hereby report on simple simulations of synthetic WISPR J-maps constructed for various scenario of

transient solar wind release in terms of blobs. This is based on Monte-Carlo simulations of blobs with varying numbers, release frequencies, speeds, and launch longitudes. We compare our synthetic J-maps with an observed WISPR J-map taken during the fourth solar encounter of PSP and use the observed daily count of tracks in this J-map in conjuction with our synthetic J-maps in order to place constraints on the global properties of slow solar wind transient release in terms of blobs.

KEYWORDS : solar physics, solar wind

Sr No: 450

SYMPOSIUM : **4.1 Advances and Upcoming Developments in Solar and Heliospheric Physics**

What two solar cycles have taught us about changes in the solar interior (by invitation)

CORRESPONDING & PRESENTING AUTHOR:

Sarbani Basu, Yale University, USA

Helioseismic data allow us to determine the internal structure and dynamics of the Sun. These data have allowed us to map the internal structure and dynamic of the Sun in exquisite detail. Helioseismic data show changes over the solar cycle which allows us to study internal changes in the Sun. We have detailed helioseismic data over two solar cycles --- solar cycle 23 and 24. These data have revealed how solar dynamic changes with solar activity; changes in solar structure are more subtle. In this talk, I shall describe what we have learned about changes inside the Sun and describe some of the features that are still unknown.

KEYWORDS : sun: oscillation, sun: interior, sun: solar-cycle

Sr No: 451

SYMPOSIUM : **4.1 Advances and Upcoming Developments in Solar and Heliospheric Physics**

Application of Deep Learning to Solar and Space Weather Data (by invitation)

CORRESPONDING & PRESENTING AUTHOR:

Yongjae Moon, Kyung Hee University, South Korea

In this talk, we introduce our recent applications of deep learning to solar and space science data. Our major applications are (1) generation of solar farside magnetograms and global field extrapolation, (2) generation of solar UV/EUV images, (3) denoising solar magnetograms, (4) generation of modern satellite images from Galileo sunspot drawings, (5) improvement of global IRI TEC maps, (6) one-day forecasting of global TEC maps, (7) generation of high-resolution magnetograms from Ca II K images, (8) generation of super-resolution magnetograms, (9) flare classification and visual explanation, and (10) forecasting solar X-ray profiles. We discuss our results and prospects for future applications.

KEYWORDS : sun, space weather, deep learning
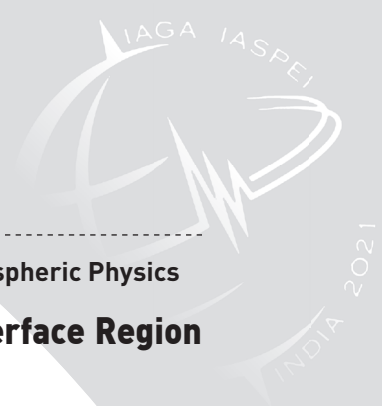
Sr No: 452

Evidence of Nanoflare-like Heating Events Observed by Interface Region Imaging Spectrograph (IRIS) (by invitation)

CORRESPONDING & PRESENTING AUTHOR:

Shah Mohammad Bahauddin, LASP, University of Colorado Boulder, USA

The heating of solar corona to several million kelvins compared to the much cooler, several thousand kelvins surface remains a mystery. One proposed mechanism is heating via a large number of small, unresolved, impulsive events called nanoflares. Each event would release energy impulsively, and the average effect would be a broad range of temperatures including a small amount of extremely hot plasma. However, detecting small scale structures and their faint, hot traces in the presence of brighter, cooler emission is observationally challenging. The enhanced spatial and temporal resolution of the solar observation satellite Interface Region Imaging Spectrograph (IRIS) has made it possible to study these structures in fine detail. IRIS has observed 'transient brightenings' in dynamic, low-lying magnetic loops, associated with strong excess line broadenings. Recently, we have discovered that the brightenings are consistent with magnetic-reconnection-mediated impulsive heating at field-line braiding sites in multi-stranded transition-region loops. The spectroscopic observations present evidence for preferential heating of heavy ions consistent with ion cyclotron turbulence caused by strong currents at the reconnection sites. Time-dependent differential emission measure distributions reveals the impulsive nature of the heating frequency and the pockets of faintly emitting 'super-hot' plasma. The observations we present and the techniques we demonstrate strengthen the possibility of ubiquitous heating by nanoflares in solar atmosphere.

KEYWORDS : solar, nanoflare, IRIS

Sr No: 453

New views of the low solar atmosphere from the Interface Region Imaging Spectrograph (IRIS) (by invitation)

CORRESPONDING & PRESENTING AUTHOR:

Bart De Pontieu, Lockheed Martin, USA

The Interface Region Imaging Spectrograph (IRIS) has been obtaining near- and far-ultraviolet images and spectra of the solar atmosphere since July 2013. IRIS is the highest resolution observatory to provide seamless coverage of spectra and images from the photosphere into the low corona. The unique combination of near- and far-ultraviolet spectra and images at subarcsecond resolution and high cadence allows the tracing of mass and energy through the critical interface between the surface and the corona or solar wind. IRIS has enabled research into the fundamental physical processes thought to play a role in the low solar atmosphere such as ion-neutral interactions, magnetic reconnection resulting from braiding, the generation, propagation, and dissipation of waves, the acceleration of non-thermal particles, and the role of reconnection, flux ropes, waves, and turbulence in flares and coronal mass ejections. Advances in numerical modeling, inversion codes, and machine learning techniques have played a key role. With the advent of exciting new instrumentation both on the ground (e.g., DKIST and ALMA), and space-based (e.g., Parker Solar Probe and Solar Orbiter), I will review new insights based on IRIS observations or related modeling, and highlight some of the outstanding challenges.

KEYWORDS : chromosphere, transition region, corona

Sr No: 454

What drives the hot solar corona? (by invitation)

CORRESPONDING & PRESENTING AUTHOR:

Lakshmi Pradeep Chitta, Max Planck Institute for Solar System Research, Germany

The outer atmosphere of the Sun, the corona is comprised of tenuous, highly ionized plasma, that is governed by magnetic fields and is heated to more than a million Kelvin. Such hot coronal plasma is thought to be powered by numerous impulsive heating events called nanoflares. What drives these impulsive nanoflares? What role does magnetic field play in coronal heating? We address these long-standing questions through multi-wavelength observations of the Sun that span from the photosphere through the corona. In this talk, we will present new results that reveal an intricate link between the impulsive coronal heating and the evolution of magnetic fields at the solar surface. In particular, we will discuss the role of magnetic reconnection, a process through which magnetic energy is liberated, in the heating of the solar corona.

KEYWORDS : sun, corona, nanoflares

Sr No: 455

A Study of Equatorial Coronal Holes during the Maximum Phase of Four Solar Cycles (by invitation)

CORRESPONDING & PRESENTING AUTHOR:

Nishu Karna, Center For Astrophysics, Harvard & Smithsonian, USA

Mahendra Karna, Nepal

Steven Saar, Center For Astrophysics, Harvard & Smithsonian, USA

William Pesnell, NASA/GSFC, USA

Edward Deluca, Center For Astrophysics, Harvard & Smithsonian, USA

The 11 yr solar cycle (SC) is characterized by periodic changes in solar activity indicators such as the number of sunspots, coronal holes, and active regions (ARs), as well as the occurrence rate of solar energetic events such as filament eruptions, flares, and coronal mass ejections. In this work, we performed a statistical study of the equatorial coronal holes (ECHs) and ARs during the maximum phase of the last four SCs: SC 21 (1979– 1982), SC 22 (1989– 1992), SC 23 (1999– 2002), and SC 24 (2012– 2015) . We compared the number of ECHs and ARs, separations between their centroids, solar wind speed, pressure, and the number of intense geomagnetic storm (IGS) data over these four cycles. We note a strong anticorrelation between the number of ARs and ECHs. We found that the number of close ARs and ECHs, solar wind speed, and the number of IGS increases with average sunspot maximum number for even cycles and decreases with average sunspot maximum for odd cycles. Also, we find strong odd– even trends in the relation between the wind properties and the numbers of close AR and ECH. These results obtained from the annual average data suggest a possible link between ECH and AR proximity and the solar wind phenomena, though odd– even trends point to the importance of other effects (e.g., Sun– Earth magnetic alignment) as well.

KEYWORDS : coronal-holes, active-regions, Solar-wind
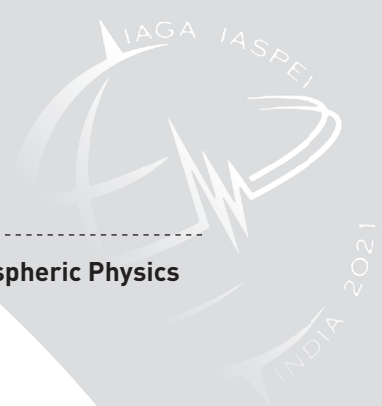
Sr No: 456

Magnetic field inference at the solar poles (by invitation)

CORRESPONDING & PRESENTING AUTHOR:

Rebeca Centeno, National Center for Atmospheric Research, USA

The measurements of magnetic fields in the Sun's photosphere is fraught with challenges derived from the limitations in the spatial resolution and the polarimetric sensitivity of the observations. This is particularly problematic at the poles of the Sun, where magnetic fields are typically weak (compared to those of active regions), and geometric projection effects make the physical area of pixels very large when observed from Earth.

The modeling assumptions underlying the interpretation of spectropolarimetric observations adds yet another layer of uncertainty to the inference of the polar magnetic fields. In this talk, we evaluate different spectral line inversion techniques and instrument stray light formulations applied to polar observations taken by the spectropolarimeter onboard Hinode. We study carefully the merit of each one of the approaches and propose a more robust methodology to analyze these datasets.

KEYWORDS :   photosphere, magnetic fields

Sr No: 457

What Have We Recently Learnt About Flare Magnetism: Observational Overview

CORRESPONDING & PRESENTING AUTHOR:

Maria Kazachenko, University of Colorado, Boulder, National Solar Observatory, USA

Continuous vector magnetic field measurements by the HMI/SDO allowed us to study magnetic field properties of many flares. In this talk I will review new observational aspects of flare magnetism described using the SDO data, including statistical properties of magnetic field changes during flares, magnetic reconnection fluxes and their rates, magnetic fluxes of flare dimmings and electric currents. I will describe how these results improved our understanding of flares and the flare/CME feedback relationship.

KEYWORDS :   solar, flares, CMEs

Sr No: 458

On Active Region Emergence Precursors (by invitation)

CORRESPONDING & PRESENTING AUTHOR:

Sylvain Korzennik, Center for Astrophysics | Harvard & Smithsonian, USA

Helioseismology has proven to be a power tools in the study of the solar interior and its changes with solar activity levels. Local helioseismic techniques allow us to focus the seismic diagnostic potential to specific area of the Sun, while the presence of magnetic features at the surface perturbs the local medium and produces an unambiguous acoustic signature.

Yet localized subsurface seismic inferences remain difficult and prone to systematic observational effects. I will review the current state of such inferences with a particular focus on detecting acoustic indicators prior to the emergence of an active region.

To this effect, I will present results from a systematic search for such pre-emergence indicators by looking at time distance travel time anomalies as well as acoustic power maps, using active regions that have emerged at low latitudes and close to the central meridian, and were observed with HMI.

By using regions that emerged near disk center, one can track the location of the emergence for days before and after the emergence time. Such data cubes of tracked surface observables can be analyzed with time-series of various length and using intensity, velocity and magnetic field measurements, to search for acoustic indicators. Since the signal is likely small and by nature non-stationary, trade-offs between temporal and spatial resolutions and careful signal filtering become key parameters in such a search.

KEYWORDS :   solar Interior, helioseismology

Sr No: 459

Using IRIS, ALMA, and the Dunn Solar Telescope to learn about (acoustic-) wave heating in the chromosphere (by invitation)

CORRESPONDING & PRESENTING AUTHOR:

Momchil Molnar, National Solar Observatory, USA
Steven Cranmer, University of Colorado, USA
Kevin Reardon, National Solar Observatory, USA

In this talk, I will present constraints on the longitudinal (e.g. compressive) and transverse (e.g. Alfvenic) wave velocity perturbations observed in the chromosphere. Better knowledge of the power in these different wave modes in different regions of the atmosphere are important inputs into models for the heating of the solar corona. By using observations at multiple viewing angles (distances from the disc center), the relative importance of these two components can be evaluated and the power in the local wave flux can be explored. This work is based on observations from the IRIS spacecraft (Mg II h & k and the Mn I 280.9 nm lines), the IBIS instrument at the DST (Ca II 854.2 nm and H-alpha lines) and brightness temperatures from ALMA. The observed phase differences between the diagnostics in these different spectral features allows us
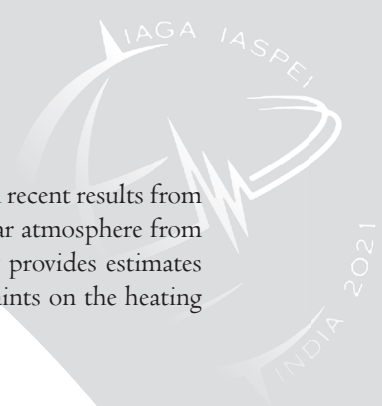
to estimate a formation height of the different lines and continua and compare them with recent results from simulations. We further combine the observations with 1D simulations of the lower solar atmosphere from the RADYN code to estimate the wave flux throughout the chromosphere. This study provides estimates of longitudinal and transverse wave power in the chromosphere, with associated constraints on the heating inputs in the middle and upper chromosphere.

KEYWORDS : chromosphere, spectroscopy, waves

Sr No: 460

SYMPOSIUM : **4.1 Advances and Upcoming Developments in Solar and Heliospheric Physics**

The Daniel K Inouye Solar Telescope and its advances for studying the solar corona (by invitation)

CORRESPONDING & PRESENTING AUTHOR:

Thomas Schad, AURA, USA

The US National Science Foundation's 4-meter aperture Daniel K Inouye Solar Telescope (DKIST) is the largest and most highly resolving optical/infrared telescope ever constructed to observe the Sun. Also, DKIST propels forward unique large-aperture coronagraphic capabilities for studying the off-limb solar corona using magnetic-dipole (M1) line spectropolarimetry. Together, these capabilities provide a powerful tool for studying the interconnected flow of mass and energy that originates in the lower atmosphere, gets transferred to and from the corona, and finally is injected into the inner heliosphere. This talk, on behalf of the DKIST science team, will highlight the advancements expected using DKIST coronagraphy, in particular for understanding the recycling of mass and energy within the closed corona, the build-up and release of magnetic energy in eruptive structures, as well as the large-scale structure and evolution of the global corona and its connections to the solar wind.

KEYWORDS : sun, coronagraphy, spectropolarimetry

Sr No: 461

SYMPOSIUM : **4.1 Advances and Upcoming Developments in Solar and Heliospheric Physics**

Coronal Pseudostreamers and Helmet Streamers: New Measurements of Plasma Properties near the Cusps (by invitation)

CORRESPONDING & PRESENTING AUTHOR:

Mari Paz Miralles, Center for Astrophysics | Harvard & Smithsonian, USA
Steven R. Cranmer, University of Colorado Boulder, USA

The role of magnetic-field topology in solar wind acceleration is an unsolved problem in solar physics. Coronal pseudostreamers differ from the more traditional helmet streamers in that they separate open field lines of the same polarity rather than the opposite polarity. Helmet streamers and pseudostreamers are believed to be sources of slow solar wind streams, despite having very different rates of superradial flux-tube expansion. Using multi-spacecraft and ground-based observations, we characterize the physical parameters of these coronal structures, and focus on their differences and similarities. Line-of-sight forward modeling

(of a range of visible-light and UV emission diagnostics) is used to investigate how the differences in magnetic topology affect the plasma properties of the coronal structures and their wind. We also aim to characterize what aspects of these structures depend directly on cusp height, no matter the polarities of the footpoints.

KEYWORDS : solar coronal streamers, solar corona, solar wind

Sr No: 462

SYMPOSIUM : **4.1 Advances and Upcoming Developments in Solar and Heliospheric Physics**

Simulations of Prominence Eruption and CME Initiation (by invitation)

CORRESPONDING & PRESENTING AUTHOR:

Yuhong Fan, National Center for Atmospheric Research, USA

We present magnetohydrodynamic (MHD) simulations of a twisted, prominence-forming coronal flux rope evolving from quasi-equilibrium to eruption. The flux rope is built up by an imposed flux emergence at the lower boundary. During the quasi-static phase of the evolution, we find the formation of a prominence-cavity system with qualitative features resembling observations, as shown by the synthetic SDO/AIA EUV images with the flux rope observed above the limb viewed nearly along its axis. The prominence condensations form in the dips of the highly twisted field lines due to runaway radiative cooling and the cavity is formed by the density depleted portions of the prominence-carrying field lines extending up from the dips. Depending on the field strength, the magnetic field supporting the prominence can be significantly non-force-free despite the low plasma-β. The prominence weight can significantly affect the stability of the flux rope and increase the loss of equilibrium height of the flux rope. The prominence draining can initiate an eruption. Finally, we will also present MHD simulations of an observed CME event using lower boundary driving conditions inferred from observed photosphere magnetic field evolution.

KEYWORDS : magnetohydrodynamics; coronal mass ejections; prominence

Sr No: 463

SYMPOSIUM : **4.1 Advances and Upcoming Developments in Solar and Heliospheric Physics**

Mapping the Sun's Alfven Zone with Inward-Flowing Plasma Parcels (by invitation)

CORRESPONDING & PRESENTING AUTHOR:

Steven Cranmer, University of Colorado Boulder, USA
Craig Deforest, Southwest Research Institute, USA
Sarah Gibson, High Altitude Observatory, USA

The Sun's Alfven surface is the point above which the solar wind speed exceeds the Alfven speed. This surface is an important critical boundary between the corona and heliosphere, and its properties affect the Sun's angular momentum evolution, the reflection of MHD turbulence, and the expansion of closed magnetic loops into the heliosphere. The upcoming PUNCH mission will map the Alfven surface and determine whether it is a steady-state structure or a more frothy "Alfven zone." In this presentation, we review existing
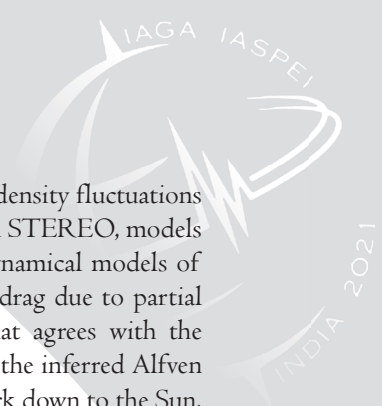
observations that attempt to locate the Alfven surface by measuring inward-propagating density fluctuations in coronagraph images. For inflowing features detected between 7 and 12 solar radii with STEREO, models of linear MHD waves could not explain their deceleration patterns. We found that dynamical models of plasma parcels that (a) accrete mass like a snowplow, and (b) experience aerodynamic drag due to partial entrainment with surrounding solar-wind flow, can become decelerated in a way that agrees with the observations. However, we found that the launch points of these parcels often sit above the inferred Alfven surface, which may require mildly supra-Alfvenic initial speeds for them to propagate back down to the Sun. This also means the parcels could be associated with nonlinear features such as reconnection-outflow jets, shocks, or shear instabilities. It is also possible that the dynamical forces on the parcels are more complex and internally structured (when near a similarly complex Alfven zone) such that they can be ducted and distorted without forming shocks.

KEYWORDS : solar corona, solar wind, magnetic reconnection

Sr No: 464

The Parker Solar Probe Solar Wind Electrons, Alphas, and Protons experiment (SWEAP): recent progress and prospects (by invitation)

CORRESPONDING & PRESENTING AUTHOR:

Michael Stevens, Smithsonian Astrophysical Observatory, USA

Launched in August 2018, the Parker Solar Probe spacecraft has completed eight full orbits of the sun, reaching a most recent perihelion distance of nearly 16 Rs. In this overview talk, I will summarize the most recent contributions of the PSP SWEAP experiment that have advanced our understanding of the non-equilibrium plasma states found in the inner heliosphere and corona, of solar wind plasma transport, and of solar wind source mechanisms.

KEYWORDS : corona, solar wind, plasma transport

Sr No: 465

Magnetosheath Microstructure: Mirror Mode Waves and Jets

CORRESPONDING & PRESENTING AUTHOR:

Xochitl Blanco Cano, UNAM, Mexico

Diana Rojascastillo, UNAM, Mexico

Luis Preisser, Österreichische Akademie der Wissenschaften, Austria

Primoz Kajdic, UNAM, Mexico

The Earth's magnetosheath is permeated with decelerated and compressed solar wind, turbulence and a variety of nonlinear waves. In addition, transient dynamic pressure (Pdyn) enhancements called magnetosheath jets can exist there. We study regions where the jets can co-exist with mirror mode waves. In particular we analized a 45 min interval when the MMS spacecraft observed a southward magnetic field (Bz < 0 nT) in the dayside magnetosheath. Under these conditions we observe jets characterized by velocity increments

and almost no density enhancements that are associated with ion distributions showing a main component and a secondary field aligned beam. The origin of such jets is related to reconnection. In contrast, other jets with more isotropic ion distributions and large density enhancements are also observed. Using MMS/THEMIS data we investigate how often can jets and mirror mode waves co-exist, and how jets, waves and ion distributions change within the magnetosheath. We find that ion bunching can occur inside some jets, and show that it is common that jets and mirror mode waves co-exist. However, the occurrence of two ion distributions inside jets is rare.

KEYWORDS : jets, magnetosheath, mirror mode

Sr No: 466

Atmospheric Gravity Waves in the Magnetized Lower Solar Atmosphere

CORRESPONDING & PRESENTING AUTHOR:
Oana Vesa, New Mexico State University, Mexico
Jason Jackiewicz, New Mexico State University, Mexico
Kevin Reardon, National Solar Observatory, USA

Atmospheric gravity waves (AGWs) are low-frequency waves driven by buoyancy forces. They are present in other stellar and planetary atmospheres, like our Earth. On the Sun, they are excited by overshooting convection and are suspected to reach and deposit energy at chromospheric heights. Recent simulations have indicated that their characteristics are sensitive to the magnetic field, with areas of strong magnetic fields suppressing their propagation or providing the basis for mode conversion into magnetoacoustic waves. Thus, this allows AGWs to be new potential seismic diagnostics in addition to commonly studied waves, such as acoustic and Alfvén waves. We can harness their untapped potential as diagnostics to sense the magnetic field and atmospheric flows in a novel way. Using high-resolution, multi-wavelength IBIS observations from the Dunn Solar Telescope and co-aligned SDO data, we investigate the characteristics of these waves throughout the lower solar atmosphere on the quiet Sun. The signatures of propagating AGWs have been observed previously at disk center. In this talk, I will explore the dynamics of these waves at disk center in addition to various locations on the quiet Sun where they have not been previously observed. This study will inform future observations of these waves, specifically on a more active Sun, using the 4-m solar telescope DKIST in the upcoming years.

KEYWORDS : gravity waves, solar atmosphere, magnetic fields

Sr No: 467

The dynamic heliosphere and its interaction with the LISM: "Ground truth" in- situ ions from the Voyagers and ENAs from Cassini (by invitation)

CORRESPONDING & PRESENTING AUTHOR:

Konstantinos Dialynas, Academy of Athens, Greece

The Voyager 1 and Voyager 2 (V1 & V2) crossings of the termination shock (TS; ~94 and ~84 AU, respectively), led to the first measurements of ions and electrons that constitute the heliosheath (HS). Their crossings of the heliopause (HP; ~122 AU and ~119 AU), pinpointed the extent of the upwind heliosphere's expansion into the Local Interstellar medium (LISM). The Cassini/INCA >5.2 keV ENA images of the celestial sphere, have placed the local V1&2/LECP measurements in a global context and have led to the discovery of a high intensity and wide ENA region that encircles the celestial sphere, called "Belt", that corresponds to a "reservoir" of particles that exist within the HS. The heliosphere forms a time-dependent, roughly symmetric obstacle to the inward interstellar flow, responding within ~2-3 yrs, in both the nose and anti-nose directions to the outward propagating solar wind changes through the solar cycle. Energy spectra from ~10 eV to 344 MeV show that the PUIs dominate the total pressure distribution inside the HS, but suprathermal ions provide a significant contribution towards maintaining the pressure balance in the HS. The combination of ENAs and ions in the HS show that the plasma beta is >>1, the ISMF upstream at the heliopause required to balance the pressure from the HS is >0.5 nT (V1 direction) and ~0.67 nT (V2 direction) and that nH~0.12/cm3. All observations, taken together, support the interpretation of a diamagnetic bubble-like heliosphere, with few substantial tail-like features.

KEYWORDS : heliosphere, cassini, voyager

Sr No: 468

Characterization of Sunspots and Solar Plages lives by the application of a 1st order Markov Chain Model

CORRESPONDING & PRESENTING AUTHOR:

Victor De Paula Vila, Ebro Observatory, Spain
Juan Jose Curto Subirats, Ebro Observatory, Spain
Teresa Sole Espuny, Ebro Observatory, Spain

We analyzed the morphological evolution of the sunspot and solar calcium plage groups recorded in the Ebro Observatory in the period 1910—1937 by using a 1st order Markov chain model in order to make predictions about several properties of these solar structures, as the probability of occurrence associated to each morphological transition, the prevalence time that these structures spend within each morphological type, the extinction-occultation forecast, the expectation that these structures have to become into a determined morphological type, and the occurrence daily rate associated to each type after a certain number of transitions. Additionally, we also analyzed the observed morphology of the structures in their appearance and extinction. Main results show that both sunspots and solar plage groups become morphologically stable after transiting to a new type. Nevertheless, this stability seems to decrease once the decay phase starts and their morphology changes into the observed type in the last stage of their evolutionary sequence. Finally,

we also studied the temporal and the spatial homogeneity of the data, concluding that both solar structures evolve with similar patterns in the northern and southern hemispheres, but both 15th and 16th solar cycles as well as each solar cycle phase, i.e., the solar minimum, the ascending phase, the solar maximum and the descending phase, present small deviations in all the analyzed properties. These deviations may affect punctually some aspects of the morphological evolution of both sunspots and solar plage groups.

KEYWORDS : Sunspots, Plages, Markov Chain Model

Sr No: 469

SYMPOSIUM : **4.1 Advances and Upcoming Developments in Solar and Heliospheric Physics**

The 7.5-year periodicity in the N-S asymmetry of sunspots and solar plages during 1910–1937

CORRESPONDING & PRESENTING AUTHOR:

Victor De Paula Vila, Ebro Observatory, Spain
Juan Jose Curto Subirats, Ebro Observatory, Spain
Ramon Julio Oliver Herrero, University of the Balearic Islands, Spain

We studied the N-S asymmetry of sunspots and solar plages from the heliophysics catalogues published annually by the Ebro Observatory during 1910—1937. The examination of the absolute and normalised N-S asymmetry indices in terms of the monthly sum of occurrences of these structures and also their sum of areas has made possible to find out a cyclic behaviour in the solar activity, in which the preferred hemisphere changes systematically with a global period of 7.5 yr approximately. In order to verify and quantify accurately this periodicity and study its prevalence in time, we also employed the RGO-USAF/NOAA sunspot data series in the period 1874—2016. Then, we examined each absolute asymmetry index time series through different techniques as the Lomb-Scargle periodogram, the CEEMDAN method, or the Complex Morlet Wavelet Transform analysis. The combined results reveal actually, that the solar activity in terms of the above-mentioned properties presents a cyclic behaviour in different time scales, consisting in two quite stable periodicities of 1.47 ± 0.10 yr and 3.8 ± 0.3 yr, which coexist with another three discontinuous components with more marked time-varying periods with means of 5.3 ± 0.4 yr, 9.0 ± 1.0 yr, and 12.7 ± 0.8 yr, respectively. Moreover, during 1910—1937, only two dominant signals with averaged periods of 4.10 ± 0.09 yr and 7.57 ± 0.08 yr respectively can be observed clearly. Finally, in both signals, periods are slightly longer for solar plages in comparison with sunspots.

KEYWORDS : 7.5-year periodicity, N-S asymmetry, solar activity
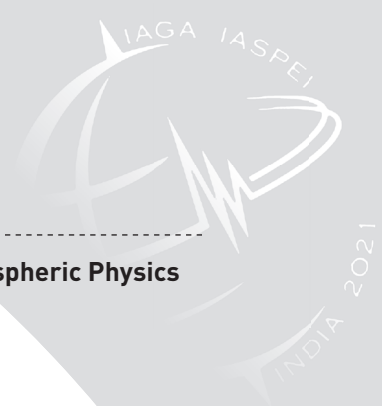
Sr No: 470

Chromospheric heating around network elements

CORRESPONDING & PRESENTING AUTHOR:

Gianna Cauzzi, AURA, USA

While it is broadly acknowledged that the interaction of magnetic field and plasma at the smallest scales plays a crucial role in chromospheric heating, many details still remain undefined. In this paper we present an observational study of the spatio-temporal heating patterns around multiple network elements, as derived from properties of the Halpha and CaII 854.2 nm lines; such patterns can help constraining the multitude of heating mechanisms currently invoked.

Expected improvements that will be made possible by the unprecedented resolution of the upcoming Daniel K. Inouye Telescope will be discussed.

KEYWORDS :   chromosphere, heating, magnetic network

Sr No: 471

An overview of the first in-situ results from Solar Orbiter (by invitation)

CORRESPONDING & PRESENTING AUTHOR:

Daniel Verscharen, University College London, UK

Solar Orbiter is the European Space Agency's latest flagship mission to study the Sun and the solar wind. After its launch in February 2020, the mission is currently in its cruise phase into the inner heliosphere. Solar Orbiter carries a suite of four in-situ instruments and six remote-sensing instruments. The group of in-situ instruments includes an Energetic Particle Detector (EPD), a Magnetometer (MAG), a Radio and Plasma Waves (RPW) instrument, and a Solar Wind Analyser (SWA). During the cruise phase, the in-situ instruments are already operational and record high-quality data of the local particles and fields.

In weekly working-group meetings, the in-situ science community has been discussing science results from Solar Orbiter since the summer of 2020. In this presentation, we will summarise a selection of the in-situ science highlights so far discussed at these working groups. We will also give a perspective on future science advances expected from the combination of the in-situ and remote-sensing instruments of Solar Orbiter.

KEYWORDS :   solar wind, in-situ science, solar orbiter

Sr No: 472

Vlasiator Advances: Global Kinetic Plasma Simulations of the Solar Wind Interaction with the Earth's Magnetic Domain (by invitation)

CORRESPONDING & PRESENTING AUTHOR:

Markus Battarbee, University of Helsinki, Finland
Urs Ganse, University of Helsinki, Finland
Yann Pfau Kempf, University of Helsinki, Finland
Lucile Turc, University of Helsinki, Finland
Maxime Grandin, University of Helsinki, Finland
Andreas Johlander, University of Helsinki, Finland
Hongyang Zhou, University of Helsinki, Finland
Maarja Bussov, University of Helsinki, Finland
Markku Alho, University of Helsinki, Finland
Maxime Dubart, University of Helsinki, Finland
Kostis Papadakis, University of Helsinki, Finland
Jonas Suni, University of Helsinki, Finland
Vertti Tarvus, University of Helsinki, Finland
Talgat Manglayev, University of Helsinki, Finland
Harriet George, University of Helsinki, Finland
Minna Palmroth, University of Helsinki, Finland

The interaction of the solar wind with the Earth's magnetic field builds up the magnetosheath and the bow shock along with a multitude of global and local plasma dynamic phenomena such as the drawn-out magnetotail. Collisionless plasmas in near-Earth space can be investigated through satellite observations, but even constellation missions provide only a few points of measurement. Simulations, on the other hand, are capable of providing both local and global spatial context to measurements of plasma phenomena.

Vlasiator is the world's most advanced kinetic magnetospheric plasma simulation, investigating global dynamics of the Earth's bow shock, foreshock, magnetosheath, magnetotail, and associated regions, in up to 6 dimensions. The hybrid-Vlasov simulation describes ions through a noise-free distribution function approach, allowing evaluation of kinetic physics at ion scales throughout the simulation domain.

We present recent advances and science results from Vlasiator, including analysis of mesoscale ion-kinetic phenomena found at the bow shock of the Earth as well as in the foreshock. We also discuss improvements to electron physics modelling in the context of the hybrid-Vlasov approach as well as the use of adaptive mesh refinement to allow 6D simulations.

KEYWORDS :   space physics, simulations, plasma physics
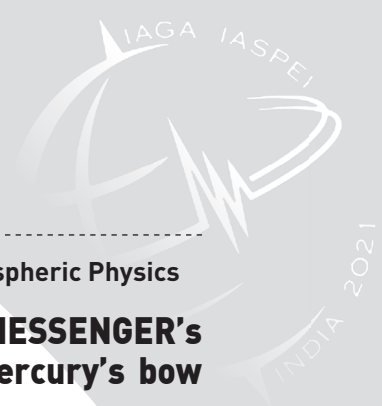
Sr No: 473

Upstream ultra-low frequency waves observed by MESSENGER's magnetometer: implications for particle acceleration at Mercury's bow shock (by invitation)

CORRESPONDING & PRESENTING AUTHOR:

Norberto Romanelli, NASA GSFC/UMBC

In this work, we present the first statistical analysis of the main properties of waves observed in the 0.05–0.41 Hz frequency range in the Hermean foreshock by the MErcury Surface, Space ENvironment, GEochemistry, and Ranging (MESSENGER) Magnetometer [Romanelli et al., 2020]. Although we find similar polarization properties to the so-called 30 s waves observed at the Earth's foreshock, the normalized wave amplitude and occurrence rate are much smaller. These differences could be associated with relatively lower backstreaming proton fluxes, the smaller foreshock size and/or less stable solar wind conditions around Mercury. In addition, we estimate that the speed of resonant backstreaming protons in the solar wind reference frame (likely source for these waves) ranges between ~1 and ~2.5 times the solar wind speed. The closeness between this range and what is observed at other planetary foreshocks suggests that similar acceleration processes are responsible for this energetic population and might be present in the shocks of exoplanets.

KEYWORDS :   ultra-low frequency waves, mercury, foreshock

Sr No: 474

Turbulent generation of magnetic switchbacks in the Alfvénic solar wind (by invitation)

CORRESPONDING & PRESENTING AUTHOR:

Munehito Shoda, National Astronomical Observatory of Japan, Japan

One of the most important early results from the Parker Solar Probe (PSP) is the ubiquitous presence of magnetic switchbacks, whose origin is under debate. Using a three-dimensional direct numerical simulation of the equations of compressible magnetohydrodynamics from the corona to 40 solar radii, we investigate whether magnetic switchbacks emerge from granulation-driven Alfvén waves and turbulence in the solar wind. The simulated solar wind is an Alfvénic slow-solar-wind stream with a radial profile consistent with various observations, including observations from PSP. As a natural consequence of Alfvén-wave turbulence, the simulation reproduced magnetic switchbacks with many of the same properties as observed switchbacks, including Alfvénic v-b correlation, spherical polarization (low magnetic compressibility), and a volume filling fraction that increases with radial distance. The analysis of propagation speed and scale length shows that the magnetic switchbacks are large-amplitude (nonlinear) Alfvén waves with discontinuities in the magnetic field direction. We directly compare our simulation with observations using a virtual flyby of PSP in our simulation domain. We conclude that at least some of the switchbacks observed by PSP are a natural consequence of the growth in amplitude of spherically polarized Alfvén waves as they propagate away from the Sun.

KEYWORDS :   solar wind turbulence, numerical simulation, magnetic switchback

Sr No: 475

Science with PUNCH: The Polarimeter to UNify the Corona and Heliosphere (by invitation)

CORRESPONDING & PRESENTING AUTHOR:

Craig De Forest, Southwest Research Institute, USA

S.E. Gibson, University Corporation for Atmospheric Research, USA

B.J. Thompson, NASA/GSFC, USA

N. Viall, NASA/GSFC, USA

S.R. Cranmer, University of Colorado, USA

A. Malanushenko, University Corporation for Atmospheric Research, USA

C. De Koning, University of Colorado, USA

M.I. Desai, Southwest Research Institute, USA

PUNCH is a NASA Small Explorer mission to study the corona and heliosphere as a single system, by making global, deep-field, 3D images of the young solar wind from the corona to the inner heliosphere. The flight segment is a constellation of four small satellites in Sun-synchronous low Earth orbit. The satellites work together as a single "virtual coronagraph" with an extremely wide field of view: from 1.5° to 45° from the Sun in all directions, all the time. Objects up to 20° from the Sun are imaged with a full polarization sequence every four minutes; the full 90° wide field of view is covered every 32 minutes. Polarization yields 3D information for each distinct feature in each image. The prime mission lasts two years with science data beginning in 2024. PUNCH data are freely available to anyone (open data policy).

The PUNCH science objectives are: (I) to understand how coronal structures become the ambient solar wind, which involves (IA) mapping solar wind flow, (IB) identifying microstructure and turbulence, and (IC) locating and understanding the Alfvén zone at the outer boundary of the corona; and (2) to understand the dynamic evolution of transient structures in the young solar wind, which involves (a) tracking CMEs and their evolution in 3D, (b) measuring CIR formation and evolution, and (c) determining dynamics of large-scale solar wind shocks.

We will present mission status, an overview of the science that drives PUNCH, and how to get involved with the mission and our international science team.

KEYWORDS :   corona, solar wind, instruments

Sr No: 476

Radial Evolution of the Ion-Scale Cyclotron Waves in the Inner Heliosphere

CORRESPONDING & PRESENTING AUTHOR:

Scott Boardsen, GPHI/NASA-GSFC, USA

Lan Jian, NASA-GSFC, USA

Leon Ofman, Catholic University/NASA-GSFC, USA

Michael Stevens, Harvard, USA

Jaye Verniero, University of California, USA

Davin Larson, University of California, USA
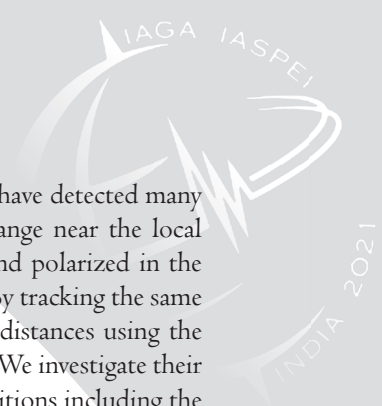
Using the high-cadence magnetic field data from Parker Solar Probe (PSP) mission, we have detected many circularly-polarized electromagnetic waves in the inner heliosphere in the frequency range near the local proton and alpha-particle cyclotron frequencies. These waves are left-hand or right-hand polarized in the spacecraft frame, and they often propagate in the direction near the local magnetic field. By tracking the same solar wind streams, we examine the properties of these waves at different heliocentric distances using the near-Sun observations from PSP and the 1-AU observations from Wind or STEREO A. We investigate their evolution in the inner heliosphere and their relationship with the solar wind plasma conditions including the ion temperature anisotropies and beam drifts.

KEYWORDS : ion cyclotron waves, phase space density, solar wind

Sr No: 477

Science using Energetic Neutral Atom Observations from IBEX (by invitation)

CORRESPONDING & PRESENTING AUTHOR:

Stephen Fuselier, Southwest Research Institute, USA

Representing the IBEX science team

The Interstellar Boundary Explorer (IBEX) has two single-pixel cameras that image the sky in Energetic Neutral Atoms (ENAs) over the energy range from 0.01 to 6 keV. The 2-year prime mission from 2009 to 2011 was tremendously successful. IBEX ENA observations during the prime mission resulted in fundamental changes in the understanding of the solar wind interaction with the local interstellar medium. Since the start of science operations, IBEX has observed ENAs continuously over more than a full solar cycle and the mission was recently extended through at least 2023. Because the ENA travel time from the termination shock/heliopause to Earth orbit ranges from more than a decade for the 0.01 keV ENAs to months for 6 keV ENAs, the extended mission has been important for understanding the time variability of all ENAs observed by IBEX. This time variability has been used to set reasonably tight limits on distances to ENA sources within the heliosphere and in the local interstellar medium. Finally, overlap of IBEX and the future Interstellar Mapping and Acceleration Probe (IMAP) mission will connect long-term IBEX ENA observations with new IMAP ENA observations at much higher sensitivity, time, and angular resolution.

KEYWORDS : interstellar medium, heliosphere, solar wind

Sr No: 478

An statistical study of the origin and the 3D propagation of small-transient events in the slow solar wind

CORRESPONDING & PRESENTING AUTHOR:

Cynthia Lopez Portela, Instituto de Geofisica, UNAM, Mexico

In this work it is presented the observational study of propagation of small-scale transients known as blobs (Sheeley et al., 1997). The minimum of the solar cycle 24 was particularly an optimal occasion to perform

an observational analysis of the detection of blobs as it has been a long quiet-period of activity. The study of the blobs' propagation has two aims: (1) to know more about their kinematic behavior and (2) to inquire about the local morphology of the solar magnetic field of their origin. The 3D analysis of propagation was based on the de-projected trajectories of blobs embedded in the continuously expanding solar corona. The selected period of observation has permitted the identification of around 100 blob-like structures detected by LASCO/SOHO and SECCHI/STEREO. In agreement with the idea that blobs are liberated from the cusps of helmet steamers (Wang et al., 1998) and considering their latitudinal distribution during the selected period of detection, the observing region in the coronagraphs was constrained to $\pm30°$ from the Sun's equator. And the inferring location of their origin in the inner solar corona was performed by the tridimensional Potential Field Source Surface (PFSS) developed by De Rosa (2003). The results of this study support previous findings that track down the origin of the slow solar wind to neighboring regions of helmet streamers and pseudostreamers (Wiegelmann et al., 1998; Wang et al., 2012; Panasenco and Velli, 2016; Sanchez-Diaz et al., 2016; Owens, Crooker, and Lockwood, 2014; Riley and Luhmann, 2012).

KEYWORDS : solar corona, solar wind, streamers and pseudostreamers

Sr No: 479

- -

SYMPOSIUM : **4.1 Advances and Upcoming Developments in Solar and Heliospheric Physics**

MAVEN observations of the Martian bow shock and foreshock (by invitation)

CORRESPONDING & PRESENTING AUTHOR:

Christian Mazelle, IRAP CNRS-University of Toulouse-CNES, France

Karim Meziane, University of New Brunswick, Canada

Without global magnetic field at Mars, its bow shock has a subsolar stand-off size and a curvature radius comparable to ion kinetic scales which raises questions related to which particle acceleration and energy dissipation mechanism can take place. The shock is also embedded well inside the neutral exosphere. Thus this is a rich example of a supercritical, mass-loaded collisionless shock that often coexists with ultra-low frequency upstream waves that are generated by the pickup ions whatever the shock geometry (including nearly perpendicular) and by foreshock backstreaming ions only for oblique geometry. We review recent results from the MAVEN spacecraft observations on the microphysics of the Martian shock and foreshock.

KEYWORDS : collisionless shock, foreshock, particle acceleration

Sr No: 480

- -

SYMPOSIUM : **4.1 Advances and Upcoming Developments in Solar and Heliospheric Physics**

Photospheric Science with the Daniel K. Inouye Solar Telescope (DKIST) (by invitation)

CORRESPONDING & PRESENTING AUTHOR:

Mark Rast, University of Colorado, USA

Construction of the National Science Foundation's Daniel K. Inouye Solar Telescope is close to completion, and instrument integration and verification at the facility are underway. With a 4m diameter primary
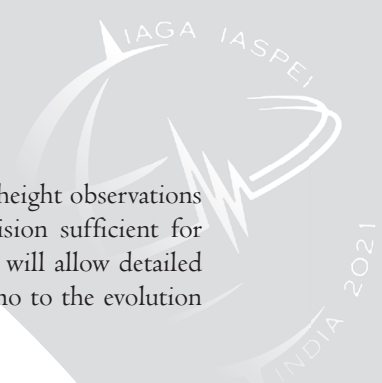
mirror, and a post-focus suite of 5 instruments, the DKIST telescope will allow multi-height observations at unprecedented spatial and temporal resolution and with spectropolarimetric precision sufficient for magnetic field determination with better than one Gauss sensitivity. These capabilities will allow detailed studies of photospheric processes ranging from the operation of the small scale dynamo to the evolution and dynamics of active regions and sunspots.

Here we focus on DKIST's anticipated contributions to our understanding of two processes that occur at the limit of observational capabilities and yet have broad importance: acoustic wave excitation and shear instability in granular downflows. Recently, data analysis techniques have been developed that should make it possible, using DKIST data, to identify individual wave sources in the photosphere. This ability may lead to new techniques in high-resolution helioseismology and allow detailed mode conversion studies based on discrete events. DKIST will also allow observations of downflows in the deep photosphere, enabling a better understanding of the degree of turbulence present there. This is important in determining the thermodynamic structure of the upper convection zone, a property critical to our understanding of the origin of the solar supergranulation. It is also critical to our understanding of the mechanisms underlying spectral line broadening which is an important uncertainty in spectropolarimetric inversions.

KEYWORDS :   photosphere, waves, turbulence

Sr No: 481

ALMA observations and spectral inversions – what can we learn about the Sun and our techniques?

CORRESPONDING & PRESENTING AUTHOR:

Ryan Hofmann, University of Colorado Boulder, USA

Kevin Reardon, National Solar Observatory, USA

Studies of the thermal structure of the solar chromosphere are typically hampered by the complexities of non-LTE radiative transfer. This issue can be addressed using observations of the millimeter continuum, which directly probes the electron temperatures in the chromosphere. In recent years, the Atacama Large Millimeter/submillimeter Array (ALMA) has made it possible, for the first time, to obtain millimeter observations of sufficient spatial resolution to supplement spectral line observations and inversions. Here, we present observations of a plage in the 3.0 mm and 1.2 mm continua with ~2 arcsecond resolution, combined with simultaneous imaging spectroscopy observations from the Interferometric Bidimensional Spectrometer (IBIS) at the Dunn Solar Telescope. We compare the observed ALMA brightness temperatures with temperatures inferred from spectral inversions using the Na D1 5896 Å and Ca II 8542 Å lines, and investigate the wide range of physical heights probed by the millimeter continuum. We find that the millimeter emission arises from a range of heights both above and below the chromospheric calcium line, depending on the local temperature profile and electron densities. We use these different diagnostics to probe the dynamics of the solar atmosphere, especially the oscillatory behaviour, and make comparison to numerical simulations.

KEYWORDS :   sun, chromosphere, inversions

Sr No: 482

The Daniel K Inouye Solar Telescope and its advances for studying the solar radiation

CORRESPONDING & PRESENTING AUTHOR:

Tetsu Anan and The DKIST Science Team, National Solar Observatory, USA

The US National Science Foundation's Daniel K. Inouye Solar Telescope (DKIST) is the largest solar optical/infrared telescope in the world and it saw first light in December 2019. DKIST reveals features in the solar photosphere and chromosphere with the highest spatial resolution, at multi wavelength ranges, and with full polarization capabilities. In addition, DKIST enables us to diagnose the solar corona off the solar limb. This talk highlights how the DKIST will improve our knowledge of the long-standing problem of chromospheric heating and of the physical mechanisms determining the radiative emission at spectral ranges forming in the higher layers of the solar atmosphere. These results are particularly important to improve our capability of modeling solar UV and EUV emission and its variability, which, in turn, is known to affect the Earth's atmosphere properties, modulate the Earth's climate, and determine the habitability of exo-planets.

KEYWORDS : sun, DKIST, radiation

Sr No: 483

The role of magnetic reconnection in coronal heating and solar wind acceleration (by invitation)

CORRESPONDING & PRESENTING AUTHOR:

David Pontin, University of Newcastle, Australia, Australia

Magnetic reconnection is a fundamental process in a plasma that allows a change of the magnetic field topology, often associated with a rapid release of magnetic energy. Here we review a few recent advances in our understanding of the importance of reconnection, both for heating the Sun's corona to its observed multi-million degree temperature, and for releasing plasma from the closed-field corona to form the solar wind.

KEYWORDS : reconnection, corona, wind

Sr No: 484

Understanding Our Heliospheric Shield: Advances in Numerical Models

CORRESPONDING & PRESENTING AUTHOR:

Merav Opher, Boston University, USA

The heliosphere is an immense shield that protects the solar system from harsh, galactic radiation. This

radiation affects not only life on Earth, but human space exploration as well. In order to understand the evolution of the heliosphere's shielding properties, we need to understand its structure and large-scale dynamics. The heliosphere is a template for all other astrospheres, enabling predictions about the conditions necessary to create habitable planets. Space science is at a pivotal point in generating new understandings of the heliosphere due to the flood of new in situ data from the Voyager 1 (V1), Voyager 2 (V2), and New Horizon spacecraft, combined with the energetic neutral atom (ENA) maps generated by IBEX and Cassini.

To date, our best large-scale computer models fail to reproduce critical observations, such as the size of the heliosphere, the plasma speeds and directions, and the width of the heliosheath.

I this talk I will review some of the existing numerical models, the differences between them and the effect that this entail in how the heliosphere is described. I will describe as well the limitations of current models and possible directions to mitigate such limitations.

I will review as well some of the efforts done in extending current models in the recently funded NASA Science Center SHIELD (Solar-wind with Hydrogen Ion Exchange and Large-scale Dynamics).

KEYWORDS : heliosphere, modeling, kinetic processes

Sr No: 485

SYMPOSIUM :   **4.1 Advances and Upcoming Developments in Solar and Heliospheric Physics**

Determining Chromospheric Structure and Stratification with Polarimetric Inversions of Non-LTE Spectral Lines (by invitation)

CORRESPONDING & PRESENTING AUTHOR:

Han Uitenbroek, National Solar Observatory, USA

The chromosphere sits in between the photosphere and the much hotter transition region and corona. It represents the initial temperature rise from the cooler lower layers and represents two important transitions of physical regimes, namely from convectively dominated photosphere to the magnetically dominated corona, and from the optically dense regime to the optically thin upper layers. These transitions are fundamental to the way the chromosphere transports energy from the photosphere to the corona. It is, therefore, critical to determine the stratification of temperature, density, ionization, magnetic field and unresolved motions in this transitional layer.

The 4-m class DKIST will be greatly extend our capabilities to determine the structure and stratification of these physical quantities in the chromosphere, not only because of its high spatial resolution, but also because of its large photon collecting area, which is critical to extract the low-percentage polarization signals that are used to determine magnetic fields remotely.

I will describe a computer code that can be used to efficiently invert spectro-polarimetric observations of chromospheric lines to determine the physical structure of the chromosphere. Because of their low densities the spectral lines that have significant opacity in these layers form under general Non-Local Thermodynamic conditions, which has to be accounted for in the inversions.

Finally, I will describe the organization of Level-2 data effort at the dKIST to run the required inversions in an automatic way for certain pre-determined observations in order to produce data sets that are ready to be used by the solar community.

KEYWORDS : sun, chromosphere, radiative transfer

Sr No: 486

Time-dependent simulations of the inner heliosphere with GAMERA model

CORRESPONDING & PRESENTING AUTHOR:
Elena Provornikova, Applied Physics Laboratory, USA
Vyacheslav Merkin, Applied Physics Laboratory, USA
Charles Arge, Goddard Space Flight Center, USA

Accurate description of the solar wind and magnetic field in the inner heliosphere is crucial for understanding dynamic plasma processes in the interplanetary medium and characterization of a background where solar coronal mass ejections and solar energetic particles propagate. Most current inner heliosphere models prescribe a steady state solution driven by a single photospheric magnetogram. In this work we demonstrate a new capability of the GAMERA (Grid Agnostic MHD with Extended Research Applications) code to model time-dependent inner heliosphere driven by a changing input from coronal WSA-ADAPT model. GAMERA model is a reinvention of the high-heritage Lyon-Fedder-Mobarry (LFM code). The distinctive features of the MHD algorithms employed by GAMERA include a highly-conservative shock-capturing scheme with very low numerical dissipation and intrinsically divergence-less magnetic field. The time-dependent inner heliosphere simulation is driven by the ADAPT-WSA solutions at 21 solar radii that are updated every 2 hrs. We describe a method to set boundary conditions in GAMERA that ensure changes of radial magnetic field at 0.1 AU specified by WSA solutions. We demonstrate time-dependent inner heliosphere simulation for a Parker Solar Probe close encounter and compare GAMERA results with in-situ observations near the Sun and at 1 AU.

KEYWORDS : inner heliosphere, simulations, solar wind

Sr No: 487

Science with Parker Solar Probe / WISPR (by invitation)

CORRESPONDING & PRESENTING AUTHOR:
Mark Linton, US Naval Research Laboratory, USA

The Wide-field Imager for Solar Probe (WISPR) is the imaging instrument on board NASA's Parker Solar Probe (PSP), launched in August 2018 with the mission of making measurements of the near-Sun plasma with gradually reduced perihelia from 35 Rs in 2018-19 to 9.8 Rs in 2025. To date PSP has successfully completed eight perihelia, with the eighth perihelion descending to just below 16 Rs.

Here we report results from the imaging observations of the electron and dust corona taken by WISPR during this first part of the mission. WISPR observations have presented us with evidence that the primordial dust orbiting the Sun is depleted near the Sun – a long-hypothesized phenomenon. In addition, WISPR has detected the circumsolar dust ring near Venus' orbit and the dust trails left behind in the orbits of active asteroid 3200 Phaethon and comet 2P/Encke, as well as images of comets themselves as they near the perihelia of their orbits about the Sun. We will review these observations and analyses, and discuss prospects for what WISPR may be able to find for us as it continues its voyage down to 9.8 Rs.

Sr No: 488

Parker Solar Probe Observations of the Solar Wind Proton-Alpha Differential flow

CORRESPONDING & PRESENTING AUTHOR:

Parisa Mostafavi, Johns Hopkins University Applied Physics Lab., USA

Robert C. Allen, Johns Hopkins University Applied Physics Lab., USA

Michael Mcmanus, Berkeley University, USA

Nour Raouafi, Johns Hopkins University Applied Physics Lab., USA

George Ho, Johns Hopkins University Applied Physics Lab., USA

Ali Rahmati, Berkeley University, USA

Jaye Verniero, Berkeley University, USA

Davin Larson, Berkeley University, USA

Solar wind proton and alpha particles are known to have different properties from one another. For example, the temperature, velocity, and density of alpha particles relative to protons can vary in a manner dependent on the solar wind type. While previous studies have investigated the evolution of the proton and alpha particles' differential velocities by comparing observations at 1 au by Wind to that at 0.3-0.7 au by Helios, Parker Solar Probe (PSP) now enables insights into these differential velocities, and relative properties, of newly accelerated solar wind very close to the Sun for the first time. In this work, we present the radial evolution of the difference between proton and alpha particle bulk velocities, densities, and temperatures observed by PSP using Solar Probe Analyzer for Ions (SPAN-Ion) and FIELDS data near perihelia when the core solar wind is in the field of view of SPAN-Ion. As has been previously observed at larger heliospheric distances, the magnitude of the proton-alpha differential speed is mostly below the local Alfvén speed and is greater for fast wind streams than for the slow solar wind. Additionally, while alpha particles typically have a higher speed than protons, the slow solar wind is sometimes characterized by higher proton speeds than alpha particle speeds. The Alpha-to-proton density ratio is also observed to be larger in the fast wind than in slow wind. Characteristics of the alpha-to-proton populations are also studied in relation to magnetic field reversals (switchbacks) observed by PSP.

KEYWORDS : parker solar probe, alpha particles, switchbacks

Sr No: 489

From the large to the small scales, and then back: On the global role of electron physics in the solar wind (by invitation)

CORRESPONDING & PRESENTING AUTHOR:

Maria Elena Innocenti, Ruhr University Bochum, Belgium

Alfredo Micera, Royal Observatory of Belgium / University of Leuven, Belgium

Elisabetta Boella, Lancaster University, UK

Anna Tenerani, The University of Texas at Austin, USA

Marco Velli, UCLA, USA

Non trivial interactions between small and large scale processes occur in most plasmas. In the solar wind however, such interactions are particularly fascinating, and require appropriate modeling developments.

In this talk, we examine how solar wind plasma expansion affects both the kinetics of the solar wind at small scales (driving microinstabilities and hence limiting the evolution of local temperature anisotropies) and heat-flux regulation at large scale.

It has been known for decades that kinetic instability can significantly contribute to heat-flux regulation at large heliocentric distances [Scime et al, 1994]. Recently, Parker Solar Probe observations have confirmed that this is the case also closer to the Sun [Halekas et al, 2020].

Heat-flux regulating instabilities, as many other in the solar wind (eg Matteini et al, 2013; Stverak et al, 2008), are influenced in their onset and evolution by solar wind plasma expansion, that modifies the background solar wind parameters with heliocentric distance, and can therefore contribute to instability stabilisation and destabilisation [Innocenti et al, 2019b].

In this work, we investigate this complex web of large-scale/ small-scale interaction through fully kinetic Expanding-Box-Model simulations performed with the newly-developed EB-iPic3D code [Innocenti et al, 2019a], where plasma expansion is self-consistently included into the model evolution. We show that, indeed, plasma expansion can indirectly contribute to heat flux regulation, by affecting heat flux regulating instabilities [Innocenti et al, 2020, Micera et al, in prep].

KEYWORDS : solar wind, electron physics, heat flux regulation

Sr No: 490

Impulsive excitation and dissipation of large amplitude slow magnetosonic waves in coronal loops: observations and modeling

CORRESPONDING & PRESENTING AUTHOR:

Leon Ofman, NASA GSFC/CUA, USA

Tongjiang Wang, NASA GSFC/CUA, USA

Slow magnetosonic waves associated with flares and impulsive flows were observed in hot coronal loops
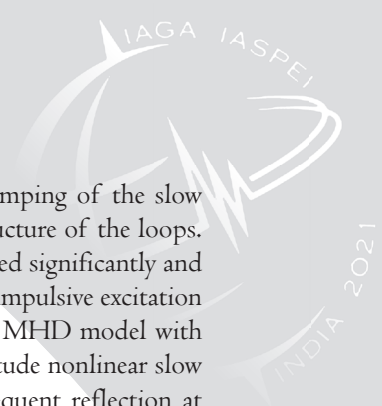
in detail by SDO/AIA, Hinode/XRT and other instruments. The excitations and damping of the slow magnetosonic waves provide information on the magnetic, temperature, and density structure of the loops. Recently, it was found using coronal seismology that the thermal conduction is suppressed significantly and compressive viscosity is enhanced in hot (T>6 MK) flaring coronal loops. We study the impulsive excitation and damping of slow magnetosonic waves in realistic coronal loop geometry using 3D MHD model with compressive viscosity and thermal conduction along the magnetic field. The large amplitude nonlinear slow magnetosonic waves are produced by upflow pulse at the loops' footpoint, and subsequent reflection at the footpoints. We find that the enhanced compressive viscosity leads to rapid formation of standing slow magnetosonic waves, followed by rapid wave dissipation. We demonstrate the mode coupling between the slow and fast mode waves. The realistic 3D model of the slow magnetosonic waves provides improved coronal seismology diagnostic of the dissipation coefficients in hot coronal loops. Our simulation results suggest that the effective transport coefficients may play a key role in the formation of standing or reflected propagating slow-mode waves observed in flaring coronal loops.

KEYWORDS :   coronal loops, magnetosonic waves, MHD modeling

Sr No: 491

Aditya Solar wind Particle EXperiment (ASPEX) on-board Aditya-L1 Mission of India

CORRESPONDING & PRESENTING AUTHOR:

Dibyendu Chakrabarty, Physical Research Laboratory, India

Many aspects of the origin, acceleration and anisotropy of solar wind particles are poorly understood till date. In order to comprehensively understand the solar and interplanetary processes and anisotropies based on solar wind measurements from the first Lagrangian (L1) point of the Sun-Earth system, it is essential to have multi-directional measurements of both low and high energy particles. In addition, it is also important to measure protons (H+, the most abundant ions) and alphas (He2+, second most abundant ion) in the solar wind separately as their differential behavior may throw light on the physical processes associated with the origin and acceleration of solar wind. Keeping these aspects in mind, Aditya Solar wind & Particle EXperiment (ASPEX) experiment on Aditya-L1 mission has been designed. ASPEX has two subsystems - Solar Wind & Ion Spectrometer (SWIS) and the Supra Thermal & Energetic Particle Spectrometer (STEPS). SWIS has two units - Top Hat Analyzer-1 (THA-1) and -2 (THA-2) looking in and across the ecliptic plane and will measure particles in the energy range of 100 eV to 20 keV. On the other hand, STEPS has six detector units pointing towards radial, Parker, intermediate (between radial and Parker), Earth, north and south directions and will measure particles in the energy range of 20 keV/n to 5 MeV/n. Therefore, ASPEX will make in-situ, multi-directional measurements of the slow & fast solar wind, supra-thermal and energetic particles in the energy range of 100 eV to 5MeV /n to address the outstanding science issues.

KEYWORDS :   aditya-L1, ASPEX, solar wind

Sr No: 492

Periodic mesoscale structures observed with Parker Solar Probe WISPR

CORRESPONDING & PRESENTING AUTHOR:

Nicholeen Viall, NASA Goddard Space Flight Center, USA

Angelos Vourlidas, Johns Hopkins University Applied Physics Laboratory, USA

Craig Deforest, Southwest Research Institute, USA

Larry Kepko, NASA Goddard Space Flight Center, USA

Russ Howard, Naval Research Laboratory, USA

Mark Linton, Naval Research Laboratory, USA

Simone Di Matteo, NASA Goddard Space Flight Center, USA

Aleida Higginson, NASA Goddard Space Flight Center, USA

Mesoscale structure in the solar wind (~tens to several thousands of Mm) are created in two possible ways: those that come directly from the Sun, and those formed through processing en route as the solar wind advects outward. Complexity arises from a competition between the imposed and injected structures that survive from the Sun and turbulence and other dynamical evolution. Understanding the source and evolution of solar wind structures is important because it contains information on how the Sun forms the solar wind and it constrains the physics of turbulent processes. Mesoscale structures also comprise the ground state of space weather, continually buffeting planetary magnetospheres. In this paper we present a case study of the first observations of periodic trains of mesoscale structures in solar wind density observed by the Wide-field Imager for Parker Solar PRobe (WISPR). Periodic trains of mesoscale structures in solar wind density have been observed close to the Sun with in situ data from the Helios spacecraft, as well as remotely in STEREO/COR2 and STEREO/HI1 white light imaging data. While some periodic density structures may be a consequence of the development of dynamics en route, many are remnants of the formation and release of the solar wind, and thus provide important constraints on solar wind models. The observation of periodic density structures so near to the Sun allows us to begin disentangling how much structure is created during solar wind formation, versus how much is due to evolution as the solar wind advects outward.

KEYWORDS :   solar wind, mesoscale structures

4.3 Space Weather and Climate Throughout the Solar System: Bringing Data and Models Together

CONVENERS: Laure Lefevre

Suiyan Fu

Noé Lugaz

Baptiste Cecconi

Mateja Dumbovic

Phillip Hess

Anna Malanushenko

Emilia Kilpua

Dibyendu Nandi

Drew Turner

Qiugang Zong

Yoshizumi Miyoshi

With the growing human technology and space exploration, understanding and modelling of space weather and climate driven by the solar activity is becoming exceedingly important.

Magnetic fields play a prominent role in driving solar activity and space weather from Sun to Earth. In the solar atmosphere, when these magnetic fields become twisted, they form twisted magnetic flux ropes, a coherent, self-confining structure, which allows them to store energy. This coherence is often invoked as a reason why bundles of magnetic flux can rise buoyantly to the solar surface to form active regions. This coherence has also been proposed as a means for storing eruptive capacity in coronal magnetic fields, and then driving solar eruptions such as flares and coronal mass ejections (CMEs). This underlying flux rope structure is used to explain the commonly observed coherence of CMEs when observed in the outer corona. As interplanetary CMEs pass over spacecraft in the heliosphere, single-spacecraft measurements are often consistent with this coherence, and have been traditionally considered evidence of twisted magnetic field structure. Flux ropes are also believed to form both at magnetopauses and in magnetotails as a consequence of the solar wind magnetic field interacting with planetary magnetospheres, and they play a key role in the transmission of mass energy and momentum within magnetospheres.

The interaction between transient solar wind events, e.g. CMEs, CIRs, and the Earth's magnetosphere would excite various types of geomagnetic phenomena, which is of great importance for the space weather research in the past several decades. Based on coordinate observations of satellites and high time resolution data obtained in recent years, progress has been made on the magnetosphere response to solar wind forcing in many aspects covered by radiation belt physics, magnetic storms and magnetospheric substorm mechanism, etc. Knowledge on the relationship between wave activities (e.g. ULF/VLF waves) and the variations of energetic particle flux in the inner magnetosphere has been greatly improved. Extensive attempts also have been made to further understand how the solar wind energy couples into the magnetosphere, leading to space weather phenomena.

The amount of scientific data from numerous missions in the heliosphere is growing rapidly, as is the number and variety of models. The availability of the large amount of data evokes novel, data driven forecasting methods and techniques. In order to use these novel methods for space weather applications, a rigorous examination of the available data, the applied techniques, and the statistical properties of the system are necessary.

In this symposium, we will explore various phases of flux rope formation and evolution from the Sun to geospace and planetary space environments, and we will explore ways in which a better understanding of this behavior can lead to improved insights into solar activity and space weather. In addition, we will explore recent progress in handling data sources, data quality issues, forecasting techniques and modelling of space weather and space climate at any point along the chain from the Sun to planets. Finally, we will explore progress from space-borne and ground-based observations, theoretical modeling and simulation studies to understand the causes and consequences of space weather phenomena in the Earth magnetosphere.

Sr No: 493

Model comparisons of CME and HSS driven Joule heating

CORRESPONDING & PRESENTING AUTHOR:

Pelin Erdemir, Istanbul Technical University, Turkey

Zerefsan Kaymaz, Istanbul Technical University, Turkey

Emine Ceren Kalafatoglu Eyiguler, Istanbul Technical University, Turkey

Lutz Rastaetter, NASA Goddard Space Flight Center, USA

Magnetic disturbances such as geomagnetic storms and substorms are known as one of the driving mechanisms of upper atmospheric Joule heating. Two main phenomena causing disturbances are coronal mass ejections (CMEs) and high speed solar wind streams (HSSs). Since the characteristics of these two solar disturbances differ, the magnetosphere is expected to give different responses. In this study, the Joule heating rates during a CME and an HSS event are examined by using MHD model. Two different magnetic storm/substorm cases, one for CME and the other for HSS, are chosen and the SWMF/BATS-R-US MHD model was run for both solar events and the resulting Joule heating rates are compared. The preliminary results show that CME driven storms and substorms have higher Joule heating ratio compared to the HSS driven ones. Following this, the storm and substorm phases for each event are identified by examining Dst and AE indices. Multiple storms and substorms are considered and the Joule heating rate corresponding to each storm and substorm phase was calculated. Comparisons indicate that the main phase of both CME and HSS storms gave the highest heating rates compared to other phases. Also, the expansion phase of the substorms during both events produced the highest heating. To form a basis for a statistical study, the number of CME and HSS events will be increased and comparisons will be expanded using MHD models and AE index method of empirical calculations. At the meeting, the results will be discussed from the geoeffectiveness of both events.

KEYWORDS : joule heating, high speed solar wind stream, coronal mass ejection

Sr No: 494

Study of Energetic Ion variations at near Earth plasma during Substorms events and associated Dipolarization using Van Allen Probes data

CORRESPONDING & PRESENTING AUTHOR:

Trunali Shah, Indian Institute of Geomagnetism, India

B. Veenadhari, Indian Institute of Geomagnetism, India

Megha Pandya, Indian Institute of Geomagnetism, India

The Earth's magnetosphere is formed by the deflection of continuously flowing solar wind and the geomagnetic field. During a geomagnetic storm, the ring current ion composition changes considerably. The quiet time ring current consists of mainly protons (H+), while the intense storm time ring current is dominated by O+ ions. On the other hand, the phenomenon of magnetospheric Substorms are responsible for the discrete injection of energetic ions at the geosynchronous orbit. In the current

studies, we intend to study the effect of the Substorm on variations of energetic ions, H+, He+, O+ in the inner magnetosphere (a geocentric distance of r <6.6 Earth Radius). So, we combinely study the substorm onset events from the year 2017-2019 using the Van Allen Probes observations. In this study we analyse H+, He+, O+ data from Helium Oxygen Electron flux (HOPE), and magnetic field data from the Electric and Magnetic field instrumentation Suit and Integrated Science (EMFISIS) instrumentation suit on board the satellite. Using this data, we study some good number of Substorm onset events for energy range of 1eV to 50keV energetic ions. We classify events into different categories based upon the L value at the onset of the Substorm. Our current studies will provide the quantification of the observed energetic ions at different energies and L-value during the Substorm. The detailed results with the analysis of statistically significant number of events and the related mechanisms will be discussed in the meeting.

KEYWORDS : substorms, dipolarization, inner magnetosphere

Sr No: 495

SYMPOSIUM : **4.3 Space Weather and Climate Throughout the Solar System: Bringing Data and Models Together**

On Developing physics-based Solar Wind Model contemplating in-situ Measurements of Aditya-L1

CORRESPONDING & PRESENTING AUTHOR:

Prateek Mayank, IIT Indore, India

Solar Wind streams, acting as a background, govern the propagation of coronal mass ejections in the heliosphere and drive geomagnetic storm activities. Therefore, predictions of the solar wind parameters are the core of space weather forecasts. Also, the structure and dynamics of the heliospheric magnetic field (HMF) are key to understanding the solar wind flow.

Typically, line-of-sight observations of a magnetogram are used to derive the HMF structure and then a solar wind model is used for forecasting solar wind parameters. Here, we present an implementation of our physics-based solar wind model aiming to complement the in-situ measurements of Aditya-L1; in particular, we will discuss our recent extension of the pilot study (Kumar et al., 2020) of data-driven solar wind prediction at L1.

We will demonstrate a detailed overview of our algorithm that incorporates coronal magnetic field modeling and the physics-based approach adopted for the inner heliosphere. We will validate our results by comparing essential thermal and dynamical properties of the solar wind at L1 and also discuss how these parameters are affected based on the choice of input magnetograms.

Finally, we will associate the output of our 3D physics-based approach to the observations from in-situ instruments of Aditya-L1, like ASPEX, PAPA and MAG.

KEYWORDS : solar wind model, aditya-L1

Sr No: 496

International initiatives to enhance space weather information architecture (by invitation)

CORRESPONDING & PRESENTING AUTHOR:

Arnaud Masson, Tpz UK for the European Space Agency, Spain

The heliophysics and space weather communities have entered the era of big data for almost a decade now. Research analysis and modelling efforts to understand system-level heliophysical processes and to enable forecast of space weather events rely largely on the preservation, accessibility and usability of diverse data products (space-based and ground-based). Information architecture, including standards for data models, metadata and data access protocols, can enhance data distribution, support data mining and data-model comparison. Since early 2020, a worldwide initiative has been setup: The International Space Weather Action Teams or ISWAT. On top of fostering international collaboration among the various scientific topics of space weather, a dedicated group was formed on information architecture. This initiative is complementary to another working group gathering major data providers in the field of heliophysics, since 2018, the International Heliophysics Data Environment Alliance (IHDEA). This talk will report achievements and on-going activities of both of these initiatives.

KEYWORDS : space weather, information architecture, data-model comparison

Sr No: 497

VirES: Data & model access for ESA's Swarm mission

CORRESPONDING & PRESENTING AUTHOR:

Ashley Smith, University of Edinburgh, UK

Martin Paces, EOX IT Services, Austria

As Swarm's product portfolio grows to better deliver on the mission's goals, we face increasing complexity in accessing, processing, and visualising the data and models. ESA provides "VirES for Swarm" [1] to help solve this problem (developed by EOX IT Services). VirES is a web-based data retrieval and visualisation tool where the majority of Swarm products are available. VirES has a graphical interface but also a machine-to-machine interface (API) for programmable use. A Python client is provided [2]. The VirES API also provides access to geomagnetic ground observatory data (INTERMAGNET), as well as forwards evaluation of geomagnetic field models to give data-model residuals. The "Virtual Research Environment" (VRE) adds utility to VirES with a free cloud-based JupyterLab interface allowing scientists to immediately program their own analysis of Swarm products using the Python ecosystem. We are augmenting this with a suite of Jupyter notebooks [3] and dashboards, each targeting a specific use case, and seek community involvement to grow this resource.

[1] VirES for Swarm: https://vires.services

[2] Python client: https://viresclient.readthedocs.io

[3] Notebooks: https://swarm.magneticearth.org

KEYWORDS : swarm, ionosphere, python

Sr No: 498

Human-efficient labeling of a solar flux emergence video dataset by a deep learning model (by invitation)

CORRESPONDING & PRESENTING AUTHOR:

Subhamoy Chatterjee, Southwest Research Institute, USA

Andres Munoz Jaramillo, Southwest Research Institute, USA

Derek Lamb, Southwest Research Institute, USA

Machine learning is becoming a critical tool for interrogation of large complex data. However, labeling large datasets is time consuming. Here we show that convolutional neural networks (CNNs), trained on crudely labeled astronomical videos, can be leveraged to improve the quality of data labeling and reduce the need for human intervention. We use videos of the solar photospheric magnetic field, crudely labeled into two classes: emergence or non-emergence of large bipolar magnetic regions (BMRs). We train the CNN using crude labeling, manually verify, correct labeling vs. CNN disagreements, and repeat this process until convergence. This results in a high-quality labeled dataset requiring the manual verification of only ~50% of all videos. Furthermore, by gradually masking the videos and looking for maximum change in CNN inference, we locate BMR emergence time without retraining the CNN. This demonstrates the versatility of CNNs for simplifying the challenging task of labeling complex dynamic events.

KEYWORDS :   sun, flux emergence, convolutional neural network

Sr No: 499

HAPI: A Standard that Enables Uniform Access to Space Weather Time Series Data

CORRESPONDING & PRESENTING AUTHOR:

Jon Vandegriff, Johns Hopkins Applied Physics Lab, USA

Robert Weigel, George Mason University, USA

Jeremy Faden, Cottage Systems, USA

Aaron Roberts, GSFC, USA

Todd King, UCLA, USA

Nand Lal, GSFC, USA

Bernard Harris, GSFC, USA

Scott Boardsen, UMBC, USA

Eric Grimes, UCLA, USA

The Heliophysics Application Programmer's Interface (HAPI) is an emerging standard for the serving of time series data, which comprises a large fraction of Space Weather data products. HAPI capitalizes on the fundamental similarities of existing services and defines a set of operations that are in fact easy for data providers to add in a non-disruptive way alongside existing access methods. Multiple data providers in the US and Europe have added HAPI access to their holdings, verifying HAPI's claim to capture essential

features. Several important science analysis codes (client readers for retrieving data) have been or are being updated to include the ability to read from HAPI servers. Wider adoption of HAPI will allow uniform access to large amounts of diverse and distributed data products associated with Space Weather. This kind of uniform access has been the holy grail of interoperability, and for time series data, HAPI offers a clear path forward. We will present highlights of the specification, and talk about adoption avenues for data providers and science data users.

KEYWORDS : data, interoperability, access

Sr No: 500

SYMPOSIUM : **4.3 Space Weather and Climate Throughout the Solar System: Bringing Data and Models Together**

PCA-MRM model for TEC over the Iberian Peninsula: performance in different space weather conditions

CORRESPONDING & PRESENTING AUTHOR:

Anna Morozova, University of Coimbra, Portugal

Teresa Barata, University of Coimbra, Portugal

Tatiana Barlyaeva, University of Coimbra, Portugal

The total electron content (TEC) over the Iberian Peninsula was modeled using a PCA-MRM models based on the decomposition of the observed TEC series using the principal component analysis (PCA) and reconstruction of the daily modes' amplitudes by a multiple linear regression model (MRM) using several types of space weather parameters as regressors. As regressors the following space weather parameters are used: proxies for the solar UV and XR fluxes, number of the solar flares of different types, parameters of the solar wind and of the interplanetary magnetic field, and geomagnetic indices. Lags of 1 and 2 days between the TEC and space weather parameters are used.

The performance of the PCA-MRM model is tested on days with different space weather conditions: quiet days, days with solar flares, and days with geomagnetic disturbances. Since MRMs were built using the "best subset" of the regressors, the set of the most significant space weather parameters for the TEC forecast was defined. These parameters are the solar UV proxy; the geomagnetic index Dst and the By component of the interplanetary magnetic field.

KEYWORDS : ionosphere, space weather, PCA

Sr No: 501

SYMPOSIUM : **4.3 Space Weather and Climate Throughout the Solar System: Bringing Data and Models Together**

Understanding our capabilities in observing and modelling coronal mass ejections (by invitation)

CORRESPONDING & PRESENTING AUTHOR:

Christine Verbeke, Royal Observatory Belgium, Belgium
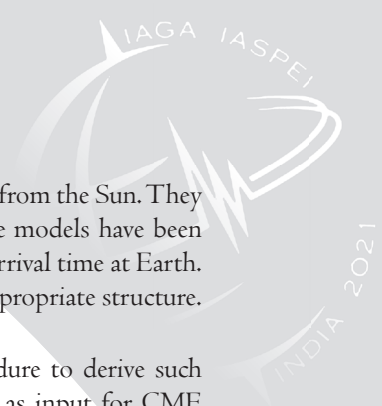
Coronal Mass Ejections (CMEs) are large-scale eruptions of plasma and magnetic fields from the Sun. They are considered to be the main drivers of strong space weather events at Earth. Multiple models have been developed over the past decades to predict the propagation of CMEs and their possible arrival time at Earth. Such models require input from observations, which can be used to fit the CME to an appropriate structure.

When determining parameters associated to the CME structure, it is common procedure to derive such kinematic parameters from remote-sensing data. The resulting parameters can be used as input for CME propagation models to obtain an arrival time prediction of the CME e.g. at Earth. However, different geometric structures and different parts of the CME structure can be fitted, and these aspects, together with the fact that most 3D reconstructions are performed by a scientist, creating a subjectivity of the fit, may lead to uncertainties in the fitted parameters. To our knowledge, so far, no large scale study has tried to map these uncertainties and how these affect the modelling of arrival time models.

As a start for this work, we focused on the effect cause by the influence and subjectivity of the performing scientist. We have designed a synthetic situation where the "true" geometric parameters are known in order to quantify such uncertainties for the first time and discuss the results. We explore further work of the associated ISSI team.

KEYWORDS :   coronal mass ejections, GCS model, error estimation
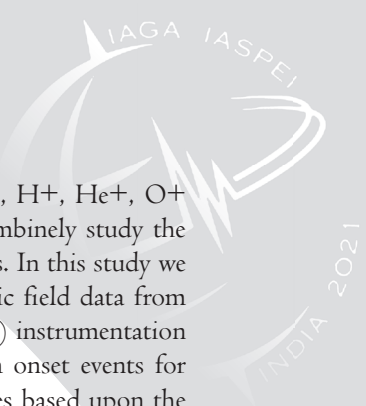
Sr No: 502

SYMPOSIUM :   **4.3 Space Weather and Climate Throughout the Solar System: Bringing Data and Models Together**

Why does the "solid-body" aerodynamic drag law work for CMEs?

CORRESPONDING & PRESENTING AUTHOR:

Debesh Bhattacharjee, Indian Institute of Science Education and Research (IISER), Pune, India

Prasad Subramanian, Indian Institute of Science Education and Research (IISER), Pune, India

Angelos Vourlidas, Johns Hopkins University, USA

Teresa Nieves Chinchilla, NASA-Goddard Space Flight Center, Greenbelt, MD (USA), USA

Niranjana Thejaswi, The University of Arizona, USA

Nishtha Sachdeva, University of Michigan, USA

Earth directed solar coronal mass ejections (CMEs) are primary drivers of space weather disturbances. The near-Earth manifestation of a CME is often termed as an interplanetary coronal mass ejection (ICME). Solar wind aerodynamic drag plays an important role in determining the dynamics of CMEs as they propagate from the Sun to the Earth. The commonly used formula for the CME aerodynamic drag is the one experienced by a solid body in a high Reynolds number flow. This is different from the aerodynamic drag formula for a bubble in a high Reynolds number flow. On the other hand, coronagraph observations suggest that CMEs are more like deformable plasma blobs than solid bodies. To investigate this apparent paradox, we analyzed in-situ data from 166 well observed ICMEs (at 1 AU) from the WIND ICME catalogue. We calculate the ratio of the energy per unit mass associated with the plasma (which includes magnetic and thermal energies) to the kinetic energy (per unit mass) due to the solar wind flow impinging on the ICME. We find a distinct enhancement of this ratio inside the ICME. This suggests that the apparent solid-body like character of ICMEs (at least with regard to aerodynamic drag) might be due to the dominance of the ICME plasma pressure over the ram pressure of the oncoming solar wind.

KEYWORDS :   magnetohydrodynamics, coronal mass ejections, solar wind

Sr No: 503

Determining and Inferring the Near-Sun Magnetic Field of Coronal Mass Ejections (by invitation)

CORRESPONDING & PRESENTING AUTHOR:

Spiros Patsourakos, University of Ioannina, Greece

The most important factor to decide the geoeffectiveness of Coronal Mass Ejections (CMEs) upon impact on geospace, is the existence of long intervals of intense southward magnetic fields therein. For this reason, a major objective of contemporary space-weather research is to assess the near-Sun magnetic field of CMEs. This is a critical information, and could be taken as input to empirical or physics-based schemes or to full MHD heliospheric codes both supplying predictions of the CME magnetic field upon impact at 1 AU. We will supply a review of current efforts aiming to determine and infer the near-Sun magnetic field of CMEs, discuss their pros and cons, and finally outline possible new paths of research.

KEYWORDS :   solar physics, space weather

Sr No: 504

A combined neural network- and physics-based approach for modeling plasmasphere dynamics

CORRESPONDING & PRESENTING AUTHOR:

Irina Zhelavskaya, GFZ Potsdam, Germany

Nikita Aseev, GFZ Potsdam, Germany

Yuri Shprits, GFZ Potsdam, Germany

In recent years, feedforward neural networks (NNs) have been successfully applied to reconstruct global plasmasphere dynamics in the equatorial plane. These neural network-based models capture the large-scale dynamics of the plasmasphere, such as plume formation and erosion of the plasmasphere on the nightside. However, their performance depends strongly on the availability of training data. When the data coverage is limited or non-existent, as occurs during geomagnetic storms, the performance of NNs significantly decreases, as networks inherently cannot learn from the limited number of examples. This limitation can be overcome by employing physics-based modeling during strong geomagnetic storms. Physics-based models show a stable performance during periods of disturbed geomagnetic activity, if they are correctly initialized and configured. In this study, we illustrate how to combine the neural network- and physics-based models of the plasmasphere in an optimal way by using the data assimilation Kalman filtering. The proposed approach utilizes advantages of both neural network- and physics-based modeling and produces global plasma density reconstructions for both quiet and disturbed geomagnetic activity, including extreme geomagnetic storms. We validate the models quantitatively by comparing their output to the in-situ density measurements from RBSP-A for an 18-month out-of-sample period from 30 June 2016 to 01 January 2018, and computing performance metrics. To validate the global density reconstructions qualitatively, we compare them to the IMAGE EUV images of the He+ particle distribution in the Earth's plasmasphere for a number of events in the past, including the Halloween storm in 2003.

KEYWORDS :   space Weather, modeling plasmasphere

Division V

5.1 Current developments of Geomagnetic observatories and integration of ground and space- based measurements

CONVENERS: Kusumita Arora

Achim Morschhauser

Katia Pinheiro

Roman Krasnoperov

Ground geomagnetic observatories play a crucial role in generating high quality and consistent long term data. On the other hand, satellites generate high quality data with global coverage. The combination of ground and satellite data has the power to open new possibilities in studying space weather, space physics, magnetosphere-ionosphere coupling, secular variation, and in geomagnetic field modeling. This session aims to bring together the most recent results from experimental and theoretical improvements of observatory and satellite data acquisition, and is also open to applications and models using these data. We invite contributions on all aspects of advances in development of new techniques and in derivation of new results from the combination of satellite and observatory data, but also from observatory data alone, in the global as well as regional context.

Sr No: 505

Evaluating Effect of Noise From Traffic on Quality of HYB Magnetic Observatory Data From Data of Lockdown Duration

CORRESPONDING & PRESENTING AUTHOR:

Kusumita Arora, CSIR-NGRI, India

Chandrashekhar Nelapatla, CSIR-NGRI, India

Manjula Lingala, CSIR-NGRI, India

Data of magnetic observatories, particularly of populous countries are increasingly contaminated by anthropogenic noise. More and more sophisticated techniques of data processing are used to eliminate this noise, nonetheless some of it cannot be removed. The main sources of noise in the data of Hyderabad (HYB) comes from the power lines and power station as well as from vehicular traffice, at distances of 1.5 and 1.0 km respectively. During the nationwide COVID-19 pandemic lockdown from 24 March to 17 May 2020, all traffic came to a complete halt including road and Metrorail. The data from this time interval gives us an opportunity to evaluate the effects of the absence of traffice generated noise sources during different geomagnetic conditions. We find that the noise level is significantly reduced in the geomagnetic field elements, especially in vertical (Z) and total field (F) components; the stability of the baselines during this period exhibits significantly more consistency than normal times. Measurements made at different distances from the main noise sources after normal traffic was resumed, provide further constraints on their influences on data quality. Such evaluations allow us to enhance noise reduction techniques from regular records to produce improved definitive data.

KEYWORDS :   magnetic observatory, definitive data, noise

Sr No: 506

Estimating historical monthly magnetic datasets based on a machine learning algorithm

CORRESPONDING & PRESENTING AUTHOR:

Seiki Asari, Japan Meteorological Agency, Japan

Masanori Kurihara, Japan Meteorological Agency, Japan

Naoto Imamura, Inc., Japan

We create optimized monthly mean datasets back to 1957 based on a machine learning algorithm. These monthly means are derived from hourly values, while the contributions from the external disturbances are reduced. A gradient boosting framework called LightGBM is used to predict the external disturbances involved in hourly means. We set several geomagnetic indices and solar zenith distance as input parameters in the machine learning model, and set external disturbances as output parameters. The model is trained by the external disturbances as suggested from a satellite field model from January 1999 to December 2015. Then we let the model predict the disturbances for 1957-1998. The monthly means are calculated by weighted mean of the hourly data, where those associated with predictions of large disturbances are accordingly down weighted.
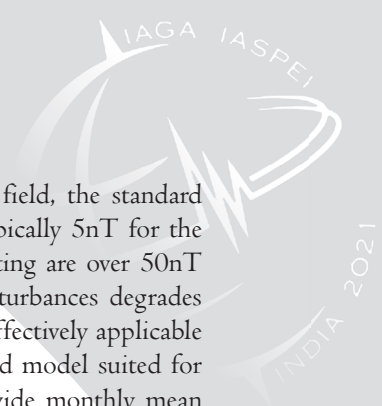
Here, we report the results for three components (XYZ) of the Kakioka magnetic field, the standard deviations of the monthly X component means are significantly reduced. They are typically 5nT for the optimized ones irrespective of the solar activity cycle, while those without the weighting are over 50nT around the solar maximum. Although the accuracy of the prediction of external disturbances degrades backwards in time as the geomagnetic indices get less reliable, the machine learning is effectively applicable to creating a historical dataset of the optimized monthly means. A historical core field model suited for describing interannual fluctuations would eventually be constructed, by using worldwide monthly mean datasets improved with the optimizing method presented.

KEYWORDS : geomagnetism, machine learning, denoising

Sr No: 507

- -

SYMPOSIUM : **5.1 Current developments of Geomagnetic observatories and integration of ground and space-based measurements**

The history of the geoelectric and atmospheric electric observations by Japan Meteorological Agency (by invitation)

CORRESPONDING AUTHOR:

Shingo Nagamachi, Japan Meteorological Agency, Japan

PRESENTING AUTHOR:

Ikuko Fujii, Japan Meteorological Agency, Japan

Shin Arita, Japan Meteorological Agency, Japan

Eiji Hirota, Japan Meteorological Agency, Japan

Seiki Asari, Japan Meteorological Agency, Japan

In February 2021, Japan Meteorological Agency (JMA) put an end to its history of the observations of the geoelectric and atmospheric electric potentials. The geoelectric observation had been operated at Kakioka, Memambetsu and Kanoya observatories since 1932, 1950 and 1948, respectively. Indeed, the latter two observatories were opened for the purpose of geoelectric observation, rather than magnetic observation. In the early times it was quite expected that the geoelectic monitoring may contribute to earthquake prediction. This unique aspect of the observation, as a mission for the society, is one of the reasons why the organized observations were continued for such a long time, from which the dataset that is rare in the world resulted. Meanwhile, since its inception in 1931, the atmospheric electric observation at Kakioka had been made persistently with a water dropper. The measurement at Memambetsu (already closed in December 2010) was originally started in 1950 with a radioactive collector and later succeeded by a field-mill in 1975. The invaluable records of these historical electric observations, together with their meta-information, are still available online at the official data service webpage of Kakioka Magnetic Observatory (https://www.kakioka-jma.go.jp/obsdata/metadata/en). In the presentation, reviewing the history of JMA's geoelectric and atmospheric electric observations, we give some specific observation records and introduce our knowledge and experiences acquired through their operations beyond decades.

KEYWORDS : observation, history, kakioka

Sr No: 508

Advanced Production of Quasi-Definitive Magnetic Observatory Data of the INTERMAGNET Standard

CORRESPONDING & PRESENTING AUTHOR:

Dmitriy Kudin, Geophysical Center of the Russian Academy of Sciences, Russia

Anatoly Soloviev, Geophysical Center of the Russian Academy of Sciences, Russia

The system for the preparation of quasi-definitive data of the INTERMAGNET standard is described. Unlike the final data, which was prepared no earlier than 1 year after the measurement, the data provided with the described system are available 1 day after the last series of absolute observations. Quasi-definitive data are used to model fast variations in the main magnetic field of the Earth and to calculate indices of geomagnetic activity. The quality of the data obtained from a comparison of the approved final INTERMAGNET data and the data from the World Magnetic Model (WMM) and International Geomagnetic Reference Field (IGRF) model is analyzed. The quality of the quasi-definitive data obtained by the proposed method of automated algorithms is shown to be comparable to the quality provided by the traditional approaches to the preparation of the final INTERMAGNET standard data.

KEYWORDS : observatory data processing, INTERMAGNET, quasi-definitive

Sr No: 509

SOK, Senegal: The opening of a new geomagnetic observatory

Abdelkader Telali, Université de Paris, IPGP, CNRS, France

Benoit Heumez, Université de Paris, IPGP, CNRS, France

Jean Pascal Rivierre, Université de Paris, IPGP, CNRS, France

Aboubacry Diallo, Institut de Recherche pour le Développement, France

CORRESPONDING & PRESENTING AUTHOR:

Vincent Lesur, Université de Paris, IPGP, CNRS, France

M'bour magnetic observatory has been operating from 1952 to the 3rd of March 2020 and the measured data have been used for numerous scientific studies. In replacement of this remarkable observatory, a new site has been selected in the neighbourhood of Niakhar, Senegal, close to the village of Sop, roughly 55km to the East of M'bour. First magnetic records are from the 9th of March 2020. Although absolute measurements have been made at this same date, due to the restriction of travels linked to the Covid-19 pandemic, weekly absolute measurements only started the 18th of March 2021. We will present the new observatory, how it was planned, built and installed, trying to limit as much as possible the impact on the agricultural activities, and adjusting for difficult environmental conditions. First elements of comparison with records from M'bour observatory will be given.

KEYWORDS : geomagnetic observatory
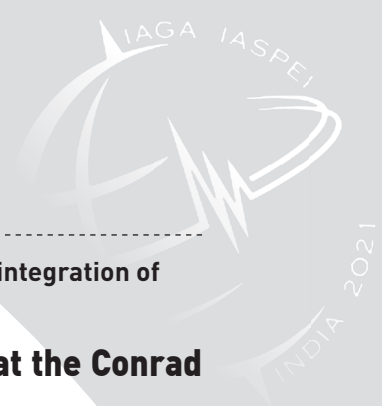
Sr No: 510

Recurring magnetic disturbances in the pT range recorded at the Conrad Observatory

CORRESPONDING & PRESENTING AUTHOR:

Patrick Arneitz, ZAMG, Austia

Niko Kompein, ZAMG, Austia

Ramon Egli, ZAMG, Austia

Roman Leonhardt, ZAMG, Austia

Barbara Leichter, ZAMG, Austia

Richard Kornfeld, ZAMG, Austia

Richard Mandl, ZAMG, Austia

The geomagnetic part of the Conrad Observatory (WIC), located at Trafelberg (Lower Austria), is equipped with a variety of sensitive magnetometers allowing for the detection of signals in the pT range. The identification of artificial signal contributions is crucial in order to guarantee very accurate and precise monitoring of geomagnetic field variations. Spectral analysis of geomagnetic time series recorded at WIC reveals recurring magnetic disturbances in the pT range. These disturbances comprise periods of 900 seconds along with higher harmonics (i.e., multiples of fundamental frequency $f0=1/900$ Hz) and are detected within magnetic scalar, vector and gradient measurements. For instance, prominent peaks are observed at a period of 75 seconds in the power spectral densities of the Y and Z components recorded with a Lemi036 sensor. Observed artificial signals can be associated with small adjustments of the mains frequency in 15-minute intervals. Furthermore, there is a correlation between variations of magnetic disturbances and power consumption, e.g., during the first lockdown due to the COVID19 pandemic in Austria. Measurements with a mobile, battery-powered station (Lemi025 sensor) placed near the entrance bear similar disturbances as regular observatory sensors, but slightly stronger. Therefore, electromagnetic disturbances most likely originate from electric currents irradiating from the mains grounding point and flowing along the main tunnel of WIC.

KEYWORDS : geomagnetic observatory time series, spectral analysis, artificial magnetic disturbances

Sr No: 511

Effects of South Atlantic Anomaly and Paraguay-Araguaia belt conductivity anomaly on Pantanal Magnetic Observatory

CORRESPONDING & PRESENTING AUTHOR:

Marcel De Oliveira, Observatório Nacional, Brazil

Rafael Amaral, ETH Zurich, Switzerland

Katia Pinheiro, Observatório Nacional, Brazil

Worldwide magnetic observatories are fundamental for the analysis of interplanetary geomagnetic events. Out of these, Pantanal magnetic observatory (PNL) is the only one in central South America. It is located in the vicinity of two distinct anomalous features: the South Atlantic Anomaly (SAA) and the Paraguay-

Araguaia belt conductivity anomaly (PACA). There was been some discussion whether these anomalies may affect magnetic data. We explore the origin of amplified H-component sudden impulses (SC(H)) in PNL, compared to nearby stations. We analyze two sudden storm commencements events, registered during September 2014 in PNL. We showed that PNL has higher values for the geomagnetic field response due to changes in the dynamic pressure of the solar wind. It was compared to a neighboring station in the central SAA, where this effect was expected to be higher considering the anomalous SAA influence only. We calculated vertical magnetic transfer functions (VTF or tippers) to investigate the possible influence of anomalous induced EM due to PACA. Tippers in PNL are larger at short periods in comparison with other deep incrusted continental observatory, which is consistent with the possible existence of a shallow crustal conductivity anomaly in this region. Both analysis corroborates with previous studies that indicate that PNL data might have amplification events associated to PACA anomaly. We suggest a detailed MT study in this region to determine the extent of this influence in PNL data.

KEYWORDS : south alantic anomaly, paraguay-araguaia belt conductivity anomaly, magnetic observatory

Sr No: 512

Higher-frequency ground magnetic field data by merging fluxgate and induction coil magnetometers at Eskdalemuir magnetic observatory.

CORRESPONDING & PRESENTING AUTHOR:

Guanren Wang, British Geological Survey, UK

Ciaran Beggan, British Geological Survey, UK

Christopher Turbitt, British Geological Survey, UK

Ellen Clarke, British Geological Survey, UK

Ground-based digital magnetic observatories have traditionally produced one-minute values, which are used in space weather research and operational models directly or through local and global activity indices. Whilst the need for one-minute values remains, measurements with a higher cadence are also becoming useful in space weather studies.

Fluxgate magnetometers are widely employed at magnetic observatories and variometer stations. Their (temperature-controlled) long-term stability is an advantage for measuring the spectrum of signals ranging from the Earth's core field through to variations caused by ionospheric and lower frequency magnetospheric signals. However, the older generation of fluxgate magnetometers has an inherent instrumental noise floor, large enough to "mask" ambient natural signals of interest in the 0.1-10Hz frequency band.

Induction coil magnetometers are optimised to capture signals at higher frequencies (0.1-100Hz) with minimal instrument noise, although stability over periods longer than a few minutes is poor. In theory, combining the long-term stability of the fluxgate magnetometer with the low-noise of the induction magnetometer, should capture the natural magnetic field for frequencies down to one-second or better.

We investigate the improvement by examining the merged time-series using data recorded by an induction coil and a fluxgate magnetometer, sited at Eskdalemuir Observatory, to produce "improved" time-series with frequencies in the 0.2 - 0.5 Hz band (periods of 2-5 seconds) for the horizontal components of the magnetic field, X and Y. We describe the data, methodology and results of our efforts to merge the data from these two complementary instruments.

KEYWORDS : fluxgate, induction-coil, magnetometer

Sr No: 513

A harmonic spline regional geomagnetic main field model over Southern Africa derived from Swarm satellite and ground based-data recorded between 2013 and 2019

CORRESPONDING & PRESENTING AUTHOR:

Emmanuel Nahayo, South African National Space Agency (SANSA) , South Africa

A regional harmonic spline geomagnetic main field model, Southern Africa Core Filed Model (SACFM-3) is derived from Swarm satellite and ground-based data in the region of the South Atlantic Anomaly (SAA) where the field intensity continues to decrease. With the help of the SACFM-3 and CHAOS-6-x9, a detailed study is conducted to shed light on the high spatial and temporal geomagnetic field variations over Southern Africa between 2014 and 2019. The results show a steady decrease of the radial component Z in almost the entire region. In 2019, its rate of decrease in the western part of the region has reached high values, 76 nT/year and 78 nT/year at Tsumeb and Keetmanshoop magnetic observatories, respectively. For some areas in the western part of the region, between epochs 2014.0 and 2019.5, the radial component Z and field intensity F show a decrease in strength, from 1.1 to 1.5% and from 0.9 to 1.3%, respectively. There is a noticeable decrease of the field intensity from the south western coast of South Africa expanding towards the north and eastern regions.

KEYWORDS :   harmonic splines, secular variation, south atlantic anomaly

Sr No: 514

Angular measurement error analysis of Declination Inclination Digital Station instrument

CORRESPONDING & PRESENTING AUTHOR:

Adam Domjan, MinGeo Ltd., Hungary
Laszlo Hegymegi, MinGeo Ltd., Hungary
Csaba Hegymegi, MinGeo Ltd., Hungary
Laszlo Merenyi, MinGeo Ltd., Hungary

Absolute magnetic measurements are performed with the usage of a classical theodolite equipped with a singel-axis magnetometer known as Declination Inclination Magnetometer (DIM).

At MinGeo Company we developed a new kind of cable-less, digital, non-magnetic DIM instrument, named as Declination Inclination Digital Station (DS). In the DS an electric theodolite, a single-axis magnetometer, a tablet and a DS application are integrated together.

Major advantages of using DS over the conventional DIMs are:
• Observer work is carried out quicker.
• Accuracy of measurement is higher.
• Personal errors involved in reading and recording are eliminated

- Calculation of magnetic meridian is automatic and accurate
- There is a template manager for observer assistance
- Enables more sophisticated absolute measurement routines
- Preliminary data processing is provided

In this presentation, methods of error analysis and detection to correct the angle measurement accuracy of DS are investigated. The DS applies digital angle encoders using a laser beam for scanning precise graduation marks etched on circular scales within in the instrument.

The angle measurement error caused by the scale graduation and circle eccentricity errors is analyzed, and an error model is built. The proposed error model is verified, and the angle measurement error can be predicted if the installation eccentricity and graduation error are known.

KEYWORDS : absolute magnetic measurement, declination inclination magnetometer, geomagnetic field vector

Sr No: 515

SYMPOSIUM : **5.1 Current developments of Geomagnetic observatories and integration of ground and space-based measurements**

Updates and Future Plans at the World Data Centre for Geomagnetism, Edinburgh

CORRESPONDING & PRESENTING AUTHOR:

Sarah Reay, British Geological Survey, UK
Susan Macmillan, British Geological Survey, UK
Simon Flower, British Geological Survey, UK
Peter Stevenson, British Geological Survey, UK
Anne Richardson, British Geological Survey, UK
John Williamson, British Geological Survey, UK
Adam Collins, British Geological Survey, UK
Ellen Clarke, British Geological Survey, UK

The World Data Centre (WDC) for Geomagnetism, Edinburgh (wdc.bgs.ac.uk) is a long-standing repository of geomagnetic data and data products. Its holdings include geomagnetic observatory time-series data, magnetic survey records, geomagnetic indices and models. Analogue records in the form of paper magnetograms, observatory yearbooks and other publications are also archived.

The WDC is a member of the World Data System and is currently applying for Core Trust Seal status. The data held on behalf of the geomagnetic community are freely accessible and openly shared.

The first step toward FAIR data principles is to make the data Findable for both humans and computers. Recently the WDC has been working with the European Plate Observing System (EPOS) to develop a metadata schema for geomagnetic observatory data. A metadata database has been populated and a webservice allowing programmatic access has been developed. The internal systems and user interface of the WDC have been updated to utilise this database. The new metadata database will be described and examples of its use given.

The WDC aims to continue to improve the services offered to the geomagnetism community. Future plans to develop support for historic digitised data sets and a new monthly mean database will be introduced.

KEYWORDS : geomagnetism, data, metadata
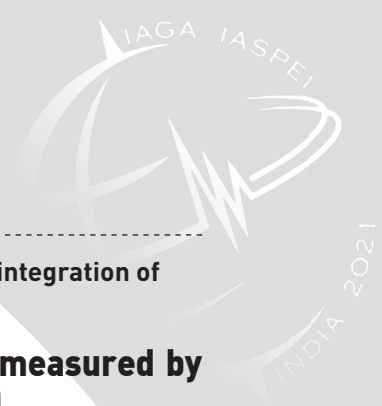
Sr No: 516

Spatial distribution of time varying geomagnetic gradients measured by different geomagnetic observatories (Comprehensive study)

CORRESPONDING & PRESENTING AUTHOR:

Andras Csontos, Mining and Geological Survey of Hungary, Hungary

Magnetic gradiometry is a widely used powerful tool to perform different geomagnetic surveys. The main purpose of the gradient measurement is to map the lateral properties and the hidden structures of the potential field.

The task of a geomagnetic observatory is completed if both the intensity and the direction of the geomagnetic field become known at one point.

On the other hand, the accuracy of the recent standard observatory instrumentation gives further chances to measure the magnetic gradients and its changes in time. The test of a simple gradient measurement by using standard observatory instrumentation was performed in a conductivity anomalous region. Similar short time fluctuations of different type of magnetic gradients were recorded by independent magnetometers.

Later we presented a comprehensive study of three geomagnetic observatories' long term dataset. We studied only the inclination readings of absolute measurement. The difference between the two absolute values of simultaneous inclination records represents the curvature of the geomagnetic field measured in the magnetic meridian plane.

We could verify that the curvature of the geomagnetic field varies in time in the selected observatories in the studied periods. We concluded that the main source of this variation of geomagnetic gradient might has effects on the internal geomagnetic field.

In this presentation we are going to characterize the variation of geomagnetic gradients in details. We are using the simultaneous data of geomagnetic observatories for this comprehensive study. The main motivation of this comparison is to get knowledge about spatial distribution of the presented phenomenon.

KEYWORDS : gradiometry, geomagnetic observatory, variation of geomagnetic gradient

Sr No: 517

Integrating ground and satellite magnetic data for equatorial-electrojet studies: importance and opportunities

CORRESPONDING & PRESENTING AUTHOR:

Gabriel Brando Soares, Observatório Nacional, Brazil

Juergen Matzka, GFZ German Research Centre for Geosciences, Germany

Katia Pinheiro, Observatório Nacional, Brazil

Achim Morschhauser, GFZ German Research Centre for Geosciences, Germany

Yosuke Yamazaki, GFZ German Research Centre for Geosciences, Germany

Cristiano Martins, UFPA Federal University of Pará, Brazil

The equatorial electrojet (EEJ) current flowing in Earth's ionosphere leads to one of the most prominent features of the geomagnetic field daily variation. The EEJ amplifies the recorded daily variation in the region of ±3° around the magnetic equator by a factor of two as compared to higher magnetic latitudes. The solar cycle, seasonal, lunar and local time variation of the EEJ magnetic signal have been widely studied using geomagnetic data from individual ground stations. Also, with the advent of space-based measurements, the EEJ longitudinal variation could be studied with much better resolution. Our study aims to show the benefit from the combined use of ground and satellite measurements to investigate the EEJ. To this end, we will present a new method to combine ground and satellite data to determine spatio-temporal characteristics of the EEJ. We will also provide an overview of the available ground and satellite data sets around the globe, and recent efforts to improve the network of equatorial stations. The perspectives and opportunities for future equatorial geomagnetic observatories and satellite data sets will also be discussed.

KEYWORDS : geomagnetic observatories, satellite data, equatorial electrojet

Sr No: 518

SYMPOSIUM : **5.1 Current developments of Geomagnetic observatories and integration of ground and space-based measurements**

Production of Quasi-definitive data and Recent Improvements at the Brazilian Magnetic Observatories

CORRESPONDING & PRESENTING AUTHOR:

Marcos Vinicius Silva, Observatório Nacional, Brazil

Achim Morschhauser, GFZ German Research Centre For Geosciences, Germany

Jurgen Matzka, GFZ German Research Centre For Geosciences, Germany

Katia Pinheiro, Observatório Nacional, Brazil

There are two magnetic observatories in Brazil: Vassouras (VSS) close to Rio de Janeiro that measures the magnetic field since 1915 and Tatuoca, located on a small island close to Belém (Pará), which started its records in 1957. VSS is part of INTERMAGNET since 1998 and TTB was recently accepted as part of this network, in 2019. The Brazilian magnetic observatories are of great importance for the global network since relevant magnetic phenomena occur: the Equatorial Electrojet in North Brazil and the South Atlantic Magnetic Anomaly. Further combination of data from magnetic observatories and satellites allows to calculate geomagnetic models that are important in a great variety of applications. In order to produce global models, the scientific community needs a fast and high-quality availability of data. Therefore, in 2008 INTERMAGNET developed a new type of data called Quasi-definitive (QD), which is expected to have similar quality as the definite data but delivered within three-months from data acquisition. The Brazilian research group started to deliver QD data from VSS and TTB in March 2020, in collaboration with staff from GFZ-Potsdam. In this work, I present recent improvements and updates at the Brazilian observatories, such as the installation of a new backup system in VSS, procedures involving the renovation of the absolute hut in TTB, baseline analysis and the methodology used to produce monthly QD data.

KEYWORDS : quasi-definitive data, magnetic observatories, baseline analysis
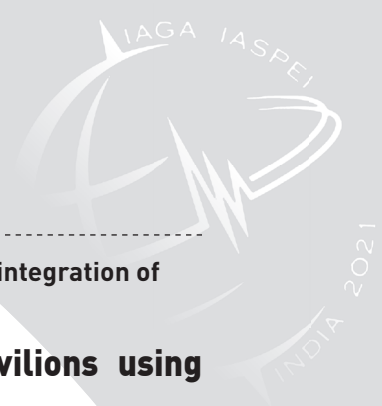
SYMPOSIUM :   **5.1 Current developments of Geomagnetic observatories and integration of ground and space-based measurements**

Design and construction of geomagnetic observatory pavilions using lightweight composite materials in the territory of Armenia

CORRESPONDING & PRESENTING AUTHOR:

Jon Karapetyan, Institute of Geophysics and Engineering Seismology after A. Nazarov

Roza Karapetyan, Institute of Geophysics and Engineering Seismology after A. Nazarov, Russia

Gevorg Poghosyan, Institute of Geophysics and Engineering Seismology after A. Nazarov, Russia

Gurgen Matevosyan, Institute of Geophysics and Engineering Seismology after A. Nazarov, Russia

Using lightweight composite construction materials based on natural minerals is a well-accepted international practice. One of the most common technologies usesbasalt and glass fibers as raw materials. The territory of the Republic of Armenia is rich with deposits of such minerals. The aim of the study is the development, design and construction of cost-effectivemodular pavilions, laboratories, cottages, and mobile stations using non-magneticlightweightcomposite materials. These new generation materials, obtained from basalt and fiberglass raw products, is a good choice for the construction of pavilions of geomagnetic observatories. The advantages of this technology include:

- Since the construction components are manufacture daresay-to-use sections, there is virtually no need for special construction equipment.
- Assembly is much faster than traditional construction (e.g. using lumber or silica brick).
- The result is robust "lightweight" structures that can be quickly dismantled or relocated if necessary.
- They are cost effective compared to traditional alternatives.
- Solar panels system may be integrated into the pavilion construction, making them smart and energy efficient scientific facilities.

The future plan is to integrate solar panels into the pavilion construction. As a result, we'll obtain smart mobile energy-efficient solutions that can be successfully applied in various sectors of the economy: urban, agriculture, emergency etc. In September 2019, not far from the town Gyumri, near the village of Gyulagarak, the deployment of a new geomagnetic observatory was finished and started its operation. The non-magnetic pavilions of this observatory, designated as "Gyulagarak", were constructed using composite modules. This observatory is the only operational one in this region.

KEYWORDS :   geomagnetic observatory, composite materials, pavilions

Sr No: 520

Automatic or remotely controlled manual absolute geomagnetic measurements with ADS-1 instrument

CORRESPONDING & PRESENTING AUTHOR:

Laszlo Hegymegi, Mingeo Ltd., Hugary

Laszlo Merenyi, Mingeo Ltd., Hugary

Janos Pazonyi, Mingeo Ltd., Hugary

Adam Domjan, Mingeo Ltd., Hugary

Csaba Hegymegi, Mingeo Ltd., Hugary

Janos Szollosy, Mingeo Ltd., Hugary

A new instrument and measurement method have been developed and realized to perform absolute declination and inclination measurement at remote places where the presence of an operator can hardly be insured. The new instrument is a rebuilt and motorized version of a widely used Zeiss nonmagnetic theodolite equipped with single axis magnetometer. It can be operated by remote manual access via internet by an operator or by autonomous manner. Movement of the telescope and alidade performed by nonmagnetic piezomotors. Original optical angle reading was replaced by an electronic digital one and the telescope is equipped with a custom made low magnetic camera. The instrument is controlled by a low-power, fan-less industrial PC. The same PC collects measurement data and ensures the connection to the internet. The PC also offers connection possibilities to a scalar absolute magnetometer and to a three component vector magnetometer. If scalar magnetometer connected, the geomagnetic field vector can be completely described at the time of the measurement. For time flag a built-in GPS receiver data is used. Power source is a 12 V battery charged from the mains or solar cell.

If no internet connection is available, the measurement repetition time can be programmed and measurement carried out automatically from time to time. Measurement data are stored in the controlling PC for later download.

Use of near and far geographic reference points (MIRA) were also examined and evaluated. Experiences with the new instrument and comparison of the results to data obtained by classical instruments are presented.

KEYWORDS : absolute geomagnetic measurement, new measurement method, unmanned operation
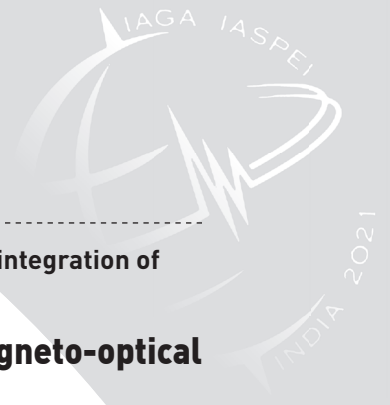
Sr No: 521

FOG-based true north measurement: compensating the magneto-optical effect

CORRESPONDING & PRESENTING AUTHOR:

Alexandre Gonsette, Royal Meteorological Institute of Belgium, Belgium

We report here on the last improvements in true north measurement based on fiber optical gyroscope (FOG).

The accurate measurement of the true north is requested for computing the geomagnetic field. In a magnetic observatory, an operator regularly performs this task during the well-known absolute measurement by pointing a reference target with the telescope of a DIFlux. The automatic system Autodif uses a similar principle. However, this method not only requires a third equipment for estimating the target azimuth but may also be hard or even impossible to perform in hostile environment leading us to explore alternatives for automatic observatories.

Improvements in FOG technology offers new opportunities that make the direct measurement of the true north potentially possible. Nevertheless, a couple of attempts based on a low cost FOG highlighted some limitations in particular due to the magneto-optical effect resulting in an error in the true north measurement.

We briefly present a true north measurement method based on FOG sensor and show how the magnetic field affects the results. We then adapt this method for compensating the magneto-optical effect taking advantage of the knowledge of the magnetic field. We finally show a couple of preliminary results obtained with a high accurate FOG sensor.

Division VI

6.1 Electromagnetic induction in Earth

CONVENERS: Alexander Grayver

Adam Schultz

Alison Kirkby

Oliver Ritter

Lindsey Heagy

Maxim Smirnov

Jared Peacock

Ute Weckmann

Electromagnetic (EM) geophysical methods are applied on scales ranging from the near surface to the deep mantle. Aspects of EM induction in geophysics include new instrumentation and data acquisition methods, mathematical and numerical improvements to data processing, modelling, and inversion, ground-based and measurements in the marine environment, airborne and satellite missions. Additionally, fundamental to all experimental geophysical applications is a sensible, reliable and modern data acquisition and handling. We are interested in studies of EM induction applied at all scales. Further, contributions in the field of EM instruments development, novel and advanced concepts of experimental design, EM and MT data processing/archiving are highly welcome. Results from EM methods are often part of multi-disciplinary studies integrating data from rock physics and other geophysical, geochemical, and geological methods to investigate complex subsurface structures and their temporal evolution. Neighbouring fields of research encompass the study of natural and controlled EM sources, geomagnetically induced currents, or geomagnetic field studies based on observatory data. This session welcomes contributions on all aspects of EM induction in geophysics.

Sr No: 522

Crustal Characterization of Portugal's mainland based on Magnetotelluric measurements

CORRESPONDING & PRESENTING AUTHOR:

Pedro Baltazar Soares, Instituto Dom Luiz, Portugal

Francisco J. Martinez Moreno, Instituto Dom Luiz, Portugal

Joana Alves Ribeiro, CITEUC, Portugal

Fernando A. Monteiro Santos, Instituto Dom Luiz, Portugal

Maria Alexandra Pais, CITEUC, Portugal

Paulo Ribeiro, CITEUC, Portugal

Antonio Mateus, Instituto Dom Luiz, Portugal

The phenomena of Geomagnetic Induced Currents (GICs) have received special attention as one of the main hazards of Space Weather. Large GICs can flow into power systems, becoming problematic or even severe enough to cause a complete system shutdown. Major factors determine GICs:(1) the strength and orientation of the electric field in the power system, depending on the ionospheric and magnetospheric currents as well as on the crust and mantle conductivity; and (2) the electric power network characteristics. The Earth's conductivity can be appraised based on geophysical measurements, providing information about the spatial distribution of conductivity in-depth and laterally. Realistic models of conductivity are obtained after processing and interpretation of Magnetotelluric (MT) soundings data.

A 3D resistivity model for Portugal mainland is reported using data from 30 broadband MT soundings spaced 50x50km. The model depicts large crustal volumes with contrasting resistivity values. The central and north parts of Portugal's mainland are typified by a high resistivity crustal domain propagating in-depth, which correlates well with the prevalence of granites and metamorphic rocks, with resistivity values ranging from $3x10^3$ to $3x10^5$ ohm.m. To the west and south, roughly corresponding to the Portuguese western shore and the South Portuguese Zone, respectively, the crustal resistivity tends to decrease unevenly to values ranging from 30 to 300 ohm.m.

The present study aims to contribute to a better understanding of the physical properties portraying the concealed crust in Portugal's mainland. In addition, the characterization of resistivity/conductivity crustal patterns is of paramount importance to improve GICs estimations.

KEYWORDS :   magnetotelluric, GICs, 3D resistivity model

Sr No: 523

Towards Accessible Large-scale Electromagnetic Inversion

CORRESPONDING & PRESENTING AUTHOR:

Seogi Kang, Stanford University, USA

Dieter Werthmller, TU Delft, Netherland

Lindsey Heagy, University of British Columbia, Canada

Douglas Oldenburg, University of British Columbia, Canada

With the latest enhancements in instrumentation and sensor technology, the volume and complexity of electromagnetic (EM) data is exponentially increasing. The number of data from a traditional ground loop EM survey is only a few tens to hundreds, whereas a modern marine controlled-source EM survey may collect more than hundreds of thousands. These EM data from various types of surveys (e.g., ground, airborne, marine, magnetotellurics) needed to be inverted to provide a three-dimensional subsurface model of electrical resistivity, which can be very useful for various types of geoscience problems including groundwater, minerals, hydrocarbon, and tectonics. However, accessibility of large-scale 3D EM inversion codes in the geoscience community is limited to some companies (e.g. oil and gas) or a few universities and institutions. Further, most of them are black-box codes limiting the users' ability to inject relevant geological or petrophysical knowledge into the inversion process. We developed an efficient 3D EM inversion algorithm that can handle large-scale EM data. The developed algorithm was constructed under the open-source geophysical inversion framework, SimPEG, where the open-source package emg3d is used as a forward modelling kernel to solve Maxwell's equations. emg3d utilizes a multigrid method to efficiently solve a large system with millions of cells, and SimPEG facilitates a modular and flexible inversion framework. To demonstrate the ability of the developed algorithm, we presented two examples: (1) marine controlled-source EM for hydrocarbon detection and (2) controlled-source audio-frequency magnetotellurics for finding minerals under the cover.

KEYWORDS : electromagnetics, inversion, open-source

Sr No: 524

Extended ModEM 3D forward modelling capabilities for space weather applications

CORRESPONDING & PRESENTING AUTHOR:

Anna Kelbert, U.S. Geological Survey, USA

Gary Egbert, Oregon State University, USA

Hao Dong, China University of Geosciences, China

Naser Meqbel, Consulting-GEO, Brazil

ModEM 3D is a parallelized Fortran magnetotelluric (MT) modeling and inversion code [Egbert and Kelbert, 2012; Kelbert et al., 2014] that is freely available for academic use, and has been widely used for 3D MT modeling and inversion by the global MT community. Some inherent approximations of ModEM 3D software are based on the traditional formulation of the MT method, and include the use of plane-wave external sources and a Cartesian approximation for regional Earth modeling. However, realistic ground-level natural geoelectric fields of consequence for space weather applications are induced in the Earth by large-scale spatially and temporally complicated ionospheric currents that intensify during geomagnetic storThese processes can be modeled within ModEM 3D by relaxing traditional MT approximations to include the use of arbitrary external source current geometry, flexible boundary conditions, and a spherical coordinate system. Other relevant developments include computational improvements that allow for high-resolution forward modeling of large spatial domains. Here, we report on our progress towards a versatile version of ModEM 3D suitable for the modeling of electromagnetic induction in the Earth in the context of large-scale space weather applications. These extensions will allow for the modeling of realistic, spatially and temporally complicated storm-time geoelectric fields. In the United States, these developments will also be used for high-resolution continental-scale forward modeling of MT impedances to create a gridded national impedance map, as detailed in the U.S. Geological Survey Geomagnetism Program Research Plan.

KEYWORDS : electromagnetic induction, magnetotelluric impedances, geomagnetically induced currents

Sr No: 525

Aurora: An open source magnetotelluric data processing package in Python linking MTH5 to EMTF XML

CORRESPONDING & PRESENTING AUTHOR:

Karl Kappler, Kappler & Associates, USA

Gary Egbert, Oregon State University, USA

Andy Frassetto, IRIS, USA

David Goldak, IRIS PASSCAL Instrument Center, USA

Lindsey Heagy, UBC, Canada

Anna Kelbert, USGS, USA

Doug Oldenburg, UBC, Canada

Jared Peacock, USGS, USA

Maeva Pourpoint, IRIS PASSCAL Instrument Center, USA

Tim Ronan, IRIS, USA

Aurora is a software package that calculates robust estimates of electromagnetic transfer functions (EMTF) from magnetotelluric time series data. It is being developed to (1) streamline generation of high-quality, exchangeable EMTFs for archiving at the IRIS data center and (2) to provide an open-source software package to the EM community that has been vetted against the legacy Egbert's EMTF codes. Aurora is a Python representation of Egbert's latest EMTF Matlab that is designed to interface with the self-descriptive MTH5 data structure for magnetotelluric time series. We use numpy, pandas, scipy, and xarray as package dependencies. Data structures at any stage along a processing pipeline can be saved for analysis and can be used as inputs for dependent computations. Comprehensive tracking of data provenance is provided within the pipeline. Data products are outfitted with MTH5 metadata which can be converted to IRIS' StationXML for surveys and EMTF XML for transfer function archiving. The Aurora software package, which will include worked example datasets, will be released via both PyPi and conda-forge in the autumn of 2021. We present an overview of these codes and outline a path forward over the following 1-2 years. The longer term vision includes capability for time and frequency domain data cleaning, data visualization, and data QC as well as novel array deployment geometries and controlled source data processing. We invite members of the community to join us in using these codes and collaborating on their future development.

KEYWORDS :   magnetotellurics, software, python

Sr No: 526

Lithospheric Architecture beneath the Southern Indian Shield Region

CORRESPONDING & PRESENTING AUTHOR:

Kusham Sandhu, IIT (Indian School of Mines), Dhanbad, India

B. Pradeep Naick, CSIR-National Geophysical Research Institute, India

A. Pratap, Oil India Limited, India

Shalivahan Srivastava, IIT (Indian School of Mines), Dhanbad, India

Kasturi Naganjaneyulu, CSIR-National Geophysical Research Institute, India

The southern Indian shield region (SISR) is an amalgamation of cratons and mobile belts. It is dominated

by the Archean Dharwar craton towards the north, Late Neoproterozoic Southern Granulite Terrain (SGT) towards the south, Neoproterozoic Eastern Ghat Mobile Belt towards the northeast, and the Arabian Sea on the western side. The northwest margin is overlain by Deccan Volcanic Province (DVP). Based on the litho-tectonics and ages, the Dharwar craton is further divided into eastern Dharwar craton (EDC) and western Dharwar craton (WDC). Several geophysical investigations (gravity, seismic tomography, deep seismic studies, heat flow, and magnetotellurics) have been carried out in the SISR by various workers emphasizing upper mantle dynamics and lithospheric thickness. Magnetotelluric data were available along with four profiles: 1) A north-south oriented approximate 800 km long pro?le (80 stations) that cut the strata of DVP, WDC, and SGT 2) Three parallel 280 km long profiles in the west-east direction (70 stations), that cut the strata of WDC and EDC. The raw data consists of time series records at about 150 MT stations within the period range of 0.01 to about 10, 000 s. The integration of available geophysical and geological studies with the new magnetotelluric data indicates that the 1) Uppermost mantle conductors in SISR correlates with the kimberlitic melt 2) Re-fertilization of mantle scar 3) Thick lithospheric root, and 4) Subduction polarity is Eastward in between EDC and WDC, and Southern polarity exists in between DC and SGT.

KEYWORDS :   lithosphere, kimberlite, re-fertilization

Sr No: 527

Numerical modeling of the electric and magnetic fields induced by ocean currents

Kosuke Fukuhara, Japan Meteorological Agency, Japan

CORRESPONDING & PRESENTING AUTHOR:

Ikuko Fujii, Japan Meteorological Agency, Japan

Magnetic variations caused by ocean currents appear as noise in magnetic observations on volcanic islands near the Kuroshio such as Miyakejima. In this study, we developed a numerical code to model the electromagnetic variations caused by the ocean current and estimated effects of large-scale ocean currents around Japan.

The code developed by Uyeshima and Schultz (2000), which calculates the induced electromagnetic field on three-dimensional spherical coordinates, was modified so as to incorporate source terms derived from ocean currents. The source term caused by the ocean current consists of the flow velocity and electric conductivity of sea water and the Earth's main magnetic field. The flow velocity, salinity and seawater temperature were obtained from MOVE model (Usui et al., 2006). The electric conductivity of sea water was calculated from the salinity, seawater temperature and water pressure. IGRF10 was used to compute the geomagnetic main field. These data are given every 10 days from April 2001 to September 2001, with the horizontal resolution of 0.1 degrees.

Calculated amplitudes of the induced magnetic field at the Earth's surface showed particularly large values on the area between the offshore of Tohoku region and Izu Islands. Around the Japan Trench, the maximum estimated amplitude was about 10 nT, due to the effect of the seafloor topography. The total force variation estimated on Miyakejima has the amplitude of about 3 nT which is roughly consistent with the observed one.

KEYWORDS :   motionally induced EM field, kuroshio, numerical study

Sr No: 528

The Necessity of Terrain Correction in Magnetotelluric Data in Himalayan Region

PRESENTING AUTHOR:

Dharmendra Kumar, IIT Roorkee, India

CORRESPONDING AUTHOR:

Arun Singh, IIT (ISM) Dhanbad, India

Mohammad Israil, IIT Roorkee, India

Broadband MT data was acquired for 39 sites along Roorkee-Gangotri (RG) profile. The 3D inversion of the dataset reveals the high resistive transverse tectonic features as Delhi–Haridwar Ridge (DHR), Mid-crustal conductor beneath the MCT zone, high resistive subducting Indian Plate and Delhi–Mahendragarh fault in Garhwal Himalaya region. In this work, we studied the role of topography on the full impedance by computing the distortion introduced by topography using homogenous halfspace. The deviations in the computed responses is due to the distortion by terrain. The static shift is observed for the period greater than 1 s, whereas for period less than 1 s, both apparent resistivity and phase shows variation with respect to period. We have calculated the percentage relative change (PRC) in data for homogenous with-topography model to flat-topography model for period greater than 1 s. Based on the PRC value, the severe distortion in 9 sites, moderate distortion in 18 sites and no distortion in rest of the sites were observed. We applied the distortion tensor stripping off technique to the distorted sites for topographic correction. The inversion of topographic uncorrected and corrected data for 39 sites was performed using the AP3DMT, a MATLAB based code. In the comparison of both the inverted models, the topographic corrected model is slightly modified in the region where the sites are distorted because of topography. The geoelectrical structures in this inverted model are relocated in terms of location and depth.

KEYWORDS :   galvanic distortion, topographic correction

Sr No: 529

Joint inversion of magnetotelluric impedance tensor and full distortion matrix

CORRESPONDING & PRESENTING AUTHOR:

Arun Singh, IIT (ISM) Dhanbad, India

Dharmendra Kumar, IIT Roorkee, India

Mohammad Israil, IIT Roorkee, India

The galvanic distortion of magnetotelluric (MT) data due to topography or small-scale surficial bodies is one of the major factors that prevents accurate imaging of the subsurface. In this study, we present a modification to AP3DMT, a MATLAB based inversion code for inverting MT and direct current resistivity data. In the new scheme, we carry out the joint inversion of MT impedance tensor data and a frequency independent full distortion matrix to circumvent the galvanic distortion problem. Several test are performed on synthetic data affected by galvanic distortion, either added numerically or due to the topography. The

test results shows that the joint inversion leads to a better conductivity model compared to the inversion of the MT impedance tensor without any correction for distortion effects. For highly distorted data, inversion without any distortion correction results in artefacts and the normalized root mean square error never reached the desired level.

KEYWORDS : galvanic distortion, joint inversion

Sr No: 530

SYMPOSIUM : **6.1 Electromagnetic induction in Earth**

Constraining crustal and upper mantle conductivity beneath islands by a joint inversion of multi-source transfer functions

CORRESPONDING & PRESENTING AUTHOR:

Chaojian Chen, ETH Zurich, Switzerland

Mikhail Kruglyakov, ETH Zurich, Switzerland

Rafael Rigaud, ETH Zurich, Switzerland

Alexey Kuvshinov, ETH Zurich, Switzerland

We simultaneously invert the magnetotelluric tippers, solar quiet (Sq) global-to-local (G2L) transfer functions (TFs), and global Q-responses aiming to obtain local 1-D crustal and upper mantle conductivity profiles beneath as many islands as practicable. Tippers and Sq G2L TFs were estimated from the observatory magnetic field data, Q-responses - from the satellite and observatory data. Quasi 1-D inversion is performed using the stochastic optimization method. The term "quasi" implies that during 1-D inversion, the 3-D forward modeling operator is exploited to account for the ocean induction effect (OIE), which is known to strongly influence the island responses. The 3-D EM modeling engines, based on a nested integral equation approach, are adopted to model OIE efficiently. We discuss the recovered 1-D conductivity structures and explore their lateral variability.

KEYWORDS : joint inversion, satellite data, observatory data

Sr No: 531

SYMPOSIUM : **6.1 Electromagnetic induction in Earth**

Three-dimensional MT inversion of the entire USArray in spherical frame

CORRESPONDING & PRESENTING AUTHOR:

Federico Munch, UC Berkeley, USA

Alexander Grayver, ETH Zürich, Switzerland

Knowledge about electrical structure of the Earth's interior is a key to understanding its thermo-chemical state and evaluate an impact of space weather events. USArray is a high quality data set of magnetotelluric measurements that addresses both of these problems. Covering ~60% of the contiguous United States on a quasi-regular 70 km spaced grid, this unique publicly available data led to the development of several quality regional 3D electrical conductivity models. However, an inversion of the entire data set demands novel multi-scale imaging approaches that can handle and take advantage of a large range of spatial scales contained in

the data and avoid distortions caused by Cartesian coordinate approximations to continental-scale surveys. By combining 3D MT modeling in spherical Earth with automatic mesh refinements techniques, we here present a preliminary 3D electrical conductivity model of the contiguous United States derived from inversion of more than 1000 USArray MT stations. The use of state-of-the-art modeling techniques based on high-order finite-element methods allows us to take into account realistic oceans and Earth's conductivity across many scales, while minimizing distortions due to geographic projections and other 'flattening' effects. This contribution discussed technical and methodological aspects and presents a preliminary conductivity model.

KEYWORDS : electrical conductivity, magnetotellurics, usarray

Sr No: 532

SYMPOSIUM : **6.1 Electromagnetic induction in Earth**

3-D inversion of MT tippers: constraining the conductivity structure beneath Australia

CORRESPONDING & PRESENTING AUTHOR:

Filippo Cicchetti, ETH Zürich, Switzerland

Alexander Grayver, ETH Zürich, Switzerland

Rafael Rigaud, ETH Zürich, Switzerland

Alexey Kuvshinov, ETH Zürich, Switzerland

Akimasa Yoshikawa, Kyushu University, Japan

Magnetotelluric (MT) tippers are responses that relate horizontal and vertical components of the magnetic field measured at a given location. Estimating MT tippers for periods up to a few hours allows us to obtain constraints on a three-dimensional (3-D) distribution of electrical conductivity down to astenospheric depths.

In this work, we estimate and invert tippers from the Australian continent. For this purpose, we combined data from several data sets. Among them is the Australian Wide Array of Geomagnetic Stations (AWAGS) project. Within this project, three components of the magnetic field were measured between November 1989 and December 1990 at 53 temporary stations. We complement AWAGS data with stations from MAGnetic Data Acquisition System (MAGDAS) project and the British Geological Survey (BGS) database.

We perform tippers' 3-D inversion using the GOFEM forward and inverse 3-D tool and spherical geometry set up; the latter eliminates potential distortions caused by cartographic projections.

The inversion of tippers is only a part of a broader project aiming to jointly invert electromagnetic induction responses of different origins and periods to obtain a 3-D conductivity model for Australia down to depths of 1500 km.

KEYWORDS : tippers, induction, Australia

Sr No: 533

Determining zone of influence of two-dimensional magnetotelluric profile data with 3D inversion: A Synthetic study

CORRESPONDING & PRESENTING AUTHOR:

Anita Devi, National Geophysical Research Institute, Hyderabad, India

Mohammad Israil, IIT Roorkee, India

Arun Singh, IIT(ISM) , India

Pravin Kumar Gupta, IIT Roorkee, India

Inverting a single MT profile data using a 3-D algorithm helps in resolving the nearby off-profile structures as compared to 2D inversion. However, there are some parameters that need to be optimized for determining the zone of influence of a profile. We define the zone of influence as the maximal distance perpendicular to the strike direction up to which an off-profile resistivity structure can be reasonably resolved. Therefore, we designed some simplified synthetic experiment to determine off-profile zone in which resistivity structure can be estimated. We performed the 3D inversion of synthetically generated full impedance tensor response for sites placed diagonally. This experiment suggests that an off-profile nearby resistivity structure can be sensed to a varying degree by the data. The zone of influence was found to be varying with resistivity, time periods, site spacing and the dimension and distance of the off-profile structures. The influence reduces as one moves away from the profile, and beyond this narrow zone of influence, the resistivity structure has no influence on the data. The optimal values of all these parameters must be explored and fixed prior to field data inversion.

KEYWORDS :   3D magnetotelluric inversion, zone of influence, off-profile features

Sr No: 534

Hydro-geophysical investigations using controlled-source electromagnetic methods in near-coastal environments (by invitation)

CORRESPONDING & PRESENTING AUTHOR:

Amir Haroon, Helmholtz Centre for Ocean Research GEOMAR Kiel, USA

Eric Attias, Hawai'i Institute of Geophysics and Planetology, University of Hawai'i, USA

Chloe Gustafson, Swansea University, UK

Kerry Key, Columbia University, USA

Rob Evans, Woods Hole Oceanographic Institution, USA

Marion Jegen, Helmholtz Centre for Ocean Research GEOMAR Kiel, USA

Sebastian Hoelz, Helmholtz Centre for Ocean Research GEOMAR Kiel, USA

Katrin Schwalenberg, BGR, Germany

Examples of seawater intrusion into coastal aquifers, groundwater-dominated coastal ecosystems, and the use of offshore freshened groundwater as a potential resource for coastal communities highlight the interconnected relationship between groundwater, oceans, and consequent societal implications. Hence, understanding the mechanisms controlling groundwater salinity distributions along coastal zones, particularly across the coastline to the offshore domain, is not only important from a resource perspective, but also

invaluable for protecting terrestrial groundwater reserves and coastal ecosystems from seawater intrusion and land subsidence. In terrestrial groundwater studies, the use of electromagnetic methods has proven effective on various spatial scales. As electromagnetic signals are sensitive to variations in pore fluid salinity patterns, several ground-based and airborne applications have been applied to understand the onshore component of coastal aquifers. However, due to a loss of sensitivity in the offshore domain caused partially by the masking effect of the conductive seawater, these inductively-coupled methodologies are ineffective in mapping groundwater pathways across the shoreline into the marine environment. Instead, ship-based galvanically-coupled controlled-source electromagnetic methods, in both time- and frequency-domain, are used for delineating sub-seafloor groundwater variations. These applications have demonstrated a high degree of sensitivity to pore fluid freshening in various settings, including siliciclastic Continental shelves (USA, New Zealand), carbonate margins (Israel, Malta), and volcanic Islands (Hawaii). This talk will present an overview of recent controlled-source electromagnetic applications and discuss future developments needed to detect, investigate, and monitor groundwater dynamics in coastal regions to assess offshore groundwater's resource potential and help safeguard terrestrial groundwater reserves in coastal regions.

KEYWORDS : hydrogeophysics, controlled-source electromagnetics, offshore groundwater

Sr No: 535

A dipping mid-crustal electrical conductor in the western part of the Delhi Seismic Zone, India, and its correlation with intraplate seismicity of the region

CORRESPONDING & PRESENTING AUTHOR:

Pavankumar Gayatri, CSIR-National Geophysical Research Institute, India

Ajay Manglik, CSIR-National Geophysical Research Institute, India

Demudu Babu Molli, CSIR-National Geophysical Research Institute, India

Narasimha Chakravarthi Nalluri, CSIR-National Geophysical Research Institute, India

The Delhi Seismic Zone (DSZ) comprising the Delhi - National Capital Region (Delhi-NCR) and neighboring areas is an active intraplate seismic region with the history of recurrent seismicity of minor-to-moderate nature. The recent seismic activity, e.g. M3.5 (2020-04-12) and M4.7 (2020-07-03) events in addition to many minor earthquakes, necessitated geophysical studies of the region for understanding of the causative mechanism(s) for the DSZ seismicity. However, very little is known about the detailed subsurface architecture and the tectonic setup of the DSZ concealed by alluvial sediments. We analyzed magnetotelluric (MT) data available at 18 locations, clustered into six groups of sites, along a 190-km-long SSW-NNE profile passing through the western end of the DSZ for regional subsurface resistivity structure. The MT method can effectively delineate the zones electrical conductivity which could be potential locales for stress concentration. Two-dimensional inversion of the distortion corrected MT impedance tensors of these sites yields a resistivity layer (~1000 ohm.m) down to 10-12 km in southern side of the profile, suggesting the subsurface extension of the Aravalli-Delhi fold belt. Importantly, the geoelectric structure yields a northward dipping electrical conductor (<10 ohm.m) down to 20-25 km in the central part of the profile. The location of the conductor shows a good correlation with the seismicity distribution both spatially and at depth. We infer that the conductor, possibly representing a zone of crustal fluids, is playing a role in the seismic activity of the DSZ, especially in its western part.

KEYWORDS : magnetotellurics, delhi seismic zone, electrical conductor

Sr No: 536

Induction in the Earth by long-term variations in the external current systems

CORRESPONDING & PRESENTING AUTHOR:

Crisan Demetrescu, Institute of Geodynamics, Romanian Academy, Russia

Venera Dobrica, Institute of Geodynamics, Romanian Academy, Romania

We find that in both external current systems and anual means time series from geomagnetic observatories and from long-term models of the main field, such as gufm1, there are present oscillations not only at the 11-year cycle time scale, but also at sub-centennial (60-90 years) and inter-decdal (20-30 years) time scales. A Hodrick-Prescott type of analysis, separating a decadal variation and a trend, has been employed. The trend has been in turn decomposed by a Butterworth filtering in the two oscillations mentioned. Moreover, these osillations are also present in the parameters of the solar activity, that is responsible for creating the external current system via the interaction of the magnetosphere and ionosphere with the variable solar wind and heliospheric magnetic field. The response of the Earth interior (core and mantle) to the oscillations in the external currents system, particularly in the ring current, is evaluated and some characterization of electrical properties of the interior is obtained.

KEYWORDS : sub-centennial oscillations, ring-current, induction

Sr No: 537

3D Electromagnetic Imaging Beneath the North Anatolian Fault Zone in the Marmara Sea

CORRESPONDING & PRESENTING AUTHOR:

Tulay Kaya Eken, Kandilli Observatory and Earthquake Research Institute (KOERI), Bogaziçi University, Turkey

Yasuo Ogawa, Tokyo Institute of Technology, Japan

Yoshiya Usui, The University of Tokyo, , Japan

Takafumi Kasaya, Japan Agency for Marine–Earth Science and Technology, Japan

M. Kemal Tuncer, Istanbul University-Cerrahpasa, Turkey

Yoshimori Honkura, Tokyo Institute of Technology, Japan

Naoto Oshiman, Kyoto University, Japan

Masaki Matsushima, Tokyo Institute of Technology, Japan

Weerachai Siripunvaraporn, Mahidol University, Thailand

The Marmara Sea, located at the northwestern Turkey, hosts the western branch of the North Anatolian Fault Zone (NAFZ) that is characterized by a complex faulting network. The NAFZ has caused a series of destructive earthquakes (>Mw7) in the 20th century. Several studies have implied that its segments in the Marmara Sea are highly prone to generate a destructive earthquake (>Mw7.2) in the near future. Hence, a proper understanding of crustal properties of the NAFZ in the Marmara region is of utmost importance to the seismic hazard assessment studies. The released energy following an earthquake depends on the accumulated stress along fault zones that is strongly controlled by the amount of fluid. Electrical resistivity is highly sensitive to deep crustal fluids, and thus electromagnetic methods are powerful tools

to image subsurface fluids in the deep crust. In this study, we have collected electromagnetic data at 25 sites in and around the Marmara Sea to elucidate 3D variation of electrical resistivity that can shed light on the brittle-ductile zones. To achieve this we performed a 3D inverse modeling on magnetotelluric data using an unstructured tetrahedral mesh with the finite element method. Our final images are able to detect resistive–conductive boundaries clearly marking the trace of the NAFZ. The region betwen Çinarcik and Central Basins is identified by high conductive anomalies at upper crustal depths (e.g. down to 10-12km). A profound resistive structure below ~15 km that is consistent with the known seismic gap is significant in this region.

KEYWORDS :   3D magnetotelluric modelling, marmara sea, north anatolian fault

Sr No: 538

- -

SYMPOSIUM :   **6.1 Electromagnetic induction in Earth**

Three dimensional magnetotelluric signatures and rheology of subducting continental crust – Insights from Sikkim Himalaya, India.

Shankaraiah Konda, Oil and Natural Gas Corporation Ltd., India

CORRESPONDING & PRESENTING AUTHOR:

Prasanta Patro, CSIR-NGRI, India

K Chinna Reddy, CSIR-NGRI, India

Narendra Babu, CSIR-NGRI, India

3D inversion of broad band MT data present variation of electrical signatures across the subducting Indian crust in Sikkim Himalaya. The vertical and horizontal geoelectric cross-sections are dominated by north-east dipping conductive zones. Two high conductivity zones (4-8 Ωm) in Lesser Himalayan Domain are explained by conductive mineral assemblage associated with abundant low saline and entrapped fluids. Another conductive feature (6-16 Ωm) in MCT Zone is in close proximity of MHT ramp and could arise from CO_2-H_2O fluid entrapment and fluids released by metamorphic reactions in ductile shear zone. High conductive anomaly (4-10 Ωm) at a depth of 5-16 Km in Greater Himalayan Sequence (GHS) is inferred due to presence of partial melts/aqueous fluids produced by present day dehydration melting of leucogranite source rocks. The constrained melt fractions are in the range of 1.4-3.8%, and less than south Tibet might be due to intrusion of frequent High Himalayan Leucogranites, low shear and radiogenic heat production (4-17 μW/m3) in Greater Himalayan Domain. However, the anomalous high conductive zone inferred with low melt and fluid fractions (5-6 wt%) corresponding to 104-105.5 Pa-s viscosity reduction associated with aqueous fluids derived by fluid absent melting. These fluids might be assisting to viscous/ductile deformation, change in crustal rheology beneath northern Sikkim Himalaya and initiate partial melting towards south Tibet. The low melt fractions and moderate viscosity of conductive mid-crustal rocks beneath GHS are insufficient to develop a melt channel to flow southward between MCT-1 and South Tibetian Detachment as envisaged in crustal channel flow model.

KEYWORDS :   magnetotellurics, 3D inversion, Sikkim Himalaya

Sr No: 539

Source effects in long-term mid-latitude magnetotelluric data

CORRESPONDING & PRESENTING AUTHOR:

Sarasija Sanaka, Institute of Geophysics Polish Academy of Science, Poland

Anne Neska, Institute of Geophysics Polish Academy of Science, Poland

The magnetotelluric (MT) method is mainly used in mineral exploration and deep crustal studies. We assume that the far field condition is fulfilled by the source signals. Anthropogenic noise which violates this far field assumption is understood well. However, some natural source signals are not homogeneous either, and awareness of the problem of source effects in MT data raises, since they can mislead interpretation of the derived resistivity models.

Natural source effects often are inferred from temporary changes in transfer functions and hence, their investigation requires long-term data. For induction arrows based on magnetic field components alone such data are available due to observatory and other monitoring-like records. For impedances that require additional measurements of electric channels, long-term data are not such readily available. Here we present an investigation of source effects based on two full magnetotelluric station data sets from Poland covering a time period of more than two years.

KEYWORDS :   magnetotellurics, source effects, transfer functions

Sr No: 540

A feasibility study on tunnel detection using the EM gradiometer method

CORRESPONDING & PRESENTING AUTHOR:

Rahul Dehiya, Indian Institute of Science Education and Research Pune, India

Clandestine tunnels pose a serious challenge to the security agencies as they facilitate drug/firearms smuggling, human trafficking, and terrorism-related activities. We present a feasibility study on tunnel detection using the EM gradiometer (EMG) method. The EMG responses are computed using a 3D EM modeling algorithm. Since the response of the tunnel is very weak compared to the primary field, the numerical accuracy of the EMG response is examined rigorously. The EMG response of various transmitter-receiver configurations is analyzed in a search for optimum instrument design. It is observed that the orthogonal transmitter-receiver configuration provides a stronger EMG response than the parallel transmitter-receiver configuration. However, the parallel transmitter-receiver configuration is suitable for depth estimation of the tunnel because the depth of the tunnel varies linearly with the peak-to-peak distance of the EMG response in the case of parallel configuration. The influence of transmitter frequency and subsurface conductivity on different transmitter-receiver configurations is also examined. Various model scenarios, such as conductive tunnel floor, conductor's presence in the tunnel, and subsurface heterogeneity, are analyzed to investigate their influence on the EMG response.

KEYWORDS :   EM gradiometer, tunnel detection, 3D modeling

Sr No: 541

Regional-to-local transfer functions in three-dimensional geomagnetic deep sounding by Sq variations

CORRESPONDING & PRESENTING AUTHOR:

Jakub Velimsky, Charles University, Czechia

The spatial configuration of the ionospheric currents precludes the use of simple local transfer functions in geomagnetic deep sounding by the solar quiet (Sq) variations. The global-to-local transfer functions, which have been introduced recently, relate the local vertical magnetic field at a particular observatory to the spherical harmonic coefficients describing the ionospheric source. The latter must be obtained by initial processing of the horizontal magnetic field measurements, and using an a-priori conductivity model.

The approach presented here introduces two novel points in this concept. First, the global spherical harmonic base is replaced on the regional scale with vector Slepian functions, concentrating the EM fields in the area of interest while still allowing to use the well developed spherical-harmonic formalism. Second, the Dirichlet boundary condition is applied in the forward problem, prescribing the total horizontal magnetic field in the Slepian base, and thus avoiding the use of an a-priori conductivity model. Such formulation allows a straightforward prediction of the regional-to-local transfer functions, which relate the vertical magnetic field at a particular point with the coefficients of the Slepian expansion of the horizontal component. Corresponding adjoint problem needed for an effective inversion is also developed.

The methodology is tested on a series of quasi-realistic scenarios for Europe with outlook towards recovery of the three-dimensional conductivity structure in the sub-continental upper mantle.

KEYWORDS : upper mantle, solar quiet variations, transfer functions

Sr No: 542

3D Lithospheric resistivity structure beneath the Rajasthan region (NW India) and geological implications

CORRESPONDING & PRESENTING AUTHOR:

Abdul Azeek K. K., CSIR-National Geophysical Research Institute, India

Veeraswamy K., CSIR-National Geophysical Research Institute, India

Prasanta K. Patro, CSIR-National Geophysical Research Institute, India

Ajay Manglik, CSIR-National Geophysical Research Institute, India

Arvind K. Gupta, CSIR-National Geophysical Research Institute, India

Prabhakar E. Rao, CSIR-National Geophysical Research Institute, India

Hanmanthu D., CSIR-National Geophysical Research Institute, India

Manoj Prabhakar B., CSIR-National Geophysical Research Institute, India

Kishore B. D. N., CSIR-National Geophysical Research Institute, India

The Rajasthan region and adjacent parts in the NW part of the Indian shield is a typical location that carries geological records of a long and protracted history of Precambrian geological evolution and Phanerozoic tectonothermal events. The Precambrian geology and the degree of geological alterations induced by the

Phanerozoic events are largely obscured by the characteristic sedimentary cover (Proterozoic to Quaternary/ recent) and flood basalt flows. We utilized long-period magnetotelluric (MT) data acquired in a grid fashion to understand the nature of lithosphere beneath the region and unfold the extent of Archean geology and Phanerozoic reworking occurred through 3D MT imaging. The 3D lithosphere resistivity structure shows conductive structures parallel as well as oblique to, and within, the regional NE-SW structural trend of the Aravalli-Delhi mountain belt in the region. The orogen parallel conductive belt seen in the deep crustal to shallow mantle depths is interpreted as the magmatic arc formed during the evolution of Delhi Fold Belt. A conductive zone imaged beneath the metallogenic North Delhi Terrane represents the mafic–silicic magmatism associated with the Proterozoic evolution of the Aravalli-Delhi Fold Belt. Highly conductive crustal and shallow mantle structures observed under the Malwa Plateau and adjacent Vindhayn basin show strong evidence of Late Cretaceous-Early Tertiary Reunion plume rise under the region and melting accompanied, which caused the Deccan flood basalt volcanism in the Indian subcontinent.

KEYWORDS : magnetotellurics, Rajasthan, resistivity structure

Sr No: 543

Electrical resistivity structure of Saurashtra region in India from magnetotelluric studies

PRESENTING AUTHOR:

Ajithabh K. S., CSIR - National Geophysical Research Institute, Hyderabad, India

CORRESPONDING AUTHOR:

Prasanta K. Patro, CSIR - National Geophysical Research Institute, Hyderabad, India

The electrical resistivity signature of the Saurashtra region in India is derived using magnetotelluric studies. Saurashtra is a part of the Deccan volcanic province (DVP), which is one of the largest continental flood basalt provinces in the world. The 2D and 3D inversions are carried out using 22 broadband magnetotelluric sites in a north – south profile in the Saurashtra. The 2D inversions are carried out using two different regularization operators, namely uniform grid Laplacian (UGL) and standard grid Laplacian (SGL) operators. The 2D output derived using the UGL operator and 3D inversion result demonstrated similar structures in the shallow sub-surface. The basalt configuration and the sub-basal Mesozoic sediments are clearly delineated. The inverted models bought out the signatures of fault zones and the crustal deformations in the study area. The similarity in the trend of the imaged faults, seismicity, and dyke patterns in Saurashtra with the Narmada–Son Lineament (NSL) region indicates the extension of NSL (line of weakness from the Precambrian time) to the Saurashtra peninsula. The Gulf of Cambay presently separates both these regions. The crustal modifications in the crustal segments due to the Deccan volcanic activity are observed in the models. The imaged fault systems are interpreted to be the preferred pathways for the magma migration during the volcanic event.

KEYWORDS : magnetotellurics, deccan volcanic province, crustal deformation

Sr No: 544

Drone-based near-surface electromagnetic and magnetic investigation of anthropogenic and archaeological structures.

CORRESPONDING & PRESENTING AUTHOR:

Tobias Bjerg Vilhelmsen, DTU Space, Denmark

Arne Doessing, DTU Space, Denmark

During the year 2020, we had a growing interest among archaeologist in an area in Falster, Denmark. Findings indicated a prehistorical fortress dating back to the early Viking Age, initial excavations in the form of small digs and pits revealed some of the fortress embankment. Due to the area's regulation and ownership, no further excavations were made. However, non-intrusive geophysical methods are still possible, and we started investigating the area with drone-based electromagnetic and magnetic methods.

In the present presentation, we use the fortress on Falster as a case study to show how drone-based electromagnetic and magnetic data can help locate potential anthropogenic and archaeological structures in the subsurface.

We use data from a magnetic sensor system and a newly developed electromagnetic sensor system. The magnetic sensor system is known from previous studies [1] but has not been used in archaeological prospecting. The electromagnetic data is collected with a multi-frequency electromagnetic sensor named GEM-2 from Geophex. We collected EM data with a line spacing of 0.5m, a sampling rate of 25Hz, drone speed of 2m/s and operate at five different frequencies.

We evaluate how to design and conduct a drone-based EM survey and the importance of a high precision GNSS positioning. We compare P- and T-mode concerning spatial coverage and survey design. We compare the magnetic and electromagnetic data and look into strengths and weakness within both datasets.

Døssing, Arne Andreasen and Jakobsen, J. 2018. WIPO Patent Application No. 2017EP68246. 2018

KEYWORDS :   drones, electromagnetic data, archaeological prospecting

Sr No: 545

A large-scale magmatic-hydrothermal system of Kusatsu-Shirane Volcano, Central Japan, revealed by broadband magnetotellurics

CORRESPONDING & PRESENTING AUTHOR:

Yasuo Matsunaga, Tokyo Institute of Technology, Japan

Wataru Kanda, Tokyo Institute of Technology, Japan

Takao Koyama, The University of Tokyo, Japan

Shinichi Takakura, The National Institute of Advanced Industrial Science and Technology, Japan

Tatsuji Nishizawa, Mount Fuji Research Institute, Japan

Kusatsu-Shirane Volcano (KSV) is an active volcano known for its significant hydrothermal activity and repeated phreatic eruptions in recent years. Geological studies estimated that frequent magmatic eruptions

occurred at Mt. Motoshirane, which constitutes the southern part of KSV, until 1500 years ago. Therefore, it is expected that the magma produced at that time has not yet cooled nor solidified, however, the location of the magma is still unknown because of no structural information in the deep underground.

To reveal the whole image of the magmatic-hydrothermal system of KSV, we conducted broadband magnetotelluric (MT) observations from 2015 to 2020 within a 20 km × 20 km area covering the entire volcanic system. Three-dimensional inversion of the MT data collected from 73 sites revealed the electrical resistivity structure of the volcano up to a depth of ~12 km below the summit.

The most remarkable feature of the model is an electrically conductive zone, which extends from a depth of 1.5 km below the summit area to a depth of ~12 km below the north-northwest of KSV. The lower part of the conductor (depth > 5 km) is moderately conductive (~20 Ωm) and the upper part (depth < 5 km) exhibits a highly conductive feature (< 1 Ωm).

The lower half is interpreted as the zone containing hydrous silicate melts and the upper half as the zone containing high-salinity brines which are strongly affected by repeated magma intrusions from the deep part. In the presentation, we will introduce the details of the interpretation.

KEYWORDS : magnetotellurics, magmatic hydrothermal system, Kusatsu-Shirane Volcano

Sr No: 546

SYMPOSIUM : **6.1 Electromagnetic induction in Earth**

An audio-frequency magnetotelluric investigation of the shallow hydrothermal system at Mt. Motoshirane, central Japan

CORRESPONDING & PRESENTING AUTHOR:

Asami Honda, Tokyo Institute of Technology, Japan

Wataru Kanda, Tokyo Institute of Technology, Japan

Takao Koyama, the University of Tokyo, Japan

Shinichi Takakura, National Institute of Advanced Industrial Science and Technology, Japan

Yasuo Matsunaga, Tokyo Institute of Technology, Japan

Tatsuji Nishizawa, Tokyo Institute of Technology, Japan

Satoshi Ikezawa, the University of Tokyo, Japan

Mt. Motoshirane is one of the pyroclastic cone groups of the Kusatsu-Shirane volcano in central Japan. Its location is about 2 km south from Mt. Shirane, which hosts the Yugama crater where phreatic eruptions were repeated. In 2018, a sudden phreatic eruption occurred at Mt. Motoshirane, which caused casualties. Since most volcanic activities had occurred around the Yugama crater, few studies were conducted at Mt. Motoshirane. A broadband magnetotelluric survey before the 2018 eruption revealed a low resistivity zone at shallow area, but it was not well constrained. X-ray diffraction analysis of the ash suggested that the source depth of the eruption reached the basement rocks. Geological studies inferred that the Neogene basement rocks are exposed around the Kusatsu-Shirane volcano, but there is no information on the depth of basement below Mt. Motoshirane.

In this study, we will show a three-dimensional resistivity structure around the craters erupted in 2018 to clarify the shallow hydrothermal system of Mt. Motoshirane. For this purpose, we conducted an audio-frequency magnetotelluric (AMT) survey in 2020. We used a three-dimensional inversion code using tetrahedral meshes to model the resistivity distribution of the volcanic edifice.

The obtained model was characterized by features similar to the apparent resistivity distribution; it roughly showed high resistivities near the surface and low resistivities at deeper levels. In the presentation, we will show the shallow resistivity structure of Mt. Motoshirane and interpret it based on the previous studies to estimate the hydrothermal system.

KEYWORDS : Mt. Motoshirane, phreatic eruption, resistivity structure,

Sr No: 547

SYMPOSIUM : **6.1 Electromagnetic induction in Earth**

Three-dimensional electrical conductivity of the world ocean and marine sediments and their effect on electromagnetic responses

CORRESPONDING & PRESENTING AUTHOR:

Alexander Grayver, ETH Zurich, Switzerland

We present new global 3-D electrical conductivity atlas of the world ocean and marine sediments. Ocean salinity and temperature data were converted to electrical conductivity by solving a thermodynamic equation of state of seawater. A sediment compaction model was used to build a 3-D electrical conductivity model of marine sediments. We show that electromagnetic responses in a wide period band, including typical ranges used in CSEM, MT and Global studies, are significantly affected by varying ocean and sediments conductivity. Incorporating this information in a model prior to inversion helps avoid artifacts and improve data fit. All data sets presented in this study are openly available.

KEYWORDS : conductivity, ocean, marine sediments

Sr No: 548

SYMPOSIUM : **6.1 Electromagnetic induction in Earth**

Evidence for compaction-induced fluid localization and stagnation from lower crustal low-resistivity zones

CORRESPONDING & PRESENTING AUTHOR:

Matthew J. Comeau, University of Muenster, Germany
Michael Becken, University of Muenster, Germany
James A. D. Connolly, ETH Zurich, Switzerland
Alexander Grayver, ETH Zurich, Switzerland
Alexey V. Kuvshinov, ETH Zurich, Switzerland
Johannes Kaeufl, ETH Zurich, Switzerland
Erdenechimeg Batmagnai, ETH Zurich, Switzerland
Shoovdor Tserendug, Mongolian Academy of Sciences, Mangilia
Sodnomsambuu Demberel, Mongolian Academy of Sciences, Mangolia

We show evidence for a conceptual hydrodynamic model of fluid localization and stagnation by thermally activated compaction from lower crustal ($>$20 km depth) low-resistivity zones. Magnetotelluric data collected across the intracontinental Bulnay region, Mongolia, was used to generate electrical resistivity models. The

models reveal low-resistivity domains (<30 ohm-m; width of ~25 km, vertical extent of <10 km) with their tops ~5 km below the brittle-ductile transition zone (BDTZ). These features are laterally extended (tube-like), ~300 km long, parallel to the Bulnay fault zone, and perpendicular to the far-field compressive tectonic stress. These low-resistivity domains are consistent with the presence of saline metamorphic fluids.

Based on the thermal structure of the crust, the hydrodynamic model predicts that fluids domains should have a vertical extent of ~9 km and their centres should be <9 km below the BDTZ. These predictions are in agreement with the resistivity models. The hydrodynamic model also gives plausible values for the activation energy for viscous creep (270-360 kJ/mol), suggesting that the mechanism is dislocation creep.

The electrical resistivity models constrain the lower crustal viscous compaction-length to be ~25 km, which is consistent with independent estimates of hydraulic and rheological properties. The model can be used to independently constrain the lower crustal effective viscosity (found to be low; e.g., ~10^{18} Pas), the fluid salinity (likely 1-0.01 wt% NaCl), and the porosity (likely 5-0.1 vol%). Overall, the results imply that it is tectonic and compaction processes that control lower crustal fluid flow, rather than lithological or structural heterogeneity.

KEYWORDS : compaction, fluid localization, lower crustal low-resistivity zones

Sr No: 549

SYMPOSIUM : **6.1 Electromagnetic induction in Earth**

MTH5: An Exchangeable and Archivable Data Format for Magnetotelluric Time Series Data with Metadata Standards

CORRESPONDING & PRESENTING AUTHOR:

Jared Peacock, US Geological Survey, USA

The lack of comprehensive metadata and data format standards for magnetotelluric (MT) time series data has impeded data sharing practices and adherence to the findability, accessibility, interoperability, and reusability (FAIR) data principles. An international collaboration led by the Incorporated Research Institutions for Seismology (IRIS) and U.S. Geological Survey have developed MTH5, a hierarchical data format (HDF5) with a comprehensive metadata standard for MT time series data. MTH5 allows an entire MT survey to be contained in a logical format described by comprehensive metadata in a single file that can be efficiently read directly from memory. The newly developed MTH5 data format will facilitate data sharing and data archival by providing a well-defined MT-specific user interface for interoperability with the existing IRIS tools and formats. IRIS is adding wideband and long period MT instruments to its pool of portable instruments for Principal Investigators, and users are required to archive any data collected at the IRIS Data Management Center (DMC). Open-source Python tools for creating MTH5 files and metadata have been developed, including tools to help researchers archive and retrieve MT data at the IRIS DMC.

KEYWORDS : magnetotellurics, HDF5, time series

Sr No: 550

Annual/Seasonal variation of induction vectors at different geological regimes of Indian sector

CORRESPONDING & PRESENTING AUTHOR:

Anusha Edara, National Geophysical Research Institute, India

We have analysed the possible annual and seasonal variations of induction vectors at different geological regimes like island observatories: MNC (Minicoy), PBR (Portblair) & CBY (Campbell Bay), at coastal observatories: ABG (Alibag) & VEN (Vencode) and inland observatories: HYB (Hyderabad). Based on 30-day period of data, the induction vectors are estimated by using 1-minute magnetic variation data for 2 years at each site by using BIRRP-code, to get the stable response in the period range of 4-140 min.

The direction of real vectors for 1000s to 3000s periods at each location indicates the direction of anomalous conductive structures. The real vectors at island sites in Lakshdweep and Andaman-Nicobar islands MNC, PBR & CBY trend towards south-east with the amplitude ranges of -0.5 to 0.5. At ABG & VEN coastal observatories, they trend to the east and south-west respectively with the amplitude range of -0.2 to 1. At inland site HYB the trend is to the north-east with the amplitude range of -0.2 to 0.2. The average annual variation of real vector amplitude ranges from 0.2 to 0.3 at island observatories, from 0.3 to 0.4 coastal observatories and and < 0.1 at inland observatories. At island sites, no seasonal pattern of variations can be inferred. At coastal sites the amplitudes of real vectors are maximum at December (Winter Solstice) and minimum at June (Summer Solstice). At inland location the real vectors are maximum at March (Vernal Equinox) and minimum at December (Winter Solstice). Qualitative inferences on the above have been attempted.

KEYWORDS :   seasonal variation, induction vectors, Indian sector

Sr No: 551

SYMPOSIUM : **6.1 Electromagnetic induction in Earth**

Magnetetotellurics: The mantle, metasomatism, and mineral deposits (by invitation)

CORRESPONDING & PRESENTING AUTHOR:

Kate Selway, University of South Australia, Australia

The magnetotelluric (MT) method has seen huge developments in the last decade. Continent-scale surveys and improved 3D inversion methods are providing unprecedented views of the resistivity structure of the upper mantle, and experimental advances allow these resistivity variations to be quantitatively interpreted in terms of mantle composition. In this talk, I will use examples from Western Australia and southern Africa to show how these results provide insights into upper mantle composition and evolution and into the formation of mineral deposits.

Highly resistive upper mantle can be interpreted within a relatively small range of compositions, which must be essentially dehydrated peridotite with no interconnected conductive phases. Less resistive upper mantle has a broader range of possible interpreted compositions, including hydrated nominally anhydrous minerals in peridotite, and interconnected conductive phases such as phlogopite or amphibole. Importantly, all the possible compositional causes for low resistivity mantle are formed during mantle metasomatism. Therefore, magnetotelluric models can be used to interpret past mantle metasomatism.

Mantle metasomatism is a necessary precondition for the formation of many major mineral deposits but this is hidden to most exploration techniques. I will discuss the conductivity signature of the mantle surrounding major mineral deposits in the Yilgarn Craton, Western Australia and the Kaapvaal Craton, southern Africa. These results illustrate how the ability of MT to model the metasomatic state of the mantle can aid in mineral exploration.

KEYWORDS :   mantle, resistivity, metasomatism

IASPEI Symposia

S1 CoSOI Observational seismology - open session seismology

CONVENERS: Torsten Dahm (Germany)

Francesco Grigoli (Switzerland)

Johannes Schweitzer (Norway)

S. Mostafa Mousavi (USA)

Aitaro Kato (Japan)

The open session of the commission of seismological observation and interpretation (CoSOI) covers a broad and diverse field of developments, approaches and application. This year, the open session comprises presentations in big data in seismology.

Freely available large datasets, including both Large-N nodal arrays and continental arrays, have greatly advanced our understanding of tectonic and earthquake processes. Combination of the big datasets, new monitoring instrumentations and novel processing methods, including improvements in rapid communication of scientific results, has led to breakthroughs in many subfields of seismology. For instance, earthquake location and large earthquake rupture processes are now routinely resolved within a few days by multiple agencies, which have led to new developments in damage impact assessment. Moreover, high performance computing has enabled machine learning being applied to massive datasets to identify previously unknown patterns. However, results of these automatized processing approaches may have errors when their uncertainties are not carefully evaluated, suggesting future research focus directions.

The session invites contributions from all fields of CoSOI including structural and earthquake seismology studies with large datasets new developments of integrating non-seismological data into seismic observations.

Sr No: 552

Version 8 of the ISC-GEM Global Instrumental Earthquake Catalogue

CORRESPONDING & PRESENTING AUTHOR:

Domenico Di Giacomo, International Seismological Centre, UK

Dmitry Storchak, International Seismological Centre, UK

James Harris, International Seismological Centre, UK

Daniela Olaru, International Seismological Centre, UK

The first version of the ISC-GEM Global Instrumental Earthquake Catalogue (1900-2009) (www.isc.ac.uk/iscgem/) was released in January 2013 (Storchak et al., 2013). The goal of the catalogue is to improve the homogeneity (to the largest extent possible, in time and space) of the earthquake parameters (especially location and magnitude) and list them along with formal uncertainties to facilitate seismic hazard and studies of seismicity of the Earth.

In 2018, the release of Version 5 marked the end of the Extension project (Di Giacomo et al., 2018) where moderate earthquakes down to ~5.5 between 1904 and 1959 were added and the catalogue extended up to 2014. Since then we started the Advancement of the ISC-GEM catalogue (www.isc.ac.uk/iscgem/advancement.php), and with this contribution we report on the latest additions to the catalogue: 1) continental earthquakes down to magnitude 5 that have occurred since 1964; 2) source mechanisms from the literature for about 1, 100 earthquakes (mostly before GCMT began in 1976) and revising earthquake parameters in light of the findings in recent and past literature; 4) station data from BCIS bulletins for earthquakes not listed in the ISS during 1950-1963.

KEYWORDS : earthquake, instrumental, catalogue

Sr No: 553

Discrimination of Tectonic and Non-Tectonic seismicity using Principal Component Analysis and Gaussian Mixture Models

CORRESPONDING & PRESENTING AUTHOR:

Akash Kharita, Indian Institute of Technology Roorkee, India

Sagarika Mukhopadhyay, Indian Institute of Technology Roorkee, India

Although many machine learning models have been proposed for event detection and location, very few models are being reported for providing automatic classification of events. Accurate classification of events is necessary to maintain the quality of earthquake catalogs and this can be a challenge in the areas where tectonic and non tectonic seismicity overlaps in space, time and magnitude. In this study, we propose a machine learning model for automatic discrimination of tectonic and non-tectonic events. This model includes the application of unsupervised machine learning technique - Principal Component Analysis (PCA) on amplified absolute frequency spectrum of Z component event series to reduce each traces of certain duration from the origin of event to 3 components. This has been observed to be able to clusterize the events having similar frequency structure, since similarity in frequency structure is the characteristic of similar source processes, this results in the distinct clusters of events having different source processes. These
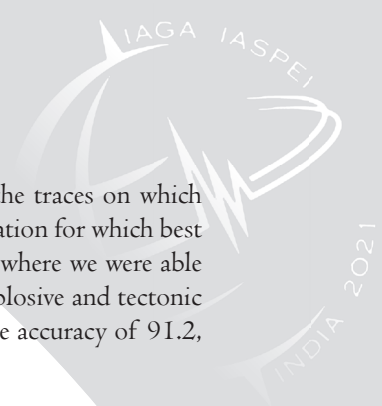
different clusters are then labelled using Gaussian Mixture Models. The duration for the traces on which PCA is applied is determined by repeating the process on different durations and the duration for which best clustering is observed is chosen. We performed 3 separate case studies using our model where we were able to discriminate 1) 600 quarry blasts and tectonic events in Lower California, 2) 598 explosive and tectonic events in Washington and 3) 600 mining blasts and tectonic events in Wyoming with the accuracy of 91.2, 92 and 89% respectively.

KEYWORDS : seismic event classification, machine learning, principal component analysis

Sr No: 554

Strong Motion Data Investigation of the 31, December 2018 Cairo-Suez Zone earthquake

CORRESPONDING & PRESENTING AUTHOR:

Asem Salama, National Research Institute of Astronomy and Geophysics | Cairo, Egypt | NRIAG, Egypt

Mohamed EL Gabry, National Research Institute of Astronomy and Geophysics | Cairo, Egypt | NRIAG, Egypt

Hesham Hussein Moussa, National Research Institute of Astronomy and Geophysics | Cairo, Egypt | NRIAG, Egypt

Mohamed Maklad, National Research Institute of Astronomy and Geophysics | Cairo, Egypt | NRIAG, Egypt

An earthquake with a magnitude Mw 3.8, 31 December 2018 struck the southern road of the Cairo-Suez zone. This earthquake was recorded at seven stations of the Nile Delta strong motion network with a minimum epicenter distance 10 km and a farther epicenter distance 302 km. This event is considered as the first recorded acceleration event near the constructions of the new capital administrative city. The maximum recorded acceleration is found at KOT station, with a value of 16.38 Gal. PGV, PGD, Pseudo acceleration curves are calculated as 0.109 cm/s, 0.114 cm, 0.0731g respectively for the same station. An intensity map is also constructed for this event, with data collected from Facebook, questionnaire, Emsc. The maximum observed intensity is (IV). The HVSR analysis is also performed for the seven stations. H/V ratios indicate that the Nile silt soils show predominant frequencies ranging from 0.5 to 2 Hz, while the quaternary sand site shows a predominant frequency of 2.3 Hz while basement rocks with 2 HZ at NUB station with the higher amplification factor at ANS & MANS stations.

KEYWORDS : strong motion, Cairo Suez, H/V ratio

Sr No: 555

ISC-EHB dataset for 1964 to 2017: Enhancing the Bulletin with ISC depth phase picks

CORRESPONDING & PRESENTING AUTHOR:

Burak Sakarya, International Seismological Centre, UK

E.R. Engdahl, University of Colorado, USA

Charikleia G. Gkarlaouni, International Seismological Centre, UK

Tom Garth, International Seismological Centre, UK

Peter Franek, International Seismological Centre, UK

James Harris, International Seismological Centre, UK

Domenico Di Giacomo, International Seismological Centre, UK

Dmitry A. Storchak, International Seismological Centre, UK

The original EHB dataset, as developed with procedures described by Engdahl et al. (1998), has been widely used in the past in various types of earth science studies. The EHB catalogue stopped in 2008, and since then the volume and quality of data has significantly improved. To take this into account we have re-constructed the ISC-EHB dataset for the period 1964-2017 with the updated criteria defined in Weston et al. (2018). Event selection for the ISC-EHB is made from the reviewed ISC Bulletin, which consists of data contributed by seismological agencies from around the world. In the past decade there has been a consistent decline in the number of depth phase picks reported to the International Seismological Centre (ISC). Depth phases are crucial for the ISC-EHB dataset as they directly influence the quality of the depth constraint. In order to address this issue, we have been routinely picking depth phases for earthquakes across the globe with mbNEIC$\geq$4.8 recorded at 28°-72° distance range and data period from April 2016. In this contribution we describe the procedures used to construct the newly refined ISC-EHB dataset covering earthquakes from 1964 to 2017. We also illustrate noteworthy features in several regions, including some of those presented in Engdahl et al. (2020). The ISC-EHB catalogue now includes 177, 416 earthquakes with prime magnitudes mb/MS>3.75 and is freely available from the ISC website. The ISC-EHB dataset will be extended beyond the year 2017 as soon as the review of each following annual ISC Bulletin is completed.

KEYWORDS : ISC-EHB, dataset, depth

Sr No: 556

SYMPOSIUM :   **S1 Observational seismology - open session seismology**

Precise aftershocks distribution of the Khankh earthquake, Mongolia

CORRESPONDING & PRESENTING AUTHOR:

Adiya Munkhsaikhan, Institute of Astronomy and Geophysics of MAS, Brazil

Ganbaatar Ariunaa, Institute of Astronomy and Geophysics of MAS, Brazil

Lkhagva Dagzinmaa, Institute of Astronomy and Geophysics of MAS, Brazil

Sereenendorj Odbayar, Institute of Astronomy and Geophysics of MAS, Brazil

Monkhor Oyunerdene, Institute of Astronomy and Geophysics of MAS, Brazil

Lkhagva Tungalag, Institute of Astronomy and Geophysics of MAS, Brazil

Ayush Dulguun, Institute of Astronomy and Geophysics of MAS, Brazil

Dorj Enkhtulga, Institute of Astronomy and Geophysics of MAS, Brazil

There are three seismic basins, Busiin-Gol, Darkhad and Khubsugul lake area, in north Mongolia. On January 11, 2021 (21:32 UTC), strong earthquake with magnitude of 6.5 (ML) occurred in the Khubsugul lake area (epicenter 51.32°N, 100.37°E), we called Khankh earthquake which is name of the nearest sum. This is the strongest earthquake that has been recorded over the 30 years of seismological observations in the Mongolian territory after the Busiin-Gol earthquake which occurred on 27th December 1991, with a magnitude of Mw = 6.5.

Many aftershocks occurred following the mainshock, up to now we detected over the 55000 aftershocks with range of local magnitude 0.1-5.5. Obtaining a precise location of the aftershock distribution is important to understand the generation mechanism of the large earthquake. The epicenter of the Khankh earthquake is located outside of the local seismic network of Mongolia. Due to this, we deployed four temporary seismic

stations in nearby Khankh seismic source zone just after two weeks of mainshock for studing the aftershock activity of this event.

In the frame work of study, we constrain the 3D velocity model and precise locations of the aftershocks using TomoDD.

KEYWORDS : khankh earthquake, khubsugul, aftershock distribution

Sr No: 557

The preliminary result of seismicity analysis for Khankh strong earthquake in Mongolia

CORRESPONDING & PRESENTING AUTHOR:

Dorjsuren Ankhtsetseg, Institute of Astronomy and Geophysics of MAS, Brazil
Adiya Munkhsaikhan, Institute of Astronomy and Geophysics of MAS, Brazil
Sereenendorj Odbayar, Institute of Astronomy and Geophysics of MAS, Brazil
Erdenetsog Nominerdene, Institute of Astronomy and Geophysics of MAS, Brazil
Munkhbaatar Dolgormaa, Institute of Astronomy and Geophysics of MAS, Brazil
Dorj Khongor, Institute of Astronomy and Geophysics of MAS, Brazil
Lkhagvasuren Sarantsetseg, Institute of Astronomy and Geophysics of MAS, Brazil

The strong earthquake with magnitude ML=6.5 (Io=7-8) occurred early in the morning on 12 January 2021 at 5:33 am local time at a shalow depth ~7-10km beneath in the middle of Huvsgul lake nearby Khankh sum, Khubsugul aimag, Mongolia. Based on the preliminary macroseismic data, it felt widely in range of intensity 2-6 included capital Ulaanbaatar, (600 km). For the recent citizens of Ulaanbaatar faced experience of feeling of strongest ground shaking since occurrence of Busiin gol earthquake (1991.12.27, ML=6.5, Io=7-8) in the west board of seistotectonic zone of Khubsugul.

The epicenter of main shock (2021.01.11, 21:32:58 UTC) is located in the western part of Doloon Uul mountain, edge of Khubsugul lake, at the distance ~29 km SW from Khankh sum. After main shock, 8 strong aftershocks with magnitude ML=4.5-5.5 in 40 minutes along the crossline of epicenter of main shock. The initial aftershocks distributed along the Khubsugul fault zone in north side of main shock and shifted to south side of main shock. The aftershock decay rate is close to 1.0.

We did probability density function analysis f(x) for catalog of Mongolian National Data Center and obtained parameters a, b, Mc value. According to the preliminary results, we observed "b value" decreased before main shock. The Khankh seismic source zone has been active.

KEYWORDS : khankh earthquake, khubsugul, macroseismic data

Sr No: 558

Landslides monitoring in the Tien Shan region by seismic stations of Central Asia

CORRESPONDING & PRESENTING AUTHOR:

Inna Sokolova, Institute of Geophysical Research NNC RK, Kazakhstan

Anna Berezina, Institute of Seismology of National Academy of Sciences of Kyrgyz Republic, Kyrgyztan

Elena Pershina, Institute of Seismology of National Academy of Sciences of Kyrgyz Republic, Kyrgyztan

Nadezhda Sokolova, Institute of Seismology of National Academy of Sciences of Kyrgyz Republic, Kyrgyztan

The features of the waveforms of a powerful landslide of November 30, 2020, GMT 23:43, in the area of the Kumtor mine, recorded by the seismic networks of Kyrgyzstan, KNET (RS RAS) and KRNET (IS NAS KR), were studied. The volume of this landslide was 12 million 825 thousand cubic meters. The landslide was recorded by a large number of seismic stations of Kyrgyzstan at epicentral distances from 36 km - TARG to 530 km - ARK.

The waveforms of another powerful landslide of September 14, 2020 in the area of the Kara-Keche coal deposit in the Naryn region of Kyrgyzstan with a volume of 800-900 thousand cubic meters were investigated. Data processing was carried out according to the records of 8 stations at epicentral distances from 58 to 226 km.

A comparison was made with the records of 7 landslides, occurred in 2004 with a volume from 800 cubic meters to 1 million cubic meters in the area of Zailiyskiy Alatau, as well as a powerful landslide in the «Kolsay Lakes» National Park on April 18, 2018, with a volume of 45-50 million cubic meters.

The dynamic and kinematic parameters of records of unusual seismic events are studied. For all recorded landslides, the dependence of the event's magnitude on the volume of the descended mass is observed. The probable factors, responsible for the landslide descent, have been investigated.

Sr No: 559

Seismicity of the Pannonian Basin: relocation with the Bayesloc algorithm using ground truth events as anchors

CORRESPONDING & PRESENTING AUTHOR:

Barbara Czecze, Eötvös Loránd Research Network, Institute of Earth Physics and Space Science, Hungary

Istvan Bondar, Eötvös Loránd Research Network, Research Centre for Astronomy and Earth Sciences, Hungary

The aim of this project was to relocate the seismic events of the entire Pannonian Basin between 1996 and 2017 to improve the view of the seismicity. The events and magnitudes in the Hungarian National Seismological Bulletin are determined with the iLoc algorithm (using 3D global RSTT velocity model). In our previous work, we clustered these events, then we applied the double-difference algorithm for the largest clusters. The combination of the iLoc and hypoDD locations served as the initial coordinates for Bayesloc.

We used hundreds of ground truth events (anthropogenic mining activity, explosions) in our Bayesloc analysis to pin down the pattern of the entire seismicity in the Pannonian Basin. We assigned different prior constraints to earthquakes, anthropogenic events, GT5 events, and presumably blast-related events. The results improved significantly, especially around the mining areas. This study well illustrates the efficiency of the usage of prior information and the Bayesloc algorithm.

KEYWORDS : bayesloc, iLoc, hypoDD

Sr No: 560

SYMPOSIUM : **S1 Observational seismology - open session seismology**

Determination of group and phase-velocity dispersion curves of Rayleigh surface waves from tidal gravimetric recordings of earthquakes

CORRESPONDING & PRESENTING AUTHOR:

Monika Wilde-Piorko, Institute of Geodesy and Cartography, Hungary

Kamila Karkowska, Institute of Geodesy and Cartography, Hungary

Przemyslaw Dykowski, Institute of Geodesy and Cartography, Hungary

Marcin Sekowski, Institute of Geodesy and Cartography, Hungary

Marcin Polkowski, Accenture, Ireland

The analysis of gravimetric recordings of earthquakes can allow improving the determination Earth's mantle structure. Tidal gravimeters are capable to detect surface waves of periods even up to 500-600 s, while a typical broad-band seismic sensor can detect them only up to the periods of 200-300 s.

This study presents the novel application of tidal gravimetric data in the determination of group and phase velocity dispersion curves of surface waves in a period range of 200-600 s. The 1 Hz sampled time series from tidal gravimeters are available in the IGETS and IRIS database. Some data has been made available thanks to courtesy of gravimetric observatories. The recordings of gravimetric stations from the area of Europe were analyzed and the consistent database of recordings of earthquakes has been created. Next, the group-velocity dispersion curves of fundamental-mode Rayleigh waves were calculated by applying the multiple filter technique. The modified Wiener deconvolution technique was used to calculate the phase-velocity dispersion curve by a two-stations method. Results obtained based on the gravimetric data were verified by applying the same procedures to the seismic data. The detailed analysis of transfer functions of instruments has been presented, too.

KEYWORDS : tidal gravimeter, surface wave, earth's mantle

Sr No: 561

CCREM: New Reference Earth Model from Coda Correlation Wavefield

CORRESPONDING & PRESENTING AUTHOR:

Xiaolong Ma, Australian National University, Australia

Hrvoje Tkalcic, Australian National University, Australia

The Earth's coda correlation wavefield has risen as a new concept in global seismology during the last decade. Resting on the principles of global-scale interferometry, it represents an abstract wavefield resulting from the cross-correlation of long-duration seismic recordings between receivers and similarity between the pairs of seismic phases. As an independent data source, a multitude of prominent features extracted from the global correlograms can be analyzed to place constraints on Earth's structure. The analysis of such features is different from interpreting either direct observations of seismic phases or free oscillations of the Earth, which can increase the deep Earth's illumination. Here we demonstrate new constraints on the Earth's radial seismic structures based on the coda correlation wavefield. The global correlogram is generated from ten selected large earthquakes, and a comprehensive dataset of correlation features is selected as observations. We fit both the travel times and waveforms of these features by computing synthetic correlograms through a series of candidate models. A preferred Earth's radial model called CCREM is proposed, which provides an optimal representation of the features in the coda correlation wavefield. The new reference model displays radially different seismic velocity structures, especially near the sharp internal boundaries compared to previous reference Earth models.

KEYWORDS : coda correlation wavefield, reference earth model, deep earth

Sr No: 562

Experimental setup of a newly converted P-wave activator to be used in the new dense P-wave seismic ground and material strength simulator

CORRESPONDING & PRESENTING AUTHOR:

Dursun Acar, ITU, Turkey

Onder Sebnem, Canakkale 18 Mart University, Turkey

Emin Demirbag, ITU, Turkey

Bedri Alpar, Istanbul University, Turkey

Caner Imren, ITU, Turkey

Hulya Kurt, ITU, Turkey

Turgay Isseven, ITU, Turkey

Neslihan Ocakoglu Gokasan, ITU, Turkey

Kadir Eris, ITU, Turkey

Gonca Orgulu, ITU, Turkey

Beril Karadoller, ITU, Turkey

Nazmi Postacoglu, ITU, Turkey

Sinan Ozeren, ITU, Turkey

Ioannis Lymperis

First destructive shock comes with P-wave in earthquake events. It causes concrete explosions that are similar to escaping of little pieces as material spreads or pressure cracks on the main mass. Weak columns are formed

as differentiated zones with rounded finite borders. It caused to inner fractures in columns just before the building collapse during S-waves or later on. Generally, P-wave source frequency interval is accepted between 1 and 11 Hz near the broken segment. In our pure P-wave experiment, the source frequency with 11 Hz are recorded with the sensors as 150 Hz as a cause of interferences. The confusion that starts with the sensors is also valid for the experiment actuators. Therefore we focused on electromagnetic actuators, instead of pneumatic and hydraulic systems that are difficult to control. The reason of that is pneumatic and hydraulic systems are not a good P-wave generator in terms of the wave direction, frequency stability and hammering velocity. In addition, these systems are not much useful because of friction and abrasion in long-term sustainability. In the experiment, we checked and eliminated the relay type electromagnetic actuators, which are carrier the heavily moving rod cores in the relay. Because the relay types are slow and non simultaneous for response to triggering circuit, we used loudspeakers with specially designed ligthweigth hammering unit in our laboratory. This experiment setting can be used for pore water, soil liquefaction and all construction technologies even in aviation or space in terms of material strength related to P-waves.

KEYWORDS : P-wave, S-wave, seismic, eartquake, actuator

Sr No: 563

SYMPOSIUM : **S1 Observational seismology - open session seismology**

Seismic monitoring of the February 7, 2021 flash flood water levels in the Dhauli Ganga river in Uttarakhand Himalaya

CORRESPONDING & PRESENTING AUTHOR:

Himangshu Paul, CSIR-National Geophysical Research Institute, India

N. Purnachandra Rao, CSIR-National Geophysical Research Institute, India

Rajesh Rekapalli, CSIR-National Geophysical Research Institute, India

D. Srinagesh, CSIR-National Geophysical Research Institute, India

Michael Dietze, GFZ German Research Center for Geosciences, India

Kristen Cook, GFZ German Research Center for Geosciences, India

River flow can generate seismic waves due to various complex processes like sediment transport, cavitation or implosion of bubbles, breaking waves due to gravity, and turbulent flow causing frictional forces against the river bed. Recent studies indicate that physical models can be developed relating seismic signals with sediment transport and turbulent flow, which enables the river monitoring remotely, using seismic data. On 7th February 2021, a rockslide event occurred in Ronti Mountain which triggered flash floods in the Rishi Ganga and Dhauli Ganga rivers in Uttarakhand Himalaya. The flash flood caused extensive damage to the hydropower projects at Rishi Ganga and Tapovan and resulted in several casualties. A network of broadband seismic stations of CSIR-NGRI is operational in this region, providing an opportunity to study the seismic records of this event. The nearest seismological station to the flood event was AUL, where the flood power was found to be concentrated in the frequency range of 0.5 and 6 Hz, and as high as -80 dB. Inversion of the data with an empirical model provided an average water level height of ~15 m during the event, with the peak water level reaching ~18 m for a duration of 4 minutes. The floodwater gauge at Joshimath corroborate with our results. In terms of far-field detection, it is observed that the flood signal clearly remains above the noise level at least up to 40 km. Further, we modelled long term seismological data to monitor water levels and compared it with precipitation data.

KEYWORDS : seismic monitoring, Rishi Ganga flash flood, turbulent flow

Sr No: 564

Seismic Bulletin for the European Arctic

CORRESPONDING & PRESENTING AUTHOR:

Johannes Schweitzer, NORSAR, Norway

Berit Paulsen, NORSAR, Norway

Galina N. Antonovskaya, N. Laverov Federal Center for Integrated Arctic Research UB RAS, Russia

Andrey V. Fedorov, Kola Branch, GS RAS, Russia

Yana V. Konechnaya, N. Laverov Federal Center for Integrated Arctic Research UB RAS, Russia

Vladimir E. Asming, Kola Branch, GS RAS, Russia

Myrto Pirli, Intependent, Norway

Recent years have shown an increased interest in Polar research and in particular in understanding tectonics and seismic hazards in the Arctic. To understand the seismic activity in the European Arctic, the seismic bulletins should be as complete as possible. We present a new seismic event bulletin for the European Arctic (70° – 90° N, -15° – 75° E), for the 24-year long period 1990 – 2013. The presentation will describe in detail the merging of the different sources taken in account for the compilation, the homogenization of the data and the relocation of the seismic events. With respect to the ISC bulletin for this region, the new bulletin contains 5, 957 new seismic events and 58, 242 new seismic onset readings from stations mostly located at regional distances. The gains are distributed over the entire study region, with the most significant contributions across the Svalbard Archipelago, along the Knipovich and northern Mohns Ridges, as well as northern Fennoscandia.

KEYWORDS : European Arctic, seismic bulletin, seismic event location

Sr No: 565

Seismological (Meta)data Licensing

CORRESPONDING & PRESENTING AUTHOR:

Jerry Carter, IRIS, USA

Most data and metadata from seismological networks are neither formally declared to be in the international public domain nor are they licensed despite the fact that GOFAIR requirements for meeting FAIR principles require that "(Meta)data are released with a clear and accessible data usage license" as one of the "Reusable" principles. (Meta)data licensing that ensures free and open access to data include public dedication tools that place the (meta)data in the international public domain (e.g., the Creative Commons public dedication tool, CC0), and licenses that require only attribution (such as CC-BY). A case is made that in the interest of pursuing free and open access to data and in promoting FAIR data principles, metadata should be declared to be in the international public domain, but that data could either be declared in the international public domain or be declared to be under a data usage license that requires nothing more than attribution of the data. Declaring requires only that the choice be communicated in a way that will be clear to people who come across the data. It is suggested that declarations should be communicated by including the license information or declaration of public domain for both the metadata and the data in the metadata as well as in the DOI (if one exists).

KEYWORDS : FAIR data principles, data licensing

S3 CoSOI & CoESM Anthropogenic seismicity

CONVENERS: Stanislaw Lasocki (Poland)

Harsh K. Gupta (India)

Beata Orlecka-Sikora (Poland)

Under suitable geological conditions, anthropic activities such as the creation of the artificial water reservoirs, underground coal and metal mining, hydrocarbon production, underground storage of CO_2, geothermal energy production, etc. can trigger/induce earthquakes. The socio-economic impact of the triggered and induced seismicity is very significant. On the one hand, the anthropogenic seismic events, though being small compared to tectonic earthquakes, are often damaging and occasionally even devastating because of their shallowness. The accurate assessment of the hazards associated with triggered earthquakes is of paramount importance. Due to anthropogenic seismic processes' relation to technological activity, which usually varies in time, this hazard assessment problem is inherently time- dependent. But the existence of this relation also opens a possibility to mitigate the related hazards through adequate modifications of the inducing industrial operations.

This symposium takes a global perspective to recognize the severity of the anthropogenic seismicity and to survey recent progress in understanding this phenomenon. We welcome both cross-sectional multi-aspect theoretical, methodological, and experimental studies as well as case histories linked to particular inducing technologies. The session will help identify cross-technology common denominators of the induced seismic processes, with specific attention devoted to approaches to hazard assessment and mitigation.

Sr No: 566

Increased earthquake activity during Hammer Drilling for the Pilot Borehole at Koyna, India

CORRESPONDING & PRESENTING AUTHOR:

Uma Anuradha Madugula, National Geophysical Research Institute, India

Rajesh Rekapalli, National Geophysical Research Institute, India

Sudheer Kolluri, National Geophysical Research Institute, India

Jagadeesh P, National Geophysical Research Institute, India

Satyanarayana Hari Venkata Subramanya, National Geophysical Research Institute, India

Among the global reservoir triggered seismicity (RTS) sites, Koyna, located near the west coast of India is an outstanding example, where the seismicity started soon after the impoundment of Koyna reservoir and has continued for the past six decades. Generally, annual loading of reservoir during the monsoon season and unloading during the rest of the year triggers earthquakes in RTS sites. The frequency of these triggered earthquakes changes with the rate of unloading. For example, for an increase of unloading rate from 0.053 to 0.170 m/day at Koyna reservoir in the 3rd week of March 2015, the weekly number of ML $\geq$0.8 increased to 25, compared to 10 in the previous week. Similar observations are presented for unloading phases during 2016, 2017 and 2018. The drilling of the 3 km deep Pilot Borehole started in December 2016 using a hammer-drilling technique, and the drilling reached sub-basalt granitic basement on 1 February 2017 with five phases of rapid drilling lasting a week or so. As this period coincides with the unloading phase of the reservoirs, we analyze the changes in the seismicity due to the additional mechanical stress from drilling. We have noticed an increase in the earthquakes during March to June 2017 with in 10 km of the Pilot Borehole site compared to 2015, 2016, and 2018. As the Koyna-Warna region is stressed close to critical, the perturbation from drilling adds to triggering of the earthquakes.

KEYWORDS : reservoir triggered seismicity, koyna, drilling, reservoir loading/unloading

Sr No: 567

Accounting for natural uncertainty within monitoring systems for induced seismicity based on earthquake magnitudes

CORRESPONDING & PRESENTING AUTHOR:

Corinna Roy, University of Leeds, UK

Andy Nowacki, University of Leeds, UK

Xin Zhang, University of Edinburgh, UK

Andrew Curtis, University of Edinburgh, UK

Brian Baptie, British Geological Survey, UK

Shale gas and geothermal power have become important energy sources worldwide, and the global demand for mined resources continues to rise. However, public concerns over risks of earthquakes in the vicinity of operational sites has increased. Traffic light systems (TLS) are often used to control our reactions to induced seismicity, and to reduce the probability of larger future events. Under a TLS, operations must stop if an earthquake with a local magnitude ML above a given threshold is detected.

However, the impact of velocity uncertainties and station site effects may be greater than a whole magnitude unit of ML, which can make the difference between a decision to continue ("green" TLS zone) and an immediate stop of operations ("red" zone). We show how to include these uncertainties in thresholds such that events only exceed a threshold with a fixed probability. This probability can be set by regulators to reflect their tolerance to risk.

We apply the new TLS both to mining-induced seismicity, and to the hydraulic fracturing induced seismicity at Preston New Road, UK, where a deterministic monitoring approach and unaccounted-for uncertainties led eventually to earthquakes with local magnitudes that resulted in the immediate cessation of fracking across the UK.

We demonstrate that with the new TLS, a red-light threshold would have been encountered earlier in the hydraulic fracturing operation at Preston New Road, UK, halting operations and potentially avoiding the later large magnitude events.

KEYWORDS : TLS, uncertainties, induced seismicity

Sr No: 568

Stochastic modelling of aftershock activity in Kiirunavaara Mine, Sweden for the estimation of strong aftershock occurrence probability

PRESENTING AUTHOR:

Drgaomir Gospodinov, Plovdiv University, Bulgaria

CORRESPONDING AUTHOR:

Savka Dineva, LKAB,Sweden

Christina Dahner Lindkvist, LKAB, Sweden

As in crustal seismicity, many mining-induced seismic events ($M \geq 1.5$) in deep underground mines, although not of large magnitude, are followed by aftershocks with certain time and magnitude distributions. Main shocks and some of the aftershocks can pose a risk to the mining operation or the personnel as they can cause damage in the rock mass. Therefore, it is important that mining activities are planned according to the probability of their occurrence. The main purpose of the present study is to apply stochastic modelling of aftershock temporal distribution for several sequences in the deep underground Kiirunavaara Mine, (Sweden) in order to estimate the evolution of strong aftershock occurrence during a sequence. The Restricted Epidemic Type Aftershock Sequence (RETAS) model was chosen for the stochastic modelling. This model considers all events with magnitude above the magnitude of completeness M0 and has the advantage of including the Modified Omori Formula (MOF) model and the Epidemic Type Aftershock Sequence (ETAS) model as its end versions, considering also all intermediate models. The obtained results show that the RETAS model versions fitted well different type of aftershock sequences. Monte Carlo simulation of the identified best-fit models was performed to forecast the probability of stronger aftershocks occurrence. For series with little or no secondary activation, the simulation of the MOF version of RETAS turned to be a practical tool for quickly determining the probability values. The applicability of the used approach was considered for re-entry protocol considerations in the mine.

KEYWORDS : mining-induced seismicty, aftershocks, RETAS

Sr No: 569

Coda wave attenuation using a unique borehole seismic network in Koyna, Western India

CORRESPONDING & PRESENTING AUTHOR:

Mallika Kothamasu, CSIR-NGRI, India

Shashidhar D, CSIR-NGRI, India

Purnachandra Rao N, CSIR-NGRI, India

Satyanarayana Hari Venkata Subramanya, CSIR-NGRI, India

About 200 earthquakes of ML 2.0 – 4.0 that were recorded at a unique borehole seismic network and also on the co-located surface seismic stations of the Koyna region, western India during 2015 – 2019 have been employed for estimation of coda wave attenuation (Qc) at central frequencies 8.0, 10.0, 12.0, 16.0, and 20.0 Hz through five lapse time windows from 20 to 60 s. For the first time for the borehole seismic stations a Qc value of 118f0.87 has been computed while the average Qc values vary from 659 at 8 Hz to 1589 at 20Hz central frequencies. On the other hand, we find for the surface seismic stations that Qc = 145f1.15, while the average Qc values vary from 798 at 8 Hz to 1790 at 20Hz central frequencies. It is inferred from this study that the obtained quality factor is strongly dependent on frequency, corroborating with the high level of seismicity of the region.

KEYWORDS : coda waves, quality factor, lapse time

Sr No: 570

The 3D aspect ratio of surface water reservoirs on the subsurface stress changes and pore pressure diffusion for induced seismicity: the Aguamilpa dam, Mexico, revisited

CORRESPONDING & PRESENTING AUTHOR:

Miguel A. Santoyo, Institute of Geophysics, National Autonomous University of Mexico, Mexico

Reservoir Triggered Seismicity (RTS) is a highly complex phenomenon when it comes to understanding the driving physical mechanisms. Among the key aspects to account for the RTS analysis is the spatiotemporal distribution of surface water loads, employing Digital Elevation Models(DEM) for the bathymetry and the time evolution of water levels; unfortunately, a detailed bathymetry is not always available.

We study the spatiotemporal evolution of the subsurface stress changes (SC) and pore pressure diffusion (PPD) as a function of the 3D configuration of the reservoir and the water level evolution of the lake. Surface loads are modelled by different theoretical 3D configurations of the lake. The theoretical bathymetry is modelled assuming a semi-ellipsoid tapered with a bidimensional cosine function. SC and PPD are calculated for a 3D half-space and different fault directions. After this, the theoretical models are compared with the actual configuration of the Aguamilpa reservoir, Mexico; This one is the third highest gravity dam and the fifth reservoir in storage capacity (6, 950 hm3) in Mexico. For this, the spacetime evolution of surface loads are computed employing the DEM before the impoundment and the observed water levels. The 3D subsurface SC and PPD from the theoretical models and from the actual reservoir configuration
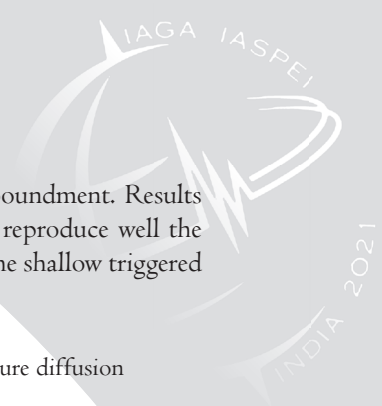
are compared with the seismic series occurred two months after the beginning of impoundment. Results show that, for different 3D configurations and specific depths, the theoretical models reproduce well the main effects from surface loads and show how these become important when analyzing the shallow triggered seismicity.

KEYWORDS : reservoir triggered seismicity, 3D lake aspect ratio, stress change and pore pressure diffusion

Sr No: 571

SYMPOSIUM : **S3 CoSOI & CoESM Anthropogenic seismicity**

Strong Ground-motion predictions from Induced Earthquakes in St. Gallen Geothermal field, Switzerland

CORRESPONDING & PRESENTING AUTHOR:

Nitin Sharma, CSIR-National Geophysical Research Institute, India

Vincenzo Convertito, Istituto Nazionale di Geofisica e Vulcanologia, Osservatorio Vesuviano, Italy

Raffaella De Matteis, Università degli Studi del Sannio, Italy

Paolo Capuano, Università di Salerno, Italy

The ground shaking whether it is due to natural or induced earthquakes, is always be a matter of concern, as long as it causes structural/non-structural damage or the human anxiety is culminated. It is well understood that industrial activities such as water injection, gas sequestration, waste fluid disposals, etc. lead to fluid pressure changes and effective stress regime, that can promote the reactivation of preexisting faults or generate new fault. Now it is becoming a usual practice to monitor induced seismicity and the consequent ground shaking while doing any kind of anthropogenic activity. Therefore, keeping in mind the importance of timely evaluation of seismic hazard and its mitigating societal benefits, the present study propose the prediction of ground-motions from specifically designed ground-motion prediction equations (GMPEs) for induced earthquakes in St. Gallen geothermal area, Switzerland.

The data analysed in this study consist of 343 earthquakes with magnitude (ML, cor) ranges between -1.17$\leq$ML, corr$\leq$3.5 and hypocentral distance from 4 km through 15 km. The data have been collected by Swiss Seismological Service in 2013 while realizing well control measures after drilling and acidizing the GT-1 well. The GMPEs for peak-ground acceleration (PGA) and peak-ground velocity (PGV) are computed. Moreover, these are the first GMPEs to incorporate strong ground motions from negative magnitude earthquakes for the analysis. The GMPEs from this study are also compared with GMPEs developed for the other induced seismicity environment. A drastic mismatch among them is also discussed.

KEYWORDS : induced seismicity, anthropogenic activity, GMPE

Sr No: 572

Ground-motion prediction equations from reservoir-triggered earthquakes at Koyna-Warna region, India

CORRESPONDING & PRESENTING AUTHOR:

Nitin Sharma, CSIR-National Geophysical Research Institute, India

Srinagesh Davuluri, CSIR-National Geophysical Research Institute, India

Shashidhar Dodla, CSIR-National Geophysical Research Institute, India

Mallika K, CSIR-National Geophysical Research Institute, India

The induced/triggered seismicity from anthropogenic sources can be a significant nuisance to a local population and in extreme cases lead to damage to vulnerable structures. This impact can limit the development of resources for clean energy like hydropower generation, geothermal power generation, etc. In order to understand the effect of ground shaking and related seismic hazard on nearby settlements analysis and development of strong ground motion models are the key tool to predict the level of ground shaking (in terms of, for example, peak ground acceleration) due to an earthquake of a certain magnitude at a particular distance.

The Koyna Warna is one of the most promising and well-established case studies of reservoir-induced seismicity in India. Eventually more significant, when the earthquake with magnitude 6.3 found to be a triggered earthquake which occurred on December 10, 1967, in the region of the said artificial water reservoir. Thus, in the present work, we develop the Ground Motion Prediction Equations (hereinafter GMPEs) for the Koyna Warna region. The GMPEs are developed for both PGA and PGVs. These GMPEs are also compared with the models developed in different induced/triggered seismicity environments around the globe.

KEYWORDS : triggered seismicity, strong ground motion, peak ground acceleration

Sr No: 573

3D velocity structure in the reservoir triggered seismic environment of Koyna, India: A Local earthquake tomography using borehole seismic network

CORRESPONDING & PRESENTING AUTHOR:

Shashidhar Dodla, CSIR-NGRI, India

Sandeep Gupta, CSIR-NGRI, India

Mallika K, CSIR-NGRI, India

Satyanarayana Hari Venkata Subramanya, CSIR-NGRI, India

This study presents results of three-dimensional velocity structure of the Koyna-Warna region of western India, a popular site of reservoir triggered seismicity, from the tomographic analysis of a unique borehole seismic network data. Arrival time data from 5167 earthquakes including micro-earthquakes are inverted for three dimensional Vp and Vp/Vs structure. The results offer image of the velocity structure with a significant velocity contrast clearly indicating the Donachiwada fault at seismogenic depths for the first time. Majority of the earthquakes occur just beneath this fault trace. An uplift of high Vp and Vp/Vs structure is found and is associated with the seismicity cluster.

KEYWORDS : tomography, koyna, borehole
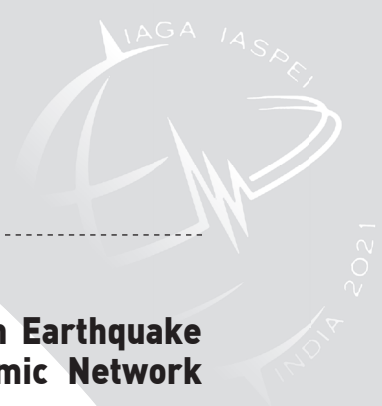
Sr No: 574

A Cross-Correlation Approach for Relative Locations of an Earthquake Sequence Recorded on the Koyna-Warna Borehole Seismic Network (Western India)

CORRESPONDING & PRESENTING AUTHOR:

Daniela Kuehn, NORSAR, Norway

Ismael Vera Rodriguez, NORSAR, Norway

Dodla Shashidhar, CSIR-NGRI, India

Kothamasu Mallika, CSIR-NGRI, India

Satyanarayana Hari Venkata Subramanya, CSIR-NGRI, India

Volker Oye, NORSAR, Norway

Seismicity triggered by impoundment of water reservoirs originates from the response of the reservoir to initial filling as well as water level changes. The Koyna–Warna region in western India is one of the most prominent examples of reservoir triggered seismicity. Within this area, an enormous number of micro-earthquakes was detected automatically on borehole records. Most of these events could not be identified on the surface network by a routine approach based on visual inspection primarily due to signal attenuation and the presence of noise. In this work, we implemented the automatic detection workflow to analyse the time series of an earthquake sequence which has a clear foreshock and aftershock activity associated with a Mw 4.0 earthquake that occurred on 3 June 2017. Further, we applied a nested grid search algorithm to constrain the absolute earthquake locations. For about one month of data, a total of ~1500 earthquakes were detected based on the automatic detection process, out of which ~1000 earthquakes were locatable. All event detections, P-wave and S-wave phase readings were manually inspected and refined to ensure their quality. Previously, only about 435 events were well-located based on the visual inspection for the same time period. Also, we analysed repeated earthquakes based on waveform similarity leading to an improvement in the relocations of earthquakes of the above earthquake sequence. The relocated seismicity aligns parallel to a deep-reaching lineament derived from recent investigations using airborne lidar measurements.

KEYWORDS :   reservoir triggered seismicity, re-location, cross-correlation

Sr No: 575

Induced Earthquakes in the Weiyuan-Rongxian Shale Gas Field, Sichuan: A Case Study of Event Cluster Initiated by Hydraulic Fracturing

PRESENTING AUTHOR:

Jinping ZI, The Chinese University of Hong Kong, Hong Kong

CORRESPONDING AUTHOR:

Hongfeng Yang, The Chinese University of Hong Kong, Hong Kong

Jinrong Su, Sichuan Earthquake Agency, China

Jiangyang Zhang, The Chinese University of Hong Kong, Hong Kong

Han Chen, The Chinese University of Hong Kong, Hong Kong

Junhao Song, The Chinese University of Hong Kong, Hong Kong

Wing Ching Jeremy Wong, The Chinese University of Hong Kong, Hong Kong

With the growing demand for energy sources and increased public concern on global warming, unconventional oil and gas such as the shale gas industry has developed rapidly in the past several years. However, rising destructive earthquakes related to hydraulic fracturing during shale gas development have been reported worldwide, posing threats to people's life and property. Thus, it is imperative to study the features and possible mechanisms of hydraulic fracturing-related earthquakes to mitigate their potential effects. The shale gas development in China mainly locates in the Sichuan basin. Here we focus on the Weiyuan shale gas field, showing a high-resolution spatial-temporal pattern of seismicity constrained from a dense temporary network.

Our temporary network was deployed from 17th April 2020 to 15th June 2020 in the Weiyuan-Rongxian shale gas field. Seismic data collected were processed by PhaseNet phase picking, REAL association, HYPOINVERSE, and HypoDD relocation with cross-correlation differential time calculated by the 3-channel sliding window cross-correlation method. Eventually, we obtained more than 5000 relocated events with magnitudes ranging from ML -1.6 to ML 3.0 in the study region. We observed a new cluster initiating on 10th May 2020, consistent with the start of hydraulic fracturing of one shale gas well nearby. The depth of induced seismicity occurred in strata slightly below the target shale layer. The seismicity migrated linearly along northwest-southeast, indicating potential reactivation of pre-existing faults. Our relocation results with unprecedented resolution indicate that the Weiyuan earthquakes were most likely induced by fracking through pore pressure diffusion.

KEYWORDS : induced earthquake, dense array

Sr No: 576

Slow slip-driven seismicity triggered by the water-reservoir impoundment

CORRESPONDING & PRESENTING AUTHOR:

Beata Orleckasikora, Institute of Geophysics Polish Academy of Sciences, Poland

Lukasz Rudzinski, Institute of Geophysics PAS, Poland

Grzegorz Lizurek, Institute of Geophysics PAS, Poland

Dorota Olszewska, Institute of Geophysics PAS, Poland

Taghi Shirzad, Institute of Geophysics PAS, Poland

One of the most important and widely-used renewable sources of energy is hydroelectric energy production by the usage of Water Reservoirs Impoundments (WRI). WRI may trigger strong earthquakes under favorable geological conditions. Hence, the socio-economic impact of reservoir-triggered seismicity is very significant. Although many studies indicate the relations between the pore pressure changes due to WRI and the observed seismicity, there is very rare to find the hydromechanical models explaining the observed processes. Here we investigate the role of hydromechanical interactions during the fault deformation to understand earthquake swarm's bursts under the pore pressure changes load due to WRI. As a natural laboratory, we selected the reservoir in Song Tranh 2 in Vietnam. Because the analyzed triggered seismicity has the swarm character, our work contributes to the further investigations of the physical mechanisms responsible for earthquake swarms and their relation to slow slip. We conclude that the small high-frequency seismic swarms accompanying WRI are driven by slow slip along the fault. They occur due to the fault temperature-controlled frictional heterogeneity. -They are the effect of slip acceleration on the seismic radiation level. The nucleating fronts expand the nucleation regime and may transition to stronger earthquakes. These results provide insights into the physical mechanisms of the seismic process triggering by WRI which may have implications in assessing the seismic hazard associated with this energy production technology.

Sr No: 577

SYMPOSIUM : **S3 CoSOI & CoESM Anthropogenic seismicity**

Challenges in discrimination between natural and anthropogenic seismicity in the South West Carpathians Bend, an active deformation area in Romania

CORRESPONDING & PRESENTING AUTHOR:

Raluca Dinescu, University of Bucharest, Romania

Mihaela Popa, National Institute for Earth Physics, Romania

Felix Borleanu, National Institute for Earth Physics, Romania

Daniela Ghica, National Institute for Earth Physics, Romania

Ioan Munteanu, University of Bucharest, Romania

Natalia Poaiata, National Institute for Earth Physics, Romania

Andreea Chircea, National Institute for Earth Physics, Romania

The South West Carpathians Bend region is characterized by shallow seismicity with moderate size earthquakes (M < 6) and a polikinetic character, highlighting significant deformation processes. The recent deformation in the region is proved by sedimentary basins bordered by intra-crustal faults. The origin and evolution of these basins is related to the N-ward tectonic transport of the Carpathian Orogen during the Paleogene-Quaternary, in the present position. With the recent development of the Romanian Seismic Network, the number of events in the Romanian earthquake catalog (ROMPLUS) shows an increasing trend and a significantly lowered magnitude detection threshold (ML~1), which led to the contamination with anthropogenic events. To increase the accuracy of seismic hazard analyses and for a better definition of the seismic activity within the study region, we put in place a methodology for identifying and removing the anthropogenic events generated by the various quarry explorations and recorded by the ROMPLUS catalog between 2015 and 2020. To discard these events, we applied modern discrimination approaches based on statistics and spectral analyses in addition to waveform cross-correlation techniques. Our results revealed a good capacity (above 85%) to differentiate between the natural and anthropogenic events that occurred in the study area. At the same time, some overlaps were also noted, indicating possible limitations of the methods for the events recorded with a low signal-to-noise ratio (SNR<5).

KEYWORDS : discrimination, seismic events, quarry blasts

Sr No: 578

Reactivations of a fault zone due to persistent seismicity in and around the Koyna-Warna area, Maharashtra, India

CORRESPONDING & PRESENTING AUTHOR:

Surajit Misra, Gauhati University, India

Manas Goswami, Gauhati University, India

Deepjyoti Goswami, Ministry of Earth Sciences, Government of India, India

The Koyna-Warna region is located in the Deccan Volcanic Province in the state of Maharashtra, India. The area has been experiencing persistent seismicity since the impoundment of the Koyna dam reservoir in 1962. The 1967 M6.3 Koyna earthquake and several thousand smaller earthquakes have hypocentres below the Deccan flood basalt pile, within the depth range of 2-10 km, and restricted over an area of ~20km x 30km. Several scientific drilling activities carried out in the study area reveal that (1) the Deccan basaltic pile has a maximum thickness of 1251 meters, and (2) the flood basalts are underlain by cratonic basement granitoid. As the hypocenters are located within the basement granitoids, deformation features preserved in them merits thorough investigations in order to understand the geological control on the seismicity of the area.

This study involves examination of physical and microstructural features of the fault zone rocks which were collected from the basement granitoids. Microstructures preserved in the rocks indicate presence of strained quartz grains, whereas, feldspars are unstrained and highly altered. Intensely fractured rocks are found at places which are either cohesive or incohesive in nature. Multiple fracture sets are found within the fault zone rocks, which are mostly filled with secondary ferruginous, siliceous, opaque and carbonate precipitations. Occurrence of cataclasites, fault breccias, fault gouge, fractures, geochemical alteration and secondary precipitations in the basement granitoid is indicative of presence of a pre-existing fault zone in the study area that has been reactivated after impoundment of the Shivajisagar water reservoir.

KEYWORDS : Koyna fault zone reactivation, brittle deformation, secondary precipitation

Sr No: 579

SEISMIC RISK – Mitigation of induced seismic risk in urban environments – evaluates induced seismic risk in urban areas of low seismicity intraplate areas

CORRESPONDING & PRESENTING AUTHOR:

Annakaisa Korja, University of Helsinki, Finland

SEISMIC RISK Working Group, University of Helsinki, Finland

Abstract : Deep geothermal energy has huge potential as environmental friendly district heat source in urban cities. A drawback is that geothermal systems can induce earthquakes that pose a previously non-existing seismic risk to the surroundings. A new project SEISMIC RISK – Mitigation of induced seismic risk in urban environments https://www2.helsinki.fi/en/projects/seismic-risk focuses on, how to evaluate, mitigate and communicate seismic hazard and risk in an urban environment in Finland? The key to risk management is in how well the process is understood and governed? This applies also to risks posed by
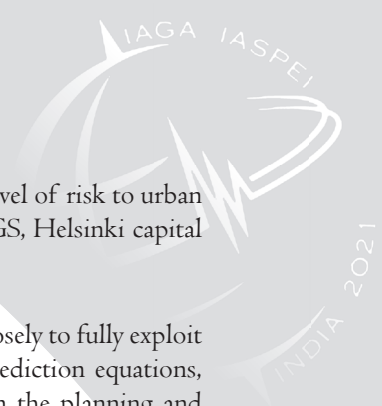
induced seismicity from enhanced geothermal system (EGS). To better understand the level of risk to urban societies, interdisciplinary data sets will be collected and modelled around Otaniemi EGS, Helsinki capital area.

SEISMIC RISK is an interdisciplinary project, where several expert groups collaborate closely to fully exploit their expertise. The project's scientific results: seismic hazard maps, ground-motion prediction equations, 3D tomographic and geological models of the capital area, surveys and interviews on the planning and regulating processes, are used to assess induced seismic risk. The risk is mitigated by evaluating soil and bedrock properties for urban planning and construction; outlining tremor and noise sensitive areas; defining new guidelines on construction of critical infrastructure; and identifying less risky areas for deep geothermal plants. The project will produce guidelines and educational material on the concepts of seismic hazard and risk, induced seismicity and its hazard and risk to urban societies for regulators, decision makers, politicians and citizens.

KEYWORDS : induced seismicity, intraplate, urban

Sr No: 580

SYMPOSIUM : **S3 CoSOI & CoESM Anthropogenic seismicity**

Assessment of potential earthquake for Koyna-Warna seismic zone and strong ground motion simulation

CORRESPONDING & PRESENTING AUTHOR:

Anup Kumar Sutar, Borehole Geophysics Research Laboratory, India
Sukanta Roy, Borehole Geophysics Research Laboratory, India
V. M. Tiwari, National Geophysical Research Institute, India

The Koyna-Warna region in western India is well known around the world for recurrent reservoir-triggered seismicity. Two distinct seismic zones, namely, Koyna Seismic Zone (KSZ) and Warna Seismic Zone (WSZ) are identified based on various geophysical studies. To understand the seismic potential of the region, we estimated the strain budget by analysing the published GPS velocities and earthquake catalogue of the region. Our analysis suggests, the rate of strain accumulation in the KSZ ($2.55E+16$ Nm/y) is estimated to be ~11 times larger when compared to the WSZ ($2.29E+15$ Nm/y). However, KSZ releases only ~20% of the accumulated energy per year, whereas, WSZ releases most of the accumulated energy in the form of earthquakes. A density model constructed from Airborne Gravity Gradiometry data as well as borehole samples test suggest, relatively higher average density and cohesive strength for KSZ compared to WSZ. Strain budget of the region suggests that the earthquake activity in KSZ may continue for a longer time whereas it may diminish in the WSZ in future. Gross strain estimates suggest, KSZ has accumulated enough strain post the 1967 M6.3 Koyna earthquake to generate an event of Mw5.8, provided the accumulated strain is released in a single event. The seismic hazard scenario in terms of peak ground acceleration (PGA) due to a potential Mw5.8 event is estimated using the stochastic simulation technique. The simulated PGA at a radial distance of ~40km from the source zone is estimated to range between 0.08 and 0.26g with an expected intensity of V-VII.

KEYWORDS : geodetic moment rate, energy release rate, peak ground acceleration

Sr No: 581

Stress Field Variations and Earthquake Source Mechanisms Associated with Wastewater Induced Seismicity in Southern Kansas, USA

CORRESPONDING & PRESENTING AUTHOR:

Amandine Amemoutou, Helmholtz Centre Potsdam GFZ German Research Centre for Geosciences, Germany

Patricia Martinez Garzon, Helmholtz Centre Potsdam GFZ German Research Centre for Geosciences, Germany

Grzegorz Kwiatek, Helmholtz Centre Potsdam GFZ German Research Centre for Geosciences, Germany

Marco Bohnhoff, Helmholtz Centre Potsdam GFZ German Research Centre for Geosciences, Germany

Justin Rubinstein, United States Geological Survey, USA

During the last decade, a surge of seismicity was observed in the conterminous USA and linked to the injection of large amounts of wastewater from oil and gas production in unconventional hydrocarbon reservoirs. We focused our study on seismicity from 2014 to 2016 in the area of elevated seismicity in southern Kansas near Harper and calculated 549 moment tensors of induced earthquakes with a moment magnitude Mw ≤ 4.9 to investigate their source mechanisms and their relation to injection activity. Our results showed approximately 17% of the analyzed events had significant non-double couple components, and these events mostly occurred near the two largest local earthquakes (the 2014 Mw 4.9 Milan and 2014 Mw 4.3 Harper earthquakes). We used these moment tensor solutions to invert for the stress field orientation and determined that most of the region lies within a transtensional stress regime, with a maximum horizontal stress σHmax trending N75°E. Moreover, in the epicentral area of the Mw 4.9 Milan earthquake, the σHmax trend is rotated to about S80°E. Locally, two areas display a change in the stress field orientation with depth, from transtensional above 5.5 km depth to strike-slip deeper in the basement. Finally by relating the resolved fault geometries to the obtained local stress field orientation, we find that most of the activated fault planes were optimally oriented to the current stress field and thus small stress perturbations caused by the water injection could lead to failure.

KEYWORDS : inversion, stress, wastewater

Sr No: 582

Influence of a gap in the filling of reservoir on seismic activity and hazard parameters in Song Tranh2 reservoir vicinity (Vietnam)

CORRESPONDING & PRESENTING AUTHOR:

Grzegorz Lizurek, Institute of Geophysics, Polish Academy of Sciences, Poland

Konstantinos Leptokaropoulos, University of Southampton, UK

Jan Wiszniowski, Institute of Geophysics, Polish Academy of Sciences, Poland

Nguyen Van Giang, Vietnamese Academy of Science and Technology, Vietnam

Izabela Nowaczyska, Institute of Geophysics, Polish Academy of Sciences, Poland

Beata Plesiewicz, Institute of Geophysics, Polish Academy of Sciences, Poland

Dinh Quoc Van, Vietnamese Academy of Science and Technology, Vietnam

Song Tranh 2 (STR2) is an artificial water reservoir located in Central Vietnam. High seismic activity has been observed in this area since the reservoir was first filled in 2011. The relation between water level and seismic activity in the area is complex. Previous studies have shown that ongoing STR2 seismic activity is an example of the delayed response type of Reservoir Triggered Seismicity, but the first phase of the activity directly after impoundment has been deemed a rapid response type. There were three stages of the reservoir filling periods: first, a period of initial impoundment, hereinafter referred to as pre-gap period (from 05/01/2011 to 10/06/2012), then a gap period (from 10/06/2012 to 31/08/2013) where reservoir impoundment stopped and water was drained to minimum exploitation level, and a third post-gap period (from 31/08/2013 to 19/06/2017). In this work, we prove that the gap in the reservoir filling results to a 2-fold rise of seismicity rate. The re-filling of the reservoir results to a drop of activity rate, roughly equal to the pre-gap period, accompanied by a significant increase of b-value. As a consequence, after the gap the exceedance probability is significantly lower in comparison to pre-gap and gap periods. The response of activity and its delay with respect to water level changes suggest that the main triggering factor is pore pressure change due to the significant water level changes observed. The findings indicate that water load and related pore pressure changes considerably influence seismic activity in this area.

KEYWORDS : reservoir triggered seismicity, water reservoir, triggered seismicity

Sr No: 583

SYMPOSIUM : **S3 CoSOI & CoESM Anthropogenic seismicity**

Insights into reservoir triggered seismicity at Koyna, India from scientific drilling investigations

CORRESPONDING & PRESENTING AUTHOR:

Deepjyoti Goswami, Ministry of Earth Sciences, India

Sukanta Roy, Ministry of Earth Sciences, India

Vyasulu V. Akkiraju, Ministry of Earth Sciences, India

The Koyna seismogenic zone in Maharashtra, India has experienced persistent seismicity for more than five decades, starting soon after the impoundment of the Koyna dam in 1962. The largest triggered earthquake of M~6.3 took place in 1967, followed by about 20 earthquakes of M5-5.9, ~200 of M≥3.5 and thousands of smaller events. Scientific drilling of a 3 km deep borehole KFD1 passing through 1247 m thick Deccan Traps and continuing1767 m in the granitic basement in one of the active seismic clusters, provided an unprecedented opportunity to determine the physical and mechanical properties of subsurface rock formation, delineate fault damage zones, and estimate stress and temperature regime in the Koyna seismogenic zone at depth. Various geophysical logs were acquired in the borehole and hydraulic fracturing tests for determining stress regime were carried out at eight depths in the crystalline basement. Salient results are as follows. (i) Seven major zones of anomalous physical and mechanical properties are delineated by geophysical data below 2100 m depth. These zones are also characterised by stress-induced shear wave velocity anisotropy. (ii) The majority of the anomalous zones are associated with breakout rotations, which are strongly suggestive of fault damage zones. (iii) The stress-depth profiles determined from hydrofrac tests indicate a strike-slip to normal faulting regime. (iv) Consistent strike azimuths of steeply dipping fractures with SHmax orientation indicate possibilities for both strike-slip and normal faulting. (v) In critically stressed Koyna region, earthquake may trigger in the favourably orientated faults/fractures with a small modification in stress regime.

KEYWORDS : reservoir triggered seismicity, rock properties, stress regime

Sr No: 584

An evaluation of surface and subsurface fracture characteristics to assess their role in water percolation in Koyna-Warna region of reservoir triggered seismicity, India

CORRESPONDING & PRESENTING AUTHOR:

Kusumita Arora, CSIR-NGRI, India

Srinu Yadavally, CSIR-NGRI, India

Gopinadh Dhulipudi, CSIR-NGRI, India

Adrien Selles, BRGM, India, France

In the Koyna-Warna seismic region, airborne LiDAR survey has produced a sub-meter scale digital elevation model (DEM), while acoustic televiewer imaging in boreholes has generated detailed geometry of structural features in each location. Combining the two, provides a view of the fracture network, which are observed on surface and observed in boreholes. The surface morphology is characterized by regional fracture zones, which appear as lineaments, on the one hand and more localized and scattered fractures on the other, which align with drainage patterns and geomorphological valleys. The layouts of such features are compared with patterns of drilling induced and natural fractures detected in boreholes located on the Deccan Plateau and adjoining Konkan plains, both from basalt and underlying basement formations. It is found that the dominant geometries on surface and boreholes are aligned. Deviations are also noted, which vary at different locations. We have attempted to associate the fracture parameters with seismicity patterns.

KEYWORDS : geomorphology, fracture pattern, triggered seismicity

Sr No: 585

59 Years of Continued Reservoir Triggered Seismicity (RTS) at Koyna, India

CORRESPONDING & PRESENTING AUTHOR:

Harsh Gupta, National Geophysical Research Institute, India

RTS began in the vicinity of the Shivaji Sagar Lake, soon after its impoundment by creating the Koyna Dam in 1962. The largest scientifically accepted RTS event of M 6.3 occurred at Koyna on 10 December 1967. Over the years, 22 M ~5 and several thousand smaller earthquakes have occurred in the region. Detailed studies of RTS sequences carried out in the 1970s led to delineating common characteristics of RTS events that also help in differentiating RTS sequences from normal earthquake sequences. The mechanism of RTS is not well understood due to the lack of near field studies. Koyna was found to be the most suitable site for such investigations in detailed discussion meetings held during the International Continental Drilling Program (ICDP) supported workshop held in India in 2011. The suggested additional work to be carried out was undertaken from 2011 to 2014 and discussed in the second ICDP Workshop held in 2014. A 3 km deep Pilot Borehole was spudded in December 2016 and completed in June 2017, followed by a post-operation ICDP workshop in October 2017. A few salient features of the work carried out in the last 59 years are presented.

KEYWORDS : reservoir triggered seismicity (RTS)

Detection of fault and fracture zones in a 3 km deep scientific borehole in the Koyna Seismogenic Zone, western India from chemical and noble gas isotope data and geophysical logs

Nagaraju Podugu, Ministry of Earth Sciences, India

Satrughna Mishra, NMDC, India

Thomas Wiersberg, GFZ German Research Centre for Geosciences, Germany

CORRESPONDING & PRESENTING AUTHOR:

Sukanta Roy, Ministry of Earth Sciences, India

The Koyna region has experienced recurrent reservoir-triggered seismicity (RTS) since the impoundment of Koyna dam in 1962. To investigate the genesis of RTS, a major programme involving scientific deep drilling and near-field observations is underway. A critical gap in understanding arises due to the relatively poor characterization of subsurface fault zone(s) and their spatial extent. In the wake of the 1967 M6.3 Koyna earthquake, a ~200 m wide and ~4 km long, NNE trending Donichawadi fissure zone was mapped between Nanel in the north and Kadoli in the south. The trend is consistent with the seismicity in the area during the past decades. To investigate further, in 2017, online gas monitoring, gas extraction and analyses was conducted during the course of drilling a 3 km deep borehole, ~5 km south of Kadoli. The study revealed anomalous formation gases CO_2, CH_4, H_2 and He, predominantly below 2100 m depth, with significant helium enhancement (4.6-7.6 ppmv above atmosphere). Fault damage zones delineated from geophysical well logs correspond with the zones of helium enhancement, indicating that the borehole punctured multiple fracture zones. The helium concentrations are remarkably consistent with those recorded over the surface fissures near Kadoli during 1996-97. $3He/4He$ ratios reveal that helium is a mixture of atmospheric and crustal radiogenic components with no mantle contribution. Thus, multiple lines of evidence suggest that the Donichawadi fissure zone is the surface manifestation of a crustal fault which extends southward from Kadoli and is permeable even after 50 years of the 1967 earthquake.

KEYWORDS : Koyna seismogenic zone, helium, fault damage zones

Unusual Seismic Activity in North-East British Columbia During Anthropogenic and Operational Quiescence: Characteristics, Causes and Consequences

CORRESPONDING & PRESENTING AUTHOR:

Rebecca O. Salvage, University of Calgary, Canada

David W. Eaton, University of Calgary, Canada

389 seismic events were detected from April to August 2020 within the Kiskatinaw area of British Columbia, encompassing a period of almost no hydraulic-fracturing operations due to a downturn in the economic market brought about by the COVID-19 pandemic. During this time period, observed seismicity had a maximum magnitude of ML1.2 but lacked temporal clustering that is often characteristic of hydraulic-

fracturing induced sequences. Hypocenters occurred within a corridor orientated NW-SE with focal depths close to the target Montney formation (<2.5 km). Based on the Gutenberg-Richter relationship, we estimate that a maximum of 21% of the detected events during lockdown may be attributable to natural seismicity, with a further 8% possibly due to dynamic triggering of seismicity from teleseismic events and 6% due to ongoing operations at a local waste-water disposal well. However, the remaining ~65% of events cannot be attributed to these primary activation process and have no obvious trigger (e.g. enhanced pressurization at the onset of seismicity). We deem this to be latent seismicity, which shows an unusually long delay following its activation processes. We can exclude direct pore-pressure diffusion and poroelastic phenomena as a cause of this seismicity, since there is no clear pattern of temporal or spatial migration, nor evidence of a fluid pressure diffusion front. Aseismic creep on weak surfaces such as faults, in response to tectonic stresses or from fault weakening, in addition to trapped elevated pore-pressures at depth could play a role in stress re-loading to sustain the observed unusual pattern of seismicity.

KEYWORDS : hydraulic fracturing, aseismic slip, British Columbia

Sr No: 588

SYMPOSIUM : **S3 CoSOI & CoESM Anthropogenic seismicity**

A seismic event three years after hydrofracturing in Wysin, Poland

CORRESPONDING & PRESENTING AUTHOR:

Stanislaw Lasocki, Institute of Geophysics PAS, Poland

Lukasz Rudzinski, Institute of Geophysics PAS, Poland

Antek K. Tokarski, Institute of Geological Sciences PAS, Poland

Beata Orlecka Sikora, Institute of Geophysics PAS, Poland

Shale gas hydrofracturing (HF) operations in Wysin, Poland were multidisciplinary monitored in the European Union SHEER project framework. These observations included precise monitoring of seismicity, carried on before, throughout, and after horizontal drilling and fracking. However, the seismic system recorded only two weak events, from which one only might link to technological activities. Three years after the end of all exploration activities in Wysin, on 15 June 2019, an M2.8 event occurred close to this HF site. The analysis of clast-fracturing in gravels indicates that the Pomerania region, where the Wysin site is, was visited by M5+ earthquakes even in the late Pleistocene. So faults in the area are expected to be pre-stressed. However, the return periods of the seismicity in this region are very long since there is no record in historical documents of an earthquake occurring there in the last 1000 years. In this connection, it is an extreme little probability that the space-time coincidence of the earthquake from 2019 and the HF activities occurred at random. On the contrary, this coincidence suggests a triggered origin of the studied seismic event. The event was located close enough to the previous HF activities to be triggered. However, the three-year delay time is much longer than the ever observed lag time for the earthquakes triggered by HF operations and makes this event exceptional.

KEYWORDS : hydrofracturing, triggering seismicity, delay time

S4 CoSOI Seismic scattering and absorption, ambient noise, and monitoring Earth's structure

CONVENERS: Hisashi Nakahara (Japan)

Ulrich Wegler (Germany)

Jayant N. Tripathi (India)

Seismic scattered waves or coda waves carry rich information on heterogeneities within the Earth. Amplitude information from coda waves has been used to estimate the spatial distribution and the frequency dependence of the strength of scattering attenuation and intrinsic absorption in the Earth. Recently, ambient noise cross-correlation has also been used to study seismic structure in the Earth thanks to the development of seismic interferometry. Time-lapse imaging or monitoring of the Earth has been conducted using tiny changes in phase information of cross-correlation functions of ambient noise and coda waves. Increasing the spatial and temporal resolutions of the imaging will help to understand the Earth's heterogeneities and dynamics. In this session, we would like to widely invite presentations related to theoretical and observational studies of attenuation, coda waves, ambient noise, and their applications to the imaging and monitoring Earth's heterogeneous structure.

Sr No: 589

Source strength and distribution of microseism energy inferred from ambient noise recorded by the Gujarat seismic network, India

CORRESPONDING & PRESENTING AUTHOR:

Monika Bhatia, Institute of Seismological Research, India

Rajesh Rekapalli, National Geophysical Research Institute (NGRI), , India

M. Ravi Kumar, National Geophysical Research Institute (NGRI), , India

Mohit Agrawal, Indian School of Mines (IITISM) , India

Seismic Ambient Noise that primarily originates from Oceans, Rivers and anthropogenic activities, contains information related to the source processes as well as the travel path. Seismologists widely use this noise to delineate the crustal structure and its variation beyond the limited resolution offered by the earthquake waveforms. In this study, we analyze the continuous ambient noise data recorded by the Gujarat Seismic Network (GSNet) during 2015 to decipher the spatial temporal variation in the primary and secondary microseism energies and their source directionality. The Probabilistic Power Spectral Densities (PPSD) and single station polarization techniques are used for this purpose. Overall, the noise levels at frequencies 0.01 to 10Hz are within the limits of global new high and low noise models. The results from PPSD suggest that the ambient noise level at short and long periods conforms with the global high in the coastal regions of the southern part of Gujarat. However, the noise levels in the northern part match with the global mean. The results suggest consistent high noise levels during the monsoon and post monsoon period. The azimuths at individual stations estimated using polarization technique suggest that the Indian Ocean and Arabian Sea are the prominent sources of ambient noise in the Gujarat region. A seasonal variation can also be discerned from the polarized signal. In addition, spatial averages of the ambient noise levels in the primary and secondary microseism bands suggest possible association of ambient noise levels with the subsurface characteristics and regional faults in the study area.

KEYWORDS : ambient noise, microseism, noise polarization

Sr No: 590

Adjoint tomography with full envelope for scattering and intrinsic attenuation

CORRESPONDING & PRESENTING AUTHOR:

Tuo Zhang, GFZ German Research Centre for Geosciences, Germany

Christoph Sens Schoenfelder, GFZ German Research Centre for Geosciences, Germany

To investigate the small-scale heterogeneity of the medium below resolution limits of the waveform tomography, the envelopes of high-frequency seismic waves have been used to derive a statistical description. We present a mathematical framework for the full envelope inversion that is based on a forward simulation of seismogram envelopes and an adjoint (backward) simulation of the envelope misfit. Our approach is based on the Radiative Transfer Equation. The forward problem is solved by modelling the 2-D multiple
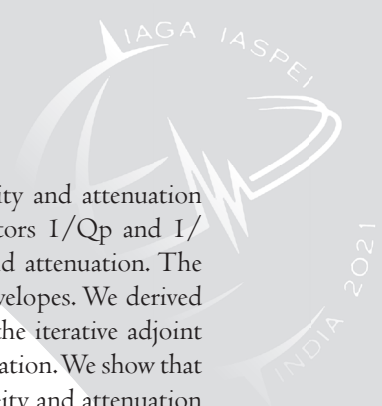
nonisotropic scattering in a random elastic medium with spatially variable heterogeneity and attenuation using the Monte-Carlo method. The fluctuation strength ⬜ and intrinsic quality factors $1/Q_p$ and $1/Q_s$ in the random medium are used to describe the spatial variability of scattering and attenuation. The misfit function is defined as the differences between the full observed and modelled envelopes. We derived the sensitivity kernels corresponding to this misfit function that is minimized during the iterative adjoint inversion. We have applied this algorithm in some numerical tests in the acoustic approximation. We show that it is possible in a rigorous way to image the spatial distribution of small scale heterogeneity and attenuation separately using seismogram envelopes. Our analysis shows that the relative importance of scattering and attenuation anomalies need to be considered when the model resolution is assessed. The inversions confirm, that the early coda is important for imaging the distribution of heterogeneity while later coda waves are more sensitive to intrinsic attenuation.

KEYWORDS : adjoint tomography, scattering and absorption inversion, radiative transfer theory

Sr No: 591

Formulation of the SPAC method for strain, rotation, and tilt

Takeshi Nishimura, Tohoku University, Japan

CORRESPONDING & PRESENTING AUTHOR:
Hisashi Nakahara, Tohoku University, Japan
Kentaro Emoto, Tohoku University, Japan

Spatial auto-correlation (SPAC) method has been applied to ambient seismic noise measured by arrays of translational seismometers for inverting phase-velocity dispersion curves of Rayleigh or Love waves for shallow S-wave velocity structure. Recently, it is becoming possible to observe wave spatial gradients such as strain, rotation, and tilt owing to the development of dense seismic networks and improving measurement technologies. Therefore, in this study, we extend the formulation of the SPAC method to strain, rotation, and tilt. We derive analytical expressions of cross spectra and coherence of the strain, rotation, and tilt components that are measured on the free surface. According to the results, both Rayleigh and Love waves contribute to most components of strains. The exceptions are areal strain and the vertical axial strain on the free surface that are affected by only Rayleigh waves. Only Rayleigh wave contributes to the tilts and rotations around the horizontal axes on the free surface, too. On the other hand, only Love wave contributes to the rotation around the vertical axis. Therefore, different kinds of the wave spatial gradients are helpful to separate Rayleigh and Love waves correctly. For practical applications, the analytical expression for the radial axial strain component will be applied directly to distributed acoustic sensing (DAS) data measured with straight sections of a fiber optic cable. Dense observations of rotation and tilt may still be difficult to carry out at present. However, analytical formulations in this study will be useful for the future.

KEYWORDS : SPAC method, strain, rotation

Sr No: 592

Heterogeneity of active volcanoes in Japan as inferred from the peak ratio analysis of scattered teleseismic P waves

CORRESPONDING & PRESENTING AUTHOR:

Gugi Ganefianto, Tohoku University, Japan

Hisashi Nakahara, Tohoku University, Japan

Takeshi Nishimura, Tohoku University, Japan

Small-scale medium heterogeneities in the subsurface can scatter seismic waves. One stochastic approach to quantify the scattering strength and the small-scale medium heterogeneity is the peak-ratio estimation that utilises the peak amplitude ratio between the transverse envelope and the total envelope of teleseismic P-wave records.

Analysis of the Hi-net seismometer network data in Japan (Nishimura, 2012) has shown that stations around tectonically active regions such as active faults and volcanoes show higher peak-ratios. However, Hi-net stations are not actually located on the volcanic edifice. In this study, we more specifically examined the peak-ratio at 47 volcanoes in Japan using seismometers maintained by the Japan Meteorological Agency (JMA).

For the 0.5-1, 1-2, 2-4, 4-8 Hz bands, peak-ratios at the JMA stations range from approximately 0.16-0.44, 0.22-0.52, 0.24-0.54, 0.30-0.60, respectively. The results are approximately twice as large as those of the Hi-net data. From the t-test, we confirmed that these differences are statistically significant at the 99.9% confidence level. We also investigated the differences between the JMA surface and borehole stations. The former peak-ratios are 22%, 49%, 64%, and 26% larger than the latter at the four frequency bands, respectively. The differences are also statistically significant at the 99% confidence level. We speculate that besides the possible intensification of small-scale heterogeneities at shallow depths, scattering can also be induced by the free-surface effect along with the topographic irregularities.

KEYWORDS :   Heterogeneity, Seismic-Scattering, Volcanoes

Sr No: 593

Ambient noise tomography applied to a passive seismic data set from Cachar fold belt, lower Assam, northeast India

CORRESPONDING & PRESENTING AUTHOR:

Bharath Shekar, Indian Institute of Technology Bombay, India

Gollapally Mohan, Indian Institute of Technology Bombay, India

Sunil Kumar Singh, Oil and Natural Gas Corporation Limited, India

We apply ambient noise tomography to a passive seismic dataset from Cachar fold-belt in lower Assam, northeast India. The Cachar region is a currently active producer of hydrocarbons with several producing oil and gas wells. Active seismic data from the region was of poor quality and a passive seismic survey was carried out by Oil and Natural Gas Corporation Limited to image the broad subsurface structures. A network of 65 wideband seismometers covering an area of about 2400 sq km continuously recorded data from February to November, 2011. The data were cross correlated with geometrical normalisation and phase-weighted stacking was performed to estimate noise cross correlation functions in a frequency band of 0.2 to 0.5 Hz for all possible receiver pairs. Frequency-time analysis was performed on the noise cross correlation functions to estimate group arrival times between pairs of stations. The group arrival times were inverted for group velocity maps using eikonal tomography. Metropolis algorithm was used to invert the group velocity maps as a function of frequency for the S-wave velocity distribution. The S-wave velocities are correlated with the structural features in the region, with high and low velocities corresponding to tight anticlines and broad synclines, respectively. P-wave stacking velocity cubes and post stack time migrated sections from a part of the region also support the structural interpretation from ambient noise tomography. Ambient noise tomography can serve as a useful tool for reservoir characterization and can help in the planning of targeted active seismic surveys.

KEYWORDS :   ambient noise, interferometry, tomography

Sr No: 594

SYMPOSIUM :   **S4 CoSOI Seismic scattering and absorption, ambient noise, and monitoring Earth's structure**

Lg wave attenuation characteristics for the Indian Shield

PRESENTING AUTHOR:

Reshma K. S., CSIR-NGRI, India

CORRESPONDING AUTHOR:

Prakash Kumar, CSIR-NGRI, India

Bhaskar Illa, CSIR-NGRI, India

Srinagesh D., CSIR-NGRI, India

Lg waves are defined as the multiply reflected shear waves or higher mode surface waves, and are prominent phase in the seismogram at a regional distance and have an average velocity of 3.5 Km/s. Insensitivity of Lg for source characteristics makes it an ideal tool to study large-scale crustal variation such as attenuation estimation. In this study, lateral variation of Q (Quality factor) and its ε dependency for 1 Hz frequency is estimated for the Indian Shield using Lg waves using Two-station method. Here we collected data from 238 earthquakes, recorded in 117 seismometers deployed over the Indian Shield, which are maintained by CSIR-NGRI, NCS and Geoscope. 2421 waveforms obtained after the pre-processing, is inverted to estimate Qo. A checkerboard test is being performed to ensure the resolution of our image. The results show that Lg-Q varies from the range ~50-650 with its frequency-dependent parameter ε of 0.6 as average. The values obtained for the cratonic region, sedimentary region and rift valleys where most of the Indian shield lies, is in broad agreement with the values estimated for other similar tectonic regimes globally by various researchers. Also, we have compared the Lg-Q values with available crustal thickness, heat flow and Vp/Vs ratio for the Indian shield. We suggest that the attenuation scenario in the Indian crust is mainly controlled by both composition and temperature.

KEYWORDS :   attenuation, lg waves, two-station method

Sr No: 595

Two decades continuous monitoring of seismic velocity change at Parkfield to identify its origins

CORRESPONDING & PRESENTING AUTHOR:

Kurama Okubo, National Research Institute for Earth Science and Disaster Resilience, Japan

Brent Delbridge, Los Alamos National Laboratory, USA

Marine Denolle, University of Washington, USA

We study the long-term evolution of the San Andreas Fault near the rupture area of the Parkfield EQ and infer changes in the fault zone material properties using continuous monitoring of seismic velocity change (dv/v). The observed temporal variations are found to result from both tectonic and environmental contributions. Our results are consistent with previous studies that found a co-seismic drop in dv/v at the time of the 2004 Parkfield earthquake followed by a logarithmic post-seismic recovery. We further evaluate the recent variation in dv/v to investigate if the recovery follows the logarithmic healing model. We process nearly two decades (2002-2020) of ambient seismic noise recorded by 3-components seismometers from the Berkeley Seismological Laboratory's High-Resolution Seismic Network. We employ several strategies to ensure that the stacked cross-correlation functions are stable and of high quality. We also perform case studies to evaluate the effects of work flows on the dv/v measurement, which includes removal of transient signal, temporal/spectral normalization, methodology of dv/v measurement (e.g. stretching vs mwcs), and the choice of reference period. The combinations of data workflow in estimating the time series of dv/v indicate the robustness of the dv/v time series. We explore in detail the various characteristics of the dv/v time series: co-seismic drop, logarithmic recovery and linear trends. We discuss the potential origins of these variations in noise source perturbation due to the varied tremor rate observed in Parkfield, and strain change due to quasi-static deformation at depth.

Sr No: 596

1 D velocity model for Delhi and surrounding region using Local event observed by Dense Seismic Network

CORRESPONDING & PRESENTING AUTHOR:

RAJAT PASRICHA, National Centre for Seismology (NCS), Ministry of Earth Sciences (MoES), New Delhi, India

Sanjay K Prajapati, National Centre for Seismology (NCS), Ministry of Earth Sciences (MoES), New Delhi, India

Shankar Pal, National Centre for Seismology (NCS), Ministry of Earth Sciences (MoES), New Delhi, India

High-precision earthquake location is of importance in a seismically active region like Delhi where seismic database is prerequisites for tectonic interpretation and seismic hazard assessment. We have derived a P– wave 1D velocity model for Delhi region which may help in constraining earthquake locations and can be used as initial reference model for 3D seismic tomography. The inversion is carried out using 140

well locatable events together with 620 P wave observations and 443 S wave observations during 2000-2018 provided by national seismological network maintained and operated by National Seismological Centre (NCS). The program VELEST has been used to constrain final velocity model using P and S phases of the events located by a local network of 17 stations deployed in and around Delhi. VELEST uses an algorithm which is based on damp least-squares method which estimates the 1D velocity model along with revised hypocenter co-ordinates and station corrections. We have used initial velocity model published by IASP91 (Kennett et al, 1991) as a priori 1D velocity models to arrive at the final model of Delhi region. The P wave velocity ranges from 5 km/s to 8 km/s to a depth of 70 km. The Moho is located at around 38 km from the surface.

KEYWORDS : seismic velocity, earthquake, hypocenter, P-wave

Sr No: 597

Heterogeneities of short-period S wave attenuation field in lithosphere of the Indian plate, Himalaya and South Tibet and their relation to seismicity

CORRESPONDING & PRESENTING AUTHOR:

Yuri Kopnichev, Schmidt Institute of Physics of the Earth of the Russian Academy of Sciences, Russia

Inna Sokolova, Institute of Geophysical Research NNC RK, Kazakhstan

We have been studying ?haracteristics of the attenuation field in the lithosphere of the South Asia. Recordings of local earthquakes, obtained by station NIL were analyzed. We considered ratios of maximum amplitudes of Sn and Pn waves within the distance range of ~300-1900 km. A total number of ~200 earthquake seismograms were processed. It was established that as a whole lower attenuation is observed in the uppermost mantle under the Indian Plate (for meridian profile oriented in direction to the source zone of large Bhuj earthquake of 26/01/2001 (Mw=7.7)). Considerably higher attenuation corresponds to the regions of the Himalaya and especially South Tibet. It was shown that increased attenuation is observed in the source zone of the recent large Nepal earthquake of 25/04/2015 (Mw=7.8). At the same time lower and intermediate attenuation takes place in the source zones of large and great interplate events (Mw=7.0-8.1), occurred in the Himalaya region in 1897-1930. From the other hand, essentially lowered attenuation corresponds to the source zone of the intraplate Bhuj earthquake. New results agree with earlier obtained data, which testify to mantle fluids concentration below source zones prior to large interplate earthquakes, and also to fluids ascending into the earth's crust after these events. Zones of high attenuation were picked out in the regions of West Himalaya and central Pakistan, where large earthquakes did not occur for a long time. It is supposed that processes of large seismic events preparation can proceed there.

KEYWORDS : S-wave attenuation field, mantle fluids, Himalaya

Sr No: 598

Mapping S wave attenuation in the region of the North Tien Shan using seismogram coda for local earthquakes and quarry blasts

CORRESPONDING & PRESENTING AUTHOR:

Yuri Kopnichev, Schmidt Institute of Physics of the Earth of the Russian Academy of Sciences, Russia

Inna Sokolova, Institute of Geophysical Research NNC RK, Kazakhstan

We have been mapping short-period shear wave attenuation field in the lithosphere of the North Tien Shan. We analyzed seismograms of local earthquakes and quarry blasts, recorded by six stations installed in the area of Almaty city and its close. Characteristics of common S coda envelopes for various sectors relative to seismic stations are described. Sections of the attenuation field for the stations considered are constructed. Characteristics of the attenuation field to the north of Zaili deep fault zone (at the southern outskirt of Kazakh platform) and to the south of it (in mountain areas) are compared. This allows us to make conclusions on difference of deep-seated fluid content in these areas. We created maps of the attenuation field in various depth ranges and at different azimuths for all stations. We found zones of highest attenuation, where processes of preparation for large earthquake could occur.

KEYWORDS : S-waves attenuation field sections, large earthquakes, deep-seated fluids

Sr No: 599

Apparent-stress scaling of the 2016 Kumamoto earthquake sequence in SW Japan from coda-derived source spectra

CORRESPONDING & PRESENTING AUTHOR:

N Subhadra, CSIR-National Geophysical Research Institute, India

S Padhy, IIT-Roorkee, India

P Martin Mai, KAUST, Saudi Arabia

G Rengin, LLNL, USA

Mayeda K, LLNL, USA

We study the source scaling relation for the 2016 Kumamoto foreshock-mainshock-aftershock sequence in SW Japan by analysing 171 local-to-regional earthquakes ($3.6 < Mw < 7.1$) recorded by 14 F-net broadband stations deployed in Kyushu Island. We employ the coda- source spectral method developed by Mayeda et al. (2003) that uses empirical corrections to obtain stable moment-rate spectra. The Coda Calibration Tool, a free Java-based tool that is available via GitHub, was used to estimate dynamic source parameters such as moment-magnitude, corner frequency, radiated seismic energy, and apparent stress. We compare apparent stress scaling results from prior Japanese sequences and examine the difference in scaling relationship between foreshocks and aftershocks using the results obtained. The likely increase in energy-to-moment ratio in this sequence, and hence departure from self-similarity, provides constraints in accurately predicting the ground motion from future large earthquakes in the region.

KEYWORDS : 2016 Kumamoto earthquake, source process, source spectra, energy-moment scaling, self-similarity
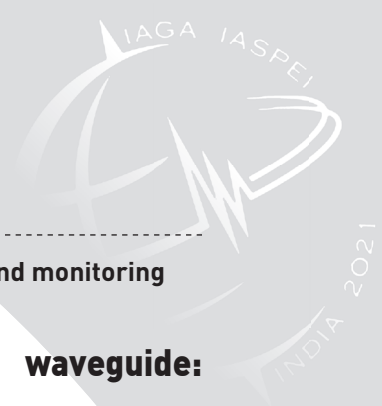
Sr No: 600

Revisiting multiple-scattering principles in a crustal waveguide: equipartition, depolarization and coda normalization

CORRESPONDING & PRESENTING AUTHOR:

Gregoire Heller, Institut de Recherche en Astrophysique et Planétologie, France

Ludovic Margerin, Institut de Recherche en Astrophysique et Planétologie, France

The goal of this study is to clarify the complex interplay between volume and surface scattering in crustal waveguides and how it impacts the crustal energy propagation. To carry out this task, we have incorporated a rigorous description of wave polarization in the context of Monte-Carlo simulations of the multiple-scattering process, by introducing a 5-dimensional Stokes vector.

In our study, we examine key multiple-scattering principles: (1) equipartition (2) depolarization, (3) coda normalization. In full elastic space, (1) predicts isotropic energy fluxes and a ratio between P- and S-wave energies equal to $\beta^3/(2\alpha^3)$; (2) predicts that energy of SV- and SH-waves are equal; (3) stipulates that the energy in the long lapse-time coda depends only on the source size.

Through extensive parametric studies, we find that, in the presence of interfaces, the isotropy of the wavefield is systematically broken and the energy ratios are shifted to the detriment of P-waves and in favor of SV-waves. This implies that a residual shear-wave polarization is preserved in the waveguide. We also show that the source mechanism leaves significant imprint on the Lg coda excitation, especially when comparing an explosion and a shear dislocation with equal magnitudes. Equipartition, depolarization and coda normalization principles are violated especially if the effects of crustal reflections are stronger than scattering by random inhomogeneities. While these principles remain fundamental guides to our understanding of the coda, their application requires a good a priori knowledge of the attenuation properties of the crust.

KEYWORDS : coda, scattering, polarized waves

Sr No: 601

Estimation of the shallow small-scale heterogeneity by using the dense DAS data

CORRESPONDING & PRESENTING AUTHOR:

Kentaro Emoto, Tohoku University, Japan

Hisashi Nakahara, Tohoku University, Japan

Takeshi Nishimura, Tohoku University, Japan

Mare Yamamoto, Tohoku University, Japan

Kodai Sagae, Tohoku University, Japan

Gugi Ganefianto, Tohoku University, Japan

Yabu Katsuhiro, Tohoku University, Japan

Recently, the distributed acoustic sensing (DAS) is spread quickly in seismology. The DAS brings a significant improvement in the spatial density of measurement points. These spatially dense data allow us to investigate the small-scale heterogeneity at shallow depths. We conducted DAS observation and collected the strain rate along the national route 4 in Miyagi Prefecture, Japan for about 1 month in 2020. The length of the fiber optic cable is 49 km and the channel interval is a 5 m. Due to the heavy traffic, the vehicle signal is dominant over whole channels. We divide channels into segments with 200 channels. We calculate the cross-correlation functions (CCFs) of 5-minute noise record including the traffic signal in each segment. Then we stack all CCFs over one month. In several segments, we could retrieve clear Rayleigh wave propagation. In the DAS observation, there are many combinations of the same channel intervals. We regard CCFs having the same channel interval as the ensemble of the Rayleigh wave propagating in random small-scale heterogeneous media. By using this ensemble, we calculate the ratio of the coherent and incoherent energy. This ratio decreases with the increase of the channel interval and it decreases to $1/e$ at about 100 m. This distance is related to the scattering mean free path. By calculating the ratio at every segment, we can estimate the scattering mean free path at very shallow ground along the fiber optic cable even if the vehicle noise is dominant.

KEYWORDS : DAS (distributed acoustic sensing), small-scale heterogeneity, noise CCF

Sr No: 602

Ambient Noise Tomography of Barmer-Sanchor rift in northwestern India

CORRESPONDING & PRESENTING AUTHOR:
Santhoshkumar Gundu, Indian Institute of Technology, Bombay, India
Satish Maurya, Indian Institute of Technology, Bombay, India
Mohan Gollapally, Indian Institute of Technology, Bombay, India

The Barmer-Sanchor rift is a 300km long northwest-southeast trending feature in the western segment of the Malani igneous province (MIP) that adjoins the Aravalli Delhi fold belt in northwestern India. Ambient noise data from 29 broadband three-component seismic stations that were operated in an area of 40000 km2 in MIP during 2009-2018 was used. The seismic interferometry technique was employed to characterize the crustal structure beneath the Barmer-Sanchor rift using ambient noise. The cross-correlation functions for the vertical and transverse component seismograms were generated and stacked to produce linear and phase weighted stacks of noise correlation function between each possible station pair. A total of about 500 noise correlation functions were generated. The fundamental mode group velocity dispersion curves for Rayleigh and Love waves were computed for the time periods 5s to 30s using the frequency-time analysis method. The dispersion measurements (~250 paths) at each period were regionalized with a 30km lateral correlation length to produce regionalized maps of group velocity perturbations. In both the Rayleigh and Love tomography maps, the rift is characterized by low group velocity anomalies (-4% to -12%) in the period range 5 to 15s. Barmer and Sanchor stations indicate much larger lowering of velocities suggesting thicker sedimentation in these regions relative to the rest of the rift. The discrepancy in local Love-Rayleigh wave group velocities anomaly at periods of 25s to 30s suggesting presence of radial anisotropy in the crust. The regionalized maps clearly delineate the geometry of the rift and characterize the anisotropy.

KEYWORDS : malani igneous province, barmer-sanchor rift, ambient noise tomography

Sr No: 603

Enhancing the Extraction of Surface-wave Dispersion Curves from the Traffic Signal in DAS Data

CORRESPONDING & PRESENTING AUTHOR:

Katsuhiro Yabu, Tohoku University, Japan

Hisashi Nakahara, Tohoku University, Japan

Kentaro Emoto, Tohoku University, Japan

Takeshi Nishimura, Tohoku University, Japan

Distributed acoustic sensing (DAS) that turns an existing fiber-optic cable into an array of strain sensors is becoming popular in seismology. Stacking data from 33 passing cars on a busy road, Yuan et al. (2020) retrieved Rayleigh-wave dispersion curves at several sections of a fiber-optic cable. Here, we develop a space-time stacking method to obtain dispersion curves along a long cable consecutively by giving chase to moving vehicles.

We use DAS data along a 50km-long section of the national route 4 in Miyagi Prefecture, Japan. The channel interval and gauge length are 5 m, and the total number of channels is 9854. First, we select dozens of vehicles running at constant speeds on the record section. Setting a space-time window with 250 m long and approximately 1 s duration in front or rear of a vehicle, we calculate a dispersion curve from an amplitude-normalized record section by the multichannel analysis of surface waves. Shifting the space-time window to chase each vehicle, we stack dispersion curves for several space-time windows within every 100 m long section. That enhances the SNR of the traffic signal at the cost of reducing the spatial resolution. Further conducting the stacking over several vehicles on average, we end up with dispersion curves consecutively along the cable.

The first higher mode was found to be predominant from 7 to 13 Hz. The fundamental mode appears from 3 to 13 Hz at some sections.

Our method will be useful for site characterization along a long cable.

KEYWORDS : DAS, traffic signal, site characterization

Sr No: 604

Evaluation of frequency-dependent attenuation mechanisms in Garhwal Himalaya based on a modified MLTWA for a layered model

CORRESPONDING & PRESENTING AUTHOR:

Simanchal Padhy, Indian Institute of Technology Roorkee, India

Subhadra Nampally, CSIR-National Geophysical Research Institute, India

Accurate estimates of attenuation mechanism obtained with a realistsic earth model are important for

ground-motion prediction at high frequencies (>1 Hz). We evaluate them for Garhwal Himalaya in 1.5-24 Hz by comparing observed and calculated coda envelopes with a modified Multiple Lapse Time Window Analysis (MLTWA); the model includes both uniform and layered half-space geometries with leakage of energy into the mantle included. Observed envelopes are obtained from the 1999 Chamoli earthquake aftershock sequence, while calculations include both the analytical and numerical Monte Carlo solutions of radiative transfer equation in 3-D acoustic media with multiple isotropic scattering (Hoshiba 1997). Our approach uses empirical scaling factor compensating for the unrealistic uniform structure by systematically comparing analytical and numerical envelopes for a suite of two-layered earth models (DelPezzo and Bianco 2010). Attenuation parameters are estimated from the best fit by trial and error forward modelling. By doing so, we correct for the bias in estimates resulting from the use of a uniform structure. Results show a strong frequency dependence of the intrinsic absorption. The best fittings are characterized by intrinsic and scattering coefficients for the uniform model greater than those for the layered one by a factor of ~3.0-5.0 and ~1.5-2.0, respectively, depending on frequency. We test the effect of mantle leakage on the estimates. Frequency-dependent absorption is not required to explain the leakage characterized by an exponential decay, in agreement with previous studies (Dominguez and Davis 2013).

KEYWORDS : 1999 chamoli earthquake, intrinsic and scattering attenuation, MLTWA

Sr No: 605

Coseismic changes in attenuation and its anisotropy

CORRESPONDING & PRESENTING AUTHOR:

Shuhei TSUJI, Nagoya University, Japan

Koshun Yamaoka, Nagoya University, Japan

Ryoya Ikuta, Shizuoka University, Japan

We found an anisotropic change in attenuation associated with seismic ground motions in dataset obtained in the experiment using an artificial seismic source, ACROSS. The dataset we analyzed was obtained by Ikuta et al. (2002) at the Awaji ACROSS test site from 2000 to 2001. We calculated variations in amplitude using the ratio of power of the transfer functions to that of the reference transfer function. In this calculation, we estimated power of noise on the transfer functions using characteristics of ACROSS signals and removed it to reduce effect of temporal change in noise level from the estimated change in amplitude. As a result, we found a coseismic decrease in amplitude at the 2000 Western Tottori Earthquake (WT) and the 2001 Geiyo Earthquake (GY).

Since Ikuta and Yamaoka (2004) suggest crack opening as a cause of the coseismic changes in velocity by anisotropy analysis, we compared coseismic change in amplitude in principal axes of coseismic delay of the S wave. As a result, a greater decrease in amplitude is obtained in the larger axis of the velocity anisotropy for both depths at WT, although no significant difference was observed for either depth at GY. This result suggests that the direction of greater attenuation corresponds to that of larger delay. That is consistent with laboratory experiments with cracked and saturated media.

KEYWORDS :   crack orientation, artificial seismic source, amplitude change

Sr No: 606

Preliminary scattering and attenuation properties of the Martian Lithosphere

CORRESPONDING & PRESENTING AUTHOR:

Sabrina Menina, Institut de Physique du Globe de Paris, France

Ludovic Margerin, Institut de Recherches en Astrophysique et Planétologie, France

Taichi Kawamura, Institut de Physique du Globe de Paris, France, France

Philippe Lognonne, Institut de Physique du Globe de Paris, France

Jules Marti, Institut de Recherches en Astrophysique et Planétologie, France

Melanie Drilleau, Institut Supérieur de l'Aéronautique et de l'Espace, France

Marie Calvet, Institut de Recherches en Astrophysique et Planétologie, France

Nicolas Compaire, Institut Supérieur de l'Aéronautique et de l'Espace, France

Raphael Garcia, Institut Supérieur de l'Aéronautique et de l'Espace, France

Foivos Karakostas, Istituto Nazionale di Geofisica e Vulcanologia, Italy

Nicholas Schmerr, University of Maryland, USA

Martin Van Driel, ETH Zurich, Sweizerland

Simon C. Stahler, ETH Zurich, Sweizerland

Matthieu Plasman, Institut de Physique du Globe de Paris, France

Domenico Giardini, ETH Zurich, Sweizerland

Sebastian Carrasco, Institute of Geology and Mineralogy, Russia

Brigitte Knapmeyerendrun, Institute of Geology and Mineralogy, Russia

Gregory Sainton, Institut de Physique du Globe de Paris, France

William T. Pike, Imperial College London, UK

William B. Banerdt, Jet Propulsion Laboratory, USA

Since its deployment at the surface of Mars in 2019, the SEIS seismometer of the NASA-InSight mission has detected hundreds of small magnitude seismic events. In this work, we investigate the attenuation properties of the Martian lithosphere using one specific family of events known as Very-High-Frequency (VF) events, which primarily contain energy above 1.5 Hz. We selected a set of VF events with a coda duration of at least 200s and a signal-to-noise ratio (S/N) greater than 2 at 2.5 Hz. We used elastic radiative transfer theory to perform a series of inversion of seismogram envelopes in a half-space geometry. The good fit between synthetic and observed envelopes confirms that multiple scattering of elastic waves released by internal sources is a plausible explanation of the high-frequency events characteristics. We quantify scattering and attenuation properties of Mars and highlight the differences/similarities with the Earth and the Moon. The dependence of the inferred attenuation/scattering parameters with hypocentral distance suggest a stratification of attenuation properties inside Mars. The albedo, i.e. the contribution of scattering to the total attenuation, derived from VF events is found to be very high which we interpret as a signature of a mostly dry medium. This result agrees with the study of Clifford et al. (2010) which suggests that the upper crust could be dry in the equatorial region near the InSight station. By the time of the meeting, we hope to present the first results of envelope modeling based on elastic radiative transport in a stratified medium.

KEYWORDS : attenuation, multiple-scattering, martian-lithosphere

Sr No: 607

Investigating the Causes of Unrest at Aluto Volcano, Central Main Ethiopian Rift, with

CORRESPONDING & PRESENTING AUTHOR:

Corinna Roy, University of Leeds, UK

Andy Nowacki, University of Leeds, UK

Xin Zhang, University of Edinburgh, UK

Andrew Curtis, University of Edinburgh, UK

Brian Baptie, British Geological Survey, UK

Rift volcanoes worldwide present significant hazard to people from eruptions, but also provide resources such as geothermal energy. Aluto in the Central Main Ethiopian Rift is an example and the site of Ethiopia's first geothermal electric power plant. Over the last 15 years at least, Aluto has undergone repeated, large (several cm) inflation and deflation episodes.

The subsurface cause of this surface deformation is variously speculated to be magma recharge of a mush-like body at ~5 km depth, swelling of a clay cap at ~1 km, or hydrous fluid loss at ~3 km. An improved interpretation of unrest at volcanoes and risk assessment requires that we identify the location, geometry and size of possible magma bodies, pathways and the amount of partial melt.

We use a reversible-jump Markov chain Monte Carlo approach to perform a fully nonlinearised joint inversion of local seismic P- and S-wave travel times, and surface wave dispersion data from empirical Green's functions, for the location of earthquakes and the velocity of the subsurface. The retrieved posterior probability of earthquake parameters and seismic velocity provide rigorous distributions of the covariance of the earthquake and velocity parameters. Hence, it is possible to probabilistically relate the imaging of the volcano's interior to the candidate physical processes occurring within it.

We observe regions of elevated V_p/V_s (> 1.8) at around 5km depth, which we interpret as partial melt. We use the posterior probability distribution of the seismic velocities to estimate the melt fraction using elastic medium theory.

KEYWORDS : ambient noise, monte carlo

Sr No: 608

Subsurface crustal velocity structure of the Garhwal and Kumaun Himalaya based on ambient noise array dispersions

CORRESPONDING & PRESENTING AUTHOR:

Sanjay Verma, Wadia Institute of Himalayan, Geology, Dehradun, India

Naresh Kumar, Wadia Institute of Himalayan Geology, Dehradun, India

Devajit Hazarika, Wadia Institute of Himalayan Geology, Dehradun, India

Dilip K Yadav, Wadia Institute of Himalayan Geology, Dehradun, India

Ajay Paul, Wadia Institute of Himalayan Geology, Dehradun, India

Sanjit Paul, IIT ISM, Dhanbad, India

The northwest Himalaya is in a seismically active zone and last three decades witnessed moderate to strong earthquakes in the Garhwal-Kumaon Himalaya, viz. 1999 Chamoli (Mb 6.8), 1991 Uttarkashi (Mb 6.6), 2011 64km east of Pithoragarh (5.5ML), 2017 45km WSW of Joshimath (5.2ML), however, crustal seismic structure and geometry beneath this region are poorly understood. We have included Garhwal, Kumaun from the boundary of the Kali river and part of the Indo-Gangetic plain of Panjab and Haryana regions in the study for subsurface crustal structure investigation. This study presents the high-resolution 3-D shear (S-wave) velocity up to crustal depth by applying non-linear inversion of Rayleigh wave dispersions from 4 to 27 s that are extracted from ambient noise cross-correlation. The S-wave velocity features vary from ~2.3 to ~3.4 km/s which correspond to sub-surface tectonic deformation, structural formations, and crustal thickness in high mountain zones. Low-velocity zones in S-velocity compared to adjacent parts are detected in the uppermost crust of the frontal Himalaya and parts of the Indo-Gangetic plain. This low velocity may correspond to thick sediment deposits in the low elevation plains transported from high elevation mountain zones of Himalaya. In contrast, the part of Himalaya and southern Tibet towards the north exhibit higher velocity suggesting the uppermost crustal part constituted by the older rocks. With the increase of depth, the spatial variation in the velocity of the whole study region decreases indicating the presence of Indian plate strata.

KEYWORDS : garhwal and kumaun himalaya, rayleigh wave, seismic tomography

Sr No: 609

Seismic interferometry applied to the record of the SEIS-InSight seismometer on Mars to monitor velocity changes in the subsurface

CORRESPONDING & PRESENTING AUTHOR:

Nicolas Compaire, ISAE-SUPAERO, France
Ludovic Margerin, OMP-IRAP, France
Raphael F. Garcia, ISAE-SUPAERO, France
Marc Monnereau, OMP-IRAP, France
Marie Calvet, OMP-IRAP, France
Simon C. Stahler, ETHZ, Switzerland
Nikolaj L. Dahmen, ETHZ, Switzerland
Philippe Lognonne, IPGP, USA
W. Bruce Banerdt, JPL-Caltech, USA

The SEIS seismometer deployed at the surface of Mars in the framework of the NASA-InSight mission has been continuously recording the ground motion at Elysium Planitia for more than one martian year. In this work, we investigate the seasonal variation of the near surface properties using both the background vibration and a particular class of high-frequency seismic events. We present measurements of relative velocity changes over one martian year and discuss the potential origins of the observed temporal variations.

Several families of high-frequency seismic multiplets have been observed at various periods of the martian year. These events are highly diffuse allowing us to use coda waves interferometry techniques to measure relative travel-time changes according to their time of occurrence. While in some families a stretching of the coda waveform is clearly observed, in other families we observe either no variation or a clear contraction of the waveform. These various behaviors correspond to different seasons in the sunlight conditions at the InSight landing site.

Consistent observations come from the background vibrations above 5Hz. We observe a frequency band structure in the power spectral density of consecutive martian day. We show that this band structure can be created by the presence of seismic waves reflected in the subsurface. It is therefore the equivalent in the frequency domain of an autocorrelogram and it can be used to measure relative travel-time changes. These measurements are in very good adequacy with the seismic multiplets and point toward a thermo-elastic behavior of the martian near surface.

KEYWORDS : SEIS-InSight, seismic interferometry, monitoring

S6 CoSOI Collection, interpretation and publication of paleo and historical earthquake data

CONVENERS: Paola Albini (Italy)

Kenji Satake (Japan)

Jian Wang (China)

Javed N. Malik (India)

Evidence of global seismic activity from instrumental records covers about one century, too short a period to catch the recurrence interval of large earthquakes. Historical seismological studies and macroseismic intensity data have significantly expanded backwards in time our knowledge of the seismic behaviour of many areas in the world. Paleoseismological studies of inland active faults, as well as coastal geological studies on tsunami deposits or marine terraces, and marine geological studies on deep-ocean turbidites, have provided important information for the past occurrence of pre-instrumental earthquakes, too.

The combination of data deriving from these three domains would result in a better vision of the long- term seismicity, which may be utilized for long-term forecast. However, challenges are still posed to researchers on how to best derive earthquake parameters from originally non-seismological observations of earthquake effects, as it is the case of both macroseismic and geological data.

This session welcomes contributions suggesting new prospects related to these topics, such as case studies of historical and paleoseismological records, their unfiltered association to specific events as well as their usual parameterization in seismological terms, or their combination with modern instrumental data, or any further issue on long term seismicity analysis and forecast of moderate and especially of large earthquakes.

Sr No: 610

Estimation of the Parameters of Two Historical Earthquakes with a New Attenuation Equation in Yunnan Province, China

CORRESPONDING & PRESENTING AUTHOR:

Guoliang LIN, Yunnan Earthquake Agency, China

Jian Wang, Institute of Geophysics, China

Yunnan province is in southwest China, where the seismicity has been active since ancient times. Generally, the uncertainty of historical earthquake parameters is larger. In order to amend the parameters of historical earthquakes, we have developed a new intensity attenuation equation.

From 2000 to 2018, there are 25 instrumentally recorded earthquakes with Ms 5.0 to 6.6 in Yunnan. The parameters of those earthquake events including epicentral location and magnitude are determined with high accuracy. Meanwhile, total intensity values of 1, 345 intensity data points have been carefully assessed by survey. With both accurate earthquake parameters and valuable intensity data, a new intensity attenuation equation has been established. The result shows the optimal intensity magnitude MI can be calculated from the mean of $Mi=(I-2.1113+0.0412\Delta i+1.3717lg\Delta i)/1.1641$. By adapting the method proposed by Bakun and Wentworh (1997) for determining earthquake source parameters directly from historical intensity data, we have tested retrospectively the new attenuation on the 25 instrumentally recorded earthquakes. Then this attenuation has been applied to deal with the parameters of two historical earthquakes, the 26 February 1713 Xundian earthquake and the 11 May 1909 Huaning earthquake. Our results reduced the uncertainty of previously estimated parameters which were large. The amended parameters will be valuable for seismic hazard analysis and earthquake disaster reduction.

KEYWORDS : intensity data, attenuation equation, historical earthquake

Sr No: 611

How authoritative are the pre-modern descriptive catalogues by von Hoff (1840), Perrey (1845-1850) and Mallet (1858)? An overview

CORRESPONDING & PRESENTING AUTHOR:

Paola Albini, INGV-Istituto Nazionale di Geofisica e Vulcanologia, Italy

Pre-modern descriptive catalogues have been used to populate the preinstrumental section of parametric catalogues since the late 1960s. The most used at a global scale are the descriptive earthquake lists by von Hoff (1840), Perrey (1845-1850), and that in a tabular format by Mallet (1858), all covering the period from Antiquity to about 1850. Because their authors were considered authorities on this issue, often to the point of becoming reliable sources in themselves, modern catalogue compilers trusted without checking the overall reliability of their catalogues. Although historical seismology investigations fixed many flaws and mistakes in early translations of earthquake effects into earthquake parameters, the question of how accurately these three authors selected their sources is still open and deserves to be dived into. The global
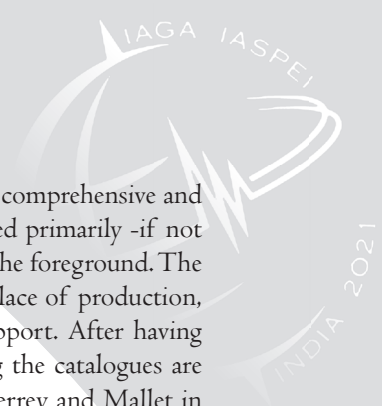
catalogues of von Hoff, Perrey and Mallet have been individually analysed to compile a comprehensive and commented list of the sources on which they relied upon. Conversely to analyses focused primarily -if not exclusively- on their seismological content, here the sources of earthquake records are in the foreground. The hundreds of items these three authors collected are examined with respect to date and place of production, type, embraced time-windows and areas in relation to the earthquake records they support. After having merged and compared these three sets of sources, differences in their use in compiling the catalogues are evidenced, to catch how they influenced the accuracy of the catalogues by von Hoff, Perrey and Mallet in describing the global seismicity up to mid-nineteenth century.

KEYWORDS :   descriptive catalogues, historical seismology, global seismicity

Sr No: 612

Why Shaking Intensities Provide Only Weak Constraint on Seismic Moment

CORRESPONDING & PRESENTING AUTHOR:

Susan Hough, US Geological Survey, USA

Recent studies have demonstrated good consistency between instrumental ground motion parameters and intensity values from on-line data-collection systems for moderately large earthquakes. We consider whether the intensity distributions of two of California's largest historical earthquakes — 1872 Owens Valley and 1906 San Francisco -- are consistent with predicted intensities from a modern ground motion model. For the 1906 earthquake, applying this approach to an extensive intensity data set yields an optimal intensity magnitude of 7.9, the same value estimated previously from seismic and geodetic data. The intensity-based magnitude of the 1872 earthquake is, however, higher than the moment magnitude estimated from geologic observations, providing evidence that it was a high stress drop event. This in turn suggests a moment towards the upper end of the range implied by scaling relations, given the estimated surface rupture length. We note that, for historical earthquakes especially but also for recent earthquakes, intensity data provide an integrated measure of shaking at relatively high frequencies, i.e., a few Hz to 10 Hz. Given the strong dependence of high frequency shaking on stress drop and its relatively weak dependence on seismic moment, simple relations predict that an intensity-based magnitude can be a full unit higher or lower than the moment magnitude. In the absence of constraints on rupture dimension, this uncertainty is likely irreducible. We further note, however, that the "failure" of intensity data to reflect moment magnitude could be viewed as a failure of moment magnitude to reflect ground motions at frequencies of engineering concern.

KEYWORDS :   historical earthquakes

Sr No: 613

Amending the parameters of historical earthquakes with the knowledge of historical administration zoning

CORRESPONDING & PRESENTING AUTHOR:

Jian WANG, Institute of Geophysics, CEA, China

For the catalog of historical earthquakes, the problem is that the errors of parameters are larger generally. Many reasons can bring the larger errors. In ancient China, macroseismic data are mainly available from the government annals. Generally, the damage descriptions of lower tier government were detailed relatively, which should be handed up to higher tier governments. In this process, the contents of the documents might be simplified. Nowadays, the annals of higher tier governments might be remained with higher likelihood. In some cases, the earthquake damage descriptions from the high tier government annals are so concise that the specific place names were omitted, even the names of towns where the damage might have actually occurred. The intensity data point (IDP) was assigned to the capital town of the high-tier government, which might lead to large uncertainties in the historical earthquake parameters. In this situation, knowledge of historical administration zoning can supply the additional information to find the right site of IDP, which will helpful to amend the parameters of the historical earthquake. As an example, one historical earthquake in the Ming Dynasty is analyzed. With the nonseismological information, including historical administration zoning, right site of the IDP was determined. This is the key step to solve the dispute and reduce the parameter uncertainty. In this process, we emphasize the important of understanding historical records in the historical time period and local scenario, so the historical administration zoning is indispensable knowledge.

KEYWORDS : historical earthquake, intensity, China

Sr No: 614

Evaluation of Damage Descriptions Around Mt. Hiei During the 1830 Kyoto Earthquake

CORRESPONDING & PRESENTING AUTHOR:
Yasuyuki Kano, The University of Tokyo, Japan
Junzo Ohmura, The University of Tokyo, Japan
Kiyomi Iwahashi, Kokugakuin University, Japan

Attenuation relationships for seismic intensity are proposed based on recent dense observation of seismic intensity. One of the key parameters of the prediction of seismic intensity distribution based on attenuation relationship is site amplification factor. GIS-based standardized ground-condition map including geomorphologic classification with mesh size of 250 m was incorporated in the relationships. The relationships help understand distributions of damage or shaking recorded in historical documents. To evaluate the location and magnitude of the 1830 Kyoto earthquake, we examined the diaries recorded at temples in and around Mt. Hiei as well as historical documents recorded around Kyoto. Several diaries describe damage or shaking intensity at the top and side of Mt. Hiei and at the side of Lake Biwa. We
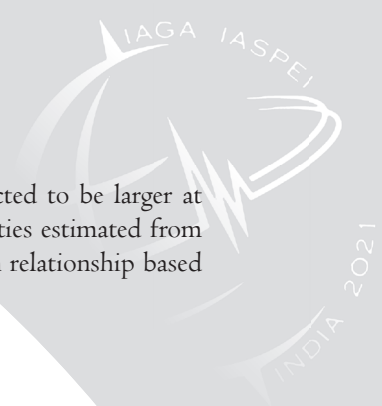
can find relatively small damage or shaking at the top. The site amplification is expected to be larger at the hillside or the side of the lake because of alluvial soil deposits. The seismic intensities estimated from descriptions in diaries are consistent with the intensities predicted from the attenuation relationship based on modern observation and site amplification factor.

Sr No: 615

Use of Earthquake Environmental Effects in Intensity Assignment for Large, Fennoscandian Earthquakes

Paivi Mantyniemi, University of Helsinki, Finland

CORRESPONDING & PRESENTING AUTHOR:

Mathilde Sorensen, University of Bergen, Norway
Ruben Tatevossian, Russian Academy of Sciences, Russia

Earthquake environmental effects (EEEs) are earthquake consequences to the surrounding natural environments, such as landslides or disturbances in water bodies. EEEs were compiled for the earthquakes of 1626, 1759, 1819, and 1904 in the Fennoscandian Peninsula, northern Europe. The principal source of information was the contemporary newspaper press. Macroseismic questionnaires collected in 1759 and 1904 were also consulted. We prepared maps showing newly discovered EEEs together with previously known EEEs and analyzed their spatial distribution. We assigned intensities based on the 2007 Environmental Seismic Intensity (ESI) scale to 27 selected localities and compared them to intensities assigned based on the 1998 European Macroseismic Scale. While the overall agreement between the scales is good, intensities may remain uncertain due to the sparsity of written documentation. The collected data sets are most probably incomplete but still show that EEEs are not unprecedented cases in the target region. The findings include landslides and rockfalls as well as cascade effects with a risk potential and widespread water movements up to long distances. The winter earthquake of 1759 cracked ice over a large area. This investigation demonstrates that the ESI scale has practical importance and can supplement the traditional intensity scales, also in regions with infrequent EEEs.

Sr No: 616

On the Modern and Possible Prehistoric Earthquake Activity near Walden Pond, Massachusetts

CORRESPONDING & PRESENTING AUTHOR:

John Ebel, Boston College, USA
Katrin Monecke, Wellesley College, USA

Daniel Brabander, Wellesley College, USA

Brad Hubeny, Salem State University, USA

Francine Mccarthy, Brock University, Canada

A locality centered on the town of Acton, Massachusetts has averaged a small earthquake once every 2.8 years over the past several decades. The largest recent earthquake in this local seismic zone had magnitude 3.1 in 1985. Precise hypocenters of 4 microearthquakes less than magnitude 1.0 since 2017 suggest that these earthquakes are taking place within the Nashoba terrane between the Clinton Newbury and Bloody Bluff faults at depths between 2 and 7 km with a roughly NNW-SSE spatial trend. A focal mechanism computed for a magnitude 3.1 1985 earthquake shows thrust faulting on a NW-SE fault plane. Thus, the earthquakes around Acton do not appear to be associated with the major mapped faults of the area but rather show an orientation similar to that of minor, NW-SE cross faults. The paleoseismicity model of Ebel et al. (SRL, 2000) inferred that the modern earthquake activity centered at Acton may be aftershocks of an earthquake of about magnitude 6.3-6.7 sometime between 399 and 867 years ago. Nashoba Hill, located in the town of Westford just north of Acton, is named after the Indian word "Nashoba" meaning "hill that shakes", perhaps due to earthquake activity in precolonial times. An analysis of sediments in Walden Pond near Acton show possible strong earthquake shaking at the pond about 800 years ago. The pond sediment data and the paleoseismicity analysis both indicate the occurrence of a precolonial earthquake of about magnitude 6.5 somewhere in or near Acton, Massachusetts area about 800 years ago.

KEYWORDS : paleoseismicity, paleoseismology, sediments

Sr No: 617

SYMPOSIUM : **S6 CoSOI Collection, interpretation and publication of paleo and historical earthquake data**

Origin Time of the 1854 Tokai Earthquake Recorded on Logbook of Russian Frigate Diana

PRESENTING AUTHOR:

Reiko Sugimori, The University of Tokyo, Japan

Kazuko Ariizumi, The University of Tokyo, Japan

CORRESPONDING AUTHOR:

Kenji Satake, The University of Tokyo, Japan

The 23 December 1854 Tokai earthquake (M~8), followed by Nankai earthquake by ~30 hrs, occurred along Nankai trough and caused widespread damage due to ground shaking and tsunamis. At the time of earthquake, a Russian frigate, Diana, was anchored in the Shimoda Bay and experienced the earthquake and tsunami. The frigate was damaged and eventually wrecked. Two Japanese historical documents reported that strong shaking occurred in Shimoda after 8 o'clock and before 10 o'clock, reflecting the 2 hr unit of the timekeeping system used in Japan. The crew reports of the frigate, reported in contemporary newspapers in English all mentioned that an earthquake first shook the ship severely, and they observed the tsunami entered the bay at around 10: 00 in local time. The time of the earthquake, however, was reported at 9:15 in Shanghai and American newspapers (The North-China Herald, The Daily Union), while at 9:45 in British newspapers (The Times, The Illustrated London News). We found that the original logbook of Diana archived at Russian State Naval Archive, Saint Petersburg, recorded that the earthquake occurred "at 3/4 of 10th hour, " indicating that it was 9:45. The former newspapers seemed to have based on the information provided by the crew of American
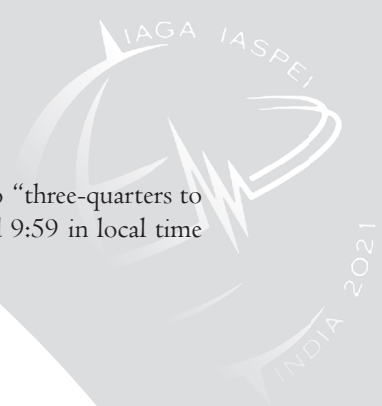
frigate which was also in Japan, but the time might have been erroneously translated into "three-quarters to ten." More precisely, the above time expression should be interpreted between 9:45 and 9:59 in local time (138°57' E), corresponding to between 0: 30 and 0:44 on Greenwich Mean Time.

KEYWORDS :   1854 Tokai earthquake, Russian frigate, origin time

Sr No: 618

Aftershock Activity of the 1596 Earthquake in Kinki Region of Japan Revealed by Diaries

CORRESPONDING & PRESENTING AUTHOR:

Junzo Ohmura, Earthquake Research Institute, University of Tokyo, Japan

Miki Hamano, Ritsumeikan University, Japan

On September 5, 1596, an earthquake of Mj7.5 occurred in the Kinki region of Japan. The aftershocks continued until April of the following year (Usami 2013). There are several diaries from the same period that record the aftershocks, and the "Tokitsune-Kyo Ki" is particularly detailed. In this diary, there are four different description for the magnitude of the tremors. However, it is difficult to distinguish the different magnitudes of the tremors from the description.

In this study, we tried to distinguish the magnitude of the earthquake motion by comparing it with other records of the diary. In "Tokitsune-Kyo Ki", there are many descriptions of "Sho-do (small movement)". However, on the days when major earthquakes occurred, "Chi-do (Ground movement)" tended to be used.

These comparisons revealed that the expressions for earthquake motion in this diary are "Chi-do (Ground movement)", "Sho-chi-do (Small ground movement)", "Sho-do (Small movement)", and "Zishin (Earthquake)" in order of magnitude. Based on this analysis of the aftershock activity, the activity declined after January 10, 1597, about four months later. After February 3, about five months later, the word " Chi-do (Ground movement)" meaning the maximum, disappears. After that, the number of " Zishin (Earthquake)", meaning the smallest, increases. At the same time, the number of recorded earthquakes was found to be decreasing.

KEYWORDS :   aftershock activity, diary, expression of vibration

S7 CoSOI National and Regional Earthquake Data Centers: Highlights and Challenges

CONVENERS: D. Srinagesh (India)
                       Dmitry Storchak (UK)

National and regional seismic operational centers play an important role in monitoring for natural earthquakes, volcanic eruptions, and other phenomena, such as induced seismicity. The products generated by these centres, from raw waveforms to earthquake catalogues are used by a wide variety of stakeholders, including researchers, emergency management agencies, policy makers, educators, regulators, and the general public.

This session focuses on the important role that earthquake centres play in advancing scientific study, especially as it relates to local and regional hazard; integrating new technological advances in data acquisition and processing; and communicating earthquake hazard and risk.

We welcome contributions describing new and evolving networks, data policies and data sharing, new processing algorithms, hazard assessments, and novel education and outreach initiatives. Other topics that highlight current advances and challenges for earthquake operation centres are also of interest.

Potential outcomes of the session may include summary publications, organized advocacy, and frameworks for closer collaboration.

Sr No: 619

Data Management System (DMS) for CSIR-NGRI Seismological Data

CORRESPONDING & PRESENTING AUTHOR:

Pavan Kumar Vengala, CSIR-National Geophysical Research Institute, India

Srinagesh D, CSIR-National Geophysical Research Institute, India

Seismological data collection, analysis and archiving are important to our understanding of the naturally occurring Earthquakes and how they are changing with the time. Properly archived and documented Data Management System will help the present and future researchers. Seismology group of CSIR-NGRI is having more than 300 digital broad band seismic stations in different Networks. Archiving and retrieval of data from above stations is huge task and to overcome this DBMS facility is one of the best solution. A Centralized recording facility (Data Management Center) is called for, that can handle inputs from multiple seismic stations, storage in a secure database, authentication and authorization based access, easy retrieval of data and providing outputs in multiple formats. This facility is designed on a Scalable Database Management System that has a user-friendly Web based front end, using PHP for scripts, on a Linux platform with MySQL as the RDBMS at the backend. The above mentioned system is deployed on one of the dedicated server in CSIR-NGRI. The main moto for designing of this facility is to create basic layer for fetching inputs for Data science, Artificial Intelligence and Machine learning.

KEYWORDS : DBMS, data science, machine learning

Sr No: 620

Rebuild of the ISC Bulletin (by invitation)

CORRESPONDING & PRESENTING AUTHOR:

Dmitry Storchak, International Seismological Centre (ISC), UK

James Harris, International Seismological Centre (ISC) , UK

Kathrin Lieser, International Seismological Centre (ISC) , UK

Domenico Di Giacomo, International Seismological Centre (ISC) , UK

The International Seismological Centre (ISC) provides the Bulletin which is regarded as the most long-term and comprehensive catalogue of instrumentally recorded seismicity on a global scale, primarily based on seismic reports from ~150 observatories and data centres worldwide. The Bulletin is used in a wide range of geophysical studies. It includes the most comprehensive set of measurements from permanent and temporary networks. The Bulletin also serves as a foundation for specialised datasets such as the ISC-GEM catalogue, ISC-EHB dataset, IASPEI GT-List and ISC Event Bibliography.

Despite a fairly strict approach to preserving operational procedures over the last ~50 years, changes were inevitable to achieve the best accuracy of earthquake parameters. The last fundamental change in procedures has affected the data years 2011 and beyond (Bondár and Storchak, 2011). To achieve compatibility in earthquake hypocentres and magnitudes through the entire period, we had to rebuild the earlier part (1964-2010).

The entire reviewed part of the ISC Bulletin (1964-2018) is now based on the same 1D velocity model, ak135, and the same earthquake and magnitude computation procedure (iscloc). We give an account of notable changes in the Bulletin from the removal of poorly constrained events to the addition of many small events, based on additional reports from permanent and temporary seismic deployments. As a result, the rebuilt ISC Bulletin has 17% more seismic arrival times from 21% more stations (Storchak et al., 2020). Another important feature was an inclusion of ~12, 000 ISC source mechanisms based on reported first motion polarities (Lentas, 2018).

KEYWORDS : ISC, bulletin, rebuild

Sr No: 621

Advancing Nordic seismological collaboration with Nordic EPOS - A FAIR Nordic EPOS Data Hub (by invitation)

CORRESPONDING & PRESENTING AUTHOR:

Annakaisa Korja, University of Helsinki, Finland

Kuvvet Atakan, University of Bergen, Norway

Peter H. Voss, GEUS, USA

Michael Roth, University of Uppsala, Sweden

Kristin Vogfjord, Icelandic Meteorological Office, Iceland

Elena Kozlovskaya, University of Oulu, Finland

Eija Tanskanen, University of Oulu, Finland

Niina Junno, University of Helsinki, Finland

Nordic EPOS - A FAIR Nordic EPOS Data Hub – is a consortium of the Nordic geophysical observatories financed by NordForsk. Partner organizations are delivering on-line data to EPOS Thematic Core Services. Nordic EPOS enhances and stimulates the active Nordic interactions related to Solid Earth Research Infrastructures (RIs) in general and EPOS in particular. Nordic EPOS develops expertise and tools designed to integrate Nordic RI data and to enhance their accessibility and usefulness to the Nordic research community. Together we can address global challenges with Nordic data.

The Nordic EPOS is organized into Tasks and Activities. The project has seven main TASKs: I - Training in usage of EPOS-RI data and services; II - Nordic data integration and FAIRness; III - Nordic station management of seismological networks, IV - Induced seismicity, safe society; V - Ash and gas monitoring; VI - Geomagnetic hazards, and VII - Communication and dissemination. The activities within the TASKs are workshops, tutorials, demos and training sessions (virtual and on-site), and communication and dissemination of information on EPOS data and metadata at local, national and international workshops, meetings, and conferences. For more information see https://www2.helsinki.fi/en/infrastructures/nordic-epos.

In seismology, NORDIC-EPOS is particularly active in standardizing observatory practices and databases, especially in following EPOS metadata standards, in increasing expertise in seismic hazard assessment for intraplate regions, in preparing a seismic hazard map for the Nordic countries and in expert capacity building in monitoring of induced seismicity in urban areas.

KEYWORDS : nordic, seismological data, FAIR

Sr No: 622

Mongolian National Data Center

CORRESPONDING AUTHOR:

Lkhagva Tungalag, Institute of Astronomy and Geophysics of MAS, Mangolia

PRESENTING AUTHOR:

Dorj Enkhtulga, Institute of Astronomy and Geophysics of MAS, Mangolia

Sereenendorj Odbayar, Institute of Astronomy and Geophysics of MAS, Mangolia

Adiya Munkhsaikhan, Institute of Astronomy and Geophysics of MAS, Mangolia

Mongolian National Data Center (MNDC) was established in 2007 as a section of the Institute of Astronomy and Geophysics (IAG). The main role of the MNDC is the monitoring and analyzing for signals, data archiving, delivery strong earthquakes information, international data exchange, studying seismic activity. Currently, geophysical stations are running at 50 sites in Mongolia, including seismic array stations. All the data is being transmitted in real-time to MNDC by radio modem and VPN via internet. Current seismological database consists of, 1900-1963 historical database, 1964-1994 analog database, 1995-2006 analog and digital database, and 2007 to present digital database.

"Seiscomp3" automat program that localization events such as natural earthquake, mining and nuclear explosion has been being run in the MNDC since 2015. The automat program is operated at the following 3 levels. Teleseismic, Regional earthquakes and early warning. Using automat detection algorithm, it allows us to create an alarm and send e-mail and phone messages, after audible signal alerts in MNDC when an earthquake with a magnitude of more than 3.5 occur in regional level. In addition, that system is being configured to automat plotting that shake map and focal mechanism

KEYWORDS : Mongolian national data center, database, automat

Sr No: 623

Arctic earthquake data and recommendations outcome from the INTAROS project

Zeinab Jeddi, University of Bergen, Norway

Mathilde B. Sorensen, University of Bergen, Norway

Finn Danielsen, Nordic Foundation for Development and Ecology, Denmark, Denmark

Christian Ronnevik, University of Bergen, Norway

Jan Michalek, University of Bergen, Norway

Tine B. Larsen, Geological Survey of Denmark and Greenland, Denmark

Trine Dahl Jensen, Geological Survey of Denmark and Greenland, Denmark

CORRESPONDING & PRESENTING AUTHOR:

Peter Voss, Geological Survey of Denmark and Greenland, Denmark

From 2016 to 2021, the INTAROS project examined monitoring gaps related to earthquakes and

other seismic events in the Arctic region and provided examples of how to close these monitoring gaps. Stakeholders were engaged through the project, and policy briefs and information sheets were developed for policy makers, regulators and the general public, giving recommendations on how to handle natural hazards with a seismic signature. Earthquake data was collected using Ocean Bottom Seismometer (OBS) systems at several locations in the North Atlantic, citizen based monitoring (CBM) was initiated in both Greenland and Svalbard, and an earthquake bulletin and a station catalog were constructed for the region. The outcomes, data, bulletin and catalog, are now available through the INTAROS iAOS (integrated Arctic Observing System https://catalog-intaros.nersc.no/), including a bulletin web service providing various search options and output options such as QuakeML and Nordic Format. In this presentation, we will provide information on how to access the data and give examples using the data. The CBM units (Raspberryshake) were shipped to local residents in Greenland, where they were deployed, providing important contributions to the seismic monitoring of the region and new knowledge on the local ambient seismic noise levels. The CBM units in Svalbard, were installed in public buildings with a high noise level, thus providing limited data on the seismic monitoring in the region, but important information on the challenges in sensor installations in buildings in permafrost areas.

KEYWORDS : Arctic, earthquake, monitoring

Sr No: 624

The Chilean Seismic Observation System (by invitation)

CORRESPONDING & PRESENTING AUTHOR:

Sergio Barrientos, University of Chile, Chile

Chile extends for about 4300 km, from approximately 17.5°S to 56°S, covering a variety of terrain and climates. More than 110 six-component seismological stations (BB + strong ground motion) distributed along the country, including two devices installed in the Chilean Pacific Islands and those part of the Integrated Plate Boundary Observatory in northern Chile transmit their data in real-time to the the National Data Center at the University of Chile located in Santiago.

To rapidly characterize size and extension of large earthquakes in the near field (because de the main thrust region is mostly concentrated between the trench and the coast with an average width of about 150 km) the monitoring system includes real-time GNSS capabilities, both on-site position estimations as well as at a central server. In near-real-time applications, as well as in the near field, unsaturated direct-displacement-estimations based on GNSS observations become critical for determination of fault finiteness of M ~ 7 (or larger) earthquakes that affect the coastal part of the country, with their associated significant tsunamigenic potential. Examples of these capabilities will be presented, such as the signals recorded for some large earthquakes taking place in this part of the world.

Continued efforts on integrating new tools to rapidly characterize large events and efforts on development, as well as implementation, of a prototype earthquake early warning system will be presented. Evolution of the SARS-CoV-2 pandemic and its consequences on the field and headquarters operations of the National Seismological Center (CSN) will also be discussed.

KEYWORDS : seismic networks, rapid earthquake characterization

Sr No: 625

Towards improved ML estimation through station correction factors for the National Observatory of Athens catalogue

CORRESPONDING & PRESENTING AUTHOR:

Olga Joan Ktenidou, National Observatory of Athens, Greece

Antonia Papageorgiou, National Observatory of Athens, Greece

Konstantinos Boukouras, National Observatory of Athens, Greece

The National Observatory of Athens (NOA), Greece, does not -to date- use station-specific correction factors when it comes to estimating local magnitudes (ML) in its routine seismicity monitoring and earthquake location. Station correction factors have been estimated for part of NOA's stations as part of an earlier study (Skordylis et al., 2016) which was performed across all networks in Greece using data up to 2013. However, those were not implemented in deriving the NOA catalogue in recent years. Today, the NOA network has grown significantly, almost by 50%, and re-evaluating station behaviour and deviations is now a timely task. This work considers NOA data up to 2020 and the entirety of the network's stations, and presents the first preliminary results from ML residuals analysis. In cases of stations whose amplitudes deviate significantly, a correlation is sought with the existing knowledge about local site conditions at the recording stations. It is hoped that this study will help improve and harmonise future routines for ML estimation in the NOA catalogue.

KEYWORDS : earthquake location, Greece, station conditions

S8 CoSOI Advances in geophysics, atmospheric science, and signal analysis for monitoring the CTBT

CONVENERS: Keith L. McLaughlin (USA)
             Inna Sokolova (Kazakhstan)
             Alexander Smirnov (Kazakhstan)

The Comprehensive Nuclear-Test-Ban Treaty (CTBT) distinguishes itself from other international agreements by establishing a verification regime that includes the International Monitoring System (IMS) and the International Data Centre (IDC). The IMS is a global, multi-physics network of sensors that record seismic, hydro-acoustic, infrasound, and radionuclide signals that are generated by nuclear explosions. The first two decades of the CTBT focused on installation of the IMS network and implementation of robust IDC processing for detection and characterization of signals recorded on the IMS.

This symposium calls for contributions of state-of-the art methods and observational studies that advance CTBT verification science across all geophysical sensor technologies. For example, recent remote sensing INSAR observations have contributed insight into deformation by underground explosions. We seek contributions in the areas of source physics, signal propagation, and signal analysis. Source physics studies improve understanding of the nuclear explosion source and features that distinguish them from non-nuclear anthropogenic sources and natural sources. Signal propagation studies include characterization of Earth's interior, the oceans, and the dynamic atmosphere. Of particular interest are advances in predictive propagation of infrasound signals in the dynamic atmosphere, acoustic-seismic conversion, and hydroacoustic-seismic conversion. Analysis includes methods to detect, characterize, and associate signals generated by common sources. Of particular interest are methods to simultaneously analyse and fuse observations across multi-physics data sets. Additionally, we invite reports on efforts to collect and analyse the wealth of historical data.

Sr No: 626

On new aftershocks of the DPRK nuclear tests detected in April 2021

CORRESPONDING & PRESENTING AUTHOR:

Ivan Kitov, CTBTO, Austia

Ronan Le Bras, CTBTO, Austia

Christos Sagagiotis, CTBTO, Austia

Haijun Wang, CTBTO, Austia

Dozens of aftershocks have been detected by seismic stations of the International Monitoring System (IMS), particularly KSRS and USRK, as well as non-IMS stations (e.g. MDJ and SEHB), since the fifth underground announced nuclear test (DPRK5, IDC mb=5.1) was conducted on September 9, 2016 at the DPRK test site. The highest aftershock activity was observed after September 3, 2017, when the sixth underground test (DPRK6, IDC mb=6.1) was conducted. The aftershock sequence decayed following approximately the Omori law with the last significant event in June 2018 and resumed in January and March 2019. The multi-master method based on waveform cross-correlation, using some of the aftershock waveforms as templates, was developed and calibrated with the events detected after the time of DPRK5. When applied to the period of the most intensive aftershock activity it showed robust detection down to magnitudes 1.0 to 1.5. No events were detected at the area of the DPRK test site by the multi-master method after April 2019, until five new aftershocks were detected between April 18 and 20, 2021. The signals from these latest aftershocks are more similar (in the cross-correlation sense) to the events observed immediately after the DPRK5 and to those observed in March 2018 and April 2019.

KEYWORDS :   aftershocks, nuclear tests, seismic waves

Sr No: 627

Review I09BR Infrasound Detection

Brandow Neri, Seismological Observatory of Brasilia University, Brazil

CORRESPONDING & PRESENTING AUTHOR:

Lucas Barros, Seismological Observatory of Brasilia University, Brazil

Arthur Macedo, Seismological Observatory of Brasilia University, Brazil

Leticia Assuncao, Seismological Observatory of Brasilia University, Brazil

Infrasound monitoring is one of the four technologies used by the International Monitoring System to verify compliance with CTBT. Shallow atmospheric and underground nuclear explosions can generate infrasonic waves that can be detected by infrasonic networks. Of the 60 infrasonic stations proposed by CTBT, one has been installed in Brazil since 2001. As the last nuclear tests were underground and on the Asian continent, the Brazilian infrasound station, I09BR did not detect it. However, there are several other sources of infrasound signals detected by it (mine blast, bolides, thunderstorm, human activity). This work aims to present the results of the analysis of data, highlighting the main signal sources that the I09BR station has been registering over the years.

KEYWORDS :   Brazilian monitoring, infrasound sources

Sr No: 628

Large chemical explosions of the Soviet period (1957-1988) on the territory of Kazakhstan as ground truth events

CORRESPONDING & PRESENTING AUTHOR:

Inna Sokolova, Institute of Geophysical Research NNC RK, Kazakhstan

Irina Aristova, Institute of Geophysical Research NNC RK, Kazakhstan

Alexandr Velikanov, Institute of Geophysical Research NNC RK, Kazakhstan

Darkhan Komekbayev, Institute of Geophysical Research NNC RK, Kazakhstan

In Soviet time, large chemical explosions were conducted on the territory of Kazakhstan with different purposes (industrial, scientific purposes, military). The parameters of these explosions are known quite well, but can be precised by special investigations using contemporary methods. Further these explosions can be used as ground-truth events for the calibration of the regional seismic networks in Central Asia. These explosions are: investigative explosions "Kabulsay" in the south of Kazakhstan, Arys 19.12.1957, yield 1000 t; double explosions for construction of a mudflow dam near Almaty: Medeo 21.10.1966, (1689 t and 3604 t) and Medeo 14.04.1967 (3940 and 1944 t); investigation explosion "Massa" near Almaty, 28.11.1981 (251 t); investigative explosions in Central Kazakhstan of 9 ton yield Chemex-1 2.09.1987 and Chemex-2 3.09.1987. In addition, on the territory of Semipalatinsk Test Site there were 175 chemical explosions conducted for military and scientific purposes; the parameters are known for ~30 explosions. For these explosions, using the historical analog seismogams and published data, the source parameters were precised, the catalogue and seismic bulletin were compiled. The kinematic and dynamic parameters of records were investigated, regional travel-time curves were constructed. The seismic effect of the investigated explosions was compared with that of other large chemical explosions conducted on Central Asia territory.

KEYWORDS : ground truth events, large chemical explosions, Central Asia

Sr No: 629

Application of explosions records of 1997-2002 conducted on the territory of the Semipalatinsk Test Site for seismic calibration tasks

Natalya Mikhailova, Institute of Geophysical Research NNC RK, Kazakhstan

CORRESPONDING & PRESENTING AUTHOR:

Inna Sokolova, Institute of Geophysical Research NNC RK, Kazakhstan

Irina Aristova, Institute of Geophysical Research NNC RK, Kazakhstan

From 1997 to 2000 at the former Semipalatinsk Test Site there was a series of explosions aimed at destructing the nuclear tests infrastructure at Balapan and Degelen sites. On September 14, 2002 there was another explosion within the On-Site Inspection training. The explosion records received from temporary and permanent seismic stations were used for the seismic calibration tasks.
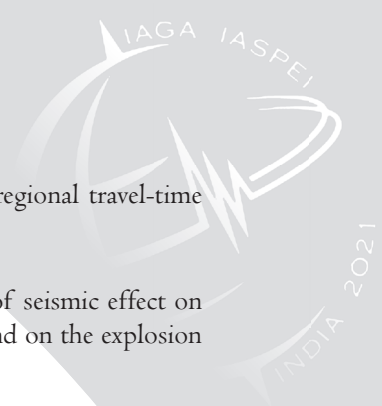
The data of the calibration explosion series in 1997-2002 were used to construct a regional travel-time curve that is currently applied by KNDC for seismic events location.

For each explosion, the energy class and magnitude were determined, the dependence of seismic effect on explosion yield, depth of charge, characteristics of medium in the field of explosion, and on the explosion mechanism were studied.

The received results should be considered at the planning of next calibration experiments.

KEYWORDS : semipalatinsk test site, calibration explosions

Sr No: 630

SYMPOSIUM : **S8 CoSOI Advances in geophysics, atmospheric science, and signal analysis for monitoring the CTBT**

Infrasound Generation From The 2017 DPRK Underground Explosion

CORRESPONDING & PRESENTING AUTHOR:
Keith Mclaughlin, Leidos, USA
Jeff Stevens, Leidos, USA

We use the Rayleigh Integral (see Pierce 1981) with numerical results of Stevens and O'Brien (2018) to compute far-field infrasound from the September 3, 2017 DPRK underground explosion. Stevens and O'Brien's (2018) 3D non-linear simulation with topography, non-linear deformation, and spall predicts enhanced spall on Mt. Mantap's southern flank. The spall asymmetry and southern flank inclination enhances southerly radiation with a distinctive modulated spectral spall signature.

We analyzed recordings at IMS array IS45 to the northwest and ROK KIGAM arrays to south and southwest (KSGAR, CHNAR, KMPAR, YPDAR, and BSDAR). We computed transmission loss (TL) using NCPAprop infrasound propagation codes and the G2S atmospheric model (wind and temperature profiles). Eigenray propagated amplitudes to IS45, CHNAR, KMPAR and YPDAR are comparable to observations. Parabolic equation (PE) TL agrees with IS45 observations, but overestimates attenuation to arrays south and southwest. Stratospheric arrivals at multiple arrays exhibit modulated spectra consistent with the spall signature (0.5 Hz spectral peak).

Pierce, A. D. (1981) Acoustics, An Introduction To Its Physical Principals and Applications, McGraw Hill, 534 pages.

Stevens, J. L. and M. O'Brien (2018), "3D Nonlinear Calculation of the 2017 North Korean Nuclear Test, " Seismological Research Letters, 89, 2068-2077. doi: 10.1785/0220180099.

KEYWORDS : infrasound, spall, explosion

S9 CoSOI Cryoseismology

CONVENERS: Myrto Pirli (Norway)

Masaki Kanao, (Japan)

Paul Winberry (USA)

Douglas Wiens (USA)

Insight into cryospheric dynamics is of utmost importance to a wide spectrum of scientific fields, from glaciology and polar climate research to projections of sea level rise. During the last decade, a growing volume of literature has been establishing cryoseismology as a very appropriate interdisciplinary tool to answer questions on diverse dynamic processes in the cryosphere, from ice-shelf crevassing and iceberg detachment, to glacier surging, basal stick-slip and tidally induced grounding-line migration, as well as phenomena related to subglacial water flow. In addition, techniques such as seismic interferometry and H/V spectral ratios of ambient noise have been emerging as potent tools to gain knowledge on the structure of shallow ice layers and changes in the permafrost.

We invite contributions on all topics of cryoseismological research, covering both the Arctic and Antarctica, as well as mountain glaciers in temperate climates.

Sr No: 631

Cryoseismologic studies for polar environment - recent progress of Japanese contribution

CORRESPONDING & PRESENTING AUTHOR:

Masaki Kanao, National Institute of Polar Research, Japan

Majority areas of Antarctica and Greenland are under the thick ice sheet and characterized by evolving cryosphere surroundings. In the polar region, associated with the recent trend on climate change such as global warming, glacier relating earthquakes are increasing during this 21st century. In this paper, a decade of progress in "Cryoseismology" at bi-polar regions is reviewed by focusing on the contribution from Japanese researchers. In particular, the specific cryoseismic events are treated, which occurred in the coastal area of East Antarctica, around the Lützow-Holm Bay, together with the coast and whole inland area of Greenland. As the major scientific results, frequency-overtone signals in the harmonic cryoseismic tremors were analyzed by assuming constant sources, suggesting inter-glacial asperities that generate characteristic tremors. Infrasound source locations were also determined by using the array deployment at the coastal regions in the Antarctic. In contrast, characteristics of glacial earthquakes and seismic interferometry approach has been conducted so as to achieve the fine structure of the Greenland Ice Sheet (GrIS) in particular the basal condition beneath the ice sheet.

KEYWORDS : cryoseismology, climate change, polar regions

Sr No: 632

Swell-Triggered Seismicity at the Near-Front Damage Zone of the Ross Ice Shelf (by invitation)

CORRESPONDING & PRESENTING AUTHOR:

Richard Aster, Colorado State University, USA

Bradley Lipovsky, University of Washington, USA

Peter Bromirski, University of California, San Diego, USA

Peter Gerstoft, University of California, San Diego, USA

Andrew Nyblade, Penn State University 16802, USA

Douglas Wiens, Washington University, USA

Ralph Stephen, Woods Hole Oceanographic Institution, USA

A 2014–2017 deployment of broadband seismographs on the Ross Ice shelf, which included three stations sited, approximately, 2 km from the ice front, reveals prolific swell-associated triggering of discrete near-ice-front (magnitude≥0) seismic subevents, for which we identify three generic types. During some strong swell episodes, subevent timing becomes sufficiently phase-locked with swell excitation, to create prominent harmonic features in spectra calculated across sufficiently long time windows via a Dirac comb effect, for which we articulate a theoretical development for randomized interevent times. These events are discretely observable at mnear-front stations, have dominant frequency content between 0.5 and 20 Hz, and, in many cases, show highly repetitive waveforms. Matched filtering detection and analysis shows that events occur at a low-background rate during all swell states but become particularly strongly excited during large amplitude swell at rates of up to many thousands per day.

The superimposed elastic energy from swell-triggered sources illuminates the shelf interior as extensional (elastic plate) Lamb waves that are observable more than 100 km from the ice edge. Seismic swarms show threshold excitation and hysteresis with respect to rising and falling swell excitation. This behavior is consistent with repeated seismogenic fracture excitation and growth within a near-ice-front damage zone, encompassing fracture features seen in satellite imagery. A much smaller population of distinctly larger near-front seismic events, previously noted to be weakly associated with extended periods of swell perturbation, likely indicate calving or other larger-scale ice failures near the shelf front.

KEYWORDS : seismology, ice shelves, ocean swell

Sr No: 633

SYMPOSIUM : **S9 CoSOI Cryoseismology**

Icequakes in Patagonia - Chile Approximation based on seismic analysis with passive networks in the Magallanes Region - Chile

CORRESPONDING & PRESENTING AUTHOR:

Edgardo Casanova, Universidad de Magallanes, Chile.

Gino Casassa, Universidad de Magallanes, Chile.

Ricardo Jana, Instituto Antártico Chileno, Chile

Sergio Barrientos, Universidad de Chile

INTRODUCTION

Glacier quakes occur by flow and mechanical deformations associated with basal sliding, surface fracturing, water transport in their internal and basal layers, frontal calving and other processes resulting from forces interaction. Several techniques have been developed to analyze the tremors of glaciers, however, elements such as temporal resolution, spatial coverage, the complexity of access and others, often limit the possibilities of systematic monitoring for some glaciers, as like those located in the Southern Patagonian Icefield.

Methods

In this research, data from 13 seismic broadband stations both permanent and part of temporary deployment are used to identify the seismicity (locate events, describe its frequencies and analyze variables to allow a better characterization of the triggering process).

To correlate the seismic analysis with the glacial dynamics, surface ice flow velocity will be studied of glaciers that concentrate a large number of earthquakes, thus presenting more elements to study the basal sliding, stick-slip processes and surface deformation in the generation of seismic signals.

In cases where seismic signals are attributed to frontal calving events the analysis is supported with optical satellite images and terrestrial photography to correlate the recorded seismic signals with the identification of precursory crevasses in the glacier front and the occurrence of nearby floating icebergs.

Results

The reference seismic catalog is being generated, along with preliminary identification of calving events in photographs, satellite images and seismic recordings.

Conclusion

The research allows the recognition. of icequakes events in the study glaciers, being a first approximation of subsequent more detailed studies.

KEYWORDS : cryoseismology, Southern Patagonian Ice Field, remote sensing

Sr No: 634

Improved early-warning of subglacial floods based on seismological data (by invitation)

CORRESPONDING & PRESENTING AUTHOR:

Eva Elbi, University of Potsdam, Germany

Christopher Bean, Dublin Institute for Advanced Studies, Ireland

Kristin Vogfjord, Icelandic Meteorological Office, Iceland

Bergur Einarsson, Icelandic Meteorological Office, Iceland

Finnur Palsson, University of Iceland, Iceland

Glaciated areas host subglacial or glacier dammed lakes that accumulate glacial meltwater, geothermal meltwater and precipitation. Eventually, these lakes drain and cause devastating floods in the glacial foreland. In Iceland, these floods drain subglacially and are visually detected once they enter the glacial river. However, at this point they already travelled several tens of kilometers beneath the ice. We demonstrate how to advance early-warning potential through the analysis of four such floods in a glaciated region of Iceland. Comparing exceptional multidisciplinary hydrological, GPS and seismic ground vibration (tremor) data, we show that array analysis of seismic tremor can be used for early location and tracking of the subglacial flood front. We find that an order of magnitude larger floods travel twice as fast. Furthermore, the timing and size of the impending flood might be estimated based on the tremor amplitude prior to it entering the river system. Advanced warnings of between 20 to 34 hours are achieved for floods with peak discharges in the range of $3000 \text{ m}^3/\text{s}$ to $210 \text{ m}^3/\text{s}$, respectively.

KEYWORDS : volcano-seismology, subglacial floods, early-warning

Sr No: 635

Constraining Floating Ice Shelf Structures by Spectral Response of Teleseismic P-Wave Coda: Ross Ice Shelf, Antarctica

CORRESPONDING & PRESENTING AUTHOR:

Thanh Son Pham, Australian National University, Australia

Hrvoje Tkalcic, Australian National University, Australia

The recent deployment of a broadband seismic array on the floating ice shelf in the Antarctica's Ross sea presents a great opportunity to study the shelf structure using broadband seismic data. In this study, we develop a further improvement of the P-wave coda autocorrelation method, which proved capable of characterizing grounded ice-cap structures. Ice shelves are floating ice sheets connected to a landmass, and in order to decipher their structures, a water layer has to be added to the problem.

We construct the power spectrum stacks of P-wave coda data, waveform records that immediately follow P arrivals, in the spectral domain, which are equivalent, via a Fourier transform, to widely used autocorrelograms in the time domain. At half of temporary seismic stations under consideration, we report prominent resonant peaks in the spectral autocorrelograms, associated with the ice-water configuration of the ice shelf. The lack of clear resonant pattern for the rest of the stations is suspected due to a high

noise level in the icy environment and significant lateral heterogeneity at the local scale. Subsequently, we develop a formalism to explain the observed resonance and devise a grid-search scheme to estimate ice- and water-thicknesses underneath the stations. Our water-thickness estimates agree well with the previously documented measurements, but there is a discrepancy in the ice thickness results. Therefore, the method has a great potential to complement the existing ice-shelf model, to be used in future monitoring applications of ice shelves, or near-future space exploration to icy planets.

KEYWORDS : P wave coda; autocorrelation; Antarctica

Sr No: 636

SYMPOSIUM : **S9 CoSOI Cryoseismology**

Tracking moulin re-awakening with glacial seismicity at the Russell Glacier, Greenland

CORRESPONDING AUTHOR:
Bernd Kulessa, Swansea University, UK
Glenn Jones, Swansea University, UK

PRESENTING AUTHOR:
Kate Swan, University of Leeds, UK
Corinna Roy, University of Leeds, UK
Andy Nowacki, University of Leeds, UK

Moulins collectively move large amounts of water from the surface to the base of ice sheets, potentially affecting their basal dynamics. However, understanding of how and when moulins re-activate at the start of a melt season is limited, causing high uncertainties in moulins' role in controlling ice flows. We examine data recorded in summer 2011 by a seismic-geodetic deployment in the Russell Glacier on the west Greenland ice sheet. Six geophones were placed around a moulin which formed in 2010, 50 km from the land termination of the glacier.

Many thousands of seismic events are identified using an STA/LTA algorithm to pick onsets and an event association procedure. This catalogue shows multiple peaks in seismicity in June, which we attribute to moulin reactivation. Increases in noise before and during this period appear to relate to increased surface cracking and water flow, as evidenced by a strong 24-hour periodicity in the seismicity.

For a number of large events, we manually pick seismic arrivals and locate the events. Preliminary results suggest most seismic activity occurs either at depth directly below the surface expression of the moulin, or near the surface to the east, where surface water flows west into the moulin. The locations suggest possible englacial seismicity distal to the moulin, also to the east, suggesting a network of melt-carrying structures within the ice which coalesce at the moulin to deliver water rapidly to the glacier bed. Further work will verify how this activity changes through time and how the moulin reactivates.

KEYWORDS : moulin, glacier, cryoseismology

Sr No: 637

Seismic Monitoring for Accurate Spatio-Temporal Location and Possible Early Warning of Himalayan Geo-Hazards

CORRESPONDING & PRESENTING AUTHOR:

Purnachandra Rao, National Geophysical Research Institute, India

Rajesh Rekapalli, National Geophysical Research Institute, India

Kristen Cook, German Research Centre for Geosciences, Germany

Michael Dietze, German Research Centre for Geosciences, Germany

Himangshu Paul, National Geophysical Research Institute, India

D. Srinagesh, National Geophysical Research Institute, India

Virendra Tiwari, National Geophysical Research Institute, India

Niels Hovius, German Research Centre for Geosciences, Germany

Conventionally seismic networks have been used for earthquake monitoring and related studies. However, recent developments have hinted at a greater role of these networks for detection, location and early warning of a suite of geohazards like rockslides, avalanches, debris flow, Glacial retreats, floods, etc. The recent catastrophes in Himalaya on 7 February 2021 and 23 April 2021 associated with rockslide and glacial outburst respectively claimed over a hundred lives, demonstrating the urgent need for development of a real time detection and early warning system for hazard mitigation in the Himalaya. The 7 Feb event was recorded on several stations of the dense seismic network of CSIR-NGRI set up in the Uttarakhand region and our analysis suggests the detectability of landslide, debris flow and flood signals above the threshold noise levels as compared to the event of 23 April. Analysis of the seismic data also enables tracking of the mass transport during flood. Based on these observations, it appears feasible to develop a Geo-Hazard Early Warning system for the Himalayan region through integrated analysis of real time data from seismological networks, supported by satellite and water level data. An in-depth analysis of several such events from the past with the help of AI/ML tools may possibly enable us to develop a framework for an early warning system that alerts the downstream communities shortly after event initiation.

KEYWORDS : geohazard, seismic network, early warning

S10 CoSHRSGM Site and Source Modeling for Urban Seismic Microzonation Studies

CONVENERS: Prantik Mandal (India)
Utpal Dutta (USA)

During the last two decades, the world had witnessed several devastating earthquakes at various places, e.g., 2001 Mw7.7 Bhuj (India), 2004 Mw9.3 Sumatra (India), 2005 Mw7.6 Kashmir (India), 2008 Mw7.9 Wenchuan (China), 2010 Mw7.1 Canterbury (New Zealand), 2011 Mw9.0 Tohoku (Japan), and 2015 Mw7.9 Kathmandu (Nepal). These earthquakes caused not only substantial damages to buildings, dwellings, and other critical infrastructural facilities due to poor construction practices but also were responsible for the loss of thousands of human lives. With the rapid growth in seismic instrumentation and advancement in data communication, the dense seismic monitoring at many high-risk urban areas is currently in operation to minimize infrastructural losses and casualties by adopting better engineering practices based on knowledge gained from the analysis of recorded seismic data. The seismic microzonation of these urban areas is studied using accurate assessment of the site and local source characteristics, which form the basis of the preparedness to mitigate the earthquake hazard and help to develop an earthquake resilient society. To reflect the modern advancements in the modeling of earthquake data for rapid assessment of the site and, source processes associated with large devastating earthquakes, and to foster inter-disciplinary and international exchange and cooperation, this session focuses on, but not limited to, the following topics:

Seismogenesis of devastating large earthquakes, 2) Evaluation of seismic hazards associated with large earthquakes, 3) Study of source scaling of earthquakes, 4) Microzonation studies including site response, shallow Vs30m and hazard mapping at a local scale, 5) Impact of soil non-linearity during large earthquakes.

Sr No: 638

Assessment of Soil Liquefaction characteristic based on Shear Wave Velocity measurements beneath the soil of the NCR Delhi, India: An Implication of Designing Earthquake Resilience Structures.

CORRESPONDING & PRESENTING AUTHOR:

Himangshu Sekhar Mandal, National Centre for Seismology, India

Sasi Kiran Gera, National Centre for Seismology, India

Om Praksh Mishra, National Centre for Seismology, India

An attempt has been made to understand the soil liquefaction characteristic based on shearwave velcities(V_s) beneath the soil of National Capital Territory(NCT) Delhi, India. Down Hole Test(DHT) was conducted at 25 selected sites over a sprawl of 1483sq.km area. The Vs data were measured at each site at @1.5m interval down to the depth up to 30m. A volume of about 500 Vs data points are collected from all these 25 sites. The Vs data are stress corrected and are used to estimate the strength of the soil in the form of Cyclic Resistance Ratio(CRR). On the otherhand the Cyclic Stress Ratio (CSR) is estimated from the Surface Peak Ground Acceleration and the Coefficeient of Stress Reduction Factor. The Factor of safety(FS) is estimated from the ratio of CRR and CSR with Magnitude Scale Factor (MSF) for a given moment magnitude of earthquake. Here, we have considered maximum moment magnitude value of 7.5 corresponding to MSF=1.0. Golbally, it is known that, if FS<1.0 then soil can liquefy else it can't. However, study shows that value of FS alone is not indicate the complete liquefaction; to over come this situation, probability of liquefaction(PL) is introduced in this study for better understanding the soil liquefaction criteria. Results shows that western part of Delhi located on older alluvium soil has lesser chances of liquefaction then the eastern part of Trans-Yamuna areas of Delhi. These results may be useful for the designing to counter measure of liquefaction for designing earthquake resistance structures over the NCR Delhi.

Sr No: 639

Improved Treatment of Site Amplification in the 6th Generation Seismic Hazard Model of Canada

CORRESPONDING & PRESENTING AUTHOR:

John Adams, Natural Resources Canada

Michal Kolaj, Natural Resources Canada

Stephen Halchuk, Natural Resources Canada

Canada's 6th Generation seismic hazard model has been released (https://doi.org/10.4095/327322), and is proposed for use in the still-pending 2020 National Building Code of Canada. The new model includes recent advancements in our understanding of: recurrence of great subduction earthquakes; revisions

in the geometry of deep inslab earthquakes; inclusion of newly-discovered potentially-active faults; and the adoption of new ground motion models. Moreover, the model has now been fully transitioned from legacy software to the OpenQuake platform. For the first time in Canada, seismic hazard is now computed directly for various site conditions and provided to the end-user for their specific Site Class and/or Vs30 (time-averaged shear wave velocities in the upper 30 m of the crust). This approach removes the need for separate site amplification look-up tables in the building code, improves the reliability of the results and simplifies the way end-users will determine seismic design values. Because of the computational load, direct calculation at each users' location and its Vs30 is impracticable. Instead three levels of interpolation from pre-computed values are used: interpolation of the hazard curve at discrete hazard values to get the hazard at the required probability; interpolation in space between adaptive-grid calculated values at circa 35, 000 points, and interpolation between fifteen Vs30 values to get hazard at the site's Vs30. In most cases the interpolations give values within a few percent of the direct-calculated values, i.e., trivially different in an engineering sense. Interestingly, the somewhat large uncertainty in Vs30 determinations seldom translates into similarly large errors in the final hazard values to be used.

KEYWORDS : seismic, hazard, amplification

Sr No: 640

Implementation of an updated seismic source model for South Africa

CORRESPONDING & PRESENTING AUTHOR:
Vunganai Midzi, Council for Geoscience, South Africa
Thifhelimbilu Mulabisana, Council for Geoscience, South Africa
Brassnavy Manzunzu, Council for Geoscience, South Africa

Presented here is a report on a new seismic source model updated from the previous model used in the 2020 version of the seismic hazard maps of South Africa. The identification and characterization of seismic sources process requires the interpretation of available seismological, geophysical, geological and tectonic data. The updated seismic source model employed updated data, new data types and source parameters that reflect the current state of knowledge of earthquake occurrence in the region. Presented is a comprehensive description of the different delineated seismic sources, made up of 27 area source zones as well as three fault sources (Kango, Dreylingen / Hebron and Tshipise / Bosbokpoort faults). Using the above mentioned data as well as a focal mechanism database, we characterised all identified seismic sources. Parameters determined include recurrence parameters (b-value, a –value and maximum expected magnitude), predominant focal mechanism for each source, seismogenic depth and earthquake depths values as well as recurrence rates for the fault sources. Given the epistemic uncertainty associated with most of these parameters, alternative values were determined that were implemented in the hazard calculations using a logic tree technique. The proposed seismic source model and its related parameters has now been implemented in preliminary seismic hazard calculations for South Africa. On comparing the new hazard results, it is clear that the new source model has significantly affected the calculated seismic hazard of the country. Further sensitivity investigations continue to be made to completely assess its impact.

KEYWORDS : seismic sources, seismicity, seismic hazard

Seismic potential of megathrust in the Kumaun-Garhwal region of NW Himalaya: implications from geodetic and seismic strain rates

CORRESPONDING & PRESENTING AUTHOR:

Sapna Ghavri, Bihar Mausam Seva Kendra Society, Planning and Development Department, Patna, India

Sridevi Jade, CSIR-4PI, India

We analysed the geodetic and seismic strain rates for composite analysis of seismic hazard potential of the Kumaun-Garhwal region of Northwest Himalaya. The principal geodetic strain rate is estimated using plate motion measurements at 144 Global Positioning System (GPS) sites reported in past ~ 20 years in the region. A modified least square inversion approach that utilizes a distance-based scale factor on the uncertainty in the velocity data is applied to get a reliable estimate of geodetic strain rate. Results indicate extensive compression in the region with a mean rate of -113 nano strain/year towards NNE in the Higher Himalaya. The principal seismic strain rate is calculated from the focal mechanism solutions of the earthquakes in the region using the Kostrov formulation. We analysed the geodetic strain rate together with seismic strain rate using seismicity catalogue of 50, 220 and 700 years and found that the orientation of principal strain rates are consistent with each other. However, the seismic strain rate estimated from 700 years catalogue is comparable with geodetic strain rate indicating the high accumulation of elastic strain energy in this region. Analysis of strain budget using geodetic and seismic moment rates of this region, suggest a large amount of stored strain energy of ~5E+21 Nm in the past 700 years which has the potential to generate a megathrust earthquake (($Mw \geq 8$)) in the present scenario.

KEYWORDS :   strain, geodetic, seismic

Nonlinear Site Response Observed at Strong-Motion Stations in Anchorage, Alaska from the 2018 Mw 7.1 Anchorage Earthquake

CORRESPONDING & PRESENTING AUTHOR:

John Thornley, Golder Associates, UK

Utpal Dutta, University of Alaska Anchorage, USA

John Douglas, University of Strathclyde, UK

Zhaohui Joey Yang, University of Alaska Anchorage, USA

On 30 November 2018 the population of southcentral Alaska was impacted by the most damaging earthquake since the devastating 1964 Great Alaska Earthquake. While much of the damage experienced in 2018 was related to nonstructural failures, there were observations of ground failure throughout Anchorage, which is Alaska's most populous city. Since the 1990s a network of digital strong-motion stations has been installed across Anchorage and that network recorded numerous earthquakes in the years prior to the 2018 event and several aftershocks. The generalized inversion technique (GIT) is used to evaluate the spectral amplification for events greater than Mw 4.5. The results of the smaller earthquakes are compared with the results from the Mw 7.1 2018 event to evaluate which strong-motion stations experienced nonlinear

site effects as a result of the damaging event. As an additional verification, a recent Mw 7.1 earthquake, the January 2016 Iniskin Earthquake, which was felt in Anchorage with an epicenter of 260km away, is also used to evaluate the site response nonlinearity. The results of this study indicate that the sites with shallower soil over rock, which are also stiffer, did not experience nonlinear site response. However, as the depth of soil increased the nonlinear site response became much more evident. This was especially evident at sites with soft soil. The comparison with the 2016 Iniskin event also shows similar results. The findings from this study can be used to further understand the variability of site response across Anchorage.

KEYWORDS :   microzonation, site effects, nonlinear response

Sr No: 643

- -

SYMPOSIUM :   **S10 CoSHRSGM Site and Source Modeling for Urban Seismic Microzonation Studies**

Impact of site amplification on seismic hazard disaggregation

CORRESPONDING & PRESENTING AUTHOR:

Michal Kolaj, Natural Resources Canada

John Adams, Natural Resources Canada

Stephen Halchuk, Natural Resources Canada

Disaggregation of seismic hazard values is required in order to understand the predominant sources of hazard and is a necessary tool for the selection of design earthquakes for scenario-based assessments, representative time histories, and other engineering studies. Canada's 6th Generation seismic hazard model (CanadaSHM6) was released in 2020 and is currently proposed for the 2020 edition of the National Building Code of Canada. A major change in CanadaSHM6 is the move from a single-reference condition (Site Class C) to directly calculating and providing to the end-user hazard values for their specific site condition as parameterized by either Site Class or Vs30 (time-averaged shear wave velocities in the upper 30 m of the crust). Similarly, while disaggregation was only previously possible for the single reference condition, users can now disaggregate hazard for their site's specific site conditions. This is especially important for soft soil sites, where the shape of the disaggregation can be highly influenced by the degree of non-linear response to strong shaking. This presentation will show CanadaSHM6 disaggregations computed using the OpenQuake engine and how the shape of the disaggregation and the key parameters (such as the mean magnitude, distance and epsilon) vary as a function of site conditions for key localities in Canada.

KEYWORDS :   seismic hazard, disaggregation, Canada

Sr No: 644

- -

SYMPOSIUM :   **S10 CoSHRSGM Site and Source Modeling for Urban Seismic Microzonation Studies**

Energy-based method to estimate corner periods of response spectra reflecting the physics of strong ground motions

CORRESPONDING & PRESENTING AUTHOR:

Ayushi Tiwari, NGRI, India

Srinagesh Davuluri, NGRI, India

Asha Kiran, IITM, India
Murty CVR, IITM, India

Characteristics of earthquake ground motions are captured in the 5% damped response spectra and represented by Tripartite Graph (TGs) having acceleration-, velocity-and displacement-sensitive regions. The shape of the TG is influenced by source, path, and site characteristics. Hence, for the same earthquake event, the TGs are different in the near- and far-fields; energy released during the earthquake, fault rupture mechanics, attenuation of motions from fault to recording station and the attenuation/amplification of motions by the geological and geotechnical strata at recording stations determine the two corner periods on the TG separating the three regions.

This paper presents engineering characteristics of strong ground motions at different sites, which are controlled by the physics of the source, path, and site effects. Qualitative and quantitative influences on the Tripartite Graphs of ground motions are presented: (a) in the near- and far-fields; and (b) in rock, shallow soil, and deep sediment strata. A quantitative method is proposed (using specific energy of ground shaking) to identify the corner periods on the TG, which are compared with those obtained by the conventional method (using PGA, PGV, and PGD). The corner periods are close to each other in the near-field, and well separated in the far-field and close to each other at the rock stratum, and well separated in the deep sediment stratum. The second corner period, which defines the design displacement response spectrum at a site, is affected by corrections applied to strong ground motions, and hence extra care is needed while applying such corrections.

KEYWORDS :   response spectra, corner periods, strong ground motion

Sr No: 645

SYMPOSIUM :   **S10 CoSHRSGM Site and Source Modeling for Urban Seismic Microzonation Studies**

Lithospheric block-and-fault dynamics modelling: What did we learn about large earthquake occurrences and seismic hazard? (by invitation)

CORRESPONDING & PRESENTING AUTHOR:
Alik Ismail Zadeh, Karlsruhe Institute of Technology, Germany
Alexander Soloviev, Russian Academy of Sciences, Russia

Understanding of lithosphere dynamics, tectonic stress localisation, and large earthquake occurrences would assist in seismic hazard assessments. Numerical modelling of lithosphere dynamics and earthquake simulations have been changing our view about localisations of large earthquakes in a system of major regional faults and about the recurrence time of the earthquakes. Here we overview the thirty-year efforts in modelling of lithospheric block-and-fault dynamics allowing to study how the blocks react to the lithospheric plate motion, how stresses are localised and released in earthquakes, where large seismic events occur, what is the recurrence time of these events, and how fault zones properties influence the earthquake dynamics. A few key factors influencing the earthquake sequences, clustering, and magnitude are identified including lithospheric plate driving forces, the geometry of fault zones, and their physical properties. We illustrate the effects of the key factors by analysing block-and-fault dynamics models applied to earthquake-prone regions. This work was partially supported by the Russian Foundation for Basic Research (grant 20-55-18008).

KEYWORDS :   tectonic stress; seismicity; earthquake simulation

Sr No: 646

Study the effects of soil layering on the basin-edge induced surface waves and aggravation factor

CORRESPONDING & PRESENTING AUTHOR:

Sanjay Kumar, CSIR-Natiioal Geohysicsl Research Institute, India

The current practice of seismic microzonation in most of the countries to transfer the bed rock motion to the surface using one-dimensional (1-D) S-wave response of a soil column. Theoretical and observational studies have revealed that basin-edge, subsurface topography and strong lateral discontinuities (SLD) can induced surface waves. The 1-D response of a soil layer was inadequate to explain the observed damage due to basin edge induced surface waves in Santa Monica during the 1994 Northridge earthquake and in Kobe basin during the 1995 Kobe, Japan earthquake. Therefore, the incorporation of 2D/3D site effects in seismic microzonation is essential. The Aggravation factor (AF) at different locations computed just by taking the ratio of spectra of response of 2D basin model to the 1D response that is normally accounted for in building codes. Our simulated results shows largest values of average AF of the order of 1.91 and 2.49 at an offset of 30 m from SLD and basin-edge models. The shape of spectral aggravation factor is highly variable with offset from SLD/basin-edge, which may be due to the dispersive nature of Love waves. Based on the trend of decrease of AAF and the maximum strain with offset from the basin-edge, we can qualitatively inferred that the effects of induced Love wave may reduce to a negligible value after a travelled distance of 6.5-10.0. (where is the wavelength corresponding to the fundamental frequency F0 of a soil layer).

Sr No: 647

Simultaneous estimation of site response and source parameters of reservoir-triggered earthquakes using data from borehole seismic network in the Koyna-Warna seismic zone, Maharashtra, India

Satyanarayana Hari Venkata Subramanya, CSIR-NGRI, Hyderabad, India

CORRESPONDING & PRESENTING AUTHOR:

Prantik Mandal, CSIR-NGRI, Hyderabad, India
D Shashidhar, CSIR-NGRI, Hyderabad, India
Arti Devi, CSIR-NGRI, Hyderabad, India
D Srinagesh, CSIR-NGRI, Hyderabad, India

The horizontal components of S-wave data from 25 Koyna-Warna events (Mw 2.0–4.0) recorded at five borehole seismograph sites were analyzed to estimate the site response and source parameters. In the 0.2–1.8 Hz frequency band, the high site response values (1.73-1.85) were observed to be associated with the regions west of the Warna reservoir. In the 3–7 Hz frequency band, the average site response estimates suggest a maximum value of 1.91 at the UBH site (near the Warna reservoir) and a minimum value of 1.7 at
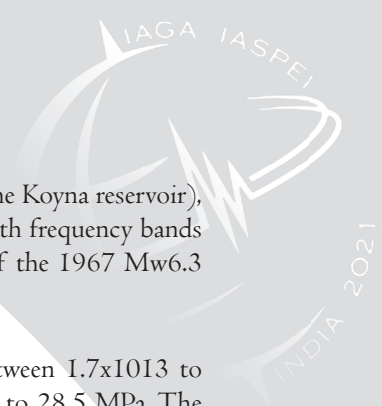
the NBH site on the western side of the Warna reservoir. While at the RBH site (near the Koyna reservoir), SR at 3-7 Hz shows a value of 1.74. At the FBH site, average site response values at both frequency bands reveal a high value of 1.85, which lies in the SW extension of the main fissure zone of the 1967 Mw6.3 Koyna earthquake.

The modelled seismic moment (Mo) and source radius (r) of earthquakes are in between 1.7×10^{13} to 3.2×10^{15} N-m and 119 to 355 m, respectively, while stress drops (Ds) vary from 1.6 to 28.5 MPa. The estimated relation $Mofc3.5 = 1.1 \times 10^{17}$ Nm/s3 between the moment and corner frequency agrees well with the relation for the other seismically active areas in the world. The modelled stress drops and seismic moment are found to satisfy the following relation:

$$\log10Mo(N\text{-}m) = 13.32 + 0.9184 \log10Ds\ (MPa).$$

Also, modelled Zuniga parameters (e>1) suggest a frictional overshoot stress drop rupture model for the Koyna-Warna earthquakes.

KEYWORDS : site response, source parameters, simultaneous inversion

Sr No: 648

Strong Motion Estimation in Costa Rica at Specific Sites Using Spectral Inversion Method

PRESENTING AUTHOR:

Nathalie Esquivel, Costa Rica

CORRESPONDING AUTHOR:

Toshiaki Yokoi, Building Research Institute, Japan

Takumi Hayashida, Building Research Institute, Japan

We performed the spectral inversion to separate the source, path, and site effects using strong ground motion records from facilities as essential as powerhouses and hydroelectric dams of Costa Rica. We conducted the spectral inversion technique adapted for a sparsely observed strong motion dataset. The results were used to estimate acceleration spectra of the strong ground motion at specific sites in and around the intensity anomaly that appeared during the 2012 Sámara earthquake of Mw 7.6. To ensure the quality, we incorporated the broadband station JTS of IRIS/IDA to estimate the source spectra' acceleration levels of six events. Then conducted the spectral inversion by using them as the reference events. We introduced two consistency checks: one to confirm the correctness of the input data; another to verify the output using synthetic spectra. The consistency checks were used in an interactive mode by elimination of suspicious data and inversions. For the final inversion, the source spectra of the reference events were also regulated by considering the site effect for one-dimensional SH-wave propagation at the site of the lowest site effect. We obtained the frequency-dependent quality factor $Q = 179f0.5598$ for the northern and central parts of Costa Rica. We introduced the formulation utilizing the outputs from the spectral inversion to reproduce the acceleration spectra of old earthquakes at sites that were not available during them. We tested this formulation for the 2012 Sámara earthquake at specific sites. We obtained the synthetic spectra consistent with the anomalous intensity distribution reported at that time.

KEYWORDS : site effect, synthetic acceleration spectra, spectral inversion

Sr No: 649

Non-ergodic Ground Motion Models Using Neural Networks

CORRESPONDING & PRESENTING AUTHOR:

Tomohisa Okazaki, RIKEN, Japan

Nobuyuki Morikawa, National Research Institute for Earth Science and Disaster Resilience, Japan

Asako Iwaki, National Research Institute for Earth Science and Disaster Resilience, Japan

Hiroyuki Fujiwara, National Research Institute for Earth Science and Disaster Resilience, Japan

Naonori Ueda, RIKEN, Japan

Ground motion models (GMMs), empirical relationships between ground-motion intensity and a few variables including magnitude and distance, play an essential role in probabilistic seismic hazard analysis. In the past decades, data-driven approaches such as neural networks (NNs) have been increasingly applied. However, these applications are mostly limited to "ergodic" models that do not consider geographical variation of ground motions. We present "non-ergodic" GMMs that perform site-specific and path-specific predictions using NNs.

Okazaki et al. (2021, BSSA) proposed a site-specific GMM that learns site properties from observational records. A key structure is the one-hot representation of sites, which specifies categorical variables in an equivalent way. This enabled the model to obtain site-specific responses at data-rich sites as well as to maintain stability at data-poor sites, which lead to a considerable reduction of residuals.

The site term obtained by the above model turned out to include path and source effects. Therefore, we attempted to decompose contributions of the three effects using the following step-by-step procedure: (1) constructing an ergodic GMM using basic input variables; (2) extracting the source term from its residuals by inputting earthquake locations; (3) extracting the path term from its residuals by inputting earthquake and site locations; and (4) extracting the site term from its residuals by inputting the one-hot representation of sites. The constructed path-specific model exhibited good performance, and we discuss seismological implications of the obtained source, path and site terms.

KEYWORDS : ground motion model, neural network

S1 1 CoEGP Earthquake Generation Process & Forecasting Models

----

CONVENERS: Eleftheria Papadimitriou (Greece)

Alexey Zavyalov (Russia)

David Rhoades (New Zealand)

Rajender Kumar Chadha (India)

Petr N. Shebalin (Russia)

It is known that the process of destruction is not a momentary act, but there is a process taking place in time and space. In preparation of macro-destruction destruction process is going through a number of levels (stages), starting with the micro-scale and ending on macro-scale, including earthquake focal area. In this symposium, we invite researchers to discuss the results and directions for further research on the physics of seismic process - from experiments in laboratory conditions, rock bursts in mines and in seismically active regions during the preparation of strong earthquakes.

Special emphasis will be given to quantitative physical models of the seismic process at different scales, describing the origin of the future earthquake source and its evolution in time and space, observations on earthquake triggering by other earthquakes or nearby faults, and synchronization between nearby faults with positive stress coupling, fault system interactions controlling earthquake occurrence, the connection of smaller magnitude seismicity with stress changes as expressed through the Rate/State model, calculation of stress changes from changes in earthquake occurrence. Modeling and simulations across a wide range of spatial and temporal scales provide a better understanding source processes and interactions, and advance predictive capabilities.

Contributions are invited on all aspects of models designed to forecast earthquake occurrence in time and/or space. The development of earthquake forecasting models is being facilitated by the improvement of data and modelling inputs. Some modeling efforts are focussed on short term clustering of earthquakes, others on the time-varying probability of rupture of major fault sources, and others on the space-time-magnitude variation of the rate of earthquake occurrence in extended regions. Models can be statistical or physics based. Data inputs include the past earthquake catalogue, known or inferred dates of previous fault ruptures, modeled physical variables such as stress accumulation and strain rates, and proposed precursory phenomena. Improved methods to test the performance of forecasting models are being developed. Reports on the application of forecasts to inform the public or in support of earthquake counter measures planning are welcome.

Sr No: 650

Precursory clustering of seismicity in a parameter space before the M8.2 Chiapas, Mexico, 2017 earthquake

CORRESPONDING & PRESENTING AUTHOR:

Stanislaw Lasocki, Institute of Geophysics PAS, Poland

Vassilis Karakostas, Aristotle University of Thessaloniki, Greece

Eleftheria Papadimitriou, Aristotle University of Thessaloniki, Greece

F. Ramon Zuniga, Universidad Nacional Autónoma de México, Mexico

Our earlier studies indicated that great earthquakes might be preceded by clustering of smaller events if these events were observed in parameter spaces. In the aftermath, we investigated here the possible clustering among 1153 M4.5+ seismic events that occurred in the 18.5 years preceding the Chiapas M8.2 earthquake, from 1.01.1999 until the main shock occurrence on 8.09.2017. The events were parameterized by dt, dr, m, where, for every event, dt and dr are the time-lapse and the orthodromic epicentral distance between this and its preceding event, respectively, and m is the magnitude of this event. To render the dt, dr, m parameters comparable, we transformed them to equivalent dimensions. The degree of clustering of an ensemble of seismic events in the space of the transformed dt, dr, m was quantified by the average distance among these events and was evaluated in sliding data windows. We received distinct long-term changes of the degree of clustering comprising: (i) a decreasing trend from the beginning of the study period to the middle of 2007, (ii) a steady increase between the middle of 2007 and the end of 2014, and (iii) a comparatively faster decrease until the mainshock. These variations of the degree of clustering were definitely different regarding the systematic trends and extreme amplitudes from the degree of clustering changes obtained for permutations of the recorded event series, which proved the statistical significance of the detected precursory clustering.

KEYWORDS : Chiapas 2017 earthquake, precursory clustering, transformation to equivalent dimensions

Sr No: 651

Evaluation and retrospective forecast testing of short-term seismicity in Eastern Aegean Sea (Greece) by means of an epidemic type stochastic model

CORRESPONDING & PRESENTING AUTHOR:

Christos Kourouklas, Aristotle University of Thessaloniki, Greece

Ourania Mangira, Aristotle University of Thessaloniki, Greece

Rodolfo Console, Istituto Nazionale di Geofisica e Vulcanologia, Italy

Eleftheria Papadimitriou, Aristotle University of Thessaloniki, Greece

Vassilios Karakostas, Aristotle University of Thessaloniki, Greece

Maura Murru, Istituto Nazionale di Geofisica e Vulcanologia, Italy

The short–term earthquake clustering properties in the Eastern Aegean Sea (Greece) area are investigated through the application of an epidemic type stochastic model (Epidemic Type Earthquake Sequence; ETES). The occurrence of the recent large main shocks in 2017 Mw=6.4 Lesvos, Mw=6.6 Kos and 2020 Mw=7.0
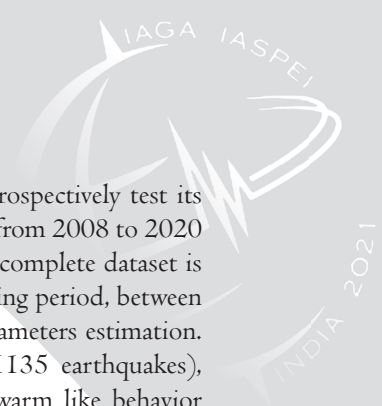
Samos offer the opportunity not only to evaluate the clustering model but also to retrospectively test its forecast skills. The analysis is performed with an earthquake catalog covering the period from 2008 to 2020 and including 2332 events with a completeness magnitude threshold of Mc=3.1. The complete dataset is separated into two distinctive subcatalogs. The first subcatalog is employed for the learning period, between 2008/01/01 to 2016/12/31 (N=1197 earthquakes) and is used for the model's parameters estimation. The second subcatalog covering the period from 2017/01/01 to 2020/11/10 (1135 earthquakes), includes the large earthquakes sequences. The estimated model parameters imply a swarm like behavior during the learning period, indicating the ability of earthquakes of small to moderate magnitude above Mc to produce their own offsprings, along with the stronger earthquakes. The retrospective forecast test of the model is investigated in the three aftershock sequences, where the lack of foreshocks resulted in low predictability of the main shocks. Immediately after the main shocks occurrence, the model adjusts with notable resemblance between the expected and observed aftershock rates, particularly for earthquakes with M≥3.5.

KEYWORDS : epidemic type model, aftershock sequences, short-term earthquake occurrence probabilities

Sr No: 652

SYMPOSIUM : **S11 CoEGP Earthquake Generation Process & Forecasting Models**

Space-Time Trade-off of Precursory Seismicity in EEPAS Forecasting of New Zealand and California Earthquakes

CORRESPONDING & PRESENTING AUTHOR:
David Rhoades, GNS Science, New Zealand
Sepideh J. Rastin, GNS Science, New Zealand
Annemarie Christophersen, GNS Science, New Zealand

'Every Earthquake a Precursor According to Scale' (EEPAS) is a medium-term earthquake forecasting model. EEPAS performs well for seismically active regions, including New Zealand (NZ) and California, and has been used for practical forecasting in NZ for a decade.

An EEPAS forecast is formed by accumulating contributions from past earthquakes to the expectation of future earthquakes. It is based on the precursory scale increase (Ψ) phenomenon and predictive scaling relations for time, magnitude and area. For a given mainshock, an identification of Ψ is represented by precursor magnitude, precursor time and precursory area. An automatic search algorithm finds multiple identifications of Ψ for most mainshocks. A trade-off between precursor time and area is observed amongst such Ψ identifications. We look for corresponding trade-offs in fitting the EEPAS model to the NZ and California catalogues. EEPAS parameters are fitted with a sequence of fixed values for the time and scaling parameters, in which the respective temporal and spatial scales vary by a factor of a hundred.

Results confirm the existence of the space-time trade-off in the EEPAS parameters fitted to both catalogues, with large spatial scales being associated with small temporal scales and vice versa.

We conclude that the space-time trade-off is an intrinsic feature of precursory seismicity. It exists independently of other factors, such as the regional strain rate, that may affect the predictive scaling relations and EEPAS model fitting.

KEYWORDS : earthquake forecasting, precursory seismicity, statistical seismology

Sr No: 653

Modeling the nonlinear influence of seasonal variations on geophysical processes and possible examples of such influence in real data

CORRESPONDING & PRESENTING AUTHOR:

Vladimir Zhuravlev, Schmidt Institute of Physics of the Earth, Russian Academy of Sciences, Moscow, 123242, Russia

The features of temporal realizations of various geophysical fields and their seasonal variations-seismic catalogs, noise at receiving stations, gps variations, magnetic field, and apparent electrical resistance are considered. An overview of the presence of a seasonal signal in real time series of various geophysical parameters is given. A wide variety of seasonal signals has been established even for the same geophysical process; examples of the absence of a season or the doubtfulness of its presence are given. Examples of the nonlinear contribution of the season are considered. Mechanisms for creating artificial time series are considered. A multiplicative model of a mixture of random noise and Flicker noise with various types of seasonal variations and other periodic components is considered. Various cases are shown when the season has a visible contribution to the model. A model for creating a random catalog of events is considered and the noise hypothesis of the appearance of a season in such a catalog is estimated. For this, modulation of such a catalog with a periodic seasonal signal was used. The noise hypothesis was tested both for events that did not fall under the noise and for those that were above the noise. When assessing the accuracy of the selection of the expected useful signal, the analysis of the possibility of filtering seasonal variations in both natural and artificial time series is carried out. The use of such methods for our earlier study of periodicity in various geophysical processes is critically examined.

KEYWORDS : long-term series of observations of geophysical parameters, analysis of spectra, seasonal mean variations

Sr No: 654

Studies of the spectrum of variations in the flow of seismic events about a calendar month

CORRESPONDING & PRESENTING AUTHOR:

Vladimir Zhuravlev, Schmidt Institute of Physics of the Earth, Russian Academy of Sciences, Moscow, 123242, Russia

For the analysis, the catalogs of earthquakes in Japan, Turkey, and the Azores were used. The spectra of the streams of such events are calculated. For weak earthquakes, the presence of a significant period of about 30 days was established.

By the method of epochs, monthly daily numbers of earthquakes were constructed for the environment. The estimate of the possible influence of the lunar tide was checked using the Harvey formula. In the general case, the amplitudes of the monthly mean curves were comparable with those similar to those according to the Harvey formula. However, in some cases, the Harvey amplitude exceeded the amplitudes of the monthly mean curves. Thus, the observed effect can be interpreted as the influence of certain monthly industrial cycles on seismicity or noise at stations, as well as the influence of the lunar tide components with periods of about 30 days. The impossibility of distinguishing between industrial impact and tide is probably due to the width of the extremum of the period of about 30 days on the spectrum and insufficient resolution.

However, the very existence of the spectrum extremum about 30 days is beyond doubt. Its identification is the more reliable, the weaker the earthquakes used for the calculations were. For Turkey, it turned out to be possible to show the great significance of the indicated spectrum peak for events from maritime territories.

KEYWORDS : Catalogs of earthquakes, lunar tide

Sr No: 655

SYMPOSIUM : **S11 CoEGP Earthquake Generation Process & Forecasting Models**

Nowcasting Earthquakes by Visualizing the Earthquake Cycle with Machine Learning: A Comparison of Two Methods

CORRESPONDING & PRESENTING AUTHOR:

John Rundle, University of California, USA
Donald Turcotte, University of California, USA
Geoffrey Fox, Indiana University, USA

The earthquake cycle of stress accumulation and release is associated with the elastic rebound hypothesis proposed by H.F. Reid following the M7.9 San Francisco earthquake of 1906. However, observing details of the actual values of time- and space-dependent tectonic stress is not possible at the present time. In two previous papers, we have proposed methods to image the earthquake cycle in California by means of proxy variables. These variables are based on correlations in patterns of small earthquakes that occur nearly continuously in time. The purpose of the present paper is to compare these two methods by evaluating their information content using decision thresholds and Receiver Operating Characteristic methods together with Shannon information entropy. Using seismic data from 1950 to present in California, we find that both methods provide nearly equivalent information on the rise and fall of earthquake correlations associated with major earthquakes in the region. We conclude that the resulting timeseries can be viewed as proxies for the cycle of stress accumulation and release associated with major tectonic activity.

KEYWORDS : nowcasting, machine learning

Sr No: 656

SYMPOSIUM : **S11 CoEGP Earthquake Generation Process & Forecasting Models**

The matrix of earthquake's genetic code – is the Etalons seismofluidogeodynmic (SFGD) "portrait" of the earthquake's focus

CORRESPONDING & PRESENTING AUTHOR:

Ramida Keramova, Azerbaijan National Academy of Sciences (RSSC at ANAS), Azerbaijan

In Azerbaijan the year-round monitoring of the seismogeodynamic regime of fluids (SFGD) spends during 1979-2021. It was established a new patterns: the final stage of earthquake's preparation is 1÷16 days; combinations of the different informative parameters of water form a reference SFGD "portrait" of a concrete seismic foci. "Portrait" is stable because water has energy-informational field - "memory". The liquid-crystal structure of its molecules archives information from the "water-rock" system, remembers-accumulates and transmits it back.

KEYWORDS : earthquake's genetic code

S12 CoEGP Interdisciplinary observations of Pre-Earthquake processes: A new approach towards Earthquake prediction studies

CONVENERS: Dimitar Ouzounov (USA)
Sergey Pulinets (Russia)
Katsumi Hattori (Japan)
Patrick Taylor (USA)

This session concerns the multi-disciplinary observations related to earthquakes, which would lead to an understanding of the physical processes preceding earthquakes. Some new results were obtained from modeling of the atmosphere-ionosphere connection and analyses of seismic records (foreshocks/aftershocks), geochemical, electromagnetic, and thermodynamic processes related to stress changes in the lithosphere, along with their statistical and physical validation. Recent large magnitude earthquakes in Asia, Central America and Europe have shown the importance of these various studies in the search for earthquake precursors either for short-term forecasting or predictions. This session will provide the next development of the topics presented in the new AGU Geophysical Monograph published this year. Presentations will include but are not limited to: observations; modeling and analyses; seismic, geochemical and electromagnetic thermodynamic processes; and case histories related to stress changes in the lithosphere along with their statistical and physical validation. Presentations on the latest developments in earthquake predictability and prospective testing associated with major earthquakes are welcomed.

Sr No: 657

The reality of operational, distance forecast of the strong earthquakes – simultaneously for different regions of the world only by the year-round monitoring of the seimogeodynamical fluids in Azerbaijan

CORRESPONDING & PRESENTING AUTHOR:

Ramida Keramova, Azerbaijan National Academy of Sciences (RSSC at ANAS), Azerbaijan

In 2019 were certified two "Automated Technologies No.1 and No.2 for the operational, distance seismic forecasting in any region of the world, only on the basis of year-round monitoring of seismogeodynamical regime of the fluids (SFGD) in Azerbaijan". Daily seismic forecasting performs: a) simultaneously for coordinates the foci of earthquakes completely different of azimuths; b) the intervals of main seismological parameters: coordinates; magnitude; depth, time realization earthquakes. Monitoring performs at 27 objects during 1979-2021.

KEYWORDS :   The reality of operational, distance forecast of the strong earthquakes

Sr No: 658

A multiparametric and multi-satellite investigation of possible seismic precursors in the lithosphere, atmosphere and ionosphere of the 28 January 2020 Mw=7.7 Jamaica earthquake.

CORRESPONDING & PRESENTING AUTHOR:

Dedalo Marchetti, Jilin University, China
Kaiguang Zhu, Jilin University, China
Angelo De Santis, Istituto Nazionale di Geofisica e Vulcanologia, Italy
Xiaodan He, Jilin University, China
Alessandro Piscini, Istituto Nazionale di Geofisica e Vulcanologia, Italy
Saioa A. Campuzano, Instituto de Geociencias IGEO (CSIC-UCM), Spain
Gianfranco Cianchini, Istituto Nazionale di Geofisica e Vulcanologia, Italy
Serena D Arcangelo, Universidad Complutense de Madrid – UCM, Spain
Domenico Di Mauro, Istituto Nazionale di Geofisica e Vulcanologia, Italy
Mengxuan Fan, Jilin University, China
Adriano Nardi, Istituto Nazionale di Geofisica e Vulcanologia, Italy
Martina Orlando, Istituto Nazionale di Geofisica e Vulcanologia, Italy
Loredana Perrone, Istituto Nazionale di Geofisica e Vulcanologia, Italy
Dario Sabbagh, Istituto Nazionale di Geofisica e Vulcanologia, Italy
Xuhui Shen, National Institute of Natural Hazards, MEMC, China
Maurizio Soldani, Istituto Nazionale di Geofisica e Vulcanologia, Italy
Ting Wang, Jilin University, China
Jiami Wen, Jilin University, China
Zining Yu, Jilin University, China

Yiqun Zhang, Jilin University, China

Zeren Zhima, National Institute of Natural Hazards, MEMC, China

On 28 January 2020 at 19:10 UTC a Mw 7.7 earthquake occurred in the Caribbean sea, very close to Jamaica Island, so mostly occupied by the sea: this circumstance brings to a very interesting situation to investigate possible precursors over the sea by the so-called Lithosphere – Atmosphere – Ionosphere Coupling (LAIC) effects.

The present study is not only another earthquake analysis, but also the occasion to implement and improve the previous techniques applied successfully to about 20 single case studies in already published works.

A new technique for detection of atmospheric anomalies is tested by focusing the analysis on the fault rupture segment. We find that some anomalies increase their statistical significance while others are not anomalous anymore. We propose that this information can be precious to distinguish the more probable seismo-induced atmospheric anomalies.

The ionosphere has been investigated by the ESA Swarm constellation and China Seismo Electromagnetic Satellite (CSES-01). An increase of ionospheric anomalies has been detected about 50 days before the earthquake. Furthermore, a clear increase of the ionosphere electron density inside the Dobrovoslky's area 39 days before the earthquake has been commonly detected by CSES-01 and Swarm-B. Such electron density increase is compatible in time to the one found for Mw=7.5 Indonesia 2018 earthquake (Marchetti et al., JAES 2020) and little less than the anticipation time of the electron density detected about one month before the Ridgecrest earthquake (De Santis et al., Front. Earth Sci. 2020). This is in agreement with the empirical Rikitake (1987) law.

KEYWORDS :   CSES, ionospheric precursors, LAIC

Sr No: 659

The spatiotemporal evolution of atmospheric/ionospheric pre-earthquake anomalies in association with the preparation zone

CORRESPONDING & PRESENTING AUTHOR:

Dimitar Ouzounov, Chapman University, USA

Sergey Pulinets, Russian Academy of Sciences, Russia

JY Liu, National Central University, Taiwan

Katsumi Hattori, Chiba University, Japan

Patrick Taylor, NASA GSFC, USA

Menas Kafatos, Chapman University, USA

We studied the temporal and spatial evolution between Thermal Radiation Anomalies (TRA); Ionospheric total electron content (TEC); and; abnormal patterns of radon data and their relationship with earthquake preparation zones (EPZ). For the estimates of each EPZ, we use Dobrovolsky et al. (1979) and Bowman et al. (1998), where the EPZ radius scales exponentially with earthquake magnitude, especially for Mw ≥ 6.0 and larger. This gives a broader study of larger magnitudes earthquakes and TRA and TEC anomalies. We analyzed 10 large (M>6) earthquakes (2004-2019) for TRA and TEC anomalies in each of the EPZ zones. Our results show evolutionally patterns in the appearance of pre-earthquake transient effects in the

atmosphere and ionosphere, with a short time-lag, from hours up to a few days, and scalable with a magnitude estimate at their unusually far distance from the epicenter (for the M7+ events). The spatial characteristics of pre-earthquake anomalies were associated with the larger area but always inside the preparation-activation region estimated by Dobrovolsky-Bowman. The pre-earthquake pattern of the atmosphere and ionosphere signals, revealed by a simultaneous analysis of satellite, GPS/TEC, Satellite Earth observations, and ground data, all suggesting that these earthquakes follow a global recognizable spatial pattern of TRA and TEC.

KEYWORDS :   precursors, thermal anomaly, LAIC

Sr No: 660

Variation of underground Rn flux near surface using Multi-channel Spectrum Analysis: Discrimination of Meteorological Effects

CORRESPONDING & PRESENTING AUTHOR:

Katsumi Hattori, Chiba University, Japan

Kazuhida Nemoto, Chiba University, Japan

Haruna Kojima, Chiba University, Japan

Chie Yoshino, Chiba University, Japan

Akitsugu Kitade, Chiba University, Japan

Recently, there are many papers on electromagnetic pre-earthquake phenomena such as geomagnetic, ionospheric, and atmospheric anomalous changes. Ionospheric anomaly preceding large earthquakes is one of the most promising phenomena. Lithosphere-Atmosphere-Ionosphere Coupling (LAIC) model has been proposed to explain these phenomena. In this study, to evaluate the possibility of chemical channel of LAIC by observation, we have developed and installed the new Rn mesurement system, which can be observe atmospheric Rn concentration, underground Rn concentration (GRC) at Asahi station, Boso, Japan, togather with a weather station. Since the atmospheric electricity parameters are very much influenced by weather factors, it is necessary to remove these effects as much as possible. In this aim, we apply the MSSA (Multi-channel Singular Spectral Analysis) to remove these influences from the variation of GRC and estimate the underground Rn flux (GRF). We investigated the correlations between GRF and heavy precipitation and between GRF and the local seismic activity around the station. The preliminary results show that there is a tendency of correlation between GRF and heavy rain and between GRF and local seismicity within an epicenter distance of 50 km from the station.

KEYWORDS :   underground Rn flux, MSSA, discrimination of meteorological effects

Sr No: 661

The Global Electric Circuit and Global Seismicity

CORRESPONDING & PRESENTING AUTHOR:

Sergey Pulinets, Space Research Institute (IKI) , Russia

Galina Khachikyan, Institute of Ionosphere, Russia

Evgeny Mareev, Institute of Applied Physics, Russia

Basing on the catalogue of earthquakes with M≥4.5 for 1973-2017, the UT variation with an amplitude of ∼ 10% in the number of earthquakes was revealed and compared with the UT variation in the gradient of the atmospheric electric potential (Carnegie curve), whose amplitude is ∼ 20%. It is shown that amplitude of the UT variation in the number of deep earthquakes is larger compared to that for crustal earthquakes, and that it is ahead of the UT variation in the gradient of the atmospheric electric potential by ∼ 2 hours. The linear regression equation between UT variations in the number of deep earthquakes and the electric potential gradient with the correlation coefficient R = 0.86 is obtained. It is shown that the maxima in UT variations of the atmospheric electric field gradient (Carnegie curve), ionospheric potential and seismic regime as well, observed around ∼ 17-19UT and ∼ 07UT, are synchronized with the time when the geomagnetic poles in the southern and northern hemispheres, respectively, "look" in the tail part of magnetosphere, from where the injection of accelerated charged particles takes place; the main minimum around ∼ 03UT is timed to the time when the geomagnetic pole in the southern hemisphere, located in the longitudinal sector of the highest seismicity, turns out of the tail part of the magnetosphere. The results support the idea that the processes of earthquake preparation are coupled with the processes of functioning of the global electric circuit and the generation of atmospheric electric field.

KEYWORDS : carnegie curve, global seismicity, global electric circuit

Sr No: 662

Spatiotemporal analysis of microseismicity clusters in central Ionian Islands (Greece)

CORRESPONDING & PRESENTING AUTHOR:

Polyzois Bountzis, Aristotle University of Thessaloniki, Greece

Anastasios Kostoglou, Aristotle University of Thessaloniki, Greece

Eleftheria Papadimitriou, Aristotle University of Thessaloniki, Greece

Vasileios Karakostas, Aristotle University of Thessaloniki, Greece

The spatio-temporal evolution of seismicity of an accurately relocated earthquake catalog in the central Ionian Islands, Greece, is explored, by the systematic identification of the earthquake clusters in 3-D space over the period September 2016–December 2019. A raw dataset of manually picked phases from a dense seismic network was relocated using the double difference method and a cross correlation algorithm, resulting in 13, 632 earthquakes with a completeness magnitude as low as Mc = 1.5. The clustering procedure engages a temporal stochastic point process, the Markovian Arrival Process (MAP), for an initial separation

of the background seismicity from potential seismic excitations, using the changes in the seismicity rate and a density-based clustering algorithm, DBSCAN, for the detection of elevated spatial density areas. A high concentration of temporally persistent clusters is identified along the western coastline of Lefkada Island, in the parallel step-over faults between the two major fault branches of the Kefalonia Transform Fault Zone and in the Myrtos Gulf area in Kefalonia. The clusters are spatially correlated to the positive static stress changes induced by the coseismic slip of the Mw6.5 November 17, 2015 Lefkada main shock. Multiple secondary faults of the Kefalonia segment can be revealed and the dominant triggering mechanisms can be illuminated contributing towards the understanding of the regional faulting properties and mechanics, an outcome that cannot be achieved solely by studying the large earthquakes, due to their rarity.

KEYWORDS : earthquake cluster detection, Central Ionian Islands (Greece), Stress transfer

Sr No: 663

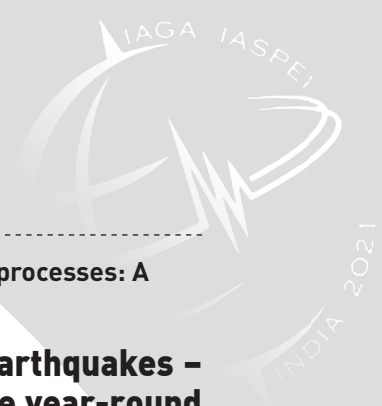SYMPOSIUM : **S12 CoEGP Interdisciplinary observations of Pre-Earthquake processes: A new approach towards Earthquake prediction studies**

Earthquake precursor signatures over multiple earthquakes from magnetotelluric data: a case study from Koyna–Warna seismoactive region, India.

CORRESPONDING & PRESENTING AUTHOR:
Venkata Vijaya Kumar Pachigolla, NGRI, India
Vishal S Rawat, Kurukshetra University, India
Prasanta K Patro, NGRI, India
A K Gupta, NGRI, India
Narendra Babu, NGRI, India

Koyna-Warna seismogenic zone is located in the Deccan traps, Western India, familiar for Reservoir Triggered Seismicity (RTS). To understand earthquake generation mechanisms, two magnetotelluric (MT) stations were established for continuous monitoring of electric and magnetic field components in Koyna - Warna seismoactive region. The co-seismic behaviour of the MT time series recorded at 15 Hz sampling frequency is analysed for the earthquake occurred on November 24, 2007 with a magnitude of 4.6. The wavelet analysis brings out sharp enhancement in the amplitude of the signal at 3-6 Hz frequency band related to the onset of the main shock of the earthquake. The amplitude spectra also show an unusual behaviour during the main shock of the earthquake. Based on amplitude spectra and wavelet analysis conclude that 3-6 Hz band is very useful in the identification of seismoelectromagnetic fluctuations during the earthquake. To understand the precursory signatures of the several earthquake magnitudes (Mw) ranging from 3.9 to 4.9 analysed using spectral polarization ratio technique. A significant anomaly was observed few hours before each earthquake using this technique. The anomalous behaviour correlates with solar activity (Dst index). The unusual behaviour before the earthquake is not related to the solar-terrestrial effect and it is related to the precursory signature. The presence of RTS and complex tectonics in the Koyna- Warna region suggests that both electrokinetic and seismic dynamo are the probable mechanisms play an important role in generation of co and pre seismic electromagnetic signals.

KEYWORDS : wavelet, seismoelectromagnetic, amplitude spectra, spectral polarization ratio.

Sr No: 664

Identifying Correlation between Magnitude of Uttaranchal region Earthquakes and Aperiodic components of Solid Earth tides and anomalous drop in Relative Humidity

PRESENTING AUTHOR:

Senthil Kumar M, SASTRA Deemed to be University, India

CORRESPONDING AUTHOR:

Venkatanathan Natarajan, SASTRA Deemed to be University, India

The earth's rotation will continue to be influenced in order to get synchronized the rotation of the sun, moon, and earth caused by the tidal friction. Variations in the rotational speed of the earth have impacted the tectonic plates collision due to their differential inertia. As a result, these stresses gradually create seismic strain, where, when exceeded a threshold level in a seismically active area, an earthquake has been triggered. In recent times, SSA is a comparatively new and efficient time series analysis technique. In this work, we choose the Uttaranchal (India) region earthquakes. Eight earthquakes are taken into consideration and analysis of ten years' time period prior to the earthquake date with respect to the lunar phase, we have identified that there is an abnormality in SET. All earthquakes have observed an aperiodic component on the sixth eigenfunctions. For a range of longitude, when the percentage of eigenfunction increases, the magnitude of earthquakes gets increases. From the daily observation of RH, anomalous drop was observed 45 days to 24 days before the earthquake. All the anomalies were observed only after the SET was triggered. Also, the irregularity observed in SET is complementary to the anomalous RH. From this investigation of these earthquakes, we observed that four have the same behaviors, and others behave differently. It is concluded that the irregularity in SET and anomalous drop in RH can be correlated with the magnitude of the earthquake and also influenced by the location of an impending earthquake at the micro-level.

KEYWORDS : solid earth tide, relative humidity, singular spectrum analysis

Sr No: 665

Chain of Lithospheric - Atmospheric - Ionospheric precursors of earthquakes: some case studies

CORRESPONDING & PRESENTING AUTHOR:

Angelo De Santis, Istituto Nazionale di Geofisica e Vulcanologia, Italy

Saioa A. Campuzano, CSIC-UCM, Spain

Gianfranco Cianchini, Istituto Nazionale di Geofisica e Vulcanologia, Italy

Serena D Arcangelo, Università Complutense Madrid, Spain

Domenico Di Mauro, Istituto Nazionale di Geofisica e Vulcanologia, Italy

Dedalo Marchetti, Jilin University, China

Adriano Nardi, Istituto Nazionale di Geofisica e Vulcanologia, Italy

Martina Orlando, Istituto Nazionale di Geofisica e Vulcanologia, Italy

Loredana Perrone, Istituto Nazionale di Geofisica e Vulcanologia, Italy

Alessandro Piscini, Istituto Nazionale di Geofisica e Vulcanologia, Italy

Dario Sabbagh, Istituto Nazionale di Geofisica e Vulcanologia, Italy

Maurizio Soldani, Istituto Nazionale di Geofisica e Vulcanologia, Italy

Earthquakes release a huge energy in few seconds, after the sudden rupture of a volume of crustal rocks along the involved fault. During the preparation phase of the impending earthquake, even if this energy is mostly stored as potential energy, another (usually smaller) part of the energy is available to produce some effects. These effects can be generally relevant in the different layers in the seismogenic area or above, i.e. Lithosphere, Atmosphere and Ionosphere (LAI), in the framework of the so-called LAI coupling (or simply LAIC). In this presentation, we will show some examples of earthquakes with M6+, where a sequence of effects at the different geolayers occurs in the preparation of the imminent earthquakes. It is this chronological synchronicity that will point to a possible earthquake prediction, together with other features we already found in past studies of seismic, atmospheric and ionospheric data analyses.

KEYWORDS : earthquakes, precursors, LAIC

Sr No: 666

SYMPOSIUM : **S12 CoEGP Interdisciplinary observations of Pre-Earthquake processes: A new approach towards Earthquake prediction studies**

Solid earth tides and Anomalous OLR Prior to the Northern Sumatra region Earthquakes (=M6.0)

PRESENTING AUTHOR:

Ramya Jeyaraman, SASTRA Deemed to be University, India

CORRESPONDING AUTHOR:

Venkatanathan Natarajan, SASTRA Deemed to be Univeristy, India

To forecast earthquakes on short-term basis scientists are examining on different precursory parameters. In this work, the authors analyse the characteristics of precursory signatures such as Solid earth tides (SET) and outgoing longwave radiations (OLR). Eleven earthquakes (1989 to 2021) occurred within 75 km radius of December 26, 2004 earthquake were considered for this study. In order to identify the epicentre of impending earthquakes, the authors have made spatial analysis of epicentral region prior to the occurrence of earthquakes. Different sized of rows and columns were analysed around the epicentre. It was found that the higher OLR flux was observed for 3° x 3° region compared to 11° x 11° region. The anomalous OLR flux index was observed that 1 to 4 months prior to the occurrence of the earthquake, probably due to the increased tectonic movement. It is also inferred that there exists a correlation between depth and the geometry of the fault associated with it and the anomaly obtained. Using Singular Spectral analysis, M2 component of SET for the preceding 10 years was analysed for the all 11 earthquakes. It is found that the percentage of aperiodic component of Eigen function increases with increase in magnitude. Hence, OLR and Solid Earth Tides can be considered as a precursor to analyse the earthquake in terms of time, location and magnitude.

KEYWORDS : outgoing longwave radiation, solid earth tides, singular spectral analysis

Sr No: 667

SYMPOSIUM : **S12 CoEGP Interdisciplinary observations of Pre-Earthquake processes: A new approach towards Earthquake prediction studies**

The geomagnetic variations and their relation to seismic energy release in the Vrancea seismic zone.

CORRESPONDING & PRESENTING AUTHOR:

Andrei Mihai, National Institute for Earth Physics, Romania

Iren Moldovan, National Institute for Earth Physics, Romania

Victorin Toader, National Institute for Earth Physics, Romania

Alexandra Muntean, National Institute for Earth Physics, Romania

Anica Otilia Placinta, National Institute for Earth Physics, Romania

This study investigates the relationship between anomalous geomagnetic variations and the occurrence of the intermediate-depth earthquakes. To distinguish the global magnetic variations from possible seismo-electromagnetic variations in a seismic area like Vrancea zone, the data recorded at MLR Seismological Observatory, situated inside the seismogenic zone were analyzed comparatively with the data recorded at SUA National Geomagnetic Observatory, located outside the Vrancea zone (150 km South-Est from Vrancea zone). The geomagnetic data were also correlated with the daily geomagnetic indices taken from NOAA for identification of solar storms. The anomalous variations can be observed at MLR on one component of the magnetic field (By) and the magnitude of these variations differ from year to year. Geomagnetic representations were plotted beside the seismicity that accompanied these variations and the geomagnetic indexes. The cumulative energy graphs are used to compare the geomagnetic anomalies with the earthquake energy release. Thus, alongside cumulative seismic energy, we also plot graphs with daily energy release. The result shows a strong link between the magnitude of these variations and the seismic activity. A significant variation is accompanied by larger earthquakes. The variations recorded on By component show two patterns: a) variations recorded on the By component that agree with small decreases/increases recorded over long periods (smooth variation); b) variations on By that varies quite a lot over long periods with step like decreases/increases (step-like variation).

KEYWORDS : geomagnetic variations, seismic energy, Vrancea zone

Sr No: 668

A possible slow-slip-event in Vrancea (Romania) seismic zone

CORRESPONDING & PRESENTING AUTHOR:

Andrei Mihai, National Institute for Earth Physics, Romania

Apostol Andrei, National Institute for Earth Physics, Romania

Iren Adelina Moldovan, National Institute of Earth Physics, Romania

Victorin Emilian Toader, National Institute of Earth Physics, Romania

Boudewijn Ambrosius, Delft University of Technology, Netherland

Alexandra Muntean, National Institute for Earth Physics, Romania

A large stress build-up was observed between 2012-2013 by using the magnetotelluric phase splitting effect from biolocation reaction around Covasna fault, situated in the immediate vicinity of Vrancea seismogenic zone, but no large earthquake was recorded. The stress oscillation was considered to be a precursor of large SSE lasting for about 1 year, between 2013 and 2014 that released the accumulated stress. To validate this postulation, GPS network data were exploited. A downward displacement for stations located in the epicentral region of intermediate-depth earthquakes and in the Focsani Depression was found during 2013-2014. The SSE during this period lead to the creation of a seismic gap in the year 2015-2020 at a depth of 150 km for intermediate-depth earthquakes with Mw > 4.0. This seismic gap is probably a precursor for the forthcoming seismic event in Vrancea.

The release of stress produced by slow-slip-events might also be an explanation for the variation of time window between Vrancea large earthquakes. In the last 300 years the window of time for two consecutive large and destructive intermediate-depth earthquakes in Vrancea was between 36 and 102 years. That's why it is very important to identify SSEs, at least for the period when GPS recordings are available.

KEYWORDS :   slow slip event, seismic, stress oscillation

SI3   CoESG & SEDI Seismic structures in the mantle

CONVENERS: Christine Thomas (Germany)

Barbara Romanowicz, (France/USA),
Sebastian Rost (UK)

Stéphane Rondenay (Norway)

Dynamic processes and mineralogical changes generate seismic observables that can be used to infer the current state of the mantle. Seismic studies of interfaces in the mantle provide constraints on composition, temperature and flow. Seismic tomography provides evidence for regional and local changes of temperature and composition and images dynamic processes driven by convection and plate tectonics. Combinations of global, regional and local studies of Earth's mantle highlight differences and connections between different tectonic regimes in the mantle. Together with constraints from mineral physics, geochemistry and geodynamics, seismological studies contribute to our understanding of the dynamics and evolution of the deep Earth shaping our planet. This session invites contributions from all areas of seismology investigating the structure of the Earth's mantle from the lithosphere to the core-mantle boundary aiming to image the dynamics and structure of the planet.

Sr No: 669

X-discontinuity beneath Indian Shield – Evidence for remnant Tethyan oceanic slab in the upper mantle

PRESENTING AUTHOR:

Uppala Srinu, CSIR – National Geophysical Research Institute, India

CORRESPONDING AUTHOR:

Prakash Kumar, CSIR - National Geophysical Research Institute, India

Chinmay Haldar, Wadia Institute of Himalayan Geology, India

M Ravi Kumar, CSIR - National Geophysical Research Institute, India

D. Srinagesh, CSIR - National Geophysical Research Institute, India

The X-discontinuity is an intermittent seismic discontinuity observed at some locations around 250 to 350 km depth. Several mineralogical and petrological mechanisms have been put forth to explain its occurrence. Because of the large depth variability, it is difficult to explain its origin invoking a single mineralogical phase transformation. In order to investigate this discontinuity beneath the Indian shield, we analyzed 10216 P wave receiver functions at seismological stations deployed on the Indian shield and Himalaya. We observed the presence of X-discontinuity as a sporadic and thin feature, in the depth range of 246 to 335 km, with a sharp shear velocity jump of 2.5-3.6%. It neither bears a clear tectonic affinity nor has any correlation with the transition zone discontinuities. Interpreting its origin due to a single mineralogical change requires a large spatial variation in the mantle temperature. Therefore, we suggest that the observed widespread X-discontinuity beneath the Indian shield owes its origin to two mechanisms i.e., orthoenstatite to High-pressure clinoenstatite transformation which shifts to lower pressures (~2 GPa) due to the presence of water (0.13 wt% H_2O) in $MgSiO_3$ and the formation of stishovite at 8-11 GPa due to excess silica in an eclogitic component derived from the Tethys oceanic lithosphere subducted during lower Eocene. The presence of such discontinuity could allow tracking of subducted material within the upper mantle providing a measure of mantle geochemical heterogeneity.

KEYWORDS : X-discontinuity, receiver functions, Indian shield

Sr No: 670

Automated Slowness Vector Measurement and Identification of Multipathed Arrivals through Bootstrapping and Cluster Analysis

CORRESPONDING & PRESENTING AUTHOR:

James Ward, University of Leeds, UK

Michael Thorne, University of Utah, USA

Andy Nowacki, University of Leeds, UK

Sebastian Rost, University of Leeds, UK

Slowness vector measurements of seismic arrivals have been used to analyse a range of mantle phenomena from ultra-low velocity zones (ULVZs) to large low-velocity provinces (LLVPs) to subducted slabs. Array techniques, commonly used to make slowness vector measurements, are limited by the subjective visual

inspection of observations and it is challenging to determine the uncertainties contributed by array geometry, local structure and noise. We present a method to automatically identify seismic arrivals in slowness space and measure their slowness vector properties with uncertainty estimates to address these limitations. To do this, we bootstrap sample the waveforms recorded at the array in question, therefore also creating random sub-arrays in each sample, then use linear beamforming to measure the coherent power at a range of slowness vectors. In each bootstrap sample, we take the top N peaks from the respective power distributions. The peaks from all bootstrap samples are gathered and we use density-based clustering algorithm DBSCAN to identify clusters of slowness vectors. From these clusters, the slowness vector properties of the arrival can be found by the mean of the points in the cluster and the uncertainties by the point distribution. The DBSCAN parameters were tuned using 2489 observations of SKS and SKKS arrivals. Then, we applied the method to identify high-frequency PKP precursors, indicative of ULVZ structure, and low-frequency multipathed Rayleigh wave arrivals. This method allows much larger datasets to be processed and allow large scale observations of multipathing locations to be made.

KEYWORDS : array seismology, body wave, multipathing

Sr No: 671

Upper mantle flow under the Arunachal Himalaya from shear wave splitting

CORRESPONDING & PRESENTING AUTHOR:

Sunil K. Roy, CSIR-National Geophysical Research Institute, India
M. Ravi Kumar, CSIR-National Geophysical Research Institute, India
V. Venkatesh, CSIR-National Geophysical Research Institute, India

An array comprising 36 broad-band seismic stations was deployed along two profiles in the Arunachal Himalaya to decipher the small-scale variations in the structure of the crust and upper mantle. Analysis of the SKS, SKKS and PKS waveforms recorded by this network yielded a total of 71 well constrained splitting and 120 null measurements. Results reveal variable fast polarization azimuths (FPAs), with those along profile 1 located in the central part, being primarily oriented along the NE and ENE-WSW directions. This can be due to anisotropy forged as a result of finite strain induced by compression. The slightly larger delay times for measurements in the southern part of profile 1, require contribution from both the lithosphere and asthenosphere. The FPAs along profile 2, in the easternmost part of Arunachal Himalaya, are oriented E-W and ENE-WSW in the northern part, and NW-SE and NNW-SSE in the southern part. Further, the FPAs, deviate from the APM and/or the regional tectonic fabrics and depend on back azimuth. This can be attributed to a combined effect of absolute plate motion-related (APM) strain and finite strain induced by compression, and/or mantle flow. Our observations affirm the hypothesis that the Eastern Himalayan syntaxis hosts a slab gap for mantle flow, and the slab roll-back results in a westward deviation of the flow (Liu et al., 2019).

KEYWORDS : shear wave splitting, Eastern Himalaya, upper mantle deformation

Sr No: 672

Contact of the Samoan plume with the Tonga subduction from intermediate and deep-focus earthquakes

CORRESPONDING & PRESENTING AUTHOR:

Pavla Hrubcova, Institute of Geophysics CAS, Czechia

Vaclav Vavrycuk, Institute of Geophysics CAS, Czechia

The Tonga subduction zone in the southwest Pacific is the fastest convergent plate boundary in the world with the most active mantle seismicity. This zone shows unique tectonic features including Samoan volcanic lineament of plume-driven origin near the northern rim of the Tonga subducting slab. The proximity of the Samoa hotspot to the slab is enigmatic and invokes debates on interactions between the Samoa plume and the Tonga subduction. Based on long-term observations of intermediate and deep-focus Tonga earthquakes reported in the Global CMT catalog, we provide novel detailed imaging of this region. Accurate travel time residua of the P and S waves recorded at two nearby seismic stations are inverted for the P- and S-wave velocities and their ratio, and reveal pronounced lateral variations. In particular, they differ for the southern and northern parts of the Tonga subduction region. While no distinct anomalies are detected in the southern Tonga segment, striking low-velocity anomalies associated with high Vp/Vs ratio are observed in the northern Tonga segment close to the Samoa plume. These anomalies spread through the whole upper mantle down to depths of ~600 km. Together with a fast extension of the northern back-arc Lau Basin, slab deformation and geochemical enrichment in the northern Tonga region, they trace deep-seated magmatic processes and evidence an interaction of the Tonga subduction with the Samoa plume.

KEYWORDS :   Tonga subduction zone, Samoa plume, upper mantle structure

Sr No: 673

Imaging D" using shear waves and transdimensional hierarchical Bayesian inversion

CORRESPONDING & PRESENTING AUTHOR:

Sima Mousavi, The Australian National University, Australia

Hrvoje Tkalcic, The Australian National University, Australia

Rhys Hawkins, Utrecht University, Netherland

Malcolm Sambridge, The Australian National University, Australia

Tomographic images of the D" layer are critical for understanding energy exchange across the core-mantle boundary (CMB), the most prominent compositional discontinuity within the earth. Various studies have documented significant heterogeneities on different spatial scales and a wide range of physical and chemical features. While there has been a consensus on the inferred long-scale structures, there are notable differences in the lowermost mantle's tomograms of the lowermost mantle, stemming from the use of different imaging methods and datasets. Significant limitations include subjective choices of model parameterizations and regularization and the absence of accounting for data noise that can lead to either over- or under-fitting the data. The major limitation of deep earth tomography has been the explicit parameterization of the region of interest, which faces inherent problems of either over-smoothing the data or allowing for overfitting.

Following our previously performed P-wave tomography, we perform an S-wave tomography of the D″ using an improved Bayes algorithm in which explicit parameterization and regularization are avoided. Spherical Voronoi cells are now implemented for an implicit parameterization of the model space. We utilize the most comprehensive, global, ScS-S differential travel time dataset measured through a waveform correlation and augment it with a new subset of data from specially targeted source-receiver geometries including the temporary deployments in Australia. We present a new S-wave tomogram of the D″ layer accompanied by model uncertainty. We interpret it in the context of the existing P- and S-wave tomographic models of the lowermost mantle.

KEYWORDS : tomography, ScS-S, core mantle boundary

Sr No: 674

SYMPOSIUM :   **S13 CoESG & SEDI Seismic structures in the mantle**

Evidence for strong topography of the mid-mantle reflector

CORRESPONDING & PRESENTING AUTHOR:
Morvarid Saki, University of Münster, Münster, Germany
Christine Thomas, University of Münster, Münster, Germany
Rafael Abreu, University of Münster, Münster, Germany

There is mounting evidence for the presence of a seismic reflector in the mantle at a depth of around 1000 km, however, the cause for this reflector is not yet well established and published observations show a range of depth estimates for the structure. Here we investigate this seismic reflector beneath the North Atlantic using a large number of PP and SS underside reflections. We analyze over 2600 earthquakes with MW ≥ 5.7 and use array seismic methods to improve the visibility of the small-amplitude reflected signals. The measured time lag between PP/SS arrivals and their corresponding precursors on robust stacks are used to estimate the depth of the reflector. Our results reveal the presence of mid-mantle structure beneath the North Atlantic in a depth range of ~700 to 1300 km, consistent for both P and S wave observations. The reflector depth is shallower than 1000 km beneath the southern part of the investigation area and deepens seemingly abruptly towards the northern part of the North Atlantic. We find polarity variations in a region of strong depth change which we assume to be due to wave interference. Using 3D waveform modelling we implement models with strong topography and show that a large step in reflector depth over a short lateral distance, as imaged with our dataset, can be resolved and that variations in precursor polarity can indeed be observed in the region of strong topography confirming our assumption of wave interference.

KEYWORDS : Atlantic Ocean, mid-mantle reflector, PP and SS precursors

Sr No: 675

SYMPOSIUM :   **S13 CoESG & SEDI Seismic structures in the mantle**

Evidence of low-velocity anomaly beneath the Barmer-Sanchor rift, NW India from Teleseismic P- wave Tomography

CORRESPONDING & PRESENTING AUTHOR:
Saju D S, Indian Institute of Technology Bombay, India
Mohan Gollapally, Indian Institute of Technology Bombay, India
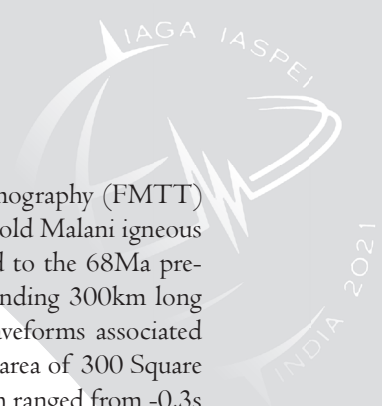
P wave teleseismic tomography was carried out using the fast marching teleseismic tomography (FMTT) algorithm to explore for imprints of volcanism in the upper mantle beneath the 750 My old Malani igneous province(MIP) in northwestern India. MIP also hosts several alkaline complexes linked to the 68Ma pre-Deccan volcanism which are preserved along the flanks of the northwest-southeast trending 300km long Barmer-Sanchor rift in MIP. Nearly 8000 P phase arrival times were picked from waveforms associated with 933 teleseismic events recorded at 29 broadband stations that were deployed in an area of 300 Square kilometres. Adaptive stacking was used to estimate the travel time relative residuals, which ranged from -0.3s to +0.9s. An elliptically shaped low-velocity anomaly (-1% to -4%) is imaged down to a depth of 200 km beneath the Barmer-Sanchor rift. The anomaly is 250km long and 150km in width in the upper mantle and is prominent in the depth range 80-160km, where the velocity reduction is maximum (-3% to -4%) relative to the AK135 velocity model. It is likely that the ancient, weak lithosphere beneath the rift facilitated the channelling of the magma from the Deccan volcanism, which resulted in thermal imprints and reduced velocities. Alternatively, compositional imprints in terms of the carbonated metasomatic mantle due to Pan African volcanic events and Neo-Proterozoic subduction may also cause a reduction in velocities.

KEYWORDS :   low-velocity anomaly, teleseismic P wave tomography, Deccan volcanism

Sr No: 676

SYMPOSIUM :   **S13 CoESG & SEDI Seismic structures in the mantle**

Seismic evidence for partial melt below tectonic plates

CORRESPONDING AUTHOR:

Eric Debayle, LGL TPE, France

Thomas Bodin, LGL TPE, France

PRESENTING AUTHOR:

Stephanie Durand, LGL TPE, France

Yanick Ricard, LGL TPE, France

The seismic low velocity zone (LVZ) of the upper mantle is generally associated with a low-viscosity asthenosphere that plays a key role for the dynamics of plate tectonics. However, its origin remains enigmatic, some authors attributing the reduction in seismic velocity to a small amount of partial melt, and others invoking solid-state mechanisms near the solidus, or the effect of volatile contents. Observations of shear attenuation provide additional constraints to unravel the origin of the LVZ. Here, we report the discovery of partial melt within the LVZ from the simultaneous interpretation of global 3D shear attenuation and velocity models. We observe that partial melting down to 150-200 km depth beneath mid-ocean ridges, major hotspots and back-arc regions feeds the asthenosphere. A small part of this melt (<0.30%) remains trapped within the oceanic LVZ. The amount of melt is related to plate velocities and increases significantly between 3 and 5 cm.yr-1, similarly to previous observations of mantle crystal alignement underneath tectonic plates. Our observations suggest that by reducing viscosity, melt facilitates plate motion and large-scale crystal alignment in the asthenopshere. Melt is absent under most of the continents.

KEYWORDS :   tomography, seismic attenuation, partial melt

Sr No: 677

Imaging deep mantle structure beneath Alaska using full waveform tomography

CORRESPONDING & PRESENTING AUTHOR:

Daniel Frost, UC Berkeley, USA

Barbara Romanowicz, UC Berkeley, USA

Alaska has a complex subduction history, the remnants of which should be present down to the lowermost mantle. Inconsistencies between regional and global tomographic models likely result from methodological limitations and limited sampling. Our understanding of the tectonic history of the Northern Pacific is incomplete. Furthermore, travel times of core-sensitive waves observed in Alaska are inconsistent with global data. Improved models of the Alaskan mantle will help solve these issues.

Travel time tomography has limited capacity to resolve complex mantle structure. In contrast, Full Waveform Inversion, which seeks to explain every wiggle of the seismogram, can account for multipathing and wavefront healing that mask strong heterogeneity like slabs and mantle wedges. By spatially restricting the inversion to a "box" we can couple different seismic wavefield solvers and compute the wavefield outside the box only once, while performing multiple inversion iterations inversion within the box, thus reducing computation time (e.g. Masson and Romanowicz, 2018ab). This enables using higher frequency body waves, sharpening existing images of seismic wavespeeds and radial anisotropy.

We apply Full Waveform "box" tomography to Alaska. In a first step, we combine a fast 1D solver for computations outside the box (DSM, Geller and Ohminato, 1994) and a regional 3D solver inside the box (RegSEM, Cupillard et al., 2012). We show our work to build starting models for the inversion, data selection, and preliminary results. In a following step, we compare the results obtained using a 1D solver or a 3D solver and 3D mantle outside of the box.

KEYWORDS : Alaska, tomography, full waveform inversion

Sr No: 678

Modelling of scattering and reflections in the lowermost mantle beneath north-eastern of South America

CORRESPONDING & PRESENTING AUTHOR:

Vanessa Hiemer, Institute for Geophysics

Christine Thomas, Institute for Geophysics

The D″ region is characterized by a variety of structures at many different scales, ranging from small-scale scatterers and ultra-low velocity zones to the large-low shear velocity provinces beneath the Atlantic and Pacific. Another prominent structure is the D″ reflector that has been found in many regions. The focus of this study is on the lowermost mantle where PKP precursors and PdP reflections originate. The PdP waves result from the reflection at the top of the D″ discontinuity and the precursors to PKPdf from scattering of the PKP phase at either the entry into the core or exit from the core. We aim to model these precursors
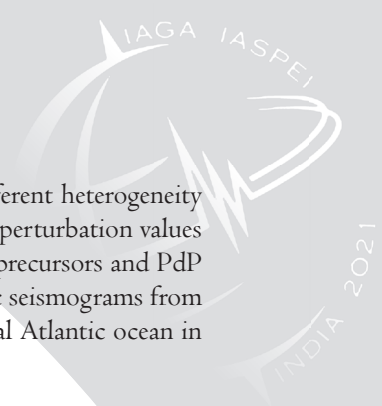
and reflections, using the axi-symmetric spectral element method AxiSEM. Testing different heterogeneity models for the D″ region, composed of scatterers with different correlation lengths and perturbation values for the seismic wave velocity, we find that some of our models can produce both, PKP precursors and PdP reflections, while others only produce PdP or PKP precursors. We compare our synthetic seismograms from the models to the data covering the north-eastern part of South America and the central Atlantic ocean in order to determine the best fitting lowermost mantle structure.

KEYWORDS : lowermost mantle, scattering, reflections

Sr No: 679

Exploring the Upper Mantle Using Surface-Wave Diffraction (by invitation)

CORRESPONDING & PRESENTING AUTHOR:

Petr Kolinsky, University of Vienna, Austria
Goetz Bokelmann, University of Vienna, Austria
Alparray Working Group, ETH

Stripe-like patterns of surface-wave arrival angles have been observed at dense networks around the world. Measurements from the AlpArray have allowed to develop the hypothesis that alternating stripes of positive and negative deviations are interference patterns caused by surface-wave diffraction by distant velocity anomalies. We use a simple modeling approach to describe the interaction of the wavefield with such anomalies. We invert the patterns of Rayleigh waves generated by earthquakes in the South Atlantic Ocean and observed on the AlpArray network in Europe. Our study has indicated that the causative anomaly is located in Central Africa, matching the upper-mantle low velocity region under the volcano-capped swells of the Cameroon volcanic line. A qualitative match of modeling the Yellowstone plume with observations from USArray suggests that the interference pattern can be used to infer the presence (and perhaps spatial extent) of the plume-like bodies in the upper mantle. We observe similar patterns in essentially every teleseismic wavefield recorded by the AlpArray network. This raises the question of the generality of this kind of observation. Is it indeed always present? Is every wavefield distorted by an anomaly somewhere along the propagation path? As these plume-like velocity anomalies distort the wavefield even when they are located significantly off the direct great circle path, we use the modeling to show that this is indeed possible. This approach allows studying distant anomalies no matter whether they are placed under the continents or the oceans, which is especially useful for regions with sparse station coverage.

KEYWORDS : surface waves, diffraction, upper mantle

Sr No: 680

Imaging the meso-scale structure and dynamics of the upper mantle beneath the Atlantic ocean

CORRESPONDING & PRESENTING AUTHOR:

Federico Munch, UC Berkeley, USA

Barbara A. Romanowicz, UC Berkeley, USA

Curtis D. Williams, University of California Davis, USA

Maxwell L. Rudolph, University of California Davis, USA

Sujoy Mukhopadhyay, University of California Davis, USA

Over the last decades, seismic tomography has provided important constraints on the long-wavelength structure of the mantle and its planform of convection. However, the dynamic interaction of tectonic plates and deep mantle circulation at intermediate wavelengths (below plate-scale) is yet not well understood. In particular, a better understanding of the oceanic upper mantle could potentially help unraveling the relationships between different scales of mantle convection, hotspot volcanism, and surface observables (e.g., MORB geochemistry and bathymetry). Here, we present a new tomographic model of the shear-wave velocity and radial anisotropy structure underneath the southern Atlantic ocean constructed from the inversion of surface and body waves waveforms down to 40s period. Preliminary results suggest the existence of quasi-periodically distributed low-velocity regions in the upper mantle (200–350 km depth) organized in horizontally elongated bands parallel to the direction of absolute plate motion. These structures are believed to indicate the influx of material from deep mantle sources (i.e. plumes) which is deflected horizontally beneath oceanic plates (French et al, 2013). Moreover, we explore the relationship between these low-velocity regions to features observed in geodynamic simulations, as well as different surface observables (e.g., subsidence rates, dynamic topography, gravity, and geochemical signals along mid-ocean ridges) to investigate links between seismic velocities, mantle temperature, composition, and mantle flow beneath mid-ocean ridges and ocean basins.

KEYWORDS : full waveform inversion, Atlantic Ocean

Sr No: 681

Inferring relationships between temperature, bulk composition and wave speeds using Mixture Density Networks (by invitation)

CORRESPONDING & PRESENTING AUTHOR:

Ashim Rijal, Utrecht University, Netherlands

Laura Cobden, Utrecht University, Netherlands

Jeannot Trampert, Utrecht University, Netherlands

Carlo Mans, Utrecht University, Netherlands

The study of seismic data provides vital information on the internal structure of the Earth. Information such as variation of wave speeds has shown the presence of seismically distinct structures (e.g. LLSVPs) in the Earth's mantle. In order to determine the thermochemical properties and dynamic relevance of these structures, it is crucial to understand the relationship between wave speeds and temperature/composition.

The relationship becomes non-linear when we include multiple physical properties and hence, a simple linear scaling to go from seismic observables to thermal or chemical structure may be inappropriate. In this study we use a neural network based approach to implicitly learn the non-linear mapping between temperature, bulk composition (expressed in terms of 6 oxides: SiO_2, MgO, Al_2O_3, FeO, Na_2O, CaO) and wave speeds. Wave speeds are calculated for 1000 randomly-chosen bulk compositions at lower mantle temperatures and pressures using thermodynamic modelling software. We train the neural network using wave speeds and pressure (depth) as the input, and temperature and composition as target outputs. The network then approximates probability density functions for temperature and composition, for a given input of P- and S-wave speeds. The posterior probability density function allows us to interpret seismic tomography models in terms of physical parameters, crucially, with uncertainties on the inferred bulk compositions and temperatures. We further investigate the joint probability density function between different oxides (and temperature) to account for any possible trade-off/correlation between parameters.

KEYWORDS : seismology, thermochemical structure, neural networks

Sr No: 682

SYMPOSIUM : **S13 CoESG & SEDI Seismic structures in the mantle**

Constraints on the state of the Mantle Transition Zone beneath the Alpine region using Ps receiver functions

CORRESPONDING & PRESENTING AUTHOR:

Saikiran Tharimena, University of Vienna, Austia

Matthew Agius, Università degli Studi Roma Tre, Italy

Gyorgy Hetenyi, University of Lausanne, Switzerland

Goetz Bokelmann, University of Vienna, Austia

The Mantle Transition Zone (MTZ), the region between 410 km and 660 km depth, is vital for the Earth's thermal and chemical evolution. The structure of the Mantle Transition Zone (MTZ), viz. its thickness and seismic anomalies could hold clues to its current thermal and chemical state. We image the MTZ seismic structure with P-to-S (Ps) receiver functions using data from 723 stations from 2016 − 2020, covering a much larger area of the Alpine region than previously imaged. Events with magnitude > 6 Mw, and a distance range of 35 to 80 degrees were used. Seismic records were pre-processed to remove instrument response, filtered using a zero-phase second order Butterworth filter with cut-off frequencies at 0.02 and 0.5 Hz, followed by rotation to radial and transverse components. Ps receiver functions were computed by deconvolving traces with clear P-wave phase from the radial component using iterative time domain deconvolution and extended time multi-taper frequency domain deconvolution. Waves with clear P-, P410s, and P660s were selected and migrated to depth using regional 3D surface wave tomography model, and then back projected onto a 3D grid. The Alpine MTZ shows evidence for subduction of the European plate in the western Alps. Punctuated anomalies beneath the Alpine region, indicated by the deflection of the 410 km and 660 km discontinuities, show evidence of slab from past subduction events reaching the MTZ, consistent with previous regional studies. Further analysis could provide clues to the dipping orientation of the subducted slab.

KEYWORDS : receiver functions, AlpArray, mantle transition zone

Sr No: 683

New insights on the structure and composition of the lower mantle from global adjoint tomography (by invitation)

CORRESPONDING & PRESENTING AUTHOR:

Laura Cobden, Utrecht University, Netherlands

Wenjie Lei, Princeton University, USA

Jingyi Zhuang, Lamont-Doherty Earth Observatory, USA

Ashim Rijal, Utrecht University, Netherlands

Carlo Mans, Utrecht University, Netherlands

Renata Wentzcovitch, Lamont-Doherty Earth Observatory, USA

Jeannot Trampert, Utrecht University, Netherlands

Jeroen Tromp, Princeton University, USA

Full-waveform inversion methods are ideal for constraining the Earth's fine-scale seismic properties, although they are computationally expensive. Here we present an interpretation of one of the first global "full-waveform" tomography models, generated using adjoint methods (Lei et al., GJI 2020). Since the P- and S- wave speed structures have been constrained simultaneously and in the same frequency band, we are able to jointly interpret them, which in turn enables us to distinguish variations in temperature from chemical or phase changes. We combine thermodynamic modelling with statistical methods in order to reconstruct the frequency distributions of the wave speeds at each depth in the lower mantle. At the top of the lower mantle, the wave speed distributions can be fit by simple changes in temperature and bulk composition. With increasing depth, an additional mechanism is required to reconcile the P-wave speed structure with the S-wave speed structure. We consider the relative roles of the iron spin transition in ferropericlase versus changes in the bulk Mg/Si ratio. In parallel, we apply machine-learning techniques that allow us to map three-dimensional variations in wave speed into probabilistic variations in temperature and mineralogy.

KEYWORDS :   tomography, mantle, spin-transition

Sr No: 684

Towards a new anisotropic tomographic model of the Earth's mantle using the SOLA method

CORRESPONDING & PRESENTING AUTHOR:

Federica Restelli, Royal Holloway University of London, UK

Paula Koelemeijer, Royal Holloway University of London, UK

Christophe Zaroli, University of Strasbourg, France

Ana Ferreira, University College London, UK

A robust physical interpretation of tomographic images remains difficult as model amplitudes are often biased and uncertainties not always quantified. In particular, an agreement amongst anisotropic models is still lacking even on the longest wavelengths. The interpretation of seismic anisotropy is of great importance, because it provides information about mantle flow, and therefore insights into the thermal state, composition and mechanical properties of the mantle.
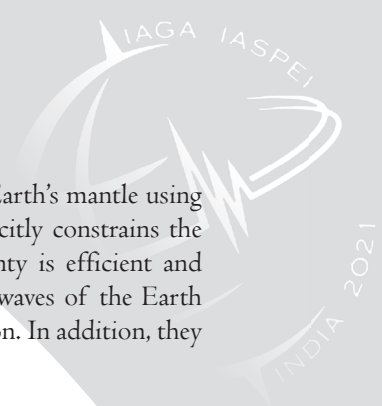
To address these issues, we aim to build a new anisotropic tomographic model of the Earth's mantle using the SOLA method (Zaroli, 2016). SOLA, based on a Backus-Gilbert approach, explicitly constrains the amplitudes to be unbiased while the computation of model resolution and uncertainty is efficient and inherent to the method. We focus our inversions on normal mode data, the standing waves of the Earth observed after very large earthquakes, which are not affected by an uneven data distribution. In addition, they are directly sensitive to both Vs and Vp anisotropy.

Here, we briefly introduce the SOLA method and we discuss results from isotropic inversions in terms of model estimates, uncertainties and resolution. We also show our initial work towards inverting for anisotropic velocities.

KEYWORDS : tomography, anisotropy, uncertainties

Sr No: 685

SYMPOSIUM : **S13 CoESG & SEDI Seismic structures in the mantle**

Light, dense-cored LLVPs constrained by seismic, geodetic and geodynamic constraints

CORRESPONDING & PRESENTING AUTHOR:

Paula Koelemeijer, Royal Holloway University of London, UK

Fred Richards, Imperical College London, UK

Mark Hoggard, Australian National University, Australia

Sia Ghelichkhan, Australian National University, Australia

Harriet Lau, University of California Berkeley, USA

Accurate estimates of density variations are essential for modelling mantle flow and to distinguish between a thermal or compositional origin of mantle heterogeneity. Particularly, constraining the density of the Large-Low-Velocity-Provinces (LLVPs) is important as their properties have major implications for the long-term evolution of the mantle. However, resolving LLVP density via seismological observations is not straightforward. Body wave data are indirectly sensitive to density, while the sensitivity of Earth's normal modes is relatively small and trades off with topography on the core-mantle boundary (CMB). Consequently, few models of lower mantle density exist, with recent studies based on specific normal modes (Koelemeijer et al., 2017) and tidal data (Lau et al., 2017) drawing opposite conclusions.

Here, I first review seismological efforts from the last decades to constrain the density of the LLVPs. I discuss how the spatial extent of any dense material may be restricted to smaller regions within the LLVPs. In addition, I discuss our current knowledge of the large-scale CMB topography, which also provides insights into the nature of the LLVPs. Finally, I present results from recent investigations in which seismological observations are combined with geodetic and geodynamic constraints that offer complementary sensitivity to lower mantle density. Specifically, we show that the presence of a dense basal layer is consistent with normal mode and tidal data, while giving an improved fit to observations of dynamic surface topography and the geoid. Together, these results point towards primarily thermal LLVPs with deep, spatially confined dense material present at their base.

KEYWORDS : density, LLVPs, CMB topography

Sr No: 686

Mineralogy, Fabric, and Deformation Across the Southwestern Border of the African LLSVP

CORRESPONDING & PRESENTING AUTHOR:

Angelo Pisconti, Westfälische Wilhelms-Universität Münster, Germany

Christine Thomas, Westfälische Wilhelms-Universität Münster, Germany

Recent advances in seismic anisotropy studies that jointly use reflections and shear wave splitting have proven to place tight constraints on the plausible anisotropic and deformation scenarios in the D" region. We apply this novel methodology to a large area of the D" region beneath the South Atlantic, in proximity and within the African LLSVP. This area of the mantle is characterized by a transition from fast to slow velocity anomalies and it is thought to be the location of deep-seated plumes responsible for hotspot volcanism. Attempting to probe the composition and deformation along the LLSVP borders may provide key information on mantle dynamics. By analyzing seismic phases sampling this region, we detect a D" discontinuity over a large area beneath the South Atlantic, extending the available knowledge on the geographical distribution of such discontinuity. Shear wave splitting observations suggest that anisotropy is present in this region of the mantle, in agreement with previous studies. We model the observations considering lattice preferred orientation and shape preferred orientation of materials expected in the D" region. A regionalization in terms of mineralogy, phase transition boundaries and deformation directions is required by the data. Two main domains of mineralogy and deformation are found, with aligned post-perovskite outside the LLSVP which is then replaced by aligned bridgmanite within the LLSVP. The scenario depicted by this study agrees well with the available information for the composition of the LLSVP and with the increase of vertical deformation direction expected to occur along the LLSVPs borders.

KEYWORDS : D", seismic anisotropy, LLSVP

Sr No: 687

Mapping Seismic Reflectors in the Mid-Mantle Within Tethys Anomaly

CORRESPONDING & PRESENTING AUTHOR:

Federica Rochira, WWU Muenster, Germany

Christine Thomas, WWU Muenster, Germany

Seismic reflectors have been detected throughout the mid-mantle at different depths, but for some of them, their origin remains poor understood. Whether they are related to current or past subducting slabs, upwelling regions or deformation processes is still a matter of debate. In this study, we aim to investigate the presence of structures in the mid-mantle. We search for seismic signals travelling off great circle path that is connecting the source with the receiver. The dataset consists of events located in Indonesia and in Japan, recorded at the broadband stations in Morocco, Namibia and Germany. By applying seismic array techniques, we measure the slowness, backazimuth and traveltime of the out-of-plane arrivals. These parameters provide the information to locate the reflection source regions and then, to map seismic heterogeneities in the Earth's mantle. We back-trace the out-of-plane arrivals as P-to-P, S-to-P or P-to-S phases and find that most of the detected reflectors are located in the mantle at depths shallower than 1500 km. Additionally, the positions

of mid-mantle reflectors correlate with the edges of high velocity anomalies beneath southern Asia, as seen in tomographic images. These high-velocity anomalies have been interpreted as remnants of fossil slabs due to the subduction of the Tethys Ocean. Amplitudes, polarities and frequency dependence of the seismic waves are used to further investigate the seismic structures.

KEYWORDS :   mantle processes, subduction processes, South Asia

Sr No: 688

- -

SYMPOSIUM :   **S13 CoESG & SEDI Seismic structures in the mantle**

The Nazca Slab and the Upper Mantle Discontinuities under Southern Peru

CORRESPONDING & PRESENTING AUTHOR:

Xyoli Prezcampos, Instituto de Geofísica, Universidad Nacional Autónoma de México, México

In southern Peru, we create a common conversion stack from receiver functions (RFs) that are back-projected along their ray path according to the iasp91 velocity model. The 410 and the 660 discontinuities are observed at about the same depth as for the iasp91 model but in the south, a valley on the 410 and a hill on the 660 topography are observed beneath the region where the Nazca slab steepens its dip. Another hill on the 660 topography is present at the northern end of the flat slab. These two regions are the thinnest regions of the transition zone indicating the mantle is the warmest here. The 660 generally shows a low topographic relief to the west of the change in slab dip, corresponding to the thickest region of the transition zone and hence the coolest. In addition to the 410 and the 660, we identify other seismic discontinuities at depths 261 ± 12 km and 495 ± 10 km. The later one is not ubiquitously observed. Another discontinuity can be sporadically seen between 280 and 400 km depth.

KEYWORDS :   mantle transition zone, mantle discontinuities, receiver functions

Sr No: 689

- -

SYMPOSIUM :   **S13 CoESG & SEDI Seismic structures in the mantle**

Mantle structure beneath Indian Ocean Geoid Low: Constraints from Receiver function study using OBS-array

CORRESPONDING & PRESENTING AUTHOR:

Sanjay Singh Negi, National Centre for Polar and Ocean Research, India
Amit Kumar, National Centre for Polar and Ocean Research, India
Lachit K Ningthoujam, National Centre for Polar and Ocean Research, India
Dhananjai K Pandey, National Centre for Polar and Ocean Research, India

A pronounced large scale geoid anomaly with high-amplitude (-40 to -106 m) on earth straddle the Indian ocean. The lowest geoid height in the Indian ocean, compared to the geoid lows beneath other parts of world has led to the hypothesis of the presence of low density and low velocity anomalies in the mid- and upper mantle and high velocity anomalies near the base of the mantle (Reiss et al 2017; Ghosh et al., 2017; Rao et al., 2020). To image the mantle transition zone discontinuities beneath the Indian Ocean Geoid Low (IOGL) we obtained P- receiver functions using passive OBS array data from the IOGL region. We observe a major depression in 410 km and 660 km depth discontinuities. This indicates a hot mantle material regime,

in which the majorite garnet to perovskite transition may become dominant at 660 km depth. We attribute this shift behind observed depression at 660 km transition boundary (Hirose, 2002). This scenario is only possible above 1527 K (Hirose, 2002) and requires minimum excess temperature range of 200-300 K (Jenkins et al., 2016). Our findings are in good agreement with the excess temperatures estimated by Reiss et al., (2017) in the central IOGL region. Our new results suggest a garnet dominant hot mid-mantle anomaly towards the center of the geoid low. The outcomes from our present study in combination with global tomography models (French and Romanowicz, 2015; Simmons et al., 2010) offer new avenues towards exploring a rising mantle plume in the Indian Ocean.

KEYWORDS :   mantle discontinuities, Indian Ocean Geoid low, transition zone

Sr No: 690

SYMPOSIUM :   **S13 CoESG & SEDI Seismic structures in the mantle**

Eikonal tomography of North American upper mantle using multi-mode surface waves

CORRESPONDING & PRESENTING AUTHOR:
Kazunori Yoshizawa, Hokkaido University, Japan
Hitoshi Matsuzawa, Hokkaido University, Japan
Fanchi Lin, University of Utah, USA

A new radially anisotropic 3-D S-wave speed model in North America is constructed using multi-mode eikonal tomography. We employ a hybrid approach utilizing the multi-mode dispersion measurements for event-station paths with nonlinear waveform inversions (Yoshizawa & Ekström, 2010) and the eikonal tomography (Lin et al., 2009).

We first measure average phase speeds along source-receiver paths for 710 teleseismic events (2007-2015, Mw≥5.8) and seismic stations in the U.S., including USArray. Travel-time fields for each mode and period are then used to obtain phase speed distributions for each event from the horizontal gradient of travel-time fields, which are stacked for all events to reconstruct multi-mode phase speed models in the U.S. A radially anisotropic 3-D S-wave model is constructed using the joint inversions of local multi-mode dispersion curves of Rayleigh and Love waves.

The final 3-D model reflects the local-scale features beneath the U.S., such as the slow velocity anomalies in the western U.S. and New Madrid Seismic Zone. Owing to the use of higher modes, we can image the whole depth range of the upper mantle. The estimated Lithosphere-Asthenosphere Transition from the vertical gradient of the S-wave model shows the rapid change of lithospheric thickness in the east and west of the Rocky Mountains, suggesting the cratonic keels at around 200-250 km depth. Radial anisotropy indicates SH>SV anomalies in the shallow lithosphere. However, some locations, such as the Cascadia Range and Superior Craton below 300 km depth, show SV>SH anomalies, indicating vertical mantle flow underneath these regions.

KEYWORDS :   surface waves, higher mode, eikonal tomography

Sr No: 691

Subsurface Velocity Structure beneath the Indian Ocean Geoid Low Region Using Surface Wave

CORRESPONDING & PRESENTING AUTHOR:

Amit Kumar, National Centre for Polar and Ocean Research, MoES, Goa, India

Sanjay Negi, National Centre for Polar and Ocean Research, MoES, Goa, India

Lachit Ningthoujam, National Centre for Polar and Ocean Research, MoES, Goa, India

Dhananjai Pandey, National Centre for Polar and Ocean Research, MoES, Goa, India

The Indian Ocean Geoid Low (IOGL) is an enigmatic phenomenon that is yet to be convincingly understood. A wide range of hypotheses have been proposed by researchers to explain the source of this geoid anomaly. However, its connection with the upper, mid and lower mantle needs a detailed understanding and appropriate depth estimates could be assigned to this feature. Our investigation aims to estimate the deep subsurface velocity structure within the IOGL region. We utilize the fundamental mode Rayleigh wave, because these are generally well excited by shallow focused earthquakes. We considered earthquake records with magnitude>5.5 that occurred at depth<100 km at regional/teleseismic distances. Although ocean bottom seismometer (OBS) data is often noisy as compared to onshore observations; average phase velocity between the period range of 30 to 200 s are retrieved reasonably well underneath an array of 17 OBSs. Inversion of estimated dispersion curves demarcates the Moho depth ~18 km (below sea level), lithosphere asthenosphere boundary (LAB) at ~55 km depth and depth interval of low velocity zone below the LAB. Results from our modelling, at variance with some earlier studies, suggest presence of a prominent low velocity zone beneath the IOGL region. Our ensued detailed investigations would fill the requisite gaps in precise determination of the vertical velocity variations underneath the IOGL region and consequently improve our understanding of the possible causes behind such anomalous features.

KEYWORDS :   phase velocity, OBS, IOGL

SI4   CoESM & CoSOIEarthquake Source Mechanics

CONVENERS: Satoshi IDE (Japan)
Keisuke ARIYOSHI (Japan)
Daniela KÜHN (Norway)
Seok Goo SONG (Korea)
Anna SKORKINA (Russia)

Recent high quality seismic and geodetic observations provide large volumes of broadband data, which enable accurate determination of earthquake source parameters (locations, magnitudes, durations, moment tensors, etc.) and detailed imaging of rupture processes emerging from slow background processes. Further, techniques for solving inverse problems have improved substantially in the recent past. Abundant information from these analyses is the basis for studying a variety of earthquakes including swarms, tectonic and volcanic events as well as induced events, and to seek the governing laws and conditions for rupture initiation, growth, and arrest. It also provides useful input to estimate the stress state, fault geometry, and fluid movement around seismic regions. The entire earthquake process from long-term tectonic loading and slow nucleation to rapid rupture propagation with strong motion radiation is now studied using numerical simulations. The validity of assumptions in these simulations is tested by data analysis and laboratory experiments supported by several drilling projects. In this symposium, we invite contributions on data analysis and interpretation of earthquake parameters and source processes, on improvement and validation of routine analysis techniques, on theoretical and numerical modeling of dynamic ruptures and earthquake sequences, and observational and experimental studies on the physics of earthquakes.

Sr No: 692

High-frequency source parameters for earthquakes of the Russian Far East

CORRESPONDING & PRESENTING AUTHOR:

Anna Skorkina, IEPT RAS, Russia

Kamchatka network of digital broadband seismic stations (D0 in FDSN), deployed in 2006–2010, provides the completeness magnitude of ~3.5 for most of the region. It also allowed applying the spectral approach to obtain high-frequency parameters as corner frequencies (up to three corner frequencies), moment magnitudes (the threshold is ~3.5), and spectral stress drop. Input data set, with appropriate SNR, includes >1000 earthquakes that occurred in 2010–2017 in different gulfs near Kamchatka (Avacha Gulf, Kronotsky Gulf, Gulf of Kamchatka, and near the Bering). Earthquakes of the Bering fault zone can be characterized by a two-corner frequencies model [Brune, 1970], while sources of other studied areas have a three-corner shape [Gusev, 2013, 2014]. No clear indication of spectral stress drop dependence on the seismic moment is found. The study was supported by a grant from the Russian Science Foundation (project 20-17-00180).

Sr No: 693

Theoretical Properties of Source Time Functions based on a Stochastic Differential Equation

CORRESPONDING & PRESENTING AUTHOR:

Shiro Hirano, Ritsumeikan University, Japan

INTRODUCTION

Many seismic source inversion analyses and recent classification of the inversion results have revealed that Source Time Function (STF) during earthquakes satisfies some empirical laws that (1) STFs are dominantly non-negative, continuous, compactly supported, and unimodal, (2) amplitude Fourier spectra of STFs are approximated by ω^2-model, (3) time-integration of STFs are proportional to t^3, and (4) The probability distribution of their total moment follows the Gutenberg-Richter law. Considering the complexity of earthquake source processes, traditional source modellings do not explain these properties, and some stochastic modelling would contribute to our understanding.

METHODS

We model STFs as a convolution of two solutions of the Bessel process, which describes non-negative distribution by using a stochastic differential equation. Some properties of the STFs are derived mathematically, while others are investigated numerically.

RESULTS

By applications of known mathematical results on the Bessel process, we could prove that our model satisfies the properties (1), (2), and (4). We found that the dimension parameter of the Bessel process must be zero for (4). Numerical simulations statistically reproduce all four properties.

CONCLUSION

The empirical laws (1) to (4) can be interpreted within our model. The most important discussion is on the physical meaning of the convolution of two solutions of the Bessel process. Because STF is a convolution of stress drop rate over the entire fault surface and self-impedance of the fault, we regard that these two are Bessel process.

KEYWORDS : source time funciton, earthquake source spectra, stochastic differential equation

Sr No: 694

SYMPOSIUM : **S14 CoESM & CoSOI Earthquake Source Mechanics**

Waveform-based probabilistic moment tensor inversion of shallow small-magnitude earthquakes (M←3.2) in North German gas fields

CORRESPONDING & PRESENTING AUTHOR:

Daniela Kuehn, GFZ, Germany

Martina Rosskopf, GFZ, Germany

Gudrun Richter, GFZ, Germany

Jose Angel Lopez Comino, Universidad de Granada, Spain

Gesa Petersen, GFZ, Germany

Torsten Dahm, GFZ, Germany

We implement a novel, probabilistic full waveform moment tensor inversion ("Grond", Heimann et al., 2018) to shallow micro-earthquakes occurring close to gas fields in Northern Germany. The method allows to investigate uncertainties arising from simplified 1-D velocity models and errors in locations. As a consequence of applying automated waveform-based data processing it is crucial to identify stations with erroneous transfer functions, gain factors or component orientation in advance.

In addition, the correct interpretation and modelling of high-frequency body waves becomes essential for low magnitude earthquakes that usually do not contain sufficient surface wave energy for standard moment tensor inversion. However, the appearance and coda phases of high-frequency body waves are strongly controlled by the site structure and, if applicable, depth of the borehole stations. For example, the existence of unknown high velocity layers above a reservoir may lead to misinterpretation of source location and mechanism (Kraaijpoel and Dost, 2012).

We apply the inversion method to events in the region of Langwedel (Lower Saxony), the largest of which is the ML 3.2 20th Nov 2019 earthquake, recorded on both BVEG and GRSN networks, comprising short period and broadband stations of different instrument types. Among others, we focus on the preparatory tasks of checking the station and data quality, partly by employing automated tools ("AutoStatsQ", Petersen et al., 2019), as well as on building 1-D velocity models. We compare findings to results of a rupture directivity analysis in the manner of López-Comino et al. (2021).

KEYWORDS : probabilistic moment tensor inversion, station quality control, small-magnitude earthquakes

Sr No: 695

Tectonic regimes and stress patterns in the Vrancea Seismic Zone: insights into intermediate-depth earthquake nests in locked collisional settings

CORRESPONDING & PRESENTING AUTHOR:

Laura Petrescu, National Institute for Earth Physics, Romania

Felix Borleanu, National Institute for Earth Physics, Romania

Mircea Radulian, National Institute for Earth Physics, Romania

Alik Ismail Zadeh, Karlsruhe Institute of Technology, Germany

Liviu Matenco, Universiteit Utrecht, Netherlands

Earthquake nests are anomalous clusters of seismicity located far from active collisional systems in intraplate, locked suture zones, or the deep part of relic subducted slabs, challenging classic earthquake generation mechanism theories. The Vrancea Seismic Zone in Romania is such an upper-mantle seismic nest located in the SE Carpathians, releasing the largest strain in continental Europe. To better understand earthquake generation processes and the relationship with lithospheric deformation, we estimate earthquake source parameters in and around Vrancea between 2014 and 2020, and determine the stress field via focal mechanism inversion and unsupervised machine learning. In the crustal domain, maximum horizontal stress is in agreement with surface fault kinematics and GPS-derived S-SE trending horizontal plate velocities relative to Eurasia, implying that tectonic stress is vertically coherent on a crustal scale. Inside the seismogenic body vertical tension and an overall compressive regime dominates, implying that vertical elongation may be the driving mechanism for brittle failure and that stress is transmitted along the sinking slab to the surface. However, the retrieved stress ratios are low: ~0.2 for mantle earthquakes Mw>4 and ~0.4 for Mw<4, challenging the brittle failure assumption. Increased pore fluid pressure has been shown to lower stress ratios, implying that dehydration embrittlement may contribute to generating intermediate-depth seismicity in the Vrancea slab. Comparisons with seismic tomography and anisotropy studies show excellent correlations between maximum horizontal stress directions, possible slab strike orientation, and seismic anisotropy, especially below ~130km depth, suggesting ambient mantle flow may also promote in-slab stress build-up and seismic potential.

KEYWORDS :   intermediate-depth earthquakes, stress inversion

Sr No: 696

Earthquake Rupture Pathways Determined by Bedrock Structure – The Mw 6 Petermann Ranges Earthquake in Australia

CORRESPONDING & PRESENTING AUTHOR:

Januka Attanayake, University of Melbourne, Austalia

Tamarah King, University of Oxford, UK

Mark Quigley, University of Melbourne, Austalia

Tao Mo, University of Melbourne, Austalia

Abraham Jones, University of Melbourne, Austalia

Gary Gibson, University of Melbourne, Austalia

David Belton, University of Melbourne, Austalia

Mike Sandiford, University of Melbourne, Austalia

Despite located in the Indo-Australian plate interior, the Australian continent experiences a Mw $\geq$ 6 earthquake approximately every 8.5 years on average. The 20 May 2016 Mw 6 Petermann Ranges Earthquake (PRE) in central Australia is the largest surface-rupturing onshore event to have occurred in nearly 27 years in Australia with a shallow hypocentre (< 5 km). We used field measurements, geodetic observations (Interferometric Synthetic Aperture Radar (InSAR) and differenced digital elevation models (dDEMs)), and high-quality teleseismic and local waveform datasets to determine precise rupture characteristics of PRE.

Our field measurements, along with geodetic observations, delineate a 21 km long linear two-segment surface rupture trace (SRT) with deformation zones 7 km and 3 km wide, respectively, on the hanging and foot wall sides and variable vertical displacements up to 0.96 m along SRT. We estimated a strike of 294° $\pm$ 29° of the causative fault from field and geodetic measurements and a dip of ~30° from precisely located aftershocks. Despite the expectation of a high crustal strength, the stress drop ($\Delta\tau$) of 2.2 MPa is markedly lower than that estimated for other Australian events (> 15 MPa) from teleseismic methods. This low $\Delta\tau$ and an estimated low radiation efficiency of ~25% (total radiated energy = 1.8 x 10^{13} Nm) are attributed to rupture propagation along weaker (low $\Delta\tau$) yet intact (low radiation efficiency) phyllosilicate-rich foliations subparallel to the causative fault plane. Recognition of bedrock control of earthquake nucleation is thus important to understand intraplate seismicity.

KEYWORDS : intraplate earthquakes, stress drop, bedrock structure

Sr No: 697

SYMPOSIUM : **S14 CoESM & CoSOI Earthquake Source Mechanics**

Relationship of preseismic, coseismic, and postseismic fault ruptures of large interplate earthquakes with slow-earthquake activity along the Japan Trench

CORRESPONDING & PRESENTING AUTHOR:

Hisahiko Kubo, National Research Institute for Earth Science and Disaster Resilience, Jpan

Tomoaki Nishikawa, Disaster Prevention Research Institute, Kyoto University, Japan

To improve our understanding of the interactions between regular earthquakes and slow earthquakes along the Japan Trench, we investigated the spatial relationship of slow-earthquake activity with the preseismic, coseismic, and postseismic fault ruptures of interplate earthquakes off the Iwate and Ibaraki coasts, Japan, including two large interplate aftershocks of the 2011 Tohoku earthquake: the 2011 off Iwate earthquake (MW 7.4) and the 2011 off Ibaraki earthquake (MW 7.8). We found that the coseismic ruptures of these earthquakes did not overlap with the active areas of slow earthquakes, while their foreshocks and aftershocks occurred in slow-earthquake-prone areas. Moreover, the 2011 off Iwate earthquake and the previous M7-class events shared common fault rupture characteristics: coseismic rupture occurred in a common asperity area, and afterslip with many aftershocks was triggered in the active area of slow earthquakes. This study demonstrates that large earthquakes off the Iwate and Ibaraki coasts feature similar rupture behaviors, spatially complementary distributions of coseismic ruptures with slow-earthquake activity and foreshock and aftershock activities within and around slow-earthquake-prone areas. This information is useful in considering future large earthquakes along the Japan Trench.

KEYWORDS : regular earthquake, slow earthquake, Japan trench

Sr No: 698

Toward Moment-Tensor Inversion Advancement Through Incorporating Earth Structure Uncertainty

CORRESPONDING & PRESENTING AUTHOR:

Thanh Son Pham, Australian National University, Australia

Hrvoje Tkalcic, Australian National University, Australia

Full-waveform moment-tensor (MT) inversion is often used for moderate earthquakes at regional scales, in which simulated waveforms by a structural model are matched with observed seismograms. Therefore, the used structural model's accuracy plays a critical role in retrieving reliable characterization of the seismic sources. Seismic velocity structures, often described through 1D models, are inaccurate, and there is always an inevitable discrepancy between predicted waveforms and the observations due to the imperfection of Earth models. This discrepancy accounts for a significant portion of the theory uncertainty considered in the MT inversion problem. This study investigates a method to incorporate Earth structure uncertainty alongside the data-noise uncertainty in the full-waveform MT inversion scheme. The uncertainty in the Earth model is employed via the structure-uncertainty covariance matrix, which is numerically estimated. Our synthetic experiments demonstrate the importance of accounting for the theory uncertainty in the full-waveform MT inversion, especially for high-frequency seismograms. The method is further applied to real-data examples from volcanic events in Long Valley Caldera and Bardarbunga to scrutinize the previous results. We conclude that careful consideration of the Earth model's uncertainty must become an integral part of future MT inversion efforts and necessary for understanding complex earthquake sources.

KEYWORDS : moment tensor; inverse problem; uncertainty

Sr No: 699

Probabilistic Point Source Modelling at the ISC

CORRESPONDING & PRESENTING AUTHOR:

Thomas Garth, International Seismological Centre, UK

Karin Sigloch, University of Oxford, UK

Dmitry Storchak, International Seismological Centre, UK

Earthquake moment tensor solutions are produced by a wide range of global or regional seismic monitoring agencies, many of which are reported to and curated by the International Seismological Centre (ISC). This overview of reported moment tensors demonstrates the variation of mechanisms reported for a single earthquake, that arises in part due to the variety of methodologies that are applied, but also reflects the inherent uncertainty in the point source representation of the earthquake source. Here we outline the techniques behind the new ISC-PPSM (International Seismological Centre – Probabilistic Point Source Model) catalogue, which employs a probabilistic inversion strategy to constrain the earthquake point source (moment tensor, source time function and depth), along with their inherent uncertainties. The result is an ensemble of earthquake point source models that can account for the body wave observations informing the inversion. The joint consideration of this well-fitting ensemble enables insights into trade-offs such as the interdependence of STF length and earthquake depth. This improves depth resolution, particularly

for shallow (< 40 km deep), remote earthquakes of moderate magnitude (Mw 5.8 − 7.2), where no clear depth phases can be observed. Shallow earthquake depth estimates from ISC-PPSM therefore can be used to constrain earthquake depths in the ISC-bulletin that would otherwise be uncertain or fixed to a default depth. Finally, we demonstrate typical ISC-PPSM results for a number of illustrative earthquakes, and discuss potential uses of this new, open access ISC product.

KEYWORDS : earthquake sources

Sr No: 700

Non-DC earthquakes in 2017 swarm in Reykjanes Peninsula, SW Iceland: Sensitive indicator of volcano-tectonic movements at slow-spreading rift

Jana Doubravova, Institute of Geophysics CAS

CORRESPONDING & PRESENTING AUTHOR:
Pavla Hrubcova, Institute of Geophysics CAS, China
Vaclav Vavrycuk, Institute of Geophysics CAS, China

The analysis of the 2017 earthquake swarm along the obliquely divergent Reykjanes Peninsula plate boundary revealed the most frequent focal mechanisms corresponding to main activated fault, which relates to transform faulting of the North Atlantic Rift in Iceland. Detailed double-difference locations, focal mechanisms and non-double-couple (non-DC) volumetric components of seismic moment tensors indicate an activation of three fault segments suggesting continuous interactions between tectonic and magmatic processes. They are related to inflation/deflation of a vertical magmatic dike and comprise: (1) shearing at strike-slip transform fault with left lateral motion; (2) collapses at normal faulting with negative volumetric components due to magma/fluid escape, and (3) shear-tensile opening at oblique strike-slip faulting with positive volumetric components connected to flow of trapped over-pressurized fluids. The identification of three regimes of complex volcano-tectonic evolution in divergent plate movement proves an enormous capability of the non-DC volumetric components to map tectonic processes in such settings.

KEYWORDS : non-double-couple components of moment tensors, Reykjanes Peninsula SW Iceland, volcano-tectonic evolution

Sr No: 701

Stress field in the Tohoku region, Japan and its relationship with faults of recent earthquakes (2)

CORRESPONDING & PRESENTING AUTHOR:
Ayaka Tagami, Research Center for Prediction of Earthquakes and Volcanic Eruptions, Graduate School of Science, Tohoku University, Japan
Miu Matsuno, Research Center for Prediction of Earthquakes and Volcanic Eruptions, Graduate School of Science, Tohoku University, Japan
Tomomi Okada, Research Center for Prediction of Earthquakes and Volcanic Eruptions, Graduate School of Science, Tohoku
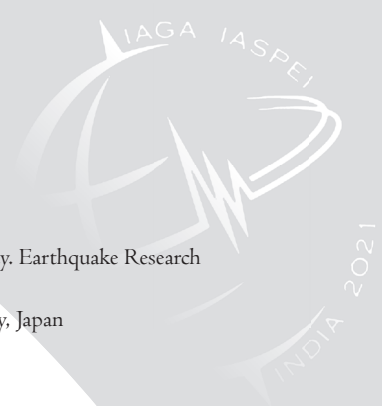
University, Japan

Shinichi Sakai, Earthquake Research Institute, University of Tokyo, Japan

Mako Ohzono, Institute of Seismology and Volcanology, Graduate School of Science, Hokkaido University. Earthquake Research Institute, University of Tokyo, Japan

Kei Katsumata, Institute of Seismology and Volcanology, Graduate School of Science, Hokkaido University, Japan

Masahiro Kosuga, Graduate School of Science and Technology, Hirosaki University, Japan

Yoshiko Yamanaka, Graduate School of Encironmental Studies, University of NAGOYA, Japan

Hiroshi Katao, Research Center for Earthquake Prediction, Disaster Prevention Research Institute, Kyoto University, Japan

Takeshi Matsushima, Institute of Seismology and Volcanology, Faculty of Sciences, Kyushu University, Japan

Hiroshi Yakiwara, Nansei-toko Observatory for Earthquakes and Volcanoes, Kagoshima University, Japan

Takashi Nakayama, Research Center for Prediction of Earthquakes and Volcanic Eruptions, Graduate School of Science, Tohoku University, Japan

Satoshi Hirahara, Research Center for Prediction of Earthquakes and Volcanic Eruptions, Graduate School of Science, Tohoku University, Japan

Toshio Kono, Research Center for Prediction of Earthquakes and Volcanic Eruptions, Graduate School of Science, Tohoku University, Japan

Shuichiro Hori, Research Center for Prediction of Earthquakes and Volcanic Eruptions, Graduate School of Science, Tohoku University, Japan

Toru Matsuzawa, Research Center for Prediction of Earthquakes and Volcanic Eruptions, Graduate School of Science, Tohoku University, Japan

Group For The Aftershock Observations Of The Off The Pacific Coast Of Tohoku Earthquake, Japan

INTRODUCTION

Many high-angle reverse fault planes are distributed in northeastern Japan. It is known that these faults planes were caused by the tensile stress field during the formation of the Japan Sea (Okamura and Kato, 2000). It is frequently observed that tectonic inversion of old normal faults (with high dip angle) occurs acting as reverse faults (e.g., Okamura et al., 1995).

In this study, we focused on three large to moderated-sized earthquakes that occurred in the inland area of northeastern Japan (the 1998 Mjma 6.1 Shizukuishi earthquake, the 2008 Mjma 7.2 Iwate-Miyagi Nairiku earthquake, and the 2003 Mjma 6.4 northern Miyagi earthquake). We estimated the stress field around the three earthquakes and investigated the relationship between the stress fields and the fault planes.

DATA AND METHODS

We use focal mechanism (moment tensor) data from the National Institute for Earth Science and Disaster Resilience (NIED) of Japan and focal mechanisms estimated from P-wave initial motions from Okada et al. (2019). For estimating the regional stress field, we deploy the stress tensor inversion method (Michael, 1984, 1987). For estimating the likelihood of slip, we use the Slip Tendency analysis (Morris et al., 1996).

RESULT AND CONCLUSION

The estimated stress fields were mostly reverse fault type. All the westward dipping planes showed lower ST values suggesting these earthquakes occurred along the fault planes unlikely to slip in the estimated stress fields. High pore fluid pressure and/or low friction coefficient could cause the unfavorable slip.

KEYWORDS : slip tendency, northeast Japan, stress field

Sr No: 702

Seismotectonic implications of the earthquakes sequence generated in the Southern Carpathians, Orsova June-July 2020 (Romania)

CORRESPONDING & PRESENTING AUTHOR:

Andrei Mihai, National Institute for Earth Physics, Romania
Eugen Oros, National Institute for Earth Physics, Romania
Anica Otilia Placinta, National Institute for Earth Physics, Romania
Iren Adelina Moldovan, National Institute for Earth Physics, Romania

The paper presents the results of the macroseismic and instrumental study of the seismic sequence produced in the western part of the Southern Carpathians, from June 25 to July 6, 2020. The main shock of the sequence occurred on June 25, 2020 at a depth of 16 km, had the moment magnitude $Mw = 4.1$, and was preceded by a foreshock with $Mw = 3.2$ produced 3 hours before. The causative fault is a transcurrent fault, lateral-right, oriented NE-SW (Cerna - Jiu Fault). The sequence has 16 earthquakes with magnitude $Mw = 1.6-4.1$ distributed in a narrow area (8x13 km) elongated approximately in the NS direction and is concentrated in the depth range of 14-21 km. The solutions of the focal mechanisms, calculated from the polarities of the P waves and the ratio of the amplitudes of the S / P waves, are characterized by predominantly detached faults, the P axes constantly oriented N760E on the direction of the maximum horizontal stress in the Intra-Carpathian space. The macroseismic data partially confirm both the attenuation relationship of the macroseismic intensity with the hypocentral distance and the acceleration-intensity conversion algorithm.

The results obtained in this paper bring additional information and solutions of great value to improve the procedures of real-time intensity estimation and the acceleration-intensity conversion algorithm necessary for the realistic evaluation of the local seismic hazard and risk.

KEYWORDS : earthquakes, macroseismic intensity, focal mechanism

Sr No: 703

Broadband slow earthquakes

CORRESPONDING & PRESENTING AUTHOR:

Satoshi Ide, The University of Tokyo, Japan

Since around 2000, various slow geophysical phenomena have been discovered in subduction zones and other rapidly deforming tectonic regions, worldwide. Depending on the observation frequencies/periods, they are named as tectonic tremors, low frequency earthquakes (LFE), very low frequency earthquakes (VLFE), and slow slip events. Most of them occurred almost simultaneously at almost the same location, with similar mechanism consistent with regional tectonic deformation. Ide et al. (2007) hypothesized the existence of a unified broadband phenomena called slow earthquakes, sharing a scaling relation different from that for ordinary fast earthquakes.

While tremor and LFE are separated from the VLFE frequency range by microseism noise, nearfield borehole observation of shallow tremor and VLFE revealed that the spectrum of these phenomena are continuous from 0.01 to 10 Hz (Kaneko et al., 2018). We can also retrieve broadband signals by stacking many LFE records as shown in Cascadia (Ide, 2019) and Nankai (Masuda et al., 2020). Thus, we can now interpret tremor and VLFE as partial component of broadband slow earthquakes.

The broadband slow earthquakes are probably controlled by random diffusional mechanism. Brownian slow earthquake model (Ide, 2008; Ide and Yabe, 2019) is a stochastic model that can explain the various characteristics of broadband slow earthquakes, such as the scaling relation between seismic moment and duration, the small ratio between seismic energy and seismic moment, slow diffusional migration pattern, and size-frequency statistics. Some regional differences can be explained by the geometrical constraint of tremor zones in Nankai, Cascadia, and Mexico (Ide and Maury, 2018).

KEYWORDS :   slow earthquakes, tectonic tremor, stochastic model

S15   CoTCS Structure of the lithosphere

CONVENERS: Prakash Kumar (India)
             Gabi Laske (USA)
             Ulrich ACHAUER (France)
             Walter Mooney (USA)

The lithosphere has preserved a record of the evolution of a multitude of Earth systems. The lithosphere-asthenosphere boundary is of fundamental importance in understanding the mantle dynamic processes. Recently many usages of the term lithosphere have been introduced based on seismic- wave velocities, seismic anisotropy, attenuation, electrical conductivity and compositions of mantle- rock samples. However, there is no general consensus on its nature in various geological units and its relation with the crust-mantle and mid-lithospheric discontinuities. Advances in seismology have resulted in much richer and more complex picture of the lithosphere than ever before. But ever new images and models also generate many new questions and varied interpretations. A partial list of questions includes the process of lithospheric formation and modification, the presence of fluids and/or partial melt, the geometry of crustal faults at depth, lithospheric modification by lateral flow, the existence and origin of seismic anisotropy and the age and physical properties of the Moho and mid-crustal discontinuities, nature of lithosphere-asthenosphere boundary etc. We welcome research contributions from various fields on regional and global scales, particularly those with a multi-disciplinary perspective to understand the crustal, lithospheric structure and lithosphere-asthenosphere system.

Imaging the crustal and upper mantle discontinuities beneath the Malani Igneous Province, NW India

CORRESPONDING & PRESENTING AUTHOR:

Gowthami Bandlamudi, Indian Institute of Technology Bombay, India

Mohan Gollapally, Indian Institute of Technology Bombay, India

The crustal and upper mantle discontinuities beneath the Malani igneous province(MIP) in northwestern India, adjoining the Aravalli-Delhi fold belt (ADFB), were imaged using P receiver functions. The MIP is a Neoproterozoic igneous province in the Marwar craton that has witnessed several volcanic episodes since the Malani bimodal volcanism. A total of 3904 receiver functions were constructed by iterative time-domain deconvolution technique using 1744 teleseismic events with magnitude $\geq$ 5.5 that were recorded at 21 broadband stations deployed in an area of 300 km². The delay times for the Pms conversion from the Moho vary from 4.0s to 5.72s at stations in MIP. The shear velocity structure was estimated by inverting the stacked RFs using the neighbourhood algorithm, and, the H-k method was utilized to estimate the crustal thickness and Poisson's ratio. The average crustal thickness and Poisson's ratio vary from ~35 $\pm$ 1 km and 0.28$\pm$0.01 beneath the Barmer rift to 42 $\pm$ 2km and 0.27$\pm$0.01 in the region adjoining the ADFB. The lower crustal shear velocities range between 3.9 km/s to 4.1km/s, indicating magmatic underplating. Overall the Poisson's ratios indicate intermediate crustal composition. The P410s and P660s time lags are delayed by $\approx$0.6s relative to those predicted by the IASP91 standard earth model, while the difference (P660s – P410s) is 24s suggesting an unperturbed mantle transition zone. The delays can be attributed to reduced seismic velocities in the uppermost mantle, possibly related to lithospheric thinning or thermal/compositional variations associated with the imprints of pre-Deccan volcanism beneath MIP.

KEYWORDS :   malani igneous province, receiver function, crust and upper mantle

The influence of multi-scale heterogeneity on surface-wave phase speeds and apparent radial anisotropy

CORRESPONDING & PRESENTING AUTHOR:

Yunao Xu, Hokkaido University, Japan

Kazunori Yoshizawa, Hokkaido University, Japan

Takashi Furumura, The University of Tokyo, Japan

Recent studies on high-frequency scattering and P wave reflectivity have suggested the existence of fine-scale heterogeneity of horizontally elongating laminated structure in the upper mantle (Kennett 2015; Kennett & Furumura, 2016), which may cause changes in long-period surface wave phase speeds and generate apparent radial anisotropy.

To investigate the effects of such heterogeneity on long-period surface waves, we performed a series of 2-D finite-difference method simulations of seismic waves in the heterogeneous structures. The inter-station measurements of fundamental-mode Rayleigh wave phase velocity are then performed to quantify the effect of elongated heterogeneity on long-period surface waves.

Results showed that horizontally elongated fine-scale heterogeneity could cause a non-negligible velocity drop for the fundamental-mode Rayleigh wave. The effects of increased strength of heterogeneity, enlarged the characteristic scale of heterogeneity, and increased thickness of the heterogeneous layer all lead to the increase of velocity reduction. A multi-scale heterogeneity model including both fine-scale (<10 km scale correlation distance) and medium-scale (10-100 km scale) heterogeneity has shown that it will create a more substantial velocity drop than fine-scale alone, especially in a shorter period range (30-60 s). By introducing such multi-scale heterogeneity, we can reproduce a significant velocity drop (2~2.5%) for long-period surface waves with a reasonable strength of fine-scale heterogeneity. This result fits well with earlier studies on this issue (e.g., Kennett et al., 2017), which may help to explain the rapid changes in anisotropic properties near the continental Mid-Lithosphere Discontinuity (MLD).

KEYWORDS : heterogeneity, seismic anisotropy, surface wave

Sr No: 706

SYMPOSIUM : **S15 Structure of the lithosphere**

Rayleigh wave tomography from ambient seismic noise in SE Canada and the NE USA

PRESENTING AUTHOR:

Omid Bagherpur Mojaver, GEOTOP, University of Quebec in Montreal (UQAM) , Canada

CORRESPONDING AUTHOR:

Fiona Darbyshire, GEOTOP, University of Quebec in Montreal (UQAM) , Canada

Stacking long duration cross-correlation of ambient seismic noise for pairs of broadband seismic stations results in emergence of inter-station Empirical Green's Functions (EGFs). A collection of calculated inter-station EGFs can be analysed in a surface wave tomography approach to obtain phase velocity variations in a region. In this study, we use ambient seismic noise vertical component recordings between 2013 and 2015 to obtain Rayleigh wave phase velocities sensitive to crustal depths beneath SE Canada and the NE USA. Our study area covers the Phanerozoic northern Appalachians and the Proterozoic eastern Grenville Province that together have experienced ~1 billion years of tectonic evolution. Our phase velocity maps suggest complex variations of seismic structure across the study area with generally slower velocities in the Appalachians than the Grenville domain. The observed patterns of velocity variations at different periods provide us clues to discuss tectonic implications. The slow anomalies recovered across the Gulf of Saint Lawrence and along the Appalachian-Grenville boundary are interpreted as resulting from a very thick sedimentary basin and a step-like Moho geometry beneath those regions respectively. We also assess directional and seasonal variations of ambient seismic noise over the two-year course of our datasets used in this study, and investigate its effect on reliability of our tomography models.

KEYWORDS : ambient seismic noise tomography, Northern Appalachians, Eastern Grenville Province

Sr No: 707

Using Receiver Functions to estimate the preliminary Moho and Vp/Vs in Northern Amazon Craton, Brazil.

Bruno Bezerra, IG - University of Brasilia, Brazil

Aline Araujo, University of São Paulo, Brazil

CORRESPONDING & PRESENTING AUTHOR:

George Franca, University of Brasilia, Brazil

The Amazonian Craton in Brazil is so hard to access, but in the last years after the implemented seismograph Brazilian network, several studies were performed. However, there are still areas to be explored such as the Northern Amazonian Craton. Then, we are using receiver functions to estimate Moho and Vp/Vs to collaborate with discussions about the results geologically, regarding its age, composition, and seismicity. We used four seismographic stations installed in Para state. In the Receiver Function technique the teleseismic is used to image the discontinuity structures underneath isolated seismic stations. The resulting receiver function is obtained by removing the effects of source and structure path effects. Once we have the receiver function traces, we follow up with the H-k Stacking method. It is literally the stacking of all the data generated in the receiver functions, which will plot a diagram relating Moho and the Vp/Vs ratio. We can use it to estimate the values for the Moho and the Vp/Vs for the region of a given station. A preliminary average thickness of the regions Northern and Southern to the Amazonian Craton was obtained, varying from 40 to 45 km in both directions of the craton. Among the results, we can also find values for the Vp/Vs varying from 1.70 to 1.74. Those results are important to define the location of earthquakes happening in and around the Amazonian Craton more accurately and to provide us a better comprehension of the crust in this province.

KEYWORDS : receiver function, Vp/Vs, crustal thickness

Sr No: 708

Elusive nature of the Dharwar lithosphere, India: A geochemical perspective

CORRESPONDING & PRESENTING AUTHOR:

Tarun Khanna, CSIR-National Geophysical Research Institute, India

Magmatism in the cratonic interiors is consequential to asthenospheric upwelling accompanied by interaction with the sub continental lithospheric mantle, and the overlying continental crust. Magmatic emplacements eluding such interactions are an extremely rare and intriguing phenomenon that warrants in depth investigations. Prolonged scavenging of the lithosphere by upwelling asthenospheric mantle melts can substantially weaken the lithospheric keel of a craton. Consequently, it triggers lithospheric erosion, thinning and extension resulting into continental rifting and subsequent break-up. Besides the geophysical investigations, which provide significant insights into the nature of a sub continental lithosphere, petrological studies potentially examine the volley of magmatic processes that culminated into shaping it. The evolution of such magmatic processes can therefore be constrained by carrying out geochemical studies in the mafic dikes that are emplaced within the cratonic provinces of the Earth. Rationale being that the geochemical

signatures, which are well preserved in the mafic dikes, not only provide an important window into the precursor crust-lithosphere-asthenosphere interaction processes, but also enable us to understand the geodynamic evolution of the craton through space and time. Apparently, the lithosphere beneath the Dharwar craton was either very frail or incapacitated to participate in the process, or perforated to channelize deep seated fractures to act as potential conduits for magma transport. In this contribution, two such rare and unique magmatic events of ~2.5 Ga and ~2.2 Ga from the western and eastern parts, respectively, of south India are presented to describe the elusive nature of the lithospheric mantle beneath the Dharwar craton.

KEYWORDS : lithospheric erosion, mafic dikes, Dharwar Craton

Sr No: 709

- -

Crustal anisotropy in Arunachal Himalaya inferred from splitting of local S waveforms

PRESENTING AUTHOR:

Undapalli Nanajee, CSIR – National Geophysical Research Institute, India

Sunil K. Roy, CSIR – National Geophysical Research Institute, India

CORRESPONDING AUTHOR:

M. Ravi Kumar, CSIR – National Geophysical Research Institute, India

Crustal shear wave anisotropy of Arunachal Pradesh, located in the eastern Himalaya, is investigated by analysing splitting of steeply incident (i c ≤45°) direct S-phases of local earthquakes, recorded at 19 stations. The 84 high-quality splitting measurements reveal that the delay times between fast and slow waves range from 0.02 to 0.4 s, and clustered between 0.05 and 0.11 s. The smallest delay times are found at stations located in the westernmost part of Arunachal Himalaya. A large variation in the Fast Polarisation Azimuths (FPA) is found among the stations, with a dependence on the back azimuth of the S-wave. The observed FPAs are either parallel to the horizontal compressive stress or the structural fabric. For the stations located in the westernmost part of Arunachal Himalaya, the FPAs obtained from SW azimuth are mainly oriented along the NW-SE or NNW-SSE direction, which is parallel/subparallel to the maximum horizontal stress. For the majority of stations located in the central and eastern parts, the FPAs are mostly oriented along the NE direction, parallel to the structural fabric. In the easternmost part of Arunachal Himalaya, there is a variation in the orientation of FPAs from south to north, which seems associated with the variation in structural fabric. In the southern part, the structural fabric is orientated along the NE direction while the northern part experiences a clock-wise rotation associated with the Siang window. The normalized time delay beneath the region is around 0.007 s/km and does not show depth dependence.

KEYWORDS : seismic anisotropy, shear-wave splitting, crust

Exploring the depth variation of crustal discontinuities and Lithosphere-Asthenosphere Boundary beneath the tectonically stable Central India

CORRESPONDING & PRESENTING AUTHOR:

Himangshu Paul, CSIR-National Geophysical Research Institute, India

D. Srinagesh, CSIR-National Geophysical Research Institute, India

Central India (between 20°N and 27°N latitudes) comprises well-known cratons and fold belts like the Bundelkhand craton, parts of Bastar and Singhbhum Craton, Delhi-Aravalli, Satpura and Singhbhum fold belts. The formation age of the Cratons is older (2.5–3.5 Ga) while the fold belts were formed later (1.7–1.9 Ga). It is expected that these Cratonic characteristics are preserved in Central India as it is relatively stable compared to the tectonically active Himalaya in the north or Mesozoic magmatic episodes in the south. We wanted to study if these different cratons have similar crustal and lithospheric characteristics and how did the formation of fold belts affect them. About 20 seismological stations are being operated within Central India by NCS, New Delhi, and CSIR-NGRI, Hyderabad. We modelled the 1D shear velocity of the crust and lithosphere beneath these stations by inverting the P-receiver functions (PRF). The crustal discontinuities were identified by inverting high-frequency RFs (low pass 2 Hz) whereas Lithosphere-Asthenosphere Boundary (LAB) depth is obtained by joint inversion of PRF (lowpass 0.5 Hz) and Rayleigh wave dispersions. The depth variation of the Moho was found to be independent of the tectonic provinces. However, we found that the LAB depth was shallower beneath Singhbhum and Bundelkhand Craton (~120 km) while beneath the Delhi-Aravalli, eastern Satpura, and Singhbhum fold belt it was relatively deeper (~140 km). They could either indicate delamination or thinner Indian Cratons. We also found significant depth differences in the intra-crustal layer across the region.

KEYWORDS :   lithospheric structure, Central India, receiver function inversion

Improving the Signal-to-Noise ratio of Converted seismic wave data using the Seislet Transform

PRESENTING AUTHOR:

Bijayananda Dalai, CSIR- National Geophysical Research Institute, Uppal Road, Hyderabad-500007, India

CORRESPONDING AUTHOR:

Prakash Kumar, CSIR- National Geophysical Research Institute, Uppal Road, Hyderabad-500007, India

Xiaohui Yuan, Deutsches GeoForchungsZentrum GFZ, Telegrafenberg, Potsdam 14473, Germany

Seismic or Seismological data commonly contain various types of noises that most of the times lead to an ambiguous interpretation of subsurface. In order to improve the signal-to-noise ratio, a number of methods exist which have their own advantages and limitations. Here we utilize a robust sparsity enhancing tool, i.e. the Seislet Transform (ST), to de-noise the receiver function data by applying the regularization. The ST is primarily characterized by the plane wave destruction method combined with the wavelet-lifting scheme. Therefore, the locally dominant event slopes are obtained precisely and then the components of lifting scheme such as update and predict operators decompose the data into multiscale orthogonal basis and the

basis-functions are oriented along the dominant events following the local linearity. As a result of which, the ST achieve the highest compressional capability, consequently, signal can be effectively compressed in the small scale and the random noise spreads in the whole transform domain. As per the fact that, the signal and noise have different characteristics, signal and noise separation in the Seislet Transform domain is achieved by simply applying a structural filtering approach i.e. the thresholding operator. The method is first tested on synthetic data contaminated with various amount of noise and then on the real field data.

KEYWORDS : receiver functions, de-noise, seislet transform

Sr No: 712

SYMPOSIUM : **S15 Structure of the lithosphere**

Seismic structure and its implications on the chemical composition of the continental crust: from the continental US to global estimates (by invitation)

CORRESPONDING & PRESENTING AUTHOR:

Weisen Shen, Stony Brook University, USA

Siyuan Sui, Stony Brook University, USA

The chemical composition of the continental crust plays a key role in our understanding of the crust-mantle diffraction, formation, and evolution of the continents, as well as the thermal budget of Planet Earth. But the accurate quantification of the composition, especially for the deep crust, has been challenging due to the ambiguities in its seismic signatures (e.g., P velocity). However, the lab measurements show that the silica content of most metamorphic and igneous rocks in the crust follow a simple trend in the Vs and Poisson's ratio. Based on this trend, we combine the high-resolution 3-D Vs model and a new map of Poisson's ratio of the crystalline crust measured by the Earthscope/USArray to construct a 3-D model of SiO2 wt% for the continental US. In this model, variations correlated with the surface geology and tectonism are found at both the local and regional scales. Benchmarks with locally collected xenoliths in central and north Montana also show high consistency. Additionally, we found that the deep crustal composition of the continental US is highly consistent with that of the mafic, globally collected crustal xenoliths, rather than the more intermediate high-grade metamorphic terranes. Finally, we show that the crustal Poisson's ratios collected across major continents, however, indicate a slightly different composition compared with the continental US, suggesting that a better estimate of the continental crustal composition shall be performed by sampling all continents systematically.

KEYWORDS : continent, crustal composition

Sr No: 713

SYMPOSIUM : **S15 Structure of the lithosphere**

A new Rayleigh wave phase velocity database for North America

CORRESPONDING & PRESENTING AUTHOR:

Satish Maurya, Indian Institute of Technology Bombay, India

Barbara Romanowicz, University of California, Berkeley, USA

We present a new set of high-quality (~35, 000 paths) Rayleigh wave phase velocities measurements for North America, using a roller-coaster algorithm (Beucler et al., 2003). The method measures the single-station average phase velocities of the surface waves along the great circle path. It solves a non-linear problem in the least-squares sense with the help of a priori information. In general, a 1D reference model works well for teleseismic earthquakes, and does not influence the results much, especially for an event with an epicentral distance greater than ~50o. However, for regional events and to sample more complex areas of the continent, we change our reference model for every path to a model obtained by trans-dimensional inversion (Haned et al., 2015) of the global dispersion dataset of Ekström (2011) along the given great-circle path. The seismic networks considered include USArray, Alaska Array, Canadian National Network, and other existing temporary and permanent seismic broadband stations. From the new dispersion dataset obtained in the period range 34-240 s, we obtained local phase velocity maps by regionalization with a lateral correlation length of 250km. These regionalized dispersion maps present geographical consistency with previous studies. Moreover, short-period (34 - 40s) local dispersion curves connect well (within ~1-2%) with the local ambient noise dispersion curves (5-40s) from USANT15 (G. Ekström, 2017) which extend this dispersion dataset to the period band (5-240s) within the conterminous United States. These data will be of interest for imaging high-resolution crustal and upper-most mantle structure.

KEYWORDS :   North America tomography, high-resolution dispersion data, non-linear inverse problem

Sr No: 714

SYMPOSIUM :   **S15 Structure of the lithosphere**

Lithospheric layering beneath the Indian cratons from surface wave tomography studies

CORRESPONDING & PRESENTING AUTHOR:

Satish Maurya, Indian Institute of Technology Bombay, India

Jean Paul Montagner, Institut de Physique du Globe de Paris, France

M. Ravi Kumar, CSIR-National Geophysical Research Institute, India

The lithospheric structure beneath cratons is the most debated issue. Owing to the weak velocity contrast at the Lithosphere-Asthenosphere Boundary (LAB), techniques using converted phases (e. g. P and S-receiver functions) cannot detect it unambiguously. In comparison, surface wave tomography allows mapping of the gradient layers like LAB and the mid-lithospheric discontinuity (MLD) more effectively, in terms of their isotropic/anisotropic nature. Recently, a 3D-seismic anisotropic (VSV - shear wave velocity and azimuthal anisotropy) lithospheric model (Maurya et al., 2016) was derived for various Indian cratons by inverting ~25, 000 Rayleigh wave group and phase velocity dispersion measurements in the 16s-250s period range. The model parameters were determined down to 300km using a trans-dimensional approach for VSV and azimuthal anisotropy using first-order perturbation theory. The two best resolved parameters (VSV and ψG- fast axis direction) in the tomography model show an intermediate layer (~80-110km) within the cratonic lithosphere, which can be interpreted as an MLD and LAB beneath the Indian cratons. We observed significant variations (120-250km) in the LAB beneath the Indian continent. The MLD was found beneath cratons where the lithosphere is thicker than >150km. A cratonic keel could be delineated beneath central India.

KEYWORDS :   surface wave tomography, Indian cratons, lithospheric layering

SI8 CoTCS & ILP Task Force CoLiBrI Integrated seismological studies of the continental lithosphere - what we can learn from seismic anisotropy and other geophysical methods about the (micro-) plate structure and fabrics

CONVENERS: Jaroslava Plomerova (Czech Republic)
             Juan Carlos Afonso (Australia)
             Nicola Piana Agostinetti (Austria)

Seismology tools help to decipher complex structure and fabrics of continental lithosphere, which was formed in different geological cycles and plate forming processes, including accretion of plate fragments, collisions, subductions, break off, spreading of micro-plates and their consequent amalgamation into new continents. Seismic tomography snap shots of the present lithosphere state, in combinations with results from other seismological results, e.g., from seismic anisotropy at different scales or modelling mantle dynamics, and inevitably in interdisciplinary approach considering, e.g., gravity, petrology, GPS and other measurements in integrated geophysical modelling, allow us to image the current detailed structure of the continental lithosphere and to improve our understanding evolution and history of the continental lithosphere. Contributions on integrated seismological studies of the continental lithosphere are welcome.
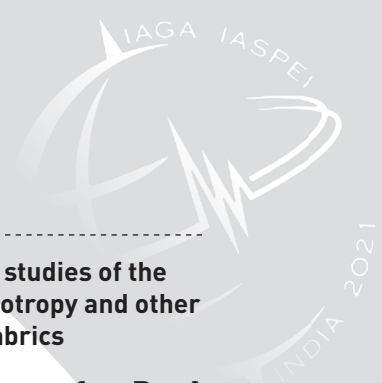
Sr No: 715

Modelling of Anisotropy in the Lithosphere and Asthenosphere for Real Earth Cases: A Critical Assessment of the Impact on SKS Measurements

CORRESPONDING & PRESENTING AUTHOR:

Gaelle Lamarque, LabexMer, IUEM, France

Nicola Piana Agostinetti, Università di Milano Bicocca, Italy

We investigate the effects of realistic Earth's lithospheric structures on measurements of SKS seismic waves birefringence, which could be perturbed by different factors. We present SKS measurements recorded in four different tectonic settings. For each case, a realistic lithospheric structure is assumed and synthetic SKS splitting measurements are compared with the field observations. Our results show that: (a) in a simple case, where anisotropy is aligned in both the lithospheric mantle and the asthenosphere, the SKS measurements can be safely interpreted as dominantly related to asthenospheric mantle flow; (b) in case of multi-layer anisotropy in the lithospheric mantle, SKS measurement can corresponds to a combination of the different fast axis orientations and intensities of the anisotropic layers, dominated by the layer with stronger anisotropy; (c) across orogens, where highly anisotropic $\geq 10\%$) crustal sections are present, a relevant per cent (30-40%) of SKS measurement can be explained by crustal contributions, with an additional challenge related to the different direction of retrieved and expected symmetry axis; and finally (d) in subduction zones, even in absence of mantle corner flow, subducted crust materials can interplay with the overriding plate to generate an interpretable SKS observation. We conclude that complex crustal and/or lithospheric anisotropy can lead to erroneous SKS splitting parameters interpretations in terms of mantle deformations. We show in particular that complex crustal anisotropy can produce both important time delay and back-azimuthal pattern. We also confirm that SKS splitting parameters do not allow to identify the presence of more than two anisotropic layers in the mantle.

KEYWORDS :   SKS anisotropy, crust, lithospheric structure

Sr No: 716

Lithospheric structure and active deformation beneath the NW Himalaya, India: Seismotectonic Implications (by invitation)

CORRESPONDING & PRESENTING AUTHOR:

Shubhasmita Biswal, Indian Institute of Technology Kharagpur, India

Sushil Kumar, Wadia Institute of Himalayan Geology, India

William Kumar Mohanty, Indian Institute of Technology Kharagpur, India

An integrated approach using major seismological tools was undertaken to understand the nature and behavior of the Indian lithosphere beneath the NW Himalaya. The study includes the determination of the optimal 1D crustal velocity model for the upper crust, to quantify the characteristic of the Indian

lithosphere as evidenced from the Shear wave splitting phenomenon, the estimation of the frequency-dependent attenuation characteristics, and the existence of Low-Velocity Zone (LVZ) beneath the NW Himalaya region. The study describes a 15 layer 1D velocity model for the Kinnaur-NW Himalaya and the relocated seismicity highlighted the active deformation underneath this particular section. Shear wave splitting signifies a significant fast polarization azimuths (FPA) orientation along the ENE-WSW direction. The average trend of the FPAs at each station indicates that the seismic anisotropy is primarily caused due to strain-induced deformation in the top ~200 km of the upper mantle as a result of the ongoing Indo-Eurasian collision. A contribution from the mantle flow in the direction of the Indian plate motion is also possible. The frequency-dependent characteristics observed from coda wave analysis concludes for the heterogeneous and sheared crust due to ongoing India-Eurasia convergence. 3D velocity inversion has been performed to investigate the subsurface structure and seismogenic layers in and around the source zone of the 1975 Kinnaur earthquake (M6.8) in the NW Himalaya. The study region exhibits low P-wave velocity (Vp) including an LVZ, indicating the presence of fluid or any partial melting strata in the middle crust of the lithosphere.

KEYWORDS :   anisotropy, tomography, attenuation

Sr No: 717

Upper Mantle Anisotropy and LAB Changes along the Bohemian Massif-Eastern Alps north-south transect (central Europe)

CORRESPONDING & PRESENTING AUTHOR:

Jaroslava Plomerova, Institute of Geophysics, Czech Acad. Sci., Czechia
Ludek Vecsey, Institute of Geophysics, Czech Acad. Sci., Czech Republic
Helena Zlebcikova, Institute of Geophysics, Czech Acad. Sci., Czech Republic
Gyorgy Hetenyi, Institute of Earth Sciences, University of Lausanne, Switzerland

Body-wave recordings from passive seismic experiments AlpArray-EASI (2014-2015) and AlpArray Seismic Network (2016-2019) are evaluated for studies of the upper mantle large-scale anisotropy and modelling the lithosphere-asthenosphere boundary (LAB) beneath the Bohemian Massif and the Eastern Alps. We analyse P-wave traveltime deviations and shear-wave splitting parameters of core-mantle refracted shear waves (SKS) at 240 broad-band stations in about 200 km broad and 540 km long band along 13.3° E longitude. Anisotropic signals in body waves are consistent within sub-regions and often sharply changes at tectonic boundaries. We invert the parameters for 3D self-consistent anisotropic-velocity models of the mantle lithosphere domains assuming hexagonal symmetry with inclined 'slow' or 'fast' axes. Along with directional dependence of body-wave anisotropic parameters we interpret such characteristics by fossil fabrics in the continental mantle lithosphere with generally in 3D oriented (inclined) symmetry axes. The AlpArray data improve significantly the LAB depth estimates in Europe. The European lithosphere, steadily thickening southward from the Eger Rift in the Bohemian Massif, collides with the Eastern Alpine keel of the northward dipping Adriatic plate, as it is modelled also in teleseismic P-wave tomography.

KEYWORDS :   mantle-lithosphere, anisotropy, LAB
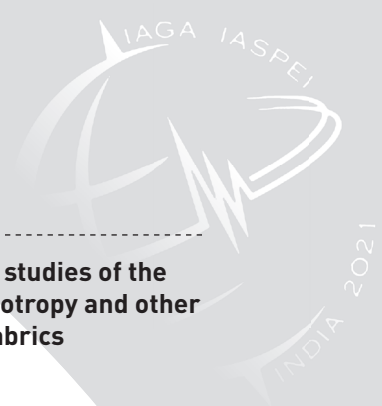
Sr No: 718

Transversely isotropic lower crust of the Bohemian Massif

CORRESPONDING & PRESENTING AUTHOR:

Jiri Kvapil, Institute of Geophysics of the Czech Academy of Science, Czech Republic

Jaroslava Plomerova, Institute of Geophysics of the Czech Academy of Science, Czech Republic

The Bohemian Massif (BM) represents the easternmost relic of the Variscan orogenic belt in central Europe. The massif was formed during the large-scale collision of supercontinents Laurasia and Gondwana approximately between 500 and 250 Ma. The Variscan orogenic processes are preserved in its tectonic structure as a collage of microplates and relics of magmatic arcs. A new 3-D shear wave velocity model from ambient noise tomography (Kvapil et al., 2021) provides a regional-scale image of velocity distribution in the BM crust. A significant feature of this model is the velocity-drop interface (VDI) modelled in the lower part of the crust. We explain this feature by anisotropic fabric of the lower crust, which is characterized as vertical transverse isotropy with the low-velocity being the symmetry axis. The VDI is often interrupted around the boundaries of the crustal units, usually above locally increased velocities in the lowermost crust. Due to the NW-SE shortening of the crust and the late-Variscan strike-slip movements along the NE-SW oriented sutures preserved in the BM lithosphere, the anisotropic fabric of the lower crust was partly or fully erased along the boundaries of original microplates. These weakened zones accompanied by a velocity increase above the Moho, which indicate an emplacement of mantle rocks into the lower crust, can represent channels through which portions of subducted and later molten rocks have percolated upwards providing magma to subsequently form granitoid plutons.

KEYWORDS : anisotropic fabric of the lower crust, Bohemian Massif, ambient noise tomography

Sr No: 719

Seismic anisotropy of the upper mantle beneath the Polish Sudetes from shear-wave splitting analysis

CORRESPONDING & PRESENTING AUTHOR:

Julia Rewers, Institute of Geophysics, Polish Academy of Sciences, Poland

Piotr Sroda, Institute of Geophysics, Polish Academy of Sciences, Poland

The main goal of the passive seismic experiment AniMaLS (Anisotropy of the Mantle beneath the Lower Silesia) is to study the upper mantle structure beneath the Polish part of the Sudetes (the NE margin of the Variscan orogen). The lithosphere in this region is characterized by existence of distinct geological units with complex tectonic history. The upper mantle beneath this area has been poorly studied until now. We present the results of the upper mantle seismic anisotropy study with shear-wave splitting method, one of the most common tools to obtain seismic anisotropy parameters. The data set was collected by 23 broadband stations located in the Polish Sudetes, between the Elbe Fault in SW and the Odra Fault in NE,

with ~30 km inter-station spacing. The stations were operating continuously for ~2 years (Oct 2017 to Oct 2019). The data set was supplemented with records from 8 permanent stations of Czech and Polish Seismological Network. We used records of SKS and SKKS phase to determine the upper mantle anisotropy using minimum energy and rotation-correlation methods. We obtained average δt ~1.2 s and fast velocity axis largely in WNW-ESE direction, turning more to NW-SE in the Eastern Sudetes area. The results are compared with other shear-wave splitting measurements in adjacent areas and with results of uppermost mantle anisotropy modelling based on Pn traveltimes from wide-angle seismic experiments conducted in this part of the Bohemian Massif. We discuss possible lithospheric and asthenospheric contributions to the observed anisotropy.

KEYWORDS : seismic anisotropy, passive seismic experiment, sudetes

Sr No: 720

SYMPOSIUM : **S18 CoTCS & ILP Task Force CoLiBrI Integrated seismological studies of the continental lithosphere - what we can learn from seismic anisotropy and other geophysical methods about the (micro-) plate structure and fabrics**

Comprehensive receiver function analysis of the Pannonian Basin and its surrounding regions

CORRESPONDING & PRESENTING AUTHOR:

Daniel Kalmar, Eotvos Lorand University, Hungary

Gyorgy Hetenyi, University of Lausanne, Switzerland

Attila Balazs, ETH Zürich, Switzerland

Istvan Bondar, Research Center for Astronomy and Earth, Hungary

We present the results of P-to-S receiver function analysis to improve the 3D image of the sedimentary layer, the upper and lower crust in the Pannonian Basin area. The Pannonian Basin hosts deep sedimentary depocentres superimposed on a complex basement structure and it is surrounded by mountain belts. We processed waveforms from 221 three-component broadband stations. As a result of the dense station coverage, we were able to achieve so far unprecedented spatial resolution in determining the structure of the crust. We applied a three-fold quality control process; the first two being applied to the observed waveforms and the third to the calculated radial receiver functions. The radial receiver function provides information about crustal structures and velocity conditions. The tangential receiver function indicates crustal dip and anisotropy. This work is the first uniform and comprehensive receiver function study of the region.

The S-wave velocity structure of the area, which we determined by the non-linear inversion method at each station, where data were sub-divided into back-azimuthal bundles based on similar Ps delay times and tangential receiver functions. The 1D inversion provided the depth of the discontinuities, shear-wave velocities and Vp/Vs ratios of each layer per bundle.

We developed a 3D visualization method based on natural neighbour interpolation to obtain the 3D crustal structure from the local inversion results. We present the sedimentary thickness map, the first Conrad depth map and an improved, detailed Moho map, as well as the first upper and lower crustal thickness maps obtained from receiver function analysis.

KEYWORDS : Pannonian Basin, receiver functions, crustal structure
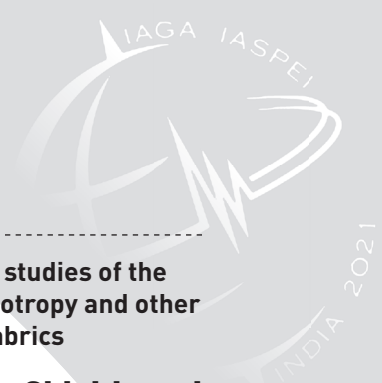
Sr No: 721

Exploring Seismic Anisotropy of the Eastern Canadian Shield and its Margins: Evidence From Shear Wave Splitting and Surface Wave Tomography

CORRESPONDING & PRESENTING AUTHOR:

Fiona Darbyshire, Université du Québec à Montréal, France

The eastern Canadian Shield and its surroundings record a complex history of craton formation and evolution, orogenesis, and rifting. These large-scale tectonic processes likely result in "fossil" anisotropic fabric preserved within the continental lithosphere. Present-day mantle convective flow below the lithosphere can cause lattice-preferred orientation of anisotropic minerals such as olivine, and thus presents a second possible source of upper-mantle seismic anisotropy.

Observations of seismic anisotropy made across the eastern Canadian Shield and its margins include shear wave splitting measurements and regional-scale surface wave tomography studies that solve for azimuthal anisotropy. In northern Canada, azimuthal variation of shear wave splitting parameters suggests the presence of multiple anisotropic layers in the upper mantle, and dipping fabrics associated with Paleoproterozoic orogenesis. Anisotropy within the Superior craton is both laterally and vertically variable. Large splits in the western Superior appear to be related to an alignment of fabrics within the cratonic keel and the sublithospheric mantle. In the central Superior, which has experienced multiple episodes of hotspot-lithosphere interaction, anisotropy is weaker. In eastern Canada, we see variations in anisotropy across the Grenville Front, and significant variability within the Appalachian domains. Along the St. Lawrence valley, the dominant fast-polarisation orientation varies only slightly, and may reflect a more regionally pervasive, perhaps sublithospheric, contribution.

We examine the anisotropy measurements in the context of other geological/geophysical data, as well as numerical models of mantle convection, to improve our understanding of the sources of seismic anisotropy associated with lithospheric and sublithospheric processes beneath eastern Canada.

KEYWORDS : seismic anisotropy, Canadian Shield, geodynamics

Sr No: 722

Shear wave splitting and mantle anisotropy beneath the Malani igneous province, Northwestern India (by invitation)

CORRESPONDING & PRESENTING AUTHOR:

Saju D S, Indian Institute of Technology Bombay, India

Mohan Gollapally, Indian Institute of Technology Bombay, India

The 750 Ma Neoproterozoic Malani igneous province(MIP) hosts the igneous suites that are explained as anorogenic magmatism linked to crustal melting during extension or to an active hot spot and also as an Andean type active margin during fragmentation of Rodinia. MIP comprises the Barmer and Sanchor rifts on the west, the 850 Ma Erinpura granite on the east adjoining the NE-SW trending Proterozoic Aravalli-Delhi fold belt and hosts the 68Ma pre-Deccan alkaline complexes. The seismic anisotropy at 29 stations deployed in a 300 square kilometer in MIP is estimated using 441 splitting measurements of SKS, SKKS and PKS phases. The delay times range between 0.5-2.1 s, with the average delay time being 1.1s. The fast polarization directions (FPD) are in the APM direction, rift parallel and perpendicular, and parallel to the orogen (ADFB). The FPD in the NE direction coincides with the APM direction implying that shearing at the base of the lithosphere is a causative mechanism. The rift exhibits FPD in the N-S and NNE-SSW direction, the former is possibly due to the orientation of the melt bodies associated with the Deccan volcanism along the rift axis, and the latter is rift perpendicular coinciding with the extensional direction of the rift. The Erinpura granite indicates FPD in the NE direction parallelling the ADFB and increase in the delay times, suggesting effect of lithospheric fabric together with mantle flow. The anisotropic signatures reflect significant contribution from the inherited fossil fabric and the asthenospheric flow.

KEYWORDS :   malani igneous province (MIP), seismic anisotropy, Deccan volcanism

Sr No: 723

- -

SYMPOSIUM :   **S18 CoTCS & ILP Task Force CoLiBrI Integrated seismological studies of the continental lithosphere - what we can learn from seismic anisotropy and other geophysical methods about the (micro-) plate structure and fabrics**

Stony Brook's Collaborations with Czech Scientists

CORRESPONDING & PRESENTING AUTHOR:

Robert Liebermann, Stony Brook University, USA

Forthe past halfcentury, I have been fortunate in maintaining collaborations with Czech scientists in the Czech Republic [formerly Czechoslovakia] from the Geofyzikální ústav -GFU [Institute of Geophysics] of the Československá akademie věd-CSAV [Czechoslovak Academy of Sciences]. These collaborations have included exchange visits by me to Prague [Praha] and convening international workshops in 1976, 1986 and 1996 in castles used by the CSAV as well as visits by Czech colleagues to Stony Brook University. The objective of this report is to relate this history and to illustrate the scientific advances, particularly in sound velocities in minerals, which resulted from these collaborations. This report is dedicated to the memory of Vladislav Babuška.

KEYWORDS :   mineral physics, high pressure, high temperature, anisotropy and lateral heterogeneity of the earth's
                     mantle.

SI9 CoTCS Intraplate Seismicity: Distribution, properties and causes

CONVENERS: D. Srinagesh (India)

Ramesh P. Singh

Won-Young Kim (S. Korea / USA)

Lars Ottemöller (Norway)

Stéphane Rondenay (Norway)

Vineet Gahalaut

Intraplate seismicity in many parts of the world significantly contributes to seismic hazard. While intraplate seismicity today is well monitored by permanent and temporary seismic networks to observe the spatial and temporal distribution, low activity rates prevent us from obtaining a more complete picture, especially when it comes to large earthquakes. And while source studies provide mechanisms and other physical parameters, exact causes for intraplate earthquakes can be difficult to identify as often one deals with a combination of different processes. Earthquakes in the plate interior regions are not frequent however, the loss of lives and property for these earthquakes is almost comparable to that in the plate boundary regions especially in developing countries. This is mainly due to higher population density, built up environment not adhering to earthquake safety and lower hazard perception amongst people living in the plate interior regions. We anticipate contributions from different parts of the world that will allow us to discuss differences and similarities with the aim to get a better understanding overall.

Sr No: 724

Coda Envelope Moment Magnitudes and Source Scaling for the Western Quebec Seismic Zone, Canada

CORRESPONDING & PRESENTING AUTHOR:

Allison Bent, Natural Resources Canada, Canada

Kevin Mayeda, US Air Force, USA

Jorge Roman Nieves, US Air Force, USA

Justin Barno, Lawrence Livermore National Laboratory, USA

Obtaining reliable moment magnitudes (Mw), the preferred magnitude for hazard assessments, for small earthquakes that make up the bulk of most earthquake catalogs has been historically problematic. Modeling methods based on long-period waveforms cannot be applied to smaller earthquakes. Mw's for these are usually determined by applying conversion relations, which may not have been validated for the complete range of magnitudes, for the myriad of magnitude scales in the catalog. The coda envelope method has emerged as one of the most promising and stable techniques for direct determination of moment magnitude for small earthquakes. The coda, consisting of scattered waves, is only minimally affected by radiation pattern enabling the method to provide stable results with sparse or azimuthally unequal networks. Recent improvements to the software by Lawrence Livermore National Laboratory to facilitate the process, in particular the previously laborious step of station calibration, make it attractive for use as a standard magnitude. Calibration for the Western Quebec Seismic Zone in eastern Canada has been completed. The long coda envelopes resulting from low attenuation have shown that this is an ideal region for the application of the method and highlighted the importance of regional calibrations. Tests on a suite of earthquakes in the magnitude 3-4 range resulted in stable Mw measurements. The data set will now be expanded and a minimum magnitude for application determined. Apparent stresses for this region were notably and consistently high. The expanded data set will be used to fine tune the source scaling relationships.

Sr No: 725

A study of recent Assam earthquake of 28 April 2021 (M 6.3) in the Eastern Himalaya and its tectonic implications

Naba Kanta Borah, CSIR-NGRI, India

CORRESPONDING & PRESENTING AUTHOR:

Srinagesh D, CSIR-NGRI, India

Sunil Kumar T. C, CSIR-NGRI, India

Pavan Kumar V, CSIR-NGRI, India

During last one century Kopli fault zone in Northeast India has witnessed several moderate to major earthquakes including 1950 earthquake of magnitude 8.6 and January 2016 earthquake of the magnitude 6.7 in Imphal. Recently an earthquake of Ms 6.3 occurred in the Kopli fault zone on 28 April 2021 at 02:21:28 (UTC). CSIR-NGRI is operating network of 10 Seismological stations in and around Kopili fault zone and recorded both the main and after-shock events. The estimated
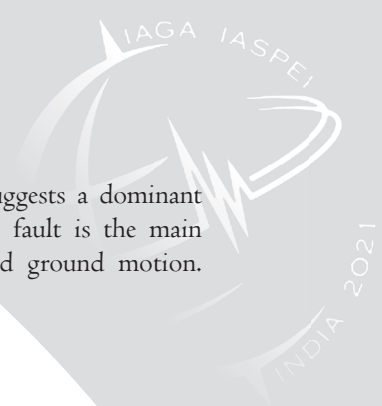
focal depth for this event is 30 km and focal mechanism solutions for this event suggests a dominant strike slip mechanism with dextral motion. These studies indicate the active Kopili fault is the main cause for this earthquake. We shall be discussing about the earthquake source and ground motion.

KEYWORDS : kopli fault, ground motion, focal mechanism

Sr No: 726

SYMPOSIUM : **S19 Intraplate Seismicity: Distribution, properties and causes**

Crustal Deformation beneath the Kumaon-Garhwal Himalaya using shear wave splitting analysis of Local Earthquakes

CORRESPONDING & PRESENTING AUTHOR:

Pavan Kumar Vengala, CSIR-National Geophysical Research Institute, India

Srinagesh D, CSIR-NGRI, India

Prantik Mandal, CSIR-NGRI, India

Naresh B, CSIR-NGRI, India

Solomon Raju P, CSIR-NGRI, India

The Kumaon-Garhwal Himalaya is located in the region of convergence between the Indian and Eurasian plates, and we used shear wave splitting analysis to map upper crustal anisotropy underneath it. We used local earthquakes recorded at 51 three-component broadband stations from a semi-permanent seismic network operated by CSIR-NGRI from 2017 to February 2020. The observed delay times (δt) range from 0.018 to 0.29s with a mean delay of 0.1s. Within the depth range of 20–25 km, the observed delay times indicate a significant scatter, implying that the source of anisotropy may be the upper crust. The computed normalized delay times show a mean value of 1.1 ms/km, within the Outer Lesser Himalaya (OLH) and the region south of it while North of OLH this value increases to 5.8 ms/km. These values suggest the crack densities of 0.0043 and 0.022 with shear wave velocity anisotropy of 0.68% and 2.47 %, revealing that the observed crustal anisotropy is parallel to stress-aligned micro cracks. In this study we found two dominant directions with one direction parallel to maximum horizontal stress direction, suggesting that the upper-crustal anisotropy is essentially influenced by the regional or local stress field. The other dominant direction is observed to be sub-parallel to the structural trends. Our results suggest that observed upper crustal anisotropy in the Inner Lesser Himalaya and North of it, is dominated by stress-induced anisotropy, whereas South of it is mostly controlled by regional structures.

KEYWORDS : shear wave splitting, crustal anisotropy, normalized delay time

Sr No: 727

SYMPOSIUM : **S19 Intraplate Seismicity: Distribution, properties and causes**

Crustal Structure of Northeast India as Evidenced by Receiver Function Imaging and Gravity modelling:Tectonic Reconstruction and Geodynamic Implications

CORRESPONDING & PRESENTING AUTHOR:

Sanjay Prajapati, National Centre for Seismology, Ministry of Earth Sciences, New Delhi 110003, India

Sowrav Saikia, National Centre for Seismology, Ministry of Earth Sciences, New Delhi 110003, India

B.R. Arora, Former Director, Wadia Institute of Himalayan Geology, Dehradun, India

P-wave receiver function technique is applied to teleseismic earthquake data from 19 broad-band stations in Northeast India. Synthesis of inverted shear wave velocity structure together with gravity modelling permits to map the structural configuration of various tectonic blocks. The thickening of crust and formation of the fluid-filled low-velocity layer above the top of the down-going Indian plate, i.e. Main Himalayan Thrust (MHT), are the coherent features of plate collision zones. Fluid-induced modulation of frictional coupling explains the nucleation of large and major earthquakes on the MHT. Similarly, the progressive westward propagation of rocks recycled from the Indo-Burmese subduction zone fuel the growth of ~10 km thick Indo-Burmese Wedge (IBW) that carpets the 2-layered crust comprising thick delta sediments overlying the mafic crust continuing eastwards from the Bay of Bengal. Further, the crust beneath Himalayan foredeep is marked by large-scale complexities, both in structure and composition. Under the western-BRV, cutting across the uplifted Shillong Plateau, thin (32-35 km) felsic (low Poisson ratio) crust with embedded ~5 km thick high velocity/density layer (HVL) accounts for the gravity high prevailing from the southern margin of the Shillong Plateau to the Lesser Himalaya. The imaged HVL symbolises a Pre-Himalayan structure on the Proterozoic passive margin of India. Reactivation of its base due to part absorption of plate convergence at the Dauki fault could be supporting the uplift of the Shillong Plateau. In contrast to the W-BRV, the narrow crustal strip along the Upper Assam Basin in the E-BRV is marked by pronounced gravity low, high Poisson ratio, which coupled with low-high velocity dual layer in deep crust is viewed as intrusive slice of the mafic crust that exists beneath the IBW.

KEYWORDS :   Northeast India, Eastern Himalayan, Indo-Burmese arc

Sr No: 728

SYMPOSIUM :   **S19 Intraplate Seismicity: Distribution, properties and causes**

Intraplate seismicity in Nordland, northern Norway: insight from seismic tomography and hypocenter relocation (by invitation)

CORRESPONDING & PRESENTING AUTHOR:

Hasbi Ash Shiddiqi, University of Bergen, Norway

Lars Ottemoller, University of Bergen, Norway

Stephane Rondenay, University of Bergen, Norway

Felix Halpaap, University of Bergen, Norway

Sofie Gradmann, Geological Survey of Norway, Norway

Jan Michalek, University of Bergen, Norway

The Nordland region, in Northern Norway, has relatively high seismicity rate despite being situated within a stable continental region. The seismicity is distributed along the coast of Nordland, and along the shelf edge. However, the causative mechanism of earthquakes in the region is still debated. An investigation of the mechanism requires high-resolution images of the crust. Therefore, we developed high-resolution 3-D VP and VP/VS ratio images of the crust in Nordland using seismic travel-time tomography. We identified a localized, ~10 to ~15 km Moho step which coincides with the extent of the coastal seismicity. Furthermore, the tomography results show local VP/VS ratio anomalies within two seismic swarm locations, namely Jektvik and Steigen areas, indicating the presence of fluid. Furthermore, we relocated the hypocenters using the double-difference relocation technique and computed focal mechanism solutions of selected earthquakes. The relocated hypocenters and focal mechanisms are used to study the distribution of Jetkvik swarms. The focal mechanisms are dominated by coast-parallel normal and normal oblique faulting

mechanisms, indicating an extensional regime. Even though the regional stress field is compressive, the local extensional regime is likely produced by a local flexure of the crust. The Jetkvik swarm occurred in an area with no known faults and formed three main clusters, where the swarms started in the central cluster, and migrated over time to the northern and southern clusters. The relocated seismicity in Jetkvik swarm shows northwest dipping planes similar to the structural trend in the region.

KEYWORDS : seismic tomography, intraplate seismic swarm, Northern Norway

Sr No: 729

- -

Symposium : S19 Intraplate Seismicity: Distribution, properties and causes

Numerical modeling of seismic wave propagation for Koyna (1967) and Latur earthquakes (1993)

CORRESPONDING & PRESENTING AUTHOR:

Yellapragada Meenakshi, IIT Madras, India

STG Raghukanth, IIT Madras, India

Estimating strong ground motion characteristics associated with the intraplate regions has a paramount significance in the seismic hazard and risk assessment studies. Major and devastating intraplate earthquakes occurred in the Southern Peninsular region of India. Peninsular India (PI) is considered as stable continental region (SCR) with low to moderate seismicity. PI region gained its attention after the occurrence of notable events like the Koyna and Khillari earthquakes. Numerical modeling of ground motion is considered a realistic alternative in the absence of ground motion data. In this paper, two numerical models are developed to generate ground motions for the Koyna earthquake (Dec 10, 1967 - Model 1) and the Khillari earthquake (Sep 29, 1993 - Model 2), using the spectral element method. The seismic wave speeds, density, and attenuation for these regions are obtained from the literature. To study the influence of topography on ground motion amplification, a 30 m high-resolution topography is incorporated. In these models, the earthquake source is characterized by a random slip field. For Model-1, the simulated time histories are compared with the recorded data, and further, peak ground velocity (PGV) contours are plotted to show the effect of ground motion in the neighboring cities. In Model-2, the PGV as well intensity (MSK) contours are plotted to estimate the intensity of the damage. In addition to this, the peak ground residual displacements (PGRD) are presented to understand the extent of ground motion due to the selected earthquakes.

KEYWORDS : ground motion, intraplate seismicity, synthetic simulations

Sr No: 730

- -

SYMPOSIUM : **S19 Intraplate Seismicity: Distribution, properties and causes**

The impact of aftershocks on seismotectonics of 2017 Moiyabana, Botswana earthquake

CORRESPONDING & PRESENTING AUTHOR:

Thifhelimbilu Faith Mulabisana, ITES, University of Strasbourg, France

Mustapha Meghraoui, IPG, Strasbourg, France

Vunganai Midzi, Council for Geoscience, South Africa

The 3 April 2017 MW 6.5, Moiyabana (Botswana) earthquake occurred in the continental interior of the African previously considered as stable. We analysed the mainshock and aftershock sequence based on a records from a local seismic network. The earthquake rupture geometry is constrained with more than 1, 000 aftershocks recorded over a period of three months and from the InSAR analysis of Sentinel-1 images (ascending orbit). mechanism solutions of the mainshock and aftershocks display predominance of NW-SE trending and NE dipping normal faulting. Stress inversion of focal mechanisms obtained from the mainshock and aftershock database are compatible with a NE-SW extension under normal faulting regime. The InSAR study shows fringes with two lobes that have a 4 to 6 cm coseismic slip on a NW-SE elongated and 30-km-long surface deformation consistent with the mainshock location and normal faulting mechanism. The modelling of surface deformation provides the earthquake rupture dimension at depth with ~ 1 m maximum slip on a fault plane striking 315°, dipping 45°, -80° rake and with Mo 7.12 1018 Nm. The occurrence of the 2017 Moiyabana earthquake, followed by an aftershock sequence in the central Limpopo belt classifies the intraplate region as an active plate interior. We demonstrate the impact aftershock sequence has in inferring the fault geometry at depth, as well as the stress associated with the Moiyabana earthquake.

KEYWORDS : seismotectonics, earthquake, fault

Sr No: 731

SYMPOSIUM : **S19 Intraplate Seismicity: Distribution, properties and causes**

Micro-seismicity of the Mesamavida crustal fault (Central Chile) through a local seismic network

CORRESPONDING & PRESENTING AUTHOR:

Martin Riedel, Universidad de Concepción, Chile

Andres Tassara, Universidad de Concepción, Chile

Matteo Lupi, University of Geneva, Switzerland

Elliot Jiwani Brown, University of Geneva, Switzerland

A network of 12 short period seismometers covering an area of 25 by 35 kilometers was deployed between July 2020 and January 2021, surrounding the recently discovered Mesamavida Fault, in the Chilean Precordillera. It is the southernmost manifestation of the West Andean Thrust Fault, a west verging structure uplifting the Andes mountain belt. Paleoseismic studies show the Mesamavida Fault can produce 6.12 < Mw < 7.35 earthquakes with a thousand year return period. However, it is not known whether it is currently active or if it is potentially dangerous. To solve these questions, a seismic catalog was built with the obtained data, containing over 2500 earthquakes with 63 of them occurring within the network. Of these, 13 follow the fault scarp and occurred between 5.1 and 26.5 kilometers depth. The data will be then used to create a 1D local velocity model, selecting the best quality earthquakes, which must meet the following criteria: (1) have an azimuthal GAP < 180° (2) have an RMS < 0.5 and (3) be detected by at least 4 stations. This model will allow us to relocate the earthquakes and reduce location error, thus providing a clearer fault geometry. Furthermore, focal mechanisms of the local earthquakes will shed light on the fault kinematics, and their magnitudes paired with a b-value analysis will provide a better understanding of the return period of larger earthquakes.

KEYWORDS : crustal micro-seismicity, west andean thrust fault, mesamavida fault

Sr No: 732

Implication of GPS and Seismic strain rates in the Kachchh, India (by invitation)

Sapna Ghavri, Patna Secretariat, India

CORRESPONDING & PRESENTING AUTHOR:

Rajeev Kumar Yadav, National Geophysical Research Institute Hyderabad, India

Sridevi Jade, CMMACS (CSIR-4PI) Bangalore, India

Quantitative measure of surface crustal rates within an active Intraplate zone is challenging as low rate of tectonic deformation may be perturbed by several non-tectonic factors of the region such as continental hydrological mass variations, atmospheric pressure load, non-tidal ocean loading and so on. Kachchh paleo-rift basin located in the western side of rigid Indian plate interior experienced several major earthquakes in the past with the latest being the 26 January 2001 earthquake and continues to be seismically active till date. Displacement time series obtained from continuous GPS (Global Positioning System) measurements in the Kachchh region are used to estimate the accumulated strain in this region using a modified least-square inversion of velocity field data in the region. The seismic strain rate is estimated from the past seismicity and fault mechanism of the significant earthquakes (Mw>2.5) in the region from 350 years of earthquake catalogue. GPS and seismic strain rates of Kachchh paleo-rift basin give lower (~900 years) and upper (~1700 years) bounds on the recurrence interval of major earthquakes capable of causing severe damage in the region. Our study indicates that 2001 Bhuj earthquake has reactivated major faults in the region resulting in strain accumulation pointing to probable occurrence of future damaging earthquakes in Kachchh paleo-rift basin.

KEYWORDS : intraplate deformation, principal strain rate, Kachchh Paleo-rift basin

Sr No: 733

Pre-eruptive crustal electrical structure and tectonics in the region of recent earthquake swarm activity at Palghar, Maharashtra, India

CORRESPONDING & PRESENTING AUTHOR:

Pavankumar Gayatri, CSIR-National Geophysical Research Institute, India

Narasimha Chakravarthi Nalluri, CSIR-National Geophysical Research Institute, India

Ajay Manglik, CSIR-National Geophysical Research Institute, India

The Deccan Volcanic Province covering western part of the Indian peninsular shield experiences a moderate level of intraplate seismicity including swarm-type activities. Recently, such a swarm activity has been observed in the Palghar region, about 120 km north of Mumbai. This activity started in November 2018 and is continuing. We have carried out a magnetotelluric (MT) study during Feb.- Mar.2019 across the seismogenic region to delineate the subsurface structure to understand the possible cause for the seismic activity. Broadband MT data were acquired at 18 sites along a 35 km long E-W profile with average station spacing of 2 km, analyzed for distortion, and inverted by a 2-D inversion algorithm. The geoelectric structure yields shallow (~5 km) and U-shaped upper-crustal (10-12 km) moderate conductivity zones. A good correlation of the hypocentral distribution of the seismic events with the shallow conductor broadly indicates possible role of fluids (either meteoric or of crustal origin) in the genesis of the Palghar swarm

activity. To understand the confined nature of the swarm activity and lateral extent of the conductors, we have covered another MT profile about 50 km south of the swarm activity region. The 2-D model for this dataset suggests continuation of those conductors further south with wider lateral separation. A combined interpretation of the results of these two profiles shall provide an improved understanding of the nature of the Palghar swarm activity.

KEYWORDS : magnetotellurics, Palghar, Deccan Volcanic Province

Sr No: 734

- -

SYMPOSIUM : **S19 Intraplate Seismicity: Distribution, properties and causes**

GNSS-derived strain and uplift rates in Central Europe and their correlation to intraplate seismicity (by invitation)

CORRESPONDING & PRESENTING AUTHOR:

Torsten Dahm, GFZ German Research Centre for Geosciences, Germany

Zhiguo Deng, GFZ German Research Centre for Geosciences, Germany

Sebastian Hainzl, GFZ German Research Centre for Geosciences, Germany

A central question of seismic hazard analysis is to understand where and how often intraplate damaging earthquakes can occur. With continuous satellite-based distance measurements (GNSS and SAPOS stations) over decades and highly developed processing methods, horizontal velocities of the Earth's surface smaller than 0.2 mm/a can be resolved today. This means that spatially dense measurement networks can be used to quantify the deformation and possible temporal changes not only at plate boundaries but also within a plate and to compare them with the current seismicity. Deformation within a plate can be related, for example, to processes in the Earth's mantle, diffuse or zonal shearing along structural zones of weakness, or the rotation of rigid crustal blocks.

We derive for the first time dense, high-precision network solutions at 876 GNSS stations in Germany and adjacent areas and combine them with solutions of neighbouring countries. Local and regional uplifts are up to ~2 mm/a and correlate with the collision zone of the Alps and Cenozoic volcanism in Germany. In addition, an unknown uplift region is detected in the East German Basin. The uplift zones north and east of the Alps correlate with low S-wave anomalies in the upper mantle related to the extended system of Eifel mantle upwelling. First results indicate possible transients in GNSS time series, the cause of which is still unclear. The observation that intraplate seismicity in Central Europe correlates with increased deformation rates from GNSS solutions in some areas but not in other zones is also unclear.

KEYWORDS : intraplate seismicity, strain rates, uplift rates

Sr No: 735

Spatial and Temporal variation of seismic attenuation in the Palghar region of western India

CORRESPONDING & PRESENTING AUTHOR:

M. Shekar, CSIR-National Geophysical Research, India

D. Srinagesh, CSIR- National Geophysical Research, India

G. Suresh, CSIR- National Geophysical Research, India

B. Naresh, CSIR- National Geophysical Research, India

K. Swathi, CSIR- National Geophysical Research, India

D. S. Vitthal, CSIR- National Geophysical Research, India

Arti Devi, CSIR- National Geophysical Research, India

G. Vikas, CSIR- National Geophysical Research, India

V. Mahalaxmi Naidu, CSIR- National Geophysical Research, India

R. Vijaya Raghavan, CSIR- National Geophysical Research, India

We study, the spatial and temporal variation of seismic wave attenuation for Palghar source region located in Deccan Volcanic Provence. We analyzed 1283 earthquakes ($1.5 < ML < 4.2$) since February 2019 to November 2020 recorded by a network of six stations, which are installed by CSIR-NGRI. We employ the single back scattering method (Aki and Chouet 1973), and calculated coda wave attenuation (Qc) at frequencies 1.5, 3, 6, 12 and 24 Hz for lapse time windows of 20 to 60 sec. We observe the temporal variation of Qc at higher frequencies ($f > 6$Hz), for a five-month window and a decrease in Qc is observed. This may be to permeability changes in the medium since 2019 to 2020. However, the temporal variation of Qc is not similar at each station. The region shows high attenuation, $Qc = 126.62 \pm 41.68$ f 1.11 ± 0.06 for 35s lapse time and high frequency parameter (~ 1) which is usually observed in seismically active regions.

Sr No: 736

Strain rate and seismicity analysis in the Central Seismic Gap of the NW Himalayan arc using continuous and campaign mode GPS measurements

CORRESPONDING & PRESENTING AUTHOR:

Saroj Kumar Mondal, CSIR-NGRI, Hyderabad, India

Vineet Kumar Gahalaut, CSIR-NGRI, Hyderabad, India

Rajeev Kumar Yadav, CSIR-NGRI, Hyderabad, India

Joshi K Catherine, CSIR-NGRI, Hyderabad, India

Amit Kumar Bansal, CSIR-NGRI, Hyderabad, India

Several devastating earthquakes occurred in the past along the Himalayan collision zone and many more are expected in this orogenic belt due to continuous accumulation of strain energy along the locked Main Himalayan Thrust (MHT) region. Central Seismic Gap probably has the higher potential of generating megathrust earthquakes in comparison to the other two Gaps (Kashmir and Assam gaps) along the Himalayan arc because of its longer period of elastic energy build-up since last great earthquake. Geodetic

measurements for longer period of observations have opened the new pathways to understand the crustal deformation along the complex faults system and its pattern of variation in different region. Here we estimate the secular velocity of 30 continuous Global Positioning System (GPS) sites in the Kumaun-Garhwal region, installed by CSIR-NGRI, and 7 continuous sites from the neighbouring western Nepal region. We estimated the variation in strain rate of the region using these sites along with 58 published campaign mode data to understand the heterogeneity of strain rate in the study area. Change in the strain rate from northwest to southeast along the Main Central Himalaya (MCT) shows negative correlation with seismicity during this interseismic period of study. The shear strain rate of up to 90 nanostrain/yr is observed in the study area. We observed the western part of Garhwal Himalaya has a higher strain than the eastern and Kumaun Himalaya.

KEYWORDS : Himalaya, GPS, strain rate and earthquakes.

Sr No: 737

Recent seismicity in Center North of Mato Grosso State – Brazil

CORRESPONDING & PRESENTING AUTHOR:

Lucas Barros, Seismological Observatory of Brasilia University, Brazil
Juraci Carvalho, Seismological Observatory of Brasilia University, Brazil
Marcelo Rocha, Seismological Observatory of Brasilia University, Brazil
George Franca, Seismological Observatory of Brasilia University, Brazil
Aline Oliveira, Seismological Observatory of Brasilia University, Brazil
Brandow Neri, Seismological Observatory of Brasilia University, Brazil
Darlan Fontenele, Seismological Observatory of Brasilia University, Brazil
Leticia Assuncao, Seismological Observatory of Brasilia University, Brazil

Earthquake in the Center North of the Mato Grosso State – Brazil was first detected in January 1955, in the current Nova Maringa town (6.2 mb and MM IV-V) intensity at 380 km from the source. This was the largest earthquake ever detected in the entire Stable Continental Interior of the South American plate. In 1959, with the arrival of the first inhabitants to the region of Porto dos Gaúchos, earthquakes were felt with an estimated magnitude of up to 4.0mb. With the installation of regional stations in the Brazilian Amazon in 1980, earthquakes continued to be detected in Porto dos Gaúchos. In March 1998, an earthquake of magnitude 5.2 mb (MM VI) was detected, and its aftershocks were studied with a local seismic network. It was determined a focal mechanism of WSW-ENE transcurrent regime, with about an extension of 5 km. In 2005, another 5.0 mb (MM V) earthquake occurred in the same fault and with the same focal mechanism. Studies of seismic wave attenuation, crustal structure with shallow seismic refraction, and local receiver function allowed us to determine an accurate 1D velocity model for the area. In December 2015, a new seismic area in Tapaporã was identified. The largest magnitude was 4.0 mb. New seismic areas were also identified in 2015 in Juara and Brasnorte, and in 2016 in Nova Maringa. All these seismogenic areas are in the Parecis Phanerozoic Basin. In this work, we present the results of studies carried out with a new local seismic network.

KEYWORDS : seismicity, brazilan seismicity
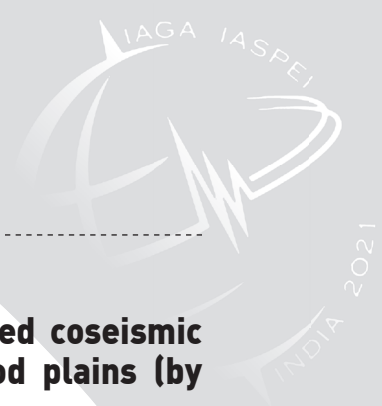
Sr No: 738

M6.3 Assam earthquake in Kopili Fault zone and associated coseismic liquefaction and ground deformation in Brahmaputra flood plains (by invitation)

Shibu Rajkhowa, CSIR-National Geophysical Research Institute, India
Nilesh K Jaiswara, CSIR-National Geophysical Research Institute, India
Prabha Pandey, CSIR-National Geophysical Research Institute, India
N K Borah, CSIR-National Geophysical Research Institute, India
D Srinagesh, CSIR-National Geophysical Research Institute, India

CORRESPONDING & PRESENTING AUTHOR:

Anand K Pandey, CSIR-National Geophysical Research Institute, India

On April 28th, 2021, a M6.3 earthquake struck the Brahmaputra plain in the Kopili Fault zone with a series of aftershocks. The recorded PGA value for the main event was 0.2 recorded at Tezpur about 40 km from the epicenter; whereas for the M 4.2 earthquake (aftershock), the recorded PGA is 0.007 for the station installed in the vicinity of the mainshock epicenter. The meizoseismal zone, south of the epicenter, experienced widespread earthquake-induced liquefaction and associated ground deformation with the development of lateral spreading, sand dykes and vents, and soft-sediment deformation. Extensive development of ephemeral sand-water springs and fountains of different dimensions along the rat holes and dried river beds is observed. We present results of the post-earthquake survey documenting size, geometry, and extent of liquefaction feature through trenching investigations revealing the subsurface architecture of sand blows and feeder-dykes from the source sand and water table depth in the region. The strong ground shaking and liquefaction induce deformation, and building tilting is observed mainly in the Brahmaputra plains with a shallow water table and saturated sand beds. We combine detailed geologic investigations with strong ground motion data to infer the liquefaction-triggering threshold and geological controls on the surface manifestation of liquefaction at the study site. The same is analysed in light of the empirical relationship suggesting the M 5.5 earthquake threshold that produces liquefaction and associated ground deformation. The result is also discussed in light of paleo-liquefaction records in the region.

KEYWORDS : liquefaction, PGA, Kopili Fault zone

Sr No: 739

Seismotectonic significance of the 2019–2020 Palghar seismic swarm, Maharashtra, India in the context of Intraplate earthquake

PRESENTING AUTHOR:

Sunilkumar T. C., CSIR-National Geophysical Research Institute, India

CORRESPONDING AUTHOR:

Srinagesh D., CSIR-National Geophysical Research Institute, India
Sunil K. Roy, CSIR-National Geophysical Research Institute, India
Shekar M., CSIR-National Geophysical Research Institute, India

This study deals with the seismogenic behaviour of the Palghar region, Maharashtra, India with the swarm sequence begining in November 2018 and still continouing. The swarm activities in general, have distinct characteristics from a typical foreshock-mainshock-aftershock pattern and are mostly associated within an area of volcanic, geothermal activity, magma injection, and fluid diffusion. Although rare and responsible for only a small fraction of the world's stress-energy release, the Stable Continental Region(SCR) earthquakes can cause widespread damage. To investigate a few fundamental characteristics and possible reasons, We study the focal mechanism, stress field together with crustal anisotropy, and thus providing a better picture of the seismogenic behaviour of the SCR-swarm. The estimated focal mechanisms of the 22 events (ML>3.5) are mostly showing normal mechanisms or with strike-slip components on nearly N-S fault plane, having significant Non-DC part and a normal stress regime is observed. The crustal anisotropy study shows N-S and NNE-SSW oriented fast polarisation azimuths (FPAs) parallel in the northern and southern clusters respectively, and concurrent with the maximum horizontal stress direction(SHmax). It seems due to the regional stress field, micro-cracks are aligned together along the SHmax resulting in "stress-induced anisotropy". The mafic intrusive body below the Palghar region induces large crustal stress that has triggered the seismic activity in the region.

KEYWORDS : earthquake swarm, focal mechanism, crustal anisotropy

Sr No: 740

Implications of tectonic and seismic framework of Delhi, National Capital Region of India: inferences from previous knowledge to future perceptions

CORRESPONDING & PRESENTING AUTHOR:

Babita Sharma, National Centre for Seismology, Ministry of Earth Sciences, India

O.P. Mishra, National Centre for Seismology, Ministry of Earth Sciences, India

The proximity to the active faults of Delhi NCR of India along with its strategic geographical and geomorphological settings is a subject of conversation or curiosity currently to comprehend on to the seismic resilient society to live in. Evidently, Delhi NCR may be affected due to the far field earthquakes associated with the inter-plate seismicity of the Indian plate in addition to the near field earthquakes with in. The behavior pattern of seismicity is to be understood clearly for Delhi NCR to recognize the implications of the sudden changes in the subsurface of crustal interior in terms of active tectonics of the region. It is now well established that the earthquakes have a tendency to arise along strained segments of faults subsequent to the dominant stress fields which is anticipated for Delhi NCR also in past and future as well. Considering the viewpoint of the ordinary settings of this region, the present study is an insight to learn the inconsistency of the seismicity patterns along with the influence of the maximum credible earthquakes both for near and far field conditions for their implications to comprehend the seismic hazard more elaboratively. The response analysis of recorded ground motions of long period and short period waveforms exhibit a clear distinct behavior in form of amplification and corresponding predominant period. Accordingly, in terms of near and far field earthquakes, the most vulnerable areas are the North Eastern region of Delhi NCR which lie in proximity to the flood plains of Yamuna river and alluvial deposits of younger origins of the foreland basin. However, the ground motions might have the characteristics to enforce the liquefaction and resonance impact in the foreland basin which in turn is adverse for the built environment in the study region. The demarcation of the study region affected by distinct seismicity patterns, is very important to understand the shaking behavior of the different kinds of infrastructures in case of near field and far field earthquakes to appropriately utilize and strengthen the new buildings and existing infrastructures in the study region.

KEYWORDS : Delhi NCR; maximum credible earthquake, response analysis; near field seismicity; far field seismicity

Sr No: 741

Recent occurrence of earthquakes in and around Delhi: Source mechanism and ground motion parameters

CORRESPONDING & PRESENTING AUTHOR:

G. Suresh, National Center for Seismology, New Delhi, India

Ravi Kant Singh, National Center for Seismology, New Delhi, India

Kapil Mohan, National Center for Seismology, New Delhi, India,

We studied the source parameters of local earthquakes ($3 \leq M \leq 4.5$) that have occurred in the National Capital Region (NCR) since April 2020 that also produced ground motions in the region. The focal mechanisms of the earthquakes reveal that most of events associated with predominantly strike-slip faulting. Analysis of a number of events shows that one of the nodal planes has a NE-SW strike, which suits to be the fault plane since the mapped geological structures in the region have a similar orientation. The trend of P- and T- axes of all events are oriented roughly towards NS and EW , respectively, while the plunge of the T-axis is nearly horizontal. Moment rate spectra of the earthquakes retrieved from records of the recorded events, which are reasonably well fit with the Brune ω^2 source model for the stress drop estimated up to 13 MPa. Discussion on PGA, PGV and PGD of these events along with felt intensity reports received from the mobile app and NCS website will be made during the presentation. Seismic amplification factor of the strata has been made by applying the method of standard spectral ratio (SSR) and we found that the estimated site effects correspond to the soft-site amplification of the sub-surface formation, which has strong bearing on the extent of seismic shaking.

KEYWORDS :   recent occurrence of earthquakes in and around Delhi

S22 ASC & CoSHRSGM Seismicity and seismic induced hazards in Asia

CONVENERS: Harsh K. GUPTA (India)

Paramesh Banerjee (Singapore)

Zhongliang WU (China)

Ruben Tatevossian (Russia)

Gary Gibson (Australia)

Toshiaki Yokoi (Japan)

Li Li (China)

In the first 20 years of the 21st Century, the number of human lives lost and quantum of economic losses due to earthquakes and the resultant tsunamis have far exceeded the similar losses in the entire 20th Century. This in spite of all the technological and scientific developments. Asia is particularly vulnerable to such losses, accounting for more than 70% human lives lost globally to earthquakes and tsunamis. Short term earthquake forecasts are not yet available. Even if such a forecast becomes possible, can the entire population of a major city be evacuated? We therefore need to develop earthquake resilient societies by spreading awareness including creating earthquake scenarios, carrying out mock-drills, involving government and public participation. Excellent tsunami warning facilities have been created following the disastrous 2004 Mw 9.2 Sumatra earthquake.

In the past 10 years, new technologies have been injected into earthquake observation and data analysis. New instrument, based on optical fiber demodulation are used to note down the ground motion and strain of the crust. Unconventional seismographs are recording new parameters such as rotational components of seismic waves. AI, machine learning and big data techniques are used to deal with earthquake recordings. Contributions are invited to address the issue of making Asian societies resilient to earthquakes and tsunamis and suggestions for future work as well as to address the issue of new technologies in observation and new methods in data processing.

Sr No: 742

Geodynamics and seismic studies in Central Seismic Gap: Initiatives in NRSC

CORRESPONDING & PRESENTING AUTHOR:

Priyom Roy, National Remote Sensing Centre, ISRO, India

Tapas Martha, National Remote Sensing Centre, ISRO, India

Kirti Khanna, National Remote Sensing Centre, ISRO, India

K.Vinod Kumar, National Remote Sensing Centre, ISRO, India

Concern lies over the 500–800 km long segment, of Garhwal–Kumaun Himalaya, where no major earthquake has happened for last ~200 years. This zone is referred to as the 'Central Seismic Gap'. NRSC/ISRO has constructed CORS and has undertaken campaign mode observations along major Himalayan thrusts belts (HFT/MBT/MCT and ISSZ) within this Central Seismic Gap. Two Continuously Operating Reference Stations (CORS) are currently operational in Manali and Dehradun. In addition, eight campaign mode stations have been established in two transects of Himachal Pradesh and Uttarakhand. The CORS at Dehradun and Manali recorded a cumulative north-eastward movement of 232 mm and 179 mm over approximately 5 years (2014-19) respectively, translating to a yearly movement of ~ 49mm/yr and ~38 mm/yr. The crustal shortening of ~ 11 mm/yr between the stations located on either side of major Himalayan thrust systems (MBT and MCT) indicating potential strain build-up. GPS Campaign data results along the Roorkee-Dehradun-Mussouri-Uttarkashi-Bhatwari section, has recorded velocities of ~44.3 mm/yr to ~49.8mm/yr, uptoUttarkashi. Thereafter between Uttarkashi and Bhatwari there is sharp change in velocities, from ~ 44.3 mm/yr to ~ 62.8 mm/yr. The Chandigarh-Pinjore-Shimla-Sundernagar-Manali Transect, show similar inhomogeneity in velocities. These campaign stations were upgraded to CORS under phase II of the study (except Roorkee and Mussoorie). The velocities are modelled with GRID STRAIN code in Matlab© and indicate towards longitudinal strain accumulation along the MCT between the campaign stations of Uttarkashi and Bhatwari. This region correlates to low 'b' value and have recorded minor earthquakes in recent past.

KEYWORDS :   geodynamics and seismic studies in Central Seismic Gap

Sr No: 743

Results of the operational, transregional, remote forecast of strong earthquakes in the Hindu Kush seismogenic zone based on the year-round SFGD monitoring in Azerbaijan

CORRESPONDING & PRESENTING AUTHOR:

Ramida Keramova, Azerbaijan National Academy of Sciences (RSSC at ANAS), Azerbaijan

The results of remote, operational seismic forecast of strong earthquakes in the Hindu Kush seismogenic zone were obtained using two "Automated technologies of forecasting in any region of the world only on the basis of year-round monitoring of the seismogeodynamic fluid's regime (SFGD) in Azerbaijan (1979-2021)". These technologies were certified in 2019. Before 1÷16 days of the earthquakes, were determined "intervals" of the main seismological parameters: coordinates; magnitude; depth, time. The reliability are 80÷85 %.

KEYWORDS :   results of the operational, transregional, remote forecast of strong earthquakes

Sr No: 744

Remote Triggering in Arunachal Pradesh, Northeastern India during the April 6, 2010, Mw7.8 Sumatra Earthquake

CORRESPONDING & PRESENTING AUTHOR:

Tony Saini, National Geophysical Research Institute, India

Abhey Ram Bansal, National Geophysical Research Institute, India

N. Purnachandra Rao, National Geophysical Research Institute, India

Venkatesh Vempati, National Geophysical Research Institute, India

Remote triggering also known as dynamic triggering is observed in many parts of the world during or after the passage of surface waves of large teleseismic earthquakes. The remote triggering is found mainly in geothermal, volcanic areas, regions disturbed by anthropogenic activities or extension regions. Very few studies found triggering in convergent or collision regions, like in Arunachal Himalaya in the current study, which is seismically active due to the collision of Indian and Eurasian plates. The CSIR-Nation Geophysical Research Institute installed a dense network of 20 broadband stations during the year 2012. We analysed waveform data of 24 hours duration during 34 teleseismic events that generated dynamic stresses $\geq$ 1kPa in the region. We find dynamic triggering in the region only during April 6, 2010, Mw 7.8, Sumatra earthquake in the forms of earthquakes and tremors. However, other earthquakes like (1) Tohoku, Mw9.1, March 11, 2011, (2) Indian Ocean, Mw8.6, April 11, 2012, and (3) Nepal Earthquake, Mw7.8, April 25, 2015, which generated large dynamic stresses, did not trigger seismicity in the region. The criticality of the region and directions of incoming waves are found to play a critical role in triggering seismicity in the region.

KEYWORDS :   N-E Himalaya, dynamic triggering, Indian Ocean Earthquake

Sr No: 745

Modern Seismology in China: Centennial Retrospect

CORRESPONDING & PRESENTING AUTHOR:

Zhongliang Wu, Institute of Earthquake Forecasting, China Earthquake Administration, China

Li Li, Institute of Geophysics, China Earthquake Administration, China

Long Wang, Institute of Earthquake Forecasting, CEA, China

Shi Che, China Earthquake Administration, China

Team CSES, China Earthquake Administration, China

The field investigation to the December 16, 1920, great earthquake in Haiyuan, organized in 1921, was regarded as the beginning of modern seismology in China. With the consistent endeavor of seismologists of several generations, Chinese seismology has been playing an active and contributive role not only in Asia but also all over the world. This presentation reviews some of the important milestones in the last 100 years, with the China Seismic Experimental Site (CSES) as the new start.

KEYWORDS :   China seismology, China seismic experimental site

Tectonic block model of continental earthquakes in China: 20 years retrospection

Long Wang, Institute of Earthquake Forecasting, China Earthquake Administration, China

CORRESPONDING & PRESENTING AUTHOR:

Zhongliang Wu, Institute of Earthquake Forecasting, China Earthquake Administration, China
Yongxian Zhang, Institute of Earthquake Forecasting, China Earthquake Administration, China
Zhigang Shao, Institute of Earthquake Forecasting, China Earthquake Administration, China

At the beginning of the 21st century, the 'tectonic block model', described by hierarchical tectonic blocks, was proposed to explain the distribution of continental earthquakes in China. The boundaries of blocks were determined by geological, geophysical, and geodetic observations. The hypothetical model implies that large earthquakes, especially those greater than M8.0 should occur in the boundary zones. This hypothesis has been tested correctly by the seismicity in Mainland China in the past 20 years. Up to now the model has been playing an active role in seismic hazard assessment and earthquake forecast in China. The model also fostered the base of the China Seismic Experimental Site (CSES). With new technology emerging and data accumulating, it is possible to update the model into new version, e.g., from 2D to 3D by considering variables of deep structures such as crust channel flow, and evolving from kinematic pattern into dynamic by computational geodynamics. Besides, during the last two decades, several multi-disciplinary researches in North China, Tibetan Plateau, and other regions provided new data and new understandings for the improvement. We suggest that the updated model could be applied to continental regions for international collaborative and comparative studies. Furthermore, combined to earthquake disaster scenarios, the model should contribute directly to the reduction of earthquake disaster risk. This presentation summarizes the progresses and discusses the prospectives.

KEYWORDS : tectonic block, continental seismicity, earthquake forecast

Parameters of Some Strong Earthquakes in Central Asia in the Second Half of the 19th Century derived from macroseismic data

CORRESPONDING & PRESENTING AUTHOR:

Ruben Tatevossian, Institute of Physics of the Earth, RAS, Russia
Nina Mokrushina, Institute of Physics of the Earth, RAS, Russia
Roman Vakarchuk, Institute of Physics of the Earth, RAS, Russia

Materials on felt earthquakes in Samarkand and Fergana regions (Republic of Uzbekistan) in 1868–1892 are presented based on original sources of information not used before. The epicentre location and magnitude for the earthquakes April 7, 1869, and March 2, 1892, are evaluated for the first time; for the other two earthquakes (April 3, 1868, and September 18, 1892), the uncertainty of previously published solutions is significantly reduced. Reduction of uncertainties of former solutions is achieved due to the formalized method of epicentral and magnitude assessment, which works successfully with sparse datasets. One of the restrictions on the entire set of solutions is association of the epicenter with certain

active tectonic structures. This criterion is used only for selecting the preferable solution from the entire set of solutions obtained solely from macroseismic data. The complete set of solutions is retained and can be used to analyze the accuracy and objectivity of the preferable solution.

Sr No: 748

SYMPOSIUM : **S22 ASC & CoSHRSGM Seismicity and seismic induced hazards in Asia**

Seismic evidence of the Pop - up tectonics beneath the Shillong Plateau area of Northeast India

CORRESPONDING & PRESENTING AUTHOR:
Ajay P. Singh, National Centre for Seismology, Ministry of Earth Sciences, India
O.P. Singh, Geological Survey of India (GSI) , India
Ajeet P. Pandey, Ministry of Earth Sciences (MoES) , India
O.P. Mishra,, Ministry of Earth Sciences (MoES), Lodhi Road, India

Three-dimensional seismic tomography (Vp, Vs, s) of the Shillong Plateau region has been performed using high-quality arrival times of the body wave phases recorded at a dense temporary seismic network. The technique is used to understand the crustal heterogeneities and also its implication to pop-up tectonics characterizing evolution of the Shillong Plateau. In the present study, we investigated an area covering approximately 150 — 100 sq km that revealed seismicity to be confined in a depth range = 60 km. A high velocity perturbation in the upper crust appears to be responsible for intense small to moderate seismic activity in the region. Crustal seismic velocities inferred from 3-D tomography showed significant lateral heterogeneities between crust and upper mantle beneath the Shillong Plateau. The high velocity zones in the uppermost crust, interpreted as Shillong plateau, acts as a geometric asperity where interseismic strain may accumulate. A low velocity zone in the lower crust probably play a major role to accommodate the stresses generated due to plate separation; culminating into future sources of great earthquakes. The geological faults are well imaged in the cross-sections and support the concept of Pop-up tectonics beneath the Shillong Plateau of NE India.

Sr No: 749

SYMPOSIUM : **S22 ASC & CoSHRSGM Seismicity and seismic induced hazards in Asia**

Tsunami hazard evaluation of Gulf of Aqaba

CORRESPONDING & PRESENTING AUTHOR:
Asem Salama, National Research Institute of Astronomy and Geophysics, Cairo, Egypt, NRIAG, Egypt
Mohamed Gabry, National Research Institute of Astronomy and Geophysics, Cairo, Egypt, NRIAG, Egypt
Hesham Hussein Moussa, National Research Institute of Astronomy and Geophysics, Cairo, Egypt, NRIAG, Egypt
Iman Farag Abu El Nadr, National Research Institute of Astronomy and Geophysics, Cairo, Egypt, NRIAG, Egypt

Large historical earthquakes with magnitudes of $6 < M \leq 7.3$ struck the Gulf of Aqaba, including the earthquakes of 363, 1068, 1212, 1312, 1588, 1778, and 1900 AD. On November 22, 1995, a large earthquake with a magnitude of 7.3 struck the Gulf of Aqaba, causing a small tsunami that hit the Egyptian port of Nuweiba, as well as the Elite and Aqaba beaches. The epicenter of this earthquake occurred between Aragonese and Eliat basins in the Gulf of Aqaba's central region. The long period of low seismicity, especially for significant events at the southern part of Arnona fault, has resulted in the creation of a potential seismic gap, with a future Mw 7.2 earthquake, which is expected to cause a tsunami in coastal cities of Saudi Arabia, Egypt. In this study, we use Mirone version 2.10 software to calculate the maximum wave height at the Gulf of Aqaba cities. The two tested scenarios are focused on the Aragonese fault of the November 22, 1995 earthquake, and the Aronan fault earthquake of 1212 AD in the Aqaba basins. The November 22, 1995 scenario produces a maximum wave height of 1 meter at Nuweiba city, 0.8 meter at Dahab city and 1.5 meter at Elat city. Whereas the Arnona fault scenario results in a maximum wave height of 0.7 m in Dahab, 0.5 m in Nuweiba coastal city of Egypt and 0.5 meter in Magna city of Saudi Arabia with less impact on north Aqaba and Elat cities.

KEYWORDS : Gulf of Aqaba, tsunami hazard, historical seismicity

Sr No: 750

SYMPOSIUM : **S22 ASC & CoSHRSGM Seismicity and seismic induced hazards in Asia**

Stress drop variations of reservoir triggered earthquakes at Koyna-Warna: A case study

CORRESPONDING & PRESENTING AUTHOR:

Chitta Ranjan Mahato, CSIR-National Geophysical Research Institute, Hyderabad, India

We have developed a new python code for the spectral ratio technique for estimation of earthquake source parameters of local earthquakes. The spectral ratio technique uses the concept of empirical green's function (EGF). A small earthquake almost from the same location with a similar focal mechanism and magnitude sufficiently lower than the target earthquake have been used as an EGF. This technique effectively accounts for the path and site effects, thus contribute unbiased estimates and it also tackles the trade-off between corner frequency (fc) and attenuation (Q) of traditional spectral fitting method. Here we investigated the dependence of stress drop on seismic moment associated with a new cluster of earthquakes (0.5-4.0ML) that occurred during June 2017 at Koyna-Warna, western India, a popular site of reservoir triggered seismicity. A total of 368 P-wave spectra have been used in this study for this purpose. Data from both surface broad-band and short-period borehole seismic networks are utilized. The stress drop varies from about 0.01-14 MPa, while median value of stress drop follows a constant drop scaling as widely accepted for natural tectonic earthquakes. Also, we analysed 450 P-wave spectra from the well-known clusters of the study region.

KEYWORDS : Koyna, green's function, spectral ratio technique

Sr No: 751

Developing an Earthquake Resilient Society in the vicinity of Himalaya

CORRESPONDING & PRESENTING AUTHOR:

Harsh K. Gupta, National Geophysical Research Institute, India

The Himalayan region has witnessed devastating earthquakes in the past. During a very active seismic activity phase, 4 earthquakes of M ~ 8 occurred during a span of only 53 years. These include the Shillong (1897), Kangra (1905), Bihar- Nepal (1934), and the Assam (1950) earthquakes. No such earthquake has occurred since the 1950 Assam earthquake. Earthquakes usually repeat. To develop an earthquake resilient society, it helps to develop an earthquake scenario, depicting, what would happen if an earlier earthquake repeats today? An earthquake scenario was built by the National Disaster Management Authority in collaboration with other agencies for the repeat of the 1905 Kangra earthquake. If this earthquake occurred in the middle of the night, ~ 0.8 million lives could be lost in Himachal Pradesh, Punjab, Haryana, and the Union Territory of Chandigarh. This information was shared with the state and central authorities of India, followed by a year-long preparation in preparing the above-mentioned four states to develop earthquake resilient society. A mega mock drill was conducted for the occurrence of the earthquake, virtually, at 11 am on 13 February 2013. Observations were conducted on pre-selected locations to assess the preparedness to mitigate the effects of such an earthquake. The participation of state and central government machinery and the public was very encouraging and pointed out the shortcomings that need to be addressed. A similar exercise was carried for the 8 north-east Indian states for the repeat of the 1897 Shillong earthquake. Results of these exercises are presented.

KEYWORDS :   earthquake resilient

Sr No: 752

Probabilistic Seismic Hazard in Uttarakhand Himalaya

CORRESPONDING & PRESENTING AUTHOR:

Daya Shanker, Indian Institute of Technology Roorkee, India
Shubham Singh, Indian Institute of Technology Roorkee, India
Komal Soni, Indian Institute of Technology Roorkee, India

Seismic hazard analysis involves the quantitative estimation of ground shaking at a particular site for a specific region. Study on Probabilistic Seismic Hazard Analysis (PSHA) has been carried out for Uttarakhand Himalaya. This the most seismically active Indian Himalayan areas, where seismically active faults, MCT, MBT and MFT are passing through it and making the region hazardous due to earthquakes occurrence. The contributions of smaller local faults cannot be ignored because the Yamuna Fault near Haridwar and Alaknanda Fault near Rudraprayag make the region more seismic potential. The CRISIS 2015 has been used for Seismic Hazard computation. For PSHA study, at mcro level area has been divided into grid size of 0.2° x 0.2°. The seismicity parameters and attenuation models have been used as input parameters to computed seismic hazard is in terms of PGA for 20%, 10% and 2% probability of exceedance in 50 years which are equivalent to return periods of 225, 475 and 2475 years respectively.

KEYWORDS :   probabilistic seismic hazard

Sr No: 753

On the spatio-temporal variation in b-value After 25 April 2015 Gorkha, Nepal earthquake

CORRESPONDING & PRESENTING AUTHOR:

Daya Shanker, Indian Institute of Technology Roorkee, India

Ram Krishna Tiwari, Tribuvan University, Kirtipur, Kathmandu, NEPAL

Harihar Paudyal, Tribhuvan University, Bharatpur, Chitwan, NEPAL

In the present investigation spatial-temporal distribution of b value along the cross section of width 20 km for five faults (Judi fault, Thaple fault, Kathmandu fault, Motihari-GauriShanker fault and Motihari-Everest fault located the Central Himalaya) was studied as a precursor phenomenon to a physical preparation for the main rupture. The earthquake data compiled from the ISC and USGS catalogues for a period 2015/04/25 to 2020/09/15 were used in analysis. The variation of the b-value along faults were reported ranging from 0.85 to 0.94 which is less than global average value of 1. The results indicate high stress condition of the faults advocating the potential regions for the future weak to moderate earthquakes. These significant low b-values are also co-related to thrust faulting patterns in the region. The spatial variation of b-value indicates low b value areas in the limited scale which are high stress area having the potentiality to generate the future large earthquake. The temporal variation of b value shows the certain fluctuations on b-value during the period of 25 April to 12 May events. Afterwards, the b value seemed to be stable around 1 to 1.5. The high b-value around 2.0 observed for Kathmandu fault might correspond to earthquake swarms during the earthquake period. The tendency relation between b-value and faulting patterns was found along the Faults. The low b-value observed for faults is in agreement with thrust faulting pattern in the region, might be useful for the evaluation of seismic hazard and earthquake forecasting.

KEYWORDS :   b-value distribution, cross section, seismic hazard analysis

Sr No: 754

Comprehensive Report on September 28, 2018 Indonesian Tsunami

PRESENTING AUTHOR:

Nazeel Sabah, Indian Institute of Technology Roorkee, India

CORRESPONDING AUTHOR:

Daya Shanker, Indian Institute of Technology Roorkee, India

On 28th September 2018, at 18:02:44 (Indonesia Central Standard Time) a strong tsunami accompanied an earthquake of Mw 7.5 and left the state of Central Sulawesi worst affected. The tsunami was quite unprecedented as the quake was spawned by a strike-slip fault (Palu-Koro fault). Usually, strike-slip faults displace land horizontally and not vertically and hence typically do not lead to a tsunami. Present article sheds some light on the geological, geographical and tectonic details of the island country which are of paramount importance in understanding the causes and mechanisms of earthquakes and tsunamis in the region as well as factors such as submarine landslips and the shape of the bay are being discussed by the scientific community as a causative to the disproportionate damage caused. Based on the various tsunami

catalogues from 1500 to date, the details of casualties and other associated damages collected by various sources, observed foreshocks (as high as Mw 6.1) and aftershocks (more than 150 in number), estimates are done for causes, maximum magnitudes and water heights observed during the tsunamis and the total fatalities. The post-tsunami geotechnical investigation also advocates liquefaction damage and landslide events experienced by the region.

KEYWORDS : submarine landslip, bay resonance, funnelling

Sr No: 755

- -

SYMPOSIUM : **S22 ASC & CoSHRSGM Seismicity and seismic induced hazards in Asia**

Crustal seismic attenuation in Kumaon Himalaya, India from Lg Q inversion

CORRESPONDING & PRESENTING AUTHOR:

Mahesh Prasad Parija, CSIR-National Geophysical Research Institute Hyderabd, India
Sudesh Kumar, CSIR-National Geophysical Research Institute Hyderabd, India
Arjun V.H., CSIR-National Geophysical Research Institute Hyderabd, India
Sandeep Gupta, CSIR-National Geophysical Research Institute Hyderabd, India

The crustal seismic attenuation structure along the Tanakpur- Dharchula- Dharma transect is studied first time by using Lg wave spectra method on densely spaced 32 broadband seismographs along ~200 km long profile in Kumaon sector of the northwest Himalaya from five regional earthquakes of M ≥ 4.0. The NE-SW profile extends between Indo Gangetic Plain in the southwest to Tethys Himalaya in the northeast. The lateral variability in the seismic attenuation structure is derived through inversion of 64 high quality two-station measurements out of total possible 94 two-station pairs. The region has Qo estimates ranging from 63±2 to 203±25, with the lowest value in the Lesser Himalaya and the highest across some part of the Indo Gangetic Plain and Siwalik Himalaya. The results do not show significant variations across the Higher Himalaya and the Tethys Himalaya. The strong attenuation reported consistently along the entire profile covering four different lithotectonic units highlights the role of lesser Himalayan duplex thrust sheets present beneath the area, which imbricates small scale crustal heterogeneities that cause strong attenuation of the Lg spectra beneath the lesser Himalaya. The presence of trapped fluids/partial melts and leucogranites can be major factors responsible for strong Lg attenuation beneath the Kumaon Himalaya

KEYWORDS : attenuation, Himalaya, quality factor

Stress transfer and accumulation on the Main Himalayan Thrust (MHT) since 1905: Implications for seismic hazard

CORRESPONDING & PRESENTING AUTHOR:

Mahesh Prasad Parija, CSIR-National Geophysical Research Institute Hyderabd, India

Sushil Kumar, Wadia Institute of Himalayan Geology, India

Shubhasmita Biswal, Indian Institute of Technology Kharagpur, India

The along-strike terminations of seismic ruptures on the Main Himalayan Thrust (MHT), western Himalayan segment due to four earthquakes of magnitude (Mw) ≥ 6.6 in the period 1905-2019 are investigated using the Coulomb stress transfer. For the 1975 Kinnaur earthquake (Mw 6.8), we observed that stress perturbations are controlled by the secondary fault structures, which generated stress heterogeneities within the study area and have limited the mainshock rupture propagation in the NW-SE direction along strike, impeding the rupture to reach the Himalayan front. We also observed that the ramp geometry of the MHT played a significant role during the 1991 Uttarkashi and 1999 Chamoli earthquakes, inhibiting the seismic ruptures to accelerate towards the surface. Besides, the geometry marks the presence of complex Lesser Himalayan duplexes, which accumulates the resultant coseismic stress from the two earthquakes. The Coulomb stress modeling from all of the studied earthquakes suggests a lateral increase in stress interactions along the strike for the 1905 Kangra, the 1991 Uttarkashi and the 1999 Chamoli events and across the strike for the 1975 Kinnaur earthquake in the western Himalaya. Finally, we infer that tectonic loading of the MHT dominates the present-day stress perturbations in the western Himalaya.

KEYWORDS :   coulomb stress, duplex, main Himalayan thrust

S24 IHFC Towards 60 years of activity of the International Heat Flow Commission

CONVENERS: Sukanta Roy (India)
Robert N. Harris (USA)
Sven Fuchs (Germany)
Massimo Verdoya (Italy)

The International Heat Flow Commission, constituted under the IASPEI in 1963, will celebrate its 60th anniversary at the next IUGG General Assembly in 2023. The activities of the Commission span all aspects of geothermal studies and linkages to the Earth sciences. Initially, the focus of the IHFC was on the acquisition of heat-flow data through temperature-depth measurements and thermal properties of rocks in a variety of geologic and tectonic regimes to constrain the thermal structure of the Earth. Since that time heat-flow studies have become fundamental for a number of applications in seismology, volcanology, geodynamics, geothermal energy, past climate change, hydrology and other fields. The goal of this symposium is to highlight the accomplishments of heat-flow studies and their role in understanding a wide range of Earth processes. The contributions to the symposium will include critical reviews identifying key-knowledge gaps as well as recent work in all aspects of geothermal investigations.
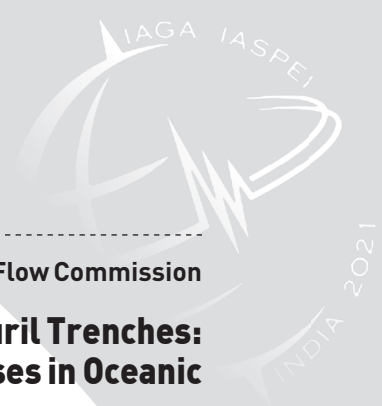
Sr No: 757

Heat Flow Anomalies on the Seaward Side of the Japan and Kuril Trenches: Implications for Fluid Circulation and Heat Transport Processes in Oceanic Crust of the Incoming Pacific Plate

CORRESPONDING & PRESENTING AUTHOR:

Makoto Yamano, The University of Tokyo, Japan

Kouta Sasaki, Kozo Keikaku Engineering Inc.Japan

Yoshifumi Kawada, Japan Agency for Marine-Earth Science and Technology, Japan

Masataka Kinoshita, The University of Tokyo, Japan

High and variable heat flow values, anomalous for the seafloor age of the incoming plate, are pervasively observed on the outer rise of the Japan Trench. We recently conducted heat flow measurements on the seaward side of the westernmost part of the Kuril Trench and found a contrasting feature: most of the obtained values are normal for the seafloor age. The broad high heat flow zone seaward of the trench can be attributed to efficient heat transport by pore fluid circulation in a permeable layer developed through fracturing of the oceanic crust due to plate bending. Nearly normal heat flow off the Kuril Trench may result from lower average permeability in less fractured crust, which suppresses large-scale fluid circulation. It is consistent with the observation that the anomaly in the seismic velocity structure, probably due to fracturing and water penetration, is more significant off the Japan Trench than off the Kuril Trench.

On the seaward slope of the Japan Trench, where normal faults are well developed, heat flow data has been rather sparse. We also conducted heat flow measurements in this area around faults with large surface displacement. At around 39°N, values obtained in the faulted area are, on average, lower than those on the outer rise, indicating that fluid circulation pattern in the oceanic crust may have changed associated with development of normal faults. Local variations were found in the vicinities of fault escarpments, possibly related to focused fluid flow along faults.

KEYWORDS :   heat flow, fluid circulation, outer rise

Sr No: 758

How to Calculate Heat Flow from Geothermal Heat Pump Data

CORRESPONDING & PRESENTING AUTHOR:

Ladislaus Rybach, Institute of Geophysics ETH Zurich, Switzerlands

The basic ingredients to calculate heat flow are temperature gradient and thermal conductivity (k). Such data can be obtained from boreholes. Geothermal heat pump systems are now installed more and more in many countries for space heating and cooling, most of them with borehole heat exchangers (BHE). Special borehole measuring set-ups and procedures are used in construction areas to determine the site specific average thermal conductivity k (TRT method) or the thermal conductivity profile (k(z), ETRT method). Such data are needed for design calculations. At the same time, the borehole temperature profile T(z) is also measured. With these data in hand, heat flow can be calculated.

Data from several BHE sites in Switzerland have been acquired, analyzed, and processed. First, the borehole temperature data for z > 100 m are plotted to display the T(z) trends, then average k or k(z) are taken from the TRT or ETRT records and reports. Finally, the local heat flow is calculated either with the average l and the average gradient or with the Bullard plot technique, which uses k(z). In the latter, layer-wise integrated thermal resistivities (delta zi/ki) are plotted against measured temperatures at corresponding depths.

The method is demonstrated by examples from BHE sites in the Zurich region/Switzerland. The "shallow" heat flow values elaborated by these means are in the range 80 to 100 mW/m2 and fit reasonably well with the general Swiss heat flow trends, determined from deep (> 1 km) borehole data.

KEYWORDS :   borehole heat exchanger, temperature log, thermal conductivity log

Sr No: 759

SYMPOSIUM :   **S24 IHFC Towards 60 years of activity of the International Heat Flow Commission**

Geothermal regime of the Koyna seismogenic zone, Deccan Traps, India constrained from measurements in the deep crystalline basement

CORRESPONDING & PRESENTING AUTHOR:

Sukanta Roy, Ministry of Earth Sciences, India
Deepjyoti Goswami, Ministry of Earth Sciences, India
Vyasulu V Akkiraju, Ministry of Earth Sciences, India
Nagaraju Podugu, Ministry of Earth Sciences, India

The geothermal regime in the western part of the Deccan Traps is constrained from equilibrium temperature measurements in the crystalline basement rocks down to 1.5 km depth beneath the Koyna seismogenic zone, combined with thermal conductivity and radiogenic heat production measurements on core samples. The contrast in gradient between Deccan basalt and granite-gneiss basement (26.5 mK m-1 and 15.7 mK m-1 respectively) is consistent with the contrast in thermal conductivity between the two rock types (1.6 Wm-1K-1 and 2.8 Wm-1K-1 respectively), yielding near identical heat flow of 43 mW m-2 over the two lithologies. The low heat flow in Koyna region is consistent with previous determinations in the southern parts of the Deccan Traps as well as the adjoining Dharwar craton to the south, which confirms that thermal transients potentially associated with the ~65 My old Deccan volcanism have decayed and heat flow is in equilibrium with crustal radiogenic heat production. Radiogenic heat production of the basement rocks, combined with the new geological constraints from scientific drilling lead to improved estimates of temperature in the crust. While temperature considerations allow for a deeper (>25 km) seismic-aseismic transition, the seismicity in the region is restricted to the uppermost 10 km of the crust only. Lack of seismic activity at greater depths may indicate the insignificant role of reservoir at those depths. Additionally, the new datasets provide constraints to infer the background thermal regime in the adjoining West Coast group of hot springs located near the western margin of Koyna seismogenic zone.

KEYWORDS :   Koyna seismogenic zone, heat flow, crustal temperatures

Sr No: 760

Renovating the Global Heat Flow Database: Status, current and future actions

CORRESPONDING & PRESENTING AUTHOR:

Sven Fuchs, Helmholtz Centre Potsdam - GFZ German Research Centre for Geosciences, Germany

The Global Heat Flow Database (GHFDB) is fostered and maintained by the International Heat Flow Commission (IHFC) for nearly 60 years now. From the very beginning, periodic revisions of the GHFDB were carried out to update the heat flow database entries and the underlying scientific methods according to the state of the science and database technology at the time. The digitization and evolution of technological concepts over the past decades and the increasing scientific demand for quality-assured and authenticated data cumulated in the start of a further fundamental database revision in 2019. Here, we want to illustrate the reasons of the revision and present the community-driven efforts to unravel associated challenges of the revision process, and provide an overview on the status of the on-going work based on a global collaboration of heat-flow scientists.

The database revision so far included (i) the collaborative development of a new database structure that substitutes the former database structure from 1976, (ii) the transformation of data to this new structure and the release of the converted GHFDB 2021 containing about 74.548 heat flow entries, and (iii) the start of the Global Heat Flow Data Assessment Project, designed to scrutinize and reassess the stored heat flow data according to the new structure that most often requires a detailed assessment of relevant meta data from the original publication. This review process is supported by over 65 geoscientists worldwide and still ongoing, and we welcome further researchers willing to contribute to this undertaking.

KEYWORDS :   heat flow, global heat flow database, international heat flow commission

Sr No: 761

Resource assessment and productivity predictions in unconventional geothermal systems

CORRESPONDING & PRESENTING AUTHOR:

Paromita Deb, RWTH Aachen University, Germany

Geothermal energy comprises utilization of earth's natural heat for producing electricity and for direct uses. Being a steady power generation source, with negligible carbon footprint, geothermal energy can play a key role in meeting the global energy demand in a safe and sustainable manner. However, in spite of the tremendous energy generating potential, geothermal energy production has been limited due to geographical constraints as well as high production costs. With fossil fuel and other renewable technologies offering quicker capital returns and immediate profit, the investment in geothermal wells, which are equally expensive, has been limited. To compete with fossil fuels and other renewable energy resources, geothermal energy exploitation requires development of unconventional resources such as Enhanced Geothermal Systems (EGS) and Super-Hot Geothermal Systems (SHGS), which offer efficient, economic and geographically unconstrained production possibilities. While EGS requires artificial stimulation, SHGS are temperature fields, usually

characterized by hot and shallow magmatic sources. In this study, we focused on three fundamental aspects for confident predictions of resource quality and production potential in unconventional geothermal systems (i) temperature assessment in volcanic field with active magmatic heat sources responsible for super-hot geothermal resources, (ii) uncertainty in temperature prediction due to uncertain modeling parameters and (iii) verifying the predictive capabilities of numerical codes used for designing EGS. The different aspects are studied implementing both numerical modeling and experimental methods. Apart from establishing workflows for reliable temperature predictions in exploration geothermal fields, our code verification study establishes confidence in two independent, coupled hydraulic fracturing simulators.

KEYWORDS : super-hot geothermal resources, enhanced geothermal system, hydraulic fracturing experiments and simulations

Sr No: 762

Heat-flow offshore Haiti and in the Caribbean plate

CORRESPONDING AUTHOR:

Frederique Rolandone, Sorbonne Universite, France
Presenting Author: Jeffrey Poort, Sorbonne Universite, France
Francis Lucazeau, IPGP, France
Sylvie Leroy, Sorbonne Universite, France

Heat-flow in the Caribbean is poorly known and generally low in the major basins and the Greater Antilles arc, but with some high values in active zones, like in the Cayman trough or in the Lesser Antilles Arc. We present new heat-flow data for offshore Haiti, which is part of the Greater Antilles arc. We obtain heat-flow estimates from 12 in situ measurements and from Bottom Simulating Reflector (BSR) along 7 seismic profiles acquired during the marine geophysical and geological survey HAITI-SIS. Both methods suggest a regionally low heat-flow, respectively 46±7 mWm-2 and 44±12 mWm-2, consistent with older data from the Greater Antilles arc. However, high heat-flow, with locally high values exceeding 80 mWm-2, was measured locally near faults, in particular the E-W strike-slip Septentrional–Oriente fault zone (SOFZ) and small reverse faults south of it. Predictive heat-flow mapping suggests this is a pervasive feature along the strike of the SOFZ. Away from the faults, heat-flow in the Greater Antilles falls to a regional heat-flow low. This uniformly low value across continental and oceanic domains is most probably related to a low radiogenic content of the continental crust. This low heat-flow pattern is confirmed at the scale of the Caribbean. Two exceptions are found in the tectonically active regions of the Lesser Antilles arc and Cayman trough. The new Caribbean heat-flow map shows that the only places that stand off to the low background heat-flow are the active zones of subduction, crustal accretion and large-scale transform faults.

KEYWORDS : heat-flow, Carribean, fault

Sr No: 763

Experimental based enhancement of theoretical approach for determining the thermal conductivity of reservoir rocks

CORRESPONDING & PRESENTING AUTHOR:

Zakhar Pichugin, Skolkovo Institute of Science and Technology, Russia

Maria Kalinina, Sergo Ordzhonikidze Russian State University for Geological Prospecting, Russia

Evgeny Chekhonin, Skolkovo Institute of Science and Technology, Russia

Irina Bayuk, Schmidt Institute of Physics of the Earth of the Russian Academy of Science, Russia

Yuri Popov, Skolkovo Institute of Science and Technology, Russia

Information on the rock thermal conductivity is necessary for heat flow determination as well as for modeling in the petroleum industry (thermal methods of enhanced oil recovery, basin and petroleum systems modeling), geothermal energy industry, civil and underground geophysics, and radioactive waste disposal. To account for spatial and temporal variations of thermal conductivity, special theoretical models of rock thermal conductivity are applied. The most widely used model – the weighted geometric mean (so-called Lichtenecker's model) – is believed by many specialists to be relevant.

We performed an analysis of the vast experimental data for different rock types including argillites, dolomites, limestones, sandstones, and siltstones (20 collections, 1765 rock samples, 33% of the samples studied at different saturation states - with air, oil, and water in pores) to test the Lichtenecker's model. The analysis showed that Lichtenecker's model systematically underestimates significantly (up to 53%) measured thermal conductivity values for porous and fractured reservoir rocks. The average error depends on rock lithology, porosity, and pore fluid and is about 20% for dry rock samples, 14% and 9% for oil- and water-saturated samples correspondingly.

Modification of the model was suggested with a correction factor following Asaad's approach. Estimations of the factor for various lithotypes, pore fluids, and porosity were performed. Interrelation between the correction factor and pore space geometry was established using the effective medium theory for rocks from carbonate reservoirs. Methodology of the correction factor determination for reservoir rock thermal conductivity modeling was developed.

KEYWORDS :   thermal conductivity, geometric mean model, theoretical modeling

Sr No: 764

The model of temperature response to external radiative forcing

CORRESPONDING & PRESENTING AUTHOR:

Anastasiia Gornostaeva, Institute of Geophysics UB RAS, Russia

Dmitry Demezhko, Institute of Geophysics UB RAS, Russia

Aleksander Antipin, Institute of Geophysics UB RAS, Russia

Today an urgent scientific problem is the developing of models describing the observed phase shifts between external radiative forcing and the induced temperature response.

We consider that this problem can be solved using the relation between the variations of the surface heat flux and ground surface temperature. Phase relation between these two parameters can be described using the model of conductive heat transfer in a homogeneous half space. According to the model, in case of harmonic oscillations in a homogeneous medium the phase shift between the variations of heat flux and temperature is constant and equals to 45°. Extending the model of conductive heat transfer to the case of a two-layer medium with an upper low thermal conductivity layer and carrying out several meteorological and actinometric measurements in diurnal and annual cycles, we have shown that the existence of such layer leads to the decrease in the phase shift value comparing with the model of a homogeneous medium (<45°).

A comparing of the model values of phase shifts with independent evidence on long time scales reveals that all the analyzed empirical data vary around a median value of 45°. An increase in the phase shift in some cases can be due to dating errors in the analysis of proxy paleotemperature records as well as the existence of a thick ice sheet at ground surface etc.

KEYWORDS : ground surface temperature, surface heat flux, phase shift

Sr No: 765

Thermal Structure of the Palaeozoic Oceanic Lithosphere in the Herodotus Basin, Eastern Mediterranean Sea

Paolo Chiozzi, University of Genoa, Italy

CORRESPONDING & PRESENTING AUTHOR:

Massimo Verdoya, University of Genoa, Italy
Elie El Jbeily, University of Genoa, Italy

It is widely accepted that the oceanic lithosphere thermal regime depends on the time elapsed from the lithosphere generation at the spreading ridge axis and the thermal relaxation from its initial condition. Two kinds of models have been classically proposed to account for the thermal structure of the oceanic lithosphere: (i) the "plate model (PM)" with a constant temperature at the lithosphere base that well accounts for the heat flow and subsidence of the seafloor; (ii) the "boundary layer model (BLM)," which is in better agreement with the seismological evidence that the lithosphere thickens away from the ridge axis. Since the plate motion has destroyed most oceanic lithosphere formed before Jurassic, these models were calibrated to the available heat-flow data that were derived from observations on <200 Myr old lithosphere. Recent studies of magnetic anomaly suggest that the lithosphere age of the Herodotus Basin might be much older, i.e. Early to Middle Carboniferous (340±25 Myr). Consequently, both PM and BLM are inapplicable to model the thermal structure of this basin. We, therefore, modelled a geotherm under the assumption of steady-state, conductive conditions. The thermal conductivity dependence upon pressure and temperature was considered, together with the radiogenic heat production estimated from crustal composition models inferred from the seismic structure. A careful revision of the available heat-flow data, corrected for the bias associated with the bottom water temperature variation and the sedimentation, provided the surface boundary condition to the thermal model.

KEYWORDS : terrestrial heat flow, ocean lithosphere, thermal structure

Sr No: 766

Terrestrial Heat Flow and Water-Loaded Depth of the Eastern Mediterranean Sea

PRESENTING AUTHOR:

Elie El Jbeily, University of Genoa, Italy

Paolo Chiozzi, University of Genoa, Italy

CORRESPONDING AUTHOR:

Massimo Verdoya, University of Genoa, Italy

We investigated the nature of the lithosphere of the Eastern Mediterranean, in the sector extending from the Ionian Sea, to the west, to Levantine Basin, to the east. Our approach combined the analysis of terrestrial heat-flow with data of bathymetry, sediment and crustal thickness derived from both global models and high-resolution local measurements. Correction for sedimentation and climatic changes were applied to infer the purely conductive steady-state geothermal flow pattern. Bathymetric data were processed by removing the subsidence caused by sediment deposition to obtain the water-loaded seafloor depth. To remove the sediment-load effect, we used porosity and density data available from drillings and corrected for the rebound effect. From the different curves of sediment bulk-density as a function of sediment thickness, we found a regional correction for the Eastern Mediterranean Sea. The resulting thermal data and water-loaded seafloor depths were then compared to reference models of continental stretching and ocean plate cooling to investigate and characterize the nature of the lithosphere. The results argue that the Levantine Basin is floored by a stretched continental crust. West of the Levantine, the Herodotus Basin seems instead characterised by oceanic type crust. In all the Eastern Mediterranean, the water-loaded seafloor depths are consistent with geological ages >250 Ma. In the Herodotus Basin, the estimated mantle heat flow is coherent with that of the oceanic Ionian lithosphere, whereas in the Levantine Basin it is comparable to that of the Sinai continental microplate

KEYWORDS : tectonic subsidence, seafloor depth, lithosphere nature

Sr No: 767

Well-log based determination of thermal properties of anisotropic formations: case studies of implementation

CORRESPONDING & PRESENTING AUTHOR:

Anuar Shakirov, Skolkovo Institute of Science and Technology, Russia

Evgeny Chekhonin, Skolkovo Institute of Science and Technology, Russia

Yury Popov, Skolkovo Institute of Science and Technology, Russia

Data on rock thermal properties are required to determine heat flow density, explore geothermal resources, design and optimize enhanced oil recovery methods, provide petrophysical support of basin and petroleum system modelling, etc. The absence of implemented techniques for in situ measurements of rock thermal properties conditioned the necessity to develop well-log-based approaches for rock thermal property determination. Well-log based approaches suggested previously for determining rock thermal properties are appropriate only for isotropic rocks. Concurrently, many rock types exhibit essential thermal anisotropy.

Therefore, well-log based determination of rock thermal properties accounting for thermal anisotropy is a task of prior concern.

The novel technique for well-log based determining rock thermal properties accounting for thermal anisotropy based on the integration of well logging and thermal core-logging data was developed and implemented. The technique encompasses the application of both advanced machine-learning techniques and enhanced theoretical modelling of rock thermal properties. The essential advantage of the developed technique is accounting for rock heterogeneity, saturation, in situ pressure and temperature in case of thermal anisotropy.

The developed technique was tested and implemented for geothermic investigations of various geological formations. From a comparison of the experimental data on rock thermal properties and well-log based prediction, it can be concluded that rock thermal conductivity and volumetric heat capacity can be determined with total uncertainties of less than 13% and 6% (for 0.95 confidence level), respectively.

KEYWORDS : well logging, thermal properties, thermal anisotropy

Sr No: 768

New data on essential vertical variations in heat flow obtained with advanced experimental technique

PRESENTING AUTHOR:

Yury Popov, Skolkovo Institute of Science and Technology, Russia

CORRESPONDING AUTHOR:

Anuar Shakirov, Skolkovo Institute of Science and Technology, Russia
Evgeny Chekhonin, Skolkovo Institute of Science and Technology, Russia
Mikhail Spasennykh, Skolkovo Institute of Science and Technology, Russia
Dzhuliya Zagranovskaya, LLC Gazpromneft Scientific and Technical Center, Russia
Zakharova Oksana, LLC Gazpromneft Scientific and Technical Center, Russia

A wide spectrum of advanced experimental approaches was used to study vertical variations in heat flow along two wells that reached thermal equilibrium. The Baleykino exploration and Bazhen parametric wells (depths of 3780 and 3203 m, drilled with coring below 1348 and 1735 m) were drilled in the Orenburg region and West Siberia (Russia) crossing unconventional hydrocarbon formations. Continuous profiling rock thermal properties (including thermal anisotropy coefficient) was performed with the field optical scanning instrument on all (1699 and 4102) recovered core samples. Additional thermal property measurements were performed with a specially developed new laser optical scanning instrument on 40 and 41 core samples (reasonably selected from continuous thermal core profiling) fluid-saturated additionally to account for induced artificial micro-fracturing and drying out of core samples during and after core recovery. The measurements at elevated temperatures were performed on 29 and 37 fluid-saturated core plugs using a combination of the DTC-300 and laser optical scanning instruments. The new well-logging based technique provided thermal conductivity data for non-coring depth intervals of 860 and 558 m, respectively. Upper and lower estimates of equivalent thermal conductivity accounted for in-situ conditions, rock fracturing, transversal and micro-anisotropy and multi-scale rock heterogeneity. An essential heat flow increase along the wells was established (by 22 and 63%) within depth intervals of 1400-2700 and 1734-3030 m, correspondingly. The new estimates of terrestrial heat flow (72.6 and 87.1 mW/m2) exceed by 114% and 55% the heat flow data obtained for the well-drilling areas with the widely-used approaches and published previously.

KEYWORDS : heat flow, vertical variations, new technique

Sr No: 769

Role of effective medium theory in expanding capabilities of experimental thermal petrophysics

CORRESPONDING & PRESENTING AUTHOR:

Irina Bayuk, Schmidt Institute of Physics of the Earth, Russian Academy of Sciences, Russia

Yuri Popov, Skolkovo Institute of Science and Technology, Russia

Raissa Romushkevich, Skolkovo Institute of Science and Technology, Russia

Evgeny Chekhonin, Skolkovo Institute of Science and Technology, Russia

Tagir Yalaev, Schmidt Institute of Physics of the Earth, Russian Academy of Sciences, Russia

Evgeny Popov, Skolkovo Institute of Science and Technology, Russia

INTRODUCTION

In this work, we demonstrate new possibilities provided by a combination of the effective medium theory (EMT) and experimental thermal petrophysics. Mainly this is important for prospecting geophysics however useful for other applications.

METHODS AND RESULTS

Among the EMT approaches we use the methods most suitable for studied rocks. One of our results is an evaluation of the pore/crack geometry of sedimentary rocks. It is helpful for revealing fractured (or damaged) zones. We demonstrate numerous examples of such evaluation using different models of pore/crack geometry incorporating a single value for the pore/crack shape or probability density functions of these values. Another problem is the estimation of thermal conductivity of mineral matrix - which is necessary for many thermal property simulators.

Among important problems that can be solved by the combination of EMT and experimental thermal petrophysics is so-called "fluid substitution" – theoretical evaluation of the thermal conductivity of rock saturated with a specific fluid or a fluid mixture provided the rock is saturated with another fluid. We show successful examples for solving this problem.

The EMT is helpful in cross-property estimation when one type of physical properties (elastic wave velocities, electric or thermal conductivity) can be predicted from another property. Specifically, we show that the EMT is a necessary tool for simultaneous evaluating the effective thermal and elastic properties of rocks from cuttings. This is of vital importance when rock samples are not available.

CONCLUSIONS

Our results show that effective medium theory greatly enhances possibilities of experimental thermal petrophysics.

KEYWORDS :   effective medium theory, thermal petrophysics

Sr No: 770

The Thermal Regime of a Vapor-Dominated Hydrothermal Field Beneath Yellowstone Lake, Yellowstone National Park, USA

CORRESPONDING & PRESENTING AUTHOR:

Robert Harris, Oregon State University, USA

Julia Favorito, The Rivers School, USA

Robert Sohn, Woods Hole Oceanographic Institution, USA

Shaul Hurwitz, U.S. Geological Survey, USA

Karen Luttrell, Louisiana State University, USA

The Hydrothermal Dynamics of Yellowstone Lake project is aimed at understanding how lake floor hydrothermal systems respond to geological and environmental perturbations at multiple timescales. We characterize a vapor-dominated geothermal field located at depths of ~100-120 m in Yellowstone Lake, Wyoming, USA, with 149 heat flux measurements made over a ~2 year interval. Measurements of both in-situ temperature and thermal conductivity as a function of depth, made with a 1-m probe via a remotely operated vehicle, are combined to compute the vertical conductive heat flux. Inside the ~55.5 x 103 m^2 bathymetric depression demarcating the vapor-dominated field the median conductive flux is 13 W m^{-2}, with a conductive output of 0.72 MW. Outside the thermal field the median conductive flux is 3.5 W m^2. We observed 49 active vents inside the thermal field, with a median exit-fluid temperature of 132 °C, and a total heat output of 29 MW. The total mass output is 56 kg s^{-1}. We find evidence for relatively weak secondary convection with a total ouput of 0.11 MW in unaltered lake floor sediments overlying an impermeable cap that traps vapor in a reservoir located ~15 m below the lake floor at a temperature of ~189 °C. The thermal output of the Deep Hole is among the highest of any vapor-dominated field in Yellowstone, due in part to the high boiling temperatures associated with the elevated ambient pressures on the deep lake floor.

KEYWORDS :   heat flow, geothermal systems

Sr No: 771

Heat Flow Evidence for Hydrothermal Circulation in Oceanic Crust at the Cascadia Deformation Front, Grays Harbor, USA

CORRESPONDING & PRESENTING AUTHOR:

Robert Harris, Oregon State University, USA

Glenn Spinelli, New Mexico Tech, USA

Accurate estimates of subduction zone temperatures are required to understand a variety of critical processes, including controls on seismogenic and aseismic behavior on subduction megathrusts. Hydrothermal circulation within subducting oceanic crust can substantially modify temperatures along the plate interface. We report 30 new conductive heat flow measurements collected just seaward of the deformation front, offshore of Grays Harbor, Washington, USA. The data were collected along Cascadia Open Access Seismic Transect Lines 4 and 5. A prominent basement high associated with a rift propagation pseudofault is imaged near the western end of Line 4. Lithospheric conductive cooling models, for 9 Ma oceanic crust, predict that heat flow should be ~175 mW m^{-2}. Just seaward of the deformation front heat flow values corrected for the
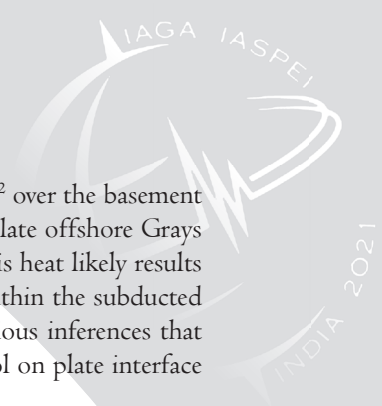
impact of sedimentation are ~200 mW m^{-2} and rapidly rise to a value of ~750mW m^{-2} over the basement high. We find that (1) hydrothermal circulation redistributes heat in the Juan de Fuca plate offshore Grays Harbor, (2) heat in addition to the basal heat flux is required to fit the data, and (3) this heat likely results from a combination of fluid flow associated from ongoing hydrothermal circulation within the subducted oceanic crust and possibly with the pseudofault. Our data and modeling support previous inferences that hydrothermal circulation within the subducting oceanic crust plays an important control on plate interface temperatures.

KEYWORDS : heat flow, subduction thrust, hydrothermal circulation

Sr No: 772

Temperature dependence of thermal conductivity for different varieties of granitoids: Implication in 1-D crustal thermal modelling

CORRESPONDING & PRESENTING AUTHOR:

Labani Ray, CSIR-National Geophysical Research Institute, India

Nishu Chopra, CSIR-National Geophysical Research Institute, India

Sikha Hiloidari, CSIR-National Geophysical Research Institute, India

Nirujogi Narsimha Naidu, CSIR-National Geophysical Research Institute, India

Varun Kumar, Indian Institute of Technology (Indian School of Mines) , India

Thermal conductivity and its variation in the Earth's interior are essential parameters to control sub-surface temperature distribution. The variation is primarily controlled by temperature and lesser extent by pressure. The temperature dependence is much higher for the upper crust compared to the lower crust. These imply the utmost necessity of detailed study for upper crustal rocks. Granitoids are one of the major constituents of the upper crust in Archaean cratons. However, granitoids have a wide range in composition and yet, data on their thermal conductivity at elevated temperatures is very much limited and a single value is commonly used to characterize the decrease in thermal conductivity with temperature for the upper crust.

We have measured thermal conductivity from 25 °C up to 300 °C by the steady-state method on thirty-four granitoid samples. These cover four compositionally different categories, e.g., alkali granite, biotite granite, granodiorite, and metasomatised granodiorite. The decrease of thermal conductivity is highest for the metasomatised granodiorite and alkali granite, intermediate for the biotite granite, and lowest for the granodiorite. The study emerged two temperature coefficient (b) values in the expression $K(T) = K(RT) x(1+bT)^{-1}$ for compositionally different granitoid. One for the alkali feldspar granite to monzogranite (1.5 x 10^{-3} K^{-1}), and another for granodiorite to tonalite to quartz diorite (0.7 x 10^{-3} K^{-1}). Considering the above two b-values for the upper crust, the 1-D steady-state thermal modeling with different heat production/thermal conductivity models shows the difference in temperature estimates at the Moho could be as much as 90 °C.

KEYWORDS : thermal conductivity, temperature coefficient, Granitoid

Sr No: 773

Tracking between ground and air temperatures: results from a 5-year long dataset collected at a Geothermal Climate Change Observatory in southern India

CORRESPONDING & PRESENTING AUTHOR:

Vyasulu Venkata Akkiraju, Ministry of Earth Sciences

Sukanta Roy, Ministry of Earth Sciences, India

Study of the relationship between surface air temperatures and ground temperatures can provide important information to better understand the geothermal signature of climate change. To carry out such studies, a geothermal climate change observatory was operated since mid-2009 in the Choutuppal campus of CSIR-National Geophysical Research Institute (17.29 oN, 78.92 oE) in southern India. The observatory is located in the regionally extensive Peninsular Gneiss rock formation. Surface temperatures along with relative humidity, precipitation, solar radiation, wind speed and direction were acquired together with ground temperature data recorded continuously at six different depths in a 1.2 m deep hole. Additionally, temperature measurements were made at different times of the year in two boreholes drilled through massive granite to 21 m and 210 m depths respectively. Analysis of ground-air temperature data for the period 2009-2014 reveals the following. (i) Air temperature changes diffuse into the granitic subsurface with associated attenuation of high frequency components and phase lag characteristic of conductive heat transfer. (ii) Ground temperatures measured in the 1.2 m and 21 m deep holes track the diurnal and seasonal changes in SAT respectively, (iii) The ground is warmer than air on average; the difference is not constant but varies between -2.1 to +7.6 oC with a mean of 3.4 ± 1.8 (SD) oC, (iv) Ground-air temperature difference is influenced by the monsoon season and incoming solar radiation. On average, the ground warms by 2.5 oC for 100 Wm-2 increases in incident solar radiation.

Sr No: 774

Anomalous Postrift Subsidence in the Bohai Bay Basin, Eastern China: Constraint from tectono-thermal modeling

CORRESPONDING & PRESENTING AUTHOR:

Qiongying Liu, Institute of Geology, China Earthquake Administration, China

Lijuan He, Institute of Geology and Geophysics, Chinese Academy of Sciences, China

Zejun Yi, Northeast Petroleum University, China

Linyou Zhang, China Geological Survey, China

The Bohai Bay Basin is the largest Cenozoic rift basin in eastern China, which exhibits a high rate of post-rift subsidence deviating from the theoretical exponentially decay trend of thermal subsidence. The driving force for this phenomenon remains an outstanding question. We quantify the spatial and temporal distribution of the anomalous post-rift subsidence by removing the thermal subsidence related to earlier stretching events from the observed tectonic subsidence. A multi-episodic finite extension model is employed to estimate the stretching factors during rifting for nine profiles and 48 wells covering the basin. Our results show that the anomalous subsidence commenced at 12 Ma and the average anomalous subsidence rate
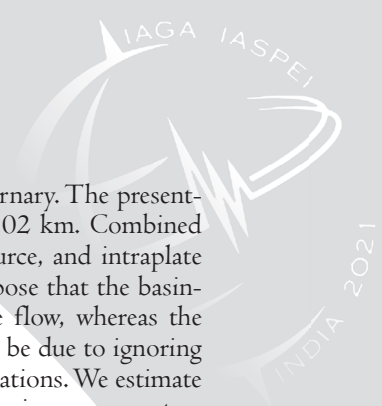
accelerated from ~19 m/Ma during the late Miocene to ~75 m/Ma during the Quaternary. The present-day anomalous subsidence exhibits an amplitude of ~400 m and a wavelength of ~102 km. Combined with previous studies, we preclude renewed rifting, fault reactivation, deep thermal source, and intraplate stresses as major mechanisms accounting for additional accommodation space. We suppose that the basin-wide anomalous subsidence may probably originate from the sub-lithospheric mantle flow, whereas the predicted dynamic topography is hundreds of meters larger than our results. This might be due to ignoring the upper mantle structure above 225-300 km depth in most dynamic topography simulations. We estimate that high-temperature anomalies between 120-200 km depth beneath the Bohai Bay Basin can generate a surface uplift of ~550 m. It implies both shallow and deep mantle processes might play important roles in shaping the surface topography.

KEYWORDS : tectono-thermal modeling; tectonic subsidence; rift basin

Sr No: 775

Thermal Data Collection in and Around Japan: Towards a Better Understanding of Thermal State of the Lithosphere and Ensuring Reliable Database

CORRESPONDING & PRESENTING AUTHOR:

Akiko Tanaka, AIST, Japan

Makoto Yamano, The University of Tokyo, Japan

Hideki Hamamoto, Center for Environmental Science in Saitama, Japan

Shusaku Goto, AIST, Japan

To provide a more reliable estimation of the subsurface temperature structure of the Japanese islands, two approaches, 1) compilations of thermal-related data and 2) measurements of thermal conductivities, are introduced.

The International Heat Flow Commission (IHFC; www.ihfc-iugg.org) of IASPEI has been fostering the compilation of the Global Heat Flow Database (GHFDB) since 1963. A new database structure for the GHFD based on the reassessment and revision of the existing global heat flow data set was just launched in 2021 [Fuchs et al., doi:10.31214/ijthfa.v4i1.62, 2021]. A new version of the database "Thermal Data Collection in and around Japan", which contains continuously updated heat flow and geothermal gradient data and adds thermal conductivity data in and around Japan, has been released in March 2019 [GSJ; https://www.gsj.jp/data/G01M/GSJ_MAP_TDCJ_2019.zip]. This contains 3670 heat flow data from 174 publications, however, many of the newly defined database fields have not been filled. We struggle to migrate and adjust to the new database structure by filling the gaps.

Better evaluation of surface heat flow, thermal conductivity data were compiled from published data and site-specific reports, and measured using the archived cores. 1961 geothermal gradient and 10130 thermal gradient data have been stored in the publication of GSJ (2019).

This study is still in progress, and we will continue to refine the thermal data using additional data and thermal proxies.

KEYWORDS : heat flow, database, thermal conductivity

Sr No: 776

Thermal conductivity at ambient and elevated temperature for the sedimentary and metamorphic rocks from the Western Himalaya, India and its implications

CORRESPONDING & PRESENTING AUTHOR:

Eswara Rao, CSIR National Geophysical Research Institute, India
Labani Ray, CSIR National Geophysical Research Institute, India
Tauheed Khan, CSIR National Geophysical Research Institute, India
Ravi G., CSIR National Geophysical Research Institute, India

The Western Himalaya region of India is primarily composed of sedimentary and metamorphic rocks of Lesser and Higher Himalayan crystalline, with few igneous intrusions. These rocks are affected by many tectonic activities during the collision of the Indian and Asian plates. Rocks are Proterozoic to Tertiary in age.

Thermal conductivity of sedimentary and metamorphic rocks from the Western Himalaya are measured using the steady-state method on 74 samples at ambient temperature and 18 samples at elevated temperature, from 25 to 300 °C. The study covers sandstone, limestone, dolostone, quartzite, phyllite, slate, and schist. Samples have been characterized based on petrography, geochemistry, petrophysical properties. Average thermal conductivity is highest (between 4 and 5 Wm-1K-1) for quartzite; intermediate (between 3 and 4 Wm-1K-1) for sandstone, limestone, dolostone, and slate; lowest (between 2 and 3 Wm-1K-1) for schist and phyllite. Studied rocks show narrow ranges in thermal conductivity for each rock type in the worldwide observed wide range showing their homogeneity in nature. Drop-in thermal conductivity with temperature is more for sandstone or limestone (30-32%) and less for phyllite or schist (14-24%). This indicates that the decrease in thermal conductivity is varied in a wide range. The variations in thermal conductivity at ambient and higher temperatures for each rock variety can be correlated well with the variation in composition from arkose to greywacke. This is the first systematic study of thermal properties for the rocks from the Western Himalaya and will be useful to derive thermal modeling and seismogenic study of this region.

KEYWORDS : thermal conductivity, sedimentary and metamorphic rocks, Western Himalaya

Sr No: 777

Features of geothermal studies of industrial wells in hydrocarbon fields

CORRESPONDING & PRESENTING AUTHOR:

Guzel Vakhitova, Bashkir State University, Russia

Rim Valiullin, Bashkir State University, Russia

Airat Ramazanov, Bashkir State University, Russia

Rashid Yarullin, Bashkir State University, Russia

Ramil Sharafutdinov, Bashkir State University, Russia

Many years of experience in temperature studies of industrial wells have shown that the success of solving problems is determined by the preparation of the well and the modes of its operation.

A well-grounded choice of downhole equipment and compliance with the measurement technology are important.

Today, the equilibrium geothermal characteristics of rocks are determined by the results of studies of long-term shut-in wells, of which there are quite a few.

As an alternative, a technology has been developed for temperature studies in wells after drilling or pending repair, followed by restoration of the equilibrium temperature of rocks from a set of measurements.

The studies are carried out with traditional downhole equipment, which is widely used in production and provides the necessary accuracy with an error of no more than 0.5 mK / m.

An alternative option is operating wells with long sump, piezometric wells and wells in the development mode.

This technology has been tested in practice, includes specific software, requirements for downhole equipment, measurement methodology, for well preparation and assessment of the quality of field data to exclude substandard measurements.

Modern distributed fiber-optic measuring systems (DTS) open up the prospect for continuous monitoring the thermal mode of the rocks. Taking into account certain advantages and existing limitations, the DTS technology will be used as an auxiliary one for areal measurements.

Practical examples of geothermal studies carried out at the fields of Russia by Skoltech, BashSU and industrial companies of the Russia are given.

KEYWORDS : geothermy, industrial wells, distributed fiber-optic measuring systems

Diamond Jubilee Symposium (by invitation)

DJ Advancing Geophysical Science – 60 Years of CSIR-NGRI, India

CONVENERS: V. M. Tiwari

CSIR-NGRI was established in 1961 with the mission to carry out basic research in geosciences and to develop the knowledge base for making informed decisions about use of geo-resources sustainably and improve preparedness and resilience to natural hazards. CSIR-NGRI has evolved in scientific vigor over the decades and has carved its niche on the global map of geo-science research organizations with its vibrant and outstanding contributions. The researchers of CSIR-NGRI have published more than 100 books, encyclopedia and ~ 5000 papers in the SCI journals, which have remarkably advanced both within the core disciplines of geophysics and across the many Earth science fields. CSIR-NGRI has also taken up a good number of research programs of global interest in collaboration involving many countries through bilateral programs as well as supports from IUGS, IUGG, IGCP, IAHS, etc. This session is planned to celebrate 60 glorious years of institute's journey and to discuss potential scientific issues that can be pursued through international collaboration in the view of global scientific challenges.

Sr No: 778

Structure of the Indian Lithosphere Research: Initiatives at the CSIR-National Geophysical Research Institute (by invitation)

CORRESPONDING & PRESENTING AUTHOR:

Vinod K Gaur, CSIR-National Geophysical Research Institute (NGRI), Hyderabad, India

Scientists at the National Geophysical Research Institute, initiated investigations of the structure of the Indian lithosphere in the late 1970s. The first quantification of the heat generation source in its various continental domains, enabled an estimate of heat flow across the Indian Moho, indicating a region of "hotter" upper mantle in the Indian shield. The state of stress in the Indian lithosphere based on olivine flow models was estimated. To address questions provoked by these early studies, about the origin of the various geological provinces and the structure of their undercarriage, a broadband seismograph was installed in the Institute's seismological observatory. Concurrently, a seismic time delay tomography experiment was designed to investigate the crust and upper mantle structure beneath the Deccan Volcanic Province, using portable, analogue seismographs that revealed a higher rigidity upper mantle underneath. Later, analysis of the Institute's broadband data yielded the first image of the elastic structure beneath the Archaean shield and was followed by experiments to investigate the crust and upper mantle structure of the wider Indian lithosphere using teleseismic receiver functions, body and surface wave tomography, and shear wave birefringence. Parallelly, gravity and magneto-telluric (MT) investigations were also designed to map the density and electrical conductivity structure of segments of the Indian lithosphere and deep mantle. Some notable features of the continental Indian lithosphere whose northern limbs were shown to have penetrated deep into Tibet from karakoram to Lhasa, include:

1. A distinct two layer lithospheric mantle beneath most of the Archean cratons and the Proterozoic Vindyhan basin. The shear velocity increase from 4.3 km/s below the Moho to a significantly higher than the normal velocity (> 4.7 km/s) at a depth of about 100 km - a feature of cold lithosphere – defies conformation to a realistic geotherm, suggesting instead, phase changes and abundance of garnet at depth.

2. The imprint of Deccan volcanism, observed as the thinning of the westernmost continental lithosphere (100-120 km), suggests limited regional extent of interaction between the Reunion plume and the Indian lithosphere.

3. Segmentation of the Indian lithosphere beneath the Ganga basin astride the Delhi-Haridwar (750 E) and the Monghyr-Saharsa (840 E) ridges creating a laterally varying and likely decoupled decollement beneath the Himalaya that would explain the varying space – time rupture sequences of great Himalayan earthquakes.

The lecture will briefly discuss the early foundations of lithospheric research at the NGRI, followed by a discussion of the notable findings about its structure.

KEYWORDS :   lithosphere, mantle, heat flow

Sr No: 779

Role of Fractals in Seismological Studies: initiatives at CSIR-NGRI (by invitation)

CORRESPONDING & PRESENTING AUTHOR:

V. P. Dimri, CSIR-National Geophysical Research Institute, Hyderabad, India

Various studies carried out across the globe reveal that many of the earth's processes satisfy fractal statistics, where space-time fluctuation patterns of dynamic systems exhibit a self similar structure. Examples range from the frequency-size statistics of earthquakes to the time series of Earth's magnetic field. It is well known that larger earthquakes are rare events and very small earthquakes are quite frequent. The Gutenburg-Richter law of earthquakes is the best example of a power law, which is termed fractal distribution. Another example in seismology is Omari's law, which describes the decay of aftershock activities with time. The fractal behaviour is well described by a fractal dimension which can be a fractional number, need not an integer. The change of fractal dimension could be a good precursor for earthquake as it is a measure of the degree of clustering of seismic events. The decrease in fractal dimension before the big earthquake is observed in several studies.

CSIR-NGRI started working on fractals during the early nineties of the last century, as can be seen in the concluding paragraph of the second chapter of a book entitled "Deconvolution and Inverse Theory (1992)", Elsevier. At first, NGRI-CSIR applied it to exploration geophysics, particularly in the potential field, developing a new approach "Scaling Spectral Method" and published these works during the 1990-s in leading international journals. Then, a national workshop entitled "Application of Fractals in Geoscience" was organized and an edited volume was released.. Earthquakes originating from different seismic zones were studied, including (1) Himalayan area particularly Uttarkashi (1991), Chamoli (1999), Nepal (2015), and North East region (2) Bhuj, Gujarat (3) Koyna, Maharashtra (4) Latur from the stable continent of India (5) Makran and Sumatra earthquakes for tsunami studies. These studies offered the foundation of forecasting earthquakes in a particular seismic zone within India. Subsequently, the fractal theory was applied to other fields of geophysics.

KEYWORDS :   fractal, power law, Omari law

Sr No: 780

Geomagnetism: 60 years at CSIR-NGRI (by invitation)

CORRESPONDING & PRESENTING AUTHOR:

Nandini Nagarajan, CSIR-National Geophysical Research Institute, Hyderabad, India

Geomagnetic observations in India have a history dating back over 200 years. Several institutions have contributed over this period, of which NGRI has a continuing, diversified and innovative approach. Salient features of NGRI 's studies have been (1) A long and complete investigation of equatorial magnetic pulsations, in the years before models of their generation and propagation were fully understood, and continuing to examine them in the light of contemporary understanding (2) Setting up and maintaining continuous monitoring of low latitude and equatorial magnetic variations, establishing characteristics of low latitude variations in quiet and disturbed periods (3) Studies of the movement of the dip equator over
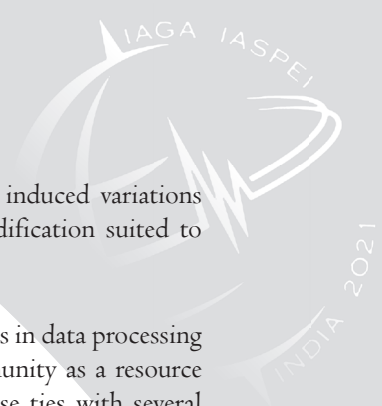
the Indian peninsula, extracting signatures of crustal electromagnetic anomalies from induced variations measured in magnetometer arrays. Developments in instrumentation, testing and modification suited to equatorial and low latitude requirements were made to obtain reliable absolute data.

NGRI has two INTERMAGNET observatories, and several remote stations. Innovations in data processing and analysis continue and the Geomagnetic team serves the INTERMAGNET community as a resource for checking and validation with required standards. In this process, the team has close ties with several groups internationally. The thrust of work in the past 10 years has been in tune with institutional objectives: magnetic variations in the sparsely studied Andaman & Nicobar islands, detailing characteristics of variability when compared to global models of the Equatorial Electrojet, constraining off-shore tectonic models using electromagnetic induction and new models of precursory and co-seismic electromagnetic signals, adapted to low latitudes, in the Kumaun Himalaya.

KEYWORDS : magnetic observatory, dip equator, quiet and disturbed periods

Sr No: 781

SYMPOSIUM :   **DJ-Diamond Jubilee Symposium**

Paleomagnetism and Electromagnetism at CSIR-NGRI (by invitation)

CORRESPONDING & PRESENTING AUTHOR:

S.K. Verma, CSIR-National Geophysical Research Institute, Hyderabad, India

Paleomagnetic studies formed an important component of CSIR-NGRI's research program right from it's inception about six decades ago. From modest beginnings the Paleomagnetic Laboratory today is well equipped with high sensitivity state of the art instruments. Major contributions include: 1) Paleomagnetic history of the drift of the Indian plate from the southern hemisphere to its present position establishing how Himalayan arc underwent different degrees of rotation with respect to the Indian Peninsula during the collision, 2) Mean pole position of several vertical sequences of Deccan Traps indicates that a drift of the Indian plate of the order of 24° took place during the entire period represented by the Deccan trap activity with only a single geomagnetic polarity transition in paleomagnetic data, and the lowest dipole moment in whole of the Cretaceous during the end Cretaceous Deccan eruption, 3) Polar wandering curve for the Indian subcontinent from Permo-Carboniferous to Lower Cretaceous studying the Rajmahal and Sylhet Traps, 4) The refined APW path for the Dharwar craton between 2367 Ma and 1886 Ma, based on paleomagnetic poles from six precisely dated dyke swarms, indicates that the craton drifted quickly with a clockwise rotation of ∼30° between 2216 Ma and 2207 Ma, suggesting that a major tectonic activity such as breakup of a supercontinent at 2.2 Ga may have been responsible for rapid drift of Dharwar craton. With modern facilities, the laboratory is now well poised to address problems in the emerging areas of Environmental magnetism, Paleointensity, Archeointensity, and Paleoclimate studies.

Electromagnetic studies have remained a vibrant area of research since the formation of CSIR-NGRI. Due to widespread applicability at different scales, Electromagnetic Exploration has remained the central theme of various research programs laying emphasis on: theoretical developments, instrumentation, laboratory modeling, field applications and large-scale regional surveys. Some of the outstanding theoretical contributions include: 1) Enhancement of EM response of a target in the presence of conducting surroundings, 2) Fundamental contribution to quantify 'Depth of Investigation (DOI)' using the behavior of Sensitivity Functions providing the theoretical basis to calculate the DOI frequently used in modern airborne EM surveys, 3) Phenomenon of response separation in Time Domain EM methods that is central to various algorithms used for the subsurface conductivity imaging, 4) Application of digital linear filters for

faster computation of EM response of arbitrarily shaped 3D conductors, 5) Joint inversion of EM (MT) and seismic data to improve resolution of low velocity layers. Concurrently CSIR-NGRI developed some world class EM instruments, namely: 1) Total field (Bz) measuring airborne Time Domain EM (ATEM) system globally acknowledged as the most advanced contemporary ATEM system, 2) Ground TEM system providing Bz measurements at selectable time range – again the most sophisticated among similar instruments in the world. The above R&D programs were complemented by the laboratory and field experiments. EM laboratory simulation studies also led to the development of a practically significant 'Null Method' based on positioning the receiver at a point with null contribution from the primary field. On the strength of this rich experience and the availability of modern EM equipment, CSIR-NGRI has carried out exploration for sulphide minerals, diamonds (kimberlites), water and other precious resources. Our Magneto-telluric (MT) team has been outstanding in designing specialized surveys for hydrocarbons, power grid transmission and in the study of sedimentary basins, cratonic structures and investigating Himalayan subduction. The CSIR-NGRI is also involved with large-scale regional HTEM surveys for atomic minerals and for aquifer mapping in water deficit regions. To cater to programs of national importance, the institute has also initiated specialized HTEM investigations for railway tunnels and roads in mountainous areas, urban planning and water supply, etc.

KEYWORDS : paleomagnetic history, MT investigations, HTEM surveys

Sr No: 782

CSIR-NGRI Investigations of the Seismic Structure of the Indian Continental Crust: A review (by invitation)

CORRESPONDING & PRESENTING AUTHOR:

M.K. Sen, Former Director, CSIR-National Geophysical Research Institute, Hyderabad, India and Institute of Geophysics, University of Texas at Austin, USA

In 1972, CSIR-NGRI started Deep Seismic Sounding studies with the primary objectives to understand the evolution of the Indian plate and the accumulation & disposition of natural resources within it. The studies are concentrated in the Dharwar craton, southern granulitic terrain, Deccan Volcanic Province, central Indian region, major basins and the Kashmir Himalayan region. Here, we present a synthesis of the crustal structure and its implications.

In general, the Indian crust has three layers with thicknesses varying from 28 to 50 km. The first crustal study along Kavali–Udipi profile shows remarkable observations in the variation of crustal thickness from 34 to 41 km corresponding to the Archaean and Proterozoic blocks of Dharwar cratons. Similarly, the seismic sections in the Aravalli, central Indian suture zone, Dharwar craton and Southern Granulite Terrain further depict magmatic underplating with paleo collision and subduction environments. The deepest Moho at ~50 km has been found in the Aravalli region.

For hydrocarbon prospecting, the basins have also been explored extensively apart from their crustal structures. These studies reveal the presence of intra-trapean mesozoics in the Cambay basin. The intriguing findings from the Bengal basin are the presence of a Hinz zone and the evidence for the trace of a mantle plume in the continental region. The first arrival travel time skip unravels a ~1.75 km thick low-velocity Gondwana layer in the Mahanadi basin and ~2.8km sediments in the intra-continental Godavari rift basin.

KEYWORDS : seismic section, crustal structure, hydrocarbon prospecting

Sr No: 783

Precambrian crust formation and evolution: insights from southern India based on 60 years of research in Geology, Geochemistry and Geochronology at CSIR-NGRI (by invitation)

CORRESPONDING & PRESENTING AUTHOR:

Y.J. Bhaskar Rao, CSIR-National Geophysical Research Institute, Hyderabad, India

Many fundamental questions concerning evolution of Earth's continental crust, such as what geodynamic processes characterise the Hadean (4.56-4.0 Ga) Earth? and since when was plate tectonics operative? remain unresolved. Global datasets on in situ zircon U-Pb ages together with Hf±O isotopic compositions for magmatic and detrital zircons from Precambrian terranes have been extremely useful in deciphering prominent mantle depletion events signifying extraction of large volumes of juvenile continental crust and its recycling - information that is critical for understanding lithospheric geodynamics in space and time. Summarised here is an overview of research at CSIR-NGRI on geological, geochemical and geochronological (mainly zircon U-Pb age–Hf isotope compositions) aspects of the Archean Dharwar craton (DC) and the Archean-Proterozoic Southern Granulite Terrain (SGT), south India, which together encompass a geologic record spanning over three billion years between ~3.6 and 0.5 Ga. The DC comprises an oblique section of ~12 km from middle to lower crust across low- to medium-grade granite-greenstone terranes divisible into the Western Dharwar Craton (WDC) and Eastern Dharwar Craton (EDC). A segment of the WDC preserving Paleo- to Mesoarchean gneisses and greenstones is characterized by 'dome and keel' structural patterns related to vertical (sagduction) tectonics. Peripheral to this 'core' are domains of Neoarchean crust that bear evidence for convergent (plate) tectonics. The zircon U-Pb age–Hf isotope data indicate (1) two major episodes of juvenile crust accretion involving depleted mantle sources at 3.45–3.17 Ga and 2.7–2.5 Ga with crustal recycling dominating the Mesoarchean record and (2) clear evidence for the operation of modern-style plate tectonics since ~2.7 Ga. The SGT is a collage of Archean and Proterozoic terranes comprising vestiges of exhumed deep crust that are enveloped by crustal-scale ductile shear zone systems. Zircon U-Pb age and Hf isotopic data for charnockite orthogneisses from these terranes indicate major events of juvenile crust addition centred around 3.45–3.17, 2.65–2.45, 2.05–1.84 and 1.0–0.9 Ga and events of crust reworking and regional granulite facies metamorphism around 2.50–2.42 and 0.57–0.52 Ga. The accretion of the Archean and Proterozoic terranes across the Palghat-Cauvery Suture zone occurred during the Ediacaran-Cambrian, possibly related to subduction processes, ocean closure, and collision within a Himalayan scale orogenic belt, described as the East African Orogen within the Gondwana Supercontinent.

KEYWORDS :   geochronology, Archaean, Proterozoic

Sr No: 784

Isostatic and Density Models of the Indian Lithosphere (by invitation)

CORRESPONDING & PRESENTING AUTHOR:

V.M. Tiwari, CSIR-National Geophysical Research Institute, Hyderabad, India

Terrestrial gravity fields are commonly utilized to determine the Earth's internal structure, and properties

to probe the dynamic processes and natural resources. The measurements of Earth's gravity field in India started in the nineteenth century which indeed facilitated the formulation of the concept of Isostasy. Gravity studies, theoretical as well as observational, have been vibrant components of the CSIR-NGRI's research endeavor, since its inception. The scientists at CSIR-NGRI have significantly contributed to the understanding of isostatic models and generation of density images under the continental and oceanic regions of the subcontinent. These studies include i) publication of a series of Gravity Maps of India with a reasonable coverage of gravity observations, tied to the international gravity reference station in 1976; ii) identification of gravity anomaly trends corroborating with the principal geotectonic trends and gravity anomalies having no correlation with surface geology iii) lateral changes in both the density and thickness of the crust and mantle lithosphere under various tectonic units of India; iv) estimation of effective strength of lithosphere and its spatial variation; v) assessment of stresses due to density anomalies in the lithosphere; vi) emplacement processes of aseismic ridges; vi) characterization of passive continental margins and several others. Some of the significant findings will be discussed.

KEYWORDS : gravity, density model, isostasy

Sr No: 785

Study of Natural and Triggered Seismicity in the Indian Peninsula (by invitation)

CORRESPONDING & PRESENTING AUTHOR:

Harsh K. Gupta, National Geophysical Research Institute, India

The establishment of a seismological observatory in 1967 at NGRI campus marked a new chapter in the advancement of observation seismology in the country. Although, missed by a whisker the observatory had a perfect inauguration when an M6.3 earthquake occurred in Koyna on December 10, 1967, a day before its operation began the next day. The aftershocks recorded by the instruments similar to the WWSSN network laid the foundation of Reservoir Triggered Studies in the India. Later, every single earthquake that occurred in the Indian Stable Shield Region (SCR) was recorded and investigated with the high quality data accrued from the observatory, which also provided guidance in field investigations. Some of these include Godavari Valley, 1969, M 5.8; Broach, 1970, M 5.8; Latur, 1993, M 6.2; Jabalpur, 1997, M 5.8; and Bhuj, 2001, M 7.8. By 1970's over 20 cases of reservoir triggered seismicity (RTS) were known. A detailed study of the RTS earthquake sequences and their comparison with normal earthquake sequences led to identification of certain common characteristics of RTS sequences which discriminate them from the normal earthquake sequences. These criteria are globally applicable. Continued studies of RTS at Koyna led to demonstrating that Koyna is an ideal site for the elusive near field studies of earthquakes. As a precursor to setting up of a borehole laboratory at a depth of ~ 7 km at Koyna for the near field study of earthquakes, a 3 km deep pilot borehole was completed in June 2017. Several international conferences were held at NGRI (Regional IASPEI Assembly, 1984; Chapman Conference on SCR Earthquakes, 1998; 2nd Asian Seismological Commission Meeting 1998; and the present IAGA-IASPEI Joint Assembly, 2021). NGRI actively participated in international projects such as the Geodynamics, International Lithosphere Program, Global Stress Map, Global Seismic Hazard Assessment Program, etc. These studies were conducted with the participation of several scientists from NGRI and in collaboration with national and international organizations. In this talk an effort is made to provide a snapshot of all these works.

KEYWORDS : reservoir triggered seismicity, Koyna, borehole

AUTHOR INDEX

Author	Pg No.
Shuji Abe	192
Rafael Abreu	504
Iman Farag Abu El Nadr	558
Dursun Acar	418
John Adams	102, 477, 480
Ademola Adelina Adetunji	70
Juan Carlos Afonso	68, 534
Oleksiy Agapitov	134
Sanchit Agarwal	189
Matthew Agius	509
Mohit Agrawal	438
Nicola Piana Agostinetti	534, 535
Lidiya Ahmed	202
Elina Aidona	254
K K Ajith	154
Tekkan Akashi	131
Vyasulu Venkata Akkiraju	576
Paola Albini	453, 454
Maria Alexandra Pais	178, 202, 391
Markku Alho	356
Khaled Ali	68
M Mahdi Alizadeh	155
Patrick Alken	109, 111, 112, 116
Robert Allen	289
Megan Allington	208
Hayley Allison	167
Bedri Alpar	418
Alparray	507
Livia Ribeiro Alves	165
Takanobu Amano	296, 334
Rafael Amaral	381
Boudewijn Ambrosius	499
Amandine Amemoutou	432
Hagay Amit	18
Petr Ammosov	128
Tetsu Anan	362
Pratyush Anand	30
Brian Anderson	189, 289
Vania Andrioli	144
Giulia D Angelo	49
Vassilis Angelopoulos	308, 312, 321, 339
Dorjsuren Ankhtsetseg	415
Aleksander Antipin	569
Alexandra Antonopoulou	330

Author	Pg No.
Galina N Antonovskaya	420
Elizaveta E Antonova	159
Tadashi Aoyama	129
Maria Theresia Apoloner	90
Andrei Apostol	499
Monica Aquino	63
Ramachandrudu Arasada	26
Aline Araujo	529
Fabiano Araujo	142
Serena D Arcangelo	52, 491, 496
Mateus Oliveira Arcanjo	147
Martin Archer	199
Ardianto Ardianto	28
Charles Arge	364
Kazuko Ariizumi	458
Irina Aristova	468
Shin Arita	379
Ganbaatar Ariunaa	414
Robin Armit	29
Patrick Arneitz	188, 228, 251, 381
Daniel Arnold	278
B R Arora	544
Kusumita Arora	50, 145, 377, 378, 434
Christina Arras	134, 135, 139, 143, 155
Anton Artemyev	312
Kazushi Asamura	164, 291, 317, 319, 323
Seiki Asari	378, 379
Nikita Aseev	167, 376
Mohsen Ghafory-Ashtiany	104
Timo Asikainen	303
Vladimir E Asming	420
Leticia Assuncao	467, 550
Richard Aster	471
Kuvvet Atakan	462
Mike Atkinson	263
Januka Attanayake	519
Eric Attias	398
Julien Aubert	120, 232
Paul Augustinus	208
Anna Avdeeva	79
Abdul Azeek	403
Naresh B	543
Padma Rao B	22, 37
Kishore B D N	403

Author	Pg No.
Lasse B N Clausen	109
Lakshmi B V	208
Narendra Babu	401, 495
Firoz Badesab	215
Mala Bagiya	48, 49, 142
Shah Mohammad Bahauddin	345
Fan Bai	247
Dmitry Baishev	304
Evelyn Baker	244
Georgios Balasis	108, 330, 333
Attila Balazs	538
Ravi Kumar Bandi	37
Gowthami Bandlamudi	527
William B Banerdt	452, 449
Sridhar Banola	50
Abhey Ram Bansal	556
Amit Kumar Bansal	513, 515,
Shanshan Bao	300
Brian Baptie	422, 450
Rajesh Kumar Barad	50, 143, 149
Teresa Barata	374
Paulo Barbosa Neto	187
Tatiana Barlyaeva	374
Justin Barno	542
Anne Barnoud	11
Sergio Barrientos	462, 472
Diego Barros	144
Lucas Barros	467, 550
Arnab Basak	341
Sarbani Basu	344
Inez Staciarini Batista	134, 142, 144
Paulo Batista	142
Josep Batlló	83, 86, 87, 89
Erdenechimeg Batmagnai	67, 407
Markus Battarbee	356
Roberto Battiston	49
Kumar Batuk	35
Gerd Baumgarten	275
Irina Bayuk	569, 573
Galina Bazilevskaya	157
Christopher Bean	473
Michael Becken	41, 67, 407
Ciaran Beggan	105, 121, 181, 182, 199, 204, 206, 236, 238, 263, 264, 327, 328, 382

Author	Pg No.
Laxmidhar Behera	61
David Belton	519
Bendeguz Bendicsek	173
Allison Bent	91, 542
Jens Berdermann	205, 271
Anna Berezina	416
Edgar Bering	98, 99
Thomas Berndt	246, 247
Francois Bertrand	109
Peter Betts	24, 29
Bruno Bezerra	529
Amarjeet Bhagat	225
Ankush Bhaskar	196, 302
Y J Bhaskar Rao	585
Veenadhari Bhaskara	317
Monika Bhatia	438
Debesh Bhattacharjee	375
Nilam Bhosale	184
Andrew J. Biggin	122, 230
Andy Biggin	118, 228
Satria Bijaksana	207, 212
Dario Bilardello	209
Zhou Bin	110
Alison Bird	102
Nikolett Biro	173
Shubhasmita Biswal	535, 563
Tapas Kumar Biswal	29
Sean Blake	196
Emma Bland	264
Pasquale Blasi	339
Eric Blinman	253
Jeremy Bloxham	15
Scott Boardsen	337, 338, 358, 373
Elizaveta Bobrovnikova	227
Thomas Bodin	505
Elisabetta Boella	366
Marco Bohnhoff	432
Goetz Bokelmann	507, 509
Robert Boldi	264
Istvan Bondar	416, 538
Olivier Bonnot	179
Richard Bono	122
Joszef Bor	263
Naba Kanta Borah	542, 551

Author	Pg No.
Ujjal K Borah	67
Olga Borchevkina	136
Felix Borleanu	429, 519
Monali Borthakur	157
Jacob Bortnik	156, 162
David Boteler	202
Konstantinos Boukouras	465
Polyzois Bountzis	494
Sebastien Bourdarie	161, 170
Zoe Adamantia Boutsi	108
Adamantia Zoe Boutsi	178, 333
Stephen Bowden	245
Alex Boyd	168, 326
Veeraiah Boylla	37
Tamas Bozoki	263, 264
Daniel Brabander	458
Gabriel Brando Soares	116, 385
Daniele Brandt	230
Ronan Le Bras	467
Aaron Breneman	293
Bill Bristow	262, 311
Peter Bromirski	471
Maxwell Brown	255
Vera Yesutor Tsali Brown	147
William Brown	117, 238
Sean Bruinsma	193
Antoine Brunet	170
Oleg Budanov	264
Jayashree Bulusu	50, 287, 298
James L Burch	339
Dalia Buresova	179
Ricardo Arlen Buriti	130
Daniel Burk	85
Kaitlynn Burkhard	85
Alan Burns	136, 151, 157, 274, 300
Maarja Bussov	356
Pavel Butyrin	85
Natalia Buzulukova	309
B Naresh	549
Sribin C	37
Sunil Kumar T C	542
Xuguang Cai	157, 300
Iver Cairns	337
Marie Calvet	449, 452

Author	Pg No.
Jaziel Campelo	187
Enrico Camporeale	173, 329
Xyoli Perez Campos	60, 100
Saioa A Campuzano	52, 233, 237,491, 496
Victoria Canillas	184, 204
Xochitl Blanco Cano	351
Luisa Capannolo	163
Paolo Capuano	425
Vincenzo Carbone	49
Alberto Molina Cardin	237
Joao Cardoso	178
Alba Fisher Carles	194
Carolina Carmo	141, 187
Alexander Carrasco	144
Sebastian Carrasco	449
Jerry Carter	420
Antonio De Jesus Mendoza Carvajal	100
Aline Guimaraes Carvalho	205
Juraci Carvalho	550
Edgardo Casanova	472
Gino Casassa	472
Florencia Castillo	185
Manuel Catalan	33
Gianna Cauzzi	355
Anny Cazenave	11
David Cebron	17
Rebeca Centeno	347
Jose Cepeda	103
Swarnapriya Ch	35
Ronan Chagas	144, 187
Supriya Chakrabarti	152
Aude Chambodut	197
Brian Chandler	15
Liao Chang	240, 246, 247
Loren Chang	101, 126
Subhamoy Chatterjee	373
Charikleia	415
Jorge Chau	276
Nilesh Chauhan	137
Louis Chauvet	179
Carlos Chaves	40
Shi Che	556
Evgeny Chekhonin	569, 571, 572, 573
Chaojian Chen	396

Author	Pg No.
Han Chen	427
Lijen Chen	309
Long Chen	125
Sony Chen	141, 144, 187
Ting Chen	245
Bingjun Cheng	106
Chio Cheng	337
Lei Cheng	309
Marina Chernigovskaya	128
Peter Chi	189, 190
Lung Chih Tsai	155
Odonbaatar Chimed	42
Vladislav Chinkin	274, 325, 326
Paolo Chiozzi	570, 571
Andreea Chircea	94, 429
Lakshmi Pradeep Chitta	346
Jeremy Chittenden	181, 199
Anita Di Chiara	101
Hanjin Choe	20, 33
Yujin Choi	33
Nishu Chopra	575
Vyron Christodoulou	327
Annemarie Christophersen	487
Arnaud Chulliat	109, 112, 114, 226
Jaroslav Chum	179
Gianfranco Cianchini	52, 492, 496
Filippo Cicchetti	397
Oscar Cid	184
Ellen Clarke	176, 181, 206, 382, 384
Pierre Camps	243
Laura Cobden	508, 510
Mihail Codrescu	136, 271
Pierdavide Coisson	95, 109, 179
Adam Collins	182, 200, 206, 384
Matthew J Comeau	41, 67, 407
Jose Angel Lopez Comino	518
Nicolas Compaire	449, 452
James A D Connolly	407
Martin Connors	202, 304
Rodolfo Console	486
Giuseppe Consolini	108
Catherine Constable	12
Tania Contardo	250
Olivier Le Contel	338

Author	Pg No.
Vincenzo Convertito	425
Kristen Cook	419, 475
Raul Daniel Corona Fernandez	84
Alfredo Del Corpo	294, 331
Anthea Coster	189, 262
Stephen Crane	102
S.R. Cranmer	358
Steven Cranmer	348, 350
Diana Navarrete Cruz	233
Andras Csontos	385
Juan Cueto Rodriguez	161
Jun Cui	308, 321
Andrew Curtis	422, 450
Murty CVR	481
Brendan Cych	256
Barbara Czecze	416
Hanmanthu D	403
Srinagesh D	426, 441, 461, 480, 542, 543, 551
Ramesh D S	45, 48, 49, 208
Curtis D Williams	508
Ligia Alves Da Silva	159, 165
Marlos Rockenbach Da Silva	159
Ioannis A Daglis	108, 156, 172, 178
Lkhagva Dagzinmaa	414
Torsten Dahm	411, 518, 548
Nikolaj L Dahmen	452
Nourallah Dahmen	170
Christina Dahner Lindkvist	423
Darharta Dahrin	212
Lei Dai	165, 339
Bijayananda Dalai	531
Lkhagvadorj Dalaijargal	42
Edoardo Dallanave	214
Cathlea S Damayanti	212
Robert Daniel	151
Finn Danielsen	463
Dimitra Daniil	208
Fiona Darbyshire	65, 68, 528, 539
Fabien Darrouzet	161
Gauri Datar	129
Riddhi Dave	68
Christopher Davies	10, 122
Craig De Forest	358
Paromita Deb	567

Author	Pg No.
Eric Debayle	505
Akash Debnath	82
Florian Deconinck	109
Charles Deehr	334
K Deenadayalan	208, 241
Vinicius Deggeroni	134, 159
Veronique Dehant	11
Rahul Dehiya	402
Peter Delamere	339
Brent Delbridge	442
Edward Deluca	346
Sodnomsambuu Demberel	67, 407
Crisan Demetrescu	229, 317, 400
Dmitry Demezhko	569
Emin Demirbag	418
Zhiguo Deng	548
Marine Denolle	442
Richard Denton	289, 310
M I Desai	358
Ravindra Desai	199
Arwen Deuss	12
Anita Devi	398
Jos Augusto Proena Maia Devienne	246
Pawan Dewangan	31, 215
Gopinadh Dhulipudi	434
Aboubacry Diallo	380
Konstantinos Dialynas	353
Gerhard Diendorfer	188
Michael Dietze	419, 475
Dimitar Dimitrov	92
Liliya Dimitrova	90, 92
V P Dimri	582
Raluca Dinescu	94, 429
Savka Dineva	423
Anna Dmitrieva	325, 326
Venera Dobrica	229, 317, 400
Michael Dobrovolsky	325, 326
Anna Dobrynina	85
Shashidhar Dodla	426
Arne Doessing	405
Munkhbaatar Dolgormaa	415
Jaime Dominguez Rivas	100
Marie Dominique	279
Adam Domjan	383, 388

Author	Pg No.
Hao Dong	392
Xiangcheng Dong	111, 340
Ashish Dongre	225
Eric Donovan	308, 312
Jana Doubravova	522
John Douglas	479
Dragomir Dragomirov	92
Martin Van Driel	449
Melanie Drilleau	449
Alexander Drozdov	167
Maxime Dubart	356
Chandra Prakash Dubey	35
Ayush Dulguun	414
Malcolm Dunlop	111, 339, 340
Guillaume Dupontnivet	217
Stephanie Durand	505
Utpal Dutta	476, 479
Ruslan Dyagilev	85
Przemyslaw Dykowski	417
Jerome Dyment	19, 20, 31, 32, 33
Boris Dzeboev	97
Jose E Garcia	185
Richard Eastes	136, 150, 151, 157, 300
Johathan Eastwood	339
David W Eaton	435
John Ebel	457
Yusuke Ebihara	196, 301
Ala Ebrahimi	21
Anusha Edara	50, 409
Ilya Edemskiy	145
Gary Egbert	392, 393
Alv Egeland	334
Joseph Eggington	199
Ramon Egli	188, 207, 381
Eva Elbi	473
Jeffrey Eighmy	253
Bergur Einarsson	473
Tulay Kaya Eken	400
Elie El Jbeily	570, 571
Erfin Elly	28
Tom Elsden	293, 295, 296
Kentaro Emoto	439, 445, 447
Yael Engbers	118, 228
E R Engdahl	413

Author	Pg No.
Mark Engebretson	202, 289
Miles Engel	319
Scott England	151
Dorj Enkhtulga	414, 463
Lev Eppelbaum	41, 61
Pelin Erdemir	370
Kadir Eris	418
Carlos Escobar	185
Philippe Escoubet	340
Nathalie Esquivel	483
Alexander Evans	123
Rob Evans	398
Scott Evans	136
Jairo F Savian	230
Jeremy Faden	373
Paulo Roberto Fagundes	140, 147
Silvia Fajar	212
Mengxuan Fan	491
Yuhong Fan	350
Xiaomin Fang	217, 222
Julia Favorito	574
M Federica Marcucci	338
Andrey V Fedorov	420
Ian Ferguson	70
Enzo Ferrara	209
Ana Ferreira	510
Cosme Figueiredo	141
Fernando Figueiredo Santos	89
Rosa Filgueira	327
Martin Fillion	111
Christopher C Finlay	109, 117, 231
Ilya Firsov	11, 124
Ewelina Florczak	204
Simon Flower	384
Bernhard Fluche	278
Mei Ching Fok	303, 314
Raffaello Foldes	331
Darlan Fontenele	550
Sergio Fontes	40
Colin Forsyth	181
Alexandre Fournier	123
Geoffrey Fox	489
George Franca	529, 550
Daniel R Franco	230

Author	Pg No.
Peter Franek	414
Gesa Franz	57, 79
Andy Frassetto	393
Mervyn Freeman	177, 181
Daniel Frost	15, 506
Huishan Fu	339
Sven Fuchs	564, 567
Ikuko Fujii	379, 394
Akiko Fujimoto	166, 186
Hiroyuki Fujiwara	484
Mizuki Fukizawa	166
Kosuke Fukuhara	394
Martin Fullekrug	258, 260
Takashi Furumura	527
Stephen Fuselier	359
Ravi G	578
Mohamed EL Gabry	413
Vineet Kumar Gahalaut	549
Congcong Gai	245
Virsen Gaikwad	215
Gugi Ganefianto	440, 445
Morgan Ganerod	228
Shib Sankar Ganguli	82
Srinivasa Rao Gangumalla	24
Urs Ganse	356
Peng Gao	219
Susmita Garai	17
Carmen Garcia	185
Raphael F Garcia	452
Raphael Garcia	449
Rolando Garcia	276
Andreina Garcia Reyes	31, 32, 33
Jeffery Garretson	335
Thomas Garth	521
Tom Garth	413
Federico Gasperini	138
Thomas Gastine	123
Vinod K Gaur	581
Galina Gavrilyeva	128
Praveen Gawali	208
Pavankumar Gayatri	399, 547
Iklim Gencturk Akay	336
Kevin Genestreti	310, 332
Agnes Genevey	255

Author	Pg No.
Harriet George	356
Marina Georgiou	293
Sasi Kiran Gera	477
Felix Gerick	11, 120
Daniel Gershman	338
Peter Gerstoft	471
Viktor Getmanov	325, 326
Sapna Ghavri	479, 547
Sia Ghelichkhan	511
Daniela Ghica	429
Rupesh Ghodpage	127, 130
Dibakar Ghosal	30, 31
Ranjana Ghosh	73, 76
Sumit Ghosh	249
Domenico Di Giacomo	412, 414, 461
Sigiava Aminalragia Giamini	169, 170
Nguyen Van Giang	432
Omiros Giannakis	108, 178
Domenico Giardini	449
Steven Gibbons	80
Gary Gibson	519, 554
S.E. Gibson	358
Sarah Gibson	350
Barbara Giles	338
Benjamin Gill	242
Nicolas Gillet	120, 124, 232
Boris Ginzburg	41
Jesper Gjerloev	203
Matina Gkioulidou	315
Hugh Glanville	96
Alex Glocer	314
Neslihan Ocakoglu Gokasan	418
David Goldak	393
Jerry Goldstein	189
Mohan Gollapally	446, 504, 527, 539
Zeynab Golshadi	21
Ana Gomes	89
Alexandre Gonsette	389
Anastasiia Gornostaeva	569
Drgaomir Gospodinov	423
Deepjyoti Goswami	430, 433, 566
Manas Goswami	430
Shusaku Goto	577
Sofie Gradmann	544

Author	Pg No.
Dmitriy Grankin	157
Lesley Gray	269
Alexander Grayver	109, 390, 396, 396, 407
Michael Greer	99
Presley Greer	99
William Greer	189
Francesco Grieco	259
Eric Grimes	373
Hana Grison	248
Chong Guan	223
Anirban Guha	263, 264
Arindam Guha	20
Brenda Abril Nequiz Guillen	100
Ezgi Gulay	201
Monica Gulmini	230
Bryan Gunawan	99
Santhoshkumar Gundu	446
Feng Guo	106, 114
Arvind K Gupta	403, 495
Ashok Kumar Gupta	69
Harsh K Gupta	421, 554, 560, 586
Pravin Kumar Gupta	398
Sandeep Gupta	426, 562
Subramanian Gurubaran	126, 130, 136
Chloe Gustafson	398
Sigmund Guttu	268
Yohan Guyodo	210, 234
Alexei Gvishiani	325, 326
Stein Haaland	339
Robert Haaser	318
Margit Haberreiter	269
Tobias Hafner	109
L Matthew Haffner	278
Joanna Haigh	269
Sebastian Hainzl	548
Stephen Halchuk	477, 480
Chinmay Haldar	501
Chris Hall	276
Felix Halpaap	103, 544
Hideki Hamamoto	577
Miki Hamano	459
Magnus Hammer	108, 231, 238
Mohamed Hamoudi	33
Donald Hampton	99

Author	Pg No.
Yuki Haneda	238, 239
Mark Hannington	79
Ulrich Hansen	41
Brian Harding	139
Ulvienin Harlianti	212
Amir Haroon	72, 398
Bernard Harris	373
James Harris	412, 414, 461
Robert Harris	574
David Hartley	293
Gelvam Andre Hartmann	230
Hiroshi Hasegawa	310
Tadahiro Hatakeyama	230
Katsumi Hattori	55, 490, 492, 493
Kentaro Hattori	196
Rhys Hawkins	503
Hisashi Hayakawa	191, 196
Takumi Hayashida	483
Devajit Hazarika	451
Lijuan He	576
Maosheng He	276
Xiaodan He	491
Lindsey Heagy	390, 391, 393
Csaba Hegymegi	383, 388
Laszlo Hegymegi	383, 388
Balazs Heilig	168, 173, 294
Moritz Heimpel	15
Graham Heinson	66
Pavel Hejda	93
Kosuke Heki	51
Gregoire Heller	445
Peggy Hellweg	91
Susann Henkel	245
Robin Heraibi	234
Elizabeth Hernandez	99
Fatima Martin Hernandez	241
Ramon Julio Oliver Herrero	354
Gwenael Herve	255
David Heslop	243, 244, 252
Gyorgy Hetenyi	509, 536, 538
Benoit Heumez	95, 380
Michael Heyns	181
Mike Heyns	199
Alfan Hidayah Kusuma	36

Author	Pg No.
Vanessa Hiemer	506
Nana Higashio	164
Aleida Higginson	368
Mitsuru Hikishima	166
Mimi Hill	208
Sikha Hiloidari	575
Masfumi Hirahara	323
Satoshi Hirahara	523
Shiro Hirano	517
Eiji Hirota	379
Alicreance Hiyadutuje	261
Ingeborg Hjorth	208
George Ho	365
Yasuhide Hobara	44, 53, 54
Sebastian Hoelz	398
Peter Hoffmann	276
Ryan Hofmann	361
Mark Hoggard	511
Lauri Holappa	303
Richard Holme	118
Matthias Holschneider	235
Asami Honda	406
Ilja Honkonen	113, 203
Yoshimori Honkura	400
Kumiko Hori	119
Shuichiro Hori	523
Tomo Hori	172, 317
Tomoaki Hori	162, 319, 322, 323
Masahiro Hoshino	339
Keisuke Hosokawa	164, 166
Susan Hough	455
Niels Hovius	475
Russ Howard	368
Julian Hoxha	115, 118
Kornyanat Hozumi	116
Pavla Hrubcova	503, 522
Yikai Hsieh	158
Jianping Huang	106, 114
Sheng Huang	163
Joseph Huba	314
Brad Hubeny	458
Juliane Huebert	181, 182, 187, 199
Debrup Hui	305
Gauthier Hulot	105, 106, 109, 111, 114, 179

Author	Pg No.
Linda Hunt	280
Shaul Hurwitz	574
Lorraine Hwang	91, 92
Miquel Ibanez	184
Satoshi Ide	516, 525
Jose Van Den Ijssel	278
Satoshi Ikezawa	406
Ryoya Ikuta	448
Ion Ilies	90
Bhaskar Illa	82, 441
Bhaskararao Illa	38, 39
Shun Imajo	172, 186, 322
Naoto Imamura	378
Caner Imren	418
Maria Elena Innocenti	366
Ana Maria Inostroza	134
Maria Del Puy Papi Isaba	94
Takemi Ishihara	33
Miaki Ishii	84
Keiichi Ishizu	78
Mohammad Israil	395
Turgay Isseven	418
Mathieu Istas	120
Bambang H Iswanto	212
Nickolay Ivchenko	260
Kiyomi Iwahashi	456
Asako Iwaki	484
Toshihiko Iyemori	129
Sreelakshmi J	147
Tomson J K	37
Jason Jackiewicz	352
Jensen Jacob	31
Christoph Jacobi	143, 266, 270, 271, 276
Laura Jacobs	99
Sridevi Jade	479, 547
Ashish Jadhav	130
Juliana Jaen	276
Thomas Jager	109
Nilesh K Jaiswara	551
Matthew James	295
Venkata Rama Rao Jammi	37
Ricardo Jana	472
Jose Antonio Jara	86, 87
Dominique Jault	17, 120, 124, 125, 232

Author	Pg No.
Allison Jaynes	164
Zeinab Jeddi	80, 463
Marion Jegen	79, 398
Trine Dahl Jensen	463
Chintan Jethva	142
Ramya Jeyaraman	497
Yan Jia	94
Lan Jian	358
Wenping Jiang	69
Xiaodong Jiang	245
Piers Jiggens	169
Dengkui Jin	217
Andreas Johlander	339, 356
P John Kurian	29
Catherine Johnson	123
Abraham Jones	519
Chris Jones	119
Glenn Jones	474
Sarah Jones	164
Shelby Jones	253
Vania Jordanova	304, 313, 318, 319
Anders Jorgensen	173
Anju K Joshi	74
H P Joshi	142
Lilla Juhasz	173
Chae Woo Jun	319
Niina Junno	462
Liisa Juusola	180, 183
Ajeet K	259
Krishnapriya K	141
Mallika K	424, 426
Veeraswamy K	403
Joshi K Catherine	549
Sreejith K M	24
Ajithabh K S	404
Reshma K S	441
Antek K Tokarski	436
Nitin Kadam	249
Jaroslav Kadlec	248
Akira Kadokura	166
Johannes Kaeufl	407
Menas Kafatos	492
Primoz Kajdic	351
Sebastian Kaki	180, 183

Author	Pg No.
Emine Ceren Kalafatoglu Eyiguler	201, 370
Maria Kalinina	569
Daniel Kalmar	538
Tereza Kamenikova	101
Kattoju A Kamesh Raju	29
Max Van De Kamp	113
Wataru Kanda	405, 406
Shrikanth Kanekal	303
Satoshi Kaneshima	12
Jian Kang	219
Seogi Kang	391
Suk Bin Kang	302
Yasuyuki Kano	86, 456
Konstantin Kanonidi	88
Odej Kao	107, 329
Chandan Kapil	148
Karl Kappler	393
Beril Karadoller	418
Arseniy Karagodin	262
Foivos Karakostas	449
Vasileios Karakostas	494
Vassilis Karakostas	486
Deepak Karan	151
Jon Karapetyan	387
Roza Karapetyan	387
Otto Karha	96
Kamila Karkowska	417
Mahendra Karna	346
Nishu Karna	346
Ivan Karpov	136
Mikhail Karpov	136
Myriam Kars	245
Yasumasa Kasaba	320
Satoshi Kasahara	172, 291, 319, 322
Yoshiya Kasahara	166, 172, 291, 304, 319
Takafumi Kasaya	400
Mathew Kasoar	269
Hiroshi Katao	523
Ryuho Kataoka	166
Christos Katsavrias	160, 169, 170, 172
Yabu Katsuhiro	445
Kei Katsumata	523
Youri Katz	41
Kirsti Kauristie	180, 203

Author	Pg No.
Shiva Kavosi	339
Yoshifumi Kawada	565
Taichi Kawamura	449
Ben Kay	66
Zerefsan Kaymaz	201, 336, 370
Maria Kazachenko	347
Yoichi Kazama	319
Kunihiro Keika	172, 282, 291, 319, 322
Anna Kelbert	182, 392, 393
Mirjam Kellinsalmi	183
Yann Pfau Kempf	356
Ankur Kepkar	135, 155
E Lawrence Kepko	339
Larry Kepko	295, 332, 368
Ramida Keramova	489, 491, 555
Guram Kervalishvili	168, 193, 278
Kerry Key	398
Johan De Keyser	339
Galina Khachikyan	494
Aibulat Khafizov	88
Shuhab Khan	99
Tauheed Khan	578
Kirti Khanna	555
Tarun Khanna	529
Marzieh Khansari	267
Akash Kharita	412
Yuri Khotyaintsev	338
Hiroshi Kikuchi	53
Eunhwa Kim	337
Tamarah King	519
Todd King	373
Masataka Kinoshita	565
Asha Kiran	481
Kartika Kirana	212
Uwe Kirscher	207, 212
Lynn Kistler	318, 320
Akitsugu Kitade	493
Naritoshi Kitamura	338
Ivan Kitov	467
C A Kletzing	171, 323
Craig Kletzing	288
Maxim Klimenko	265
Dmitri Klimushkin	292, 293, 298
Brigitte Knapmeyerendrun	449

Author	Pg No.
Petra Koucka Knizova	126, 133
Ondrej Knopp	112
David Knudsen	308
Kenneth Kodama	242
Paula Koelemeijer	510, 511
Male Koester	245
Benjamin Kohl	89
Haruna Kojima	493
Michal Kolaj	477, 480
Petr Kolinsky	507
Sudheer Kolluri	422
Alexander Koloskov	263, 264
Mick Emil Kolster	58
Dmitry Kolyukhin	64
Darkhan Komekbayev	468
Attila Komjathy	52
Niko Kompein	188, 381
Suman Konar	73
Shankaraiah Konda	401
Yana V Konechnaya	420
C De Koning	358
Toshio Kono	523
Yuri Kopnichev	443, 444
Heidrun Kopp	79
Annakaisa Korja	430, 462
Richard Kornfeld	381
David Koronczay	173
Galina Korotova	297
Dmitry Korotyshkin	270
Monika Korte	12, 227, 235, 255
Sylvain Korzennik	348
Michael Kosch	260
Anastasios Kostoglou	494
Masahiro Kosuga	523
Mahender Kotha	215
Mallika Kothamasu	424
Daniel Kouba	133
Christos Kourouklas	486
Anna Kovylyaeva	325, 326
Takao Koyama	405, 406
Elena Kozlovskaya	462
Jonathan Krall	314
Mikhail Kruglyakov	396
Sergey Kshevetskii	132, 133

Author	Pg No.
Olga Joan Ktenidou	465
Hisahiko Kubo	520
Yasubumi Kubota	195
Harald Kuchareck	339
Dmitriy Kudin	88, 380
Dmitry Kudin	88
Daniela Kuehn	427, 518
Andrzej Kulak	263
Bernd Kulessa	474
Atul Kulkarni	116
Atsushi Kumamoto	166, 291
Amit Kumar	25, 513, 515
Dewashish Kumar	66
Dharmendra Kumar	395
K Vinod Kumar	20
Naresh Kumar	451
Pankaj Kumar	30
Prakash Kumar	24, 38, 39, 82, 441, 501, 526, 531
Rohtash Kumar	249
Sandeep Kumar	319
Sanjay Kumar	482
Santosh Kumar	26
Sudesh Kumar	562
Sushil Kumar	535, 563
Varun Kumar	575
Venkata Vijaya Kumar	66, 495
Nikhil Kumar Baranval	71
Anup Kumar Sutar	431
Komal Kumari	270
Yu Long Kung	89
Yuliya Kurdyaeva	132, 133
Masanori Kurihara	378
Satoshi Kurita	164, 186
Vladimir Kurkin	304
Muhammad Fachrul Rozi Kurniawan	28
Hulya Kurt	418
W S Kurth	171
William Kurth	337
Alexey Kuvshinov	67, 109, 396, 397, 407
Alexey V Kuvshinov	67, 408
Jiri Kvapil	537
Grzegorz Kwiatek	432
Yongxiang Li	217, 242
Christian Laag	210

Author	Pg No.
Matt Lacaire	189
Alisson Dal Lago	165
France Lagroix	210, 234
Nand Lal	373
Gaelle Lamarque	535
Derek Lamb	373
Roland Lammegger	114
Benoit Langlais	119
Gianni Lapenta	339
Giovanni Lapenta	282
Virginia Lapenta	250
Tine B Larsen	463
Brian Larson	318
Davin Larson	358, 365
Marine Lasbleis	15
Fazlul Laskar	136
Gabi Laske	77, 526
Stanislaw Lasocki	421, 436, 486
J Lastovicka	145
Jan Lastovicka	272, 273
Emanuele Laterra	40
Ralph Latteck	166
Harriet Lau	511
Benoit Lavraud	161, 339
Michael Lawson	189
Erin Lay	318
Ivan Lebedev	227
Juan Jose Ledo	185, 204
Juan Ledo	185
Thomas Lee	84
Marianne Greff Lefftz	62
Jean Michel Leger	109
Jamie Lehnen	99
Wenjie Lei	510
Barbara Leichter	101, 381
Stacey Lengyel	253
Roman Leonhardt	188, 228, 381
Konstantinos Leptokaropoulos	432
Matthew Leroy	242
Sylvie Leroy	568
Aditya Lesmana	28
Vincent Lesur	19, 33, 95, 110, 380
Sarah Letaief	243
Hui Li	134, 165

Author	Pg No.
Stefano Loppi	250
Jean Louis Pincon	338
Jeffrey Love	182
San Lu	308, 309
Xian Lu	270
Greg Lucas	182
Francis Lucazeau	568
Franzjosef Luebken	275
Maria Luisa Osete Lopez	229
Karen Luttrell	574
Ioannis Lymperis	418
John Lyon	300, 311, 335
Larry Lyons	262, 311, 312
Robert L Lysak	290
Robert Lysak	288
Ravi Kumar M	22, 37
Satyanarayanan M	66
Senthil Kumar M	496
Shekar M	551
Srihari Rao M	67
Lifeng Ma	242
Qianli Ma	163
Xiaolong Ma	13, 418
Yuzhang Ma	307
Justin Mabie	83, 97
R J Macdowall	323
Arthur Macedo	467
Kevin Mackey	85
Susan Macmillan	384
Uma Anuradha Madugula	422
Stefano Maffei	199
Pavel Mager	293, 298
Werner Magnes	106
Chitta Ranjan Mahato	559
Devika Maisnam	35
Saumen Maiti	73, 76
Vladimir Makhmutov	157
Mohamed Maklad	413
Olga Malandraki	339
A Malanushenko	358
Kothamasu Mallika	427
Alexei Malovichko	85
J Malsoma	249
Venkateshwarlu Mamilla	211

Author	Pg No.
Shiva Shankar Manche	20
Prantik Mandal	476, 452, 543
Himangshu Sekhar Mandal	477
Mioara Mandea	11, 124, 232
Richard Mandl	381
Ourania Mangira	486
Talgat Manglayev	356
Ajay Manglik	399, 403, 547
Jyrki Manninen	304
Carlo Mans	508, 510
Paivi Mantyniemi	457
Brassnavy Manzunzu	478
Paolo Marangio	327
Dedalo Marchetti	52, 491, 496
Jose Paulo Marchezi	134, 159, 165
Alex Marcuello	184, 185
Evgeny Mareev	494
Ludovic Margerin	445, 449, 452
Josep Maria Pares	241
Guy Marquis	63
Santi Marsal	185
Santiago Marsal	184, 204, 233
Tapas Martha	555
Anna Marti	185
Jules Marti	449
P Martin Mai	444
Orlando Martina	53
Cristiano Martins	386
Patricia Martinez Garzon	432
Francisco J Martinez Moreno	391
Carlos Martinis	151
Shoji Masafumi	166
Dakalo Mashao	260
Norimichi Mashiko	90
Arnaud Masson	372
Liviu Matenco	519
Massimo Materassi	49
Antonio Mateus	391
Gurgen Matevosyan	387
Shoya Matsuda	166
Kakeru Matsuki	54
Naoko Matsumoto	230
Yasuo Matsunaga	405, 406
Miu Matsuno	522

Author	Pg No.
Tomoko Matsuo	152
Ayako Matsuoka	166, 172, 186, 291, 320, 323, 324,
Masaki Matsushima	14, 400
Takeshi Matsushima	522
Hitoshi Matsuzawa	514
Toru Matsuzawa	523
Raffaella De Matteis	425
Simone Di Matteo	288, 295, 368
Vivien Matthias	276
Juergen Matzka	116, 139, 193, 385
Jurgen Matzka	386
Stefan Mauerberger	235
Domenico Di Mauro	52 , 491, 496
Satish Maurya	22, 446, 532, 533
Ved Maurya	40
Astrid Maute	145, 152
Prateek Mayank	371
Kevin Mayeda	543
Christian Mazelle	360
Francine Mccarthy	458
Phil Mccausland	256
William Mcclintock	136
Aoife Mccloskey	205
David Mccormack	102
Joseph Mcinerney	274, 278
Keith Mclaughlin	469
Michael Mcmanus	365
Claudia Medeiro	134
Amauri Medeiros	130
Domenico Meduri	122
Irina Medvedeva	128
Jennifer Meehan	197
Yellapragada Meenakshi	545
Joseph Meert	254, 257
Mustapha Meghraoui	545
Lars Mejnertsen	199
Leonarda Isabel Esquivel Mendiola	100
Qingquan Meng	217
Xing Meng	52
Sabrina Menina	449
Naser Meqbel	392
Laszlo Merenyi	383, 388
Maite Merino	86
Maria Teresa Merino	87

Author	Pg No.
Gollapally Mohan	440
Kapil Mohan	553
William Kumar Mohanty	24, 535
Omid Bagherpur Mojaver	528
Nina Mokrushina	557
Iren Moldovan	498
Mark Moldwin	202
Demudu Babu Molli	399
Momchil Molnar	348
Thiago R Moncinhatto	231
Saroj Kumar Mondal	549
Setbandhu Mondal	67
Sikha Mondal	76
Katrin Monecke	457
Marc Monnereau	452
Jean Paul Montagner	22, 533
Isabel Montanez	242
Joan Montanya	263
Fernando A Monteiro	178, 202
Remy Monville	17
Yongjae Moon	344
Robert Moore	263
Max Moorkamp	57, 60
Nobuyuki Morikawa	484
Kenji Morinaga	90
Steven Morley	318
Juliano Moro	134, 141, 144, 187
Anna Morozova	154, 374
Achim Morschhauser	116, 377, 385, 386
Matthias Morzfeld	256
Zbysek Mosna	133, 146
Parisa Mostafavi	365
Jon Mound	199
Sima Mousavi	503
Hesham Hussein Moussa	413, 558
Pablo S Moya	159
Abdul Muhari	28
Sagarika Mukhopadhyay	412
Sujoy Mukhopadhyay	508
Thifhelimbilu Mulabisana	478
Thifhelimbilu Faith Mulabisana	545
Federico Munch	396, 508
Adiya Munkhsaikhan	414, 415, 463
Ulziibat Munkhuu	42

Author	Pg No.
Andres Munoz Jaramillo	373
Alexandra Muntean	498, 499
Ioan Munteanu	429
Radhakrishna Munukutla	24, 26, 29
Judit Murakozy	343
Benjamin Murphy	182
John Murphy	89
Kyle Murphy	293
Maura Murru	486
Kalevi Mursula	303
Donal Murtagh	259
Adrian Muxworthy	244
Subhadra N	447
Purnachandra Rao N	424, 475, 556
Abdelmansour Nadji	45
Shingo Nagamachi	90, 379
Kasturi Naganjaneyulu	393
Nandini Nagarajan	582
Emmanuel Nahayo	383
B Pradeep Naick	393
V Mahalaxmi Naidu	549
Manoj Nair	98, 102
Nisha Nair	23, 25
Hisashi Nakahara	437, 439, 440, 445, 447
Aoi Nakamizo	195, 297
Satoko Nakamura	164
Takuma Nakamura	310
Shinya Nakano	330
Hiroyuki Nakata	127, 131, 162
Takashi Nakayama	523
Tsutomu Nakgatsuma	195
Pushkar Nalawade	252
Narasimha Chakravarthi Nalluri	399, 547
Subhadra Nampally	447
Undapalli Nanajee	530
Dibyendu Nandy	341
Adriano Nardi	53, 491, 496
Clezio Denardin	134, 144, 187
Nirujogi Narsimha Naidu	575
Afroditi Nasi	160, 170, 172
Venkatanathan Natarajan	496, 497
Fernando Navarro Estrada	100
Srinivas Nayak	45, 48
Cristian Neagoe	94

Author	Pg No.
Sanjay Negi	25, 515
Sanjay Singh Negi	513
Phani Chandrashekhar Nelapatla	138, 378
Kazuhida Nemoto	493
Brandow Neri	467, 550
Anne Neska	79, 402
Mariusz Neska	263, 264
Coralie Neubueser	56
Binbin Ni	316
Patrick Nicol	243
Junsheng Nie	217, 219
Jorge Roman Nieves	542
Teresa Nieves Chinchilla	375
Shabnam Nikbakhsh	267
Romina Nikoukar	168, 326
Andreas Nilsson	208
Alexander Nindos	343
Yafei Ning	307
Lachit Ningthoujam	515
Tomoaki Nishikawa	520
Koji Nishimura	166
T Nishimura	150
Takeshi Nishimura	439, 440, 445, 447
Toshi Nishimura	262, 311, 312
Yukitoshi Nishimura	308, 321
Masaki Nishino	284
Nozomu Nishitani	162, 261
Takanori Nishiyama	166
Tatsuji Nishizawa	405, 406
Michael Nisilevich	88
Paulo Alexandre Nogueira	141, 144, 187
Erdenetsog Nominerdene	415
Reiko Nomura	166, 86, 291, 322
Adam Nordsvan	213
Masahito Nose	90, 166, 186, 192, 287, 291, 323
Susan Nossal	278
Victor Novikov	200
Andy Nowacki	422, 450, 474, 501
Norbert Nowaczyk	224, 227
Izabela Nowaczyska	432
Kenro Nozaki	131
Andri Dian Nugraha	28, 36
Andi Azhar Nurdin	28
Andrew Nyblade	471

Author	Pg No.
Katariina Nykyri	285
Victoria Oancea	89, 94
Yuki Obana	186, 290
Jens Oberheide	270
Paul Obrien	195
Sereenendorj Odbayar	414, 415, 463
Leon Ofman	358, 366
Yasunobu Ogawa	164
Yasuo Ogawa	78, 400
Junzo Ohmura	456, 459
Shin Ohtani	203
Hiroyo Ohya	127, 131, 162
Mako Ohzono	523
Alexey Oinats	304
Maheswar Ojha	73, 74, 75, 76
Makoto Okada	238
Tomomi Okada	522
Tomohisa Okazaki	484
Zakharova Oksana	572
Kjellmar Oksavik	307
Kurama Okubo	442
Paul Okubo	84
Daniela Olaru	412
Doug Oldenburg	393
Aline Oliveira	550
Clara Oliveira	260
Denny Oliveira	196, 303
Marcel De Oliveira	381
Wellington P De Oliveira	230
Nils Olsen	106, 109, 114, 231
Dorota Olszewska	428
Yoshiharu Omura	158, 164
Nour Eddine Omrani	268
Hermann Opgenoorth	203
Merav Opher	362
Rona Oran	123
Gonca Orgulu	418
Yuhi Orito	131
Martina Orlando	237, 491, 496
Beata Orleckasikora	428
Eugen Oros	524
Joseph Orourke	16
Yvan Orsolini	268
Pascal Ortega	263

Author	Pg No.
Naoto Oshiman	400
Anica Otilia Placinta	498, 524
Lars Ottemoller	80, 544
Odd Helge Otteraa	268
Dimitar Ouzounov	490, 492
Ilya L Ovchinnikov	159
Oluwafisayo Owolabi	138
Shin Oyama	164
Shinichiro Oyama	166, 304
Volker Oye	427
Monkhor Oyunerdene	414
Mitsunori Ozaki	166, 304
Louis Ozeke	293
Sinan Ozeren	418
Ajeet P	558
Jagadeesh P	422
Solomon Raju P	543
Igor P Kirpichev	159
Shreedevi P R	315
Sunil P S	49
Martin Paces	372
S Padhy	444
Simanchal Padhy	447
Antonio Padilha	40
Shankar Pal	442
Duggirala Pallamraju	127, 152, 267
Minna Palmroth	286, 356
Finnur Palsson	473
Hongmiao Pan	220
Yongxin Pan	221
Anand K Pandey	551
Dhananjai K Pandey	23, 513
Laxmi Pandey	75
Prabha Pandey	551
Manoj Pandit	254
Megha Pandya	317, 370
Isabelle Panet	62
Evgeny Panov	311
Sanja Panovska	12, 117, 227
Tarun Kumar Pant	152
Tarun Pant	303
Kostis Papadakis	356
Constantinos Papadimitriou	108, 169, 170, 330, 333
Eleftheria Papadimitriou	485, 486, 494

Author	Pg No.
Antonia Papageorgiou	465
Navin Parihar	259
Mahesh Prasad Parija	562, 563
Jean Pascal Rivierre	380
Rajat Pasricha	442
Parashram Patil	130
Prasanta K Patro	65, 66, 401, 495
Spiros Patsourakos	342, 343, 376
Harihar Paudyal	561
Ajay Paul	451
Arghyadeep Paul	336
Himangshu Paul	419, 475, 530
Sanjit Paul	451
Daniel Paulescu	90, 94
Ana Roberta Paulino	130, 142
Igo Paulino	130, 142
Berit Paulsen	420
Kristoff Paulson	289
Adhitya Pavithran	298
Vladimir Pavlov	211
F Javier Pavon Carrasco	233
Francisco J Pavon Carrasco	237
Francisco Javier Pavon Carrasco	229
Mari Paz Miralles	342, 349
Janos Pazonyi	388
Jared Peacock	390, 393, 408
Courtney Peck	192
Nicholas Pedatella	136, 266
Zhaowen Pei	246, 247
Klaudio Peqini	115, 118
Regia Pereira	187
Natalia Gomez Perez	182, 200
Victoria Canillas Perez	184
Pablo Rivera Perez	229
Kristell Perot	259
Loredana Perrone	52, 491, 496
Elena Pershina	416
Joseph D Perez	309
William Pesnell	346
Gesa Petersen	518
Noel Petit	189, 190
Laura Petrescu	519
Steven Petrinec	339
Valery Petrov	88

Author	Pg No.
Eduard Petrovsky	248
Anatoly Petrukovich	338
Julia Pfeffer	11
Kevin Pham	300, 335
Tai Phan	310
Amanda Piassi	187
Giorgio Picanco	141, 144, 187
Zakhar Pichugin	569
Leonie Pick	205
Mirko Piersanti	49
Ermanno Pietropaolo	331
William T Pike	449
Polina Pikulina	265
Marcin Pilinski	192
Viacheslav Pilipenko	202
Valdir Gil Pillat	147
Megan Pina	99
Fernando J G Pinheiro	202
Fernando Pinheiro	177
Katia Pinheiro	100, 101, 116, 117, 377, 381, 386
Victor Pinto	159
Paul Piraino	89
Myrto Pirli	420, 470
Sergei Pisarevsky	214, 251
Alessandro Piscini	53, 491, 497
Angelo Pisconti	512
Anthony Pivarunas	254
Ferdinand Plaschke	338
Matthieu Plasman	449
Alain Plattner	121
Beata Plesiewicz	432
Jaroslava Plomerova	534, 536, 537
Natalia Poaiata	429
Katerina Podolska	133
Nagaraju Podugu	435, 566
Stefaan Poedts	161
Gevorg Poghosyan	387
Thierry Poidras	243
Marcin Polkowski	417
Andreas Pollinger	106, 114
Bart De Pontieu	345
David Pontin	362
Jeffrey Poort	568
Mihaela Popa	90, 94, 429

Author	Pg No.
Evgeny Popov	573
Yuri Popov	569, 573
Yury Popov	571, 572
Itay Porat	99
Nazmi Postacoglu	418
Maeva Pourpoint	393
Manoj Prabhakar	403
Erno Pracser	263
Sanjay K Prajapati	442
Sanjay Prajapati	543
M Prasad	35
A Pratap	393
Luis Preisser	351
Xyoli Prezcampos	513
John Prince	99
Awali Priyono	28
Elena Provornikova	364
Sergey Pulinets	490, 492, 494
Antti Pulkkinen	198, 303
Nanang T Puspito	28
Liying Qian	157, 272, 274, 278, 300
Murong Qin	163
Pilar Queralt	185
Mark Quigley	519
Luis Quintanar Robles	100
Dinh Quoc Van	432
Jay R Johnson	309
Mircea Radulian	519
Jonathan Rae	293, 295, 333
R Vijaya Raghavan	549
STG Raghukanth	545
Ali Rahmati	365
Shikha Raizada	150
Shibu Rajkhowa	551
Khasi Raju	66
Airat Ramazanov	579
Arianna Ranabhat	279
Eswara Rao	578
Prabhakar E Rao	403
Nour Raouafi	365
Mark Rast	360
Lutz Rastaetter	370
Sepideh J Rastin	487
Adina Vanciu Rau	94

Author	Pg No.
Jan Rauberg	168, 193, 278
Michela Ravanelli	52
Rahul Rawat	146, 263, 264, 303
Vishal S Rawat	495
Labani Ray	575, 578
Kevin Reardon	348, 352, 361
Sarah Reay	384
Rania Rebbah	154
Dario Recchiuti	288
K Chinna Reddy	67, 401
Sergio Toledo Redondo	264
G D Reeves	323
Geoff Reeves	291
Geoffrey Reeves	175
Ashton Reimer	262
Will Reis	78
Rajesh Rekapalli	4190, 422, 438, 475
Jeremy Rekier	11
Jie Ren	292
G Rengin	444
Toralf Renkwitz	276
Laysa Resende	134, 141, 144, 187
Federica Restelli	510
Alessandro Retino	338
Milos Revallo	93
Julia Rewers	537
Sara Rezaei	80
David Rhoades	485, 487
Maria O Riazantseva	159
Joana Alves Ribeiro	177, 202, 391
Paulo Ribeiro	89, 391
Yanick Ricard	505
Fred Richards	511
Anne Richardson	384
Gemma Richardson	181, 182, 200, 206
A Richmond	150
Gudrun Richter	518
Rafael Rigaud	396, 397
E Joshua Rigler	182
Ashim Rijal	508, 510
Archana RK	145
Kate Roberston	66
Aaron Roberts	373
Andrew P Roberts	220

Author	Pg No.
Kate Robertson	69
Robert Robinson	303
Marcelo Rocha	550
Federica Rochira	512
Hannah Rogers	98, 101, 121, 327
Diana Rojascastillo	351
Frederique Rolandone	568
Lucie Rolland	48
Sidorov Roman	326
Barbara A Romanowicz	508
Giuseppe Romeo	168, 326
Esmeralda Romero Hernandez	187
Raissa Romushkevich	573
Tim Ronan	393
Stephane Rondenay	544
Christian Ronnevik	463
Alexa Roosnovo	189, 190
Guillaume Ropp	110
Shindy Rosalia	28, 36
Martina Rosskopf	518
Sebastian Rost	500, 501
Michael Roth	462
Sunil K Roy	502, 530, 551
Corinna Roy	422, 450, 474
Priyom Roy	555
Sukanta Roy	431, 433, 435, 564, 566, 576
Jeffrey Royce Cox	253
Eugene Rozanov	157, 262, 265
Justin Rubinstein	432
Aleksandr Rubtsov	292
Dmitriy Rudko	211
Maxwell L Rudolph	508
Lukasz Rudzinski	428, 436
John Rundle	489
Andrei Runov	310
Christopher Russell	189, 289, 340
James Russell	276
Ladislaus Rybach	565
Pawel Rzonca	180
Sunil A S	49
Saju D S	504,539
Abhirami S G	66
Jason S Herrin	212
Steven Saar	346

Author	Pg No.
Nazeel Sabah	561
Dario Sabbagh	52, 491, 497
Nishtha Sachdeva	375
Libor Sachl	112
Kodai Sagae	445
Christos Sagagiotis	467
Sovan Saha	127, 152, 267
David P Sahara	28
Swarandeep Sahoo	10, 17, 117
Ryan Said	263
Sowrav Saikia	543
Kalachand Sain	73, 74, 75, 76
Tony Saini	556
Gregory Sainton	449
Shinji Saito	164
Yoshifumi Saito	338
Shinichi Sakai	523
Takeshi Sakanoi	164
Burak Sakarya	413
Morvarid Saki	504
Asem Salama	413, 558
Nizan Salomonski	41
Rick Saltus	102
Rebecca O Salvage	435
Malcolm Sambridge	503
Sarasija Sanaka	402
Ingmar Sandberg	161, 169, 172
Sandberg Sandberg	170
Jasmine Sandhu	293, 295
Kusham Sandhu	393
Mike Sandiford	519
Satish Sangode	225, 249, 252
Jesus Antonio Perez Santana	100
Angelo De Santis	52, 114, 237, 491, 496
Ondrej Santolik	161, 171
Rute Santos	177
Yuri Santos	230
Miguel Santoyo	84
Veronica Sanz	185
Lkhagvasuren Sarantsetseg	415
Krishna Sarkar	137
Kouta Sasaki	565
Kenji Satake	453, 458
Sumanta Kumar Sathapathy	26

Author	Pg No.
Kaoru Sato	166
Mitsuteru Sato	264
Gabriella Satori	263, 264
Stanislav Sazykin	321
Thomas Schad	349
Maximilian Arthus Schanner	235
Erik Schmaqter	271
Nicholas Schmerr	449
Florian Schmid	79
Elisabeth Schnepp	228
Christoph Sens Schoenfelder	438
Robert Scholger	228
Lucas Schreiter	278
Harald Schuh	155
Tobias Schwaiger	11, 120, 232
Katrin Schwalenberg	398
Robert Wimmer Schweingruber	338
Johannes Schweitzer	5,411, 420
Murray D Sciffer	290
Daniel Seaton	192
Onder Sebnem	418
Gopi K Seemala	146, 148, 302
Delia Iresine Bello Segura	100
Kanako Seki	291, 296, 334
Marcin Sekowski	417
Adrien Selles	434
Kate Selway	410
M K Sen	584
Moumita Sengupta	73
Nataliya Sergeyeva	88, 97
Ahmad Setiawan	36
Yosi Setiawan	232
Antrisha Setiwan	54
Robert Sewell	192
Henry Seywerd	102
Antonio Sgamellotti	249
Trunali Shah	317, 370
Anuar Shakirov	571, 572
Shengtan Shang	223
Daya Shanker	560, 561
Zhigang Shao	557
Ramil Sharafutdinov	579
Shivangi Sharan	101, 119
Babita Sharma	552

Author	Pg No.
Nitin Sharma	425, 426
Ann Shea	196
Arie Sheinker	41
Bharath Shekar	440
M Shekar	549, 551
Miaomiao Shen	222
Weisen Shen	532
Xiaochen Shen	163
Xuhui Shen	106, 113, 114, 491
Simon G Shepherd	162
Jiankui Shi	134, 144
Hasbi Ash Shiddiqi	544
Hiroyuki Shinagawa	139
Atsuki Shinbori	192
Iku Shinoahara	323
Iku Shinohara	164, 166, 172, 186, 291, 319, 323
Manabu Shinohara	166, 186
Kazuo Shiokawa	127, 162, 164, 166, 299, 304, 315
Taghi Shirzad	428
Munehito Shoda	357
Masafumi Shoji	291, 319
Khogenkumar Shoraisam	23
Rob Shore	181
Robert Shore	177
Yuri Shprits	123, 167, 376
Muhammad Shuhail	29
David Gary Sibeck	165
David Sibeck	134, 297, 302
Tarique Siddiqui	145
Roman Sidorov	325
Karin Sigloch	521
Regia Silva	144
James Simmons	99
Ajay P Singh	558
A P Singh	34
Amrita Singh	74
Anand P Singh	19,35
Anand Singh	58, 59
Arun Singh	395, 398
Ashutosh Singh	27
O P Singh	558
Rajesh Singh	156, 259
Ram Singh	50, 149
Ravi Kant Singh	553

Author	Pg No.
Satendra Singh	76
Shubham Singh	50, 560
Sunil Kumar Singh	440
Lachit Singh Ningthoujam	25
Pabitra Singha	30
Anup Sinha	254
Ashwini Kumar Sinha	146, 263, 264, 289, 302
Shipra Sinha	302
Miriam Sinnhuber	157
Weerachai Siripunvaraporn	400
Mikhail Sitnov	283
Mani Sivakandan	146
Vera Sivtseva	128
Anna Skorkina	83, 97, 516, 517
James Slavin	307
Olivia D Pita Sllim	60
Don Smart	196
Andy Smith	181
Ashley Smith	372
C W Smith	323
Ekaterina Smotrova	293
Pedro Baltazar Soares	202, 391
Pedro Soares	178
Demberel Sodnomsambuu	42
Robert Sohn	574
Inna Sokolova	416, 443, 444, 466, 468
Nadezhda Sokolova	416
Maurizio Soldani	53, 491, 497
German Sole	86
Anna Sole Castelli	194
Teresa Sole Espuny	353
Stan Solomon	278
Stanley Solomon	157, 274, 300
Alexander Soloviev	481
Anatoly Soloviev	274,380
Thanh Son Pham	14, 473, 521
Chunhui Song	217
Junhao Song	427
Rui Song	55
Komal Soni	560
Kareem Sorathia	299, 311, 335
Mathilde B Sorensen	463
Valery Sorokin	200
Luca Sorriso Valvo	338

Author	Pg No.
Thomas Sotirelis	168, 326
Nikita V Sotnikov	159
David Southwood	296
Mikhail Spasennykh	572
Simo Spassov	254
H E Spence	323
Harlan Spence	291
Glenn Spinelli	574
Courtney Sprain	122
Gokul Venu Sreebindu	24
K N S S S Srinivas	66
Gangumalla Srinivasa Rao	26, 27
Uppala Srinu	501
S Sripathi	143, 149
Shalivahan Srivastava	69, 393
Piotr Sroda	537
Simon C Stahler	449, 453
Frances Staples	293
Peter Stauning	179, 314
Cristiana Stefan	229, 317
Giovana Stefani	187
Claudia Stein	41
Peter Steinbach	173, 264
Erik Steinmetz	202
Maruna V Stepanova	159
Ralph Stephen	471
Judy Stephenson	261
Robert Sternberg	253
Jeff Stevens	469
Michael Stevens	351, 358
Peter Stevenson	384
Gunter Stober	270
Claudia Stolle	106, 107, 116, 139, 145, 152, 153, 168, 193, 278, 329
Dmitry Storchak	412, 414, 460, 461, 521
Frode Stordal	268
Marte Stromme	80
Kevin Styp Rekowski	107, 329
Jinrong Su	427
Juan Jose Curto Subirats	194, 353
Prasad Subramanian	375
Satyanarayana Hari Venkata Subramanya	422, 424, 426, 427, 482
Tulasiram Sudarsanam	154
Reiko Sugimori	458

Author	Pg No.
Siyuan Sui	532
Timofei Sukhodolov	157, 265
M Sulzer	150
Weijie Sun	308
Weiqin Sun	321
Surendra Sunda	49
Jonas Suni	356
A S Sunil	48
Pornchai Supnithi	116
G Suresh	549, 553
N Suresh	249
Eric Sutton	192
Takeru Suzuki	127
Kate Swan	474
K Swathi	549
Abdennasser Tachema	45
Ayaka Tagami	522
Hisao Takahashi	130
Kazue Takahashi	189, 285, 287, 288
Naoko Takahashi	296
Shinichi Takakura	405, 406
Yuhei Takeshita	304
Hayashida Takumi	42
Akiko Tanaka	577
Kentaro Tanaka	162
Takashi Tanaka	195, 301
Yoshimasa Tanaka	166, 186, 192
Binbin Tang	307
Eija Tanskanen	96, 267, 462
Vertti Tarvus	356
Theo Tassin	123
Ruben Tatevossian	457, 554, 557
Lisa Tauxe	251, 253, 256
Patrick Taylor	490, 492
Team CSES	556
Abdelkader Telali	380
Evdokia Tema	230
Anna Tenerani	366
Runa Van Tent	12
Mariko Teramoto	162, 166, 186, 291, 322, 323
Filipe Terra Nova	18, 230
Claudio Robustelli Test	209
Saikiran Tharimena	509
Erwan Thebault	109, 119

Author	Pg No.
Niranjana Thejaswi	375
Stephan Thiel	65, 69
Ed Thiemann	192, 279
Christine Thomas	9, 10, 12, 500, 504, 506, 512
B J Thompson	358
Alan Thomson	181, 182, 200
Michael Thorne	501
John Thornley	479
Denise Thorsen	99
Sheng Tian	293
Xingbin Tian	315
Ayushi Tiwari	480
Prabhakar Tiwari	50
Raghvendra Tiwari	249
Ram Krishna Tiwari	561
V M Tiwari	35, 431, 475, 580,585
Hrvoje Tkalcic	13, 14, 418, 473, 503, 521
Victorin Emilian Toader	499
Victorin Toader	498
Steve Tobias	119
Frank Toffoletto	299, 308, 311, 321
Yokoi Toshiaki	42
Gabor Toth	123
Chloe Tovar	99
Jeannot Trampert	508, 510
Karlheinz Trattner	340
Lorenzo Trenchi	108
Santiago Andreas Triana	11
Ricardo I F Trindade	231
Ricardo Trindade	230
Jeroen Tromp	510
Vladimir Truhlik	179
Shoovdor Tserendug	67, 407
Leo Tsibizov	325
Kanaris Tsinganos	178
Fuminori Tsuchiya	127, 131, 162, 164, 166, 291
Shuhei TSUJI	448
Masaki Tsutsumi	166, 276
M Kemal Tuncer	400
Lkhagva Tungalag	414, 463
Christopher Turbitt	382
Lucile Turc	356
Donald Turcotte	489
Drew Turner	168, 326, 369
Naveen P U	34

Author	Pg No.
Pietro Ubertini	49
Naonori Ueda	484
Satoru Ueno	192
Han Uitenbroek	363
Arban Uka	115, 118
Sasha Ukhorskiy	168, 294, 311, 326
Alexandra Ulinski	99
Norio Umemura	192
Judith Unamuno	86, 87
Maria Usanova	167, 174
Yoichi Usui	226, 238
Yoshiya Usui	400
Arjun V H	562
Bhargav Vaidya	336
Rami Vainio	338
Rajesh Vaishnav	271
Andris Vaivads	339
Roman Vakarchuk	557
Guzel Vakhitova	579
Fridrich Valach	93
Rim Valiullin	579
Jon Vandegriff	373
Perla Pina Varas	204
Roger Varney	262
Vaclav Vavrycuk	503, 522
Ludek Vecsey	536
Manuel J Aguilar Velazquez	60
Alexandr Velikanov	468
Jakub Velimsky	112, 403
Massimo Vellante	288, 294, 331
Marco Velli	366
Venkatesh Vempati	556
Pavan Kumar Vengala	461, 543
V Venkatesh	502
Ismael Vera Rodriguez	427
Christine Verbeke	374
Massimo Verdoya	564, 570, 571
Daniel Veres	210
Jerome Vergne	63
Olivier Verhoeven	119
Olga Verkhoglyadova	52
S.K. Verma	583
Sanjay Verma	451
Vishnu Kant Verma	58

Author	Pg No.
Jaye Verniero	358, 365
Daniel Verscharen	355
Oana Vesa	352
Rajiv Vhatkar	130
Nicholeen M Viall	295, 368
Louise Vick	103
Francisco Vieira	147
Luis Eduardo Vieira	134
Pierre Vigneron	109, 179
G Vikas	549
Victor De Paula Vila	353, 354
Tobias Bjerg Vilhelmsen	405
Ari Viljanen	180, 183, 203
Umberto Villante	288, 295
Antonio Villaseñor	86, 87
Sarah Vines	289
Marcos Vinicius Silva	386
Yuri Vinogradov	85
D S Vitthal	549
Anton Vogelmann	94
Kristin Vogfjord	462, 473
Peter H Voss	462
Peter Voss	80, 463
Angelos Vourlidas	343, 368, 375
Lara Wacha	210
Prasanna Waichal	46,47
Maria Walach	295
Mariatheresia Walach	293
Nehpreet Walia	334
Chengshan Wang	217
Chi Wang	134, 144, 165, 307
Chihping Wang	311
Dedong Wang	167
Guanren Wang	187, 206, 382
Haijun Wang	467
Huapei Wang	246
Jian WANG	453, 454, 456
Jie Wang	43, 106, 114
Long Wang	556, 557
Shiang Yu Wang	319
Shishun Wang	246
Tieyan Wang	340
Ting Wang	491
Tongjiang Wang	366

Author	Pg No.
Wenbin Wang	157, 300
Wenrui Wang	308, 321
Xiangyu Wang	307
Xueyi Wang	309
James Ward	501
Mako Watanabe	53, 54
Colin L Waters	290
Clare Watt	293
Dong Wei	111, 321
Robert Weigel	373
Banjamin Weiss	123
Jiami Wen	491
Renata Wentzcovitch	510
Magnes Werner	114
Dieter Werthmller	391
James Weygand	203, 283
Kathy Whaler	108, 121, 187, 204, 328
Samuel Wharton	295
Brandi Wheeler	85
Jens Wickert	135, 155
Sri Widiyantoro	28
Douglas Wiens	470, 471
Thomas Wiersberg	435
Monika Wilde-Piorko	417
Earle Williams	263, 264
Kathryn A Mc Williams	339
John Williamson	384
Michael Wiltberger	311,335
Simon Wing	168, 281, 309, 326, 332, 339
Aldo Winkler	250
Jan Wiszniowski	432
Chris Witte	85
Richard Wolf	308, 321
Wing Ching Jeremy Wong	427
R Carey Woodward	278
Cristiano Max Wrasse	130, 142
Darren Wright	295
Haonan Wu	270
Zhongliang Wu	554, 556, 557
John Wygant	288, 293
Lidong Xia	307
Tian Xiao	221
Zanyang Xing	307
Chao Xiong	106, 111, 278

Author	Pg No.
Shihua Xu	217
Yunao Xu	527
Pengfei Xue	246
Katsuhiro Yabu	445
Dilip K Yadav	451
R Yadav	39
Rahul Yadav	25
Rajeev Kumar Yadav	547, 549
Rakesh Yadav	15
Srinu Yadavally	434
Hiroshi Yakiwara	523
Olesya Yakovchuk	265
Kateryna Yakymenko	318
Tagir Yalaev	573
Tomotsugu Yamakawa	296
Kazuhiro Yamamoto	291, 322
Mare Yamamoto	445
Masayuki Yamamoto	131
Yoshiko Yamanaka	523
Makoto Yamano	565, 577
Koshun Yamaoka	448
Yosuke Yamazaki	116, 139, 140, 143, 145, 153, 193, 276, 386
Yuri Yampolski	263, 264
Maodu Yan	216, 221, 222, 223
Hongfeng Yang	427
Huigen Yang	307
Jian Yang	308, 321
Junying Yang	111
Xiaoqiang Yang	216, 218, 223
Yanyan Yang	105, 106, 113, 114
Zhaohui Joey Yang	479
Asaf Yaniv	41
Changli Yao	43
Rashid Yarullin	579
Alexey Yaschenko	200
Igor Yashin	325, 326
Anna Yasyukevich	128
Kiley Yeakel	168, 326
Giri Yellalacheruvu	29
Tim Yeoman	295
Zejun Yi	576
Toshiaki Yokoi	483, 554
Shoichiro Yokota	172, 291, 319, 322
Yoshihiro Yokoyama	129

Author	Pg No.
Shinji Yoneshima	80
Akimasa Yoshikawa	116, 131, 397
Chie Yoshino	55, 493
Kazunori Yoshizawa	514, 527
Wandi Yu	276
Yiqun Yu	313, 315
Zining Yu	491
Xiaohui Yuan	531
Jia Yue	276
Tong Yuqi	110
Ludmila Zabarinskaya	88
Alik Ismail Zadeh	481, 519
Dzhuliya Zagranovskaya	572
Alexander Zaitsev	88
Bryan Zaldivar	185
Jinbo Zan	219, 222
Elena Zanella	209
Christophe Zaroli	510
Mikolaj Zawadzki	121
Zhima Zeren	106, 114
Dawen Zhang	222
Fei Zhang	321
Jiangyang Zhang	427
Linyou Zhang	576
Qinghe Zhang	307
Shunrong Zhang	262
Tao Zhang	217, 222
Tingwei Zhang	218
Tuo Zhang	438
Weilin Zhang	217, 222
Xin Zhang	422, 450
Yang Zhang	316
Yiqun Zhang	492
Yongliang Zhang	307
Yongxian Zhang	557
Brandon Zhao	189
Xiang Zhao	243, 245
Irina Zhelavskaya	167, 324, 376
Liu Zhengkuan	144
Zeren Zhima	113, 492
Yi Zhong	220, 245
Bin Zhou	106, 114
Fei Zhou	81
Hongyang Zhou	356

Author	Pg No.
Kaiguang Zhu	491
Ping Zhu	11
Yajun Zhu	144
Jingyi Zhuang	510
Vladimir Zhuravlev	488
Jinping ZI	427
Helena Zlebcikova	536
Qiugang Zong	292, 298, 369
Siti Zulaikah	212
Zulfakriza Zulfakriza	28, 36
Juan Rodriguez Zuluaga	153
F Ramon Zuniga	486

IAGA IASPEI INDIA 2021

60
CSIR
NGRI
1961 - 2021

CSIR – NATIONAL GEOPHYSICAL RESEARCH INSTITUTE
(Council of Scientific and Industrial Research)
Uppal Road, Hyderabad - 500 007 (India)
www.ngri.org.in